SYNTHESIS, STRUCTURES, AND REACTIVITY OF BIOLOGICALLY RELEVANT SULFUR-CONTAINING COPPER(I) COMPLEXES

AN ABSTRACT

SUBMITTED ON THE NINETEENTH DAY OF SEPTEMBER 2014

TO THE DEPARTMENT OF CHEMISTRY

IN PARTIAL FULFILLMENT OF THE REQUIREMENT

OF THE SCHOOL OF SCIENCE AND ENGINEERING

OF TULANE UNIVERSITY

FOR THE DEGREE

OF

DOCTOR OF PHILOSOPHY

BY

Skylar J. Ferrara

APPROVED BY:

James P. Donahue, Ph.D.,
Chair

Russell H. Schmehl, Ph.D.

Mark J. Fink, Ph.D.

Janarthanan Jayawickramarajah, Ph.D.

Abstract

Several aspects of the bioinorganic chemistry of copper remain elusive. Low-coordinate, sulfur-containing copper sites appear to play different, yet very important roles in biology. These motifs are not well understood, but are implicated in biological copper sequestration, copper transfer, and are found as part of an active site within a particular metalloenzyme system that catalyzes water-gas shift chemistry. The work described in this dissertation details the exploratory synthesis aimed at modeling these systems.

Synthetic efforts to gain access to two-coordinate copper(I) bis(thiolato) species which model copper metallochaperones and metalloregulatory proteins are outlined in Chapter 1. To this end, the synthetic preparation of a new, bulky thiolate ligand precursor, 1-(thioacetyl)triptycene, was devised. Upon deprotection to form 1-(thiolato)triptycene, this ligand affords several new low-coordinate cuprous thiolate complexes. One particular species, $[Bu_4N][Cu(STrip)_2]$, exists as an analogue of the copper metallochaperones and metalloregulatory proteins described previously. A cyclic hexameric species, $[Bu_4N][(CuSTrip)_6(\mu_6\text{-}Br)]$, emerged from the coordination chemistry and features a new cuprous thiolate structure type. Additionally, a few organometallic copper(I) complexes bearing the triptycene ligand are discussed.

Chapter 2 describes the synthesis of new, potentially useful two- and four-coordinate copper(I) silylthiolate complexes and cuprous metallothiols. Here, synthesis and characterization of [Cu(IPr)(SH)] represents the *first* example of a two-coordinate

copper metallothiol species is reported. The reactivity of both copper(I) silylthiolates and cuprous metallothiols was explored within the context of their potential use as starting materials in an effort to construct heteronuclear species.

Chapter 3 details the synthetic efforts toward assembling a structural analogue of the metalloenzyme active site of molybdenum-dependent carbon monoxide dehydrogenase (Mo-CODH). Two synthetic methodologies, silane-mediated coupling and the reaction of terminal sulfido molybdenum species with labile copper(I) salts, were explored in this context. Several new heteronuclear cluster species containing [Mo(μ-$S)_2$Cu] rhomb core units were formed from the reactions outlined in this chapter. Conclusions are discussed with regard to the synthetic nuances associated with generating a synthetic analogue of the active site of Mo-CODH.

Multinuclear copper species bearing diamino-dithiolate (N_2S_2) ligands which formed either serendipitously via ligand exchange or by deliberate syntheses are described in Chapter 4. Copper complexes containing N_2S_2 ligands appear to stabilize or support mixed-valence cores and can access a variety of structure types. The interesting features associated with these structures are discussed and comments regarding the potential reactivity of these species are framed within a bioinorganic context.

SYNTHESIS, STRUCTURES, AND REACTIVITY OF BIOLOGICALLY RELEVANT SULFUR-CONTAINING COPPER(I) COMPLEXES

A DISSERTATION

SUBMITTED ON THE NINETEENTH DAY OF SEPTEMBER 2014

TO THE DEPARTMENT OF CHEMISTRY

IN PARTIAL FULFILLMENT OF THE REQUIREMENT

OF THE SCHOOL OF SCIENCE AND ENGINEERING

OF TULANE UNIVERSITY

FOR THE DEGREE

OF

DOCTOR OF PHILOSOPHY

BY

Skylar J. Ferrara

APPROVED BY:

James P. Donahue, Ph.D.,
Chair

Russell H. Schmehl, Ph.D.

Mark J. Fink, Ph.D.

Janarthanan Jayawickramarajah, Ph.D.

©Copyright by Skylar J. Ferrara, 2014

All Rights Reserved

DEDICATED TO MY MOTHER KATIE, AND MY LATE FATHER, CARL.

Acknowledgements

It would not have been possible to write this dissertation without the help and support of many great, caring people with whom I've known both past and present. Unfortunately, I can only specifically mention some of these people here.

First and foremost, I would like to express my sincere gratitude to my doctoral advisor, Professor James P. Donahue. Over my years at Tulane it became clear that Jim invested an enormous amount of time and energy in cultivating me as a scientist and intellect. His guidance and encouragement throughout my graduate career were integral in every achievement along the way. At his core, Jim truly cares about people, especially his students, and I have nothing but the utmost respect for this unwavering dedication to those people in his life. Thank you, Jim, I hope this is merely the beginning of a long and fruitful relationship between us.

I would like to thank the members of my dissertation committee: Professor Russ Schmehl, Professor Mark Fink, and Professor Janan Jayawickramarajah. Your valuable guidance regarding my research is much appreciated, as is your welcoming presence around the department. Your helpful discussions and kind letters of recommendation are not overlooked, and for that I'm truly grateful.

Special thanks are in order acknowledging Dr. Joel Mague's contribution to the crystallography in my dissertation, and for acting as a second advisor to me. The number of hours spent helping me to learn X-ray crystallography and offering advice are

remarkable. I'm extremely appreciative of all your help Dr. Mague. Additionally, I'd like to thank my undergraduate advisor, Professor Craig Anderson. Craig has been instrumental in encouraging me to continue along my academic path and has been a tremendous friend over the years. Without his help, none of this would have been possible.

I would like to take this opportunity to thank Professor Carol Zhang and Professor Heiko Jacobsen for their advice and friendly conversations over my time at Tulane. I'd like to especially thank Carol for all the useful career advice she's given me and for helping me in my last few months at Tulane. In addition, I wish to thank collaborators Professor Stephen Sproules (Dept. of Chemistry, University of Glasgow) for EPR measurements and Professor Kyle Lancaster (Dept. of Chemistry, Cornell University) for XAS measurements. I'm also appreciative of the administrative and other supporting staff in the chemistry department: Emelina Sanchez, Ginette Arguello, Billy Russell, Linda Chevalier, and Qi Zhao.

Perhaps those most directly relevant to my career as a graduate student are the faces I've seen on a daily basis. All past and present Donahue group members are acknowledged not only for their help academically, but for their care and humor, making the group a fun and enjoyable place to work. Dr. Upul Jayarathne, Dr. Yong Yan, Dr. Jing Gu, Dr. Amelia Neuberger, Dr. P. Chandrasekaran, Dr. Mike Reale, Angel Greene, Joel Leger, Ted Shaner, Cooper Battle, Tod Grusenmeyer, and Shane McGlynn are acknowledged for their valuable friendship. A special debt of gratitude is owed to Yong Yan and Upul Jayarathne, whom have made my graduate experience special and continue

to inspire me as I watch their paths in life unfold. I would also like to especially thank Angel Greene for her help with computational work and for her tremendous friendship during my time at Tulane.

I'm extremely appreciative of all my former students, who've taught me the value in each person existing as a dynamic individual. Everyone deserves equal attention and opportunity, as time is the only limiting factor when it comes to personal success. I've thoroughly enjoyed watching all of my former students evolve into amazing individuals regardless of the specific route they've chosen and I'm very proud of you all.

I am deeply grateful to my wonderful girlfriend, Alberta Poon. Your love and support means the world to me. Lastly, I'm truly indebted to my mother Katie, and brother Dash, for their unending love, encouragement, and support. I am unbelievably lucky to have you in my life.

TABLE OF CONTENTS

Page

ACKNOWLEDGEMENTS ii

LIST OF FIGURES xi

LIST OF SCHEMES xii

LIST OF TABLES xv

CHAPTER 1

1. INTRODUCTION 1

1.1 COPPER(I) METALLOREGULATORY PROTEINS AND METALLOCHAPERONES 2

1.2 MOLYBDENUM-DEPENDENT CARBON MONOXIDE DEHYDROGENASE 8

1.3 BIOMIMETIC CHEMISTRY 9

2. RESULTS AND DISCUSSION 11

2.1 SYNTHESIS AND REACTIVITY 11

2.2 STRUCTURES 26

3. SUMMARY AND CONCLUSIONS 38

4. EXPERIMENTAL 43

5. REFERENCES 51

CHAPTER 2

1. INTRODUCTION 58

1.1 COPPER(I) SILYLTHIOLATES 61

1.2 CUPROUS METALLOTHIOLS 65

2. RESULTS AND DISCUSSION 67

2.1 SYNTHESIS 67

2.2 REACTIVITY: ORGANIC PARALLELS? 74

2.3 STRUCTURES 79

3. SUMMARY AND CONCLUSIONS 83

4. EXPERIMENTAL 84

5. REFERENCES 90

CHAPTER 3

1. INTRODUCTION 94

1.1 CARBON DIOXIDE REDUCTION CHEMISTRY 94

1.2 MOLYBDENUM-DEPENDENT CARBON MONOXIDE DEHYDROGENASE 97

1.3 SYNTHETIC ANALOGUES OF Mo-CODH 103

2. RESULTS AND DISCUSSION 109

2.1 SYNTHETIC APPROACHES 109

2.2 SILANE-MEDIATED COUPLING APPROACH 110

2.3 REACTIONS BETWEEN TERMINAL SULFIDO MOLYBDENUM COMPLEXES AND LABILE COPPER SALTS 138

2.4 MISCELLANEOUS REACTIONS 146

3. SUMMARY AND CONCLUSIONS 147

4. EXPERIMENTAL 154

5. REFERENCES 159

CHAPTER 4

1. INTRODUCTION 165

1.1 BIOLOGICAL RELEVANCE 165

2. RESULTS AND DISCUSSION 168

3. SUMMARY AND CONCLUSIONS 187

4. EXPERIMENTAL 189

5. REFERENCES 193

APPENDIX A 196

CHAPTER 1 CRYSTAL INFORMATION 196

APPENDIX B 272

CHAPTER 2 CRYSTAL INFORMATION 272

APPENDIX C 298

CHAPTER 3 CRYSTAL INFORMATION 298

APPENDIX D 350

CHAPTER 4 CRYSTAL INFORMATION 350

LIST OF FIGURES

Chapter 1

Figure 1.1 Structural representations of metalloregulatory protein CueR. Images taken from reference 8 (with permission) and the Protein Data Bank (reference 9). "From Changela, A.; Chen, K.; Xue, Y.; Holschen, J.; Outten, C. E.; O'Halloran, T. V.; Mondragón,A. Science **2003**, 301, 1383– 1387. Reprinted with permission from AAAS." 4

Figure 1.2 Copper transport among the three main pathways within the cell. Image taken from reference 12. "Reprinted (adapted) with permission from (Pitts, A. L.; Hall, M. B. Inorg. Chem. **2013**, 52, 10387-10393). Copyright (2013) American Chemical Society." 6

Figure 1.3 Proposed pathway for the intracellular trafficking of Cu(I) by Atx1. Inset: a proposed mechanism for the exchange of Cu(I) involving two- and three-coordinate intermediates. Image taken from reference 10 with permission. "From Pufahl, R. A.; Singer, C. P.; Peariso, K. L.; Lin, S.-J.; Schmidt, P. J.; Fahrni, C. J.; Cizewski Culotta, V.; Penner-Hahn, J. E.; O'Halloran, T. V. Science **1997**, 278, 853– 856. Reprinted with permission from AAAS." 8

Figure 1.4 The native active site of molybdenum-dependent carbon monoxide dehydrogenase from Oligotropha carboxidovorans. 9

Figure 1.5 Crystallographically authenticated structure types among homoleptic monothiolate copper(I) complexes. 12

Figure 1.6 Structurally authenticated mononuclear copper(I) bis(thiolato) complexes. References 16-21. 13

Figure 1.7 Mass spectrum (MALDI-TOF) of product mixture from the attempted reaction $[Cu(STrip)_2]^{1-} + Ph_3SiSH \rightarrow [Cu(STrip)(SSiPh_3)]^{1-} + TripSH$. The inset show the presence of the desired $[Cu(STrip)(SSiPh_3)]^{1-}$ as a mixture with $[Cu(STrip)_2]^{1-}$ and $[Cu(SSiPh_3)_2]^{1-}$. 20

Figure 1.8 Mass spectrometric (MALDI-TOF) authentification of the bis(triptycyl) copper(I) monoanion. 23

Figure 1.9 ^1H NMR spectrum of [Cu(IPr)(Trip)] highlighting the correct integration corresponding to the methyne protons of the isopropyl groups of IPr and the 10H proton of the triptycyl ligand's unsubstituted bridgehead carbon 24

Figure 1.10 Cell packing diagram for triclinic polymorph of **4** illustrating the π-π stacking of anthracenyl groups and alternating disposition of thioacetyl groups. 28

Figure 1.11 Thermal ellipsoid plot of bis(9-anthracenyl)sulfide at the 50% probability level highlighting anthracene planes AB and A'B'. Hydrogen atoms are omitted for clarity. 29

Figure 1.12 Thermal ellipsoid plots of 1-(thioacetyl)triptycene **5**, tert-butyl triptycyl sulfide **8,** and anion **9** of $[Bu_4N]^+[TripS^-]$ at the 50% probability level. Hydrogen atoms are omitted for clarity. 30

Figure 1.13 Thermal ellipsoid plot (50%) of anion **10** with hydrogen atoms omitted for clarity, illustrating the π···π and CH···π interactions that enforce the small C−S···S−C torsion angle. 32

Figure 1.14 Thermal ellipsoid plots (50%) of anion **14** with view orthogonal to Cu_6 plane and side-on with triptycyl groups truncated for clarity. All hydrogen atoms are removed for clarity. Inset of **Table 1.4** showing selected structural parameters for **14**. 34

Figure 1.15 D_{3d} $Cu_6(STrip)_6$ core structure inscribed within the D_{6h} homoleptic thiolate $M_6(SR)_{12}$ structure. 36

Figure 1.16 Thermal ellipsoid plots (50%) of **13** and anion of $[Bu_4N][Cu(Trip)Cl]$ with hydrogen atoms omitted for clarity. Inset **Table 1.5** provides crystal information of $[Bu_4N][Cu(Trip)Cl]$. 37

Figure 1.17 Recreated molecular orbital diagrams for $[Cu(SMe)_2]^{1-}$ showing different mixing of Cu d orbitals with S p orbitals for geometries with a C−S···S−C dihedral angle of 180° (left) and 90° (right). "Reprinted (adapted) with permission from (Pitts, A. L.; Hall, M. B. Inorg. Chem. **2013**, 52, 10387-10393). Copyright (2013) American Chemical Society." 40

Figure 1.18 X-ray absorption near edge structure (XANES) spectra for different copper complexes, highlighting the match between resting state of native Atx1 core and that of trigonal three-coordinate dianionic tris(thiolate) model complex. Image reproduced from reference 10 with permission. "From Pufahl, R. A.; Singer, C. P.; Peariso, K. L.; Lin, S.-J.; Schmidt, P. J.; Fahrni, C. J.; Cizewski Culotta, V.; Penner-Hahn, J. E.; O'Halloran, T. V. Science **1997**, 278, 853– 856. Reprinted with permission from AAAS." 42

Chapter 2

Figure 2.1 Minimal representations of some heteronuclear metalloenzyme active sites. 59

Figure 2.2 Existing mononuclear copper(I) silylthiolates from the literature (References 31-34). 63

Figure 2.3 Structurally characterized copper metallothiols. References 40-42. 66

Figure 2.4 Crystal structures and selected structural parameters for copper(I) silylthiolate complexes. All thermal ellipsoid plots at the 50% probability level. 80

Figure 2.5 Crystal structure and packing diagram for [Cu(IPr)(SH)]. Thermal ellipsoid plot is drawn at the 50% probability level. Hydrogen atoms are omitted for clarity, except for the sulfhydryl hydrogen, which was identified in the electron difference maps near the end of the refinement and ultimately refined with appropriate distance restraints. 82

Chapter 3

Figure 3.1 Minimal representations of the metal-containing active sites of CO dehydrogenases. 98

Figure 3.2 Representative structure of Mo-dependent carbon monoxide dehydrogenase and the reaction it catalyzes. Image generated using the Protein Data Bank. 100

Figure 3.3 Active site of Mo-CODH and its proposed mechanism of CO oxidation. 101

Figure 3.4 Existing structural analogues of Mo-CODH (references 26,27, and 29). 104

Figure 3.5 ESI-MS (negative ion mode) of an aliquot taken ~5 mins. after reaction of $[MoO_2(bdt)(OSiPh_3)]^{1-}$ with $[Cu(STrip)(SSi^iPr_3)]^{1-}$ at -78°C. 116

Figure 3.6 Crystal structures of **1A** (top) and **1B** (bottom). Thermal ellipsoid plot is drawn at the 50% probability level. Hydrogen atoms are omitted for clarity. 119

Figure 3.7 Positive ion mode MALDI-MS (top) and calculated (bottom) isotope distribution pattern for $[Mo(=O)S_3(CuP^tBu_3)_3]^+$. Calculated spectrum obtained from http://www.sisweb.com/mstools/isotope.htm. 122

Figure 3.8 Crystal structure of **3**, $[MoO_2(OSiPh_3)(\mu\text{-}O)Cu(Me_4phen)(P^tBu_3)]$. Thermal ellipsoid plot is drawn at the 50% probability level. Hydrogen atoms are omitted for clarity. 124

Figure 3.9 UV-vis spectrum of **3**, 0.54 μM in THF. 125

Figure 3.10 Positive ion mode MALDI-MS of $[MoO(^tBu_4salphen)]^+$. 129

Figure 3.11 UV-vis spectrum of $[MoO(^tBu_4salphen)Cl]$, 14.6 μM in THF. 130

Figure 3.12 MALDI-MS of the product obtained from the reaction shown in Scheme 3.13. 132

Figure 3.13 Room temperature EPR spectrum of the product isolated from the reaction described in Scheme 3.13. 133

Figure 3.14 UV-vis of $[Mo(=O)S_3(CuP^tBu_3)_3Cl]$, 44.2 μM in THF. 135

Figure 3.15 ^1H NMR spectrum of $[Mo(=O)S_3(CuP^tBu_3)_3Cl]$. Full spectral width (+100 ppm to -100 ppm) showing benzene solvent residual (most downfield), P^tBu_3 (middle) and TMS (0 ppm) (top spectrum), and P^tBu_3 doublet (bottom spectrum). 136

Figure 3.16 MALDI-MS of $[Mo(=O)S_3(CuP^tBu_3)_3]^+$ from the reaction shown in Scheme 3.14 in positive ion mode. 137

Figure 3.17 Crystal structure of $[MoO(\mu\text{-}S)_3(Cu(phen))_3]^+$ cation **5**. Thermal ellipsoid plot drawn at the 50% probability level. Hydrogen atoms are omitted for clarity. 144

Figure 3.18 Cyclic voltammogram (100 mV/s scan rate, cathodic direction) of $[(phen)MoOS(OSiPh_3)_2]$ in DCM with $[Bu_4N][PF_6]$ electrolyte. 145

Chapter 4

Figure 4.1 Minimal representations of the Cu_Z active site and Cu_A site in nitrous oxide reductase from Pseudomonas stutzeri. 167

Figure 4.2 Crystal structure of $[[Cu(N_2S_2aryl)]_3(Cu_2)]$, **1**. Hydrogen atoms are omitted for clarity and all thermal ellipsoid plots are at the 50% probability level. One of two independent molecules in the asymmetric unit of the unit cell is shown. 171

Figure 4.3 Crystal structure of **2**. Hydrogen atoms are omitted for clarity, and all thermal ellipsoids are presented at the 50% probability level. 174

Figure 4.4 ^{1}H NMR spectrum of **2**. 175

Figure 4.5 ^{1}H NMR spectrum overlay. Pure spectrum of **2** (raised, back) and co-crystallized mixture from discrete synthesis (lower, front). 176

Figure 4.6 Crystal structure of **3** from two perspectives: face down (top) and side on (bottom). Hydrogen atoms are omitted for clarity, and all thermal ellipsoids plotted at the 50% probability level. 178

Figure 4.7 ^{1}H NMR spectrum of **3**. 180

Figure 4.8 Cyclic voltammogram of **3** in THF with $[Bu_4N][PF_6]$ as supporting electrolyte. 181

Figure 4.9 Frontier molecular orbitals of **3** calculated from the crystal structure coordinates of **3**. Showing the HOMO (highest occupied molecular orbital, left) and LUMO (lowest unoccupied molecular orbital, right). 183

Figure 4.10 Molecular orbital diagram for **3** displaying the HOMO, HOMO-1 (H-1), and HOMO-2 (H-2). 183

Figure 4.11 Crystal structure of cation of decacopper **4**. All hydrogen atoms removed for clarity and thermal ellipsoids plotted at the 50% probability level. 186

Figure 4.12 UV-vis spectrum of **4**, 0.14 mM in acetonitrile highlighting λ_{max} (ε_{Molar}). 187

LIST OF SCHEMES

Chapter 1

Scheme 1.1 Synthesis of 1-(thioacetyl)triptycene. 15

Scheme 1.2 Synthesis of copper(I) complexes with 1-(thiolato)triptycene. 18

Scheme 1.3 A closed, stoichiometric cycle for generating 1-(chalcoacetyl)triptycene via chalcogen insertion. E = chalcogen donor source. 25

Chapter 2

Scheme 2.1 Synthetic scheme for copper(I) silylthiolate complexes. 69

Scheme 2.2 Synthetic scheme for copper(I) metallothiols. L = neutral donor ligands, IMes = 1,3-bis(2,4,6-trimethylphenyl)imidazol-2-ylidene, IPr = 1,3-bis(2,6-diisopropylphenyl)imidazol-2-ylidene, and triphos = 1,1,1-tris(diphenylphosphinomethyl)ethane. 71

Scheme 2.3 Reactivity of organic thiols. 76

Scheme 2.4 Oxidative addition of tetraethylthiuram disulfide to [Cu(IMes)(SH)]. 77

Chapter 3

Scheme 3.1 Energetic requirements for the reduction of carbon dioxide at pH 7 in aqueous solution versus NHE, 25°C, 1 atmosphere, and 1M for the other solutes. References 4 and 5. 96

Scheme 3.2 Synthetic route to Mo-CODH analogue by Tatsumi et al. (reference 26). 105

Scheme 3.3 Synthetic route to Mo-CODH analogue by Young et al. (reference 27). 106

Scheme 3.4 Synthetic route to Mo-CODH analogue outlined by Holm et al. (Reference 29). 108

Scheme 3.5 Synthetic scheme used by Holm et al. to form a synthetic analogue of sulfite reductase (reference 40). Iron-sulfur clusters and sirohemes are minimal representations. 111

Scheme 3.6 Silane-mediated coupling scheme for formation of M−S−M' species. 112

Scheme 3.7 Coupling reaction between $[MoO_2(bdt)(OSiPh_3)]^{1-}$ and $[Cu(STrip)(SSi^iPr_3)]^{1-}$. 115

Scheme 3.8 Reaction of $[MoO_2(OSiPh_3)_2]$ and $[Cu(IMes)(SSi^iPr_3)]$. 118

Scheme 3.9 Reaction between $[MoO_2(OSiPh_3)_2]$ and $[Cu(P^tBu_3)(SSiPh_3)]$. 121

Scheme 3.10 Reaction between $[MoO_2(Me_4phen)(OSiPh_3)_2]$ and $[Cu(P^tBu_3)(SSiPh_3)]$. 123

Scheme 3.11 Reaction between $[MoO(N_2S_2aryl)(OSiMe_3)]$ or $[MoO(N_2S_2alkyl)(OSiMe_3)]$ and $[Cu(IMes)(SSi^iPr_3)]$. 127

Scheme 3.12 Synthesis of $[MoO(^tBu_4salphen)Cl]$. 128

Scheme 3.13 Reaction between $[MoO(^tBu_4salphen)Cl]$ and $[Cu(IMes)(SSi^iPr_3)]$. 131

Scheme 3.14 Reaction between $[MoO(^tBu_4salphen)Cl]$ and $[Cu(P^tBu_3)(SSiPh_3)]$. 134

Scheme 3.15 Reaction between a labile copper(I) salt and a sulfidomolybdenum complex. 138

Scheme 3.16 Reaction between $(Et_4N)_2[MoO_3S]$ and $[Cu(S93)(MeCN)[BF_4]$. 139

Scheme 3.17 Reaction between $(Et_4N)_2[MoO_3S]$ and $[Cu(IMes)(MeCN)][PF_6]$ in THF. 141

Scheme 3.18 Reaction between $[(phen)MoOS(OSiPh_3)_2]$ and $[Cu(IMes)(MeCN)][PF_6]$. 142

Scheme 3.19 Reaction between $[(phen)MoOS(OSiPh_3)_2]$ and $[Cu(Tpm^*)(MeCN)][PF_6]$. 143

Scheme 3.20 Possible general mechanism for $[Mo(\mu\text{-}S)_2Cu]$ formation. 149

Scheme 3.21 Potential reaction scenario modeling Mo-CODH reactivity. 153

Chapter 4

Scheme 4.1 Reaction affording pentacopper species **1**. 170

Scheme 4.2 Reaction affording dicopper species **2**. 173

Scheme 4.3 Synthetic route to tetracopper **3**. 177

Scheme 4.4 Synthesis of decacopper cage cluster **4**. 185

LIST OF TABLES

Chapter 1

Table 1.1	Numbering system for compound identification in Chapter 1.	15
Table 1.2	Crystal and refinement data for compounds **3**-**5**, **7**-**10**, and **13**-**14**.	27
Table 1.3	Structural parameters of $[Cu^{I}(SR)_2]^{1-}$ compounds.	33
Table 1.4	Inset of **Table 1.4** showing selected structural parameters for **14**.	34
Table 1.5	Inset **Table 1.5** provides crystal information of $[Bu_4N][Cu(Trip)Cl]$.	37
Table 1.6	Summary of Structural Data for [Cu(carbene)(SR)] Compounds.	38

Chapter 2

Table 2.1	Crystal and refinement data for compounds in Chapter 2.	79
Table 2.2	Structural parameters for copper(I) silylthiolate and metallothiol compounds.	81

Chapter 3

Table 3.1	Crystal and refinement data for compounds in Chapter 3.	113
Table 3.2	Compound number list for Chapter 3.	114

Chapter 4

Table 4.1	Crystal and refinement data for compounds in Chapter 4.	169
Table 4.2	Compound number list for Chapter 4.	169
Table 4.3	Copper-copper bond distances in **1**.	172
Table 4.4	Selected bond distances about the core of **3**.	179

Chapter 1

Synthesis, Structures, and Reactivity of Cuprous Triptycylthiolate Complexes

Introduction

Transition metal ions constitute an essential class of components in all of life across the taxonomic spectrum. However, transition metals are found in trace levels within every organism. Metal ion content exceeding "trace" amounts is toxic and potentially fatal to the cell. Thus, the sequestration, storage, and trafficking of transition metal ions is crucial for maintaining normal cell physiology. This regulation of metal ion content represents a dramatically important manifestation of coordination chemistry. The binding of metal ions in biology is dominated by hard-soft acid-base theory, where metal ions coordinate the heteroatoms of specific protein residues. Additionally, the size, shape, and electronic environment of the local binding site are critical aspects which give rise to the complexity of structures and associated functions observed in biology.

Copper is one of the handful of essential transition elements found in biological systems, where it plays a number of diverse roles with respect to both electron transfer and its Lewis acid character. Following the rise of photosynthetic organisms such as cyanobacteria, oxygen accumulated in Earth's atmosphere and oceans, leading to a decrease in solubility of iron and an expansion of the biological role of copper. Its ability to undergo one-electron redox events (specifically its copper(I)/(II) redox couple), makes copper an ideal biological cofactor; however, this ability also allows it to readily catalyze the formation of reactive oxygen species (ROS) through Fenton chemistry when "free" or

unbound within the cell. ROS, primarily as hydroxyl radical formed from free intracellular copper, can damage proteins, nucleic acids, and lipids, and can disrupt the biosynthesis of iron-sulfur clusters that are essential for the activity of numerous important cellular enzymes. As life evolved in the oxygen-rich environment, more complex roles for copper arose with concomitant trafficking pathways that evolved to ensure that most copper ions in the cell are either transiently sequestered or compartmentalized, thereby maximizing the trade-off between their biological utility and toxicity. To maintain proper homeostasis, organisms rely on copper ion binding metallochaperones, metalloregulatory proteins, and other cuprophilic constructs to move Cu(I) around as a complexed metal.

Within the context of the human body, understanding how the body maintains proper copper homeostasis is vital to prevent or cure diseases associated with a build-up or lack of copper. Diseases linked to an improper Cu(I) balance include Menkes disease[1], Wilson's disease[2], and familial amyotrophic lateral sclerosis.[3] While these diseases are genetic and cannot be cured, they can be treated. At the present, improving treatments can only be facilitated by a deeper understanding of copper transfer inside the cell. Additionally, a build-up of copper ions has been found to also be connected to Alzheimer's[4] and prion[5] diseases.

Copper(I) Metalloregulatory Proteins and Metallochaperones

Copper(I) is a soft, d^{10} metal ion, and prefers to bind other soft ions both *in vitro* and *in vivo*. A very favorable soft-soft bonding interaction exists between copper and sulfur; thus, the vast majority of copper-containing biomolecules feature at least one

sulfur atom bound in their immediate coordination sphere. Given the necessity of strict regulation of copper content by these biomolecules that bind and traffic copper(I), conserved binding motifs are observed within each class.

Metalloregulatory proteins transduce metal ion signals into changes in gene or protein expression and often function in metal ion homeostasis or detoxification. These functions are necessary since cells in the natural world consistently encounter a changing environment with fluctuations in nutrient concentrations. Cell survival requires physiological responses to such changes. Homeostatic controls rely on the presence of sensory systems that detect fluctuations in intracellular metal levels and discriminate among various metal ions. Discrimination between metal ions may be achieved through the existence of metal-specific structural motifs and/or by specific metal ion uptake and intracellular translocation to organelles containing the metalloregulatory molecules.

CueR is a metalloregulatory protein which acts as a copper-responsive genetic switch that regulates transcription of genes encoding CopA and CueO, the primary copper-export system in *E. coli*.[6] Expression of the CopA effluxer is induced when dimeric CueR binds two copper(I) ions. Thermodynamic calibration studies performed on CueR reveal a zeptomolar (10^{-21} M) sensitivity to free copper(I), which measures to significantly less than one atom per cell.[7,8] The extraordinary sensitivity and selectivity are implicated by an unusual buried metal-receptor site in CueR which constrains the metal to a linear, two-coordinate geometry and uses helix-dipole and hydrogen bonding interactions to reinforce metal binding. This coordination mode is unique among metalloproteins but ideal for an ultrasensitive genetic switch. Precluding unambiguous protein crystallographic detail, X-ray absorption spectroscopic techniques (XANES and

EXAFS) were used to adequately identify the structure of the binding sites. The two metal binding sites of dimeric CueR contain bis(cysteinate) ligation at copper(I), featuring a linear, digonally bound [S−Cu(I)−S] core.[8]

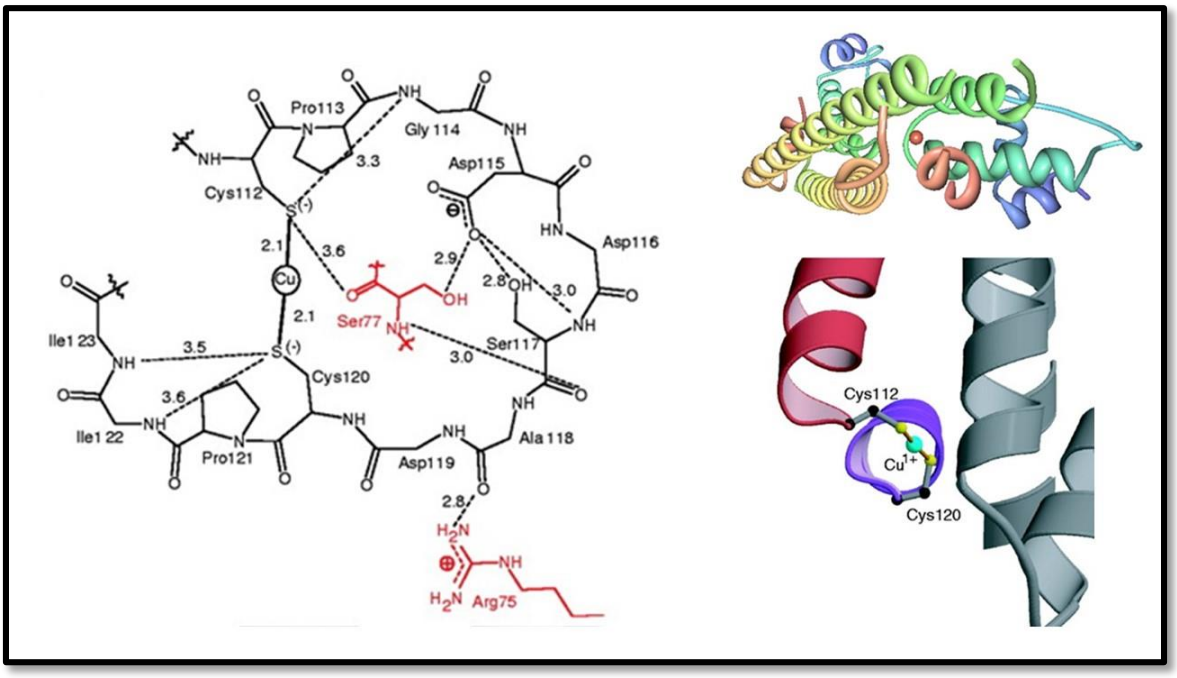

Figure 1.1 Structural representations of metalloregulatory protein CueR. Images taken from reference 8 (with permission) and the Protein Data Bank (reference 9). "From Changela, A.; Chen, K.; Xue, Y.; Holschen, J.; Outten, C. E.; O'Halloran, T. V.; Mondragón,A. *Science* **2003**, 301, 1383– 1387. Reprinted with permission from AAAS."

Four factors appear to give rise to CueR's exquisite selectivity. Divalent metal ions typically prefer higher coordination numbers than monovalent coinage metals, thus discrimination is first conferred at the level of coordinate-covalent bond formation. Cys^{112} and Cys^{120} represent the only ligating residues, giving rise to a two-coordinate geometry at the binding site. Secondly, the local environment of the binding cavity

imposes hydrophobic and steric restrictions which contribute to a shielded coordination environment. In CueR, the buried [S−Cu(I)−S] center formally bears a net negative charge (monoanion). However, charge neutralization of thiolate Cys^{120} likely arises from interactions with the positively charged end of the helix dipole and two backbone hydrogen bonds that originate from the short two-turn α helix extending from the metal binding loop. Lastly, a positively charged lysine residue, Lys^{81}, is found in the vicinity of Cys^{112}, leading to additional charge neutralization for the CueR binding sites.

Copper metallochaperones are soluble, cytoplasmic copper-binding proteins. These proteins bind copper after it enters the cell and deliver it to their corresponding recipient proteins. In yeast, Atx1 is the copper metallochaperone that delivers copper to the Ccc2 P-type ATPase.[10] Most often, copper chaperones bear significant structural similarity to their target proteins, and they frequently possess the methionine and cysteine –rich heavy metal associated MXCXXC binding motif found in metal ion translocating ATPases. X-ray absorption spectroscopy (XANES and EXAFS) has revealed the copper binding site of Atx1 to contain two cysteinate residues and a weakly bound third sulfur atom, giving rise to a structure that is intermediate between near-linear two-coordinate and trigonal three-coordinate. Atox1 is the human homologue of Atx1 and features essentially the same structural domains. In the human body, there are several pathways for copper inside the cell, and each starts with the uptake of copper(I) through a Ctr permease.[11] These high-affinity copper transporters contain methionine and cysteine binding sites (MXCXXC motif) that coordinate copper as it enters the cell. Upon entering the cytoplasm, there are three main destinations for a copper ion: the CcO (cytochrome c oxidase) enzyme in the mitochondria, the copper/zinc superoxide

dismutase 1, or the ATPase proteins in the Golgi apparatus (Figure 1.2). Copper ions are then transferred to these destinations via the metallochaperones that are specific to each path. The Atox1 metallochaperone carries copper(I) to the Golgi apparatus where it is transferred to a metal binding domain of ATP7A or ATP7B.[12]

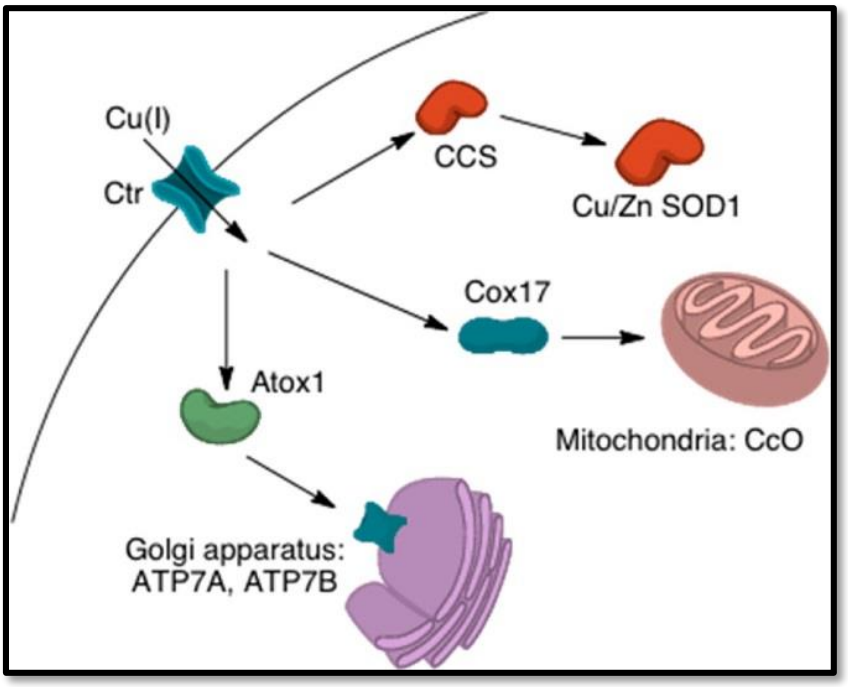

Figure 1.2 Copper transport among the three main pathways within the cell. Image taken from reference 12. "Reprinted (adapted) with permission from (Pitts, A. L.; Hall, M. B. *Inorg. Chem.* **2013**, 52, 10387-10393). Copyright (2013) American Chemical Society."

The structural and functional similarities found between Atx1 and Atox1 suggest a similar, if not identical, mechanism for copper(I) transport. A proposed mechanism begins with the binding of copper(I) to the metallochaperone in a two-coordinate fashion. A nearby receptor protein can then interact with copper bound to the metallochaperone to form a three-coordinate intermediate. Scission of one copper-sulfur bond on the metallochaperone to transiently form a two-coordinate species is followed by

coordination of a second sulfur by the receptor protein. In this way, copper is shuttled between the copper metallochaperone (Atx1 or Atox1) and the corresponding receptor protein (Ccc2 for Atx1 and ATP7A or ATP7B for Atox1) by accessing transiently formed two-and three-coordinate intermediates. This mechanism provides a route to a diffusion-driven movement of the copper(I) ion from one site in the cell to another on the basis of small differences in the binding constants of each domain for Cu(I). This sequence is essentially a vectorial process with the copper(I) ion being expeditiously passed down a local thermodynamic gradient, from Cu(I) binding sites of lower affinity to higher affinity sites, prohibiting its release into the cytoplasm. If the free energy changes for each of these steps are coupled, it has been proposed that hydrolysis of ATP by a receptor protein may provide the overall driving force by moving copper(I) ions across the vesicular membrane into a separate receptacle, where they are ultimately incorporated into ceruloplasmin (the major copper carrying protein in the blood).[10]

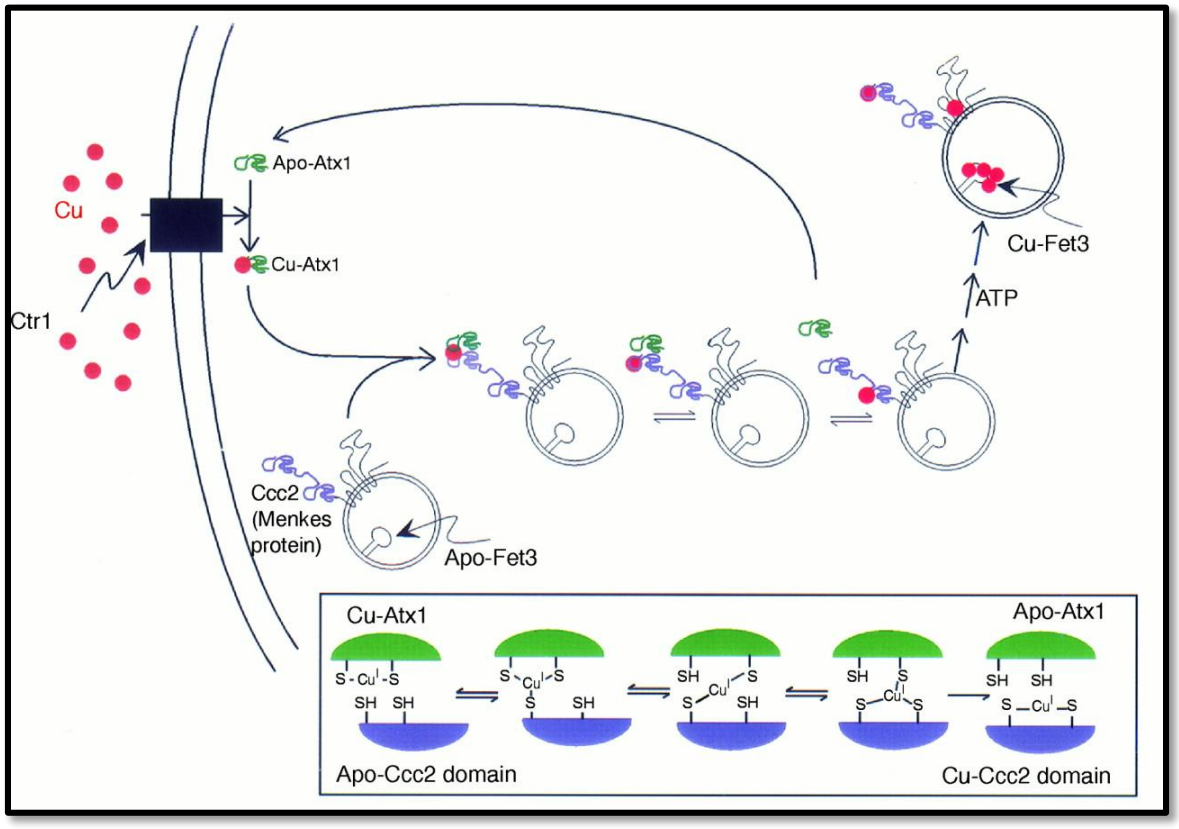

Figure 1.3 Proposed pathway for the intracellular trafficking of Cu(I) by Atx1. Inset: a proposed mechanism for the exchange of Cu(I) involving two- and three-coordinate intermediates. Image taken from reference 10 with permission. "From Pufahl, R. A.; Singer, C. P.; Peariso, K. L.; Lin, S.-J.; Schmidt, P. J.; Fahrni, C. J.; Cizewski Culotta, V.; Penner-Hahn, J. E.; O'Halloran, T. V. *Science* **1997**, 278, 853– 856. Reprinted with permission from AAAS."

Molybdenum-Dependent Carbon Monoxide Dehydrogenase

A third metallobiomolecule found in nature also features the two-coordinate, all-sulfur ligated copper(I) motif. Molybdenum-dependent carbon monoxide dehydrogenase (Mo-CODH) is an aerobic carbon monoxide (CO) oxidizing metalloenzyme system that catalyzes the reaction: $CO + H_2O \leftrightarrow CO_2 + 2H^+ + 2e^-$. Mo-CODH plays a major role in Earth's global carbon cycle, and contributes significantly to the regulation of CO content

in the atmosphere.[13] The metalloenzyme's active site is heterobimetallic and contains both copper(I) and molybdenum(VI). A molybdoenzyme fragment reminiscent of those found in the xanthine dehydrogenase-oxidase and sulfite oxidase families is tethered to a cysteinate-ligated Cu(I) ion by a single, unsupported sulfide bridge.[14,15] This unusual core structure is unprecedented in biology and represents a new functional role for this low-coordinate copper motif. The structural nuances of Mo-CODH and importance of the chemical transformations it catalyzes present a potentially rewarding challenge to the field of modern bioinorganic chemistry. Further discussion of Mo-CODH will be withheld until Chapter 3 of this dissertation.

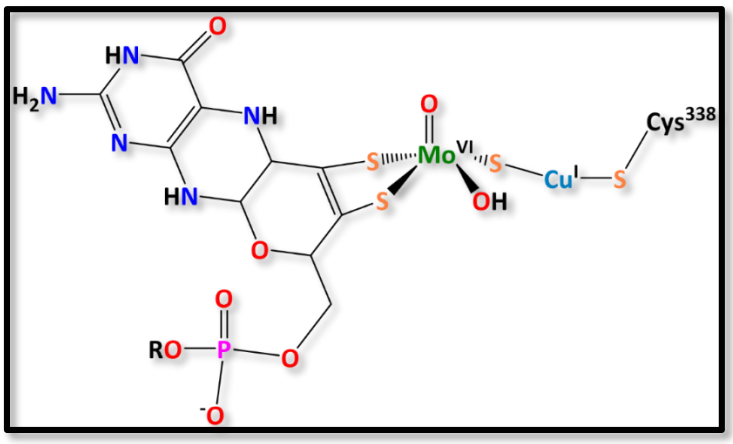

Figure 1.4 The native active site of molybdenum-dependent carbon monoxide dehydrogenase from *Oligotropha carboxidovorans.*

Biomimetic Chemistry

The complexity of biological systems often renders a detailed study of their structural and mechanistic properties very difficult. In an effort to elucidate these properties and to answer specific questions, biomimetic model chemistry can be

performed in conjunction with biochemical investigation of the natural biomolecules of interest. Modeling of metal-containing biomolecules begins with synthetic efforts to develop structural analogues. These structural analogues should closely match the geometric parameters and elemental constituency of the site of interest. Subsequent experimentation can evaluate the competency of such a structural analogue with respect to the native site's function. If the reactivity parallels that of the naturally occurring system, a functional analogue has been developed.

Removal of the cofactor from a metalloenzyme follows with complete loss of catalytic function as a consequence. Similarly, simple coordination complexes modeling metalloproteins and metalloenzymes often do not display identical reaction profiles or catalytic competency. This emphasizes the requirement of a well-orchestrated, intricate array of chemical processes and interactions necessary for proper function. Protein environments can feature steric profiles of varying scale and magnitude, complex networks of hydrogen bonding and proton relays, hydrophobic and hydrophilic compartments, and multiple and partial charges. Characteristics such as these highlight the marked difference between *in vivo* and *in vitro* chemistry. However, biomimetic chemistry can present a scenario in which efforts directed toward biological targets can lead to new, useful information with respect to the underlying coordination chemistry.

In the context of CueR, Atx1 and Atox1, and Mo-CODH, the unusual low-coordinate, sulfur rich coordination sphere about copper(I) is most reasonably due to steric constraints provided by the surrounding protein environment. Given the fundamental importance of the relatively unexplored class of low-coordinate copper(I) thiolate chemistry, these biological targets were chosen for synthetic modeling.

Described herein is the synthesis, characterization, and reactivity of a new class of low-coordinate cuprous thiolate complexes.

Results and Discussion

Synthesis and Reactivity

A rich structural diversity is found among homoleptic cuprous thiolates with simple monothiolate ligands[16-36] (see Figure 1.5). This is due to the relatively small size of the late transition element copper(I) (ionic radius of 74 pm for 4-coordinate) and the very favorable soft-soft interaction between copper(I) and divalent sulfur. These conditions allow for thiolates to flexibly bridge multiple copper ions before building charge and/or coordinatively saturating the copper(I) ions. Closed-shell, d^{10} copper(I) prefers a 4-coordinate, tetrahedral arrangement of ligands. Given the inherent steric limitations of most simple monothiolates, multinuclear clusters and occasionally polymeric species dominate product formation, which spread out the overall charge. This suggests that the steric profile of the thiolate ligand largely influences the nature of the product being formed, as multinuclear cluster species represent the major products rather than discrete, mononuclear lower-coordinate complexes. Access to homoleptic, low-coordinate copper(I) thiolates therefore requires sterically demanding ligands of considerable size.

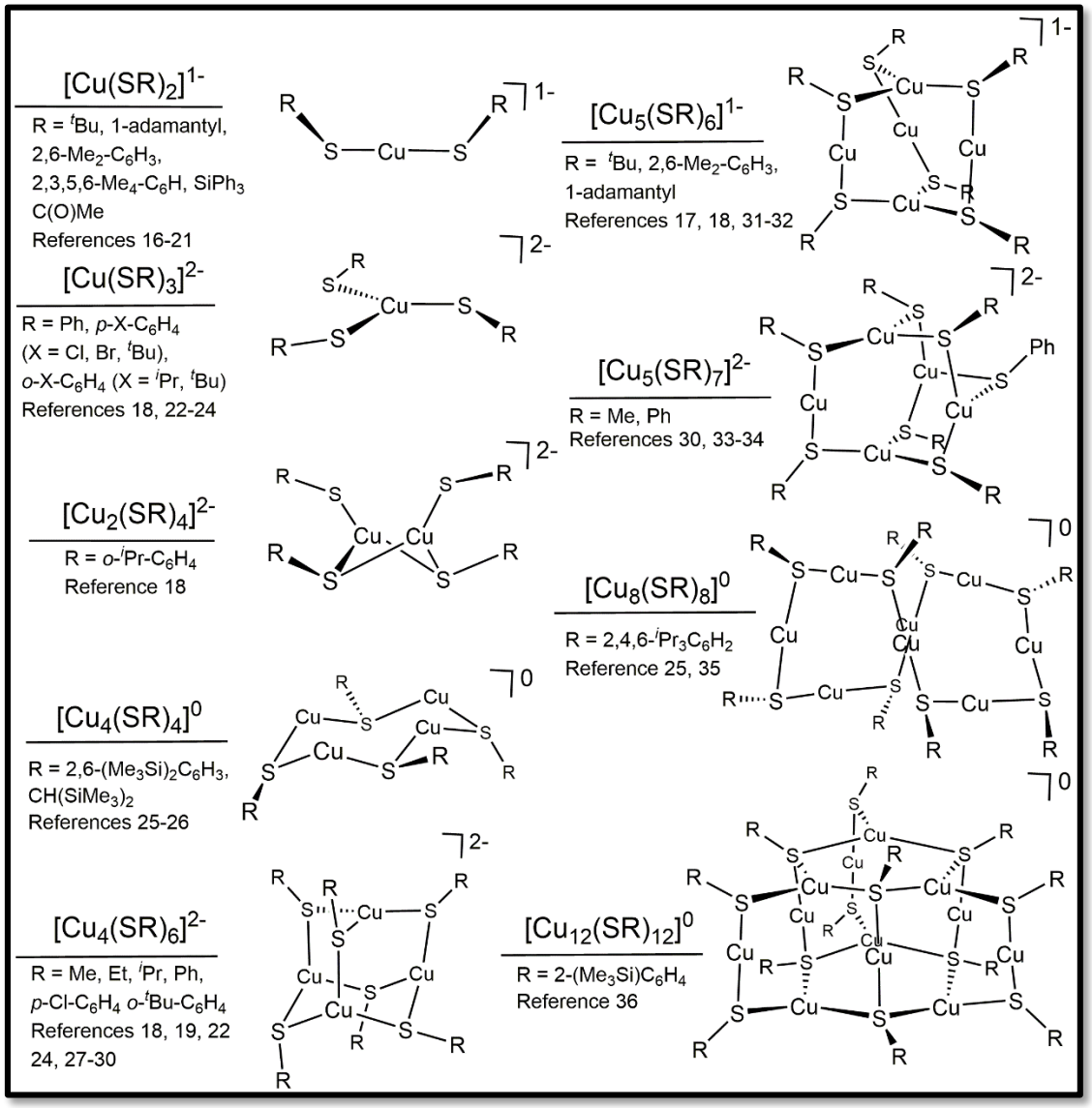

Figure 1.5 Crystallographically authenticated structure types among homoleptic monothiolate copper(I) complexes.

Two-coordinate, monoanionic copper(I) bis(thiolato) complexes represent the lowest coordination number for homoleptic cuprous thiolates. It is noteworthy that common thiolates typically access multiple structure types, often in mixture with one another, as is the case with these homoleptic two-coordinate complexes. Access to a

discrete synthetic protocol for these low-coordinate complexes should entail use of thiolate ligands featuring considerable steric bulk.

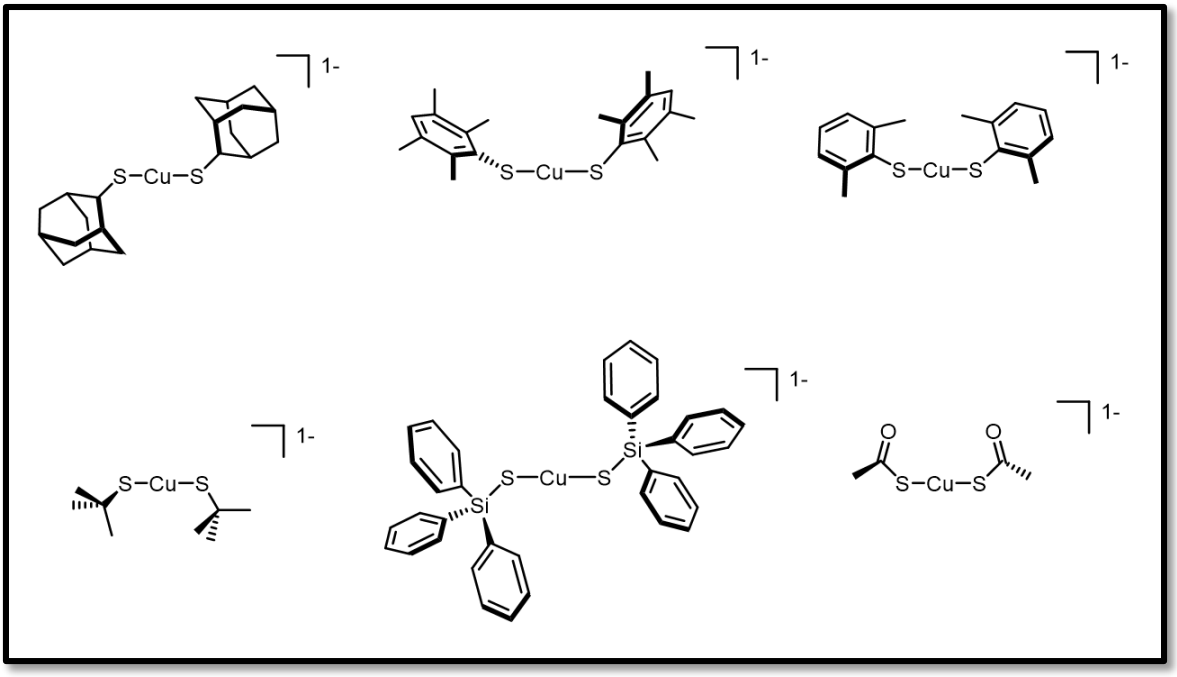

Figure 1.6 Structurally authenticated mononuclear copper(I) bis(thiolato) complexes. References 16-21.

Sterically encumbered thiolate ligands find frequent application in the synthesis of metal sites designed to feature coordinative unsaturation and display atypical reactivity.[37-40] Among those thiolate ligands with appreciable steric profile and ready access, either commercially or via a well-defined synthesis, are *tert*-butyl thiolate, 1-adamantyl thiolate, alkyl substituted thiophenolates,[41,42] and terphenyl thiolates.[43,44] A disadvantage of simpler alkyl thiolates is a degree of vulnerability toward C-S bond scission and formation of organic sulfide.[38,39] For aryl-type thiolates, a potential drawback exists with respect to their electronic difference from cysteinate, which is generally the supporting

thiolate ligand in metal-containing sites in biology. Recourse to an alkyl-type thiolate ligand with enhanced steric hindrance, stability against decomposition, and availability in usable quantity by a clear synthetic pathway is therefore desirable for further advancements in thiolate coordination chemistry, especially work with a biological motivation.

Triptycenyl 1-thiolate is a ligand that meets the foregoing criteria and would usefully fill a place in the range of options available to the inorganic coordination chemist. Any capacity of 1-(thiolato)triptycene to add something new to the extensively developed milieu of copper(I) thiolate chemistry, for example, produce a new structure type, enable improved yields, confer greater thermal stability, or selectively stabilize one structure type vs another of the same empirical formula, would speak persuasively of its broader capabilities to do new chemistry. First reported by Kawada, Iwamura, and co-workers in 1987, the preparation of 1-(thiolato)triptycene was notably unattended by any procedural detail, indication of yield, or physical characterization.[45] Later work by Nakanishi identified the molecule spectroscopically and analytically.[46] In 2009, a first report appeared describing the synthesis of a transition metal complex with 1-(thiolato)triptycene, $[Pt(PPh_3)_2(H)(STrip)]$,[47] but this contribution also did not offer any elaboration upon the synthesis of the thiol.

Efforts to prepare triptycene-1-thiol following the first reported synthesis via lithiation of 1-(bromo)triptycene and subsequent reaction with elemental sulfur produced mixtures of polysulfide species, which were difficult to resolve by chromatographic or crystallization methods. This consideration motivated an examination of an alternative route to 1-(thiolato)triptycene via the corresponding 9-anthracenyl sulfides.

9(10H)-anthracenone	**1**
bis-(9-anthracenyl)disulfide	**2**
bis-(9-anthracenyl)sulfide	**3**
9-(thioacetyl)anthracene	**4**
1-(thioacetyl)triptycene	**5**
9-(bromo)anthracene	**6**
tert-butyl 9-anthracenyl sulfide	**7**
tert-butyl 1-triptycenyl sulfide	**8**
1-(thiolato)triptycene(1-), $[STrip]^{1-}$	**9**
$[Cu^{I}(STrip)_2]^{1-}$	**10**
$[Cu^{I}(STrip)(SSiPh_3)]^{1-}$	**11**
$[Cu^{I}(STrip)I]^{1-}$	**12**
$[Cu^{I}(IMes)(STrip)]$	**13**
$[(Cu^{I}\text{-}STrip)_6(\mu_6\text{-}Br)]^{1-}$	**14**

Table 1.1 Numbering system for compound identification in Chapter 1.

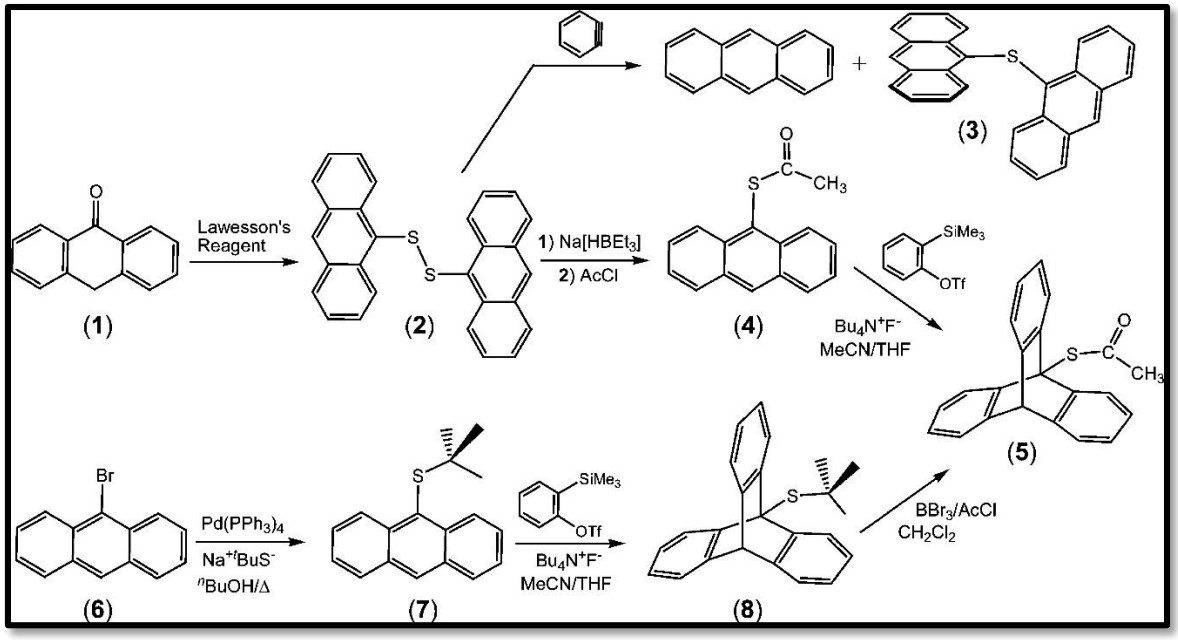

Scheme 1.1 Synthesis of 1-(thioacetyl)triptycene.

Initial efforts to prepare 1-(thiolato)triptycene proceeded by analogy to the synthesis of the corresponding alcohol as described by Wolczanski et al.[48] Thus, with Lawesson's reagent or P_2S_5, commercially available 9(10H)-anthracenone (Scheme 1.1, **1**) is conveniently converted to the corresponding thione, which then readily tautomerizes to anthracene-9-thiol. When conducted in open air, this reaction affords disulfide **2**.[49] Disulfide **2** itself does not permit direct access to the triptycenyl group, as its reaction with benzyne results in facile sulfur atom abstraction to afford predominantly anthracene accompanied by minor quantities of bis(9-anthracenyl)sulfide (**3**, Scheme 1.1). This incompatibility of the disulfide group with the powerful electrophile benzyne requires its transformation to a protected form. Reduction of **2** with $NaHBEt_3$, followed immediately by introduction of acetyl chloride produces 9-(thioacetyl)anthracene (**4**, Scheme 1.1), a similar route to which has been reported.[50]

The condensation of 9-(acetyl)anthracene with benzyne generated via the classical anthranilic acid route produces 1-(acetyl)triptycene in 33% yield.[48] However, no identifiable quantity of **5** was produced when the same conditions were employed with **4**. Typically operating under milder conditions, more recently described benzyne-generating reagents, both 2-(trimethylsilyl) phenyl triflate[51] and (phenyl) [*o*-(trimethyl)phenyl]iodonium triflate,[52] were explored as alternative sources of benzyne. An advantage of these reagents is the facile generation of benzyne by introduction of F^- at reduced temperature rather than the reflux conditions required with anthranilic acid.[53] Divalent sulfur readily reacts with electrophiles like benzyne to produce, at least transiently, betaines which subsequently fall apart to unwanted products. Here, the application of heat only serves to further this undesirable reaction. The importance of

thermal control in this system is apparently affirmed by isolation of **5** (Scheme 1.1) in 5.3% yield when 2-(trimethylsilyl) phenyl triflate is employed as benzyne precursor at reduced temperature.

The rather low yield found for the foregoing synthesis of **5** prompted some consideration for use of *tert*-butyl 1-(triptycenyl) sulfide (**8**), a successful preparation of which has been described as proceeding by Diels-Alder condensation of benzyne with *tert*-butyl 9-anthracenyl sulfide (**7**, Scheme 1.1).[54] Compound **7** in turn is readily accessed from commercially available 9-(bromo)anthracene (**6**) via a Pd-catalyzed coupling reaction with $Na^{+t}BuS^{-}$ (**6** → **7**, Scheme 1.1).[55] With protecting groups smaller or less sterically hindered than *tert*-butyl, 9-anthracenyl sulfides are prone to electrophilic attack by benzyne at sulfur and do not undergo the desired [4+2] cycloaddition. A moderate yield of ~13% is reproducibly found for the synthesis of **8** via **7**, although the reported yield is substantially higher at 36%.[54] The observed invariance of yield for **8**, regardless of the particular method by which benzyne is generated, supports the suggestion that it is inherently restricted by a kinetic competitiveness of other reaction pathways, namely betaine formation and/or condensation of benzyne to afford the 1,4 cycloadduct rather than the desired 9,10 adduct.[54]

tert-Butyl-for-acetyl group conversion proceeds in straightforward fashion via a BBr_3/AcCl dealkylation protocol described by Bjørnholm and co-workers.[56] Although this protocol was first reported as a methodology for exchange of *tert*-butyl for acetyl groups in aryl *tert*-butyl systems and has been widely applied[57] since then, the reaction as it applies to this alkyl *tert*-butyl triptycenyl sulfide system (**8** → **5**, Scheme 1.1) follows successfully and in somewhat better yield. The thioacetyl protected form of 1-

(thiolato)triptycene (**5**) is a convenient, air-stable form of this ligand that is readily deprotected with a variety of bases such as H^-, RO^-, or *n*BuLi. Thus, in three steps from commercially available **6**, usable quantities of 1-(thioacetyl)triptycene are attainable in an overall yield of 5%.

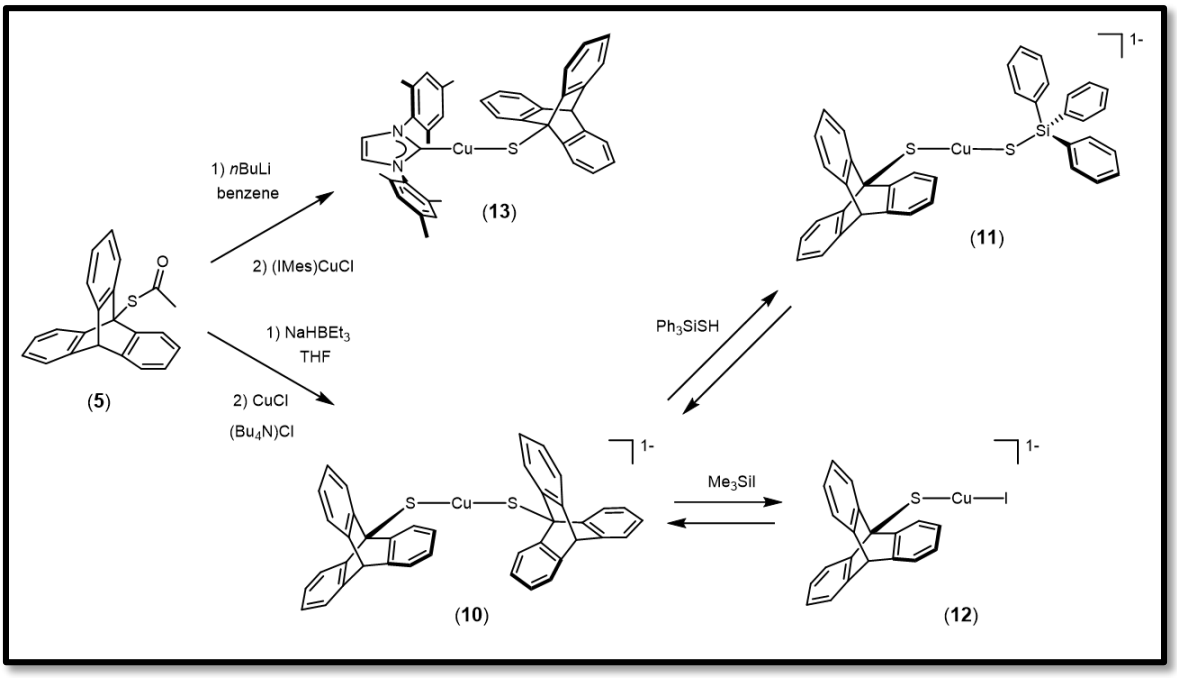

Scheme 1.2 Synthesis of copper(I) complexes with 1-(thiolato)triptycene.

Deprotection of **5** with $NaHBEt_3$ at reduced temperature under an anaerobic atmosphere cleanly and conveniently unmasks the thiolate anion. Introduction of a mixture of CuCl/$(Bu_4N)Cl$ to *in situ* generated thiolate anion in a 2:1 ratio readily affords $[Bu_4N][Cu(STrip)_2]$ in reproducible yields of ~77% (**5** → **10**, Scheme 1.2). The yield for $[Bu_4N]$**10** compares well to those for related compounds (Figure 1.6). Additionally, it is observed qualitatively that **10** is quite robust in solution under anaerobic conditions and stable against formation of yellowish colors typically associated with decomposition to

various clusters and/or cage species. This apparently enhanced stability is attributed to the 1-(thiolato)triptycene ligand's augmented steric bulk and a possible inability to support some of the structural motifs observed in the clusters of Figure 1.5, such as three-coordinate Cu(I) or the μ_3-bridging mode for thiolate ligand.

Employing a 3:1 ratio of $TripS^-$ in reaction with Cu(I) yielded no evidence for formation of a $[Cu(STrip)_3]^{2-}$ species. Mononuclear cuprous tris(thiolate) complexes have thus far only been observed with aryl-type thiolates,[18,22-24] suggesting that the moderated basicity of this class of thiolate plays a role in enabling Cu(I) to tolerate this very reducing environment. However, in the absence of a thorough understanding of the factor(s) governing selection of $[Cu(SR)_2]^{1-}$ vs $[Cu(SR)_3]^{2-}$, one must be cautious against any conclusion that 1-(thiolato)triptycene is too sterically encumbering as to be able to form any $[M(STrip)_3]^n$ species. In one instance, when $[Cu(MeCN)_4][PF_6]$ and $(Bu_4N)Br$ were used as starting materials following a similar preparation, single crystals of $[Bu_4N][(CuSTrip)_6(\mu_6\text{-}Br)]\cdot[Bu_4N][PF_6]$, $[Bu_4N]$**14**$\cdot[Bu_4N][PF_6]$, were identified by X-ray crystallography (*vide infra*). Anionic **14** represents a new structure type in cuprous thiolate chemistry. Each thiolate sulfur bridges only two copper(I) ions; thus, each Cu(I) remains linearly bound to triptycyl thiolate in a cyclic hexamer. Deliberate attempts to reproduce the synthesis of this interesting copper species unfortunately yielded only $[Bu_4N]$**10**.

The size and rigidity of the 1-(thiolato)triptycene ligand present the possibility of supporting the existence of new, low-coordinate copper(I) species that are of interest in their own right for further synthesis. To the best of my knowledge, no discrete,

heteroleptic two-coordinate copper(I) bis(thiolato) complexes exist. Thus, such a heteroleptic species containing two bulky thiolates represents an attractive target to gauge the possibilities and limitations of 1-(thiolato)triptycene.

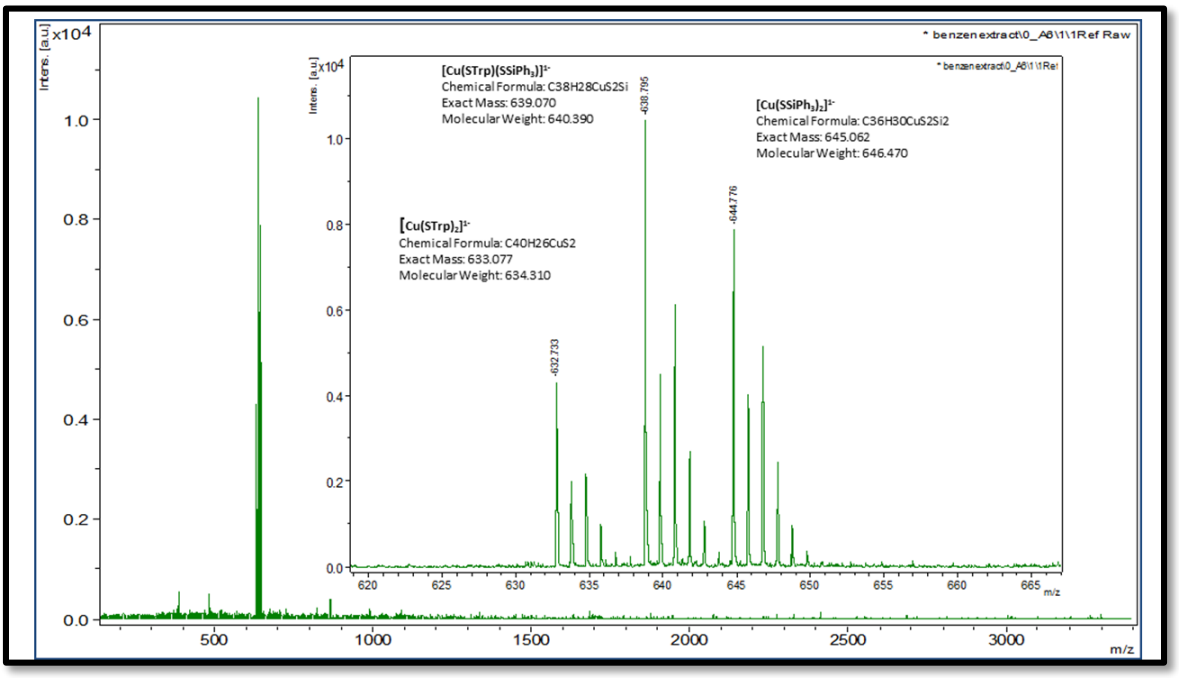

Figure 1.7 Mass spectrum (MALDI-TOF) of product mixture from the attempted reaction $[Cu(STrip)_2]^{1-} + Ph_3SiSH \rightarrow [Cu(STrip)(SSiPh_3)]^{1-} + TripSH$. The inset show the presence of the desired $[Cu(STrip)(SSiPh_3)]^{1-}$ as a mixture with $[Cu(STrip)_2]^{1-}$ and $[Cu(SSiPh_3)_2]^{1-}$.

Noting that silanethiols are more acidic than their carbon-containing congeners,[58,59] exchange of 1-(thiolato)triptycene for Ph_3SiS^- by protonolysis appeared to be a plausible route to the new heteroleptic species $[Cu^I(STrip)(SSiPh_3)]^{1-}$, **11**. Assessed by mass spectrometry (see Figure 1.7), this ligand exchange by protonolysis does indeed proceed, but only to afford a product mixture. Although a modest enrichment of **11** can be affected by extraction of the crude solid product mixture with benzene, the compound

appears to be inherently vulnerable to ligand scrambling in solution. Efforts to isolate the heteroleptic species by precipitation or crystallization seemed to drive the product equilibrium in the direction of homoleptic products, $[Cu(STrip)_2]^{1-}$ and $[Cu(SSiPh_3)_2]^{1-}$, where the high crystallinity of homoleptic **10** salts causes it to be the only retrievable species by typical crystallization methods. Within a similar context, it seemed plausible that a Si−I bond of a comparable, possibly lesser, strength than a typical Si−S bond,[60] might afford a route to heteroleptic, two-coordinate $[Cu^{I}(STrip)I]^{1-}$, **12**. Again on the basis of a mass spectrometry assay, the 1:1 reaction of Me_3SiI with **10** yields **12** and unreacted **10** as a mixture. This mixture appears to decompose over time at room temperature, and the greater crystallinity of anion **10** again militates against a selective crystallization of the heteroleptic anion of interest. One heteroleptic species that can be isolated, although it has precedent,[61,62] is [Cu(STrip)(IMes)] **13**, prepared from the reaction of $TripS^-$ with [(IMes)CuCl] (*vide supra*, Scheme 1.2). Given the propensity of cuprous bis(thiolato) species to undergo ligand scrambling, and the ease with which halides can bridge copper(I) ions, the N-heterocyclic carbene IMes was chosen for its stability, size, and solubility. Additionally, complexes similar to charge neutral **13** with simpler thiolate ligands have been used as catalysts for the hydrothiolation of activated olefins.[61]

With the successful application of precursor 1-(thioacetyl)triptycene to generate coordination complexes bearing the 1-(thiolato)triptycene ligand, alternative, more practical routes were examined in an effort to incorporate other chalcogens into this particular ligand framework. A series of 1-(chalcogenido)triptycene ligands could potentially display some interesting differences with respect to the overall coordination

chemistry and physical properties of the products containing them. While sensitive, the ease of preparation of carbanion triptycyllithium, $Li^+ Trip^-$,[63] prompted investigation into its use as a ligand. The alkyl-type carbanion $Trip^-$ lacks both β-hydrogens and readily available acceptor orbitals, which suggests that the corresponding M-C bond should be stable enough to support organometallic complexes bearing them. Reaction of triptycyllithium with either CuCl/$(Bu_4N)Cl$ or $[Cu(MeCN)_4]BF_4$/$[Bu_4N]Cl$ mixtures in a 2:1 ratio led to formation of a product mixture which contained off-white $[Bu_4N][Cu(Trip)_2]$ as judged spectroscopically (see Figure 1.8). This organometallic bis(triptycyl) copper(I) species, somewhat counterintuitively, is extremely reactive and represents only a minor portion of the product mixture. Efforts to crystallize the monoanion were unsuccessful; however, a byproduct of the reaction, $[Bu_4N][Cu(Trip)Cl]$, was characterized via X-ray crystallography. While the data collected crystallographically for $[Bu_4N][Cu(Trip)Cl]$ were not of suitable quality for publication, this complex is, to the best of my knowledge, the first copper triptycyl complex to be structurally authenticated. The sensitivity and poor yield of desirable $[Bu_4N][Cu(Trip)Cl]$ motivated a change in direction synthetically, and this complex was not explored further.

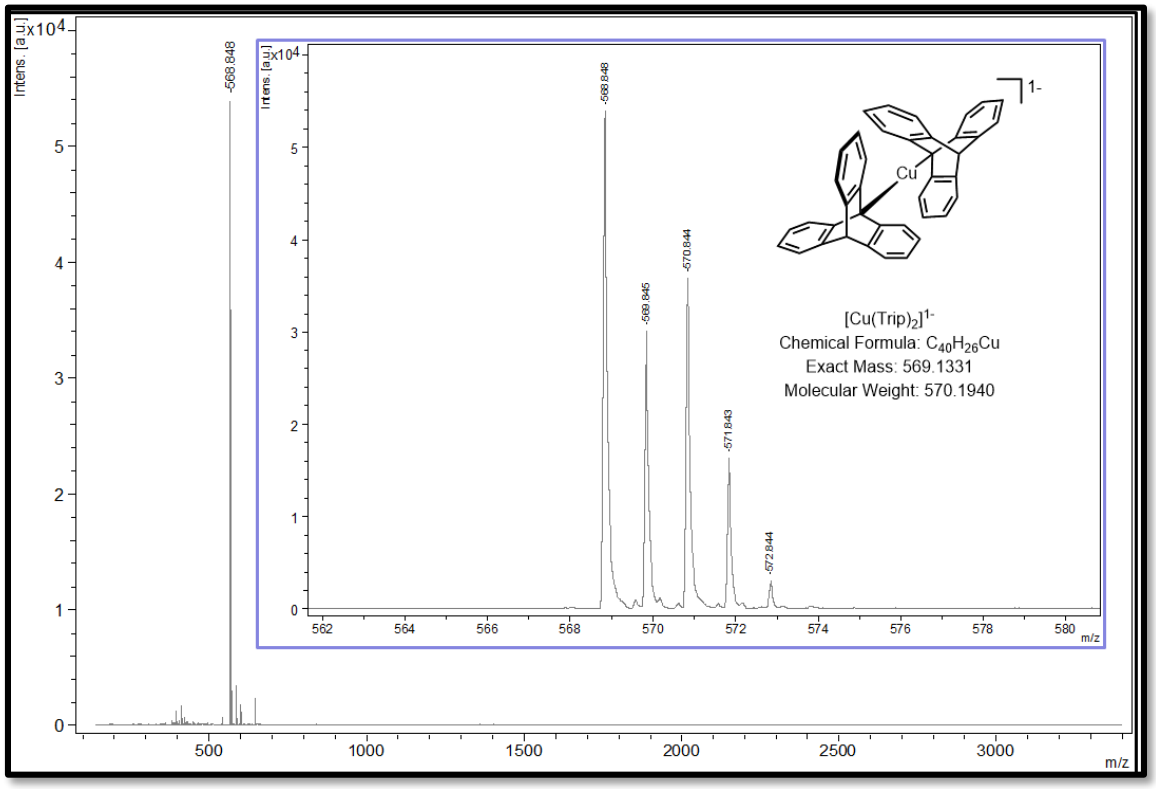

Figure 1.8 Mass spectrometric (MALDI-TOF) authentification of the bis(triptycyl) copper(I) monoanion.

Having successfully isolated low-coordinate complexes with bulky *N*-heterocyclic carbene (NHC) auxiliary ligands, this framework was explored to support the triptycyl ligand moiety. Salt metathesis reactions between triptycyllithium and [(NHC)CuCl] complexes resulted in product mixtures that contained [Cu(NHC)(Trip)] along with unreacted copper starting material and triptycene as comfirmed by ^{1}H NMR. As witnessed in previous systems (the synthesis of $(Bu_4N)[Cu(Trip)_2]$ and triptycenethiol), triptycyllithium generated *in situ* finds a way to abstract a hydrogen atom either from solvent, adventitious moisture present, or some other source to yield triptycene (TripH) during the course of the reaction. While this apparently inherent problem is hard to

circumvent, the spectroscopic evidence for formation of the desired organometallic complex was encouraging enough to test its reactivity.

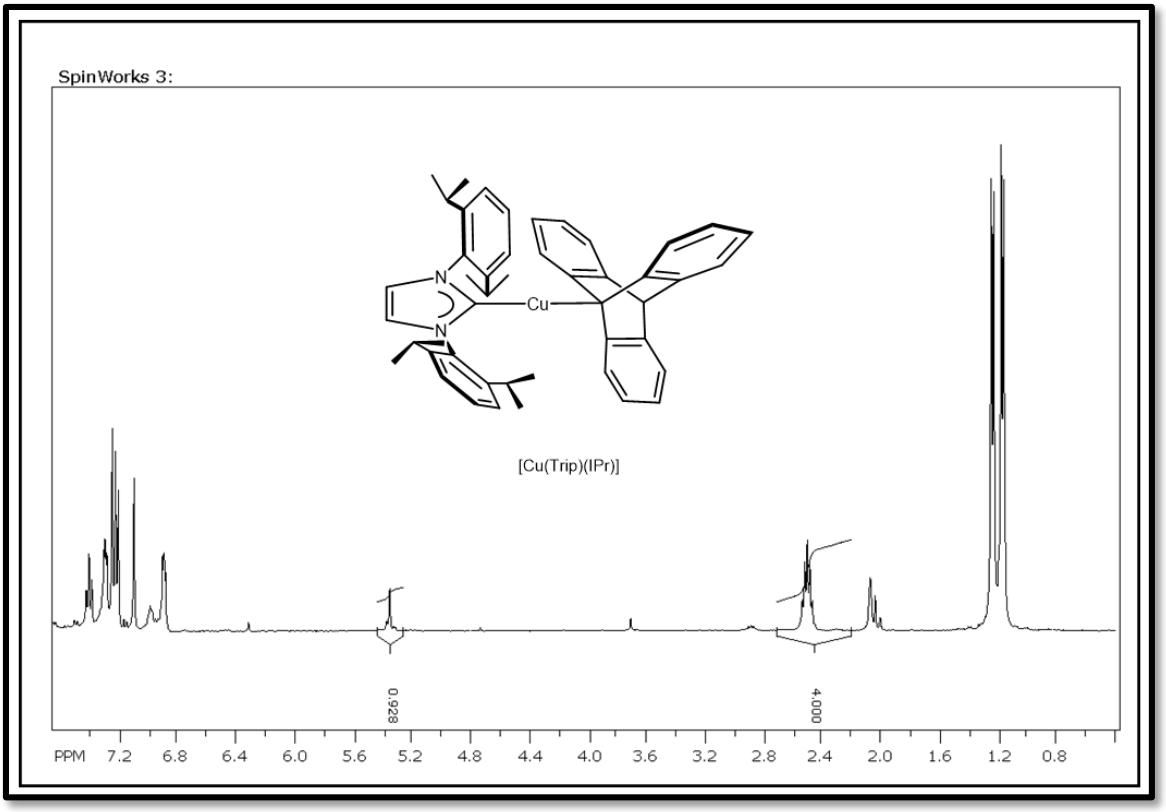

Figure 1.9 ^{1}H NMR spectrum of [Cu(IPr)(Trip)] highlighting the correct integration corresponding to the methyne protons of the isopropyl groups of IPr and the 10H proton of the triptycyl ligand's unsubstituted bridgehead carbon.

Interest in a potential series of 1-(chalcogenido)triptycene complexes, as well as the 1-(chalcoacetyl)triptycene precursor molecule, prompted us to explore the possibility of chalcogen insertion into the M-C bond of these organometallic copper(I) triptycyl complexes.

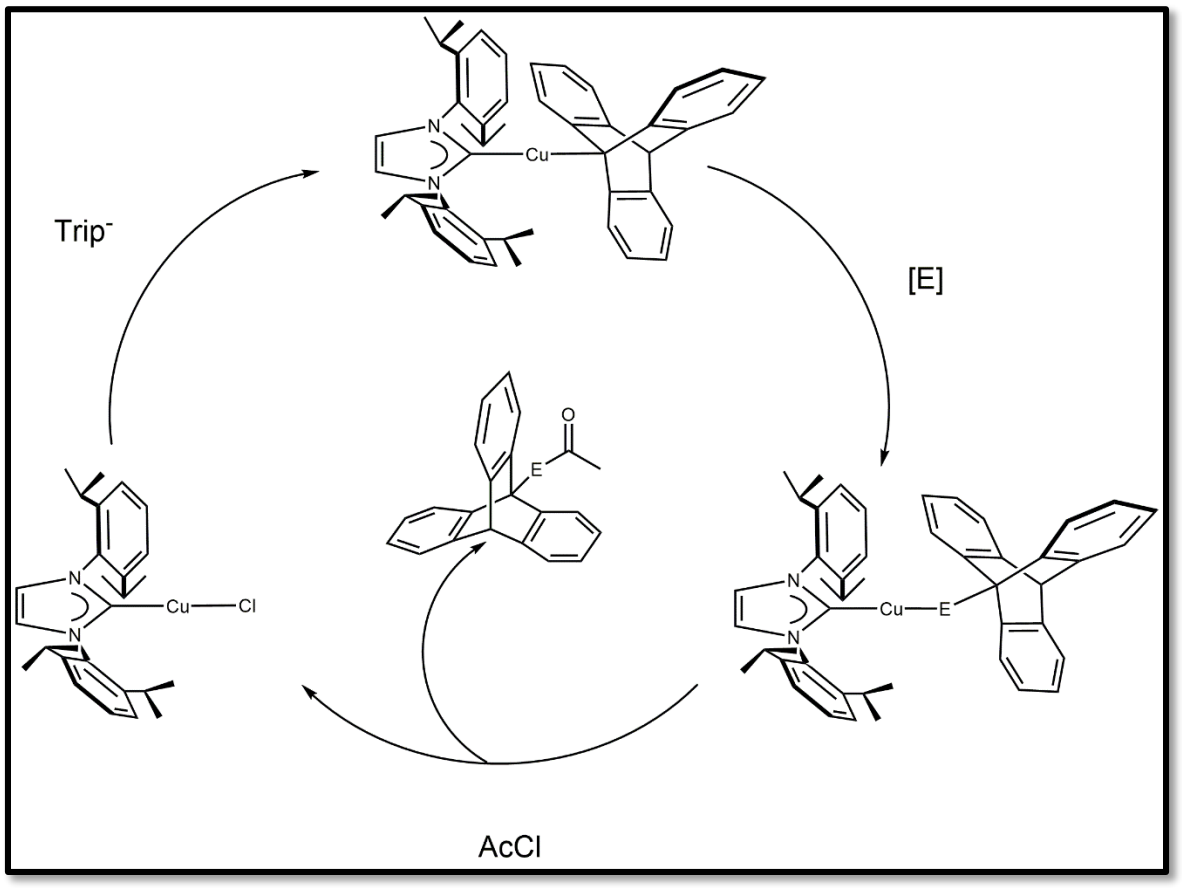

Scheme 1.3 A closed, stoichiometric cycle for generating 1-(chalcoacetyl)triptycene via chalcogen insertion. E = chalcogen donor source.

The difficulty associated with isolation of [Cu(NHC)(Trip)] species led to attempts at observing chalcogen insertion with these complex in an *in situ* manner. Thus, one could devise a closed, stoichiometric cycle for generating 1-(chalcoacetyl)triptycene based on Scheme 1.3, which would potentially allow for the investigation of chalcogen insertion into the Cu-C(Trip) bond, isolation and characterization of new 1-(chalcogenido)triptycene complexes, assembly of new 1-(chalcoacetyl)triptycene ligand precursors, and regeneration of starting material. Reaction of chalcogen donor sources

like elemental sulfur, ethylene sulfide, benzyl trisulfide, selenium powder, and tellurium powder with [Cu(NHC)(Trip)] prepared *in situ* gave complicated mixtures of products, many of which appeared to decompose over time. In one instance, addition of benzyl trisulfide to *in situ* prepared [Cu(IPr)(Trip)] yielded benzyl triptycyl sulfide (Trip-SBz) and [Cu(IPr)(SBz)] as isolated products which where determined via ^{1}H NMR. Owing to the rather miniscule amount of benzyl triptycyl sulfide afforded by this reaction, optimization of this reaction was not pursued. One-pot reactions involving the *in situ* preparation of [Cu(NHC)(Trip)], addition of chalcogen source, followed by the addition of acetyl chloride and appropriate work-up failed to produce the desired products of interest. Extraction with lower polarity solvents from the crude product mixture and/or chromatographic work-up resulted again in the observation of triptycene (TripH) as the major product formed as indicated by ^{1}H NMR. On a few occasions, acetyl triptycene (TripC(O)Me) was obtained as a fraction from column chromatography, as authenticated via its distinct chemical shifts in ^{1}H NMR (as opposed to the chemical shifts for TripSC(O)Me). This result suggests that either chalcogen insertion doesn't occur cleanly, at least within a reasonable timeframe, or the low-coordinate copper system employed is too labile, and formation of simpler, undesirable thermodynamically favored products ultimately occurs.

Structures

In conjunction with spectroscopic methods, X-ray diffraction has been used to affirm the identity of all new compounds, as well as those already known but previously

uncharacterized by crystallography.

Table 1.2 Crystal and refinement data for compounds **3-5**, **7-10**, and **13-14**.

compound	**4**	**4**	**7**	**3**	**5**	**8**
solvent	none	none	none	none	none	none
formula	$C_{16}H_{12}OS$	$C_{16}H_{12}OS$	$C_{18}H_{18}S$	$C_{28}H_{18}S$	$C_{22}H_{16}OS$	$C_{24}H_{22}S$
fw	252.32	252.32	266.38	386.48	328.41	342.48
xtl system	orthorhombic	triclinic	monoclinic	monoclinic	monoclinic	orthorhombic
space grp	*Pbca*	$P\bar{1}$	*C*2/*c*	*C*2/*c*	$P2_1/n$	$P2_12_12_1$
color,	white block	yellow block	yellow	yellow slat	colorless plate	colorless slab
a, Å	10.555(2)	8.2800(6)	25.546(1)	20.481(3)	27.442(9)	13.8394(7)
b, Å	14.071(3)	9.3040(7)	6.9794(3)	5.0204(8)	13.748(4)	15.6605(8)
c, Å	16.444(3)	16.872(1)	17.7731(8)	19.693(3)	8.789(3)	16.5178(9)
α, deg.	90	103.204(1)	90	90	90	90
β, deg.	90	96.846(1)	116.824(1)	114.562(2)	96.499(5)	90
γ, deg.	90	102.158(1)	90	90	90	90
V, Å^3	2442.2(9)	1217.7(2)	2827.9(2)	1841.6(5)	3295(2)	3579.9(3)
T, K	100	100	100	100	100	100
Z	8	4	8	4	8	8
R1,[a] wR2[b]	0.0577, 0.1374	0.0351, 0.0903	0.0362, 0.0947	0.0384, 0.0887	0.0412, 0.1047	0.0374, 0.0893
GoF	1.149	1.040	1.044	1.061	1.031	1.027

compound	$[Bu_4N]$**9**	$[Bu_4N]$**10**	$[Bu_4N]$**10**	$[Bu_4N]$**14**·$[Bu_4N][PF_6]$	**13**
solvent	none	Et_2O	C_6H_6	none	none
formula	$C_{36}H_{49}NS$	$C_{60}H_{72}CuNOS_2$	$C_{59}H_{65}CuNS_2$	$C_{152}H_{150}BrCu_6F_6N_2PS_6$	$C_{41}H_{37}CuN_2S$
fw	527.82	950.85	915.78	2803.22	653.33
xtl system	monoclinic	triclinic	monoclinic	monoclinic	triclinic
space grp	$P2_1/n$	$P\bar{1}$	$P2_1/n$	*C*2/*c*	$P\bar{1}$
color,	colorless prism	colorless prism	colorless prism	pale blue plate	colorless plate
a, Å	12.116(6)	11.5110(7)	12.841(1)	38.957(7)	8.3547(15)
b, Å	16.180(8)	16.082(1)	20.226(2)	28.740(5)	9.8990(17)
c, Å	16.321(8)	16.758(1)	18.384(1)	11.982(2)	20.568(4)
α, deg.	90	100.892(1)	90	90	78.984(2)
β, deg.	97.575(6)	105.633(1)	93.558(1)	91.710(2)	80.382(2)
γ, deg.	90	108.445(1)	90	90	80.950(2)
V, Å^3	3172(3)	2705.4(3)	4765.0(6)	13410(4)	1632.3(5)
T, K	100	100	100	100	100
Z	4	2	4	4	2
R1,[a] wR2[b]	0.0402, 0.1030	0.0614, 0.1828	0.0606, 0.1521	0.0810, 0.2026	0.0461, 0.1072
GoF	1.028	1.074	1.004	1.039	1.023

[a] $R1 = \Sigma||F_o| - |F_c||/\Sigma|F_o|$. [b] $wR2 = \{[\Sigma w(F_o^2 - F_c^2)/\Sigma w(F_o^2)^2]\}^{1/2}$; $w = 1/[\sigma^2(F_o^2) + (xP)^2]$, where $P = (F_o^2 + 2F_c^2)/3$.

9-(thioacetyl)anthracene **4** was identified in two polymorphs, a triclinic form ($P\bar{1}$) obtained by evaporation from CH_2Cl_2/hexanes and an orthorhombic form found by slow evaporation from ethyl acetate. The triclinic setting's packing arrangement of **4** is comprised of intermolecular π-π interactions that enforce columnar stacking in a direction approximately coincident with the *a* axis (Figure 1.10).

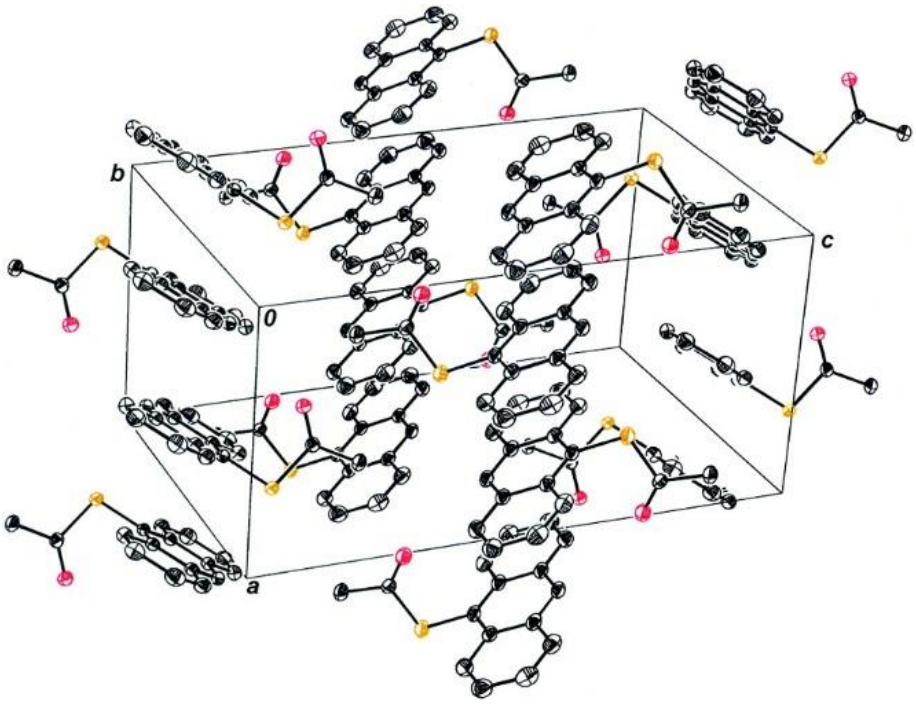

Figure 1.10 Cell packing diagram for triclinic polymorph of **4** illustrating the π-π stacking of anthracenyl groups and alternating disposition of thioacetyl groups

Each stack of molecules alternate by 180 degree rotations such that the thioester groups of adjacent molecules appear on opposite sides of the column in an orientation orthogonal to the anthracene plane (Figure 1.10). The orthorhombic polymorph completely lacks this columnar stacking arrangement. Instead, molecules are arranged as pairs with parallel anthracenyl groups and thioester groups on opposite sides of the π–π interface

but directed toward the pairing partner. These pairs of molecules are in turn related to one another by the three sets of mutually orthogonal 2-fold screw axes in *Pbca*. In contrast to the crystal packing patterns of these two polymorphs of **4**, that for **7** reveals no intermolecular π-stacking. A plausible explanation can be due to the size of the *tert*-butyl groups, which may be too close and too large to favor this otherwise more typical packing arrangement. Interatomic bond distances and angles in **4** and **7** are unexceptional.

Bis(9-anthracenyl)sulfide, **3**, obtained as an unintended product, is moderately interesting as one of the more sterically crowded organic sulfides to be structurally characterized.[62,64-66] The sulfur atom of each molecule resides on a C_2 axis such that only half the molecule is crystallographically unique. The molecule features a C-S-C angle of 104.0(1)° and a S-C bond distance of 1.786(2)Å (Figure 1.11).

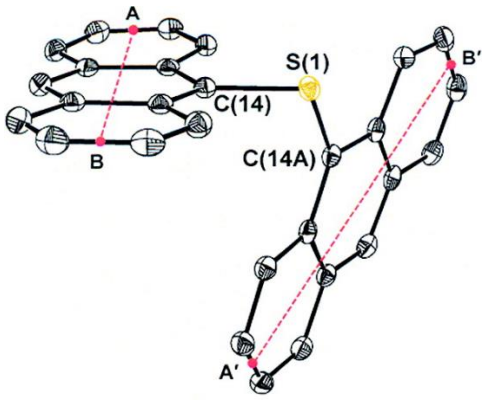

Figure 1.11 Thermal ellipsoid plot of bis(9-anthracenyl)sulfide at the 50% probability level highlighting anthracene planes AB and A'B'. Hydrogen atoms are omitted for clarity.

This C-S-C angle is smaller than the corresponding values observed in the structures of other hindered organic sulfides (106.4-119.8°),[64-67] possibly because effective π-stacking

between the anthracenyl groups in **3** offsets any energetic cost associated with contracting this bond angle. The twist between anthracenyl groups, defined here as the torsion angle between the AB and A'B' line segments (Figure 1.12) when joined at their midpoints, is 54.8°. Molecules of **3** pack in highly ordered stacks along the *b* axis of the cell using both anthracenyl groups.

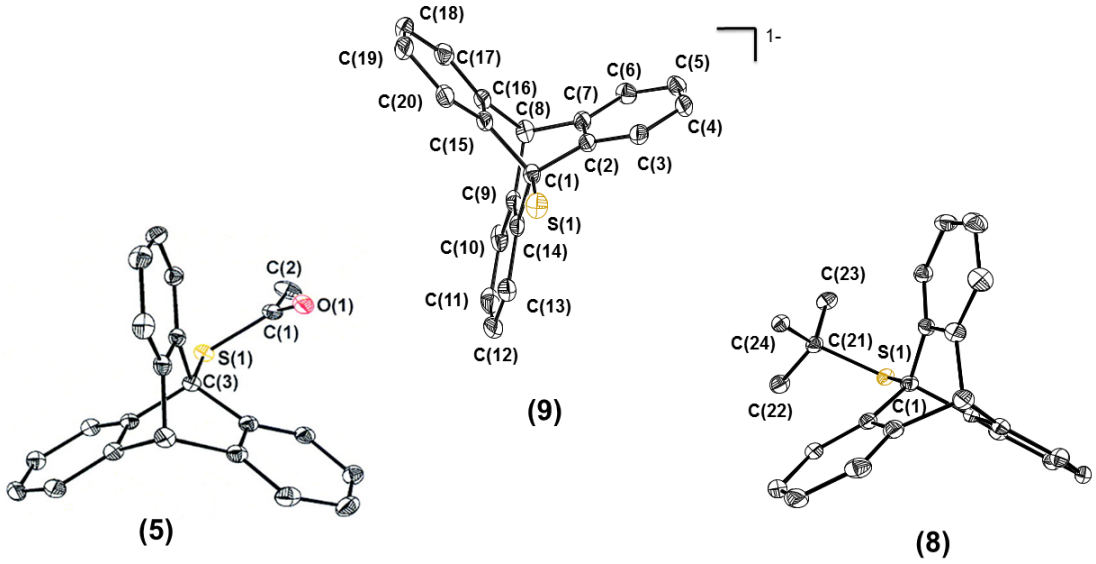

Figure 1.12 Thermal ellipsoid plots of 1-(thioacetyl)triptycene **5**, *tert*-butyl triptycyl sulfide **8,** and anion **9** of $[Bu_4N]^+[TripS^-]$ at the 50% probability level. Hydrogen atoms are omitted for clarity.

Interatomic distances and angles for **5**, **8**, and **9** reveal noting atypical. Despite their similarity in size and shape, **5** and **8** pack rather differently in the crystalline state. Molecules of **5** pack in a "head-to-head", "tail-to-tail" fashion that juxtaposes the triptycenyl groups of neighboring molecules and arranges them approximately in the plane of the *b* and *c* axes. In contrast, molecules of **8** arrange themselves approximately linearly along the *b* axis but with an alternating "up-and-down" disposition of triptycenyl

groups. The structure of $[Bu_4N]^+[TripS^-]$, $[Bu_4N]$**9**, is interesting primarily as an unperturbed thiolate anion and reference point for defining a steric cone angle for the ligand. If the angle defined by one of the ortho hydrogen atoms with the thiolate sulfur and bridgehead (ipso) carbon atoms is taken as subtending half of the steric cone angle, then this cone angle is quantified as 144.6°. This value contrasts with the cone angle value of 150° reported for the corresponding 1-(alkoxy)triptycene,[48] the difference being attributable to the C−S single bond being longer than the C−O single bond.

Anion **10**, $[Cu(STrip)_2]^{1-}$, has been characterized as its $[Bu_4N]^+$ salt in two different unit cells due to incorporation of different solvent molecules into the crystal lattice. In both cases, the anion resides on a general position in the asymmetric unit. Figure 1.13 presents a thermal ellipsoid plot of the anion from the determination with Et_2O in the lattice.

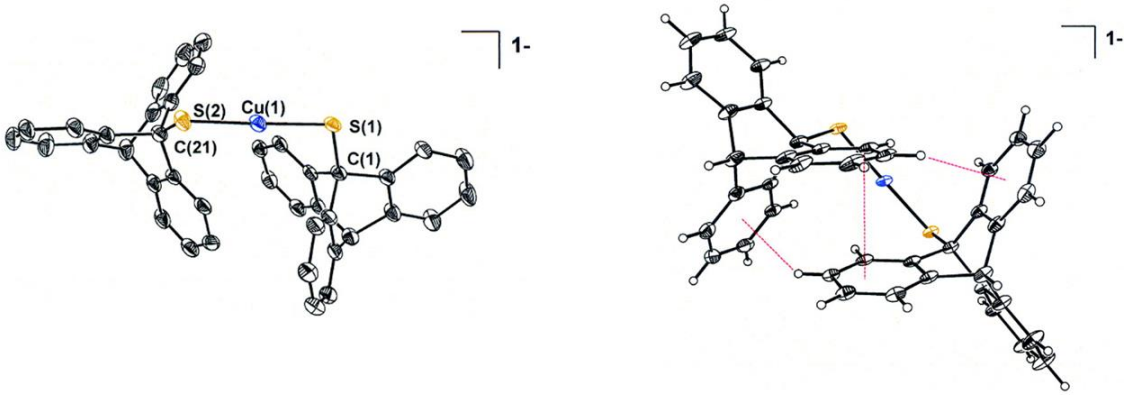

Figure 1.13 Thermal ellipsoid plot (50%) of anion **10** with hydrogen atoms omitted for clarity, illustrating the π···π and CH···π interactions that enforce the small C−S···S−C torsion angle.

Structural features for both determinations are highly similar and are presented in Table 1.3 along with corresponding data from known Cu(I) bis(thiolate) complexes of this type. One particularly noteworthy difference between **10** and the other complexes of this type is that the C−S bond distances in the former are moderately longer by ~0.01 Å. This difference is significant within the resolution limits of these data.

Table 1.3 Structural parameters of $[Cu^{I}(SR)_2]^{1-}$ compounds.

Compound	% Yield	Cu–S, Å	S–Cu–S, deg.	C–S···S–C, deg.[a]
$[Cu(STrip)_2]^{1-}$	77	2.1541(7),[b] 2.1605(7)[b] 2.1549(9),[c] 2.1624(9)[c]	177.80(3),[b] 174.88(4)[c]	44.1,[b] 37.9[c]
$[Cu(S\text{-}1\text{-}Ad)_2]^{1-}$ [17]	77	2.147(1)	180.0	180.0
$[Cu(S\text{-}^{t}Bu)_2]^{1-}$ [d, 19]	58	2.1380(7), 2.1410(6), 2.1422(6), 2.1434(6)	176.69(2), 179.54(3)	78.7
$[Cu(S\text{-}2,6\text{-}Me_2\text{-}C_6H_3)_2]^{1-}$ [18]	48	2.111(3), 2.127(1)	165.22(7)	42.1
$[Cu(S\text{-}2,3,4,5\text{-}Me_4C_6H_1)_2]^{1-}$ [16]	60	2.137(2)	178.6(1)	-[e]
$[Cu(SSiPh_3)_2]^{1-}$ [20]	52	2.1508(6)[f]	180.0[f]	180.0[f]

[a]Torsion angle between thiolate ligands. [b]Values from $[Bu_4N][Cu(STrip)_2]\cdot Et_2O$. [c]Values from $[Bu_4N][Cu(STrip)_2]\cdot C_6H_6$. [d]Two independent anions occur in the asymmetric unit of the unit cell. [e]Atomic coordinates are unavailable for this structure. [f]These values are from a structure of $[Et_4N][Cu(SSiPh_3)_2]$ determined in our laboratory. The unit cell and space group found are the same as reported by Holm and coworkers.[20]

The unanticipated closeness of the two triptycyl groups in **10** is reflected by the modest C−S···S−C torsion angles of 37.9 and 44.1° for the two independent structures. It has been suggested that the torsion angle observed for $[Cu(S^{t}Bu)_2]^{1-}$ may reflect a Cu−S π-π interaction.[19] However, the wide variation seen in this torsion angle is indicative of the governance of this parameter by crystal packing effects. In **10**, interligand π-π (~3.62 Å) and CH···π (2.84, 3.11 Å) interactions (Figure 1.13) clearly play a decisive role in enforcing this crystalline state conformation. Typical π-π and CH···π interaction energies are each 2-3 kcal/mol,[68] which collectively would afford enough stabilization to supersede a more extended conformation with larger C−S···S−C torsion angle. The presence of only four aryl-type hydrogen atoms in a 1:1:1:1 ratio indicates that this configuration seen in the crystal structure of **10** does not persist in solution. It is probable

that the juxtaposition and orientation of triptycyl groups in **10** that enable these π-π and CH···π interactions are produced at the expense of the elongated Cu−S bonds noted (*vide supra*).

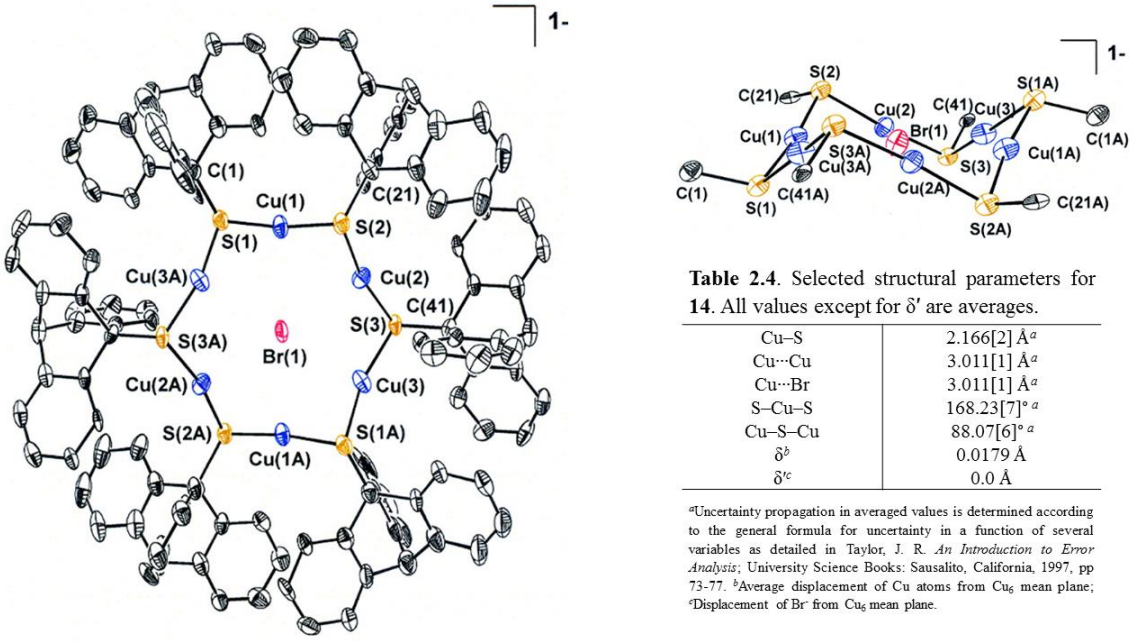

Table 2.4. Selected structural parameters for **14**. All values except for δ′ are averages.

Cu–S	2.166[2] Å[a]
Cu···Cu	3.011[1] Å[a]
Cu···Br	3.011[1] Å[a]
S–Cu–S	168.23[7]°[a]
Cu–S–Cu	88.07[6]°[a]
δ[b]	0.0179 Å
δ′[c]	0.0 Å

[a]Uncertainty propagation in averaged values is determined according to the general formula for uncertainty in a function of several variables as detailed in Taylor, J. R. *An Introduction to Error Analysis*; University Science Books: Sausalito, California, 1997, pp 73-77. [b]Average displacement of Cu atoms from Cu_6 mean plane; [c]Displacement of Br^- from Cu_6 mean plane.

Figure 1.14 Thermal ellipsoid plots (50%) of anion **14** with view orthogonal to Cu_6 plane and side-on with triptycyl groups truncated for clarity. All hydrogen atoms are removed for clarity. Inset of **Table 1.4** showing selected structural parameters for **14**.

In initial efforts to prepare $[Bu_4N]$**10** from $[Cu(MeCN)_4][PF_6]$/$[Bu_4N]Br$ starting materials, single crystals of $[Bu_4N][(CuSTrip)_6(\mu_6\text{-}Br)]\cdot[Bu_4N][PF_6]$ were isolated and identified crystallographically (Figure 1.15). This copper thiolate species can be described as a charge neutral $Cu_6(STrip)_6$ cyclic hexamer with a cyclohexane-like chair conformation. About the plane defined by the six copper(I) ions, the linear copper(I) ions reside at the midpoints of the cyclohexane line segments while the thiolate sulfur atoms, each of which bridges two copper ions, coincide with the vertices (or carbon atom

positions) of the cyclohexane chair. At the center of this cyclic hexamer, which resides on a crystallographic inversion center, sits a bromide ion such that an overall uninegative charge is conferred upon the structure. The core of this $Cu_6(STrip)_6$ structure, neglecting the conformations of the triptycenyl groups, displays D_{3d} point group symmetry. Favorable soft-soft interactions with the copper(I) ions appear to hold the bromide in place, and this interaction may play a templating role in the formation of this structure. Copper-bromide distances and other selected structural features are summarized in the Table 1.4 inset of Figure 1.14. Copper-sulfur distances in this compound are appreciably longer than those found in $[Bu_4N][Cu(STrip)_2]$, an observation that is typical when comparing bridging versus terminal thiolate ligands in homoleptic copper(I) thiolate complexes. Although not a deliberate result, the existence of this structure is useful in showing that 1-(thiolato)triptycene, while a relatively big and awkward thiolate, is nevertheless not rendered completely incapable of a bridging coordination mode. However, as the images in Figure 1.15 suggest, the ligand's cone angle is probably too wide to support any of the analogous cage structure types seen with other thiolate ligands (Figure 1.5).

The $Cu_6(STrip)_6$ hexamer does not have a prior example among copper(I) thiolate complexes, but the structure type, without the halide ion, is precedented in $[Au_6(S\text{-}2,4,6\text{-}{}^{i}Pr_3C_6H_2)_6]$.[69] A topologically related set of homoleptic thiolate complexes are cyclic hexamers of the composition $M_6(SR)_{12}$ (M = Ni^{II}, R = Me,[70] Et,[71] ^{n}Pr;[72] M = Pd^{II}, R = Et,[73] ^{n}Pr;[74] M = Zn^{II}, R = Me,[75] M = Ru^{II}, R = Me[75]). Whereas one triptycyl thiolate ligand bridges each pair of adjacent copper(I) ions in $Cu_6(STrip)_6$ with an alternating

placement above and below the Cu_6 mean plane, two thiolate ligands bridge each pair of adjacent M(II) ions in the $M_6(SR)_{12}$ structures, six being on each side of the M_6 plane.

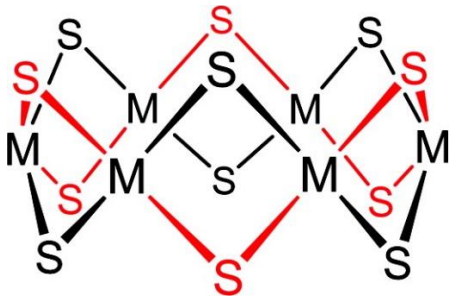

Figure 1.15 D_{3d} $Cu_6(STrip)_6$ core structure inscribed within the D_{6h} homoleptic thiolate $M_6(SR)_{12}$ structure.

Figure 1.15 illustrates how the $Cu_6(STrip)_6$ cyclohexane-type structure (black) derives from the $M_6(SR)_{12}$ by removal of alternating thiolate ligands (red) above and below the M_6 plane.

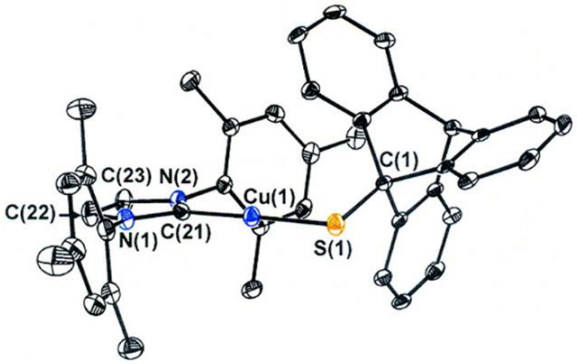

(13)

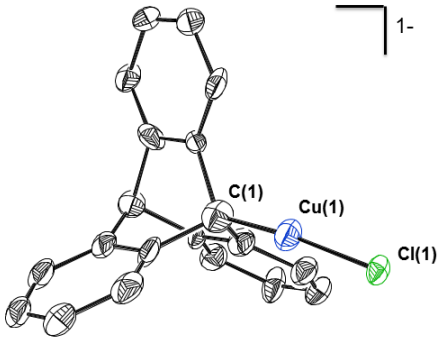

[Cu(Trip)Cl]$^{1-}$

Table 2.5 Crystal and refinement data for [Bu$_4$N][Cu(Trip)Cl].

compound	**[Bu$_4$N][Cu(Trip)Cl]**
solvent	none
formula	$C_{36}H_{49}ClCuN$
fw	594.75
xtl system	orthorhombic
space grp	$Pca2_1$
color, habit	colorless slab
a, Å	19.242(12)
b, Å	19.418(12)
c, Å	17.998(11)
α, deg.	90
β, deg.	90
γ, deg.	90
V, Å^3	6725(7)
T, K	100
Z	8
R1,[a] wR2[b]	0.1020, 0.2417
GoF	0.993

[a] $R1 = \Sigma||F_o| - |F_c||/\Sigma|F_o|$. [b] $wR2 = \{[\Sigma w(F_o^2 - F_c^2)/\Sigma w(F_o^2)^2\}^{1/2}$; $w = 1/[\sigma^2(F_o^2) + (xP)^2]$, where $P = (F_o^2 + 2F_c^2)/3$

Figure 1.16 Thermal ellipsoid plots (50%) of **13** and anion of [Bu$_4$N][Cu(Trip)Cl] with hydrogen atoms omitted for clarity. Inset **Table 1.5** provides crystal information of [Bu$_4$N][Cu(Trip)Cl].

Utilization of the steric capacity of the tryptycyl moiety afforded two-coordinate organometallic complexes **13** and [Bu$_4$N][Cu(Trip)Cl]. N-heterocylic carbene complex **13**, a compound type reported to be effective for the catalytic hydrothiolation of electron deficient olefins,[61] is also two-coordinate and linear at copper (Figure 1.16).

Table 1.6 Summary of Structural Data for [Cu(carbene)(SR)] Compounds.

Compound	Cu–C, Å	Cu–S, Å	S–Cu–C, deg.	Cu–S–C, deg.
[Cu(IMes)(STrip)]	1.892(3)	2.1491(8)	178.83(8)	103.76(8)
[Cu(^{i}Pr$_2$NHCMe$_2$)(SAr*)][a,61]	1.902(6)	2.122(2)	164.0(2)	114.44(18)
[Cu(IPr)(SPh)][b, 60]	1.895(2)	2.139(1)	178.3(1)	100.5(1)
[Cu(IPr)(SBz)][b, 60]	1.898(2)	2.127(1)	171.5(1)	112.1(1)
[Cu(SIPr)(SPh)][c, 60]	1.896(2)	2.145(2)	177.5(1)	105.8(1)
[Cu(SIPr)(SBz)][c, 60]	1.897(3)	2.121(1)	169.5(1)	110.9(3)

[a]SAr* = 2,6-bis(2,4,6-triisopropylphenyl)benzenethiolate(1-); [i]Pr$_2$NHCMe$_2$ = 4,5-dimethyl-1,3-diisopropylimidazol-2-ylidene; [b]IPr = 1,3-bis(2,6-diisopropylphenyl)imidazol-2-ylidene; [c]SIPr = 1,3-bis(2,6-diisopropylphenyl)imidazolidin-2-ylidene.

The bond angles and bond lengths about copper(I) in **13** are compared to those observed in related structures (Table 1.6). Again, it is noteworthy that the Cu-S bond length once more defines the upper end of the range and is significantly longer within the experimental resolution than the corresponding values for other related compounds. A shorter Cu−C bond length appears to correlate to the longer Cu−S bond length according to the data presented in Table 1.6. Structural data collected for [Bu$_4$N][Cu(Trip)Cl] (Figure 1.16) are of rather low quality (R1 = ~0.10), although it represents the *first* structurally characterized copper(I) triptycyl complex.

Summary and Conclusions

Chapter 1 details the synthesis of 1-(thioacetyl)triptycene that affords usable quantities of this convenient, protected form of 1-(thiolato)triptycene. A key aspect of this synthesis is a dealkylation of *tert*-butyl 1-triptycenyl sulfide via a BBr$_3$/AcCl

protocol that heretofore has seen its application limited to the unmasking of aryl thiolates that are protected as *tert*-butyl sulfides. Triptycenyl-1-thiolate readily supports two-coordinate copper(I) complexes, evident by the preparation of [Cu(STrip)(IMes)] and $[Cu(STrip)_2]^{1-}$ in good yield and by their stability. Structural characterization of $[Cu(STrip)_2]^{1-}$ as its $[Bu_4N]^+$ salt reveals longer Cu−S bond distances than in any related $[Cu(SR)_2]^{1-}$ structure and a surprising C−S···S−C torsion angle of 41° (average of two structures), both of which arise from multiple interligand π-π and CH···π interactions. The mononuclear heteroleptic species $[Cu(STrip)(SSiPh_3)]^{1-}$ and $[Cu(STrip)I]^{1-}$ were shown to be generated in solution but only in mixture with the homoleptic bis(thiolate) anions, from which they were not separable. The cyclic hexameric species $[Bu_4N][(Cu\text{-}STrip)_6(\mu_6\text{-}Br)]$ was identified as an adventitious minor byproduct in the synthesis of $[Cu(STrip)_2]^{1-}$ when soft bromide was incorporated in the $[Cu(MeCN)_4][PF_6]/[Bu_4N]Br$ starting materials, and its structure is important in establishing some of the coordination capabilities of 1-(thiolato)triptycene. Bulky 1-(thiolato)triptycene can bridge metal ions, but it is unlikely to be able to accommodate $M_x(SR)_y$ cage structures or motifs involving μ_3 thiolate. A limitation of this ligand is the very modest solubility it will confer on symmetric, charge-neutral species. Nevertheless, the improved access to this ligand provided herein should enable new, coordinatively unsaturated metal complexes to be prepared and investigated for their properties and reactivity. Thus, this ligand should provide utility to both coordination chemistry and bioinorganic chemistry communities at large.

Furthermore, in 2013 Hall and coworkers published results on rigorous electronic structures calculations for model complexes of the Atox1 metallochaperone system.[12]

These density functional theory calculations provided insight into the structure and bonding within the Atox1 system with implications regarding its transfer mechanism.

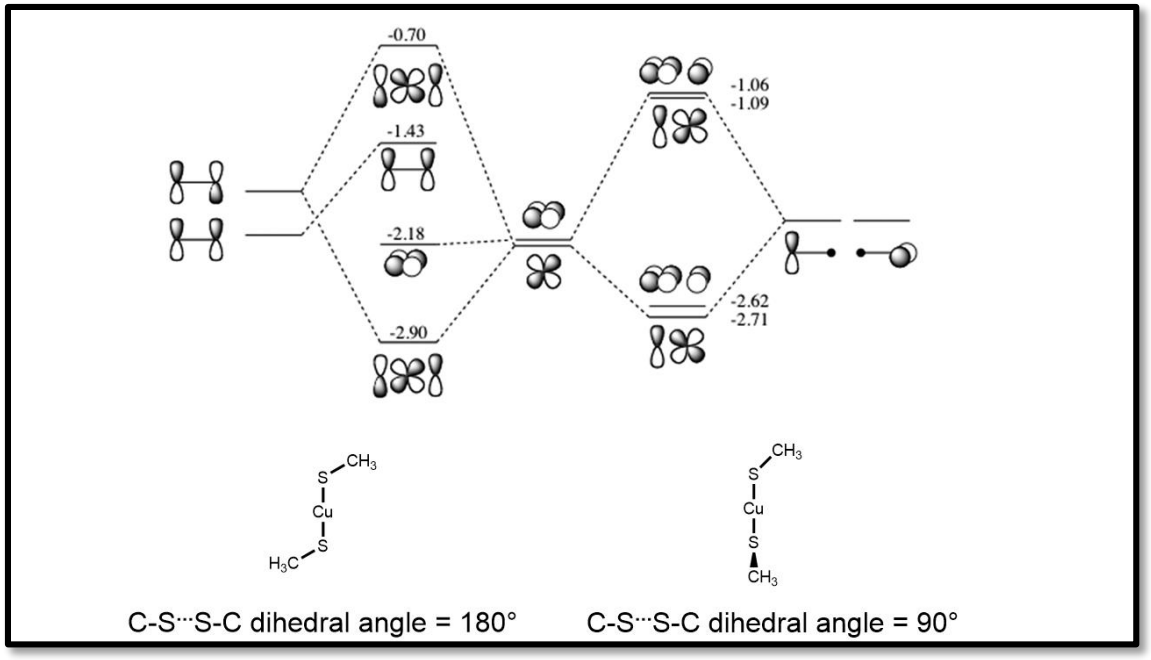

Figure 1.17 Recreated molecular orbital diagrams for $[Cu(SMe)_2]^{1-}$ showing different mixing of Cu d orbitals with S p orbitals for geometries with a C−S···S−C dihedral angle of 180° (left) and 90° (right). "Reprinted (adapted) with permission from (Pitts, A. L.; Hall, M. B. *Inorg. Chem.* **2013**, 52, 10387-10393). Copyright (2013) American Chemical Society."

The anionic model complex $[Cu(SMe)_2]^{1-}$, converged on a structure with a near-linear S-Cu-S angle and ~90° C−S···S−C dihedral angle. Planar conformations for the bis(thiolate) (dihedral of 180°) give rise to sulfur lone pairs that form symmetric and antisymmetric interactions with the corresponding Cu 3d orbitals, the latter of which interacts strongly with one of the filled Cu 3d π orbitals. In a conformation in which the dihedral angle is perpendicular (90°), sulfur lone pair orbitals interact with two Cu 3d π orbitals, where each sulfur lone pair destabilizes one Cu 3d orbital. Such a bonding

situation is destabilizing because these interactions consist of four-electron orbital-orbital repulsions, where the antibonding combination is more destabilizing than the bonding combination is stabilizing, leading to an overall net destabilization. Stability is gained by adopting a conformation geometry where these sulfur lone pair-3d orbital repulsions (Pauli) are spread out across a maximum number of orbitals. While this distribution destabilizes a greater number of 3d orbitals, the energy increment in which they are destabilized decreases, leading to a more stable structures overall. Thus, the structure with an approximately ~90° dihedral angle represents the lowest energy conformation for $[Cu(SMe)_2]^{1-}$. A simplified molecular orbital depiction of these bonding scenarios can be seen in Figure 1.17. When comparing these calculated results with reported crystal structure data for two-coordinate cuprous bis(thiolato) complexes (Table 1.3), it appears that crystal packing effects dominate the overall solid state structure for these compounds. Nonetheless, alkyl bis(thiolate) $[Cu(STrip)_2]^{1-}$ features a sub-90° C−S···S−C torsion angle, and thus represents an adequate model for CueR and Atx1/Atox1 with respect to its structural and electronic characteristics.

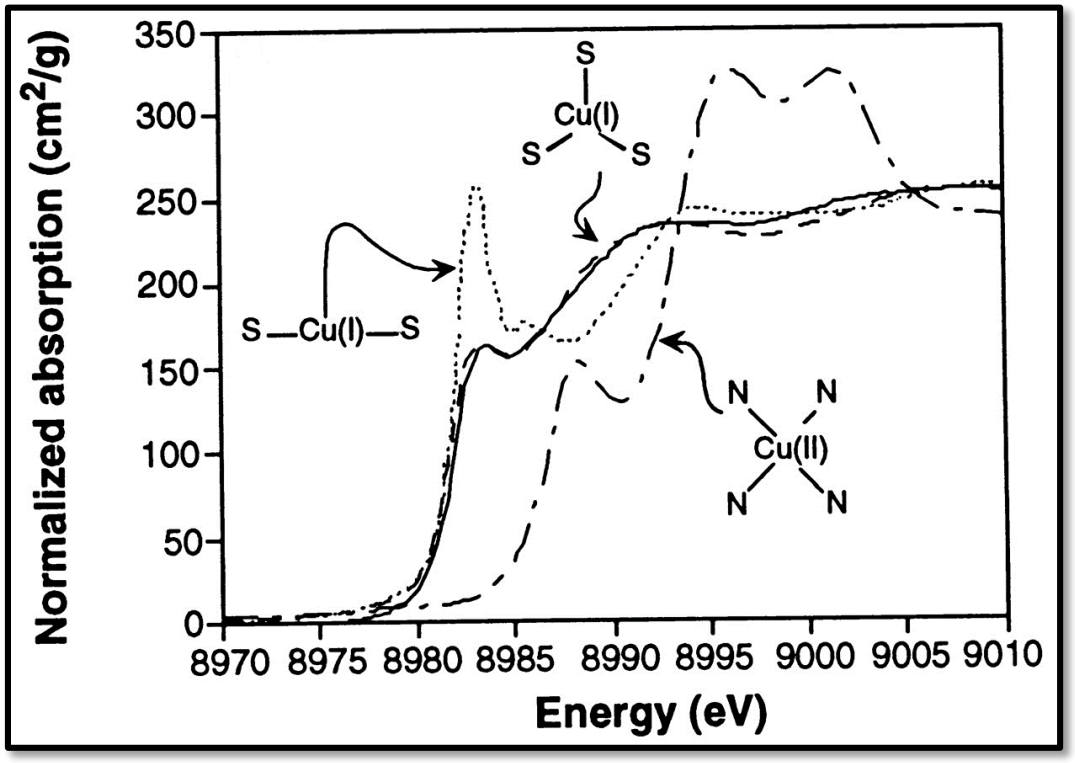

Figure 1.18 X-ray absorption near edge structure (XANES) spectra for different copper complexes, highlighting the match between resting state of native Atx1 core and that of trigonal three-coordinate dianionic tris(thiolate) model complex. Image reproduced from reference 10 with permission. "From Pufahl, R. A.; Singer, C. P.; Peariso, K. L.; Lin, S.-J.; Schmidt, P. J.; Fahrni, C. J.; Cizewski Culotta, V.; Penner-Hahn, J. E.; O'Halloran, T. V. *Science* **1997**, 278, 853– 856. Reprinted with permission from AAAS."

Moreover, in the absence of quality crystallographic data, bioinorganic chemists often use advanced forms of spectroscopy to determine the structure of metal-containing sites in biology. X-ray absorption spectroscopy (XANES, EXAFS, etc.) is often used in this respect. In a typical experiment, the spectrum from the native protein site in question is compared to spectra of discrete synthetic model complexes (Figure 1.18). Combinations of these spectroscopic techniques can provide a comprehensive description of the bonding about the core. Therefore, synthetic model complexes that satisfactorily mimic the coordination environment and electronic properties of the binding sites of

metalloproteins are of general use to the bioinorganic community. Given the straightforward, high-yielding synthesis of $[Cu(STrip)_2]^{1-}$, its stability both as a solid and in solution toward adventitious oxidation, the alkyl-type thiolate ligand binding, and its sub-90° core torsion angle in the solid state, $[Cu(STrip)_2]^{1-}$ rises to the fore as a potentially useful control in spectroscopic experiments aimed at elucidating the core properties of sulfur-containing copper(I) metallobiomolecules.

Experimental

All reactions and manipulations were performed under a pure dinitrogen or argon atmosphere using modified Schlenk techniques or an inert-atmosphere box. Literature procedures were employed for the syntheses of *tert*-butyl 9-anthracenyl sulfide,[55] $[Cu(CH_3CN)_4][PF_6]$,[76] and [(IMes)Cu(Cl)] (IMes = 1,3-bis(2,4,6-trimethylphenyl)imidazol-2-ylidene).[77] Solvents either were dried with a system of drying columns from the Glass Contour Company (CH_2Cl_2, Et_2O, tetrahydrofuran (THF)) or freshly distilled according to standard procedures[78] (MeOH, CH_3CN). Other reagents and all solvents used in column chromatography purifications were used as received from commercial sources. Silica columns were run in the open air using 60–230 μm silica (Dynamic Adsorbents). The numbering system employed in compound identification is defined in Table 1.1.

IR spectra were taken as pressed KBr pellets with a Thermo Nicolet Nexus 670 FTIR instrument in absorption mode. All NMR spectra were recorded at 25 °C with a Varian Unity Inova spectrometer operating at 400 or 100.5 MHz for ^1H and ^{13}C, respectively, and were referenced to the solvent residual. Mass spectra were obtained by

either MALDI-TOF (Bruker Autoflex III instrument) or by electrospray ionization methods (Bruker microTOF with Agilent Technologies 1200 Series LC). Elemental analyses were performed by Midwest Microlab, LLC of Indianapolis, IN.

Diffraction quality crystals of all molecular compounds were obtained by slow evaporation in the open air from the solvent or solvent mixture indicated parenthetically: triclinic 9-(thioacetyl)anthracene (CH_2Cl_2/hexanes), orthorhombic 9-(thioacetyl)anthracene (EtOAc), *tert*-butyl 9-anthracenyl sulfide ($CDCl_3$), bis(9-anthracenyl)sulfide (THF/hexanes), 9-(thioacetyl)triptycene (hexanes/EtOAc), 9-(*tert*-butyl)triptycene (CH_2Cl_2/MeOH). Suitable crystals of the ionic species that were characterized by crystallography were prepared by the small-scale vial-in-a-vial vapor diffusion technique. The following solvent pairs indicate specific combinations successfully employed as solvent/diffusing vapor for crystal growth: $[Bu_4N][STrip]$ (THF/^{t}BuOMe), $[Bu_4N][Cu(STrip)_2]\cdot Et_2O$ (THF/Et_2O), $[Bu_4N][Cu(STrip)_2]\cdot C_6H_6$ (C_6H_6/hexanes), $[Bu_4N][(Cu\text{-}STrip)_6(\mu_6\text{-}Br)]\cdot[Bu_4N][PF_6]$ (MeCN/^{t}BuOMe). The color and morphology of each crystal are indicated in Table 1.2. All crystals were coated with paratone oil and mounted on the end of a nylon loop attached to the end of the goniometer. Data were collected with a Bruker APEX CCD diffractometer equipped with a Kryoflex attachment supplying a nitrogen stream at 100 K. Full spheres of data were obtained by employing one of the two following collection routines: (1) Three sets of 606 frames in ω (0.3º/scan) with φ held constant at 0, 120, and then 240º; (2) Three sets of 400 frames in ω (0.5º/scan), collected at φ = 0.00, 90.00 and 180.00° followed by two sets of 800 frames in φ (0.45°/scan) collected with ω constant at -30.00 and 210.00°. The data collection program and frame time used for each data set were as follows: 9-

(thioacetyl)anthracene (orthorhombic): Routine 1, 30 sec; 9-(thioacetyl)anthracene (triclinic): Routine 2, 20 sec; tert-butyl 9-anthracenyl sulfide: Routine 2, 20 sec; bis(9-anthracenyl)sulfide: Routine 1, 30 sec; 9-(thioacetyl)triptycene: Routine 1, 10 sec; 9-(*tert*-butyl)triptycene: Routine 2, 25 sec; [Bu4N][STrip]: Routine 1, 30 sec; $[Bu_4N][Cu(STrip)_2]\cdot Et_2O$: Routine 2: 15 sec; $[Bu_4N][Cu(STrip)_2]\cdot C_6H_6$: Routine 1, 30 sec; $[Bu_4N][(Cu\text{-}STrip)_6(\mu_6\text{-}Br)]\cdot[Bu_4N][PF_6]$: Routine 2, 90 sec.

All data were collected under control of the *APEX2* software package,[79] except for the orthorhombic form of 9-(thioacetyl)anthracene, in which use was made of the earlier *SMART* software.[80] Raw data were reduced to F^2 values using the *SAINT*[81]or *SAINT+*[82] software, and a global refinement of unit cell parameters was performed using 1958–9988 selected reflections from the full data set. Data for the all compounds were corrected for absorption on the basis of multiple measurements of symmetry equivalent reflections with the use of *SADABS*[83]. All structure solutions were obtained by direct methods using *SHELXS*,[84] while refinements were accomplished by full-matrix least-squares procedures using *SHELXL*[85]. Both the *SHELXS* and *SHELXL* programs are incorporated into the *SHELXTL* software suite.[86] For $[Bu_4N]$ $[Cu(STrip)_2]\cdot Et_2O$ a badly disordered molecule of THF was removed with the *SQUEEZE* option in *PLATON*.[87] All hydrogen atoms were added in calculated positions and included as riding contributions with isotropic displacement parameters tied to those of the carbon atoms to which they were attached. All images were created with the use of *XP*, which also is part of the *SHELXTL* package. Final unit cell data and refinement statistics are collected in Table 1.2.

Syntheses

tert-Butyl 1-triptycenyl Sulfide, 8

A solution of 2-(trimethylsilyl) phenyl triflate (4.97 g, 0.017 mol) in 15 mL of dry MeCN was transferred via cannula to a yellow, stirring solution of **7** (4.44 g, 0.017 mol) in 40 mL of dry THF at 0 °C. Tetra-*n*-butylammonium fluoride (16.6 mL, 1 M in THF, 0.017 mol) was then added to the mixture dropwise at 0 °C, which induced a progressive fading of color to a light yellow. While being stirred for 12 h, the reaction mixture was slowly warmed to ambient temperature and then taken to dryness under reduced pressure to afford a yellow residue. This residue was dissolved in 100 mL of CH_2Cl_2. The resulting solution was washed with water (4 × 30 mL) and then dried over $MgSO_4$. This crude yellow product solution was evaporated onto silica (3.0 g), which then was dry-loaded onto a silica column packed as a slurry with *n*-pentane. The column was eluted with *n*-pentane to separate unreacted **7** (3.55 g, yellow band with streaking). Subsequent elution with *n*-pentane/CH_2Cl_2 (2:1) moved **8** as a pale yellow band. Concentration of the eluant to dryness gave **8** as a pale yellow solid (Yield: 0.78 g, 68% based on reacted *tert*-butyl 9-anthracenyl sulfide). Recrystallization from hot MeOH produced large colorless plates. R_f = 0.74 (1:2, CH_2Cl_2:*n*-pentane). ^{1}H NMR (δ, ppm in $CDCl_3$): 1.65 (s, 9H), 5.26 (s, 1H), 6.94 (m, 6H), 7.28 (d, 3H), 7.73 (d, 3H). ^{13}C NMR (δ, ppm in $CDCl_3$): 34.52, 47.43, 54.37, 65.86, 123.34, 124.14, 124.76, 125.61, 145.53, 146.43. Anal. Calcd for $C_{24}H_{22}S$: C, 84.16; H, 6.47; S, 9.36. Found: C, 84.18; H, 6.45; S, 9.25.

1-(Thioacetyl)triptycene, 5

To a stirring solution of **8** (1.02 g, 2.98 mmol) in 20 mL of dry CH_2Cl_2 and 5 mL of acetyl chloride (excess) was slowly added BBr_3 in CH_2Cl_2 (8 mL, 1 M in CH_2Cl_2, 8 mmol) at room temperature to generate a dark brown reaction mixture. This mixture was stirred at ambient temperature for 12 h, then poured into 100 mL of ice and extracted with 100 mL of CH_2Cl_2. The yellow organic phase was dried over $MgSO_4$, evaporated onto silica and dry-loaded onto a column that was packed as a slurry in hexanes. Elution of the column with CH_2Cl_2/hexanes (1:2) brought **5** forward as the first band (pale yellow). Slow evaporation of the corresponding column fraction yielded a white, crystalline product 0.69 g (Yield: 71%). R_f = 0.18 (1:2 CH_2Cl_2/hexanes). ^{1}H NMR (δ, ppm in $CDCl_3$): 2.75 (s, 3H), 5.41 (s, 1H), 6.99 (m, 6H), 7.31 (d, 3H), 7.39 (d, 3H). ^{13}C NMR (δ, ppm in $CDCl_3$): 31.94, 54.14, 63.76, 123.10, 123.84, 125.13, 126.10, 142.71, 144.91, 192.10. IR (KBr): 1699 cm^{-1} (C═O). ESI-MS$^+$: *m*/*z* 351 (M + Na^+), 679 (2 M + Na^+). Anal. Calcd for $C_{22}H_{16}OS$: C, 80.45; H, 4.91; S, 9.76. Found: C, 80.35; H, 4.96; S, 9.60.

[^{n}Bu$_4$N][Cu(STrip)$_2$], [^{n}Bu$_4$N]10

A suspension of cuprous chloride (0.031 g, 0.313 mmol) and anhydrous [^{n}Bu$_4$N]Cl (0.087 g, 0.313 mmol) in 15 mL of dry THF was stirred for 4 h at room temperature in the absence of light, during which time all components are brought into solution. A second flask containing a clear, colorless solution of **5** (0.205 g, 0.624 mmol) in 20 mL of dry THF was cooled to −78 °C, and $NaHBEt_3$ (0.65 mL, 1 M in THF, 0.65 mmol) was added dropwise to generate a yellow solution. This solution was stirred at −78 °C for 45 min

and then was allowed to warm to ambient temperature with stirring for an additional 1.5 h. After the separate mixtures were stirred for their respective allotted reaction times, the copper solution was transferred dropwise via cannula to the solution of deprotected ligand, which was cooled to −78 °C. The color of the resulting mixture progressively faded to a lighter yellow as the copper solution was added. With stirring, the reaction mixture was then slowly warmed to room temperature overnight, during which time a pale yellow solution with a white precipitate formed. The white solid was removed by filtration under N_2, and the filtrate reduced to dryness under reduced pressure. The resulting solid residue was washed with Et_2O (5 mL) and dried under vacuum to afford 0.212 g of a pale yellow solid (Yield: 77%). Crystallization via diffusion of Et_2O or ^{t}BuOMe vapor into a concentrated THF solution afforded large, colorless, block-shaped crystals. ^{1}H NMR (δ, ppm in CD_3CN): 0.96 (t, -$NCH_2CH_2CH_2\mathit{CH_3}$, 12H), 1.34 (sextet, -$NCH_2CH_2\mathit{CH_2}CH_3$, 8H), 1.58 (pentet, -$NCH_2\mathit{CH_2}CH_2CH_3$, 8H), 3.06 (t, -$N\mathit{CH_2}CH_2CH_2CH_3$, 8H), 5.41 (s, 2H), 6.79 (t, 6H), 6.89 (t, 6H), 7.28 (d, 6H), 8.26 (d, 6H). MALDI-MS$^-$: *m*/*z* 633 (anion). Anal. Calcd for $C_{56}H_{62}NS_2Cu$: C, 76.71; H, 7.13; N, 1.60. Found: C, 78.16; H, 7.29; N, 1.91.

[1,3-Bis(2,4,6-trimethylphenyl)imidazol-2-ylidene] (triptycenylthiolato) Cuprate, [Cu(IMes)(STrip)], 13

To a clear, colorless solution of **5** (0.026 g, 0.079 mmol) in 5 mL of dry C_6H_6 was added ^{n}BuLi (32 μL, 2.5 M in hexanes, 0.08 mmol) via gastight syringe at room temperature. This pale yellow solution was stirred for 2 h. A solution of [Cu(IMes)(Cl)] (0.032 g, 0.079 mmol) in 6 mL of 2:1 THF/C_6H_6 (v/v) was then slowly added via cannula to the solution of deprotected ligand. This reaction mixture was stirred for 12 h, during

which time a white precipitate formed. The white solid was separated by filtration, and the solvent was removed from the filtrate under reduced pressure to yield an off-white residue. Extraction of this product residue with 5 mL of Et_2O was followed by anaerobic filtration through packed Celite and concentration of the filtrate to about 3 mL. Colorless plate crystals formed upon standing at room temperature after 2 d (Yield: 0.018 g, 35%). ^{1}H NMR (δ, ppm in $CDCl_3$): 2.03 (s, 12H, IMes *ortho*-CH_3), 2.27 (s, 6H, IMes *para*-CH_3), 5.23 (s, 1H, STrip bridgehead), 6.80 (t, 7H, IMes *meta*-H and STrip aryl, overlapping), 6.90 (t, 3H, STrip aryl), 7.01 (s, 2H, IMes NC*H*), 7.22 (d, 3H, STrip aryl), 7.90 (d, 3H, STrip aryl). ^{13}C NMR (δ, ppm in $CDCl_3$): 18.1 (IMes *ortho*-*C*H_3), 21.3 (IMes *para*-*C*H_3), 54.1 (STrip bridgehead), 61.8 (STrip *ipso*), 122.0 (IMes *ortho*-C), 123.7 (STrip aryl-C), 124.4 (STrip aryl-C), 125.1 (STrip aryl-C), 126.0 (STrip aryl-C), 129.5 (IMes *meta*-C), 134.6 (IMes N*C*H), 135.3 (IMes *para*-C), 139.3 (IMes N*C*-*ipso*), 144.4 (STrip aryl-C), 145.6 (STrip aryl-C), 150.1 (IMes N*C*Cu). MALDI-MS$^+$: *m*/*z* 671 ($MH^+ + H_2O$). Anal. Calcd for $C_{41}H_{37}CuN_2S$: C, 75.37; H, 5.71; N, 4.29; Found: C, 75.06; H, 5.54; N, 4.40.

[^{n}Bu$_4$N][(Cu-STrip)$_6$(μ$_6$-Br], [^{n}Bu$_4$N]14

A clear, colorless solution of **5** (0.029 g, 0.088 mmol) in 5 mL of dry THF at −78 °C was treated dropwise with a solution of $NaHBEt_3$ (0.09 mL, 1 M in THF, 0.09 mmol) to produce a light yellow mixture. This solution was stirred at −78 °C for 45 min and then allowed to warm to room temperature with stirring for an additional 1.5 h. The solution was again cooled to −78 °C. A solution of $[Cu(CH_3CN)_4]PF_6$ (0.016 g, 0.043 mmol) in 5 mL of dry MeCN was then added dropwise, which progressively turned the reaction mixture to a lighter yellow color. This mixture was stirred at −78 °C for 1.5 h. A solution

of [^{n}Bu$_4$N][Br] (0.014 g, 0.043 mmol) in 5 mL of dry MeCN was slowly added. With stirring, the reaction mixture was slowly warmed to room temperature overnight. The mixture was then reduced to dryness under reduced pressure, and the solid residue was washed with 5 mL of Et_2O. The remaining solid was redissolved in dry MeCN (6.0 mL) and filtered under an atmosphere of N_2 through packed Celite. Colorless block crystals of [^{n}Bu$_4$N]**14**·[Bu$_4$N][PF_6], identified by X-ray crystallography, were obtained by diffusion of ^{t}BuOMe vapor into a concentrated MeCN solution of the crude product. Deliberate efforts to reproduce the synthesis of [^{n}Bu$_4$N]**14** typically resulted in the formation of [^{n}Bu$_4$N]**10** as the only identifiable species.

References

1) Tümer, Z.; Møller, L. B. *Eur. J. Hum. Genet.* **2010**, *18*(5): 511–518.

2) Das, S. K.; Ray, K. *Nat. Clin. Pract. Neurol.* **2006**, *2*(9), 482-93.

3) Rosen, D. R.; Siddique, T.; Patterson, D. et al. *Nature* **1993**, *362*, 59–62.

4) Huang, X.; Cuajungco, M. P.; Atwood, C. S. et al. *J. Biol. Chem.* **1999**, *274*, 37111-37116.

5) Viles, J. H.; Cohen, F. E.; Prusiner, S. B.; Goodin, D. B.; Wright, P. E.; Dyson, H. J. *Proc. Natl. Acad. Sci. USA* **1999**, *96*, 2042–2047.

6) Outten, F. W.; Huffman, D. L.; Hale, J. A.; O'Halloran, T. V. *J. Biol. Chem.* **2001**, *276*(33), 30670-7.

7) Chen, K.; Yuldasheva, S.; Penner-Hahn, J. E.; O'Halloran, T. V. *J. Am. Chem. Soc*. **2003**, *125* (40), 12088–12089.

8) Changela, A.; Chen, K.; Xue, Y.; Holschen, J.; Outten, C. E.; O'Halloran, T. V.; Mondragón, A. *Science* **2003**, *301*, 1383-1387.

9) http://www.rcsb.org/pdb/

10) Pufahl, R. A.; Singer, C. P.; Peariso, K. L.; Lin, S. J.; Schmidt, P. J.; Fahrni, C. J.; Culotta, V. C.; Penner-Hahn, J. E.; O'Halloran, T. V. *Science* **1997**, *278*, 853-856.

11) Kim, B. E.; Nevitt, T.; Thiele, D. J. *Nat. Chem. Biol*. **2008**, *4*(3), 176-185.

12) Pitts, A. L.; Hall, M. B. *Inorg. Chem.* **2013**, *52* (18), 10387–10393.

13) Mörsdorf, G.; Frunzke, K.; Gadkari, D.; Meyer, O. *Biodegradation* **1992**, *3*, 61-82.

14) Dobbek, H.; Gremer, L.; Meyer, O.; Huber, R. *Proc. Natl. Acad. Sci. USA* **1999**, *96*, 8884-8889.

15) Dobbek, H.; Gremer, L.; Kiefersauer, R.; Huber, R.; Meyer, O. *Proc. Natl. Acad. Sci. USA* **2002**, *99*, 15971-15976.

16) Koch, S. A.; Fikar, R.; Millar, M.; O'Sullivan, T. *Inorg. Chem.* **1984**, *23*, 121–122.

17) Fujisawa, K.; Imai, S.; Kitajima, N.; Moro-oka, Y. *Inorg. Chem.* **1998**, *37*, 168–169.

18) Zeevi, S.; Tshuva, E. Y. *Eur. J. Inorg. Chem.* **2007**, 5369–5376.

19) Kohner-Kerten, A.; Tshuva, E. Y. *J. Organomet. Chem.* **2008**, *693*, 2065–2068.

20) Groysman, S.; Majumdar, A.; Zheng, S.-L.; Holm, R. H. *Inorg. Chem.* **2010**, *49*, 1082–1089.

21) Sampanthar, J. T.; Vittal, J. J.; Dean, P. A. W. *J. Chem. Soc., Dalton Trans.* **1999**, 3153–3156.

22) Coucouvanis, D.; Murphy, C. N.; Kanodia, S. K. *Inorg. Chem.* **1980**, *19*, 2993–2998.

23) Garner, C. D.; Nicholson, J. R.; Clegg, W. *Inorg. Chem.* **1984**, *23*, 2148–2150.

24) Fujisawa, K.; Imai, S.; Suzuki, S.; Moro-oka, Y.; Miyashita, Y.; Yamada, Y.; Okamoto, K. *J. Inorg. Biochem.* **2000**, *82*, 229–238.

25) (a) Block, E.; Kang, H.; Ofori-Okai, G.; Zubieta, J. *Inorg. Chim. Acta* **1990**, *167*, 147–148. (b) Schröter-Schmid, I.; Strähle, J. *Z. Naturforsch., B: Chem. Sci.* **1990**, *45*, 1537–1542.

26) Hu, S.-Z. *Jiegou Huaxue* **1999**, *18*, 47.

27) Dance, I. G.; Calabrese, J. C. *Inorg. Chim. Acta* **1976**, *19*, L41–L42.

28) Dance, I. G.; Bowmaker, G. A.; Clark, G. R.; Seadon, J. K. *Polyhedron* **1983**, *2*, 1031–1043.

29) Baumgartner, M.; Schmalle, H.; Dubler, E. *Polyhedron* **1990**, *9*, 1155–1164.

30) Baumgartner, M.; Schmalle, H.; Baerlocher, C. *J. Solid State Chem.* **1993**, *107*, 63–75.

31) Dance, I. G. *J. Chem. Soc., Chem. Commun.* **1976**, 68–69.

32) Bowmaker, G. A.; Clark, G. R.; Seadon, J. K.; Dance, I. G. *Polyhedron* **1984**, *3*, 535–544.

33) Dance, I. G. *J. Chem. Soc., Chem. Commun.* **1976**, 103–104.

34) Dance, I. G. *Aust. J. Chem.* **1978**, *31*, 2195–2206.

35) Yang, Q.; Tang, K.; Liao, H.; Han, H.; Chen, Z.; Tang, Y. *J. Chem. Soc., Chem. Commun.* **1987**, 1076–1077.

36) Block, E.; Gernon, M.; Kang, H.; Ofori-Okai, G.; Zubieta., J. *Inorg. Chem.* **1989**, *28*, 1263–1271.

37) Dilworth, J. R.; Arnold, P.; Morales, D.; Wong, Y.-L.; Zheng, Y.The Chemistry and Applications of Complexes with Sulfur Ligands. In *Modern Coordination Chemistry*; Leigh,G. J., Winterton, N., Eds.; Royal Society of Chemistry: Cambridge, U.K., **2002**; pp 217–230.

38) Dilworth, J. R.; Hu, J. *Adv. Inorg. Chem.* **1993**, *40*, 411–459.

39) Blower, P. J.; Dilworth, J. R. *Coord. Chem. Rev.* **1987**, *76*, 121–185.

40) Dance, I. G. *Polyhedron* **1986**, *5*, 1037–1104.

41) Field, L.; Grunwald, F. A. *J. Org. Chem.* **1951**, *16*, 946– 953.

42) Blower, P. J.; Dilworth, J. R.; Hutchinson, J.; Nicholson, T.; Zubieta, J. A. *J. Chem. Soc., Dalton Trans.* **1985**, 2639–2645.

43) Bishop, P. T.; Dilworth, J. R.; Nicholson, T.; Zubieta, J. *J. Chem. Soc., Dalton Trans.* **1991**, 385–392.

44) Niemeyer, M.; Power, P. P. *Inorg. Chem.* **1996**, *35*, 7264–7272.

45) Kawada, Y.; Ishikawa, J.; Yamazaki, H.; Koga, G.; Murata, S.; Iwamura, H. *Tetrahedron Lett.* **1987**, *28*, 445–448.

46) Hayashi, S.; Nakamoto, T.; Minoura, M.; Nakanishi, W. *J. Org. Chem.* **2009**, *74*, 4763–4771.

47) Nakata, N.; Yamamoto, S.; Hashima, W.; Ishii, A. *Chem. Lett*. **2009**, *38*, 400–401.

48) LaPointe, R. E.; Wolczanski, P. T.; Van Duyne, G. D. *Organometallics* **1985**, *4*, 1810–1818.

49) (a) Majumdar, K. C.; Chattopadhyay, S. K.; Sen, B. K. *Indian J. Chem*. **1986**, *25B*, 1261– 1262. (b) Kansikas, J.; Sipilä, K. *Acta Crystallogr., Sect C.* **2000**, *56*, 72–73.

50) Beckwith, A. L. J.; Low, B. S. *J. Chem. Soc.* **1961**, 1304–1311.

51) Himeshima, Y.; Sonoda, T.; Kobayashi, H. *Chem. Lett.* **1983**, 1211–1214.

52) Kitamura, T.; Yamane, M.; Inoue, K.; Todaka, M.; Fukatsu, N.; Meng, Z.; Fujiwara, Y. *J. Am. Chem. Soc.* **1999**, *121*, 11674–11679.

53) Fieser, L. F.; Williamson, K. L. *Organic Experiments*, 5th ed.; D. C. Heath: Lexington, MA, **1983**; pp 246–249.

54) Nakamura, N. *Chem. Lett.* **1983**, 1795–1798.

55) Jennings, W. B.; Kochanewycz, M. J.; Lunazzi, L. *J. Chem. Soc., Perkin Trans. 2* **1997**, 2271–2274.

56) Stuhr-Hansen, N.; Christensen, J. B.; Harrit, N.; Bjørnholm, T. *J. Org. Chem.* **2003**, *68*, 1275–1282.

57) See, for example: (a) Greger, J. G.; Yoon-Miller, S. J. P.; Bechtold, N. R. *J. Org. Chem.* **2011**, *76*, 8203–8214. (b) Wen, H.-M.; Zhang, D.-B.; Zhang, L.-Y. *Eur. J. Inorg. Chem.* **2011**, 1784–1791. (c) Petersen, A. B.; Thyrhaug, E.; Jain, T.; Kilsaa, K.; Bols, M.; Moth-Poulsen, K.; Harrit, N.; Bjørnholm, T. *J. Phys. Chem. B* **2010**, *114*, 11771–11777. (d) Zeng, X.; Wang, C.; Batsanov, A. S. *J. Org. Chem.* **2010**, *75*, 130–136. (e) Babudri, F.; Farinola, G. M.; Naso, F. *Synlett* **2009**, 2740–2748. (f) Moth-Poulsen, K.; Bjørnholm, T. *Nat. Nanotechnol.* **2009**, *4*, 551–556.

58) Salinger, R. M.; West, R. *J. Organomet. Chem.* **1968**, *11*, 631–633.

59) Herman, A.; Wojnowski, W. *Struct. Chem.* **1992**, *3*, 239–244.

60) Tacke, R.; Wannagat, U. *Top. Curr. Chem.* **1979**, *84*, 1–75.

61) Delp, S. A.; Munro-Leighton, C.; Goj, L. A.; Ramírez, M. A.; Gunnoe, T. B.; Petersen, J. L.; Boyle, P. D. *Inorg. Chem.* **2007**, *46*, 2365–2367.

62) Groysman, S.; Holm, R. H. *Inorg. Chem.* **2009**, *48*, 621–627.

63) Kawada, Y.; Iwamura, H. *J. Org. Chem.* **1981**, *46*, 3357-3359.

64) Jeffrey, G. A.; Robbins, A. *Acta Crystallogr., Sect. B* **1980**, *36*, 1820–1826.

65) Bard, A. J.; Cowley, A. H.; Leland, J. K.; Thomas, G. J. N.; Norman, N. C.; Jutzi, P.; Morley,C. P.; Schlüter, E. *J. Chem. Soc., Dalton Trans.* **1985**, 1303–1307.

66) Grilli, S.; Lunazzi, L.; Mazzanti, A. *J. Org. Chem.* **2001**, *66*, 4444–4446.

67) Arnold, P. L.; Natrajan, L. S.; Hall, J. J.; Bird, S. J.; Wilson, C. *J. Organomet. Chem.* **2002**, *647*, 205–215.

68) Hayashi, N.; Higuchi, H.; Ninomiya, K. In *X/π Interactions in Aromatic Heterocycles: Basic Principles and Recent Advances*; Matsumoto, K.; Hayashi, N., Eds.; Topics in Heterocyclic Chemistry: Heterocyclic Supramolecules II 18; Springer: Heidelberg, Germany, **2009**; pp 1–35.

69) (a) Schröter, I.; Strähle, J. *Chem. Ber.* **1991**, *124*, 2161–2164. (b) LeBlanc, D. J.; Lock, C. J. L. *Acta Crystallogr., Sect. C* **1997**, *53*, 1765–1768.

70) Wark, T. A.; Stephan, D. W. *Organometallics* **1989**, *8*, 2836–2843.

71) Miyamae, H.; Yamamura, T. *Acta Crystallogr., Sect. C* **1988**, *44*, 606–609.

72) Xiao, H. L.; Jian, F. F.; Zhang, K. J. *Bull. Korean Chem. Soc.* **2009**, *30*, 846–848.

73) Thomas, P. J.; Lavanya, A.; Sabareesh, V.; Kulkarni, G. U. *Proc.—Indian Acad. Sci., Chem. Sci.* **2001**, *113*, 611–619.

74) Kunchur, N. R. *Acta Crystallogr., Sect. B* **1968**, *24*, 1623–1633.

75) Xie, M.-H.; Wang, M.; Wu, C.-D. *Inorg. Chem.* **2009**, *48*, 10477–10479.

76) Kubas, G. J. *Inorg. Synth.* **1979**, *19*, 90.

77) Goj, L. A.; Blue, E. D.; Delp, S. A.; Gunnoe, T. B.; Cundari, T. R.; Pierpont, A. W.; Petersen, J. L .; Boyle, P. D. *Inorg. Chem.* **2006**, *45*, 9032–9045.

78) Armarego, W. L.; Perrin, D. D. *Purification of Laboratory Chemicals*; Butterworth-Heinemann, Linacre House, Jordan Hill: Oxford, Great Britain, **2000**.

79) *SMART*, Version 5.625, Bruker-AXS, Inc., Madison, Wisconsin, USA, **2000**.

80) *APEX2*, Version 2008.2-0, Bruker-AXS, Inc., Madison, Wisconsin, USA, **2008**.

81) *SAINT*, Version 7.60A, Bruker AXS, Inc., Madison, Wisconsin, **2008**.

82) *SAINT-Plus*, Version 7.34A, Bruker AXS, Inc., Madison, Wisconsin, USA.

83) Sheldrick, G. M. *SADABS*, Version 2008/2, Universität Göttingen, Göttingen, Germany, **2008**.

84) Sheldrick, G. M. *SHELXS-97*, Universität Göttingen, Göttingen, Germany, **2008**.

85) Sheldrick, G. M, *SHELXL-97*, Universität Göttingen, Göttingen, Germany, **2008**.

86) (a) *SHELXTL*, Version 6.10, Bruker-AXS, Madison, WI, **2000**. (b) *SHELXTL*, Version 2008/4, Bruker-AXS, Madison, WI, **2008**.

87) Spek, A. L. *PLATON*, A Multipurpose Crystallographic Tool, Utrecht University, Utrecht, The Netherlands, **2009**.

Chapter 2

Synthesis and Reactivity of 2-and 4-Coordinate Copper(I) Silylthiolate Complexes and Metallothiols

Introduction

Since the inception of modern inorganic chemistry, much attention has been devoted to the investigation of heteronuclear metal-containing complexes.[1-6] Reasons for studying materials containing disparate metal centers are extensive but generally pertain to applications in activating substrates arising from the bifunctionality of the differing metal centers. Not only do such complexes exist as a conceptual link between materials and their constituents, but heteronuclear compounds provide the potential for exhibiting synergistic reactivity different from that which is observed for homometallic or mononuclear complexes. Traditionally, early/late heterobimetallic complexes have been constructed and examined in this regard. The chemical reactivity which underpins these compounds is based on the close proximity in which these different metal ions are placed, which may, in some cases, establish a highly polar dative bond between fragments. In such a scenario, the soft, electron-rich Lewis-basic late transition metal center may impart reductive properties upon a substrate, while the harder, Lewis-acidic early transition metal may confer oxidative effects, as it is energetically favorable to fill the early metal's vacant d orbitals. Different heterometallic systems may feature different synergistic behavior, ranging from only one metal fragment providing an "electronic tuning" role while the other fragment(s) act in a more typical fashion as the reaction center, to both

distinct fragments being involved in bond making and breaking. Moreover, the cooperative nature associated with these multinuclear assemblies present the possibility of multi-electron chemical transformations. Transformations such as these embody the ultimate goal of most efforts within the modern realm of small molecule activation chemistry.

In biology, several metalloenzyme systems contain active sites with mixed-metal cores that facilitate catalytic transformations via concerted reactivity derived from the different metal centers. Most notably among these are the nitrogenases,[7, 8] hydrogenases,[9] and carbon monoxide dehydrogenases.[10, 11]

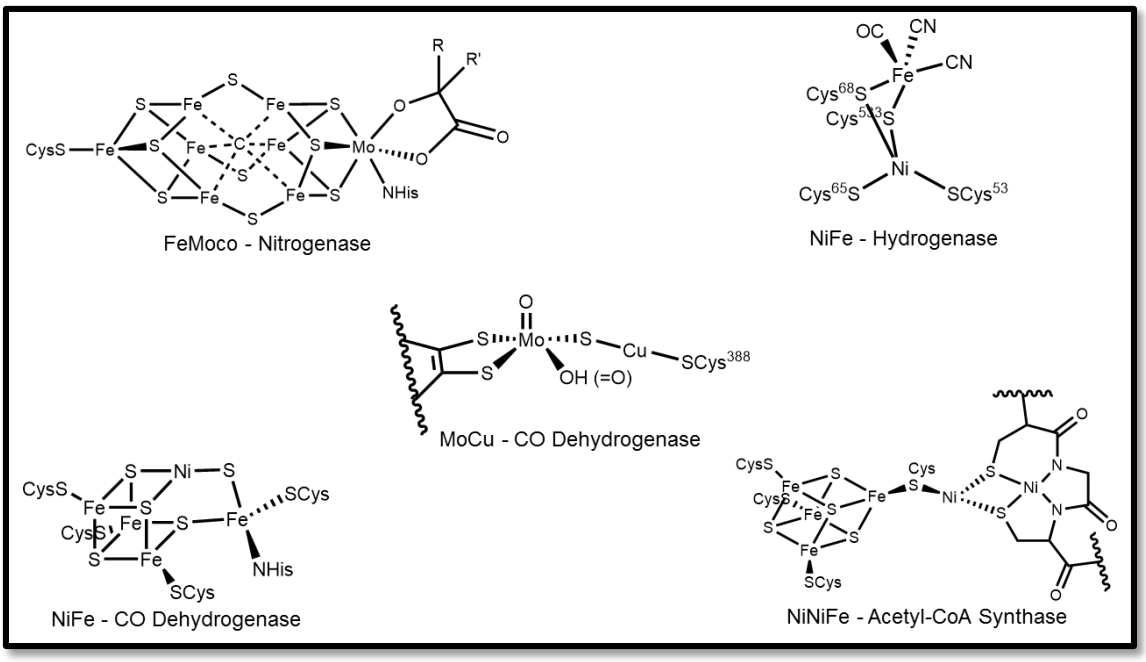

Figure 2.1 Minimal representations of some heteronuclear metalloenzyme active sites.

The combinations of different metal centers found in these metalloenzyme systems play very precise roles, which engender their overall efficiency with respect to the remarkable

chemical transformations they catalyze. A rationale behind the diversity among heteronuclear metallobiomolecules is shrouded in evolutionary history, but must, more generally, be attributed to bioavailability and selective pressure to evolve multiple biochemical pathways to secure the viability of critical cellular functions.

An interesting motif that could offer potential promise as a component within a heteronuclear framework is that of a sulfur-containing copper(I) fragment. In particular, a low-coordinate, sulfur-containing copper(I) fragment would exhibit Lewis acidity appropriate for binding and activating small molecules. The closed-shell d^{10} copper(I) ion is capable of engaging in π-backbonding with unsaturated molecular fragments, thus destabilizing the molecular fragment as electron density is pumped into its π^* antibonding orbitals. These characteristics are desirable from a reactivity standpoint for a component within a heteronuclear construct. As an auxiliary constituent, sulfur ion (as thiolate or sulfide), provides strong soft-soft interactions with copper(I), leading to an augmented covalency about the Cu(I)-S bond. Subsequently, this covalency could give rise to a high degree of electronic delocalization about the fragment, which is another advantageous behavior associated with multielectron chemical transformations.

One such heteronuclear metalloenzyme system exists which incorporates a sulfur-containing copper(I) fragment. Molybdenum-dependent carbon monoxide dehydrogenase features a two-coordinate, all sulfur-ligated copper(I) ion tethered to a molybdoenzyme-type fragment (Figure 2.1). In this system, the pendent sulfur-containing copper fragment is integral in the binding and subsequent oxidation of carbon monoxide. Additionally, the ubiquity of the sulfur-containing copper(I) fragment in homonuclear metallobiomolecules speaks persuasively to its general utility.

Given the propensity for sulfur-containing copper(I) fragments to assemble into cluster-type species (refer to Chapter 1), a synthetic rationale is necessary in order to successfully access discrete heteronuclear structures of interest. With the specific aim of creating heteronuclear species resembling that of molybdenum-dependent carbon monoxide dehydrogenase, mononuclear copper(I) complexes were explored as precursors for the delivery of sulfur-containing copper(I) fragments. Of particular interest are complexes bearing silylthiolate and sulfhydryl ligands, as they should be amenable to desilylation or deprotonation to form reduced sulfur-containing copper fragments *in situ*. These reduced fragments could form the basis of constructing particular heteronuclear species of interest. Exploratory synthesis of these underdeveloped classes of compounds is described herein.

Additionally, it should be noted that copper silylthiolates and metallothiols are of interest as precursors to binary and ternary metal chalcogen clusters,[12-16] semiconducting materials,[17] and nanomaterials.[18-20] While this chemistry is inherently related, these topics exist beyond the general scope of this chapter and will not be discussed further.

Copper(I) Silylthiolates

In order to develop a general strategy for the controlled synthesis of heteronuclear species featuring sulfur-containing copper(I) fragments, efforts have been directed toward the synthesis of isolable metal complexes of the general formula $L_xCu(SSiR_3)_y$. Motivation for the formation of silyl-functionalized metal chalcogenolate complexes is founded on the basis that E-Si bonds can be substantially weaker and thus more readily

cleaved than E-C bonds (where E = chalcogen). Differing from their carbon-containing congeners, silanes, more specifically triorganosilanes, generally feature longer and weaker Si-C bonds, where Si is less electronegative than C, leading to a more polarized Si-C bond.[21] Tetravalent silicon also contains empty d orbitals, as well as rather low-lying $\sigma^*_{C\text{-}Si}$ orbitals, which give rise to a π-accepting ability that moderates a completely different reactivity at the silicon center versus its carbon analogues.[22-25] Thus, effective cleavage of E-Si bonds can be achieved in the presence of nucleophiles containing electronegative heteroatoms, where the elimination of the triorganosilyl group by reaction with MX_n salts (X = halide, acetate, oxide, etc.) proceeds via formation of thermodynamically stable byproducts of the type $XSiR_3$. Implications of this reactivity will be further elaborated upon in detail in Chapter 3 of this dissertation. In the same manner that reagents $E(SiR_3)_2$ and $RESiR_3$ can be used as sources of E^{2-} and RE^-, respectively, $M(ESiR_3)_n$ complexes can be viewed as "protected metal chalcogenides", $[M(E)_n]^{y-}$.

Within the existing body of literature, complexes of copper(I) bearing silylthiolate ligands are rather scarce and exist as both smaller cluster-type species and discrete mononuclear complexes. In the absence of bulky, neutral donor ligands, cluster species $[Cu_4(SSiMe_2{}^tBu)_4]$[26] and $[Cu_4(SSiPh{}^tBu)_4]$[27] are produced in reacting the lithium or sodium salts of the respective silylthiolates with simple copper(I) precursors. Ligand exchange from $[(MeCN)_2Fe(SSiPh_3)_2]$ to $[Cu(MeCN)_4][PF_6]$ produced related cluster $[Cu_4(SSiPh_3)_4]$, with a planar, square arrangement of Cu(I) ions with each vertex bridged by a μ-$SSiPh_3$ ligand.[28] In the presence of phosphine coligands, dinuclear [(Me_3SiS-

$Cu)_2(\mu\text{-}Ph_2PC{\equiv}CPPh_2\text{-}\kappa^2P)_3]$[29] and $[Cu_2\{SSiMe_2)_2S\}(PEt_3)_3]$[30] are obtained from copper acetate starting materials and disilathiane and cyclotrisilathianes, respectively.

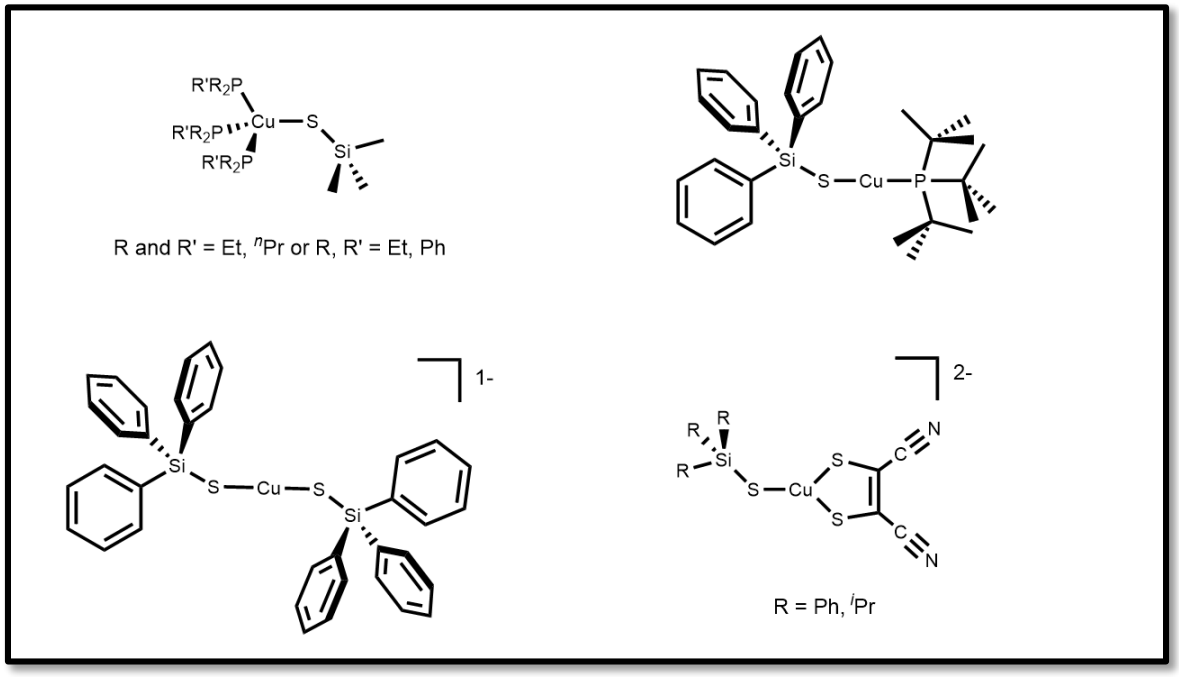

Figure 2.2 Existing mononuclear copper(I) silylthiolates from the literature (References 31-34).

Ingress to mononuclear cuprous silylthiolate complexes hinges on the use of bulky coligands or by coordinatively saturating the metal center to stabilize the mononuclear species of interest. The few known species are shown in Figure 2.2. Reaction of Cu(OAc) with excess monodentate phosphine ligands, followed by the addition of hexamethyldisilathiane ($Me_3Si\text{-}S\text{-}SiMe_3$) affords mononuclear complexes of the formulation $[(R_2R'P)_3Cu(SSiMe_3)]$ (R and R' = Et, ^{n}Pr,[31] or R = Et, Ph, R' = Et, Ph[32]). These air and moisture-sensitive, thermally labile complexes are synthesized and isolated well below room temperature. Under the conditions employed, excess phosphine

is necessary to avoid production of chalcogenolate bridged species of higher nuclearity. Three-coordinate dianionic complexes, $[Cu(mnt)(SSiR_3)]^{2-}$ (R = ^{i}Pr or Ph), are prepared in good yield by displacement of phosphine in $[Cu(mnt)(PPh_3)]^{1-}$ with R_3SiS^-.[33] These species are somewhat thermally sensitive and decompose in solution over time.

Remarkably, two-coordinate cuprous silylthiolates are known and can be prepared reproducibly (see Figure 2.2). In 2006, Fink and coworkers reported the first monomeric dicoordinate copper(I) silanethiolate, $[Cu(P^tBu_3)(SSiPh_3)]$.[34] Reaction of $[^tBu_3PCu(MeCN)][BF_4]$ with $[Ph_3SiSLi(THF)_2]_2$ in acetonitrile affords the product in excellent yield. Coordinative unsaturation at the copper center is stabilized by the combined steric demands exhibited by both the bulky triphenylsilanethiolate ligand and tri-*tert*-butyl phosphine (182° cone angle). This two-coordinate cuprous silylthiolate complex displays expected near-linear coordination about the copper center, and is fairly unstable thermally. Homoleptic, two-coordinate monoanion $[Cu(SSiPh_3)_2]^{1-}$, was reported by Holm et al. in 2010.[33] Protonolysis of $[Cu(SAd)_2]^{1-}$ (SAd = adamantylthiolate) with two equivalents of triphenylsilanethiol yields this bis(thiolato) complex in good yield. Thermally sensitive $[Cu(SSiPh_3)_2]^{1-}$ is the first reported mononuclear, two-coordinate bis(silylthiolato) complex. It should be noted, that prior to publication of this work (reference 33), successful synthesis and a crystal structure of this complex had been achieved in my hands via a different salt metathesis route. However, the yield obtained from this preparation was negligible and this result will not be discussed further.

Cuprous Metallothiols

Metallothiols, or transition metal complexes featuring distinct sulfhydryl (hydrogen sulfide, -SH) ligands represent the conceptual, and often the actual link between the coordination chemistry of sulfide (S^{2-}) and mercapto (RS^{-}) complexes. In recent years, particular interest in this chemistry arose from the understanding that these kinds of complexes should play a significant role in the catalytic hydrodesulfurization (HDS) of fossil fuels.[35, 36] Additionally, these complexes have relevance in mimicking the Claus reaction, that is, the industrially adopted process to dispose of the H_2S produced during the HDS treatment of crude oil and natural gas,[37] and are implicated (at least as transiently-formed species) in some metallobiomolecule systems in Nature.[38]

According to a review on metallothiols by Peruzzini et al. that appeared in 2001,[39] hydrochalcogenido complexes of the coinage metals were discussed as being "extremely rare" and that *no* copper species had been described thus far. Since 2001, several multinuclear species have been described, mostly with bridging sulfhydryl motifs, and only three mononuclear complexes have been fully characterized.

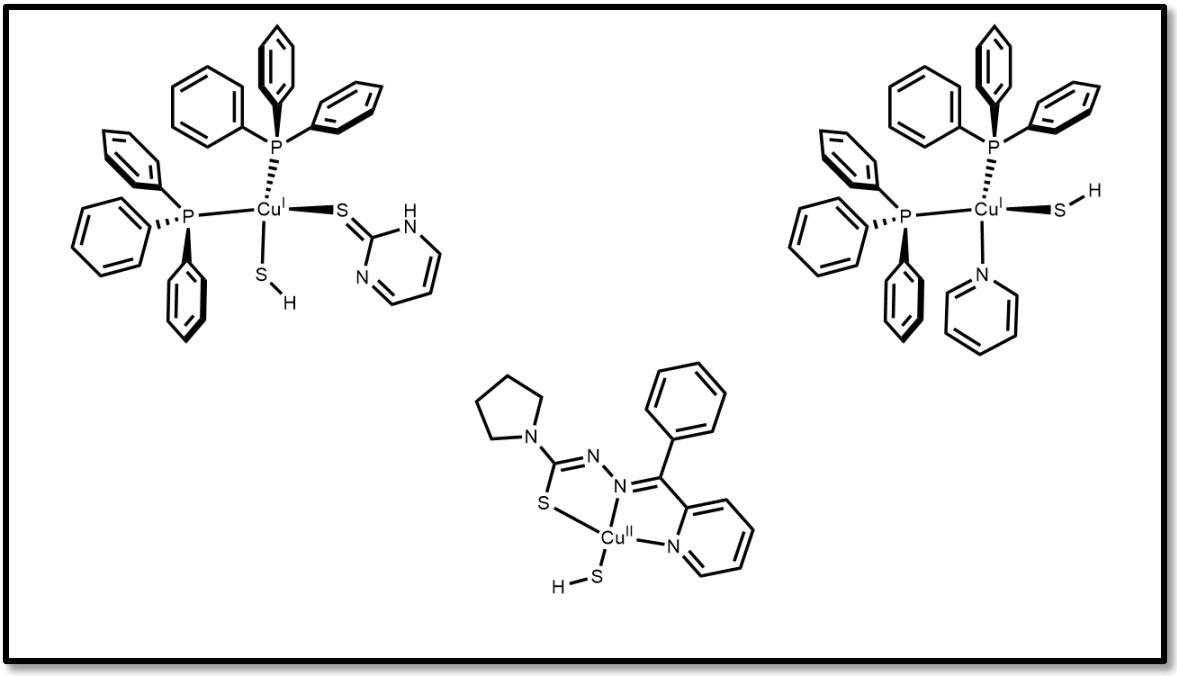

Figure 2.3 Structurally characterized copper metallothiols. References 40-42.

Of these three complexes, all are four-coordinate, and one is a copper(II) species. Square planar [Cu^{II}(BpypTsc)(SH)] was crystallographically characterized as a byproduct via decomposition of parent compound [Cu^{II}_2(BpypTsc)$_2$][SO_4] (HBpypTsc = 2-benzoylpyridine *N*(4),*N*(4)-(butane-1,4-diyl)thiosemicarbazone).[40] Tetrahedral, four-coordinate copper(I) complexes [Cu(PPh_3)$_2$(py)(SH)][41] and [Cu(PPh_3)$_2$(pmtH)(SH)][42] (pmtH = 2-mercaptopyrimidine, thione isomer) were formed as byproducts from the photolysis of [(PPh_3)$_2$Cu(trto)Cu(PPh_3)$_2$] (trto = trithiooxalate) in pyridine and the redox reaction between copper(II) sulfate or nitrate with 2-mercaptopyrimidine in the presence of triphenylphosphine, respectively.

At this point in time, the literature completely lacks preparative details for mononuclear copper(I) metallothiols. Any contributions pertaining to their synthesis,

reactivity, and physical properties would be of general interest to the coordination chemistry community at large. This chapter focuses on the synthesis and reactivity of new copper(I) silylthiolates and cuprous metallothiols.

Results and Discussion

Synthesis

In order to gain access to the desirable mononuclear copper(I) silylthiolates and metallothiols outlined above, appropriate choice of starting material and auxiliary ligand was of principal concern. Suitable auxiliary ligands should be soft and maintain a considerably large steric profile to impede the formation of multinuclear species with bridging sulfur-based ligands. Given the successful preparation and/or stabilization of both monomeric copper(I) silylthiolates and metallothiols with bulky phosphine coligands (*vide supra*), the large, facially coordinating C_3 symmetric 1,1,1-tris(diphenylphosphinomethyl)ethane (triphos) was employed. The bulky triphos ligand not only enforces a facial coordination about a tetrahedral copper(I) complex, which should allow for functionalization at the remaining vertex, but the size and rigidity of the triphos ligand should also impart additional thermal stability to the products with which it is coordinated. Fink et al. has demonstrated that use of bulky tri-*tert*-butyl phosphine can afford two-coordinate silylthiolate species.[34] By way of a modern analogy to classic phosphine-based coordination chemistry, *N*-heterocyclic carbenes (NHCs), which modulate the steric and electronic properties of their transition metal-based complexes in

a similar fashion, came to our attention as appropriate auxiliary ligand frameworks to explore in an attempt to generate new low-coordinate complexes. NHCs have an interesting push-pull electronic structure, where electron density is pulled from the bonding sp^2 hybridized singlet carbene carbon along the σ bonds to the nitrogen heteroatoms, and electron density is pushed back from the nitrogen lone pairs into the empty carbene carbon p orbital (n → 2pz). This scenario gives rise to a soft, strong σ-donating, but weakly π-accepting ligand type. Additionally, the choice of R group bound to the nitrogen heteroatoms can impart desirable solubility and steric hindrance properties to the NHC-bound complex. Nolan et al. have shown that NHC ligands can be used to effectively isolate two-coordinate copper(I) species of the type [Cu(NHC)X] (X = halide), which have been used as precatalysts in a variety of chemical transformations.[43] The ability of NHC ligands to preclude formation of more typical halide-bridged copper(I) species speaks persuasively to the applicability of NHCs with respect to isolating similar mononuclear species with sulfur-containing ligands.

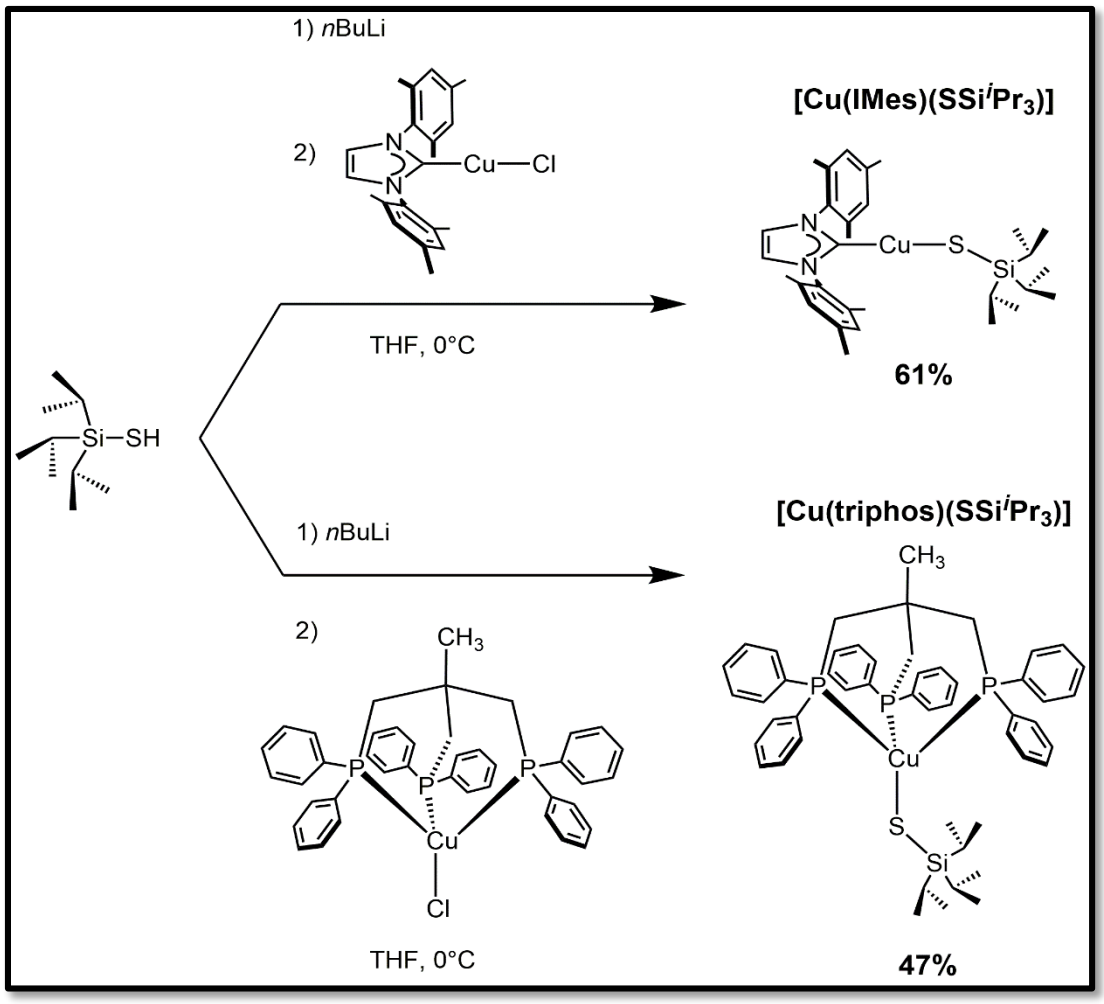

Scheme 2.1 Synthetic scheme for copper(I) silylthiolate complexes.

Silylthiolate complexes [Cu(IMes)(SSi^{i}Pr$_3$)] (IMes = 1,3-Bis(2,4,6-trimethylphenyl)imidazol-2-ylidene) and [Cu(triphos)(SSi^{i}Pr$_3$)] are formed in moderate to good yield via salt metathesis of *in situ* generated lithium triisopropylsilanethiolate with known, easily prepared metal chlorides [Cu(IMes)Cl][44] and [Cu(triphos)Cl],[45] respectively. The triisopropylsilane motif was deliberately chosen for these complexes owing to its size and solubility. Here, the size of the organic goups on the silicon center dictate how stable the resulting product complex will be. Triisopropylsilanethiolate as a

ligand appears to be an ideal choice with respect to stability, solubility, and crystallinity. The lithium salt of triisopropylsilanethiol is apparently soluble in non-polar hydrocarbon solvents, whereas starting material triisopropylsilanethiol is a liquid at room temperature. These properties allow for easy purification of the desired products of interest. Pure, colorless, crystalline material of [Cu(IMes)(SSi^{i}Pr$_3$)] is obtained by slow cooling of a filtered diethyl ether extract of the resulting residue from the crude reaction mixture. This complex is highly soluble in most common organic solvents including diethyl ether, but is very sparingly soluble in hydrocarbon solvents like pentane and hexane. In addition to being air and moisture sensitive, [Cu(IMes)(SSi^{i}Pr$_3$)] is thermally sensitive and decomposes over time at room temperature. However, it can last for several months if kept below 0°C under nitrogen or argon. Full characterization has been obtained for [Cu(IMes)(SSi^{i}Pr$_3$)], including its simple, yet distinct ^{1}H NMR spectrum. Four-coordinate [Cu(triphos)(SSi^{i}Pr$_3$)] can be obtained as a white solid via precipitation by addition of hexanes to the filtered, concentrated reaction mixture. While crystalline material is harder to access for this complex, single crystals were grown by slow cooling of a toluene/hexanes mixture. This complex is soluble in THF and acetonitrile, and fairly soluble in aromatic hydrocarbons like benzene and toluene. NMR (^{1}H, ^{13}C, ^{31}P) spectra of [Cu(triphos)(SSi^{i}Pr$_3$)] generally feature broadened signals, presumably due to dynamic binding of the triphos ligand in solution. It is well-documented that triphos has the ability to dissociate at least one ligand arm under various circumstances.[46, 47] This behavior serves to complicate absolute assignments within each spectrum, especially ^{13}C NMR. [Cu(triphos)(SSi^{i}Pr$_3$)] is completely stable at room temperature under an anaerobic

atmosphere. For this complex, the thermal stability is likely attributed to the combined steric hindrance associated with both triphos and triisopropylsilanethiolate.

Given the possible ambiguity associated with proper crystallographic assignment of terminal sulfhydryl versus terminal chloride ligand,[48] and the potential for replacement of sulfhydryl group by chloride in chlorinated solvents,[49-51] a tailored reaction scheme was devised to avoid any possible complications with respect to these issues (see Figure 2.5).

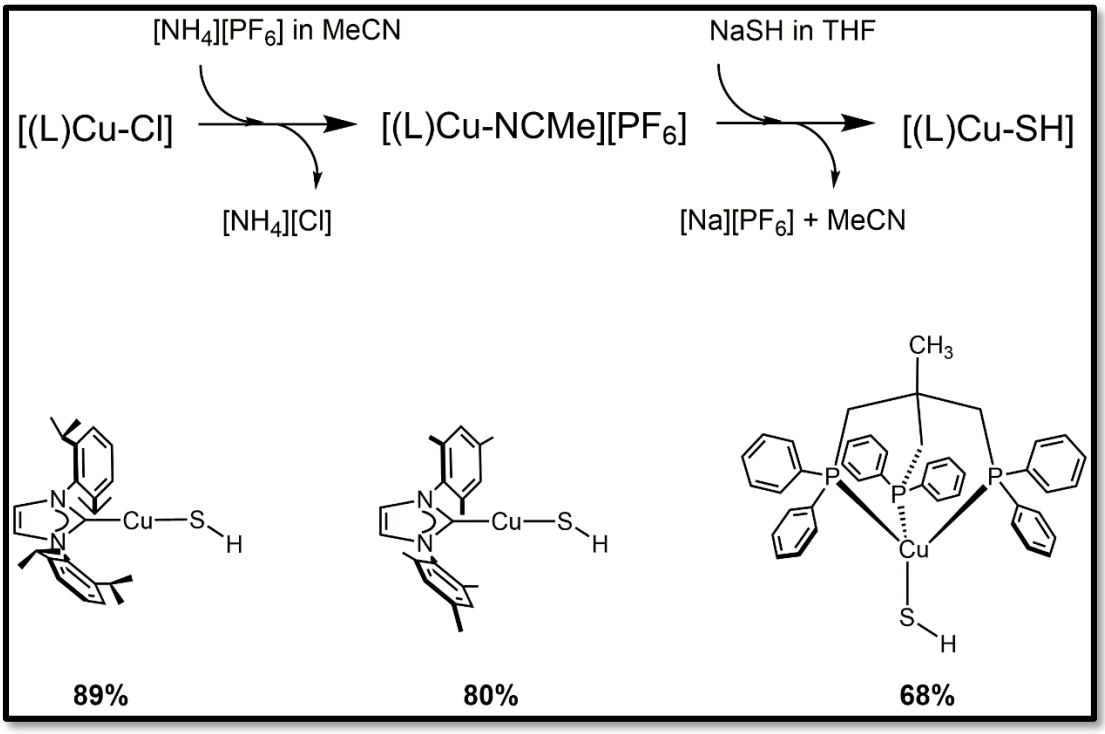

Scheme 2.2 Synthetic scheme for copper(I) metallothiols. L = neutral donor ligands, IMes = 1,3-bis(2,4,6-trimethylphenyl)imidazol-2-ylidene, IPr = 1,3-bis(2,6-diisopropylphenyl)imidazol-2-ylidene, and triphos = 1,1,1-tris(diphenylphosphinomethyl)ethane.

Following Scheme 2.2, parent metal chlorides can be conveniently converted to their acetonitrile adducts as hexafluorophosphate salts via reaction with ammonium

hexafluorophosphate in acetonitrile. This reaction is driven to product formation by the increased solubility of the product salts (as opposed to the neutral parent chloride complexes) and the complete insolubility of ammonium chloride in acetonitrile. These [(L)Cu−NCMe][PF_6] salts are then reacted with commercially available sodium hydrogen sulfide (Na^+SH^-) in THF to afford the copper(I) metallothiol complexes in good to high yield. Complexes [Cu(IPr)(SH)], [Cu(IMes)(SH)], and [Cu(triphos)(SH)] can all be conveniently crystallized by diffusing diethyl ether vapor into filtered, concentrated THF solutions of each product. Trace amounts of [Na][PF_6] tend to co-crystallize with and contaminate each colorless, crystalline sample. This byproduct can be removed simply by repeated recrystallization from the solvent combination mention above. Occasionally, crude products contain some color, presumably due to small amounts of oxidized and/or multinuclear byproduct species, but these impurities can be easily removed via crystallization. Thus, in just a few short steps, the first series of deliberately synthesized copper(I) metallothiols can be obtained. Additionally, it should be noted that [Cu(IPr)(SH)] and [Cu(IMes)(SH)] are the *first* examples of two-coordinate copper(I) sulfhydryl complexes.

Several nuances of transition metal sulfhydryl chemistry complicate proper characterization and assignment of these complexes. Within a crystallographic context, if the hydrosulfide ligand's associated hydrogen atom density cannot be detected inside an electron density map, sulfur and chlorine are not easily distinguished by X-ray diffraction. Crystallographic assignment of sulfhydryl versus chloride is usually based on trends in metal-ligand bond lengths. However, so few cuprous metallothiols have been structurally characterized that an assessment of this type is rendered difficult. To

eliminate any crystallographic ambiguity, chlorinated solvents were completely avoided in the preparation and isolation of these complexes to evade any adventitious reaction between copper(I) and chlorinated solvent. In spectroscopic terms, most metal sulhydryl complexes display no IR absorption that can be safely assigned to the stretching vibration of the S−H bond, despite the usual appearance of this band in an often empty region of the IR spectrum (~2500 cm^{-1}).[39] The lack of assigments for this band is likely a consequence of the weak intensity and broadness of this vibration. ^{1}H NMR comes to the fore as a spectroscopic technique most well-suited to confirm the identity of the sulfhydryl ligand in these complexes, given the typical appearance of the sulfhydryl proton's distinct high field chemical shift (numerous species appear at negative values vs. TMS). While not explained explicitly, a review of metallothiols from 2001[39] displays a notable amount of absent entries for sulfhydryl proton ^{1}H NMR chemical shift data for a variety of different transition metal sulfhydryl complexes. It is unclear from a perusal of the literature why certain metallothiol sulfhydryl protons show no observable signal. Perhaps some signals are obscured by other proton signals due to the variable range in which they have been observed, or it's conceivable that these signals may be significantly broadened. Unfortunately, for the series of complexes described here, no sulfhydryl proton signals are observed for any complex, even when the spectral width for the particular experiment is appropriately enlarged. Parent ions in mass spectrometry for the series also remains elusive. The two dicoordinate NHC metallothiols only display cationic peaks corresponding to $[Cu(NHC)_2]^+$, which is commonly observed as an artifact of ionization for copper(I)-NHC complexes, and only $[Cu(triphos)]^+$ is observed for the four-coordinate complex. Despite the lack of routine characterization with regard to

assignment of sulfhydryl group bound to each metallothiol, the synthetic route outlined in Scheme 2.2 provides for a qualitative confirmation of product being generated via ^{31}P NMR. Using ^{31}P NMR, the disappearance of hexafluorophosphate signal thus corresponds to metallothiol formation. The ^{1}H NMR spectrum of each product shows proton resonances corresponding only to the neutral donor ligand, which are slightly different than the analogous chloride containing species, and no signal due to coordinated acetonitrile. Complexes [Cu(IPr)(SH)], [Cu(IMes)(SH)], and [Cu(triphos)(SH)] were also analyzed crystallographically, which verified that each complex is charge neutral, monomeric, and maintains the appropriate formulation. Additionally, a satisfactory elemental analysis was obtained for [Cu(IPr)(SH)].

Reactivity: Organic Parallels?

Having in hand new copper(I) silylthiolate complexes and cuprous metallothiols, efforts were made to test their reactivity within the context of generating $[(L)Cu{-}S]^-$ fragments for potential use in forming heteronuclear species. Labilization of capping silyl group and sulfhydryl proton was attempted using common reagents utilized in analogous, well-known organic reactions. Proof of formation of $[(L)Cu{-}S]^-$, followed by trapping with a common organic electrophile, or functionalization at coordinated sulfur by other means would be suggestive of the ability of these complexes to be used for constructing more complicated heteronuclear architectures.

Given the relative ease of Si−S bond cleavage in the presence of chloride, oxide (acetate, alkoxide, aryloxide, etc), and fluoride (*vide supra*), organic reagents containing these groups were employed to unmask the $[(L)Cu{-}S]^-$ fragment. Reaction of

[Cu(IMes)(SSi^{i}Pr$_3$)] with fluoride sources [Bu$_4$N][F], 48% HF(aq), and [NH$_4$][F] in THF or diethyl ether led to complete decomposition of the starting material. This decomposition is observed as forming insoluble colored precipitates and occurs readily even at reduced temperatures and in the presence of trapping electrophiles like acetyl chloride. Addition of dry, gaseous HCl or 12N HCl to ethereal solutions of [Cu(IMes)(SSi^{i}Pr$_3$)] resulted in formation of small amounts of isolable protonated imidazolium salt IMes·HCl with attending decomposition. Imidazolium salts of this type are easily identified by ^{1}H NMR, where a small (integrates appropriately to 1H), distinct singlet appears downfield in the spectrum (δ 11.05 in CDCl$_3$ for IMes·HCl). Reaction of [Cu(IMes)(SSi^{i}Pr$_3$)] with acetyl chloride in diethyl ether yielded minor decomposition and apparent formation of [Cu(IMes)(Cl)] and ^{i}Pr$_3$SiSAc. Acetyl protected triisopropylsilylthiolate, ^{i}Pr$_3$SiSAc, was detected via ^{1}H NMR from a hexane wash of the crude product. The identity of the resulting copper(I) complex was not confirmed, but can be speculated to be [Cu(IMes)(Cl)] in terms of appropriate mass balance for the reaction. Surprisingly, addition of [Et$_4$N][OH] to [Cu(IMes)(SSi^{i}Pr$_3$)] in THF gave no reaction, whereas reaction of [Cu(IMes)(SSi^{i}Pr$_3$)] with glacial acetic acid in THF led to complete decomposition. Additionally, [Cu(IMes)(SSi^{i}Pr$_3$)] did not react with heterocumulenes like carbon dioxide and *N*,*N*'-dicyclohexylcarbodiimide.

No reaction was observed upon addition of [Bu$_4$N][F] followed by acetyl chloride to a THF solution of [Cu(triphos)(SSi^{i}Pr$_3$)]. Similarly, no reaction took place between [Cu(triphos)(SSi^{i}Pr$_3$)] and trityl tetrafluoroborate. Addition of 48%(aq) HF to a THF solution of [Cu(triphos)(SSi^{i}Pr$_3$)] resulted in extensive decomposition, where the only

isolable material obtained was found to be free triphos ligand as judged via ^{1}H and ^{31}P NMR.

With the rather extensive history of chemical reactivity associated with organic thiol species, reactions were performed to assess what parallels can be drawn with the series of copper(I) metallothiols. Scheme 2.3 outlines the classic reactions with mercaptans that were explored in this context.

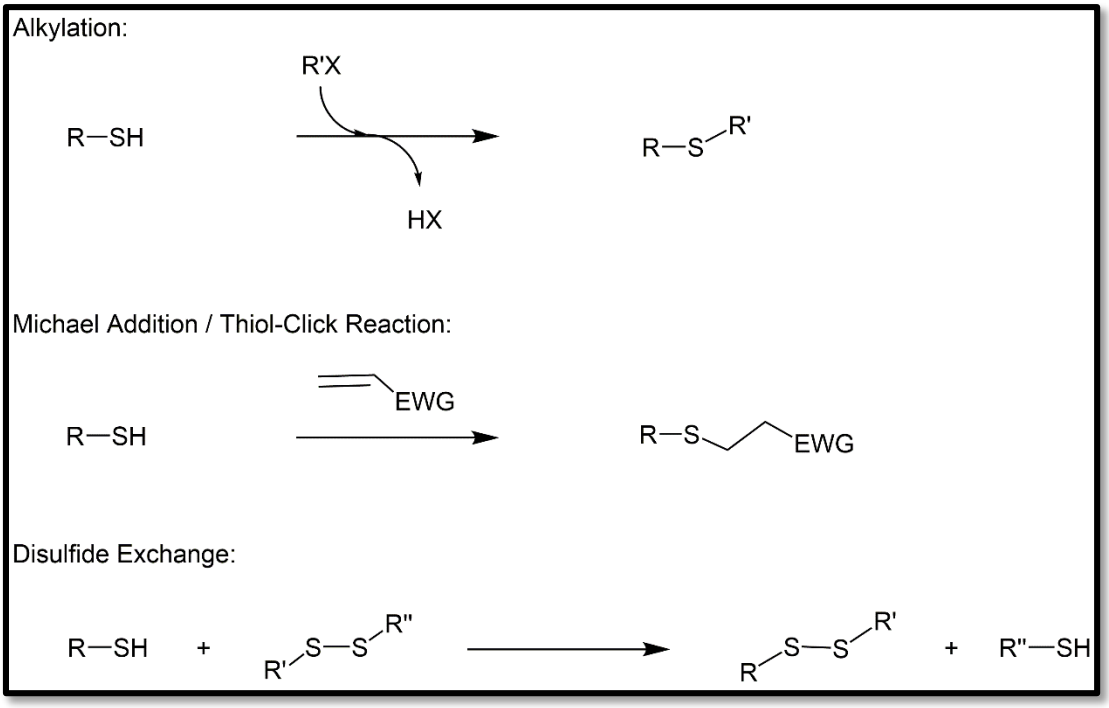

Scheme 2.3 Reactivity of organic thiols.

The reaction of [Cu(IPr)(SH)], [Cu(IMes)(SH)], and [Cu(triphos)(SH)] with methyl iodide in THF yielded no reaction, even under refluxing conditions. Addition of methyl iodide to a solution of [Cu(IPr)(SH)] in the presence of triethylamine base gave a white precipitate of (methyl)triethylammonium iodide as confirmed by ^{1}H NMR and unreacted copper starting material. A few other reactive alkyl halides were tested, but no

alkylation was observed in any experiment. Methyl acrylate and methyl methacrylate were used as Michael acceptors in attempts to add metallothiol S−H bonds across electron deficient olefins. Likewise, this series of reactions failed to yield any functionalization of the metallothiol starting materials. Attempts to effect disulfide exchange between di-*tert*-butyl disulfide or diphenyl disulfide and [Cu(IPr)(SH)], [Cu(IMes)(SH)], and [Cu(triphos)(SH)] similarly afforded no reaction. However, reaction of [Cu(IMes)(SH)] and one equivalent of tetraethylthiuram disulfide in THF produced a dark brown colored reaction mixture. Here, facile oxidative addition of tetraethylthiuram disulfide by [Cu(IMes)(SH)] with complete displacement of monodentate carbene and sulfhydryl ligands afforded known dimeric $[Cu^{II}_2(Et_2dtc)_4]$ as confirmed crystallographically (Et_2dtc = diethyl dithiocarbamate, see Scheme 2.4).[52]

Scheme 2.4 Oxidative addition of tetraethylthiuram disulfide to [Cu(IMes)(SH)].

Furthermore, attempts to deprotonate the sulfhydryl moieties in this series of metallothiols with triethylamine gave no reaction, and rather slow, partial decomposition where the only isolable species observed via ^{1}H NMR were starting material and imidazolium salts when lithium methoxide and *n*-butyllithium were employed. It should also be noted that complexes [Cu(IPr)(SH)] and [Cu(IMes)(SH)] are quite sensitive in polar protic solvents, especially alcohols, from which imidazolium salts form.

From the reactions described above, neither copper(I) silylthiolates nor cuprous metallothiols appear particularly suitable as potential precursors for constructing heteronuclear species. The instability of copper(I) silylthiolates upon attempted desilylation and the peculiar inertness of cuprous metallothiols suggest that efforts to generate $[(L)Cu{-}S]^-$ *in situ* are complicated and further reactivity in a controlled fashion may not be likely. Of the two types of complexes, copper(I) silylthiolates may potentially be useful in forming multinuclear species, given the appropriate conditions and additional metal-containing reagent(s). Efforts along these lines are presented in Chapter 3 of this dissertation. The stability of the series of copper(I) metallothiols is rather surprising. Rauchfuss et al. previously reported the reactivity of $[Cp_2Ti(SH)_2]$ and $[Cp_2Ti(\mu\text{-}SH)_2Mo(CO)_4]$.[53] In comparing the two complexes, mononuclear $16e^-$ species $[Cp_2Ti(SH)_2]$ was found to be relatively inert or react in a sluggish manner, where the sulfhydryl groups were found to be rather nonnucleophilic. In contrast, the $34e^-$ dimer $[Cp_2Ti(\mu\text{-}SH)_2Mo(CO)_4]$ featured very reactive, nucleophilic sulfhydryl moieties. Within this work, the tuned down nucleophilicity of the sulfhydryl groups in $[Cp_2Ti(SH)_2]$ was tentatively ascribed to potential S to Ti π-bonding, a scenario which is different upon rehybridization in $[Cp_2Ti(\mu\text{-}SH)_2Mo(CO)_4]$. While these systems are markedly different from the cuprous metallothiols described here, a similar, general justification (stabilization via S-to-Cu π interaction) may explain the inert behavior of these low-coordinate, $14e^-$ copper(I) metallothiol species. Without further experimentation, it remains unclear why these complexes are so inert.

Structures

Crystal information for [Cu(IMes)(SSi^{i}Pr$_3$)], [Cu(triphos)(SSi^{i}Pr$_3$)], and [Cu(IPr)(SH)] is provided in Table 2.1.

Table 2.1. Crystal and refinement data for compounds in Chapter 2.

compound	**[Cu(IMes)(SSi^{i}Pr$_3$)]**	**[Cu(triphos)(SSi^{i}Pr$_3$)]**	**[Cu(IPr)(SH)]**
solvent	none	none	none
formula	$C_{30}H_{45}CuN_2SSi$	$C_{57}H_{68}CuP_3SSi$	$C_{27}H_{37}CuN_2S$
fw	557.37	969.71	486.19
xtl system	monoclinic	monoclinic	orthorhombic
space grp	$P2_1/c$	$P2_1/n$	$Pccn$
color, habit	colorless plate	colorless block	colorless block
a, Å	19.4065(18)	14.5029(10)	10.6051(18)
b, Å	10.8938(10)	16.1500(11)	12.746(2)
c, Å	15.2754(14)	22.0822(15)	19.205(3)
α, deg.	90	90	90
β, deg.	104.834(1)	93.455(1)	90
γ, deg.	90	90	90
V, Å^3	3121.7(5)	5162.7(6)	2596.0(8)
T, K	150	150	100
Z	4	4	4
R1, wR2	0.0314, 0.0823	0.0321, 0.0870	0.0387, 0.1299
GoF	1.048	1.010	1.125

R1 = $\Sigma||F_o| - |F_c||/\Sigma|F_o|$. wR2 = $\{[\Sigma w(F_o^2 - F_c^2)/\Sigma w(F_o^2)^2\}^{1/2}$; $w = 1/[\sigma^2(F_o^2) + (xP)^2]$, where $P = (F_o^2 + 2F_c^2)/3$.

Copper(I) silylthiolates [Cu(IMes)(SSi^{i}Pr$_3$)] and [Cu(triphos)(SSi^{i}Pr$_3$)] both crystallize in the monoclinic crystal system. Large, colorless, single-crystalline plates of [Cu(IMes)(SSi^{i}Pr$_3$)] form on standing from a concentrated diethyl ether solution cooled to ~ -30°C. Selected structural parameters are found within Figure 2.4 and Table 2.2.

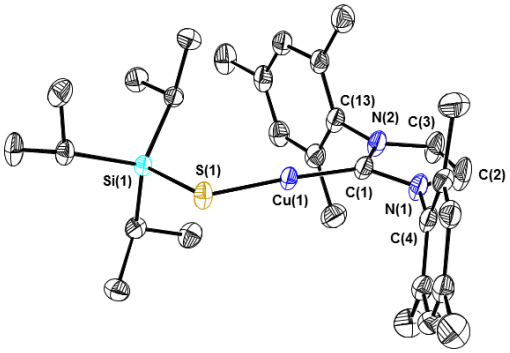

[Cu(IMes)(SSi^{i}Pr$_3$)]	monoclinic P2$_1$/c
C-Cu-S Angle (deg)	174.77(5)
Cu-S-Si Angle (deg)	102.55(2)
C-Cu Length (Å)	1.883(2)
Cu-S Length (Å)	2.1337(4)

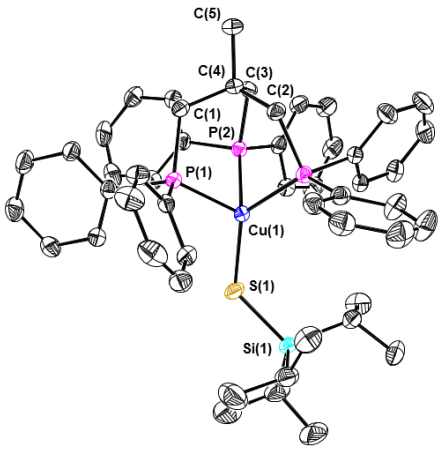

[Cu(triphos)(SSi^{i}Pr$_3$)]	monoclinic P2$_1$/n
Cu-S-Si Angle (deg)	118.93(2)
Cu-S Length (Å)	2.2670(5)

Figure 2.4 Crystal structures and selected structural parameters for copper(I) silylthiolate complexes. All thermal ellipsoid plots at the 50% probability level.

The two-coordinate species [Cu(IMes)(SSi^{i}Pr$_3$)] features a Cu−C bond distance in line with, but on the shorter end of the spectrum for, existing two-coordinate *N*-heterocyclic carbene copper(I) thiolates.[54] Likewise, its Cu−S bond distance of 2.1337(4) Å is within the normal range for *N*-heterocyclic carbene copper(I) thiolates, but shorter than existing two-coordinate silylthiolates [Cu(P^{t}Bu$_3$)(SSiPh$_3$)][34] (2.1578(11) Å) and [Cu(SSiPh$_3$)2]$^{1-}$ (2.1508(6) Å).[54] Presumably, the steric hindrance provided by *N*-heterocyclic carbene ligands differs from bulkier phosphines, which can give rise to subtle differences with respect to this parameter. [Cu(IMes)(SSi^{i}Pr$_3$)] displays a near-linear core, and a Cu−S−Si angle of 102.55(2)°, which is slightly more open than that seen in [Cu(P^{t}Bu$_3$)(SSiPh$_3$)] (97.63(5)°) and closer to that of [Cu(SSiPh$_3$)$_2$]$^{1-}$ (104.85(3)°).

Table 2.2 Structural parameters for copper(I) silylthiolate and metallothiol compounds.

Compound	Cu–S, Å
[Cu(IMes)(SSi^{i}Pr$_3$)]	2.1336(4)
[Cu(P^{t}Bu$_3$)(SSiPh$_3$)][34]	2.1578(11)
[Cu(triphos)(SSi^{i}Pr$_3$)]	2.2670(4)
[Cu(Et$_3$P)$_3$(SSiMe$_3$)][31]	2.4022(5)
[Cu(^{n}Pr$_3$P)$_3$(SSiMe$_3$)][31]	2.3970(10)
[Cu(IPr)(SH)]	2.0991(12)
[Cu(PPh$_3$)$_2$(py)(SH)][41]	2.322(1)
[Cu(PPh$_3$)$_2$(pmtH)(SH)][42]	2.3652(6)

[Cu(triphos)(SSi^{i}Pr$_3$)] features a Cu−S bond distance of 2.2670(4) Å, which is notably shorter than those observed for similar tris(trialkyl)phosphine silylthiolates characterized by Corrigan et al. (see Table 2.2), but longer than the Cu−S bond in other two-coordinate species. The longer Cu−S bond lengths for the tetrahedral, four-coordinate tris(phosphine) silylthiolates may be attributed to the enhanced sterics and an increase in the "p" character at the copper(I) center (four-coordinate vs two-coordinate).[34] Heteroleptic, mononuclear phosphine complexes typically contain LUMO orbitals with varying σ^*_{M-S} character, which can accept lone pairs (HOMO) from bound phosphines. Partial population of this σ^*_{M-S} orbital leads to weakening of the Cu−S bond and its subsequent elongation with attending ionic character. Thus, longer Cu−S bonds and wider Cu−S−Si angles are seen for these more ionic tris(phosphine) copper(I) silylthiolates than for the two-coordinate species.[55] The Cu−S−Si bond angle about

[Cu(triphos)(SSi^{i}Pr$_3$)] of 118.93(2)° is marginally narrower than angles observed for [Cu(Et$_3$P)$_3$(SSiMe$_3$)] and [Cu(nPr$_3$P)$_3$(SSiMe$_3$)].[31] This smaller angle is likely due to the geometric constraints exhibited by tridentate, facially coordinating triphos, as opposed to the "free" monodentate phosphines bound to the latter two complexes.

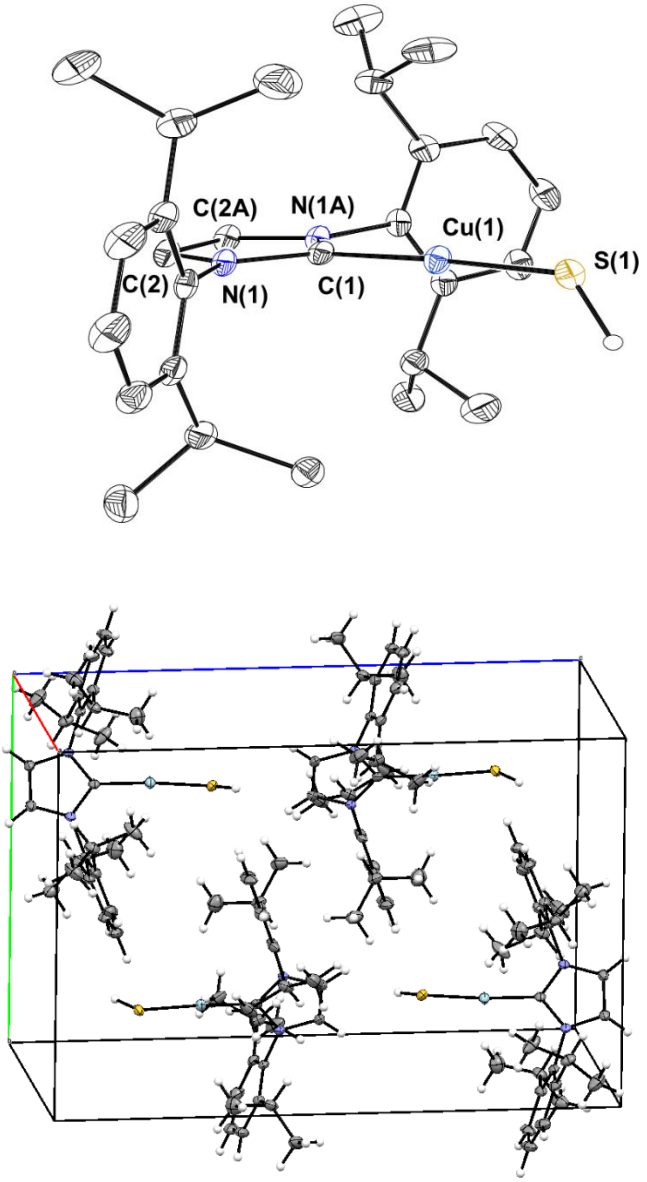

Figure 2.5 Crystal structure and packing diagram for [Cu(IPr)(SH)]. Thermal ellipsoid plot is drawn at the 50% probability level. Hydrogen atoms are omitted for clarity, except for the sulfhydryl hydrogen, which was identified in the electron difference maps near the end of the refinement and ultimately refined with appropriate distance restraints.

Cuprous metallothiol [Cu(IPr)(SH)] packs in a head-to-tail fashion in the orthorhombic crystal system and displays no close contacts or exogenous binding at copper. This complex is the *first* structurally characterized two-coordinate copper(I) metallothiol. [Cu(IPr)(SH)] features a significantly shorter Cu−S bond distance (2.0991(12) Å) compared to the other two existing four-coordinate complexes $[Cu(PPh_3)_2(py)(SH)]$[41] (2.322(1) Å) and $[Cu(PPh_3)_2(pmtH)(SH)]$[42] (2.3652(6) Å). Of particular note, this Cu−S bond length appears to be shorter than *any* transition metal-based metallothiol reported within a 2001 review on metallothiols.[39] Moreover, this bond length appears to differ (longer Cu−X, where X is either –SH or −Cl) from that reported for the analogous chloride complex [Cu(IPr)Cl][56] (2.089 Å). However, without better data, these differences are difficult to evaluate. While curiously short, it's hard to gauge any importance for this particular value within any meaningful context given the scarcity of reported structures for cuprous metallothiols. Finally, complexes [Cu(IMes)(SH)] and [Cu(triphos)(SH)] were initially mischaracterized as their chloride-containing analogues, and thus were not satisfactorily refined and will not be presented here.

Summary and Conclusions

Access to new, potentially useful two- and four-coordinate copper(I) silylthiolates and cuprous metallothiols can be effected by simple salt metathesis reactions to give the products in good to high yield. Use of triisopropylsilanethiol appears to be successful in imparting enhanced solubility, crystallinity, and stability to the set of silylthiolate complexes. Additionally, stabilization of two-coordinate sulfur-containing copper(I) complexes can be achieved readily by employing *N*-heterocyclic carbenes as auxiliary

ligands. The series of copper(I) sulfhydryl complexes reported here is the first to be synthesized deliberately, and the charge neutral complex [Cu(IPr)(SH)] is the *first* example of a two-coordinate copper metallothiol.

From a survey of their reactivity, it appears that neither cuprous silylthiolate nor metallothiol can be used to generate $[(L)Cu{-}S]^{1-}$ in a controlled fashion. Attempts to unmask silyl moieties or deprotonate sulfhydryl ligands led to significant decomposition in most cases. A rationalization for the peculiar inert behavior of the cuprous metallothiol species described here remains unclear without further experimentation and a more thorough analysis of the electronic structure of these complexes. Of the two types of complexes, copper(I) silylthiolates may potentially be of use in constructing heteronuclear architectures given the appropriate conditions. Reactions within this context are described in detail in Chapter 3 of this dissertation.

Experimental

All reactions and manipulations were performed under a pure dinitrogen or argon atmosphere using modified Schlenk techniques or an inert-atmosphere box. Literature procedures were employed for the syntheses of [(IMes)Cu(Cl)] (IMes = 1,3-bis(2,4,6-trimethylphenyl)imidazol-2-ylidene),[44] [(triphos)Cu(Cl)] (triphos = 1,1,1-tris(diphenylphosphinomethyl)ethane),[45] $[(triphos)Cu{-}NCMe][PF_6]$,[57] $[(IMes)Cu{-}NCMe][PF_6]$,[58] and $[(IPr)Cu{-}NCMe][PF_6]$[58] (IPr = 1,3-bis(2,6-diisopropylphenyl)imidazol-2-ylidene).

Solvents either were dried with a system of drying columns from the Glass Contour Company (Et_2O, hexane, toluene, benzene, tetrahydrofuran (THF)) or freshly distilled according to standard procedures (CH_3CN).[59] Other reagents were used as received from commercial sources.

All ^{1}H, ^{13}C, and ^{31}P NMR spectra were recorded at 25 °C with a Varian Unity Inova spectrometer operating at 400, 100.5, or 168.1 MHz for ^{1}H, ^{13}C, and ^{31}P respectively, and were referenced to the solvent residual (^{1}H and ^{13}C) or 85% phosphoric acid (^{31}P). The ^{29}Si NMR spectrum was taken on a Bruker Avance 300 spectrometer and was referenced to TMS internally. Mass spectra were obtained by either MALDI-TOF (Bruker Autoflex III instrument) or by electrospray ionization methods (Bruker microTOF with Agilent Technologies 1200 Series LC). Elemental analyses were performed by Midwest Microlab, LLC of Indianapolis, IN.

All crystals were coated with paratone oil and mounted on the end of a nylon loop attached to the end of the goniometer. Data were collected with a Bruker APEX CCD diffractometer equipped with a Kryoflex attachment supplying a nitrogen stream at 100 or 150 K. Full spheres of data were obtained by employing one of the two following collection routines: (1) Three sets of 606 frames in ω (0.3º/scan) with φ held constant at 0, 120, and then 240º; (2) Three sets of 400 frames in ω (0.5º/scan), collected at φ = 0.00, 90.00 and 180.00° followed by two sets of 800 frames in φ (0.45°/scan) collected with ω constant at -30.00 and 210.00°. All data were collected under control of the *APEX2* software package. Raw data were reduced to F^2 values using the *SAINT* or *SAINT+* software, and a global refinement of unit cell parameters was performed using selected reflections representing ~ 25% of the full data set. Data for the all compounds were

corrected for absorption on the basis of multiple measurements of symmetry equivalent reflections with the use of *SADABS*. All structure solutions were obtained by direct methods using *SHELXS*, while refinements were accomplished by full-matrix least-squares procedures using *SHELXL*. Both the *SHELXS* and *SHELXL* programs are incorporated into the *SHELXTL* software suite. The sulfhydryl (S−H) hydrogen atom in [Cu(IPr)(SH)] was identified in the difference maps and refined with appropriate constraints. All other hydrogen atoms were added in calculated positions and included as riding contributions with isotropic displacement parameters tied to those of the carbon atoms to which they were attached. All images were created with the use of *XP*, which also is part of the *SHELXTL* package. References for the crystallography software mentioned above can be found in Chapter 1 (references 79-87) of this dissertation. Final unit cell data and refinement statistics are collected in Table 2.1.

[1,3-bis(2,4,6-trimethylphenyl)imidazol-2-ylidene] (triisopropylsilanethiolato) cuprate, [Cu(IMes)(SSi^{i}Pr$_3$)]

To a solution of triisopropylsilanethiol (0.29 mL, 1.35 mmol) in 10 mL dry THF was added *n*-butyllithium (0.54 mL, 2.5M in hexane, 1.35 mmol) at 0°C, which was stirred for 45 min at 0°C, then allowed to warm to room temperature with stirring for an additional 1 hr. This colorless solution was then slowly cannulated into a solution of [1,3-bis(2,4,6-trimethylphenyl)imidazol-2-ylidene] copper(I) chloride [(IMes)CuCl] (0.544 g, 1.35 mmol) in 20 mL dry THF at 0°C. The reaction mixture was allowed to warm to room temperature as it was stirred for 16 hr. Removal of the solvent *in vacuo*

gave a pale yellow residue, to which 40 mL of dry diethyl ether was added with stirring. The mixture was filtered and the filtrate concentrated to ca. 20 mL. Colorless plate crystals form upon cooling to -20°C after 1 day (Yield: 0.458g, 61%). This compound is thermally sensitive, and is best stored under an inert atmosphere at -20°C. ^{1}H NMR (δ, ppm in benzene): 6.68 (s, 4H), 5.92 (s, 2H), 2.08 (s, 6H), 1.94 (s, 12H), 1.23 (d, 18H), 0.99 (sept., 3H). ^{13}C NMR (δ, ppm in benzene): 180.7, 139.3, 135.7, 134.8, 129.6, 121.5, 21.1, 19.8, 17.8, 16.0. ^{29}Si NMR (δ, ppm in benzene): 25.71. Anal. Calcd for $C_{30}H_{45}CuN_2SSi$: C, 64.65; H, 8.14; N, 5.03. Found: C, 64.40; H, 8.08; N, 5.08.

[1,1,1-tris(diphenylphosphinomethyl)ethane] (triisopropylsilanethiolato) cuprate, [Cu(triphos)(SSi^{i}Pr$_3$)]

To a solution of triisopropylsilanethiol (0.14 mL, 0.672 mmol) in 10 mL dry THF was added *n*-butyllithium (0.28 mL, 2.5M in hexane, 0.70 mmol) at 0°C, which was stirred for 45 min at 0°C, then allowed to warm to room temperature with stirring for an additional 1 hr. This colorless solution was then slowly cannulated into a suspension of [1,1,1-tris(diphenylphosphinomethyl)ethane] copper(I) chloride [(triphos)CuCl] (0.486 g, 0.672 mmol) in 20 mL of dry THF at 0°C, which brought all components into solution. The reaction mixture was allowed to warm to room temperature as it was stirred for 16 hr. This off-white solution was filtered through celite, concentrated to ca. 10 mL *in vacuo*, and precipitated with 30 mL of hexane. The white solid was collected to give 278mg (47% yield) of crude product. ^{1}H NMR (δ, ppm in benzene): 7.62 (m,br, 12H),

7.01-6.75 (m, 18H), 2.24 (s, 6H), 1.56 (d,br, 18H), 1.20 (s, 3H), 0.87 (sept., 3H). ^{31}P NMR (δ, ppm in benzene referenced to 85% H_3PO_4 internal standard): -32.3.

1,1,1-tris(diphenylphosphinomethyl)ethane Copper(I) hydrogen sulfide, [Cu(triphos)(SH)]

To a mixture of [(triphos)Cu(NCMe)]PF_6 (215 mg, 0.246 mmol) and sodium hydrosulfide (14 mg, 0.250 mmol), was added 30 mL of dry acetonitrile. The reaction mixture was stirred under nitrogen for 6 hr and evaporated to dryness *in vacuo*. 20 mL of dry THF was added to the residue. The resulting suspension was anaerobically filtered through celite and the filtrate was reduced to dryness, washed with 5mL ether, and dried *in vacuo* to afford the product as an off-white, sometimes pale orange powder (121 mg, 68% yield). Diffusion of diethyl ether vapor into a saturated acetonitrile solution of the product produces colorless plate crystals. ^{1}H NMR (δ, ppm in CD_3CN): 7.42 (m, 12H), 7.17 (m, 6H), 7.09 (m, 12H), 2.49 (s, broad, 6H), 1.57 (s, 3H). ^{31}P NMR (δ, ppm in CD_3CN referenced to 85% H_3PO_4 internal standard): -26 (broad).

1,3-bis(2,6-diisopropylphenyl)-1,3-dihydro-2H-imidazol-2-ylidene Copper(I) hydrogen sulfide, [Cu(IPr)(SH)]

To a mixture of [(IPr)Cu(NCMe)]PF_6 (200 mg, 0.313 mmol) and sodium hydrosulfide (18 mg, 0.321 mmol) was added 25 mL of dry THF. The reaction mixture was stirred for 6 hr and filtered anaerobically through celite. The filtrate was evaporated

to dryness, washed with 5 mL ether and dried under vacuum, affording 135mg (89% yield) of an off-white powder. Large, colorless block crystals can be obtained by diffusing diethyl ether vapor into a concentrated THF solution of the product. ^{1}H NMR (δ, ppm in CD_3CN): 7.57 (t, 2H), 7.44 (s, 2H), 7.41 (d, 4H), 2.57 (septet, 4H), 1.26 (d, 12H), 1.24 (d, 12H). Anal. Calcd for $C_{27}H_{37}CuN_2S$: C, 66.84; H, 7.69; N, 5.77. Found: C, 66.46; H, 7.44; N, 5.82.

1,3-bis(2,4,6-trimethylphenyl)-1,3-dihydro-2H-imidazol-2-ylidene Copper(I) hydrogen sulfide, [Cu(IMes)(SH)]

To a mixture of $[(IMes)Cu(NCMe)]PF_6$ (307 mg, 0.554 mmol) and sodium hydrosulfide (32 mg, 0.571 mmol) was added 30 mL of dry THF. The reaction mixture was stirred for 6 hr and filtered anaerobically through celite. The filtrate was then reduced to dryness *in vacuo*. The resulting solid was washed with 5 mL of diethyl ether and dried under vacuum to give 178 mg (80% yield) of an off-white powder. Colorless, column-shaped crystals form upon diffusion of diethyl ether vapor into a concentrated THF solution of the product. ^{1}H NMR (δ, ppm in CD_3CN): 7.16 (s, 2H), 6.98 (s, 4H), 2.41 (s, 6H), 1.67 (s, 12H).

References

1) Bullock, R. M.; Casey, C. P., *Acc. Chem. Res.* **1987,** *20*, 167-173.

2) Cooper, B. G.; Napoline, J. W.; Thomas, C. M., *Catal. Rev.* **2012,** *54*, 1-40.

3) Gade, L. H., *Angew. Chem. Int. Ed.* **2000,** *39*, 2659-2678.

4) Rodriguez, J. A.; Goodman, D. W., *Science* **1992,** *257*, 897-903.

5.) Stephan, D. W., *Coord. Chem. Rev.* **1989,** *95*, 41-107.

6) Wheatley, N.; Kalck, P., *Chem. Rev.* **1999,** *99*, 3379-3419.

7) Hoffman, B. M.; Lukoyanov, D.; Yang, Z. Y.; Dean, D. R.; Seefeldt, L. C., *Chem. Rev.* **2014,** *114*, 4041-4062.

8) Lancaster, K. M.; Roemelt, M.; Ettenhuber, P.; Hu, Y. L.; Ribbe, M. W.; Neese, F.; Bergmann, U.; DeBeer, S., *Science* **2011,** *334*, 974-977.

9) Lubitz, W.; Ogata, H.; Rudiger, O.; Reijerse, E., *Chem. Rev.* **2014,** *114*, 4081-4148.

10) Can, M.; Armstrong, F. A.; Ragsdale, S. W., *Chem. Rev.* **2014,** *114*, 4149-4174.

11) Dobbek, H.; Gremer, L.; Kiefersauer, R.; Huber, R.; Meyer, O., *Proc. Natl. Acad. Sci. U.S.A.* **2002,** *99*, 15971-15976.

12) McCleverty, J. A.; Meyer, T. J., *Comprehensive coordination chemistry II: from biology to nanotechnology*. Elsevier Pergamon: 2004.

13) Dance, I.; Fisher, K., *Prog. Inorg. Chem.* **1994,** *41*, 637-803.

14) Corrigan, J. F.; Fuhr, O.; Fenske, D., *Adv. Mater.* **2009,** *21*, 1867-1871.

15) Tran, D. T. T.; Beltran, L. M. C.; Kowalchuk, C. M.; Trefiak, N. R.; Taylor, N. J.; Corrigan, J. F., *Inorg. Chem.* **2002,** *41*, 5693-5698.

16) Tran, D. T. T.; Taylor, N. J.; Corrigan, J. F., *Angew. Chem., Int. Ed.* **2000,** *39*, 935-937.

17) Lewerenz, H. J., *Solar Energy Materials and Solar Cells* **2004,** *83*, 395-407.

18) Zhong, X. H.; Han, M. Y.; Dong, Z. L.; White, T. J.; Knoll, W., *J. Am. Chem. Soc.* **2003,** *125*, 8589-8594.

19) Petrov, D. V.; Santos, B. S.; Pereira, G. A. L.; de Mello DonegÃ¡, C., *J. Phys. Chem. B* **2002,** *106*, 5325-5334.

20) Castro, S. L.; Bailey, S. G.; Raffaelle, R. P.; Banger, K. K.; Hepp, A. F., *Chem. Mater.* **2003,** *15*, 3142-3147.

21) Walsh, R., *Acc. Chem. Res.* **1981,** *14*, 246-252.

22) West, R.; Barton, T. J., *J. Chem. Ed.* **1980,** *57*, 165.

23) West, R.; Barton, T. J., *J. Chem. Ed.* **1980,** *57*, 334.

24) Patai, S.; Rappoport, Z., *The chemistry of organic silicon compounds*. Wiley: 1989.

25) Auner, N.; Weis, J., *Organosilicon Chemistry I: From Molecules to Materials*. Wiley: 2011.

26. Komuro, T.; Matsuo, T.; Kawaguchi, H.; Tatsumi, K., *J. Chem Soc., Dalton Trans.* **2004**, 1618-1625.

27) Kückmann, T. I.; Hermsen, M.; Bolte, M.; Wagner, M.; Lerner, H.-W., *Inorg. Chem.* **2005,** *44*, 3449-3458.

28) Komuro, T.; Kawaguchi, H.; Tatsumi, K., *Inorg. Chem.* **2002,** *41*, 5083-5090.

29) Wallbank, A. I.; Corrigan, J. F., *Can. J. Chem.* **2002,** *80*, 1592-1599.

30) Komuro, T.; Matsuo, T.; Kawaguchi, H.; Tatsumi, K., *Inorg. Chem.* **2003,** *42*, 5340-5347.

31) Tran, D. T. T.; Corrigan, J. F., *Organometallics* **2000,** *19*, 5202-5208.

32) Borecki, A.; Corrigan, J. F., *Inorg. Chem.* **2007,** *46*, 2478-2484.

33) Groysman, S.; Majumdar, A.; Zheng, S.-L.; Holm, R. H., *Inorg. Chem. 49*, 1082-1089.

34) Medina, I.; Jacobsen, H.; Mague, J. T.; Fink, M. J., *Inorg. Chem.* **2006,** *45*, 8844-8846.

35) Startsev, A. N., *Catal. Rev.* **1995,** *37*, 353-423.

36) Friend, C. M.; Chen, D. A., *Polyhedron* **1997,** *16*, 3165-3175.

37) Drozdova, Y.; Steudel, R., *Chem. Eur. J.* **1995,** *1*, 193-198.

38) Valentine, J. S., *J. Am. Chem. Soc.* **1984,** *106*, 6463-6463.

39) Peruzzini, M.; De Los Rios, I.; Romerosa, A., *Prog. Inorg. Chem.* **2001,** *49*, 169-454.

40) Sreekanth, A.; Prathapachandra Kurup, M. R., *Polyhedron* **2003,** *22*, 3321-3332.

41) Strauch, P.; Dietzsch, W.; Golič, L., *Z. Anorg. Allg. Chem.* **1997,** *623*, 129-134.

42) Batsala, G. K.; Dokorou, V.; Kourkoumelis, N.; Manos, M. J.; Tasiopoulos, A. J.; Mavromoustakos, T.; Simčič, M.; Goli-Grdadolnik, S.; Hadjikakou, S. K., *Inorg. Chim. Acta* **2012**, *382*, 146-157.

43) Diez-Gonzalez, S.; Escudero-Adan, E. C.; Benet-Buchholz, J.; Stevens, E. D.; Slawin, A. M. Z.; Nolan, S. P., *J. Chem. Soc., Dalton Trans.* **2010**, *39*, 7595-7606.

44) McLean, A.; Neuhardt, E.; St. John, J.; Findlater, M.; Abernethy, C., *Trans. Met. Chem.* **2010**, *35*, 415-418.

45) Warad, I.; Abd-Elkader, O.; Boshaala, A.; Al-Zaqri, N.; Hammouti, B.; Ben Hadda, T., *Res. Chem. Intermed.* **2013**,*39*, 721-732.

46) Brandt, K.; Sheldrick, W. S., *Chem. Ber.* **1996,** *129*, 1199-1206.

47) Ross, A.; Sharp, P. R., *Inorg. Chem.* **2013**, *52*, 12645-12654.

48) Segal, B. M.; Hoveyda, H. R.; Holm, R. H., *Inorg. Chem.* **1998,** *37*, 3440-3443.

49) Osterloh, F.; Saak, W.; Pohl, S., *J. Am. Chem. Soc.* **1997,** *119*, 5648-5656.

50) Liu, H. Y.; Scharbert, B.; Holm, R. H., *J. Am. Chem. Soc.* **1991,** *113*, 9529-9539.

51) Goh, C.; Segal, B. M.; Huang, J.; Long, J. R.; Holm, R. H., *J. Am. Chem. Soc.* **1996,** *118*, 11844-11853.

52) Verma, S. K.; Kadu, R.; Singh, V. K., *Synthesis and Reactivity in Inorganic, Metal-Organic, and Nano-Metal Chemistry 44*, 441-448.

53) Ruffing, C. J.; Rauchfuss, T. B., *Organometallics* **1985,** *4*, 524-8.

54) Ferrara, S. J.; Mague, J. T.; Donahue, J. P., *Inorg. Chem. 51*, 6567-6576.

55) Chojnacki, J., *J. Mol. Struct.: THEOCHEM* **2008,** *862*, 112-117.

56) Kaur, H.; Zinn, F. K.; Stevens, E. D.; Nolan, S. P., *Organometallics* **2004,** *23*, 1157-1160.

57) Cain, M. F.; Hughes, R. P.; Glueck, D. S.; Golen, J. A.; Moore, C. E.; Rheingold, A. L., *Inorg. Chem.* **2010**, *49*, 7650-7662.

58) Fructos, M. R.; De Fremont, P.; Nolan, S. P.; Mar Dauiiaz-Requejo, M.; Perez, P. J., *Organometallics* **2006,** *25*, 2237-2241.

59) Armarego, W. L. F.; Chai, C. L. L., *Purification of Laboratory Chemicals*. Butterworth-Heinemann: 2003.

Chapter 3

Synthetic Efforts Toward a Structural Analogue of Molybdenum-Dependent Carbon Monoxide Dehydrogenase

Introduction

Carbon Dioxide Reduction Chemistry

The most substantial energy- and environmental-related problems facing post-industrial era society can be traced directly to carbon dioxide (CO_2) and its role within the carbon biogeochemical cycle. The relative balance between biological fixation of carbon dioxide into organic carbon and the oxidation of fixed carbon back to carbon dioxide has been significantly altered by anthropogenic sources of CO_2. Carbon dioxide is the final product of the complete oxidation of carbon, and is a main thermodynamic byproduct of the combustion of fossil fuels. Globally, an increasing demand for energy and subsequent increasing emissions of CO_2, a potent greenhouse gas, intimately parallel the inflating human population. Having already tipped the balance, further increases in CO_2 emissions are predicted to produce widespread and uncontrollable repercussions on Earth's climate and habitations.[1, 2] Furthermore, because modern life is so dependent on energy, fierce competition for nonrenewable resources, particularly fossil fuels, creates

far-reaching social, political, and economic contention.[3] Thus, it is of paramount importance to gain a better fundamental understanding of how carbon dioxide can be manipulated on a molecular level in an effort to develop technologies that can remedy environmental pollution caused by the greenhouse gas and potentially recycle it back into a useful fuel or fuel precursor.

In its ground state, carbon dioxide is a linear, $16e^-$ molecule that belongs to the point group $D_{\infty h}$. Although containing two polar C−O bonds, the vectors associated with charge separation are equal in intensity and opposite in direction, making the molecule nonpolar. Nevertheless, CO_2 retains the behavior of a species that contains two polar bonds along with their associated characteristic reactivity. Despite the nucleophilic nature of the two oxygen atoms, carbon dioxide behaves prevalently as an electrophile at carbon, given its carbon-centered π-antibonding LUMO.

The transformation of carbon dioxide into a useful product is complicated by many factors. Activation of CO_2 is challenging owing to its nonpolar characteristics. Pertaining to the reduction of CO_2 to a useful product, like lower oxide CO, it is more favorable on thermodynamic grounds to generate products via proton-coupled multi-electron events rather than single electron reductions. The energetic requirements associated with the reduction of carbon dioxide relevant to these processes are shown in Scheme 3.1 (Eqs. 1-7).[4, 5]

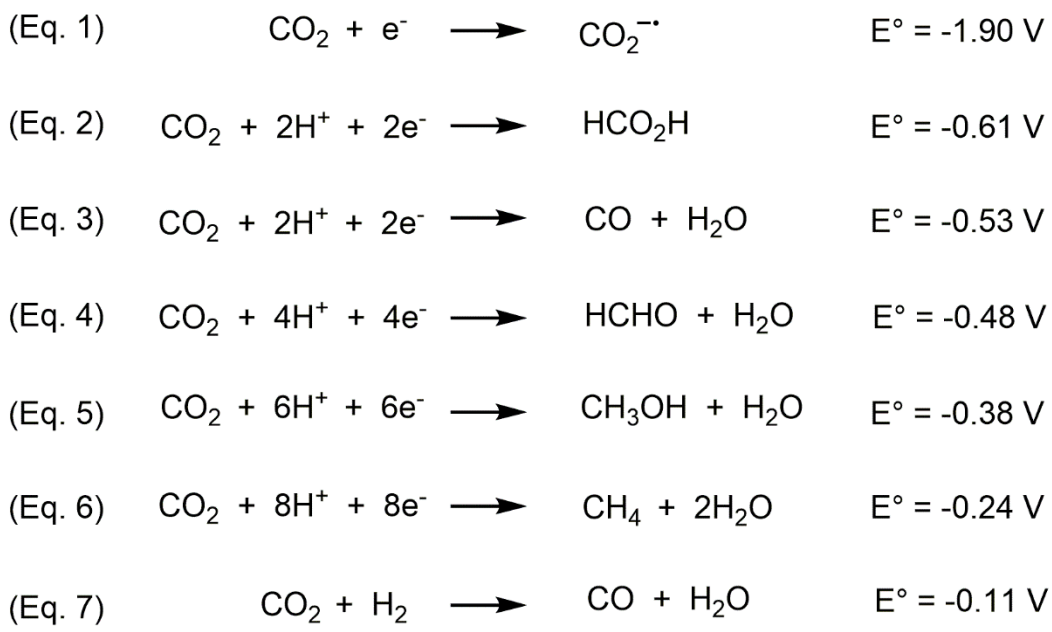

Scheme 3.1 Energetic requirements for the reduction of carbon dioxide at pH 7 in aqueous solution versus NHE, 25°C, 1 atmosphere, and 1M for the other solutes. References 4 and 5.

Very negative potentials are required for the one-electron reduction of CO_2, resulting from the large reorganizational energy required for the structural rearrangement of linear CO_2 to the bent CO_2 anion radical ($CO_2^{-\cdot}$). Therefore, an appropriate catalyst for CO_2 reduction should ideally operate near the thermodynamic potential of the reaction to be driven and bypass the highly energetically unfavorable formation of an anion radical intermediate. Carbon dioxide's thermodynamic stability and appreciable kinetic barrier for activation obstruct the development of an appropriate catalyst, and consequently, the direct production of liquid fuels from CO_2 remains a significant challenge.

An alternative strategy to direct conversion of CO_2 to liquid fuels is to convert CO_2 and H_2O into CO and H_2, respectively. Well-developed Fischer-Tropsch technologies can then be used to convert this synthesis gas (CO and H_2) into liquid fuels.

Access to syngas components can be accomplished by an industrial process called the water-gas shift reaction, which runs the reversible reaction: $CO + H_2O \rightleftharpoons CO_2 + H_2$ (Eq. 8).[6, 7] Classically, the water-gas shift reaction is operated in conjunction with the gasification of coal to produce pure hydrogen (H_2) in the forward reaction, which, by itself, is a potential commodity fuel and fuel precursor. By altering the system's conditions, this reaction can be driven to form either CO or H_2. While a feasible means for utilizing CO_2, current water-gas shift reaction systems demand a large input of energy. Crucial to its viable use within an alternative energy regime on a global scale is the development of an appropriate catalyst that can moderate this barrier for interconversion between CO and CO_2 more easily and efficiently.

Molybdenum-dependent carbon monoxide dehydrogenase

Of the six known pathways in nature, the Calvin cycle and photosynthesis are the two main contributors to global fixation of carbon dioxide, while the Wood-Ljungdahl pathway dominates anaerobic CO_2 fixation.[8] Key components intimately tied into the natural fixation of carbon dioxide are a class of metalloenzymes known as carbon monoxide dehydrogenases (CODH). CO dehydrogenases (Figure 3.1) catalyze the reversible reaction: $CO + H_2O \rightleftharpoons CO_2 + 2e^- + 2H^+$ (Eq. 9); essentially nature's version of the water-gas shift reaction. In the forward reaction, the oxidation of carbon monoxide produces carbon dioxide, which is fixed into cellular carbon, and protons and electrons. The protons generated in Eq. 9 power the synthesis of ATP via a transmembrane proton gradient, and the electrons are shuttled through an electron-transport chain where they ultimately reduce dioxygen (aerobic form) or are carried to different terminal electron

acceptors which couple to other energy requiring cellular processes (anaerobic form). In this way, organisms grow autotrophically on CO by coupling CO oxidation to CO_2 fixation.

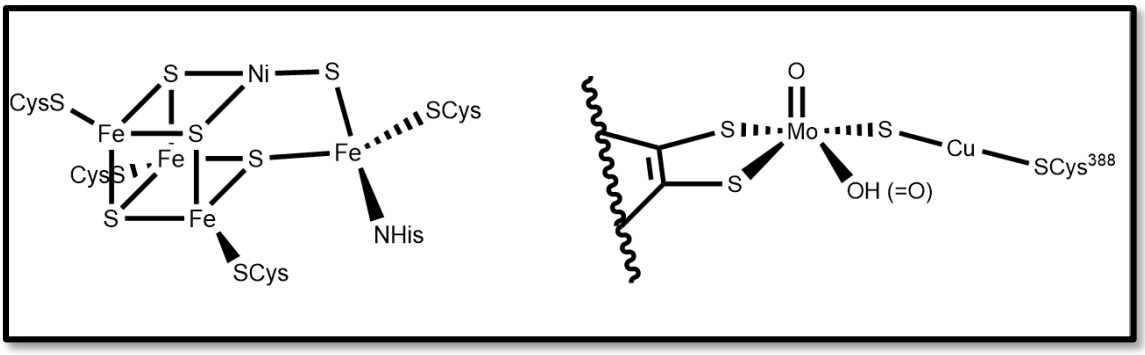

Figure 3.1 Minimal representations of the metal-containing active sites of CO dehydrogenases.

Anaerobic CO dehydrogenases employ catalytic active sites that contain iron and nickel transition elements (Ni-CODH), as shown in Figure 3.1. These metalloenzymes are the most extensively studied of the CO dehydrogenases and exist in two forms, Ni-CODH and the bifunctional Ni-CODH/ACS (ACS = Acetyl-CoA synthase). The nickel enzyme, Ni-CODH, works in tandem with hydrogenase to catalyze the formation of CO_2 and H_2 from CO and H_2O. As the fastest CODH, Ni-CODH can oxidize up to ~40,000 molecules of CO per second (CODH I from *Carboxydothermus hydrogenoformans*).[9] Carbon dioxide becomes a substrate for CODHs below ca. -0.3 V, where approximately 10 molecules of CO_2 are reduced to CO every second.[10-12] In Ni-CODH/ACS, CO is produced by CO_2 reduction at Ni-CODH, then transferred to ACS where it is used to form acetyl-CoA in the Wood-Ljungdahl pathway. Electrochemical analysis of Ni-CODH/ACS displayed efficient reduction of CO_2 to CO with almost no overpotential.[13]

Given the value of CO as a fuel precursor, a large-scale enzymatic electrocatalytic system based on Ni-CODH/ACS can be imagined, and efforts toward such a possible system are currently being investigated. However, these Ni-based metalloenzymes are extremely oxygen-sensitive, making growth, purification, and manipulation of these enzymes difficult.

The aerobic CO dehydrogenase contains transition metals molybdenum and copper (Mo-CODH), and is related to the molybdenum hydroxylases. Carboxidotrophic bacteria which incorporate this metalloenzyme metabolize CO, which is their sole source of carbon and energy.[14] In biological terms, CO is a rather potent electron donor (~1,000 fold stronger than NADH), with a relatively low half-cell potential of -0.52 V.[15] It is likely that early forms of life evolved to utilize this property of CO as an energy source. Electrons derived from Mo-CODH catalyzed CO oxidation (Eq. 9) are transported through a quinone-based electron transport chain to O_2.[16] The carbon dioxide generated during turnover is fixed into cell carbon via the Calvin-Benson-Basham pathway.[17, 18] Aerobic organisms containing CODH live in the top few centimeters of soil and have been estimated to remove ~2×10^8 metric tons of CO (~20% total atmospheric CO) from Earth's atmosphere annually,[19] characterizing their niche role within carbon's biogeochemical cycle.

Structural characterization of the most thoroughly investigated Mo-CODH, that from *Oligotropha carboxidovorans*, reveals a dimer composition with each monomer containing three subunits $(\alpha\beta\gamma)_2$. The small subunit (CoxS, 17.8kDa) has two [2Fe-2S] clusters, the medium subunit (CoxM, 30.2kDa) contains FAD, and the large subunit (CoxL, 88.7kDa) possesses the catalytic active site.[20] Significant structural and sequence

homologies exist between Mo-CODH and xanthine oxidoreductase (XOR) and other molybdenum hydroxylases,[21] thus expanding the role of molybdenum centers in biology.

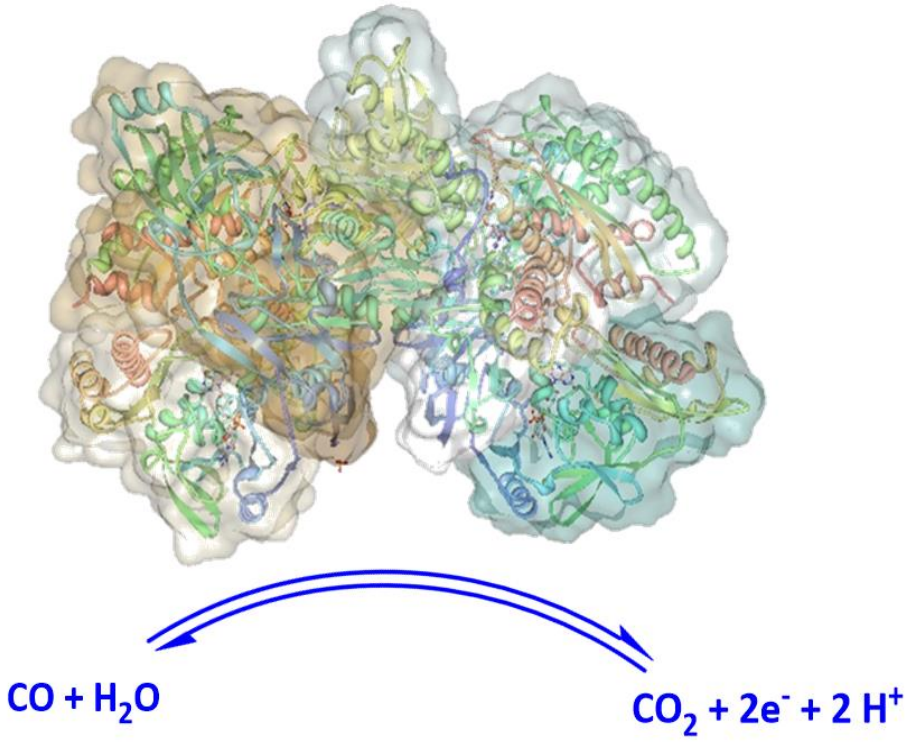

Figure 3.2 Representative structure of Mo-dependent carbon monoxide dehydrogenase and the reaction it catalyzes. Image generated using the Protein Data Bank.

The active site of Mo-CODH lies at the end of a ~6 Å wide hydrophobic tunnel approximately 17 Å below the surface of the protein.[22] Architecturally, the native active site features a unique, heterodimetallic [Mo−S−Cu] core. This core contains a square-pyramidal Mo center bound to two oxo groups (one axial and one equatorial), and three equatorial sulfur atoms. Two sulfur atoms derive from a chelated molybdopterin unit and

the remaining sulfur is a bridging sulfide, which tethers the Mo fragment to a two-coordinate Cu(I) fragment that is capped by cysteinate (Cys 388) (Figure 3.3).

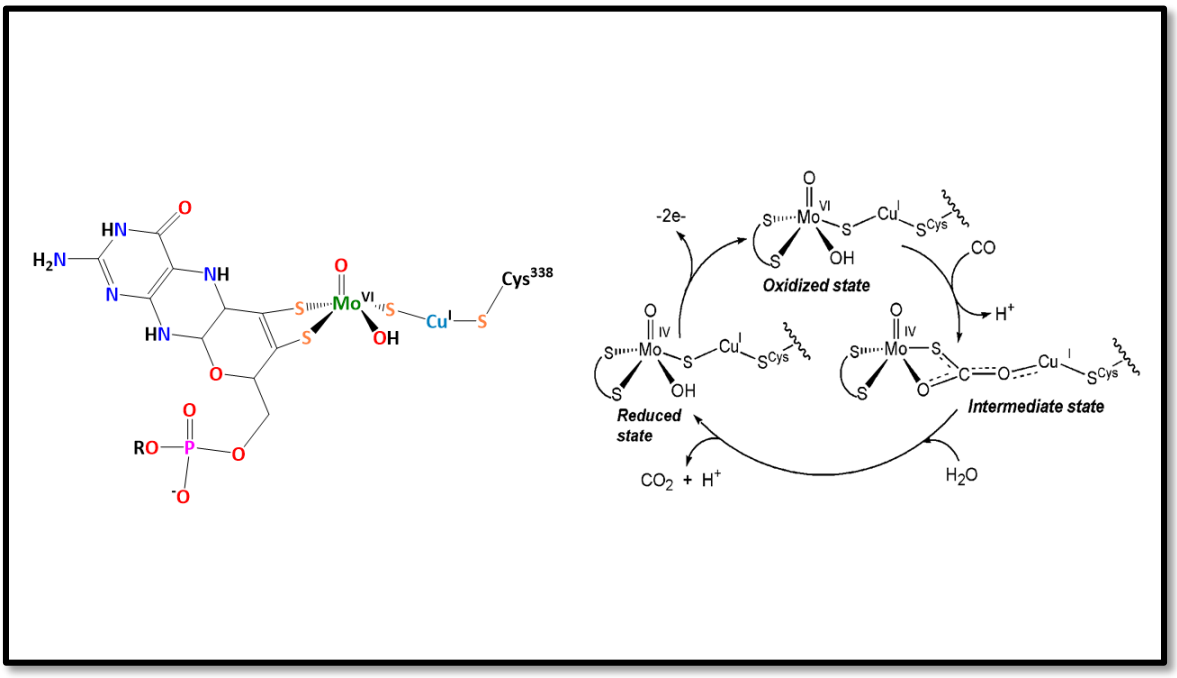

Figure 3.3 Active site of Mo-CODH and its proposed mechanism of CO oxidation.

This heterodimetallic core is unprecedented in biology and presents a synthetic challenge to biomimetic and coordination chemists alike. Despite anticipated changes in bond lengths, the reduced and oxidized states of Mo-CODH retain their overall geometry. This feature, also observed in Ni-CODH, leads to a minimal reorganization energy and is likely key to the efficiency of these metalloenzyme systems. Within the secondary coordination sphere, stabilization of charges appears to be aided by the appearance of several residues within hydrogen bonding distance of the active site.

The composition of Mo-CODH's active site can be viewed as a redox reservoir (Mo fragment) tethered to a pendant Lewis acid (low-coordinate Cu fragment) by an

unsupported, single-atom sulfide bridge. Briefly considering the active site's electronic structure, the chelating dithiolene unit from the attached molybdopterin provides effective ligand-to-metal π donation which competes with terminal oxo ligands for molybdenum's empty π orbitals. In turn, this weakens the Mo−O bonds and gives the molybdenum fragment its characteristic oxygen atom transfer behavior. The coordinative unsaturation at copper is presumed to facilitate binding of CO and additional bonding associated with the intermediate during turnover. In this way, the two fragments work in concert to efficiently catalyze the reversible reaction in Eq. 9. Much slower than Ni-CODH, the enzyme has a catalytic rate of 107 s^{-1} in the forward direction, with no information regarding its reduction of CO_2 (back reaction).[20, 23] The proposed catalytic pathway for oxidation of CO is shown in Figure 3.3. On the basis of a crystal structure incorporating *n*-butylisocyanide (inhibitor) bound Mo-CODH, it was proposed to proceed through a thiocarbonate-type intermediate.[20] However, recent computational analyses suggest that a thiocarbonate intermediate may actually lead to a deep minimum on the potential energy surface, making CO_2 release difficult.[24, 25] Additionally, these studies propose that CO oxidation could occur directly at the copper center followed by electron transfer to molybdenum via the electronic delocalization about the [Mo-S-Cu] core.

Given the importance of Mo-CODH with respect to carbon dioxide reduction and water-gas shift chemistry, an effort to understand more about this unusual system and how it efficiently operates is valuable within the context of both environmental remediation and alternative energy. In order to elucidate the mechanism by which Mo-CODH effectively moderates the barrier for interconversion between CO and CO_2, synthetic model studies should be employed. Gaining access to such information must

begin with a structural analog, which should be robust in order to rigorously analyze spectroscopically and crystallographically. Efforts along these lines form the basis of this chapter (Chapter 4), and will be discussed in detail herein.

Synthetic Analogues of Mo-CODH

The scarcity of information regarding Mo-CODH can be attributed to its only fairly recent structural characterization (2002) and the challenging synthesis required to model its core. An adequate structural analogue of Mo-CODH should feature as many of these important aspects as possible: (i) a single-atom, unsupported sulfide bridge [Mo-S-Cu], (ii) a two-coordinate, all sulfur-ligated Cu(I) ion, (iii) a *cis*-dioxo or *cis*-oxo/hydroxo molybdenum fragment, (iv) mono-dithiolene coordination at molybdenum, and (v) a square pyramidal geometry about the molybdenum center. The salient features of the active site are those directly involved in activating CO, which include the single sulfide bridge, the two-coordinate copper center, and oxo-ligation at molybdenum. Compromise with respect to any of these important features is tempered by constraints imposed by viable synthetic routes to these motifs. Since its X-ray structure solution in 2002, only a few attempts have been made to synthetically model Mo-CODH. These accounts are described below chronologically.

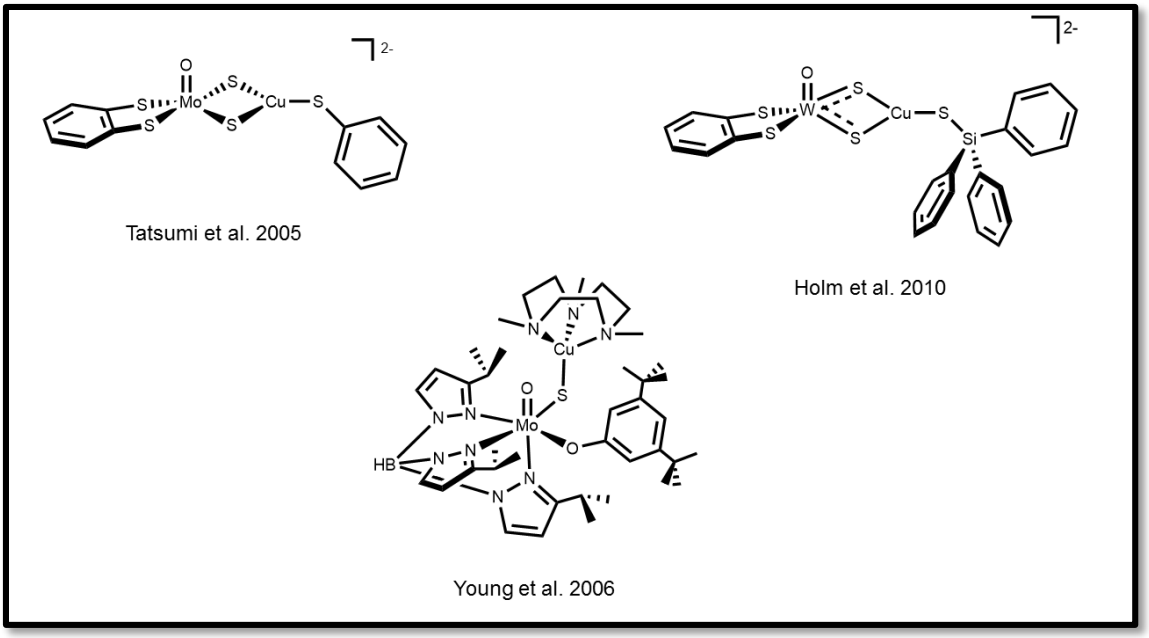

Figure 3.4 Existing structural analogues of Mo-CODH (references 26,27, and 29).

In 2005, Tatsumi et al. published a series of Mo-CODH analogues based on the use of dithiomolybdate as a starting material, given its remarkable affinity for transition metal ions.[26] Reaction between a simple copper(I) starting material like CuCN and dithiomolybdate yields dinuclear $[O_2Mo(\mu_2\text{-}S)_2CuCN]^{2-}$ in excellent yield. Salt metathesis with $K^{+}\,^{-}SPh$ to afford $[O_2Mo(\mu_2\text{-}S)_2Cu(SPh)]^{2-}$, followed by electrophilic substitution via double protonation of a terminal oxo ligand gave analogue $[(bdt)(O)Mo(\mu_2\text{-}S)_2Cu(SPh)]^{2-}$ (Scheme 3.2).

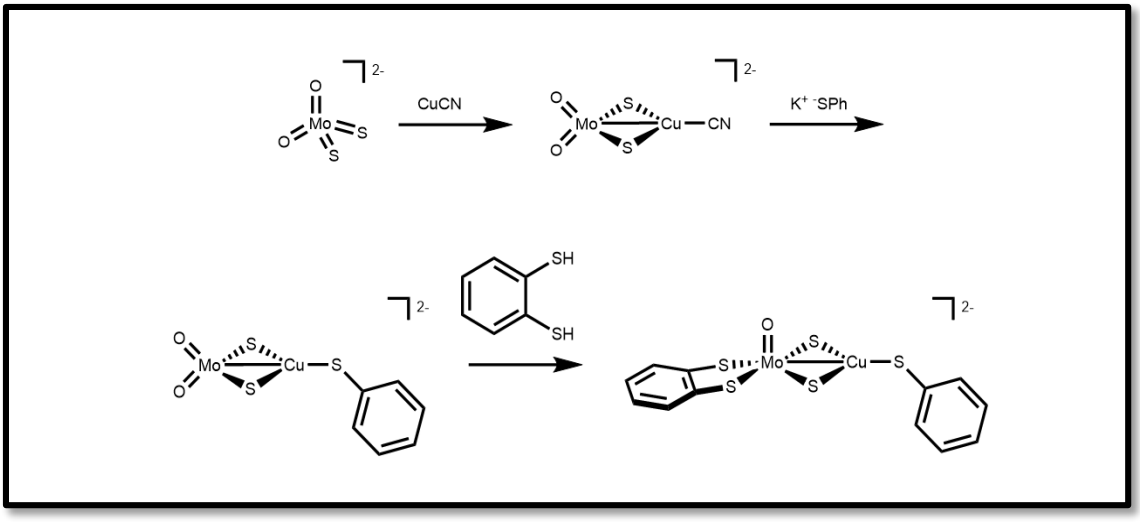

Scheme 3.2 Synthetic route to Mo-CODH analogue by Tatsumi et al. (reference 26).

This relatively simple synthetic approach to the formation of an Mo-CODH analogue complete with fully oxidized Mo(VI) in a square pyramidal geometry, mono-dithiolene coordination, terminal oxo ligation at molybdenum, and cuprous thiolate bound via a bridging sulfide has one major structural drawback – it contains two sulfide bridges between metal ions instead of one. This feature of the core apparently prevents reactivity associated with the native active site, as this model complex doesn't insert isocyanide or CO.[26] These observations call to attention the importance of the single sulfide bridge motif within the [Mo-S-Cu] core in preserving the reactivity related to the native active site.

Young et al. took a drastically different approach in modeling the active site of Mo-CODH in 2006.[27] By imposing considerable steric restraints on both Mo and Cu starting materials, they were able to synthesize the first Mo-CODH analogue that features a single sulfide bridge between the transition metal centers (Figure 3.4). The reaction of

reduced, oxosulfido species $[CoCp_2][Tp^{iPr}MoOS(OC_6H_3\text{-}3,5\text{-}{}^tBu_2)]$ with $[Cu(NCMe)(Me_3tacn)][BF_4]$ follows with displacement of labile, bound acetonitrile ligand and formation of Mo-CODH analogue species $[Tp^{iPr}MoO(OC_6H_3{}^tBu_2\text{-}3,5)(\mu\text{-}S)Cu(Me_3tacn)]$ (Scheme 3.3).

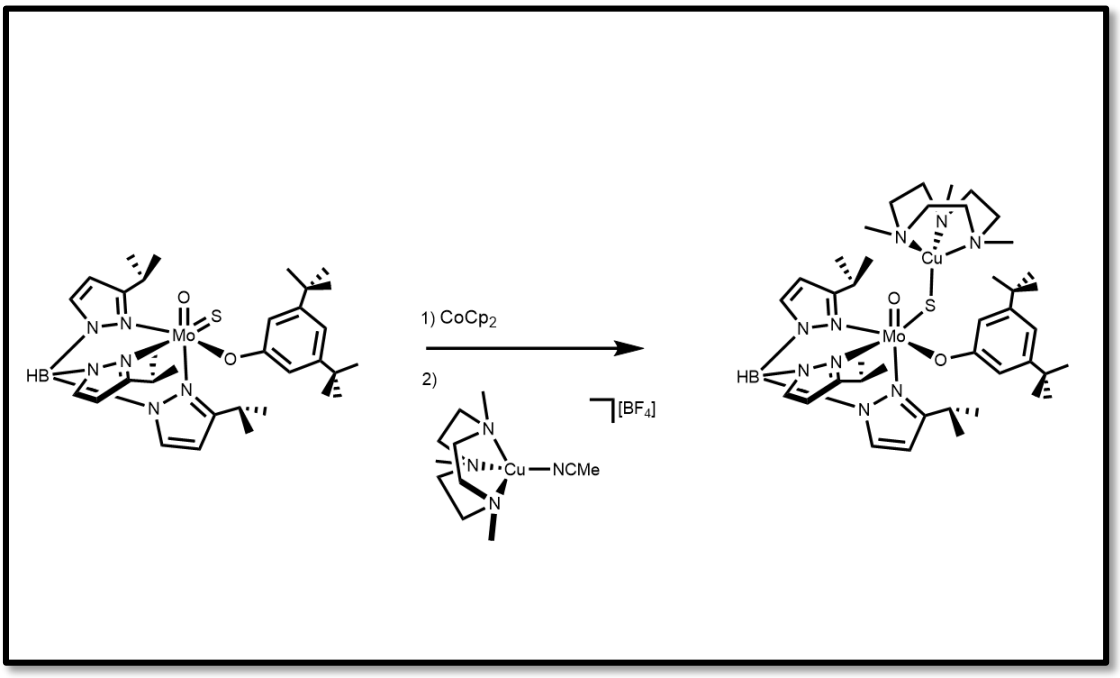

Scheme 3.3 Synthetic route to Mo-CODH analogue by Young et al. (reference 27).

This charge neutral analogue contains Mo(V) and Cu(I) and therefore models the one-electron reduced, paramagnetic form of active Mo-CODH. EPR spectra and DFT calculations indicate extensive delocalization of the SOMO over the [Mo-S-Cu] core, which suggests that this core could potentially act as a conduit for electrons. During turnover, CO could be oxidized directly at Cu, followed by two-electron transfer to Mo via the sulfide bridge.[27] While this analogue contains the integral single sulfide bridge

motif, dithiolene coordination and two-coordinate geometry at copper are absent, and the Mo(V) center is different from the native active site's resting state of Mo(VI). It should also be noted that the synthesis of this analogue is deceptively simple. Not only does the molybdenum starting material dimerize in solution, but it can also undergo intramolecular C−H activation resulting in formation of chelating mercaptophenolate species.[28] These complications caution against the general utility of this approach toward constructing an Mo-CODH analogue.

A report from Holm et al. in 2010 outlined a different approach to constructing a model system for Mo-CODH.[29] High-valent molybdenum has been shown to be unstable with respect to incoming thiolate, a process known as internal reduction, in which thiolate anions reduce high-valent molybdenum typically with attending condensation of reduced, thiolate- or sulfide-containing molybdenum fragments via bridging thiolates or sulfides.[30-32] In order to circumvent internal reduction, Holm et al. used tungsten monodithiolene starting materials in place of their molybdenum analogues, as tungsten is more stable toward incoming thiolate. In addition, the synthetic strategy applied utilizes copper(I) silylthiolates as reactants and is based on the difference of 25-40 kcal/mol between Si−S and Si−O bond dissociation energies (Scheme 3.4).[33-35] A detailed description of this general reaction type will be provided vide infra.

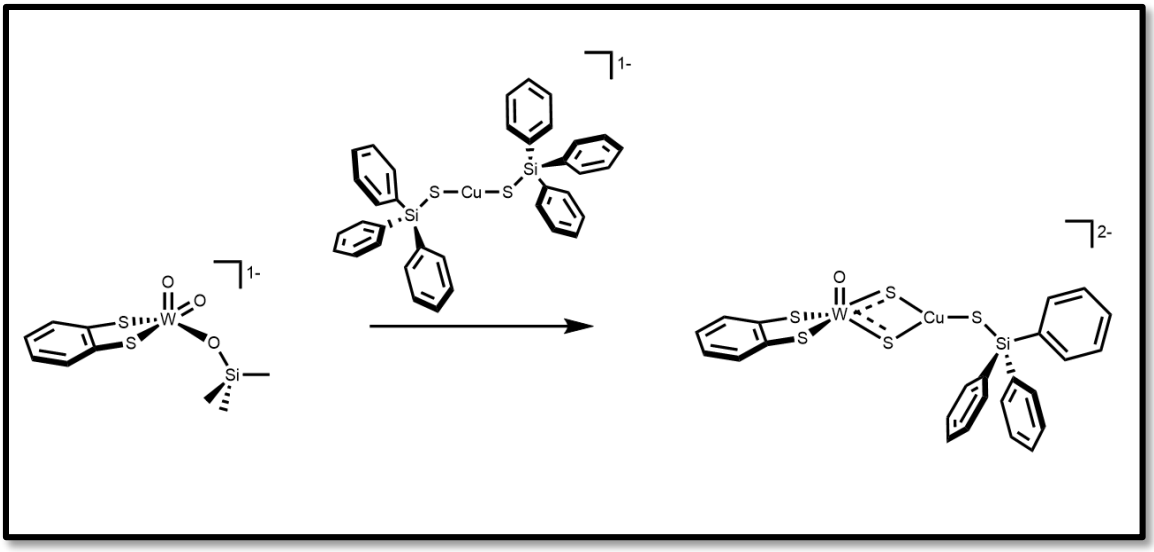

Scheme 3.4 Synthetic route to Mo-CODH analogue outlined by Holm et al. (Reference 29).

Following the synthetic route outlined in Scheme 3.4 (above) leads to formation of analogues that contain two sulfide bridges, with core units described as [W(μ-S)$_2$Cu] rhombs. Products of this formulation are the only isolable heterodinuclear species from these reactions, which are driven by the formation of stable disiloxane byproducts. The authors suggest a pathway which involves initial formation of an unstable [W(μ-S)Cu] species which undergoes rearrangement to form disulfido bridged species [W(μ-S)$_2$Cu] and anionic [WO$_3$(bdt)]$^{1-}$. Evidence for the latter species, [WO$_3$(bdt)]$^{1-}$, is provided by mass spectrometry.[29] The driving force for this rearrangement process can be ascribed to the stability of the [W(μ-S)$_2$Cu] rhomb aided by the initial formation of Si−O bonds.

Results and Discussion

Synthetic Approaches

Realization of a synthetic analogue of Mo-CODH with greater fidelity to the enzyme active site appears complicated by a number of factors. Firstly, the instability, and thus scarcity, of mixed oxosulfido molybdenum complexes unfortunately limits their use as starting materials in constructing heteronuclear complexes. Secondly, the difficulty in preparing and handling two-coordinate copper thiolate complexes also restricts their use as starting materials. Lastly, and perhaps most importantly, the propensity to form thermodynamically stable [Mo(μ-S)$_2$Cu] rhombs provides a significant challenge in gaining access to an analogue that contains a critical single, unsupported sulfide bridge between Mo and Cu. This motif is not only crucial within the context of a structural analogue, but is presumed to be necessary for any associated function relevant to the native active site.

Below are the results from attempts to form analogues of Mo-CODH, cataloged by method or synthetic approach used. It should be made clear from the start that the goal of the work described herein is to provide synthetic means to usable quantities of an isolable analogue robust enough to be characterized and analyzed by a variety of techniques. Additionally, an examination of the utility of the synthetic methods employed will be gauged with respect to the specific transformation for which they are applied. All reactions chronicled here were perfomed, handled, and manipulated anaerobically unless described otherwise.

Silane-Mediated Coupling Approach

The methodology behind the first approach toward forming a synthetic analogue of Mo-CODH is one which presents a reaction-type that is driven thermodynamically. Here, utilization of the differences in bond dissociation energies related to silicon-heteroatom bonds, specifically triorganosilane-heteroatom bonds, is directly exploited. Silicon is chlorophilic ($Me_3Si{-}Cl$ = ~113 kcal/mol), oxophilic ($Me_3Si{-}OH$ = ~133 kcal/mol), and very fluorophilic ($Me_3Si{-}F$ = ~160 kcal/mol), and thus preferentially forms bonds with these atoms under most conditions.[33] This general concept, or reaction-type, has been successfully used within the realm of modern organic synthesis. For example, an oxygen atom within an organic molecule can be silylated, followed by subsequent chemistry that would otherwise not be possible if the oxygen atom was not silylated, then the silyl moiety can be effectively removed via deprotection with a desilylating reagent like tetrabutylammonium fluoride to regenerate the original oxygen-containing group. In this way, silanes can be used effectively as protecting groups.[36] These protecting groups can usually be cleaved by acids or bases, and a common desilylating reagent employed is the fluoride anion, since the silicon-fluoride bond is the strongest of any silicon-heteroatom bond.[37, 38]

In an effort to generate sulfide-bridged motifs, protection of sulfur with a silyl group appears to be a viable means to induce coupling of two distinct metal components given its relatively weak Si−S bond ($Me_3Si{-}SH$ = ~103 kcal/mol).[39] Therefore, following a general trend in bond dissociation energies (Si−F >> Si−O > Si−Cl > Si−S), can provide a framework for reactivity to work within. Cleavage of a Si−S bond in a $MSSiR_3$ species

should occur in the presence of a M−F, M−O(R), or M−Cl species, to form a thermodynamically more stable $FSiR_3$, $(R)OSiR_3$, or $ClSiR_3$ product. Subsequent coupling of the unmasked $M-S^-$ fragment to the open coordination site on the other metal species can then occur, providing a product of M−S−M′ formulation. While other factors clearly contribute to the reactivity of two different species (Mo−O vs Mo−S bond strengths, etc.), this trend should provide a significant driving force within this context. Successful reactivity using this general concept has been demonstrated in a few previous instances. Perhaps the most elegant example of this chemistry was reported in 1996 by Holm et. al (Scheme 3.5).[40]

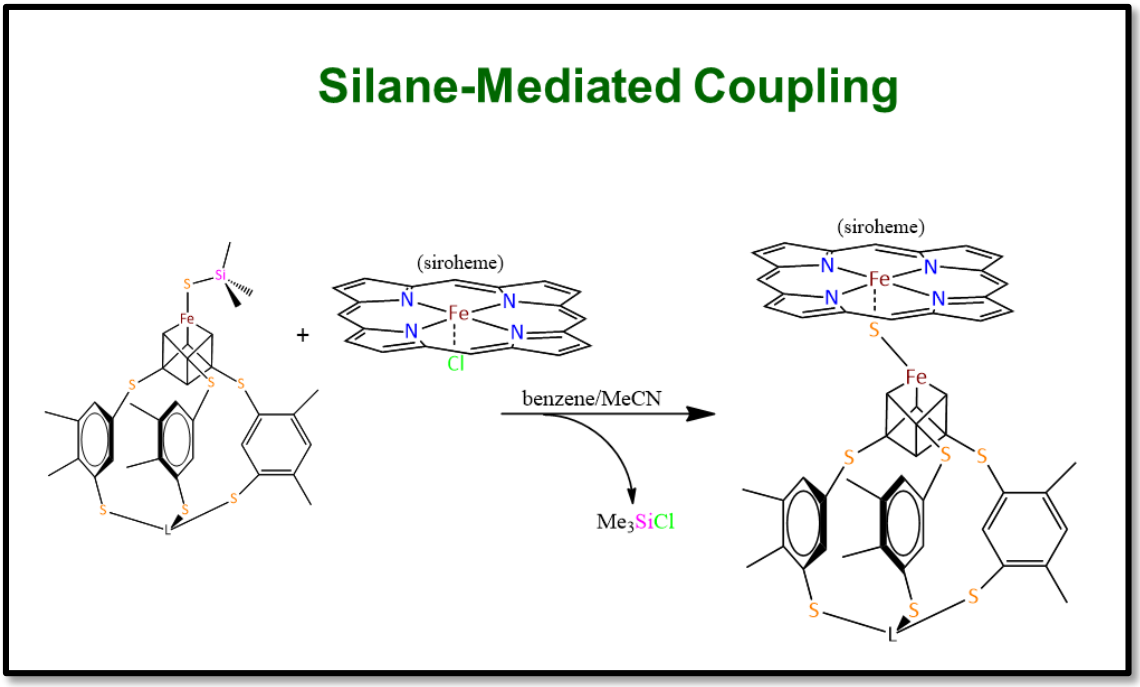

Scheme 3.5 Synthetic scheme used by Holm et. al to form a synthetic analogue of sulfite reductase (reference 40). Iron-sulfur clusters and sirohemes are minimal representations.

Reaction of a silylthiolate-appended iron-sulfur cluster with a siroheme chloride complex resulted in expulsion of trimethylsilyl chloride and formation of a $[Fe_4S_4]-S-$ferriheme

bridged assembly modeling sulfite reductase.[40] A scheme relevant to Mo-CODH modeling for this reaction-type, which will be referred to as 'silane-mediated coupling' from here on, is shown in Scheme 3.6.

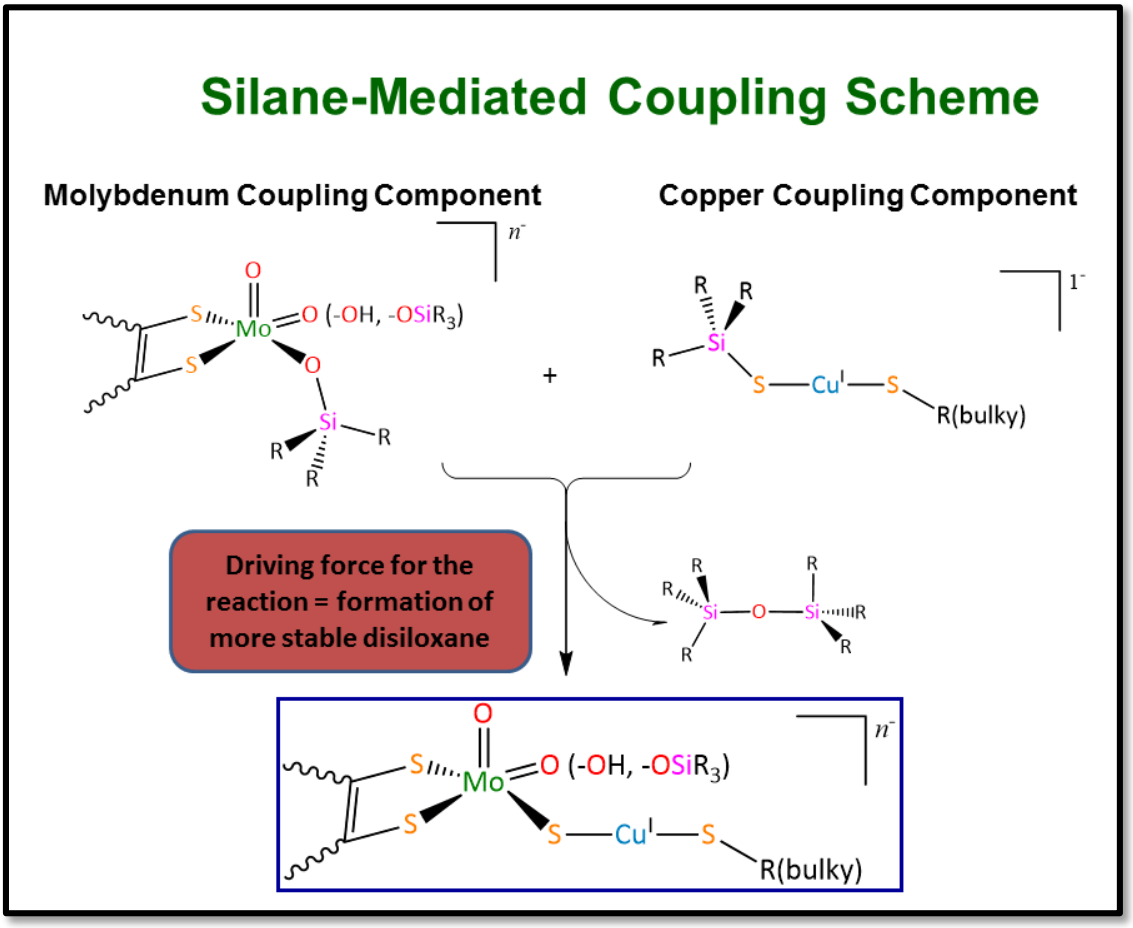

Scheme 3.6 Silane-mediated coupling scheme for formation of M−S−M' species.

Here, the example reaction shows coupling to form a disiloxane (by)product. This particular reaction-type will provide entry into these silane-mediated coupling reactions for a few reasons. Firstly, there exist at least a few siloxide-containing molybdenum complexes in the literature which appear to be suitable for starting materials. Secondly, access to low-coordinate silylthiolate complexes of copper(I) was demonstrated in the

last chapter of this dissertation (Chapter 2). Additionally, molybdenum silylthiolate complexes containing terminal oxo ligands are presumed to be unstable with respect to a potential intramolecular rearrangement to form terminal sulfide ligand and siloxide. Lastly, disiloxanes are particularly stable in comparison to silanols, silyl ethers, and silyl chlorides based on silicon-heteroatom bond strength and π-donation from two oxygen lone pairs into empty σ* orbitals on Si. This effect is what gives rise to the quasi-linear conformation of the [Si−O−Si] core in disiloxanes like hexaphenyldisiloxane.

Table 3.1. Crystal and refinement data for compounds in Chapter 3.

compound	**1A/1B**	**3**	**5**
solvent	$Ph_3SiOH \cdot 2½C_6H_6$	none	2 MeCN
formula	$C_{96}H_{103}Cu_4Mo_2N_6O_{3.64}S_{5.36}Si$	$C_{46}H_{58}CuMoN_2O_4PSi$	$C_{40}H_{30}Cu_3F_6MoN_8OPS_3$
fw	2044.98	921.48	1166.49
xtl system	triclinic	monoclinic	monoclinic
space grp	$P\bar{1}$	$C2/c$	$P2_1/c$
color, habit	orange block	yellow column	orange block
a, Å	15.106(5)	38.121(12)	15.1101(17)
b, Å	18.635(7)	9.499(3)	20.018(2)
c, Å	19.062(7)	30.459(10)	28.962(3)
α, deg.	100.487(5)	90	90
β, deg.	107.454(5)	116.922(4)	102.9060(16)
γ, deg.	105.339(5)	90	90
V, Å^3	4733(3)	9834(5)	8538.9(17)
T, K	150(2)	100(2)	100(2)
Z	2	8	8
R1, wR2	0.0368, 0.0864	0.0406, 0.1028	0.0318, 0.0663
GoF	1.026	1.095	1.042

$R1 = \Sigma||F_o| - |F_c||/\Sigma|F_o|$. $wR2 = \{[\Sigma w(F_o^2 - F_c^2)/\Sigma w(F_o^2)^2\}^{1/2}$; $w = 1/[\sigma^2(F_o^2) + (xP)^2]$, where $P = (F_o^2 + 2F_c^2)/3$.

{[$MoOS_3$(CuIMes)](μ_4-Cu)[$MoOS_3$(CuIMes)$_2$]}	**1A**
{[MoO_2S_2(CuIMes)](μ_3-Cu)[$MoOS_3$(CuIMes)$_2$]}	**1B**
[Mo(=O)S_3(CuP^tBu_3)$_3$Cl]	**2**
[MoO_2($OSiPh_3$)(μ-O)Cu(Me_4phen)(P^tBu_3)]	**3**
[MoO(^{t}Bu_4salphen)Cl].	**4**
[MoO(μ-S)$_3$(Cu(phen))$_3$][PF_6]	**5**

Table 3.2 Compound number list for Chapter 3.

To begin, $[MoO_2(bdt)(OSiPh_3)]^{1-}$ (where bdt = 1,2-benzenedithiolate) was chosen as the molybdenum coupling component since it featured square pyramidal geometry, dithiolene ligation, *cis*-dioxo ligation (apical and basal), and a siloxide ligand.[41] Reaction between $[MoO_2(bdt)(OSiPh_3)]^{1-}$ and in situ generated $[Cu(STrip)(SSi^iPr_3)]^{1-}$ (see Chapter 1 of this dissertation) led to the formation of a green colored reaction mixture up mixing (Scheme 3.7). While cuprous bis(thiolato) species are fairly unstable, it was presumed that the steric bulk provided by the triptycylthiolate ligand could stabilize a product in which the copper center maintains its two-coordinate geometry.

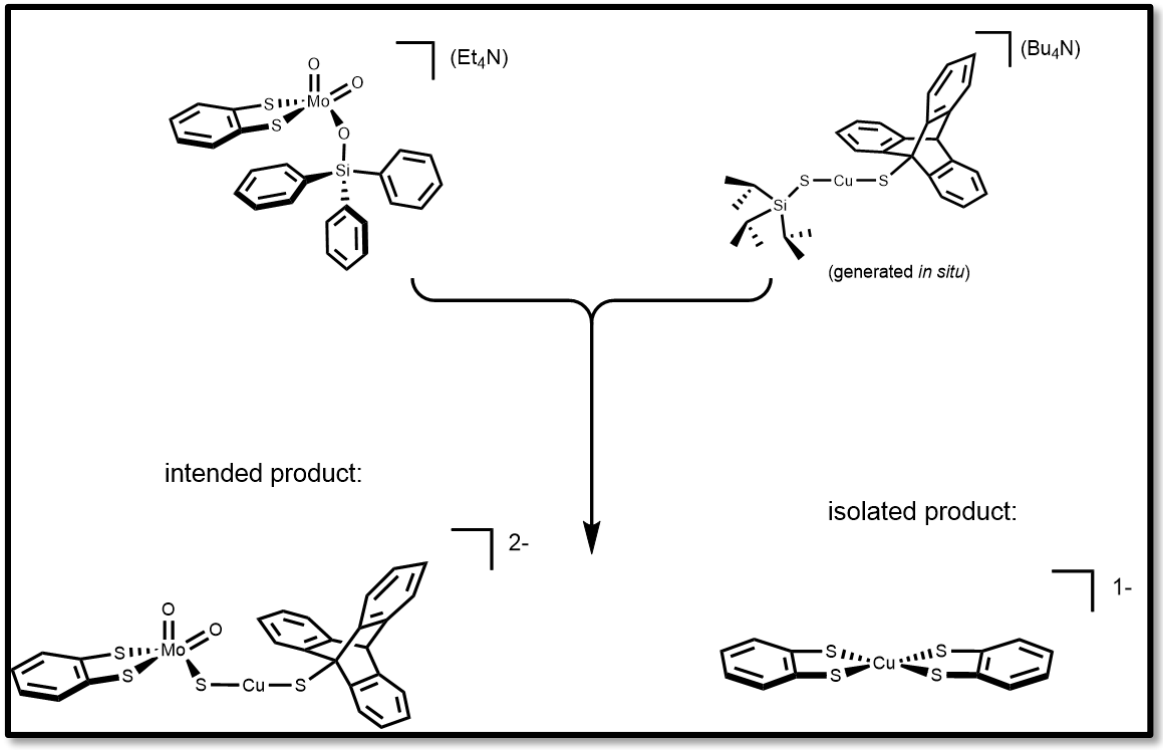

Scheme 3.7 Coupling reaction between $[MoO_2(bdt)(OSiPh_3)]^{1-}$ and $[Cu(STrip)(SSi^iPr_3)]^{1-}$.

Analysis of the product mixture appeared complex, but contained a small amount of unreacted $[MoO_2(bdt)(OSiPh_3)]^{1-}$ (characterized spectroscopically via ^1H NMR and mass spectrometry) and a new green species as the major isolable product. This green species was found to be $[Cu(bdt)_2]^{1-}$ on the basis of mass spectrometry and by crystallographic characterization. Here, ligand exchange dominates the reaction in order to effect a more favorable bonding interaction between the rather labile copper(I) center and the soft chelates provided by the benzene-1,2-dithiolate ligands.

This reaction appears to also occur independently of temperature, as reactions performed at low temperature (-78°C) gave rise to immediate formation of this green

color, which is indicative of $[Cu(bdt)_2]^{1-}$. The results from pulling an aliquot from this reaction mixture at low temperature can be seen in Figure 3.5.

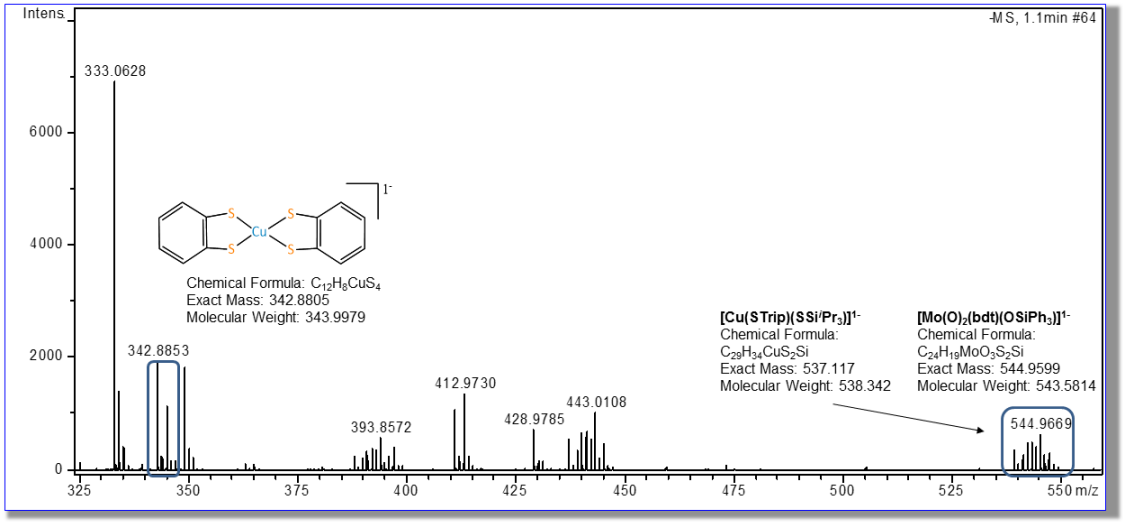

Figure 3.5 ESI-MS (negative ion mode) of an aliquot taken ~5 mins. after reaction of $[MoO_2(bdt)(OSiPh_3)]^{1-}$ with $[Cu(STrip)(SSi^iPr_3)]^{1-}$ at -78°C.

This negative ion mode ESI-MS spectrum shows formation of $[Cu(bdt)_2]^{1-}$ (left side) and the presence of unreacted starting materials (overlaid, right side) after only a few minutes stirring at low temperature. No peaks at higher molecular weight or suggestive of a species containing both copper and molybdenum were found. Choice of solvent may also be an important factor in these reactions. THF was the most often used solvent for reasons of solubility. Running the reaction in more polar acetonitrile appeared to promote the formation of $[Cu(bdt)_2]^{1-}$ and gave rise to decomposition within the product mixture. Solvent combinations of THF with other hydrocarbon solvents like benzene, or running the reaction directly in benzene heterogeneously, still produced green $[Cu(bdt)_2]^{1-}$ and led to isolation of large quantities of starting material. Other, similar

reactions between $[MoO_2(bdt)(OSiPh_3)]^{1-}$ and copper silylthiolate species (e.g. $[Cu(IMes)(SSi^iPr_3)]$, $[Cu(P^tBu_3)(SSiPh_3)]$, $[Cu(triphos)(SSi^iPr_3)]$, and $[Cu(SSiPh_3)_2]^{1-}$) led to the same formation of $[Cu(bdt)_2]^{1-}$ as the major isolable product. In one instance, from the reaction between $[MoO_2(bdt)(OSiPh_3)]^{1-}$ and $[Cu(SSiPh_3)_2]^{1-}$), hexaphenyldisiloxane was isolated from the product mixture and was characterized crystallographically and via ^{1}H NMR. Despite this appearance of the desired byproduct from the reaction, the major isolable product remained $[Cu(bdt)_2]^{1-}$.

While dithiolene coordination is present as a feature of the active site of Mo-CODH, compromise of this motif in order to avoid inhibition of desired product formation by ligand exchange must be the logical course of action synthetically. Therefore, molybdenum-based coupling components without soft chelating ligands must be used as starting materials. Particularly attractive in this regard is charge neutral, tetrahedral $[MoO_2(OSiPh_3)_2]$[42], since its coordinative unsaturation should allow for easy access with respect to the intended coupling reaction, and it would likely be amenable to further ligation following coupling. For the copper coupling component, $[Cu(IMes)(SSi^iPr_3)]$ provides an ideal starting material due to its straightforward preparation and isolation as a pure, crystalline solid, its two-coordinate geometry, and its complete solubility in diethyl ether, which allows for any unreacted starting material to be easily washed out of the reaction mixture.

Upon mixing $[MoO_2(OSiPh_3)_2]$ and $[Cu(IMes)(SSi^iPr_3)]$, an orange solution is produced, which forms immediately at both room temperature and at -78°C.

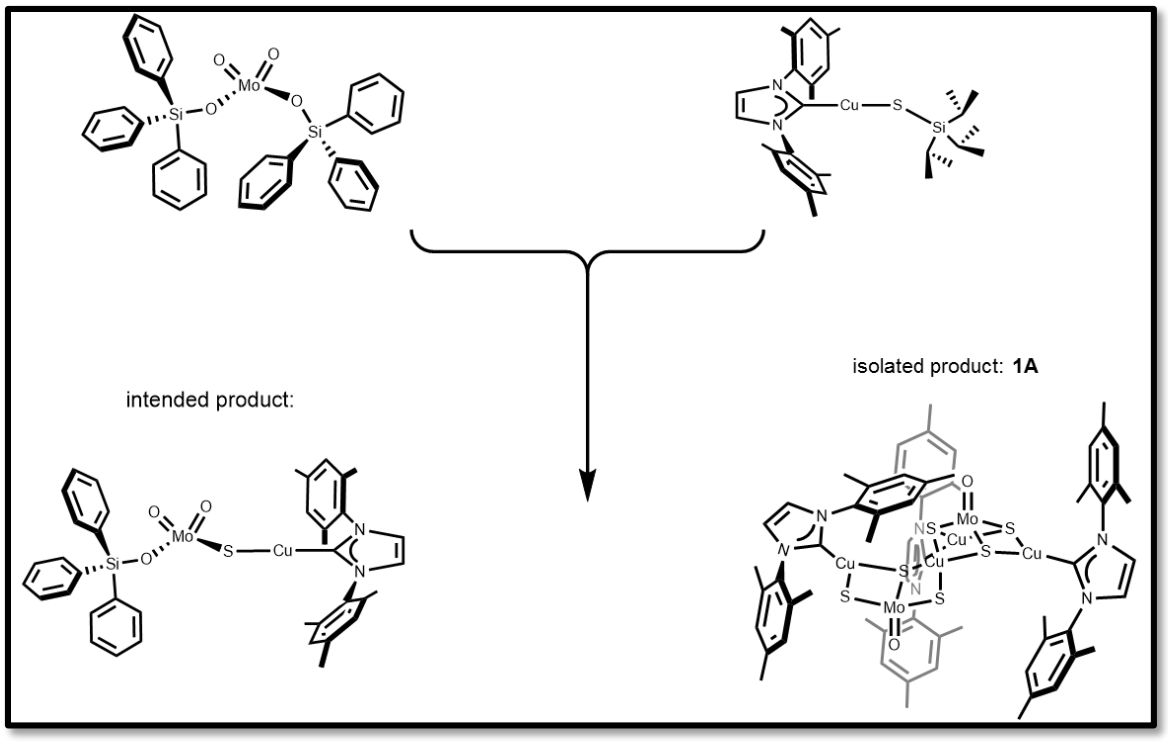

Scheme 3.8 Reaction of $[MoO_2(OSiPh_3)_2]$ and $[Cu(IMes)(SSi^iPr_3)]$.

Given that both starting materials are colorless (d^0 Mo(VI) and d^{10} Cu(I)), this orange color is presumably indicative of ligand-to-metal charge transfer (LMCT) from sulfur into the empty d orbital manifold of hexavalent molybdenum. Analysis of the product mixture gives a soluble, diamagnetic, orange solid as the major isolable product. The ^1H NMR is dominated by signals attributed to the IMes ligand, and mass spectrometry shows only $[Cu(IMes)_2]^+$, which is the typical fragment signal that arises from any complex containing a $[Cu(IMes)]^+$ unit. X-ray crystallography reveals the formulation of this orange product to be two closely related independent molecules: $\{[MoOS_3(CuIMes)](\mu_4\text{-}Cu)[MoOS_3(CuIMes)_2]\}$ (**1A**) and $\{[MoO_2S_2(CuIMes)](\mu_3\text{-}Cu)[MoOS_3(CuIMes)_2]\}$ (**1B**).

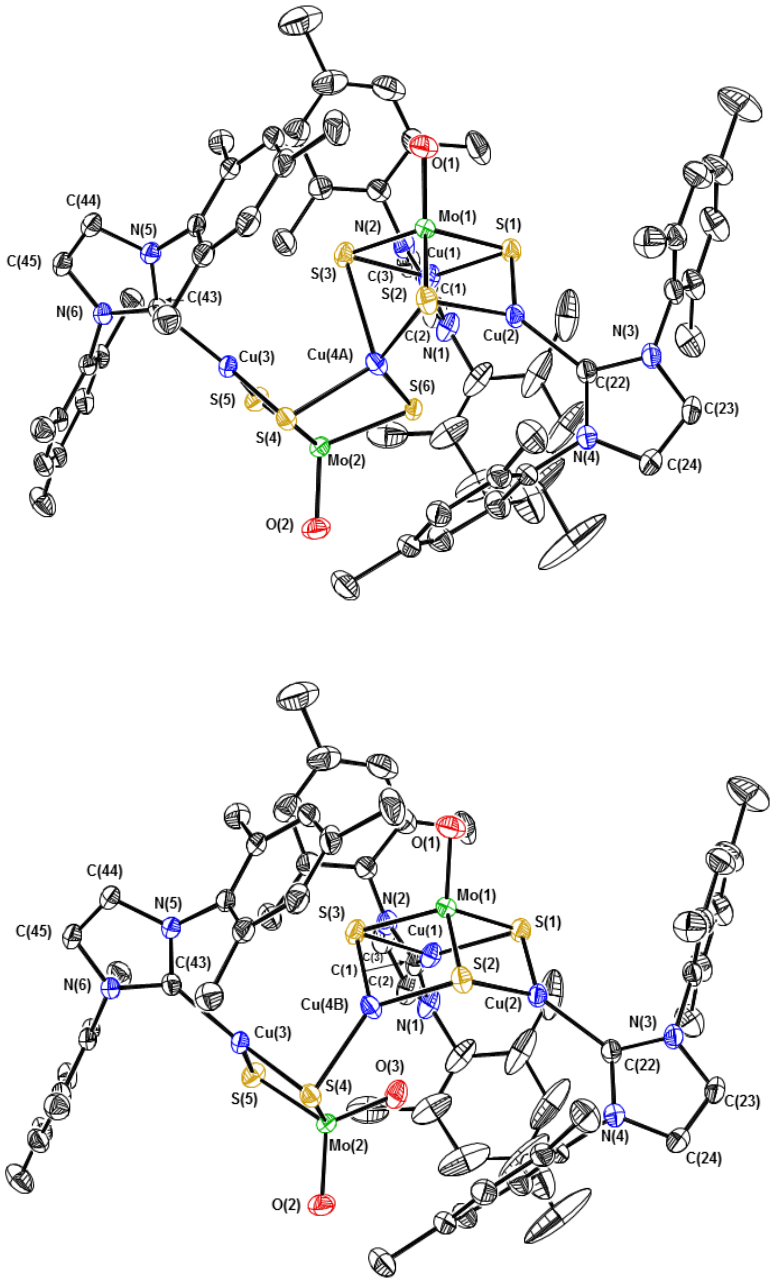

Figure 3.6 Crystal structures of **1A** (top) and **1B** (bottom). Thermal ellipsoid plot is drawn at the 50% probability level. Hydrogen atoms are omitted for clarity.

The difference between **1A** and **1B** is the coordination of the bridging copper(I) ion (Cu4) either to four sulfides (**1A**) in a tetrahedral fashion, or to three sulfides (**1B**) in a trigonal fashion, where the second voided cubane has two terminal oxo ligands on molybdenum.

Isolation of products **1A** and **1B** is highly reminiscent of the work reported by Holm et. al[29], since these products contain thermodynamically stable [Mo(μ-S)$_2$Cu] rhomb cores and suggest a non-stoichiometric reaction or facile ligand rearrangement taking place during the reaction. Additionally, a polyoxoanion byproduct, [Mo$_6$O$_{19}$][Cu(IMes)$_2$]$_2$, was isolated from this reaction and was characterized crystallographically. Polyoxoanion formation from the reaction which produces clusters **1A** and **1B**, is also suggestive of a shuffling of oxygen and sulfur atoms akin to the rearrangement observed in the system reported by Holm et. al.[29] Double voided cubane cluster products **1A** and **1B** are new complexes, however, simpler single voided cubanes of similar composition are known.[43-46] Of note structurally, one might speculate that the steric hindrance associated with the large IMes ligand might prevent formation of single unit voided cubanes, as opposed to the double voided cubanes observed here.

A similar reaction, that between [MoO$_2$(OSiPh$_3$)$_2$] and [Cu(P^{t}Bu$_3$)(SSiPh$_3$)], gives rise to product formation which parallels that seen in Scheme 3.8. Upon mixing, again regardless of temperature, an orange product mixture is immediately produced. ^{1}H NMR analysis of this orange major product is diamagnetic and shows only a doublet corresponding to the ^{t}Bu$_3$P ligand.

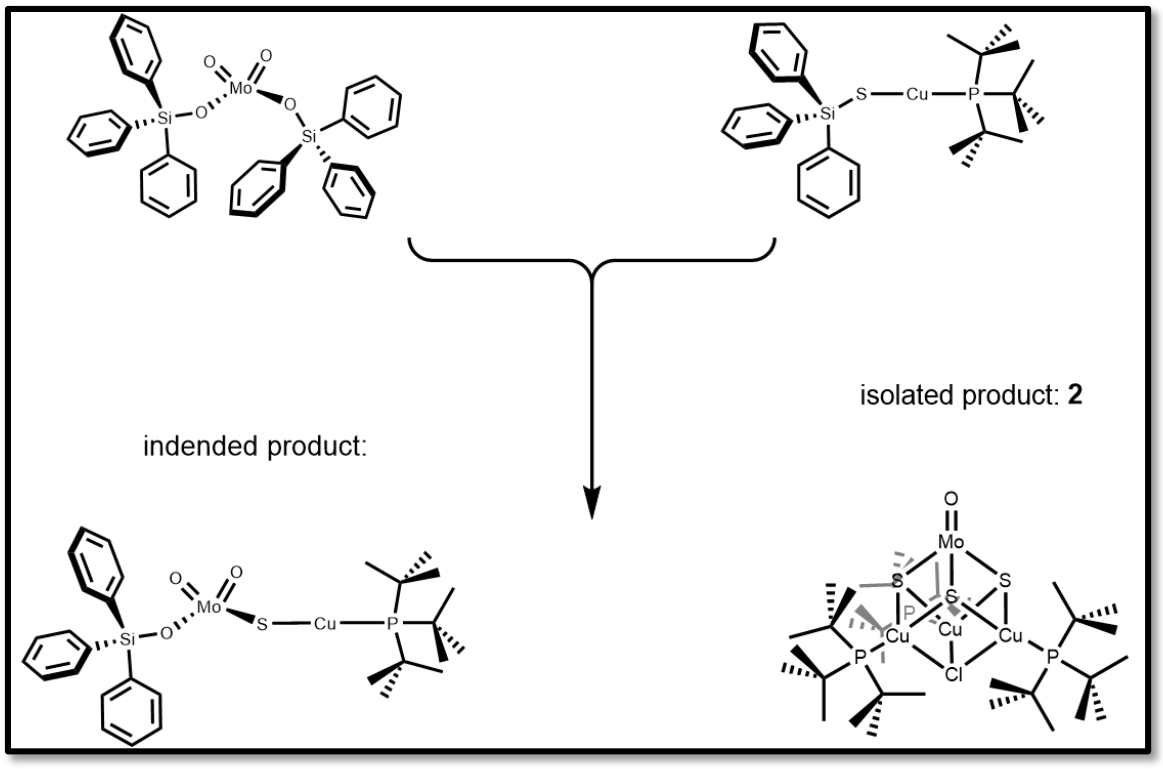

Scheme 3.9 Reaction between $[MoO_2(OSiPh_3)_2]$ and $[Cu(P^tBu_3)(SSiPh_3)]$.

Orange crystals obtained from this reaction were subjected to X-ray crystallography. A solution emerged for these crystals, which indicated a charge neutral formulation of $[Mo(=O)S_3(CuP^tBu_3)_3X]$ (**2**), where X is presumably chloride given that the reaction work-up involved a chlorinated solvent. Unfortunately, an apparent twinning problem has thus far prevented a satisfactory refinement for this structure. However, from the structure solution, we can at least identify the core of the molecule, which appears to be a charge neutral, single cubane related to **1A** and **1B**. In line with this crystallographic evidence is the mass spectrometry associated with **2**. Mass spectrometric analysis of both crystalline material and the crude product untainted by chlorinated solvent reveals a

cationic fragment described as $[Mo(=O)S_3(CuP^tBu_3)_3]^+$ as the fragment of highest molecular weight (Figure 3.7).

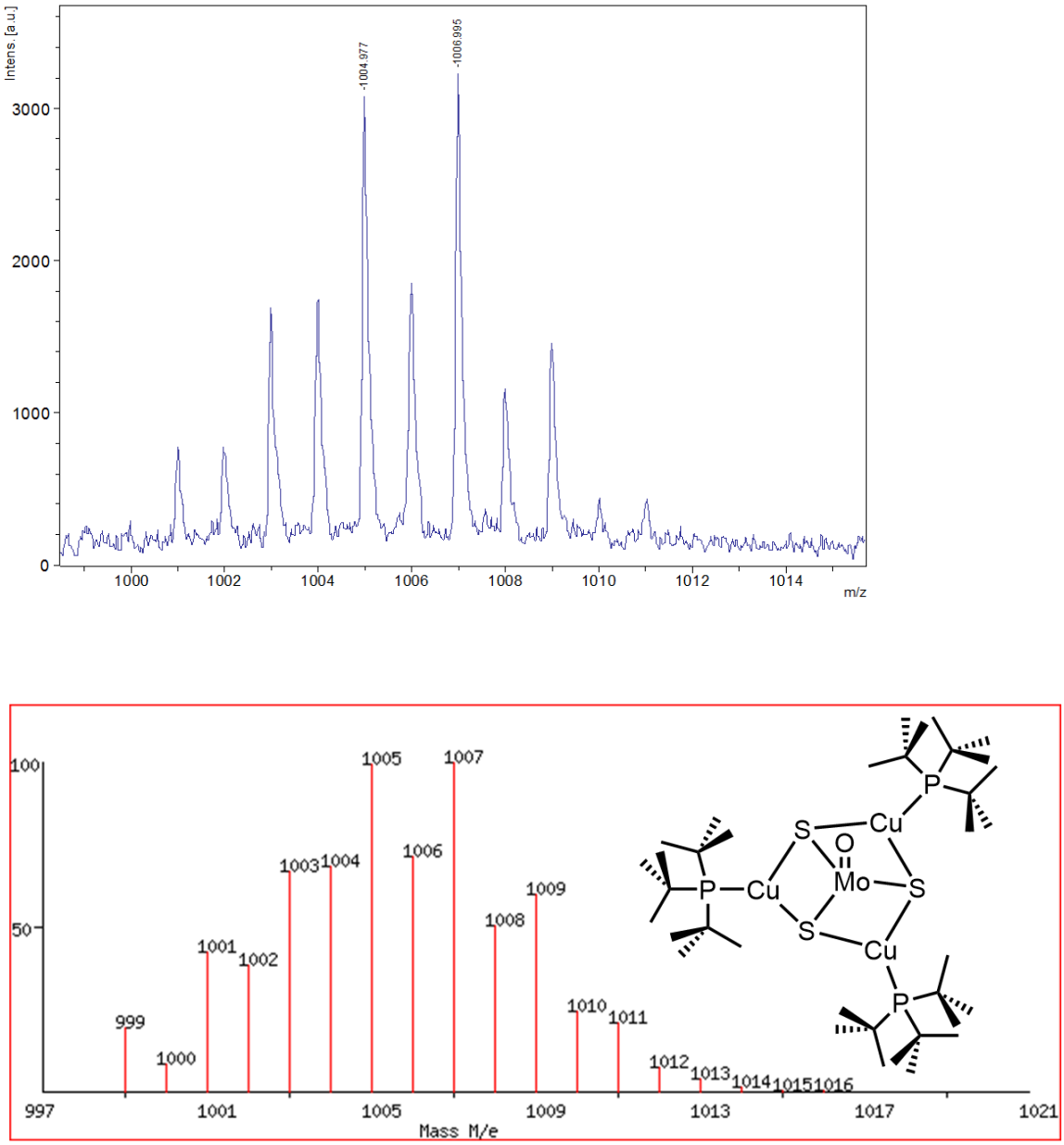

Figure 3.7 Positive ion mode MALDI-MS (top) and calculated (bottom) isotope distribution pattern for $[Mo(=O)S_3(CuP^tBu_3)_3]^+$. Calculated spectrum obtained from http://www.sisweb.com/mstools/isotope.htm.

In an effort to prevent cluster formation, a coordinatively saturated molybdenum starting material, $[MoO_2(Me_4phen)(OSiPh_3)_2]$[47] ($Me_4phen$ = 3,4,7,8-tetramethylphenanthroline), was employed as a coupling component. Here, use of a six-coordinate molybdenum coupling component with a significant steric profile should serve to tune down the reactivity in order to prevent polynuclear cluster formation. In an initial attempt, reacting $[MoO_2(Me_4phen)(OSiPh_3)_2]$ with $[Cu(P^tBu_3)(SSiPh_3)]$ led to formation of a yellow product, from which large, bright yellow crystals were produced.

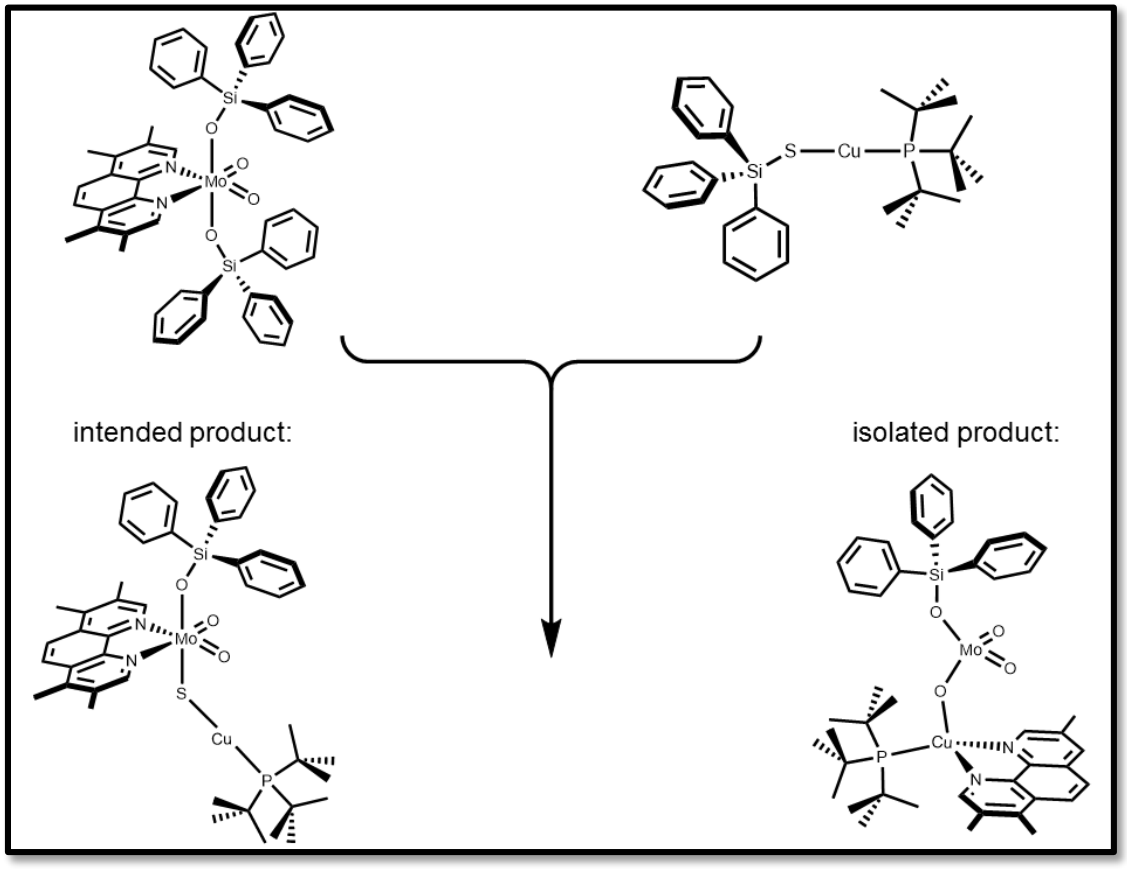

Scheme 3.10 Reaction between $[MoO_2(Me_4phen)(OSiPh_3)_2]$ and $[Cu(P^tBu_3)(SSiPh_3)]$.

Analysis of these crystals via ^{1}H NMR revealed the presence of $^{t}Bu_3P$, Me_4phen, and Ph_3SiO- ligands. X-ray crystallography disclosed the identity of the actual structure, which was found to be $[MoO_2(OSiPh_3)(\mu\text{-}O)Cu(Me_4phen)(P^{t}Bu_3)]$ (Figure 3.8), **3**.

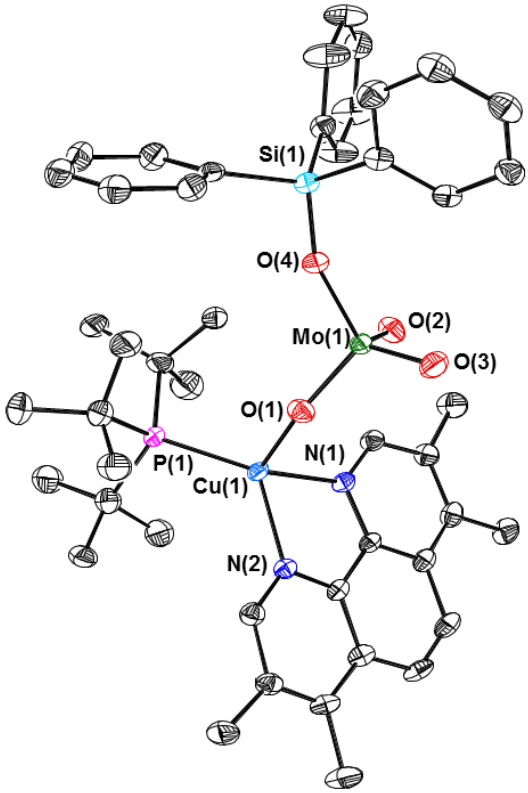

Figure 3.8 Crystal structure of **3**, $[MoO_2(OSiPh_3)(\mu\text{-}O)Cu(Me_4phen)(P^{t}Bu_3)]$. Thermal ellipsoid plot is drawn at the 50% probability level. Hydrogen atoms are omitted for clarity.

Complex **3**, $[MoO_2(OSiPh_3)(\mu\text{-}O)Cu(Me_4phen)(P^{t}Bu_3)]$, displays two tetrahedral metal centers (Mo and Cu) bound by a bridging oxo ligand, a structural motif accounted for in the literature,[48-50] where the [Mo(μ-O)Cu] core is typically part of a polynuclear framework and copper is divalent. In this reaction, Me_4phen has migrated from high-valent molybdenum to low-valent copper. The driving force behind this migration can be

attributed to the strong π-interaction between copper and the Me_4phen ligand, aided by the labilization of Me_4phen due to the strong trans influence from the terminal oxo ligands on molybdenum. Closed-shell d^{10} copper(I) can engage in π-backbonding with low-lying π* orbitals on Me_4phen in a metal-to-ligand charge transfer fashion. Presumably, this interaction gives rise to the compound's intense yellow color, as a feature is present at 388 nm in the electronic spectrum of **3** (Figure 3.9).

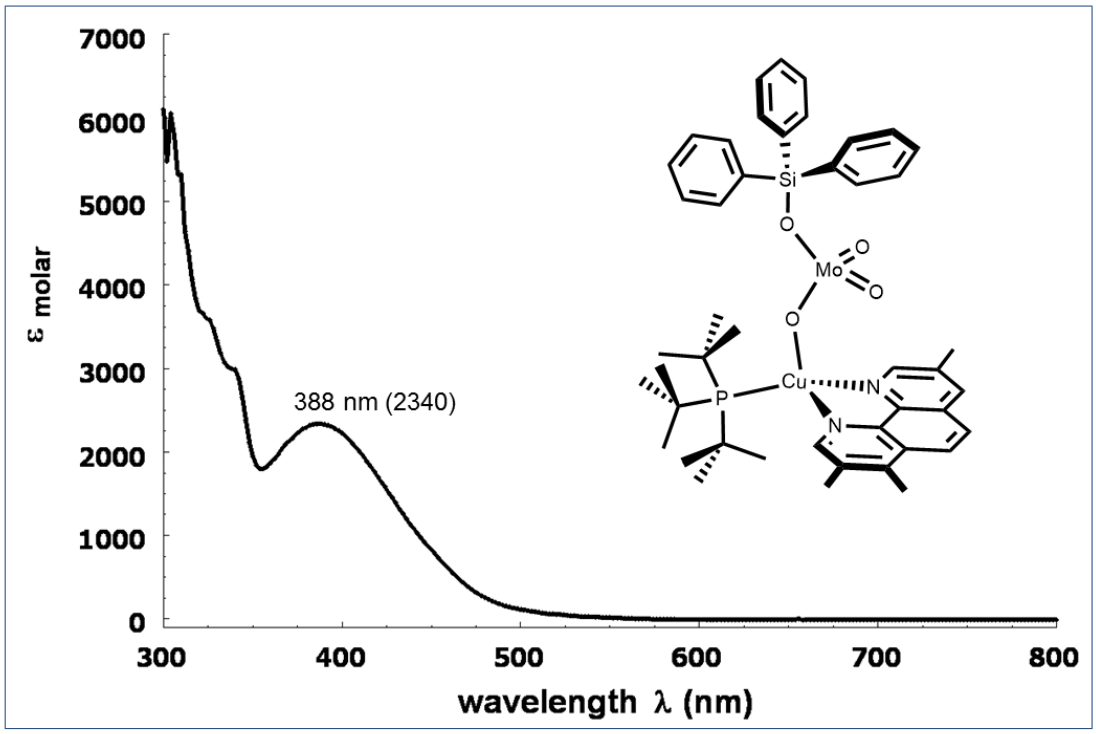

Figure 3.9 UV-vis spectrum of **3**, 0.54 μM in THF.

While complex **3** lacks a sulfide bridge, the chalcogen-bridged core is tantalizingly close to a desired structure, and offers the possibility for further manipulation in an effort to substitute bridging oxo for bridging sulfide. Unfortunately, the synthesis of complex **3** is not reproducible, and attempts to regenerate **3** synthetically appear to lead to different

cluster-type products akin to **2**, with concomitant isolation of small quantities of free Me_4phen. Additionally, a small scale reaction of **3** with hexamethyldisilathiane, $Me_3Si{-}S{-}SiMe_3$, resulted in apparent decomposition of the starting material. Moreover, reactions between other copper coupling components ([Cu(IMes)(SSi^iPr_3)] and [Cu(triphos)(SSi^iPr_3)]) and [MoO_2(Me_4phen)($OSiPh_3)_2$] gave rise to sluggish reactions, from which small amounts of orange-colored products were observed with attending isolation of large quantities of starting material, even with heating and prolonged reaction times. These orange products yielded no indication spectroscopically of a desired product but appear to be similar to the cluster species presented earlier. It is likely that the sterics associated with starting material [MoO_2(Me_4phen)($OSiPh_3)_2$] impede the general reactivity desired within the context of a silane-mediated coupling reaction.

A variety of more flexible, less sterically hindered molybdenum coupling components can be found within the works reported by Spence, Wedd, and Enemark et. al.[51-54] Complexes of the formulation [MoO(N_2S_2)X], where X is any number of anionic ligands, including oxo, chloride, thiolate, siloxide, etc., represent a series of molybdoenzyme analogues. The N_2S_2 ligand (N_2S_2aryl = *N*,*N*′-dimethyl-*N*,*N*′-bis(2-mercaptophenyl)ethylenediamine and N_2S_2alkyl = *N*,*N*′-dimethyl-*N*,*N*′-bis(2-mercaptoethyl)ethylenediamine) is a flexible tetradentate ligand framework that contains both hard nitrogen donor groups and soft thiolate donor groups. This allows the N_2S_2 ligand to stabilize metal centers in a variety of oxidation states. The most interesting complexes in this series as molybdenum coupling components are [MoO(N_2S_2aryl)($OSiMe_3$)] and [MoO(N_2S_2alkyl)($OSiMe_3$)], which contain Mo(V) centers. Individual reactions between [MoO(N_2S_2aryl)($OSiMe_3$)] or

[MoO(N_2S_2alkyl)($OSiMe_3$)] and [Cu(IMes)(SSi^iPr_3)] yield deeply colored reaction mixtures.

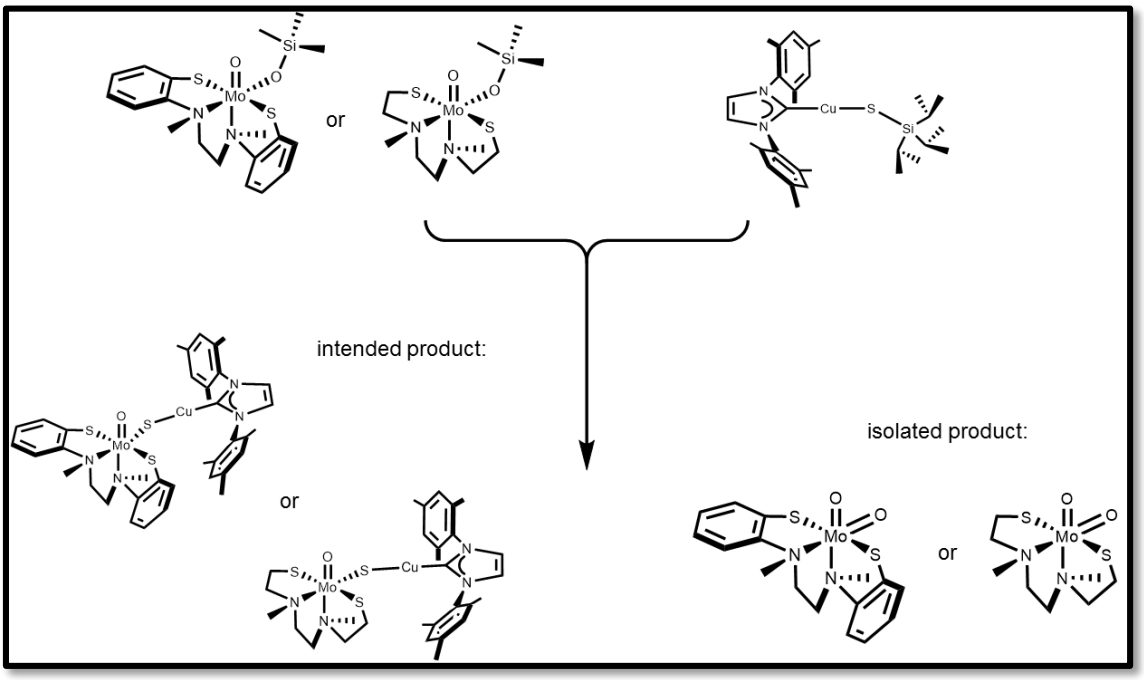

Scheme 3.11 Reaction between [MoO(N_2S_2aryl)($OSiMe_3$)] or [MoO(N_2S_2alkyl)($OSiMe_3$)] and [Cu(IMes)(SSi^iPr_3)].

Dark orange-red crystals from the individual product mixtures were characterized via X-ray crystallography, and found to be the known[51, 55] Mo(VI) *cis*-dioxo forms of the molybdenum starting materials. In these reactions, presumably, [Cu(IMes)(SSi^iPr_3)] abstracts Me_3Si radical to effect a redox reaction resulting in oxidized *cis*-dioxo molybdenum(VI) products, the reverse of which has been documented.[56, 57] It is unclear how or by which mechanism this redox reaction occurs, however, what is clear is that these reactions do not provide access to heterodinuclear species of interest within the context of Mo-CODH modeling. Also, surprisingly, reaction of the chloride precursor

[MoO(N_2S_2aryl)Cl] with [Cu(IMes)(SSi^{i}Pr$_3$)] yielded no reaction, even at elevated temperatures.

Endeavoring to prevent both ligand exchange and cluster formation, a final series of reactions were run making use of a molybdenum coupling component which contains a bulky, rigid salphen ligand framework (salphen = *N*,*N*′-bis(salicylidene)-1,2-benzenediamine). As a starting material, paramagnetic, deep orange-red (Figure 3.11), Mo(V)-containing [MoO(^{t}Bu$_4$salphen)Cl] (**4**) was generated via protonolysis of [MoO(acac)$_2$Cl][58] by H$_2$^{t}Bu$_4$salphen in good yield (Scheme 3.12, H$_2$^{t}Bu$_4$salphen = *N*,*N*′-bis(3,5-di-*tert*-butylsalicylidene)-1,2-benzenediamine).

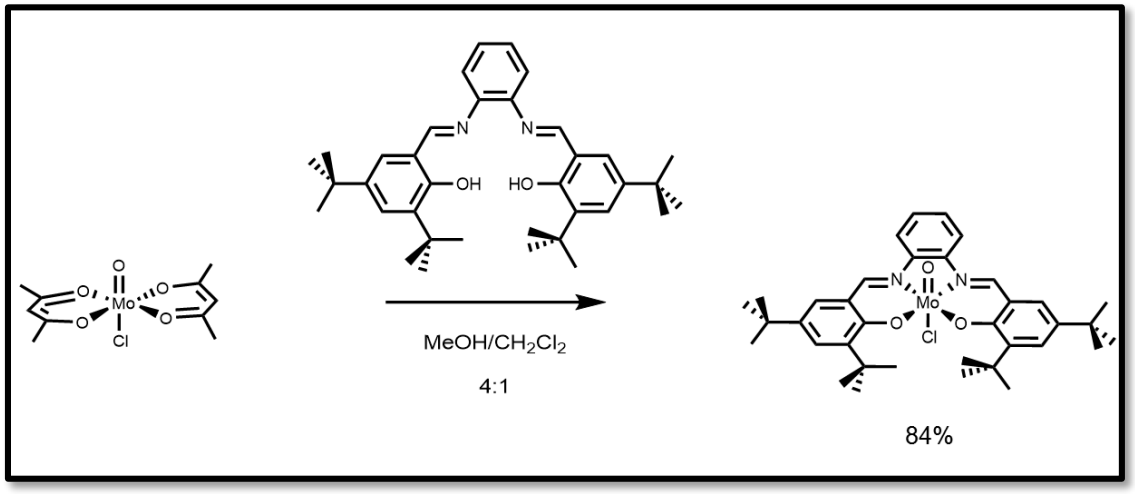

Scheme 3.12 Synthesis of [MoO(^{t}Bu$_4$salphen)Cl].

The rigid, tetradentate salphen ligand about molybdenum should stabilize against ligand exchange and allow reactivity to occur at a face of the molecule. Here, the terminal oxo ligand exerts a strong trans influence felt by the chloride ligand, making the chloride susceptible to substitution. Evidence for this behavior can be seen in the MALDI mass

spectrum (Figure 3.10), where the parent ion minus chloride is observed in positive ion mode.

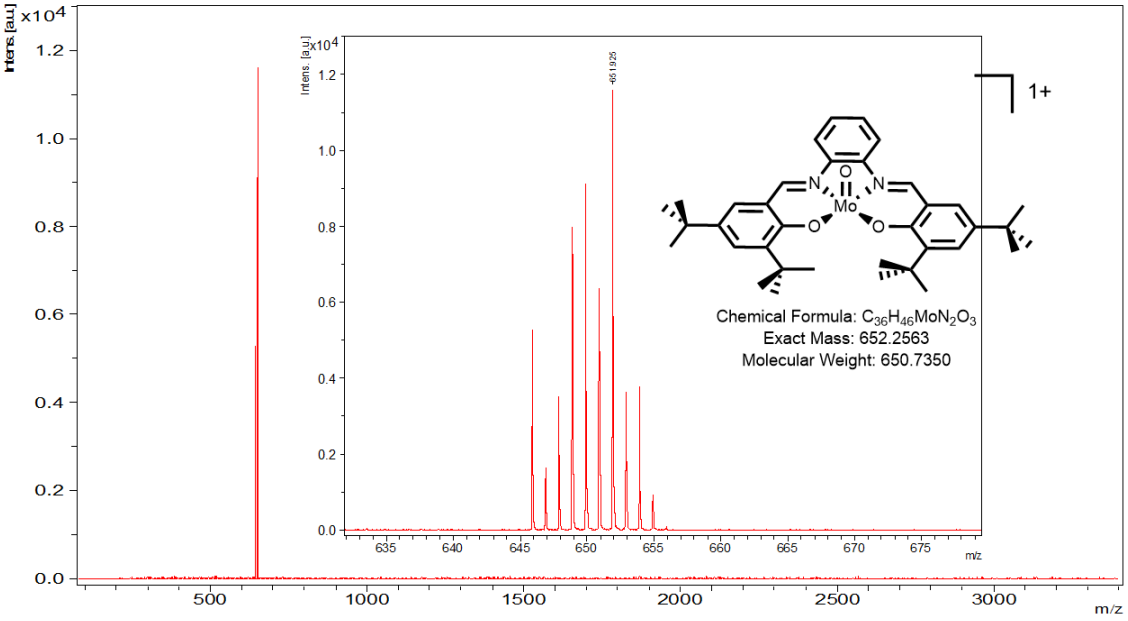

Figure 3.10 Positive ion mode MALDI-MS of $[MoO(^{t}Bu_4salphen)]^{+}$.

An additional structural feature of note, is the presence of flanking, ortho *tert*-butyl groups on the salphen ligand. These bulky groups should act to obstruct reaction between the nearby phenolate oxygen atoms and incoming silyl group. The interaction between a silyl group and a terminal oxo ligand is always a possibility within the context of a silane-mediated coupling reaction. However, monooxo molybdenum complexes are harder to silylate due to the strong, favorable π-donation from oxo to molybdenum's empty dπ orbitals. Thus, it would appear likely that the desired substitution reaction would take place at the chloride-containing face of the molecule.

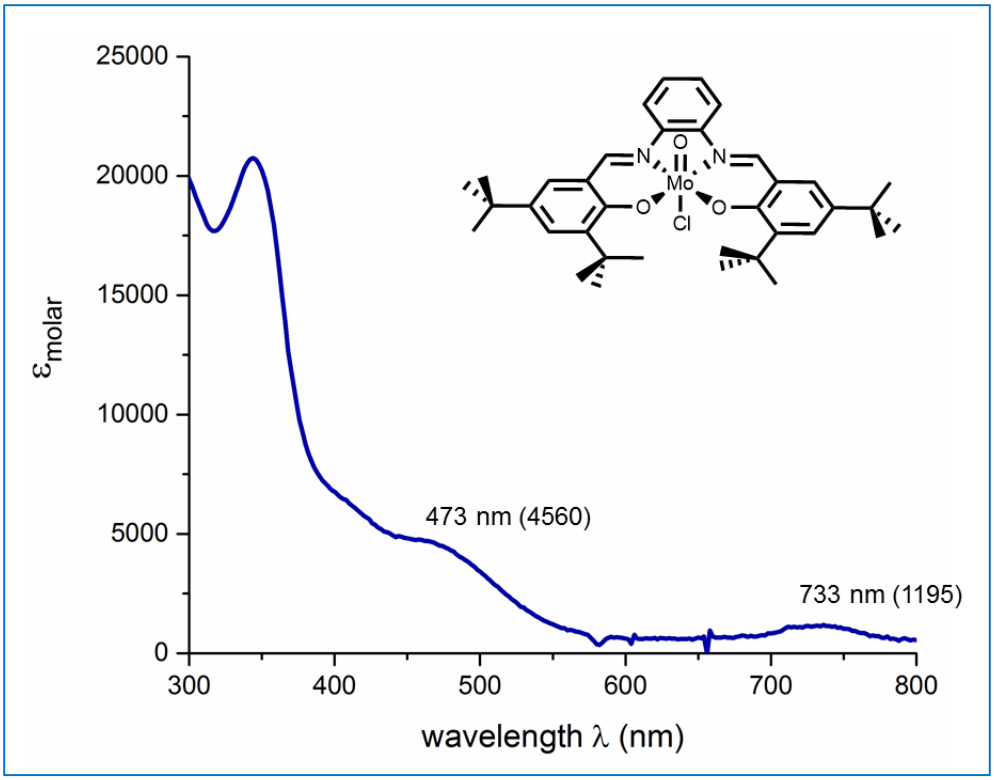

Figure 3.11 UV-vis spectrum of [MoO(^{t}Bu$_4$salphen)Cl], 14.6 μM in THF.

The reaction between [MoO(^{t}Bu$_4$salphen)Cl] and [Cu(IMes)(SSi^{i}Pr$_3$)] gave rise to a deep red-orange solution, from which a paramagnetic, uniform, dark red-orange solid is obtained (Scheme 3.13). While single crystals of the product were not forthcoming, mass spectrometry reveals the presence of two distinct fragments, [MoO(^{t}Bu$_4$salphen)]$^+$ and [Cu(IMes)$_2$]$^+$ (Figure 3.12). Again, the appearance of the fragment [Cu(IMes)$_2$]$^+$ is an artifact of ionization and indicates the presence of *at least* [Cu(IMes)]$^+$. All characterized molecules containing at least the [Cu(IMes)]$^+$ motif feature this fragment via mass spectrometry. These fragments persist after thorough washing and precipitation of the product, which suggest that a single product has been isolated and contains both Mo and Cu, each with their desired ligand components intact.

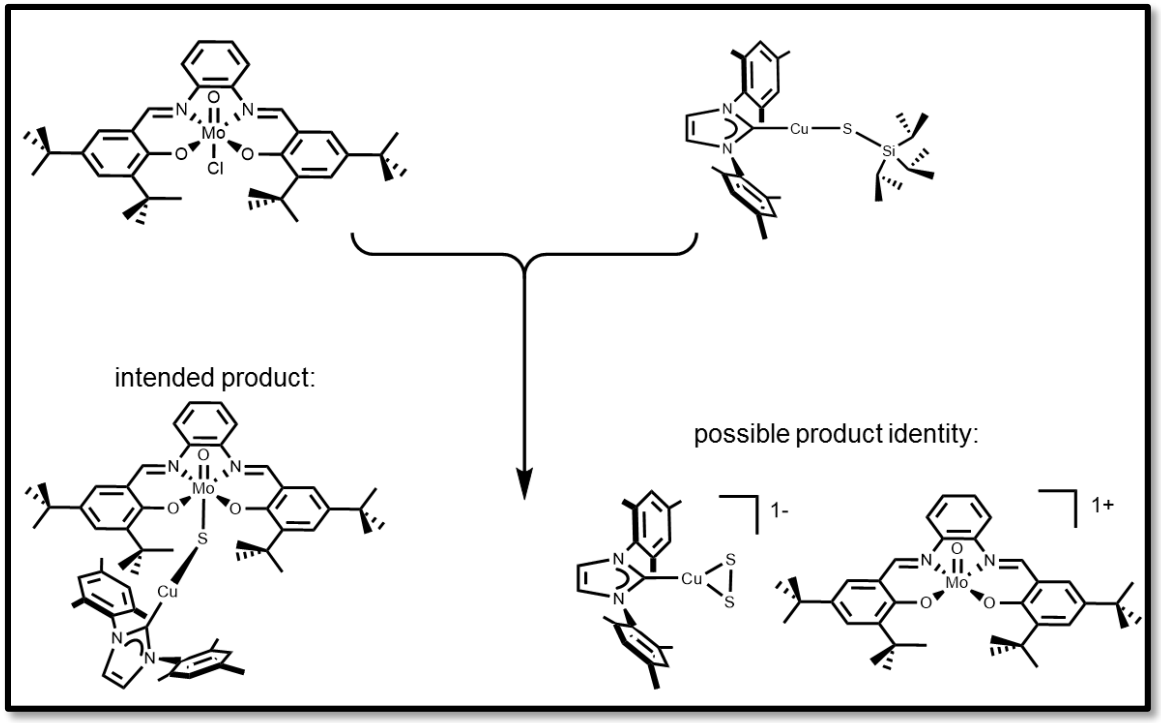

Scheme 3.13 Reaction between [MoO(^{t}Bu$_4$salphen)Cl] and [Cu(IMes)(SSi^{i}Pr$_3$)].

No additional features are present in the mass spectrum, and one might imagine the most tenuous connection within the desired product to be the fragile sulfide bridge. Moreover, the size and stability attributed to the tetradentate salphen ligand should keep the ligand anchored to molybdenum and thwart polynuclear product formation. Thus, it appeared likely that a desired product was formed. However, further structural verification was required.

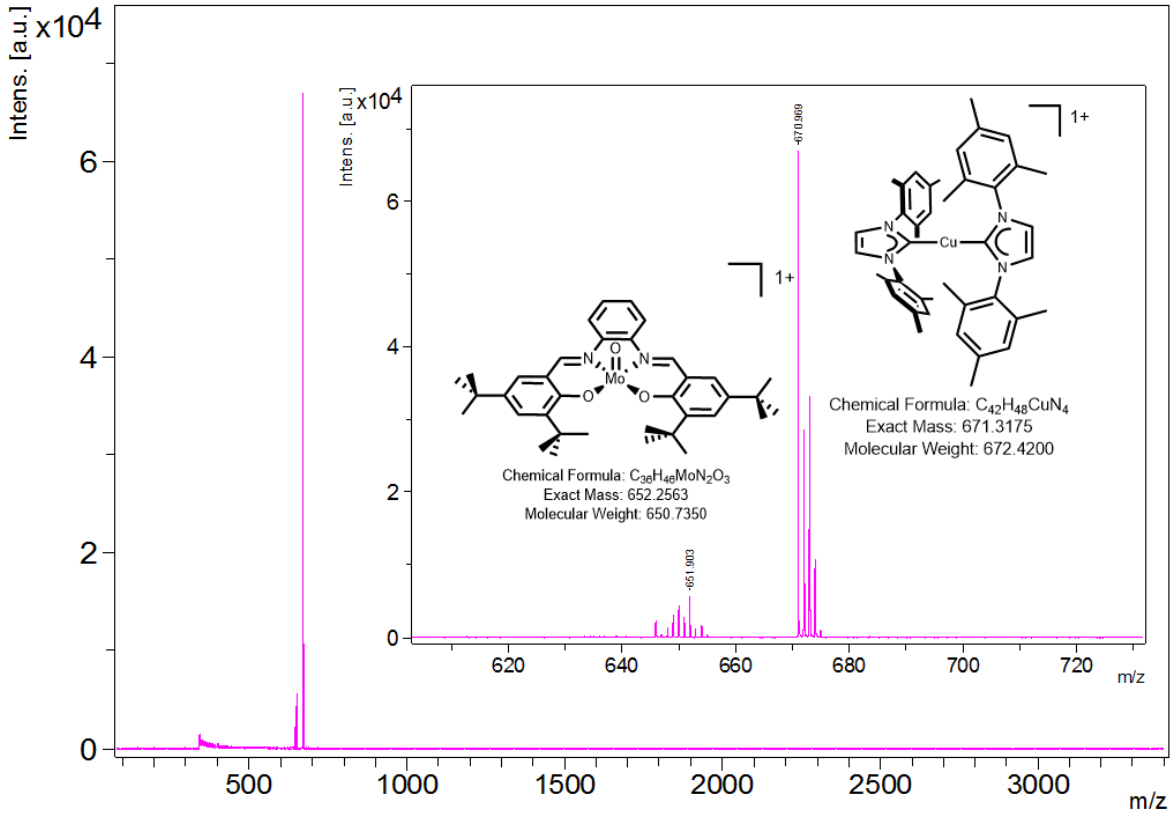

Figure 3.12 MALDI-MS of the product obtained from the reaction shown in Scheme 3.13.

For the purpose of gaining more information as to the actual identity of the product formed from the reaction described in Scheme 3.13, samples were sent to collaborators for electron paramagnetic resonance (EPR) and X-ray absorption spectroscopy (XAS) measurements. Analysis of this product via EPR reveals no evidence for hyperfine coupling to copper. Our collaborator, Professor Stephen Sproules at the University of Glasgow, describes the spectrum (Figure 3.13) as containing two, possibly three distinct Mo(V) species present in the spectrum at room temperature. These findings suggest a more complex assignment of the product, and may provide some justification for why single crystal formation remains elusive.

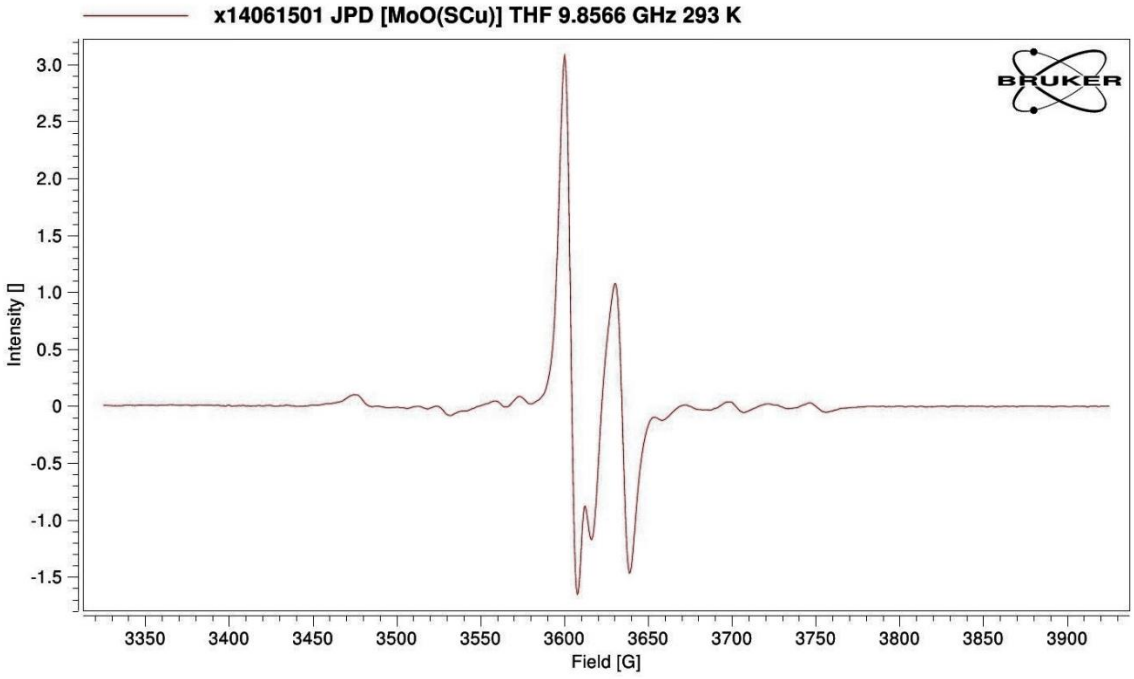

Figure 3.13 Room temperature EPR spectrum of the product isolated from the reaction described in Scheme 3.13.

XAS measurements of the same sample were performed by Professor Kyle Lancaster at Cornell University. His analysis reveals no backscattering from molybdenum at the copper K-edge. He notes that the best fit seems to indicate a three-coordinate Cu(I) ion ligated by two sulfurs (possibly disulfide) and a carbene carbon. At the molybdenum L-edge, the terminal oxo ligand is present, as is the N_2O_2 environment of the salphen ligand. However, no ligand *trans* to the terminal oxo group is visible. These results suggest that the product contains separate molybdenum and copper fragments, presumably like that pictorially represented in Scheme 3.13.

Taken together, the results provided for the reaction shown in Scheme 3.13 indicate a rather complicated product formulation which, at the time of this writing, has

still not been entirely elucidated. What is clear is that this reaction does not provide access to a structural analogue of Mo-CODH.

The reaction between [MoO(^{t}Bu$_4$salphen)Cl] and [Cu(P^{t}Bu$_3$)(SSiPh$_3$)] takes a different course. Upon mixing, a deep orange-red solution (Figure 3.14) is produced, which affords an orange-red product that is considerably more soluble than the molybdenum starting material (completely soluble in benzene, toluene, etc.).

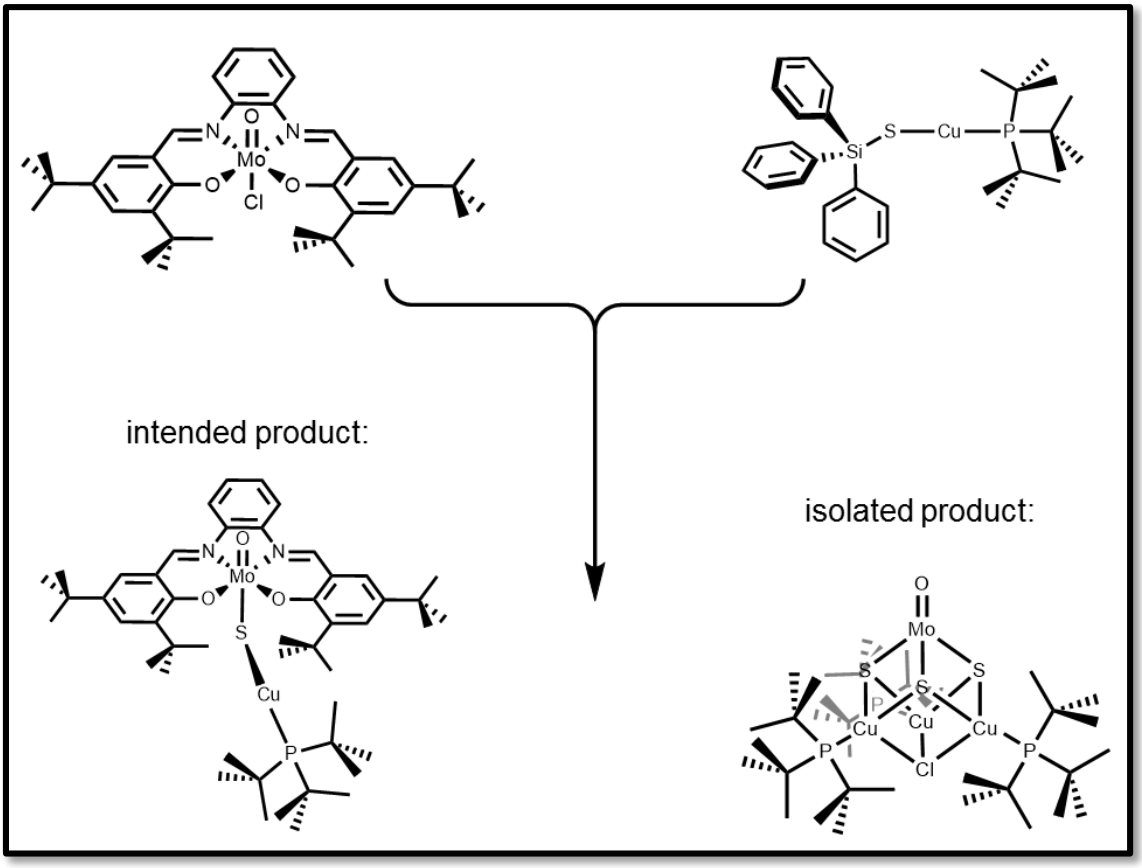

Scheme 3.14 Reaction between [MoO(^{t}Bu$_4$salphen)Cl] and [Cu(P^{t}Bu$_3$)(SSiPh$_3$)].

Crystals from this crude product were isolated and analyzed crytallographically. The crystallography reveals the product to be that of **2**, the heterocubane formulated as [Mo(=O)S_3(CuP^tBu_3)$_3$Cl] (Scheme 3.13).

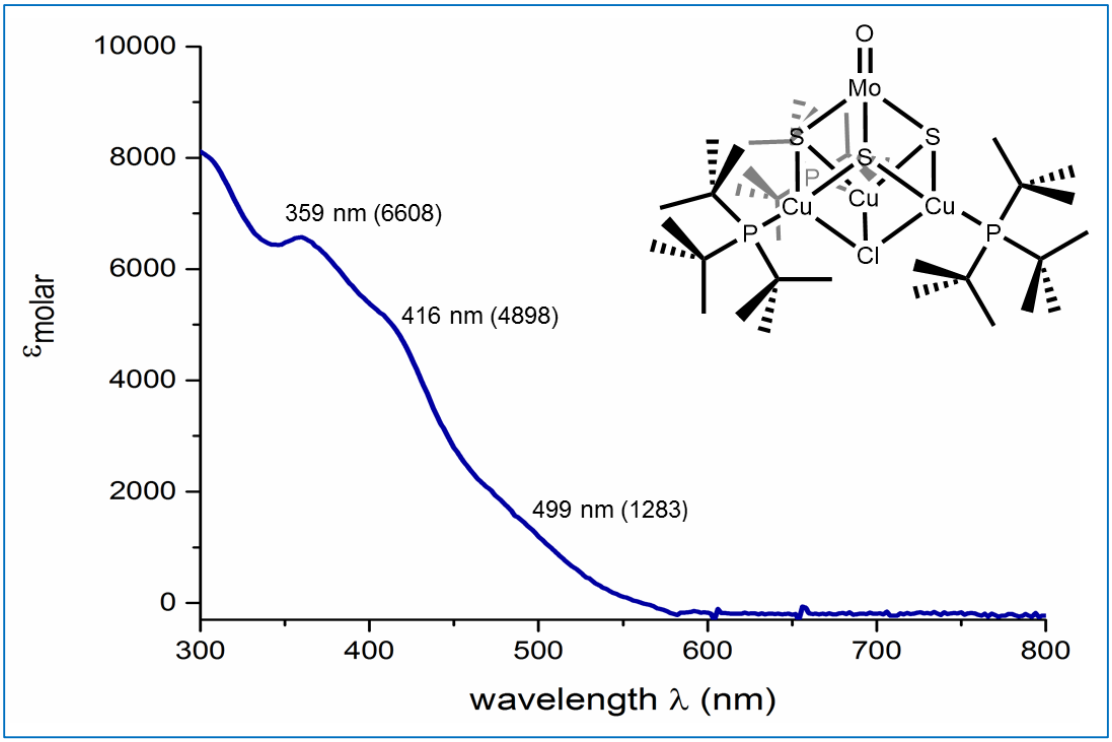

Figure 3.14 UV-vis of [Mo(=O)S_3(CuP^tBu_3)$_3$Cl], 44.2 μM in THF.

As in the previous case (*vide supra*) for **2**, the charge neutral heterocubane structure emerges from a structure solution, but cannot be properly refined. Spectroscopic evidence for **2** falls in line with the crystallography. It appears that no lower energy, weak intensity band is observed in the electronic absorption spectrum which would be indicative of a d-d transition (Figure 3.14). Furthermore, these crystals give rise to a diamagnetic ^{1}H NMR spectrum, which only contains the ^{t}Bu$_3$P associated doublet (Figure 3.15). Mass spectrometry also exhibits the isotope distribution pattern characteristic of the [Mo(=O)S_3(CuP^tBu_3)$_3$]$^+$ cation in positive ion mode (Figure 3.16).

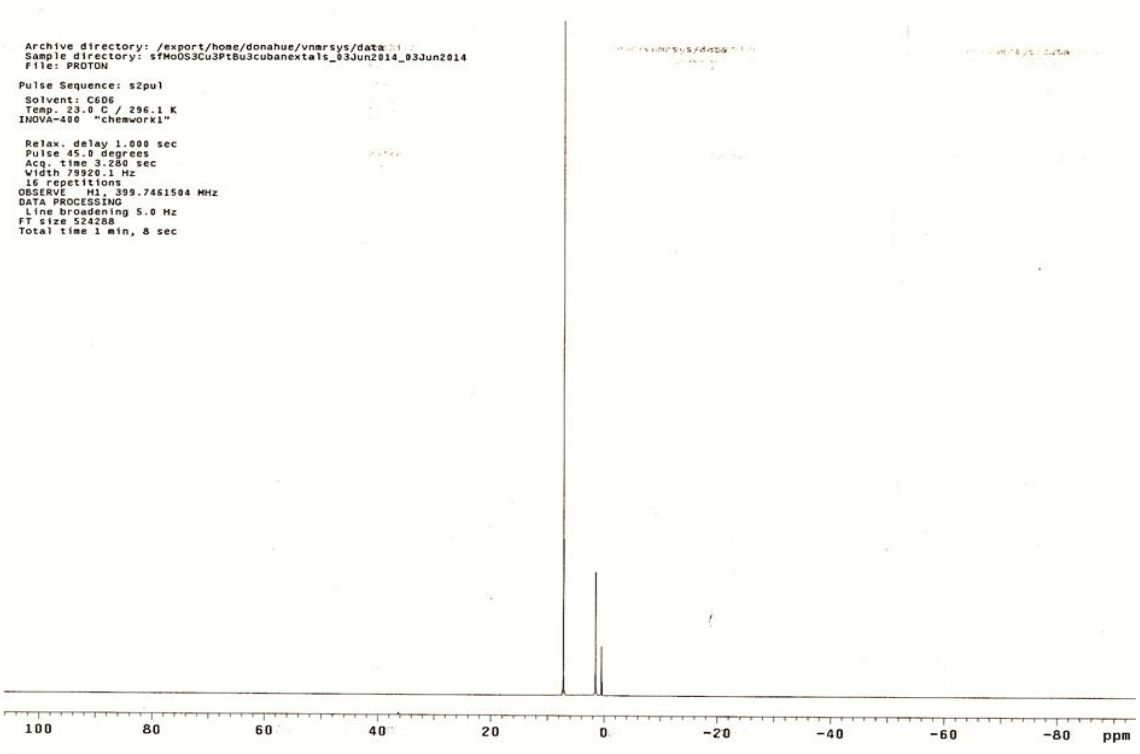

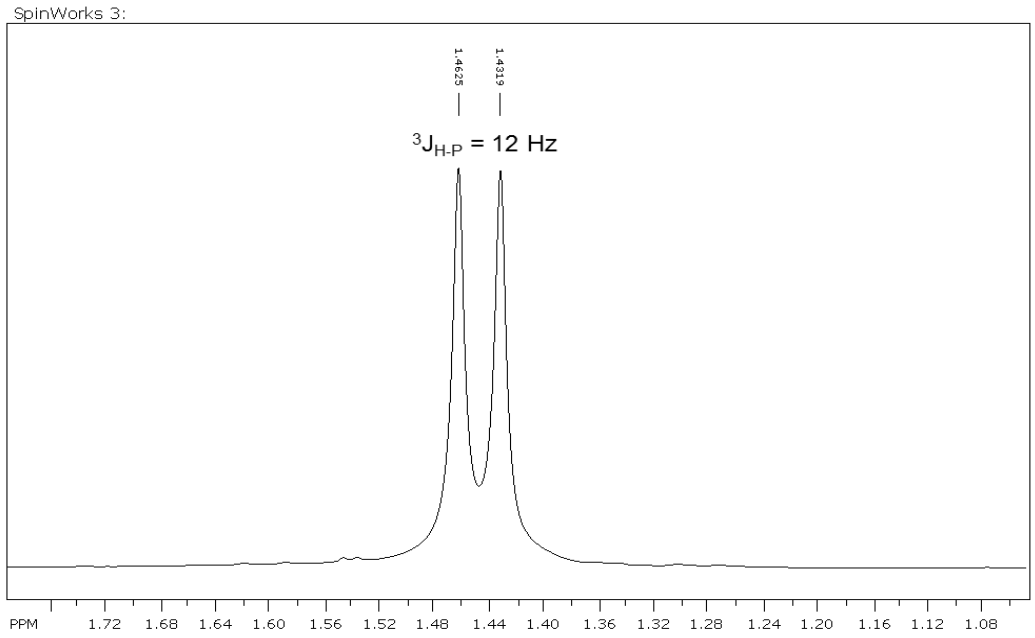

Figure 3.15 ^{1}H NMR spectrum of [Mo(=O)S_3(CuP^tBu_3)$_3$Cl]. Full spectral width (+100 ppm to -100 ppm) to display the absence of paramagnetism and showing benzene solvent residual (most downfield), P^tBu_3 (middle) and TMS (0 ppm) (top spectrum), and P^tBu_3 doublet (bottom spectrum).

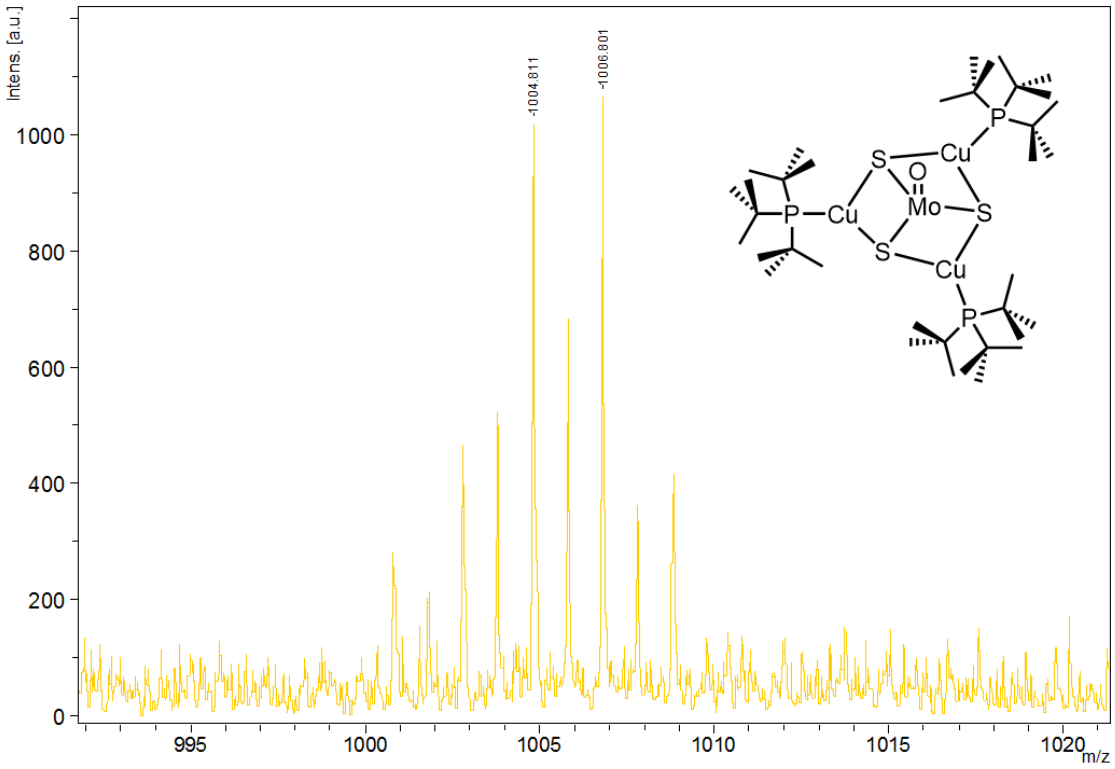

Figure 3.16 MALDI-MS of $[Mo(=O)S_3(CuP^tBu_3)_3]^+$ from the reaction shown in Scheme 3.14 in positive ion mode.

The process by which this redox reaction occurs is unclear. What is remarkable, and should not be understated, is the apparent thermodynamic driving force to not only produce $[Mo(\mu\text{-}S)_2Cu]$ rhombs, but to form this specific heterocubane product, since this particular product was generated from two very different reactions (Scheme 3.9 and Scheme 3.14). Further commentary on the silane-mediated coupling reaction methodology within the context of Mo-CODH analogue preparation will appear in the Summary and Conclusions section of this chapter.

Reactions Between Terminal Sulfido Molybdenum Complexes and Labile Copper Salts

A second synthetic approach toward constructing a model of Mo-CODH takes advantage of monovalent copper's mercaptophilicity. Soft copper(I) interacts strongly with soft sulfur ion to form stable bonding scenarios. In this context, labile copper(I) salts should react with molybdenum precursors which contain terminal sulfido groups to effectively condense the two discrete complexes into one. Essentially, a labile copper fragment should be able to coordinate to a terminal sulfido group on molybdenum. A reaction scheme for this interaction is shown in Scheme 3.15.

Scheme 3.15 Reaction between a labile copper(I) salt and a sulfidomolybdenum complex.

Evidence for this type of reactivity is found in the seminal work reported by Young et al. in the introduction of this chapter.[27] The generality of this reaction is not made clear from that report, and the simplicity of the approach warrants exploration. Numerous copper(I) salts containing a labile acetonitrile ligand of the formulation $[LCu\text{-}NCMe]^+$ exist and are accessible. These salts emerge as ideal starting materials due to the flexibility of the neutral L ligand with respect to size, denticity, and electronic effects, all which can be tuned appropriately. Unfortunately, the instability of mixed, oxosulfido

complexes of molybdenum detracts from their use within this scenario. Nonetheless, a few known complexes are accessible and form the basis for exploring this reaction-type.

The first series of reactions employed the known oxosulfido complex, $(Et_4N)_2[MoO_3S]$,[59] as the molybdenum starting material. A synthetic procedure for this monothiomolybdate exists; however, a new, simpler preparation using hexamethyldisilathiane was devised and provided usable quantities of this starting material (see the Experimental section of this chapter). The reaction between $(Et_4N)_2[MoO_3S]$ and $[Cu(S93)(MeCN)][BF_4]$[60] (S93 = 1,4,7-trithiacyclononane) gave rise to a dark orange reaction mixture with a dark orange precipitate.

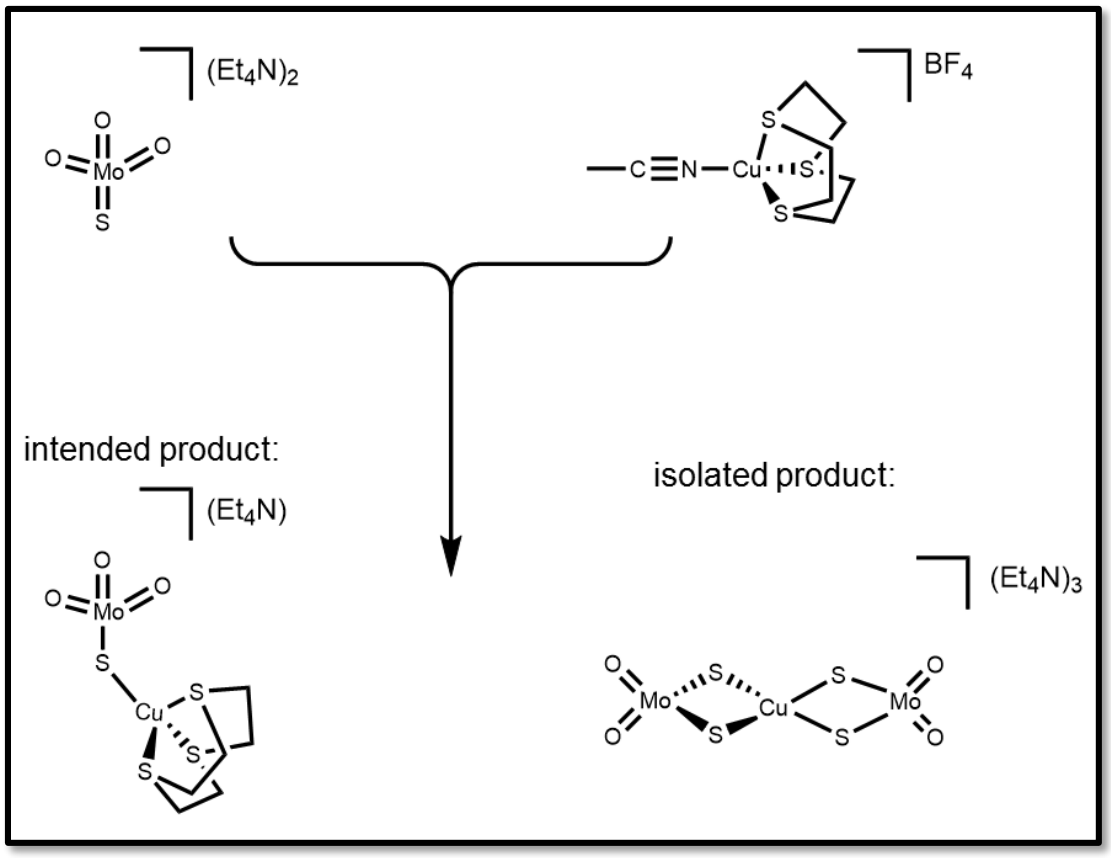

Scheme 3.16 Reaction between $(Et_4N)_2[MoO_3S]$ and $[Cu(S93)(MeCN)[BF_4]$.

The product isolated from this reaction was only very sparingly soluble in organic solvents, indicative of oligomeric or polymeric species. X-ray crystallography on a small set of crystals isolated from this reaction mixture revealed the identity of the product obtained to be trinuclear $(Et_4N)_3[O_2Mo(\mu\text{-}S)_2Cu(\mu\text{-}S)_2MoO_2]$ (Scheme 3.16). Similarly, reaction between $(Et_4N)_2[MoO_3S]$ and other copper(I) salts gave rise to dark-colored intractable products, again indicative of multinuclear, oligomeric, or polynuclear species. This result occured at both room temperature and reduced temperature and appeared to be solvent-dependent. Using acetonitrile as the solvent led to almost exclusive intractable product formation. Employing mixed MeCN/THF or pure THF as a solvent seemed to slow down the formation of intractable products but did not prevent them from forming completely. Product mixtures from THF or a MeCN/THF combination afforded smaller amounts of intractable product with mostly starting material as the other identifiable species.

In one instance, the heterogeneous reaction between $(Et_4N)_2[MoO_3S]$ and $[Cu(IMes)(MeCN)][PF_6]$[61] in THF gave rise to a yellow filtrate from which crystals of $(Et_4N)[O_2Mo(\mu\text{-}S)_2Cu(IMes)]$ were isolated (Scheme 3.17). While the isolation of this product appeared encouraging, this product was found in mixture with mostly starting material, as confirmed spectroscopically. These results suggested that $(Et_4N)_2[MoO_3S]$ was perhaps too reactive and that the combination of this starting material and labile copper(I) salts was too susceptible to cluster formation.

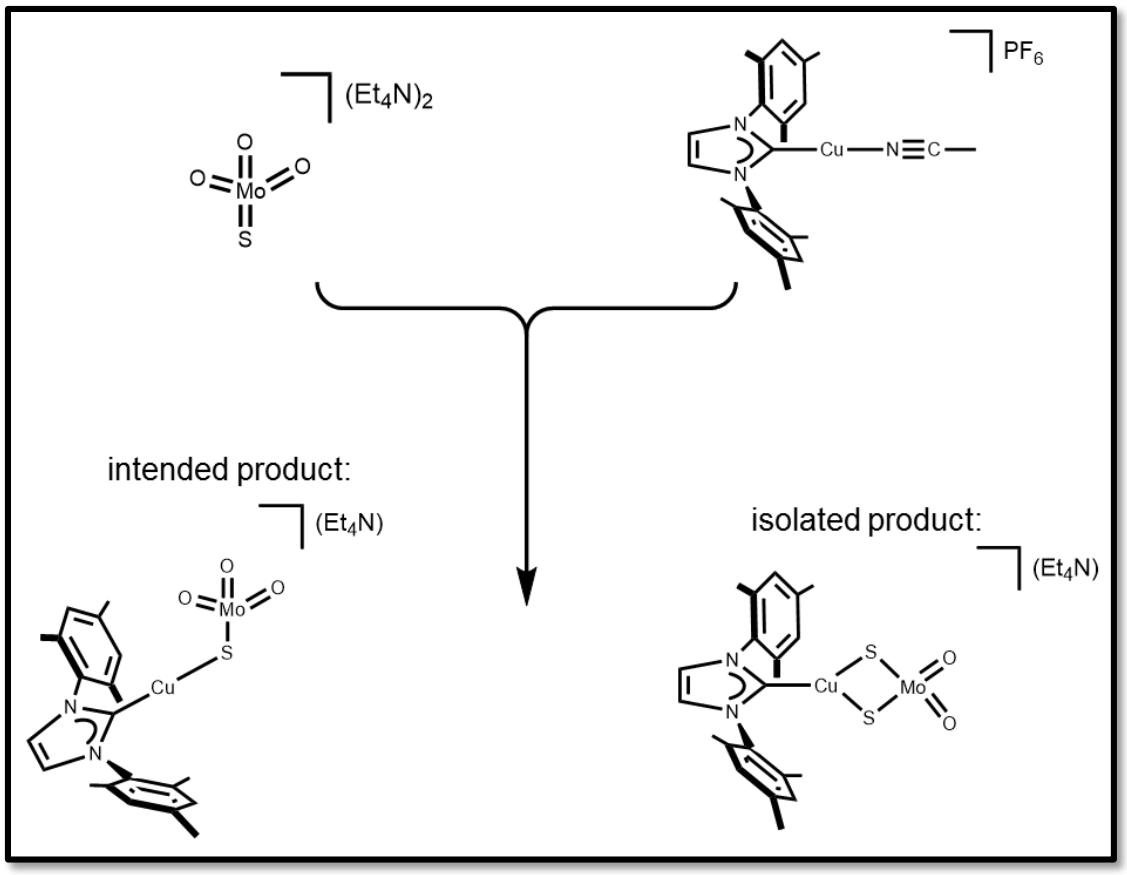

Scheme 3.17 Reaction between $(Et_4N)_2[MoO_3S]$ and $[Cu(IMes)(MeCN)][PF_6]$ in THF.

Turning to another oxosulfido molybdenum starting material that should be less prone to cluster formation, known $[(phen)MoOS(OSiPh_3)_2]$[62] was used in a series of reactions. This complex provides considerable steric hindrance and has the advantage of being more soluble in organic solvents than polar $(Et_4N)_2[MoO_3S]$. The reaction between $[(phen)MoOS(OSiPh_3)_2]$ and $[Cu(IMes)(MeCN)][PF_6]$ in DCM generated a deep orange product mixture. Analysis of the product mixture via ^1H NMR was complicated and showed the presence of what appeared to be a number of different species. What was clear from the ^1H NMR spectroscopy was that the two halves of the phen ligand were no

longer chemically inequivalent, which indicated a product containing some symmetry different from the asymmetric [(phen)MoOS(OSiPh$_3$)$_2$] starting material (Scheme 3.18).

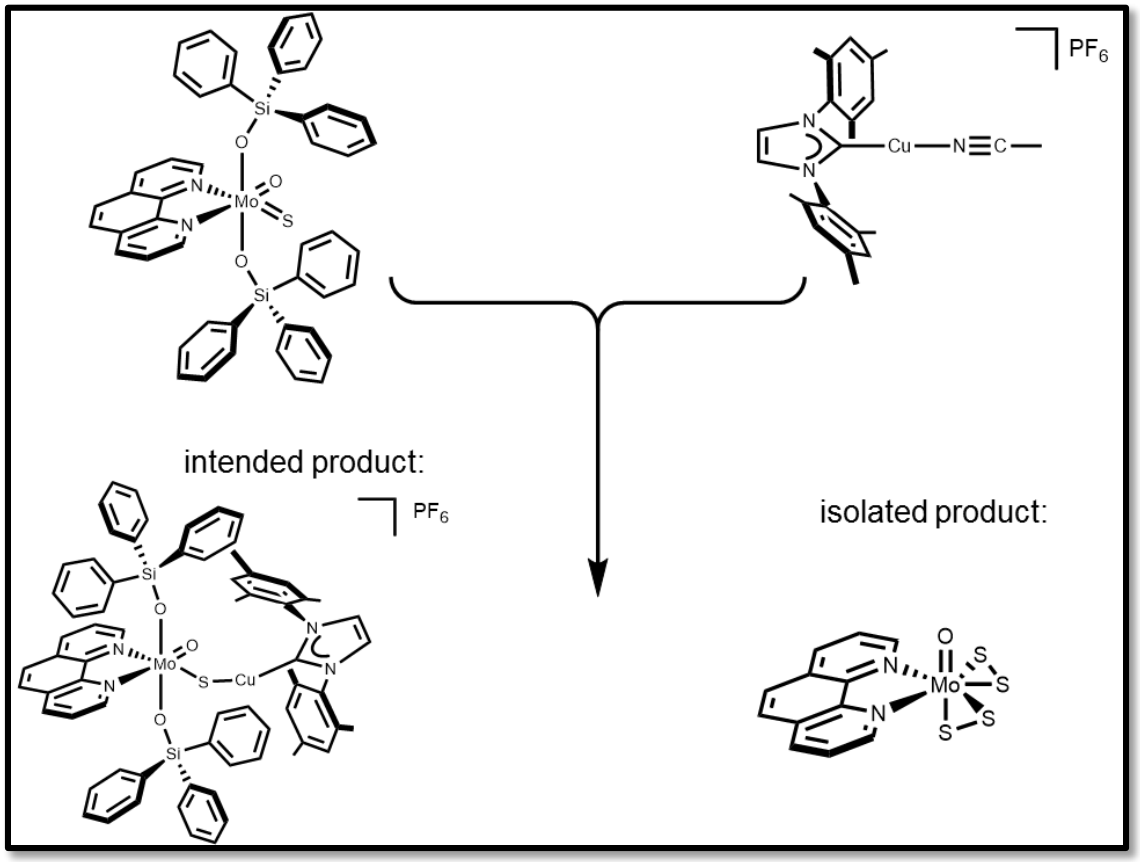

Scheme 3.18 Reaction between [(phen)MoOS(OSiPh$_3$)$_2$] and [Cu(IMes)(MeCN)][PF$_6$].

Crystals from the orange component of the mixture were analyzed crystallographically and found to be [(phen)MoO(S−S)$_2$] (Scheme 3.18). This charge neutral complex contained no copper component and indicated that a high degree of sulfur atom shuffling occured at some point over the course of the reaction.

Rationalizing that perhaps the low-coordinate nature of the [Cu(IMes)(MeCN)][PF$_6$] starting material may aid in this undesired shuffling of sulfur

atoms, a four-coordinate copper starting material was used to explore this reaction. The reaction between [(phen)MoOS(OSiPh$_3$)$_2$] and [Cu(Tpm*)(MeCN)][PF$_6$] (Tpm* = tris(3,5-dimethyl-1-pyrazolyl)methane) in DCM also afforded a dark orange reaction mixture (Scheme 3.19).

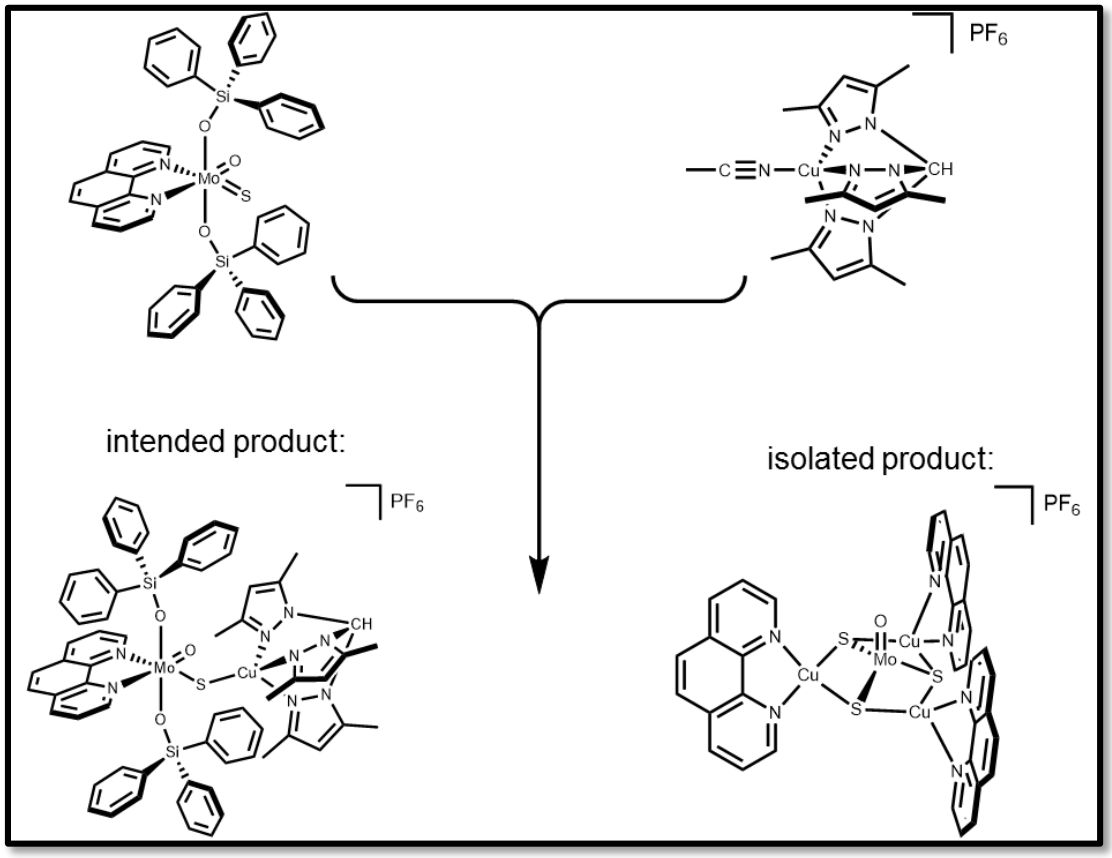

Scheme 3.19 Reaction between [(phen)MoOS(OSiPh$_3$)$_2$] and [Cu(Tpm*)(MeCN)][PF$_6$].

Again, analysis of the crude product mixture via ^{1}H NMR revealed the phen ligand to contain chemical equivalency suggestive of symmetric binding. Crystals from the deep orange product analyzed by crystallography disclosed the identity of the product species to be voided heterocubane [MoO(μ-S)$_3$(Cu(phen))$_3$][PF$_6$], **5**. Despite the steric hindrance provided by the tridentate Tpm* ligand, this reaction proceeds with complete

displacement of Tpm* and migration of phen from molybdenum to copper. As observed previously, the apparent driving force for this ligand exchange is the favorable bonding scenario between closed-shell d^{10} Cu(I) and the π-acidic phen ligand.

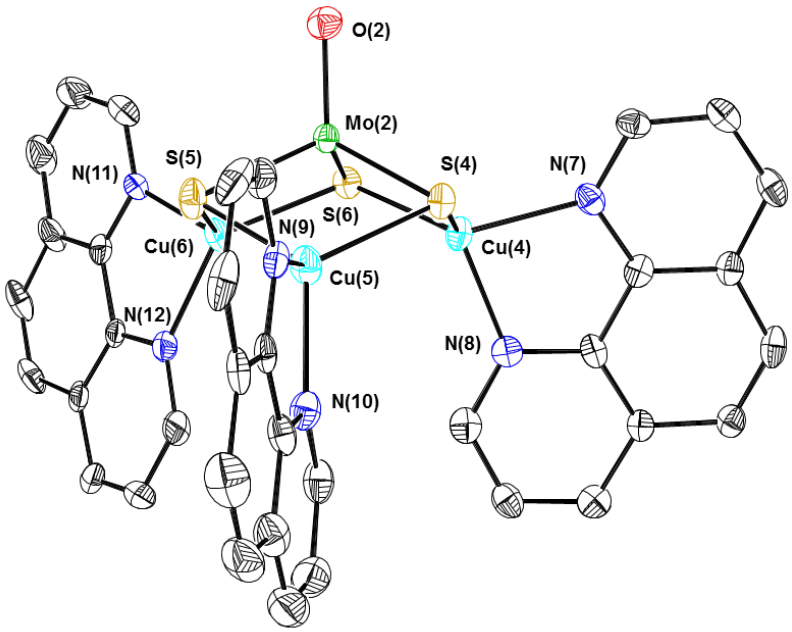

Figure 3.17 Crystal structure of $[MoO(\mu\text{-}S)_3(Cu(phen))_3]^+$ cation **5**. Thermal ellipsoid plot drawn at the 50% probability level. Hydrogen atoms are omitted for clarity.

Rationalizing that a charge neutral product may be more stable than a charged species, in line with the work reported by Young et al.,[27] a reduced form of the molybdenum oxosulfido complex was investigated. Electrochemical analysis of high-valent Mo(VI)-containing $[(phen)MoOS(OSiPh_3)_2]$ was not reported in the original work in which this complex appeared.

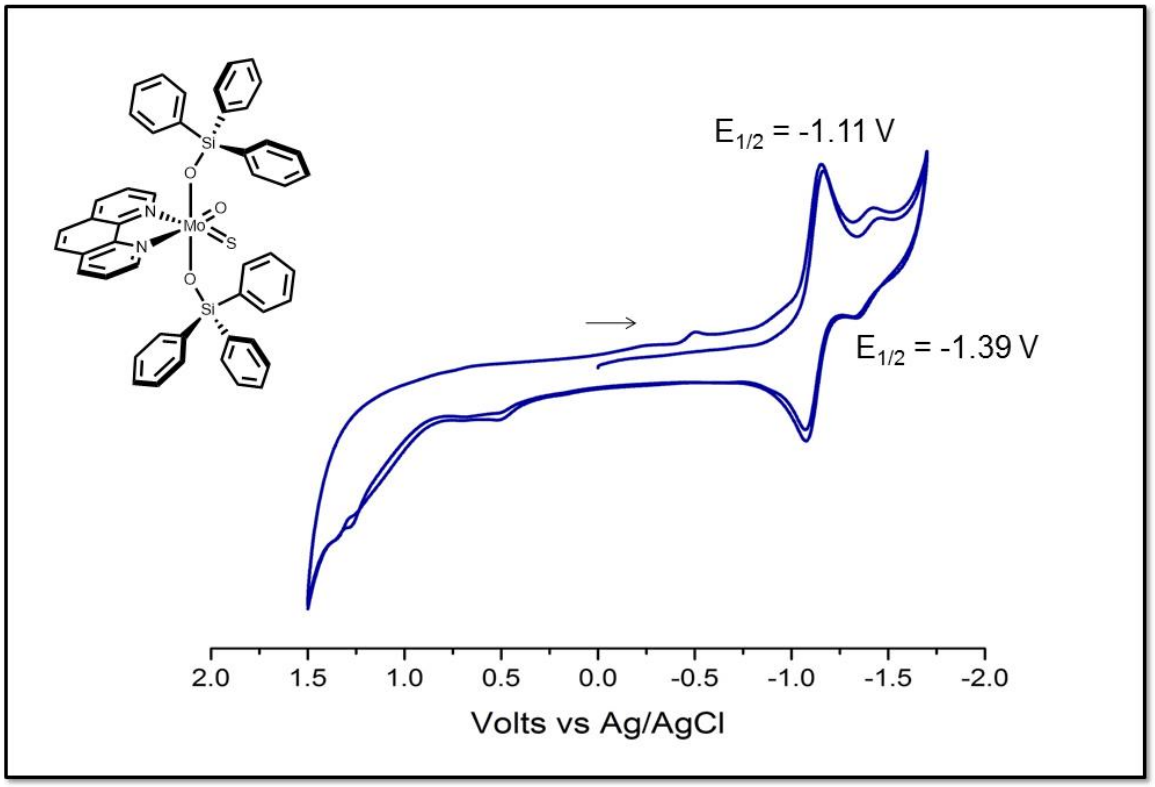

Figure 3.18 Cyclic voltammogram (100 mV/s scan rate, cathodic direction) of [(phen)MoOS($OSiPh_3$)$_2$] in DCM with [Bu_4N][PF_6] electrolyte.

Cyclic voltammetry revealed a reversible feature at $E_{1/2}$ = -1.11 V with a second, quasireversible feature at $E_{1/2}$ = -1.39 V versus Ag/AgCl. This observation indicated that charge neutral [(phen)MoOS($OSiPh_3$)$_2$] should be stable upon chemical reduction. Addition of the reducing reagent decamethylcobaltocene (Cp^*_2Co) to orange solutions of [(phen)MoOS($OSiPh_3$)$_2$] generated a deep cherry-red solution within ~15 mins. Labile copper(I) salts such as those described previously were then added to the reduced complex, which was generated *in situ*. In all reactions, complex mixtures were obtained, from which no spectroscopic evidence for a desired heteronuclear product was found. The paramagnetic nature of the crude products made ^{1}H NMR analysis difficult, and no mass spectrometric analysis displayed any species of interest. In most reactions, isolation

of yellow $Cp^*_2Co(III)$ salts dominated the accessible products obtained in the reaction work-up. In one instance, a structure solution emerged via X-ray crystallography for a red-orange colored crystal from one of the reactions. The solution indicated a [Mo−S−Co] linkage, but the identity of the molecule was polynuclear and contained no copper, so it was not further refined.

Similar to the reactivity observed in the series of silane-mediated coupling reactions, the reaction of terminal sulfido molybdenum complexes with labile copper(I) salts gave rise to species which feature $[Mo(\mu\text{-}S)_2Cu]$ rhomb cores. Even when both starting materials incorporate sterically hindering ligands, the formation of polynuclear, heterocubane or voided heterocubane structures readily occured. Further commentary on this reaction-type can be found in the Summary and Conclusions section of this chapter.

Miscellaneous Reactions

Several other attempts at synthesizing heteronuclear complexes relevant to Mo-CODH by synthetic approaches different than those described above were made, yet were unsuccessful. Some reactions involved multiple starting material components and gave rise to unique products, although not pertinent within the context of Mo-CODH modeling. A few of these products will be discussed in Chapter 4 of this dissertation.

Summary and Conclusions

From the reactions described above and more which are not cataloged here, it is evident that a general approach toward forming an analogue of Mo-CODH is not easily accessible either by a silane-mediated coupling approach or by the reaction of a terminal sulfido molybdenum species with labile copper(I) complexes. In all stoichiometric 1:1 reactions, complicated mixtures of products were formed. This result appeared to persist regardless of choice of solvent or temperature at which the reaction was run. Observed in both approaches was the tendency to form and subsequently isolate heteronuclear cluster species, predominantly of the voided heterocubane or heterocubane type. It is likely, with respect to mass balance, that polar oxomolybdenum species made up the remaining uncharacterized portion of the product mixture. These species were hard to isolate and analyze, and tended to decompose or generate molybdenum blues in the work up. Given that most cluster species were comprised of one oxomolybdenum fragment and three copper fragments, attempts to obviate these clusters from forming by introducing more molybdenum starting material also were unsuccessful. In this case, the same cluster species were produced with greater amounts of starting material recovered. Since the products described above were obtained either in low yield or were only indicative of the crystals which form from the bulk of the crude reaction mixture, yields are not presented, as they have little meaning within a preparative context here. It is possible, and perhaps quite likely, that formation of a desired species which contains a single sulfide bridge between Mo and Cu occurs. However, such a species forms quickly with respect to the reaction and eventually transforms into a more stable product as mentioned previously. Trapping of a desirable “kinetic product” was not possible by routine synthetic means,

and attempts to characterize such were not made since those efforts lie beyond the scope of the objective at hand. While all attempts to synthesize an analogue of Mo-CODH were unsuccessful, four important points emerge from the experiments performed within this context and are presented below.

1. With respect to the synthetic methodology employed for constructing an analogue of Mo-CODH, both approaches give rise to the desired chemical transformations. The silane-mediated coupling approach effectively couples a molybdenum fragment to a sulfur-containing copper fragment, which is bridged by sulfur, with concomitant release of a $R_3Si{-}X$ byproduct. Likewise, the reaction between a terminal sulfido molybdenum complex with a labile copper(I) salt leads to, in many cases, condensation to form products which contain both metal ions bridged by sulfur. However, these reactions are either not altogether very specific, or ultimately facilitate a stronger driving force for product formation, like the production of thermodynamically stable [Mo(μ-S)$_2$Cu] rhombs. Given the number of possible combinations of starting materials with respect to both approaches, it may simply be the case that a specific combination or select few specific combinations afford a desirable product, as is apparently the case with the analogue reported by Young et. al.[27] Formation of the Young analogue appears to occur under rather specific conditions, and it is noteworthy that no follow-up work was performed with it, nor have any successive analogues come from his group.

2. From the nature of the products isolated from the reactions described in this chapter, it is clear that some form of ligand scrambling occurs. This type of rearrangement seems to be consistent with that reported by Holm et. al.[29] Formation of [Mo(μ-S)$_2$Cu] rhomb-containing species is accompanied by creation of

polyoxomolybdenum species. Evidence for this is observed directly in at least one instance, where a polyoxoanion complex was recovered from the reaction which produced **1A** and **1B** (*vide supra*). It remains unclear how this shuffling of sulfur and oxygen atoms occurs mechanistically, and without experimental mechanistic studies, can only be speculated upon. If one were to speculate as to how this process happens, a rather minimal, very general can be devised and is shown in Scheme 3.20.

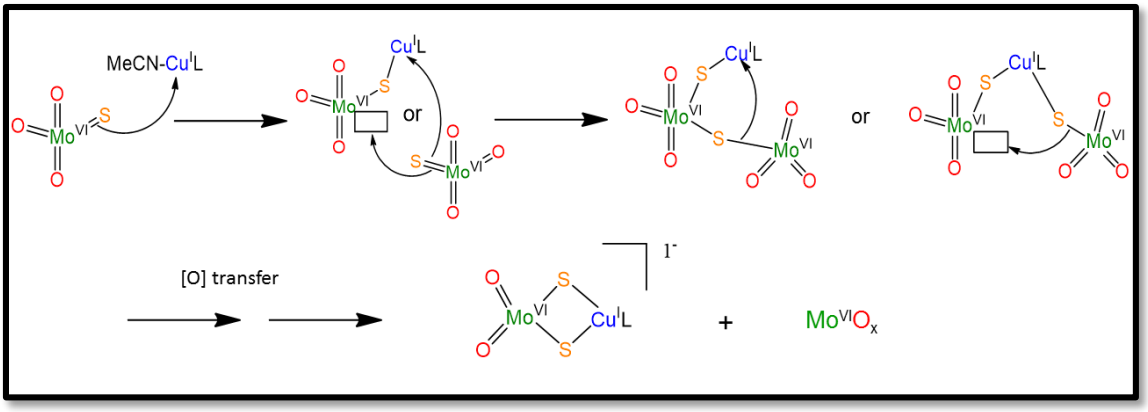

Scheme 3.20 Possible general mechanism for [Mo(μ-S)$_2$Cu] formation.

Displayed in the general scheme above, monothiomolybdate was used as a simplified starting material to show how this process may transpire. Given the simplicity of the scheme, it would not be implausible to extrapolate this scenario to more complicated starting materials, including those involved in a silane-mediated coupling. To envision a silane-mediated coupling reaction within this scheme, one could start in the second step and replace the second monothiomolybdate complex with a copper(I) silylthiolate. Here, the presence of Cu(I) ion appears to facilitate the condensation of sulfur ions about one molybdenum center to form [Mo(μ-S)$_2$Cu] rhomb motifs. Again, it should be stated that this scheme is entirely speculative.

3. Examination of the products isolated from these reactions, even under different reaction conditions, showcase the susceptibility of mixtures containing an oxomolybdenum fragment, copper(I), and a sulfur source to form heterocubanes or voided heterocubanes of the formulation $[MoOS_3(CuL)X]$ (L = neutral donor ligand, X = anionic monodentate ligand) which contain core units comprised of $[Mo(\mu\text{-}S)_2Cu]$ rhombs. These thermodynamically stable entities present a significant challenge in modeling Mo-CODH, and have been touted as problematic in previous reports by other groups.[29, 63] One can surmise that the successful construction of a core containing [Mo−S−Cu], as reported by Young et al.,[27] is attributed to the large steric profiles of each starting material. However, this appears to not be a general method for circumventing $[Mo(\mu\text{-}S)_2Cu]$ rhomb formation, as sterically hindered starting materials described in the reactions within this chapter failed to produce the desirable [Mo−S−Cu] core. What should not be understated, is the remarkable ability with which these rhomb core units form, even under drastically different reaction conditions like those described in Scheme 3.9 and Scheme 3.14. Here, the same heterocubane product, **2**, is generated even when the molybdenum starting material contains a rigid tetradentate ligand and is Mo(V). In the reaction shown in Scheme 3.14, the $[MoO(^tBu_4salphen)Cl]$ starting material undergoes oxidation (Mo(V)→Mo(VI)) and the reaction proceeds with complete displacement of the tetradentate salphen ligand to form heterocubane $[Mo(=O)S_3(CuP^tBu_3)_3Cl]$. Similarly, the reaction described in Scheme 3.19 proceeds with complete displacement of the bulky, tridentate Tpm* ligand on copper. These reactions exist as clear experimental evidence for the strong thermodynamic driving force associated with $[Mo(\mu\text{-}S)_2Cu]$ rhomb formation.

4. A final point worth highlighting is found in the way in which these molecular fragments condense to form clusters. Previous reports on Mo-CODH modeling caution against the complication of "internal reduction" at the molybdenum center, since high-valent molybdenum is unstable with respect to incoming thiolate under certain circumstances.[29, 63] In some cases, Mo(VI) fragments are reduced to Mo(V) with attending condensation of fragments through bridging mercapto moieties in the presence of thiolate anion. While this process is well documented,[30-32] it appears to not occur within the reactions described in this chapter. In fact, in no reaction is the molybdenum fragment reduced, and multinuclear species representative of products from this process were never observed. These results suggest that the presence of copper(I) ion impedes or prohibits, in some fashion, the reduction of molybdenum fragments and their subsequent condensation.

From the results obtained within this chapter, one can begin to contemplate a next direction to take within the context of Mo-CODH modeling chemistry. From the significant synthetic challenge associated with formation of a single sulfide bridged [Mo−S−Cu] core, it appears that a drastic compromise of the structural requirements needs to take place. In this respect, I can offer three possibilities in accessing discrete complexes relevant to Mo-CODH.

Firstly, it is now well documented that reactions to obtain this [Mo−S−Cu] core are dominated by ligand exchange and [Mo(μ-S)$_2$Cu] rhomb formation. To effectively prevent both, attempting to form the relevant core motif within a single molecular framework may prove advantageous. One can imagine a small macrocyclic ligand or polydentate ligand that can house both Mo and Cu, from which coupling between the two

may occur. The resulting reaction should have a kinetic advantage, since it would essentially be intramolecular. Initial attempts utilizing this approach were complicated and unsuccessful in my hands. The synthesis required to generate an appropriate macrocycle or asymmetric ligand framework to house two distinct metal centers proved very challenging. Adding to this challenge was the difficult coordination chemistry associated with placement of the two unique metal centers within the same ligand. While initial attempts were unsuccessful in this regard, development of an adequate ligand framework may present the possibility of accessing the [Mo−S−Cu] core and at least give rise to some interesting coordination chemistry.

Secondly, no real attempts to synthesize an analogue of the proposed thiocarbonate-containing intermediate have been reported. While thiocarbonate is generally rather unstable, a few molybdenum complexes containing this ligand appear in the literature.[64-66] Condensation of a molybdenum fragment and a copper fragment through a thiocarbonate bridge should prove to be more accessible synthetically, perhaps in a way that parallels the reactions reported by Takuma et. al.[26] Isolation of a discrete analogue of the proposed intermediate should provide information with regard to structure and reactivity, and ultimately afford useful commentary on the plausibility of the proposed intermediate as inferred in previous reports.[20, 22]

Finally, efforts to explore the reactivity associated with the native active site of Mo-CODH within a model complex should prove interesting. A cursory analysis of the active site reveals a two-component system – a redox reservoir (molybdenum fragment) tethered to a pendent Lewis acid (low-coordinate copper fragment). Given the synthetic challenge associated with stabilizing a sulfur ligated bridge to low-coordinate copper, it

may prove useful to replace copper with another, more stable Lewis acid. In this regard, gold(I) comes to the fore as a possible replacement, since mononuclear gold(I) thiolates are quite stable.[67] Additionally, much work has been done modeling molybdoenzymes and their oxygen atom transfer chemistry.[32, 68, 69] By attaching a particular pendent Lewis acid to an existing molybdoenzyme analogue, one might observe reactivity relevant to that which occurs in the active site. As a suitable pendent Lewis acid, ligands containing borane groups should be considered, due to their strong interaction with oxygen atoms via adduct formation. In a similar vein, work reported by Bercaw et al. shows the usefulness of coordinated pendent Lewis acids, specifically with regard to activating CO.[70] A possible reaction scenario is provided in Scheme 3.21.

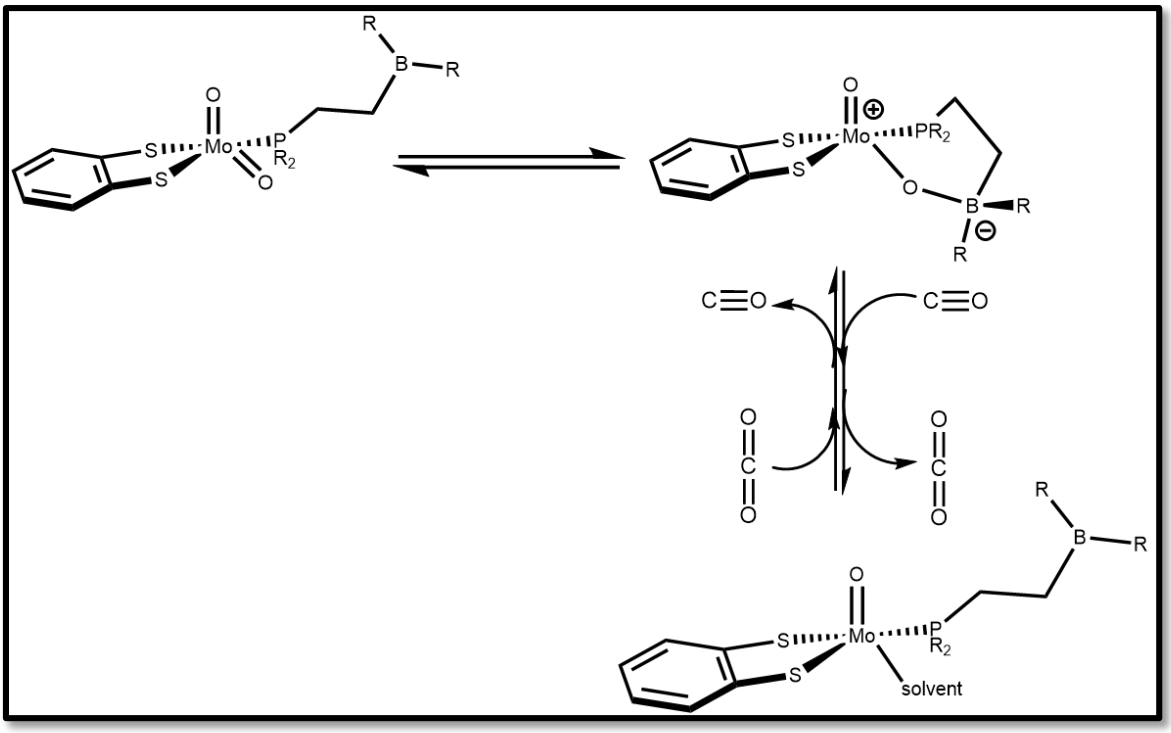

Scheme 3.21 Potential reaction scenario modeling Mo-CODH reactivity.

The reaction shown in Scheme 3.21 is *entirely* speculative, since neither starting material nor product are known complexes. However, one could imagine interesting reactivity provided one had access to systems that incorporate the general features presented above.

Experimental

All reactions and manipulations were performed under a pure dinitrogen or argon atmosphere using modified Schlenk techniques or an inert-atmosphere box. Literature procedures were employed for the syntheses of $[MoO_2(Me_4phen)(OSiPh_3)_2]$,[47] $[Cu(P^tBu_3)(SSiPh_3)]$,[71] $H_2{}^tBu_4$salphen,[72] and $[MoO(acac)_2Cl]$.[58]

Solvents either were dried with a system of drying columns from the Glass Contour Company (Et_2O, hexane, benzene, tetrahydrofuran (THF)) or freshly distilled according to standard procedures (CH_3CN).[73] Other reagents were used as received from commercial sources.

All ^1H and ^{31}P NMR spectra were recorded at 25 °C with a Varian Unity Inova spectrometer operating at 400 or 168.1 MHz for ^1H and ^{31}P, respectively, and were referenced to the solvent residual (^1H) or 85% phosphoric acid (^{31}P). UV-vis spectra were recorded at ambient temperature with a Hewlett-Packard 8452A diode array spectrometer. Electrochemical measurements were performed using a CHI620C electrochemical analyzer workstation with a Ag/AgCl reference electrode, Pt-disk working electrode, and a Pt wire as auxiliary electrode. $[^nBu_4N][PF_6]$ was used as the electrolyte. Under these conditions, the Cp_2Fe^+/Cp_2Fe couple consistently occurs at +0.50 V. Mass spectra were obtained by either MALDI-TOF (Bruker Autoflex III

instrument) or by electrospray ionization methods (Bruker microTOF with Agilent Technologies 1200 Series LC). Elemental analyses were performed by Midwest Microlab, LLC of Indianapolis, IN.

All crystals were coated with paratone oil and mounted on the end of a nylon loop attached to the end of the goniometer. Data were collected with a Bruker APEX CCD diffractometer equipped with a Kryoflex attachment supplying a nitrogen stream at 100 or 150 K. All data were collected under control of the *APEX2* software package. Raw data were reduced to F^2 values using the *SAINT* or *SAINT+* software, and a global refinement of unit cell parameters was performed using selected reflections representing ~ 25% of the full data set. Data for the all compounds were corrected for absorption on the basis of multiple measurements of symmetry equivalent reflections with the use of *SADABS*. All structure solutions were obtained by direct methods or intrinsic phasing using *SHELXS*, while refinements were accomplished by full-matrix least-squares procedures using *SHELXL*. Both the *SHELXS* and *SHELXL* programs are incorporated into the *SHELXTL* software suite. All hydrogen atoms were added in calculated positions and included as riding contributions with isotropic displacement parameters tied to those of the carbon atoms to which they were attached. All images were created with the use of *XP*, which also is part of the *SHELXTL* package. References for the crystallography software mentioned above can be found in Chapter 1 (references 79-87) of this dissertation. Final unit cell data and refinement statistics are collected in Table 3.1.

Bis(tetraethylammonium) monothiomolybdate, $(Et_4N)[MoO_3S]$

To a suspension of finely ground ammonium orthomolybdate ($[NH_4]_2[MoO_4]$, 0.40 g, 2 mmol) in 20 mL dry methanol was added tetraethylammonium hydroxide (25% in MeOH, 2.7 mL, 4 mmol) via gas-tight syringe, which brings all components into solution. This clear, colorless solution was stirred at room temperature for 30 min. and evaporated *in vacuo* to give a wet residue. Approximately 10 mL of dry ether was added with shaking to give a white solid, the ether was then cannulated off and the solid dried *in vacuo* with the aid of gentle heating. Once adequately dry, 50 mL dry acetonitrile was added to generate a fine suspension, to which hexamethyldisilathiane (0.43 mL, 2 mmol) was added dropwise via gas-tight syringe. Upon addition, a yellow color grows in progressively, and the mixture is stirred at room temperature for 12 hr. The lemon-yellow solution thus obtained is filtered and concentrated *in vacuo* to ~10 mL and 40 mL dry ether is added to precipitate a lemon yellow solid which is collected by filtration, washed with ether and dried under high vacuum. The yellow solid was dissolved in a minimum amount of dry acetonitrile and filtered through celite. Diethyl ether was introduced by vapor diffusion into the solution. After 2 days, the product was collected as 654 mg (73%) of large yellow crystals. Analytical data are identical to those found in the literature.[59] UV-vis (acetonitrile), λ_{max} nm (ε_M): 288 (14232), 386 (426). Anal. Calcd for $C_{16}H_{40}MoN_2O_3S$: C, 44.02; H, 9.24; N, 6.42. Found: C, 43.85; H, 9.18; N, 6.38.

[$MoO_2(OSiPh_3)(\mu\text{-}O)Cu(Me_4phen)(P^tBu_3)$], 3

To a fine suspension of [$MoO_2(OSiPh_3)_2(Me_4phen)$] (59 mg, 0.064 mmol) in 10 mL dry THF was added dropwise a solution of [$Cu(P^tBu_3)(SSiPh_3)$] (36 mg, 0.065 mmol) in 5 mL dry THF to generate a yellow mixture. The reaction mixture was stirred for 16 hr and filtered through celite. This filtrate was evaporated to dryness and washed with 5 mL of diethyl ether. Yellow needle crystals were produced via vapor diffusion of diethyl ether into a concentrated, filtered solution of the product in dichloromethane. It should be noted that this product was *not* deliberately reproducible. ^{1}H NMR (δ, ppm in $CDCl_3$): 8.83 (s, 2H), 8.12 (s, 2H), 7.64 (d, 2H), 7.48 (m, 5H), 7.39 (m, 3H), 7.20 (t, 5H), 2.71 (s, 6H), 2.50 (s, 6H), 1.47 (d, 27H). UV-vis (THF), λ_{max} nm (ε_M): 388 (2340).

[$MoO(^tBu_4salphen)Cl$], 4

To a mixture of $H_2{}^tBu_4$salphen (0.306 g, 0.566 mmol) and [$MoO(acac)_2Cl$] (0.176 g, 0.509 mmol) was added 20 mL of dry MeOH and 5 mL of dry DCM to immediately generate a deep red-orange solution. The reaction mixture was stirred for 4 hr and then concentrated to ~6 mL *in vacuo*. Addition of 20 mL of hexanes precipitated a red-orange solid which was collected by filtration anaerobically. The collected precipitate was washed with 5 mL of diethyl ether and 15 mL of hexanes. The product was then dried under high vacuum to give 0.294 g (84% yield) of a red-orange solid. MS^+ (MALDI-TOF, *m/z*): 652, [$MoO(^tBu_4salphen)]^+$. UV-vis (THF), λ_{max} nm (e_M): 473 (4560), 733 (1195).

[Mo(=O)S_3(CuP^tBu_3)$_3$Cl], 2

A colorless solution of [Cu(P^tBu_3)(SSiPh_3)] (0.100 g, 0.179 mmol) in 15 mL of dry THF was slowly cannulated into a solution of red-orange [MoO(^{t}Bu_4salphen)Cl] (0.123 g, 0.179 mmol) in 25 mL of dry THF to generate a deep red-orange reaction mixture which was slightly darker than the starting material in color. The reaction mixture was stirred for 3 hr and subsequently taken to dryness. The crude product residue was redissolved in 20 mL of benzene and filtered through celite anaerobically. Evaporation of the filtrate gave a deep red-orange crude solid. A few large, dark red-orange block shaped crystals were formed by diffusion of hexanes into concentrated solutions of this crude product. ^{1}H NMR (δ, ppm in C_6D_6): 1.45 (d, $^3J_{HP}$ = 12Hz, 27 H). IR (KBr, ν in cm^{-1}): 932, $\nu_{Mo=O}$. UV-vis (THF), λ_{max} nm (ε_M): 359 (6608), 416 (shoulder, 4898), 499 (shoulder, 1283). MS$^+$ (MALDI-TOF, *m/z*): 1005, [Mo(=O)S_3(CuP^tBu_3)$_3$]$^+$.

References

1) Solomon, S. B. Q., D.; Manning, M.; Chen, Z.; Marquis, M.; Averyt, K.B.; Tignor, M.; Miller, H.L. , Intergovernmental Panel On Climate Change. In Cambridge University Press: New York, NY, 2007.

2) Pollack, H. N.; Gore, A., *A World Without Ice*. AVERY Publishing Group.

3) Yergin, D., *The Quest: Energy, Security, and the Remaking of the Modern World*. Penguin Group US.

4) Halmann, M. M., Steinberg, M., *Greenhouse Gas Carbon Dioxide Mitigation: Science and Technology*. CRC Press. Ed. Lewis Publishers: Boca Raton, Fla.; 1999.

5) Sutin, N.; Creutz, C.; Fujita, E., *Comments Inorg. Chem.* **1997,** *19*, 67-92.

6) Ford, P. C., *Acc. Chem. Res.* **1981,** *14*, 31-37.

7) Laine, R. M.; Crawford, E. J., *J. Mol. Catal.* **1988,** *44*, 357-387.

8) Fuchs, G., *Ann. Rev. Microbio. 65*, 631-658.

9) Svetlitchnyi, V.; Peschel, C.; Acker, G.; Meyer, O., *J. Bacteriol.* **2001,** *183*, 5134-5144.

10) Maynard, E. L.; Lindahl, P. A., *J. Am. Chem. Soc.* **1999,** *121*, 9221-9222.

11) Heo, J.; Staples, C. R.; Ludden, P. W., *Biochemistry* **2001,** *40*, 7604-7611.

12) Kumar, M.; Lu, W.-P.; Ragsdale, S. W., *Biochemistry* **1994,** *33*, 9769-9777.

13) Shin, W.; Lee, S. H.; Shin, J. W.; Lee, S. P.; Kim, Y., *J. Am. Chem. Soc.* **2003,** *125*, 14688-14689.

14) King, G. M.; Weber, C. F., *Nat. Rev. Micro.* **2007,** *5*, 107-118.

15) Can, M.; Armstrong, F. A.; Ragsdale, S. W., *Chem. Rev. 114*, 4149-4174.

16) Wilcoxen, J.; Zhang, B.; Hille, R., *Biochemistry 50*, 1910-1916.

17) Crawford, R. L. *Microbial growth on C1 compounds: proceedings of the 4th Internat. Symposium*, Washington, 1984, American Soc. for Microbiology: Washington.

18) Bowien, B.; Schlegel, H. G., *Annu. Rev. Microbiol.* **1981,** *35*, 405-452.

19) Mörsdorf, G.; Frunzke, K.; Gadkari, D.; Meyer, O., *Biodegradation* **1992,** *3*, 61-82.

20) Dobbek, H.; Gremer, L.; Kiefersauer, R.; Huber, R.; Meyer, O., *Proc. Natl. Acad. Sci. U.S.A.* **2002,** *99*, 15971-15976.

21) Hille, R., *Chem. Rev.* **1996,** *96*, 2757-2816.

22) Dobbek, H.; Gremer, L.; Meyer, O.; Huber, R., *Proc. Natl. Acad. Sci. U.S.A.* **1999,** *96*, 8884-8889.

23) Zhang, B.; Hemann, C. F.; Hille, R., *J. Biol. Chem. 285*, 12571-12578.

24) Hofmann, M.; Kassube, J.; Graf, T., *J. Biol. Inorg. Chem.* **2005,** *10*, 490-495.

25) Siegbahn, P. E. M.; Shestakov, A. F., *J. Comput. Chem.* **2005,** *26*, 888-898.

26) Takuma, M.; Ohki, Y.; Tatsumi, K., *Inorg. Chem.* **2005,** *44*, 6034-6043.

27) Gourlay, C.; Nielsen, D. J.; White, J. M.; Knottenbelt, S. Z.; Kirk, M. L.; Young, C. G., *J. Am. Chem. Soc.* **2006,** *128*, 2164-2165.

28) Doonan, C. J.; Nielsen, D. J.; Smith, P. D.; White, J. M.; George, G. N.; Young, C. G., *J. Am. Chem. Soc.* **2005,** *128*, 305-316.

29) Groysman, S.; Majumdar, A.; Zheng, S.-L.; Holm, R. H., *Inorg. Chem.* **2009,** *49*, 1082-1089.

30) Wang, J.-J.; Groysman, S.; Lee, S. C.; Holm, R. H., *J. Am. Chem. Soc.* **2007,** *129*, 7512-7513.

31) Groysman, S.; Wang, J.-J.; Tagore, R.; Lee, S. C.; Holm, R. H., *J. Am. Chem. Soc.* **2008,** *130*, 12794-12807.

32) Enemark, J. H.; Cooney, J. J. A.; Wang, J.-J.; Holm, R. H., *Chem. Rev.* **2003,** *104*, 1175-1200.

33) Tabulated BDEs of Si-, Ge-, Sn-, P- and Se-X bonds. In *Handbook of Bond Dissociation Energies in Organic Compounds*, CRC Press: 2002.

34) Basch, H., *Inorg. Chim. Acta 252*, 265-279.

35) Leroy, G.; Temsamani, D. R.; Wilante, C., *J. Mol. Struct.: THEOCHEM* **1994,** *306*, 21-39.

36) Wuts, P. G. M.; Greene, T. W., *Greene's Protective Groups in Organic Synthesis*. Wiley.

37) Walsh, R., *Acc. Chem. Res.* **1981,** *14*, 246-252.

38) Becerra, R.; Walsh, R., Thermochemistry. In *The Chemistry of Organic Silicon Compounds*, John Wiley & Sons, Ltd: 2003; pp 153-180.

39) Chatgilialoglu, C., *Organosilanes in Radical Chemistry*. Wiley: 2004.

40) Zhou, C.; Cai, L.; Holm, R. H., *Inorg. Chem.* **1996,** *35*, 2767-2772.

41) Lim, B. S.; Willer, M. W.; Miao, M.; Holm, R. H., *J. Am. Chem. Soc.* **2001,** *123*, 8343-8349.

42) Huang, M.; DeKock, C. W., *Inorg. Chem.* **1993,** *32*, 2287-2291.

43) Hongwei, H.; Xinquan, X.; Shaofang, L.; Xiaoxing, H.; Qiangjin, W., *J. Coord. Chem.* **1995,** *35*, 299-306.

44) Shi, S.; Lin, Z.; Mo, Y.; Xin, X. Q., *J. Phys. Chem.* **1996,** *100*, 10696-10700.

45) Sarkar, S.; Mishra, S. B. S., *Coord. Chem. Rev.* **1984,** *59*, 239-264.

46) Tran, P. D.; Nguyen, M.; Pramana, S. S.; Bhattacharjee, A.; Chiam, S. Y.; Fize, J.; Field, M. J.; Artero, V.; Wong, L. H.; Loo, J.; Barber, J., *Energy & Environmental Science 5*, 8912-8916.

47) Thapper, A.; Donahue, J. P.; Musgrave, K. B.; Willer, M. W.; Nordlander, E.; Hedman, B.; Hodgson, K. O.; Holm, R. H., *Inorg. Chem.* **1999,** *38*, 4104-4114.

48) DeBurgomaster, P.; Bartholomä, M.; Raffel, R.; Ouellette, W.; Müller, A.; Zubieta, J., *Inorg. Chim. Acta 363*, 1386-1394.

49) Choi, K.-Y.; Ryu, H.; Suh, I.-H., *Inorg. Chim. Acta* **2000,** *299*, 268-276.

50) Shores, M. P.; Bartlett, B. M.; Nocera, D. G., *J. Am. Chem. Soc.* **2005,** *127*, 17986-17987.

51) Dowerah, D.; Spence, J. T.; Singh, R.; Wedd, A. G.; Wilson, G. L.; Farchione, F.; Enemark, J. H.; Kristofzski, J.; Bruck, M., *J. Am. Chem. Soc.* **1987,** *109*, 5655-5665.

52) Singh, R.; Spence, J. T.; George, G. N.; Cramer, S. P., *Inorg. Chem.* **1989,** *28*, 8-10.

53) Barnard, K. R.; Bruck, M.; Huber, S.; Grittini, C.; Enemark, J. H.; Gable, R. W.; Wedd, A. G., *Inorg. Chem.* **1997,** *36*, 637-649.

54) Wilson, G. L.; Kony, M.; Tiekink, E. R. T.; Pilbrow, J. R.; Spence, J. T.; Wedd, A. G., *J. Am. Chem. Soc.* **1988,** *110*, 6923-6925.

55) Bruce, A.; Corbin, J. L.; Dahlstrom, P. L.; Hyde, J. R.; Minelli, M.; Stiefel, E. I.; Spence, J. T.; Zubieta, J., *Inorg. Chem.* **1982,** *21*, 917-926.

56) Do, Y.; Simhon, E. D.; Holm, R. H., *Inorg. Chem.* **1985,** *24*, 1831-1838.

57) Money, J. K.; Folting, K.; Huffman, J. C.; Collison, D.; Temperley, J.; Mabbs, F. E.; Christou, G., *Inorg. Chem.* **1986,** *25*, 4583-4589.

58) Chen, G. J. J.; McDonald, J. W.; Newton, W. E., *Inorg. Chim. Acta* **1979,** *35*, 93-97.

59) Partyka, D. V.; Holm, R. H., *Inorg. Chem.* **2004,** *43*, 8609-8616.

60) Wyer, E.; Gucciardo, G.; Leigh, V.; Mueller-Bunz, H.; Albrecht, M., *J. Organomet. Chem. 696*, 2882-2885.

61) Fructos, M. R.; De Fremont, P.; Nolan, S. P.; Mar Dauiiaz-Requejo, M.; Perez, P. J., *Organometallics* **2006,** *25*, 2237-2241.

62) Thapper, A.; Donahue, J. P.; Musgrave, K. B.; Willer, M. W.; Nordlander, E.; Hedman, B.; Hodgson, K. O.; Holm, R. H., *Inorg. Chem.* **1999,** *38*, 4104-4114.

63) Majumdar, A., *J. Chem. Soc. Dalton Trans.* **2014**, *43*, 12135-12145.

64) Alvarez, R.; Carmona, E.; Marin, J. M.; Poveda, M. L.; Gutierrez-Puebla, E.; Monge, A., *J. Am. Chem. Soc.* **1986,** *108*, 2286-2294.

65) Marsh, R. E.; Clemente, D. A., *Inorg. Chim. Acta* **2007,** *360*, 4017-4024.

66) Gales, S. L.; Pennington, W. T.; Kolis, J. W., *J. Organomet. Chem.* **1991,** *419*, C10-C13.

67) Mohr, F.; Schmidbaur, H., *Gold Chemistry: Applications and Future Directions in the Life Sciences*. John Wiley & Sons: 2009.

68) Holm, R. H., *Chem. Rev.* **1987,** *87*, 1401-1449.

69) Holm, R. H., *Coord. Chem. Rev.* **1990,** *100*, 183-221.

70) Miller, A. J. M.; Labinger, J. A.; Bercaw, J. E., *Organometallics 29*, 4499-4516.

71) Medina, I.; Jacobsen, H.; Mague, J. T.; Fink, M. J., *Inorg. Chem.* **2006,** *45*, 8844-8846.

72) Weberski, M. P.; McLauchlan, C. C.; Hamaker, C. G., *Polyhedron* **2006,** *25*, 119-123.

73) Armarego, W. L. F.; Chai, C. L. L., *Purification of Laboratory Chemicals*. Butterworth-Heinemann: 2003.

Chapter 4

Polynuclear Copper Complexes Featuring Diamino-Dithiolate (N_2S_2) Ligands

Introduction

Diamino-dithiolate ligands (N_2S_2 ligands) which contain both hard nitrogen donor atoms and soft sulfur donor atoms are of significant use in the coordination chemistry community. Ligand frameworks that feature both hard and soft donor atoms can be used to stabilize transition metal complexes in unique geometries over a wide range of oxidation states. The size and constituency of the spacing groups between heteroatoms can be tuned to allow for flexibility with respect to the complex's geometry and can accommodate exogenous binding or incorporation of additional metal centers. Given the variation which can exist by synthetic means, ligands of this type can be utilized for different purposes to support a broad range of systems. Complexes bearing these ligands have appeared in reports modeling metalloproteins,[1-5] within a medicinal context,[6, 7] for potentially interesting redox and magnetic behavior,[8] and for activating carbon dioxide using a similar, yet slightly more elaborate ligand environment.[9]

Biological Relevance

Owing to the ubiquity of nitrogen and sulfur-containing amino acid residues, namely histidine and cysteine, metalloproteins tend to incorporate both or some variation of nitrogen and sulfur based ligation in binding a metal center. Within the realm of bioinorganic copper chemistry, blue copper electron transfer proteins are the most thoroughly examined.[10, 11] These proteins exist in a few different types, where the Type 1

blue copper proteins (azurin, plastocyanin, etc.) are generally found in a distorted tetrahedral, almost trigonal pyramidal geometry bound to two histidines (N-donors), a cysteinate residue (S-donor), and a methionine (S-donor). This peculiar geometry about the copper ion, which is enforced by the protein with which it is bound (entatic state), restricts the degrees of freedom associated with a structural rearrangement upon changing oxidation state.[12] For copper, this situation represents a compromise between the usual tetrahedral coordination of d^{10} copper(I) complexes and the square planar geometry of d^9 copper(II) complexes. In this way, the constrained geometry alleviates reorganizational energy coupled to the redox event taking place at copper and ultimately aids in the flow of electrons through the metalloprotein.

Another copper-containing site in biology that incorporates both nitrogen and sulfur in its immediate coordination sphere is the Cu_Z active site of nitrous oxide reductase,[13-15] along with its accompanying Cu_A electron transfer site[16-18] (Figure 4.1). Both sites consist of sulfur-bridged multicopper cores, which confer extensive electron delocalization and/or give rise to platforms from which substrates can be activated in a cooperative fashion.

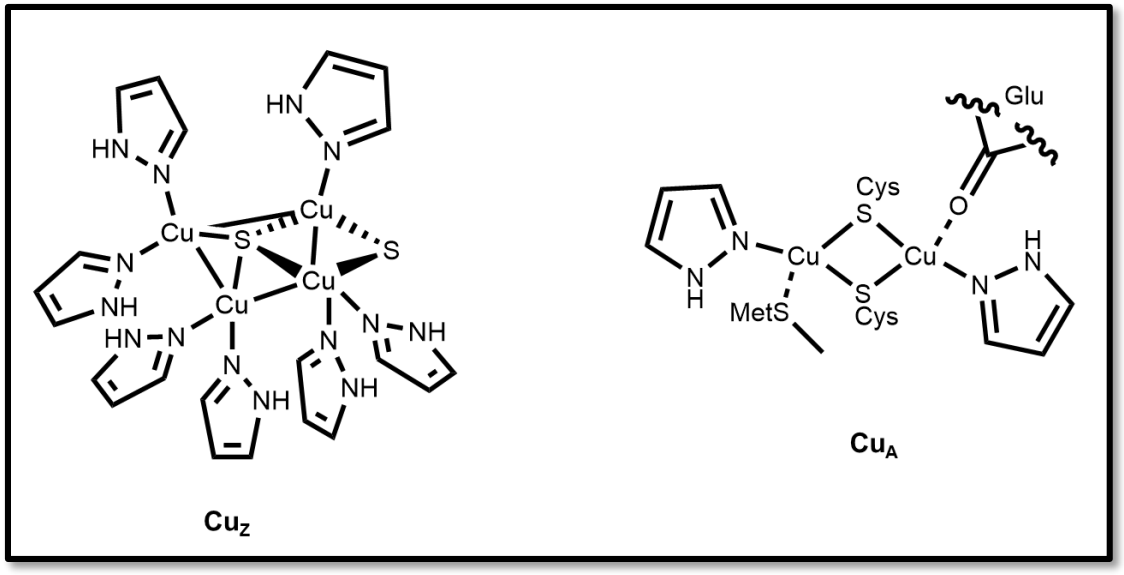

Figure 4.1 Minimal representations of the Cu_Z active site and Cu_A site in nitrous oxide reductase from *Pseudomonas stutzeri*.

Nitrous oxide reductase is the terminal enzyme in denitrification, and catalyzes the reduction of nitrous oxide to molecular nitrogen and water ($N_2O + 2e^- + 2H^+ \rightarrow N_2 + H_2O$). The Cu_Z active site consists of four copper ions in a butterfly arrangement about a central sulfide, which bridges all four copper centers. The edge of the tetranuclear site features another bridging sulfide between two copper centers. While still a topic of debate, it is presumed that the fully reduced 4Cu(I) state of the metalloenzyme is the catalytically competent state. Intimately linked to the function of the Cu_Z active site is the Cu_A electron transfer site, which facilitates the flow of electrons during turnover. The CuA site is a dinuclear copper species bridged by two cysteinates and capped by histidines, methionine, and an amino acid backbone carbonyl. Similar to the blue copper proteins, Cu_A is tuned to facilitate the flow of electrons toward the Cu_Z site.

These examples highlight the broad capability of copper ions to access interesting electronic states and subsequent reactivity when bound by nitrogen and sulfur donor atoms. Specifically, the multicopper assemblies can give rise to very important chemical transformations which may be of interest within the context of environmental remediation and industrial application, as the facile reduction of kinetically inert N_2O could subsequently oxidize an organic substrate. Few attempts have been made to model nitrous oxide reductase, and these efforts warrant further investigation.[19, 20] Cooperative substrate binding and activation by multicopper assemblies, like that proposed in nitrous oxide reductase, have appeared in a few recent reports[9, 21] and show promise within the context of modeling related systems.

While investigating the coupling reactions in an effort to form an analogue of Mo-CODH as described in Chapter 3 of this dissertation, several products were isolated that were not immediately relevant in the context of Mo-CODH modeling but interesting in their own right. These polynuclear copper complexes formed via ligand exchange from the original molybdenum-N_2S_2 species to copper. The resulting copper-N_2S_2 species formed the basis for further synthesis to generate related species, all of which are presented herein.

Results and Discussion

Multicopper species formed either via ligand exchange or directly are presented below in chronological order. Three different N_2S_2 ligands were used in the course of this work: *N*,*N*′-dimethyl-*N*,*N*′-bis(2-mercaptophenyl)ethylenediamine[4] (N_2S_2aryl), *N*,*N*′-dimethyl-*N*,*N*′-bis(2-mercaptoethyl)ethylenediamine[22] (N_2S_2alkyl), and *N*,*N*′-bis-2-

methyl-mercaptopropyl-*N*,*N'*-dimethylethylenediamine[23] (N_2S_2alkylMe$_4$). All reactions described were performed and manipulated anaerobically.

Table 4.1. Crystal and refinement data for compounds in Chapter 4.

compound	**1**	**2**	**3**	**4**
solvent	none	C_6H_6	½ Et_2O	2.25 MeCN
formula	$C_{48}H_{54}Cu_5N_6S_6$	$C_{49}H_{60}Cu_2N_4S_2$	$C_{26}H_{57}Cu_4N_4O_{0.50}S_4$	$C_{52.50}H_{102.75}B_6Cu_{10}F_{24}N_{18.25}S_8$
fw	1225.03	896.21	816.15	2402.51
xtl system	triclinic	monoclinic	monoclinic	monoclinic
space grp	$P\bar{1}$	$P2_1/c$	$P2_1/c$	Pn
color, habit	brown block	colorless block	colorless block	purple slab
a, Å	11.840(2)	12.8490(5)	13.1795(15)	14.014(3)
b, Å	20.650(4)	16.8154(7)	13.1678(15)	31.074(6)
c, Å	20.801(4)	23.0028(9)	21.683(3)	21.818(4)
α, deg.	85.228(2)	90	90	90
β, deg.	89.839(2)	96.0220(10)	103.5610(16)	90.39(3)
γ, deg.	84.436(2)	90	90	90
V, Å^3	5044.0(16)	4942.6(3)	3658.0(7)	9501(3)
T, K	150(2)	150(2)	150(2)	150(2)
Z	4	4	4	4
R1, wR2	0.0483, 0.1041	0.0514, 0.1514	0.0365, 0.0862	0.0750, 0.1672
GoF	1.035	1.025	1.037	1.137

R1 = $\Sigma||F_o| - |F_c||/\Sigma|F_o|$. wR2 = $\{[\Sigma w(F_o^2 - F_c^2)/\Sigma w(F_o^2)^2\}^{1/2}$; $w = 1/[\sigma^2(F_o^2) + (xP)^2]$, where $P = (F_o^2 + 2F_c^2)/3$.

[[Cu(N_2S_2aryl)]$_3$(μ-Cu$_2$)]	**1**
[(IPr)Cu-Cu(N_2S_2aryl)]	**2**
[((N_2S_2alkylMe$_4$)Cu)$_2$(μ-Cu$_2$)],	**3**
[Cu$_{10}$(S(CH$_2$)$_2$N(Me)CH$_2$-)$_4$(MeCN)$_8$][BF$_4$]$_6$	**4**

Table 4.2 Compound number list for Chapter 4.

Initial attempts toward forming a coupling product between [MoO(N_2S_2aryl)Cl][5] and [Cu(IMes)(SSi^{i}Pr$_3$)] led to no reaction between the starting materials (see Chapter 3). An alternative synthetic route involved a three component system, where addition of

hexamethyldisilathiane ($Me_3Si{-}S{-}SiMe_3$) to a mixture of [$MoO(N_2S_2aryl)Cl$] and [Cu(IPr)Cl] was intended to facilitate the desired coupling.

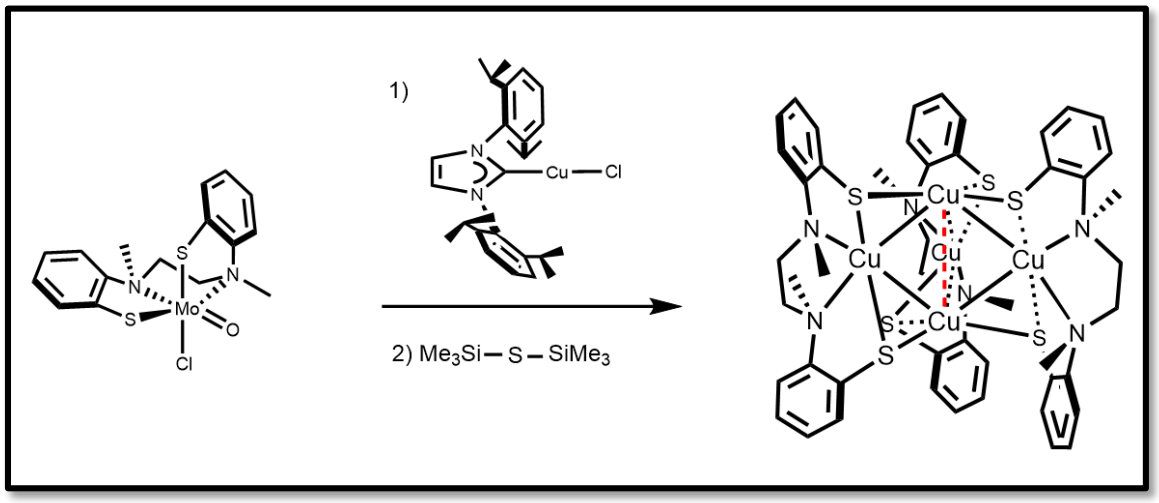

Scheme 4.1 Reaction affording pentacopper species **1**.

This reaction in THF afforded a dark mixture, from which dark brown crystals formed on standing from a combined diethyl ether/pentane wash. These crystals were analyzed by X-ray crystallography and found to be charge neutral [$[Cu(N_2S_2aryl)]_3(Cu_2)$], **1**.

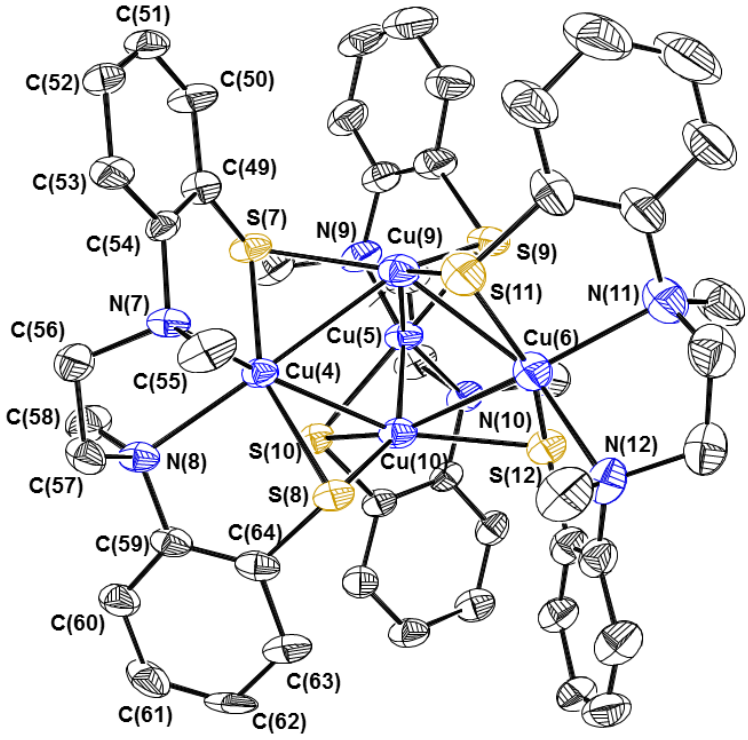

Figure 4.2 Crystal structure of [[Cu(N_2S_2aryl)]$_3$(Cu_2)], **1**. Hydrogen atoms are omitted for clarity and all thermal ellipsoid plots are at the 50% probability level. One of two independent molecules in the asymmetric unit of the unit cell is shown.

This pentacopper species, **1**, forms via ligand exchange of the Mo-N_2S_2aryl starting material to copper with complete excision of monodentate ligands on copper. The structure is comprised of three distinct Cu-N_2S_2aryl units poised around two central copper ions that are each bound by three sulfur ions from the ends of the N_2S_2aryl ligands in a distorted trigonal fashion (slightly out of plane). The charge neutral formulation of **1** indicates a degree of oxidation about the core with respect to electroneutrality, given the existence of three dianionic N_2S_2 ligands and only five copper ions. Determining the particular site of oxidation within the cluster is rendered quite difficult since the core is

not symmetric when bond lengths are analyzed (Table 4.3), which reveal subtle differences about each copper center.

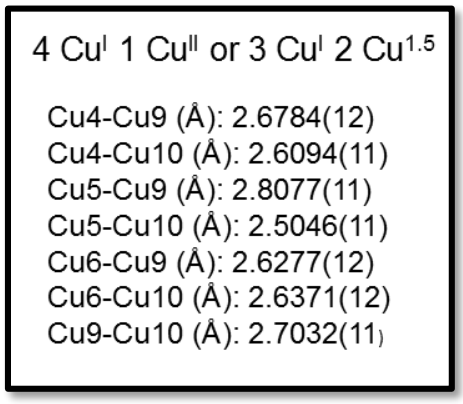

Table 4.3 Copper-copper bond distances in **1**.

All N_2S_2 ligands are folded in a manner that suggests they are bound to copper(I) ions, since discrete copper(II) ions would most certainly feature square planar coordination. Thus, this core can tentatively be described as being comprised of either four Cu(I) ions and one Cu(II) ion, or three Cu(I) ions and two Cu(1.5^+) ions. Interestingly, this structure type has some precedent.[24, 25] However, the reported pentacopper species feature three discrete square planar Cu(II)-N_2S_2 units flanking two Cu(I) ions and have an expanded core size in comparison to **1**. The occurrence of this structure type in varying degrees of oxidation suggests a potentially flexible redox interplay among structures of this general formulation. Perhaps complexes of this type, stabilized by N_2S_2 ligands, can support multi-electron redox events. Given the lack of data regarding the known complexes, and the apparent irreproducibility of complex **1** synthetically, this point remains speculative.

In a separate attempt toward a coupling reaction, an entirely different result emerged. When an equivalent of sodium triethylborohydride was added to a mixture of $[MoO(N_2S_2aryl)(SH)]$[4] and $[Cu(IPr)(OH)]$[26] an orange reaction mixture was generated.

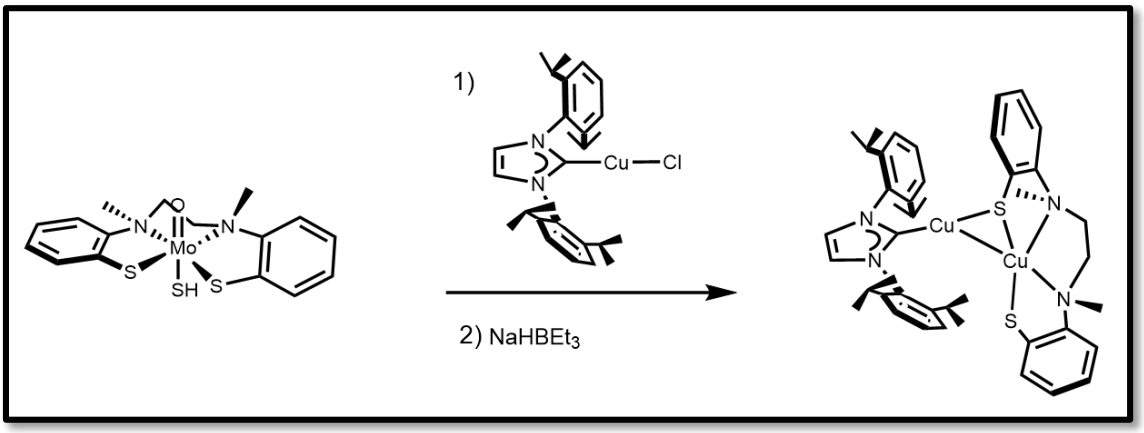

Scheme 4.2 Reaction affording dicopper species **2**.

Addition of hexanes to a pale yellow benzene extract from this crude mixture afforded large colorless block-shaped crystals on standing. X-ray crystallography revealed the identity of these crystals to be dinuclear $[(IPr)Cu\text{-}Cu(N_2S_2aryl)]$, **2**.

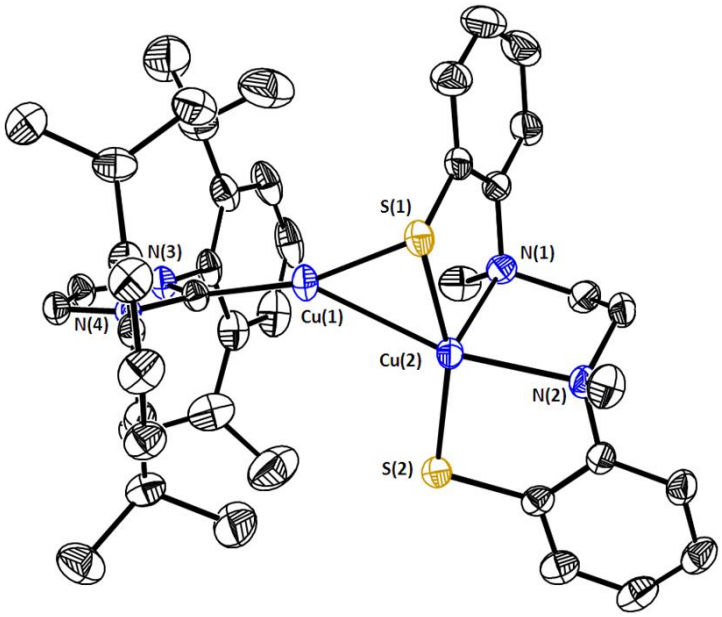

Figure 4.3 Crystal structure of **2**. Hydrogen atoms are omitted for clarity, and all thermal ellipsoids are presented at the 50% probability level.

Formation of **2** proceeds with ligand exchange, again from the Mo-N_2S_2aryl starting material to copper with excision of monodentate ligands. A labile $[Cu(IPr)]^+$ fragment generated during the course of the reaction coordinates to one sulfur on the end of the bound N_2S_2aryl ligand. Charge neutral complex **2** features two Cu(I) ions in close proximity, with a Cu−Cu distance of 2.6231(5) Å, presumably due to diminished sterics about the coordinatively unsaturated $[Cu(IPr)]^+$ unit. The diamagnetic ^{1}H NMR spectrum of **2** corroborates the assignment as containing two Cu(I) ions (Figure 4.4).

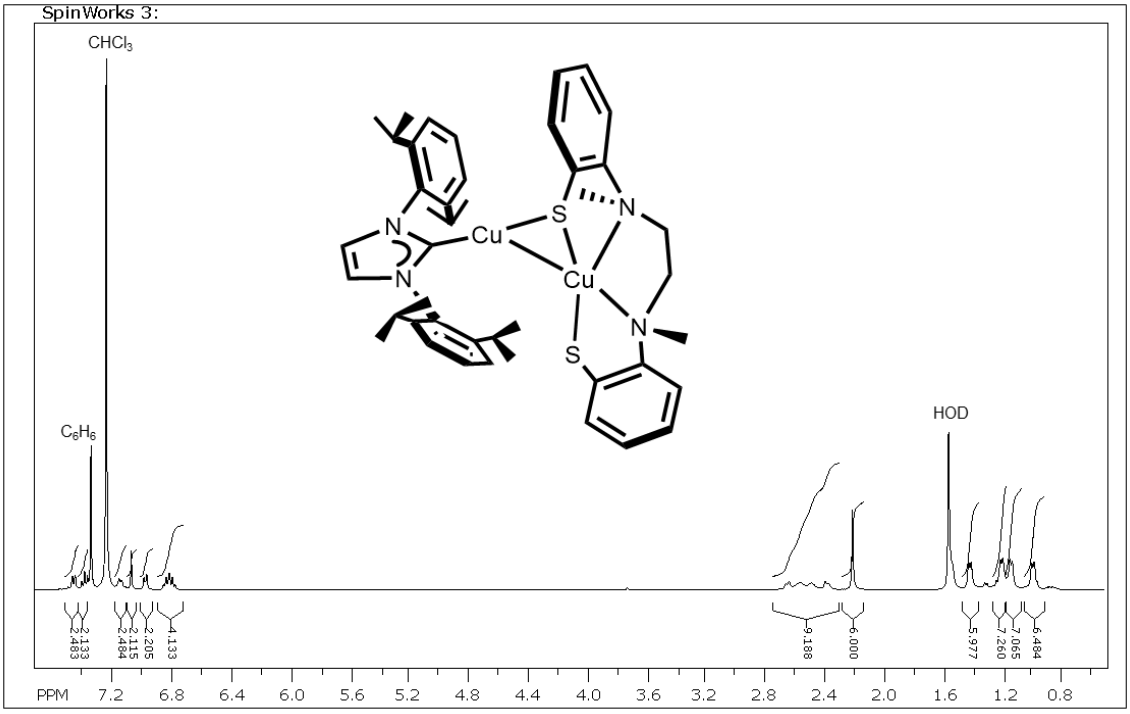

Figure 4.4 ^{1}H NMR spectrum of **2**.

Dicopper **2** displays a rather 'open' core, as the coordinative unsaturation of one copper center leaves the core accessible. One might imagine the usefulness of such an accessible core with respect to binding and activating small substrates. Thus, efforts were made to reproduce **2** synthetically. The reaction between [Cu(IPr)Cl] and half an equivalent of $Na_2N_2S_2$aryl (generated *in situ* from $H_2N_2S_2$aryl and 2 equivalents of $NaHBEt_3$) led to a mixture of products, which upon workup appear to include desired complex **2**. Unfortunately, complex **2** could not be isolated from the mixture and appeared to co-crystallize with at least [Cu(IPr)Cl] starting material as observed via ^{1}H NMR spectroscopy (Figure 4.5).

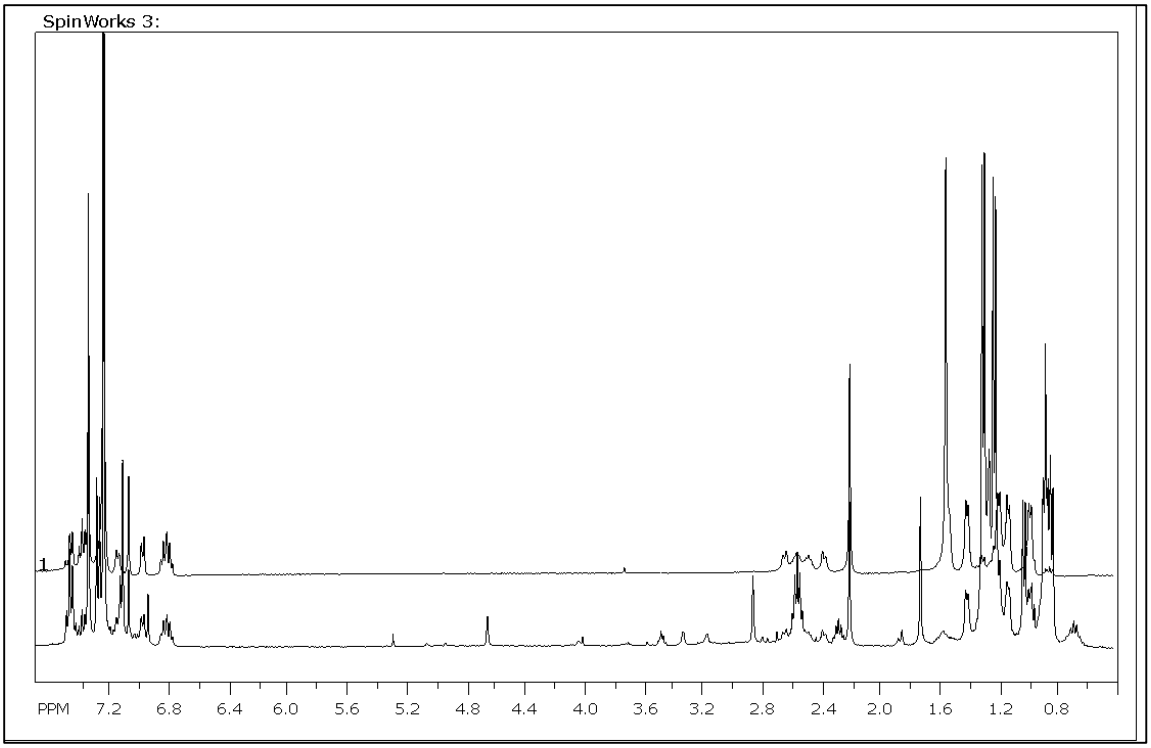

Figure 4.5 ^{1}H NMR spectrum overlay. Pure spectrum of **2** (raised, back) and co-crystallized mixture from discrete synthesis (lower, front).

A second attempt at synthetically accessing a derivative of **2**, using the N_2S_2alkylMe$_4$ ligand, yielded an entirely different result. Addition of half an equivalent of $Na_2N_2S_2$alkylMe$_4$ (generated *in situ* from $H_2N_2S_2$alkylMe$_4$ and NaHBEt$_3$) to a solution of [Cu(IPr)Cl] in THF afforded a crude orange mixture. Colorless crystals formed on standing from a combined diethyl ether/pentane extract of the crude product. These crystals were analyzed by X-ray crystallography and found to be tetranuclear [((N$_2$S$_2$alkylMe$_4$)Cu)$_2$(μ-Cu$_2$)], **3**.

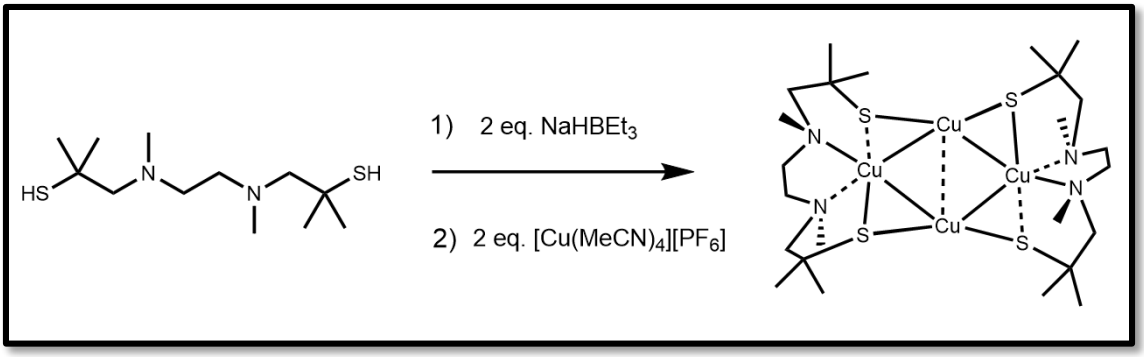

Scheme 4.3 Synthetic route to tetracopper **3**.

This tetracopper complex can be reproducibly synthesized by reacting half an equivalent of $Na_2N_2S_2alkylMe_4$ with $[Cu(MeCN)_4][PF_6]$ in acetonitrile, followed by extraction of the product into toluene, benzene, or diethyl ether. Crystals are formed, albeit in rather low yield, from low temperature solvent combinations of pentane and toluene, benzene, or diethyl ether. Complex **3** is a colorless solid that is extremely air and moisture sensitive.

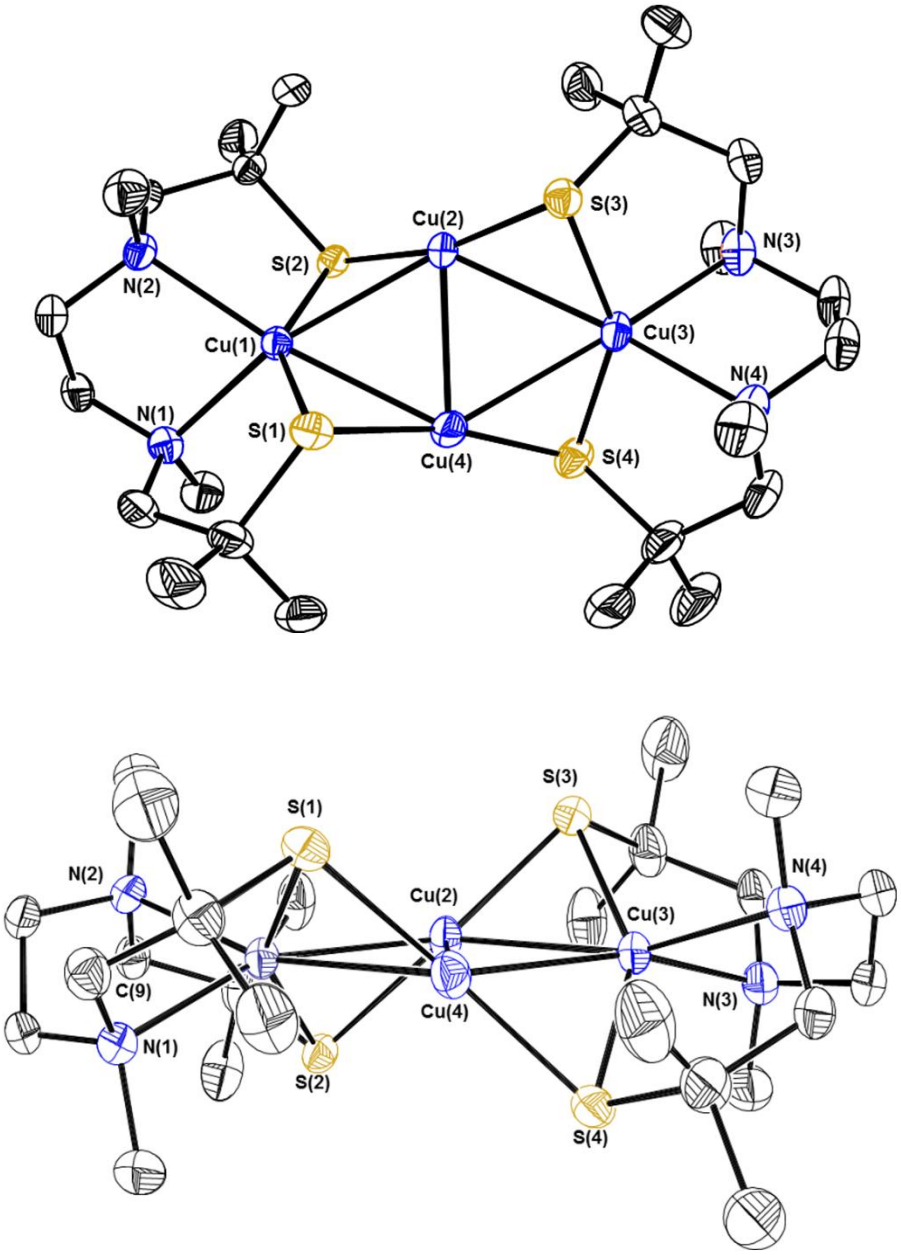

Figure 4.6 Crystal structure of **3** from two perspectives: face down (top) and side on (bottom). Hydrogen atoms are omitted for clarity, and all thermal ellipsoids plotted at the 50% probability level.

Tetracopper **3** features a planar, rhomb shaped core of Cu(I) ions, where two copper ions are bound by N_2S_2alkylMe_4 ligands in a tetrahedral fashion, and the remaining two

copper ions are perched between the sulfur ions of the ends of each N_2S_2alkylMe_4 ligand. The core consisting of copper and sulfur atoms appears to be somewhat ubiquitous in copper thiolate chemistry (see cataloged references reported by Howell),[27] and complexes bearing a similar overall composition have been reported.[28, 29]

Bond	Distance (Å)
Cu(1)-N(1)	2.203(2)
Cu(1)-N(2)	2.230(2)
Cu(1)-S(2)	2.2565(8)
Cu(1)-S(1)	2.2593(8)
Cu(1)-Cu(2)	2.5799(5)
Cu(1)-Cu(4)	2.6078(5)
Cu(2)-S(3)	2.1836(8)
Cu(2)-S(2)	2.1873(8)
Cu(2)-Cu(3)	2.5940(5)
Cu(2)-Cu(4)	2.6802(6)
Cu(3)-N(4)	2.215(2)
Cu(3)-N(3)	2.223(3)
Cu(3)-S(4)	2.2553(8)
Cu(3)-S(3)	2.2568(8)
Cu(3)-Cu(4)	2.6042(5)
Cu(4)-S(1)	2.1958(8)

Table 4.4 Selected bond distances about the core of **3**.

Metrics associated with the core of **3** (Table 4.3) fall in line with those observed previously.[28] The prochiral nitrogen donor groups impart a stereochemical configuration upon the molecule, which results from the interplay between flexibility of the N_2S_2 ligand's spacing groups between heteroatoms and the overall sterics associated with the ligand upon coordination. In **3**, the crystal structure displays the (*R*,*R*) enantiomer with respect to an absolute configuration. Necessarily this molecule exists as a racemic

mixture of both all-(*R*) and all-(*S*) enantiomers, as it crystallizes in a centric space group. These configurations appear to result from the steric constraints of the ligand as it flexes to coordinate in a tetrahedral fashion about each copper ion, leading to diametrically opposed methyl groups on each nitrogen atom of the ligands. These chiral mononuclear [Cu(N_2S_2alkylMe$_4$)] units operate pairwise as bifunctional sulfur donor ligands toward 'free' copper ions to form stable tetranuclear species with planar metal frameworks. In addition to structural considerations, the colorless appearance of **3** (no LMCT observed in the visible spectrum) and its diamagnetic ^{1}H NMR spectrum (Figure 4.7) support an assignment of the complex as containing four Cu(I) ions.

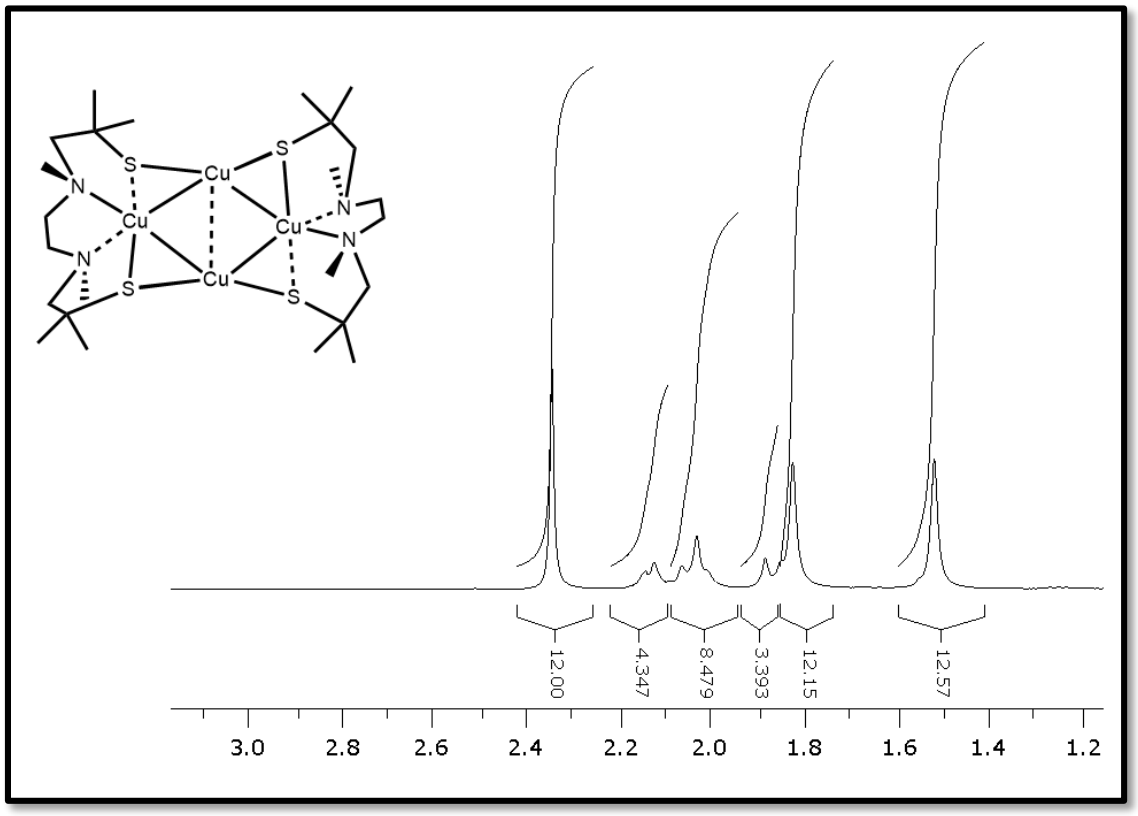

Figure 4.7 ^{1}H NMR spectrum of **3**.

While most general aspects of **3** parallel that which is reported for the few existing analoguous complexes,[28] one noteworthy deviation is the electrochemistry of **3**. Henkel et al. report that these few complexes only show irreversible oxidation events at fairly positive potentials via cyclic voltammetry measurements.[28] Cyclic voltammetry of **3** in both THF and weakly coordinating CH_2Cl_2 displays quasireversible events at mild potentials versus Ag/AgCl (Figure 4.8).

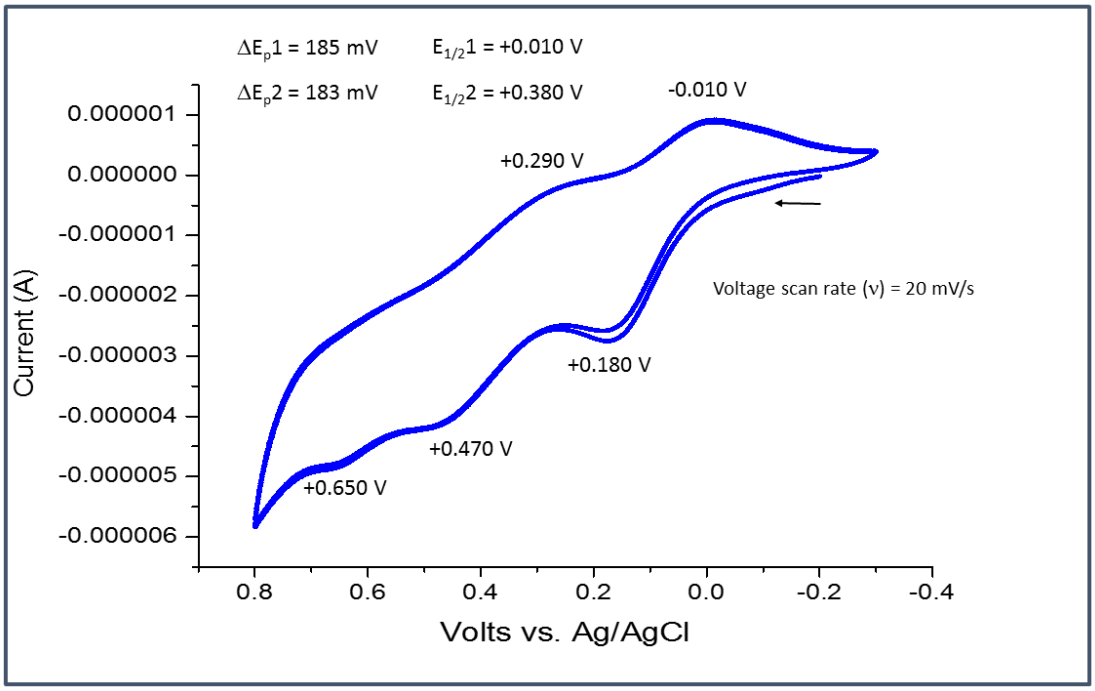

Figure 4.8 Cyclic voltammogram of **3** in THF with $[Bu_4N][PF_6]$ as supporting electrolyte.

The cyclic voltammogram of **3** features two rather broad, quasireversible waves centered around $E_{1/2}$ = + 10 mV and $E_{1/2}$ = + 380 mV with an irreversible oxidation occurring at + 650 mV. These features persist when the measurement is conducted in dichloromethane. A possible explanation for the large peak separation for the quasireversible events could come from the presumed sluggish reorientation of the ligand and core as the

[Cu(N_2S_2alkylMe_4)] units flex between a more tetrahedral and more square planar geometry upon reduction and oxidation. Nonetheless, these features seem to suggest an electronic delocalization about the core of **3** that helps stabilize the compound against degradation following electrochemical oxidation, which is the more typical behavior of cuprous thiolate species. Generally, copper(II) is oxidizing enough to transform thiolate into disulfide, and conversely, copper(I) can oxidatively add disulfide. This reactivity tends to complicate electrochemical measurements of most simple cuprous thiolate species.

Molecular orbital calculations performed at the B3LYP level of theory by my colleague Angelique Greene on the solid state crystal structure of **3**, provide additional insight into its electronic structure (Figures 4.9 and 4.10). It should be noted that these calculations were single point calculations performed using the atomic coordinates from the crystal structure. The crystal structure found for **3** was not amenable to a geometry optimization in the gas phase or solution.

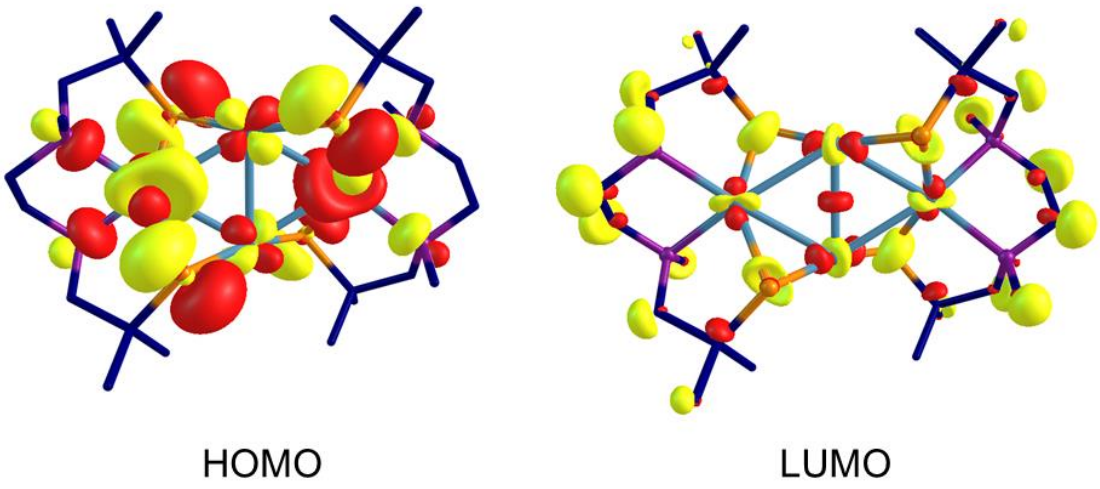

Figure 4.9 Frontier molecular orbitals of **3** calculated from the crystal structure coordinates of **3**. Showing the HOMO (highest occupied molecular orbital, left) and LUMO (lowest unoccupied molecular orbital, right).

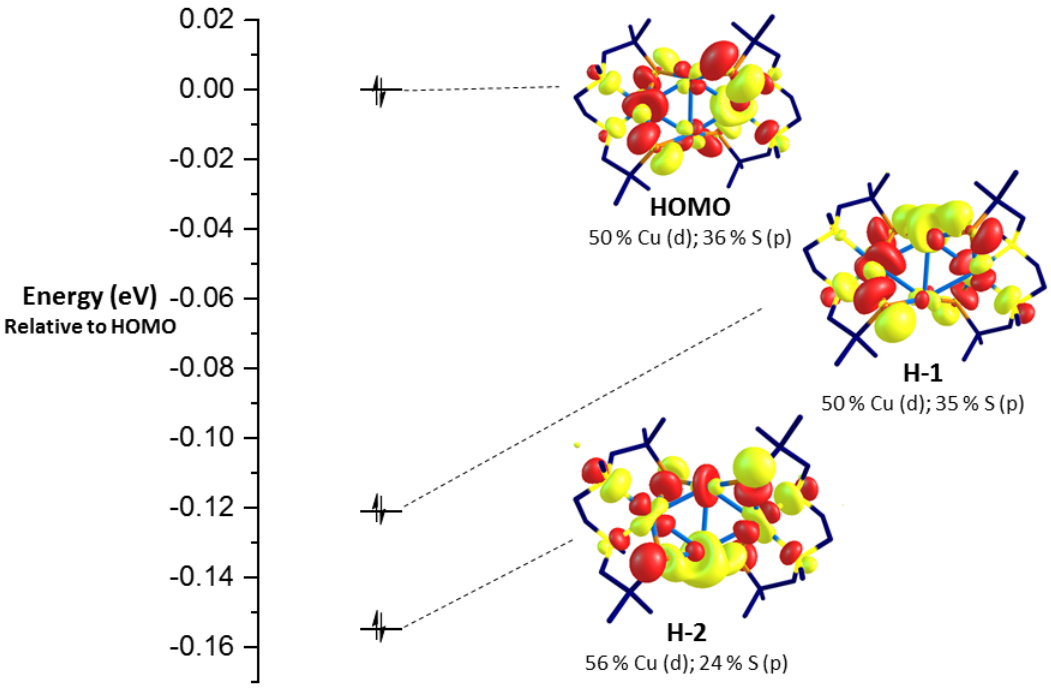

Figure 4.10 Molecular orbital diagram for **3** displaying the HOMO, HOMO-1 (H-1), and HOMO-2 (H-2).

These calculations reveal frontier molecular orbitals composed mostly of Cu d-orbital and S p-orbital character about the core of the molecule. In the HOMO, the interactions between Cu(d) and S(p) appear to be mostly antibonding. It is possible that these destabilizing antibonding interactions observed in the frontier orbitals contribute to the relative ease with which **3** is oxidized. Of additional note, is the degree of molecular orbital composition deriving from *both* the metal centers *and* ligands about the core of **3** observed in the LUMO through HOMO-2. This suggests a potentially extensive electronic delocalization over the core.

From these results, one might speculate upon the possibilities for reactions that might be accomplished with tetranuclear **3** and perhaps upon any loose analogies between **3** and the Cu_Z site of nitrous oxide reductase that may exist. Can **3** cooperatively bind and/or activate small substrates? Are two-electron transformations possible? The synthetic reproducibility of tetracopper **3** opens the door for a whole suite of potentially interesting reactions in order to gain a better understanding of its behavior.

A separate effort was made to prepare a dinuclear all Cu(I) species along the lines of that which was reported to activate carbon dioxide.[9] The reaction between the disulfide of the N_2S_2alkyl ligand and free Cu(I) salts led to a completely new result. Addition of two equivalents of $[Cu(MeCN)_4][BF_4]$ to an acetonitrile solution of the N_2S_2alkyl disulfide afforded a uniform, dark purple solution (Scheme 4.4). This color qualitatively suggests an oxidative addition of the disulfide by copper takes place, since electronic transitions in the visible spectrum due to LMCT S(p)→Cu(d) and d-d transitions are now possible given the open shell configuration of Cu(II).

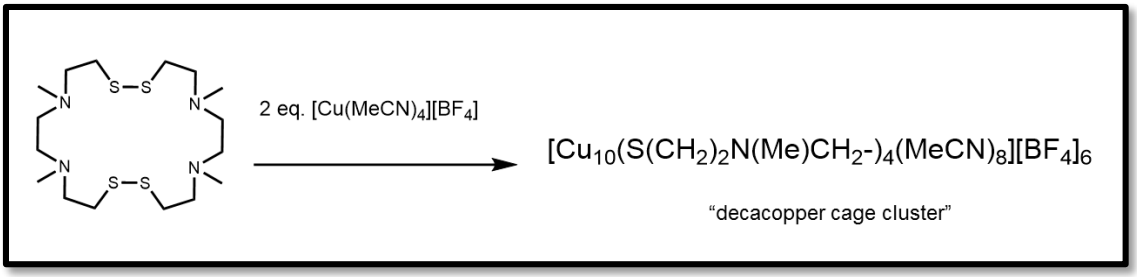

Scheme 4.4 Synthesis of decacopper cage cluster **4**.

Large, deep purple crystals are formed from diffusion of *tert*-butyl methyl ether into concentrated solutions of the crude product. These crystals were analyzed via X-ray crystallography and found to consist of a decacopper cage-type cluster species formulated as $[Cu_{10}(S(CH_2)_2N(Me)CH_2-)_4(MeCN)_8][BF_4]_6$, **4**. This reaction proceeds with oxidative addition of the N_2S_2alkyl disulfide to form a complex decanuclear cage structure. Evident within the structure (Figure 4.11) are four square planar Cu(II) [Cu(N_2S_2alkyl)] units (Cu(1)-Cu(4)), about which six Cu(I) ions sit between either two or three sulfur atoms derived from the [Cu(N_2S_2alkyl)] fragments.

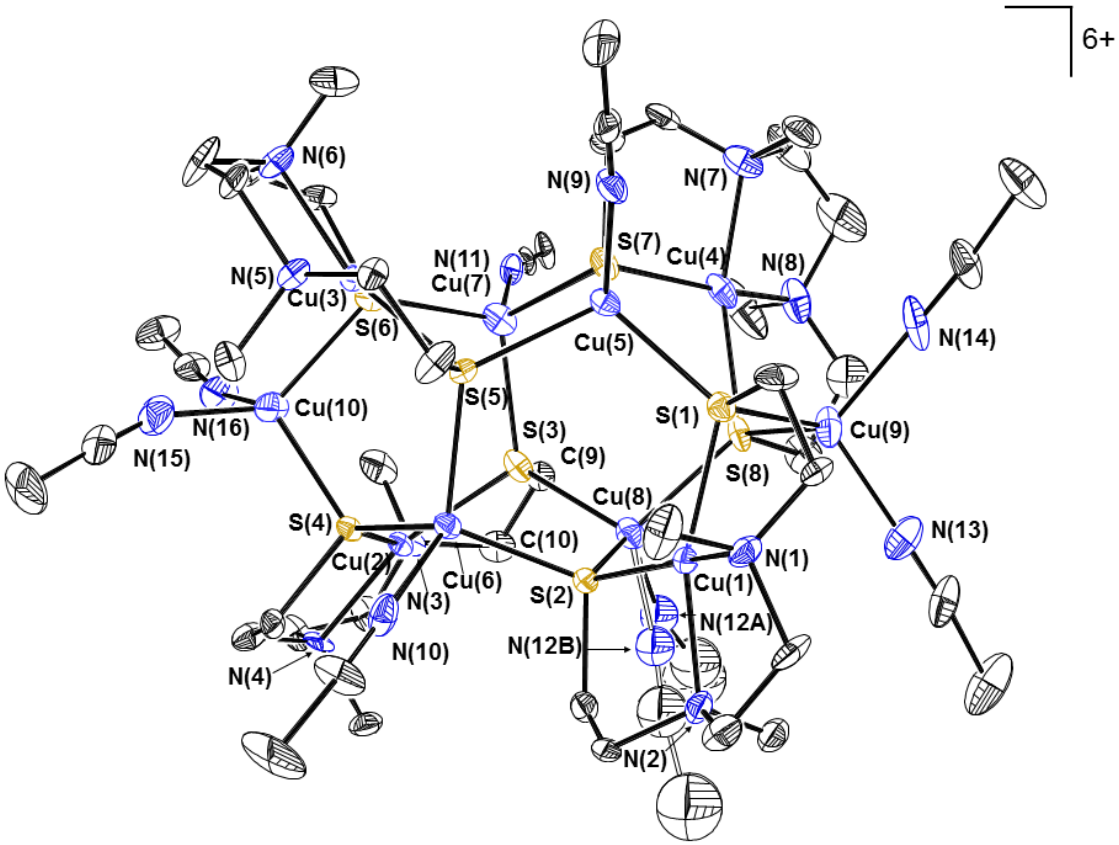

Figure 4.11 Crystal structure of cation of decacopper **4**. All hydrogen atoms removed for clarity and thermal ellipsoids plotted at the 50% probability level.

Despite the complexity of cluster **4**, this decanuclear product appears to be completely reproducible by synthetic means. Solutions of the deep purple mixture of the N_2S_2alkyl disulfide ligand and free copper(I) salts in the appropriate ratio repeatedly produce crystalline **4**, as verified by its electronic absorption spectrum (Figure 4.12).

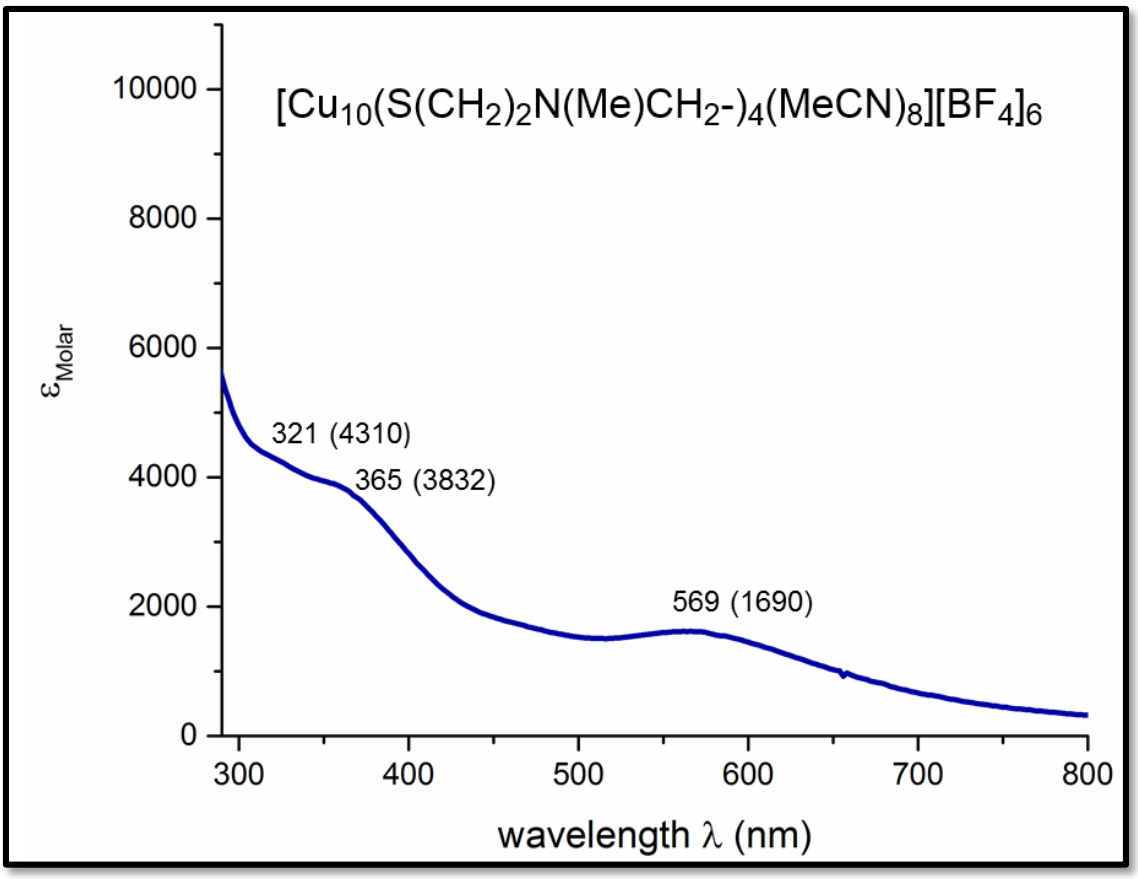

Figure 4.12 UV-vis spectrum of **4**, 0.14 mM in acetonitrile highlighting λ_{max} (ε_{Molar}).

Mixed-valence cluster **4** doesn't reveal any interesting electrochemical behavior, but its established reproducibility is suggestive of the ability of N_2S_2 ligands to support unique structures.

Summary and Conclusions

Copper complexes bearing N_2S_2 ligands formed either serendipitously via ligand exchange or by deliberate syntheses access a variety of structure types. These N_2S_2 ligands appear to stabilize or support mixed-valence cores, which may prove interesting with respect to the potential redox-flexibility and/or multi-electron transformations

possible with these cluster species. If realized, these attributes would mimic, to some extent, the complex transformations observed in nature by metalloenzyme and metalloprotein systems.

It is unclear how large a role the sterics associated with each distinct N_2S_2 ligand play in accessing one structure type versus another. The appearance of copper ions unbound by N_2S_2 ligands within each structure presented here seems to offer the possibility of interplay between structures under different conditions. For example, it may be possible to form a structure like that of **1** by reacting a structure like **3** with a mononuclear Cu(II)-N_2S_2 unit. Likewise, if the sterics were increased for the N_2S_2 ligand involved in the reaction to generate decacopper **4**, would the nuclearity of the product decrease?

Perhaps of greatest importance are the potential transformations possible by polynuclear structures of the type described in this chapter. Complexes **2** and **3** feature coordinatively unsaturated copper sites. Given the fully reduced (all Cu(I)) cores of these complexes, one can speculate as to their potential ability to bind and activate small organic substrates. Furthermore, the presence of multiple copper ions within each core opens up the possibility of cooperative binding and activation, and subsequent multi-electron transformations are conceivable. In particular, complex **3** appears worthy of continued study. Its tetracopper core superficially mimics that of the Cu_Z site of nitrous oxide reductase. Additionally, the quasireversible electrochemical events displayed by **3** seem to suggest its potential ability to release two electrons into a substrate. An open question remains as to whether, in light of the structure and electrochemical behavior of **3**, this complex can oxidatively add sulfur (S^0) to generate a core that includes a μ_4-

bridging sulfide like that observed in the Cu_Z site. Given the open framework of **3**'s core, an exploration of its reactivity may prove interesting within a bioinorganic context.

Experimental

All reactions and manipulations were performed under a pure dinitrogen or argon atmosphere using modified Schlenk techniques or an inert-atmosphere box. Literature procedures were employed for the syntheses of *N*,*N*′-dimethyl-*N*,*N*′-bis(2-mercaptophenyl)ethylenediamine[4] (N_2S_2aryl), *N*,*N*′-dimethyl-*N*,*N*′-bis(2-mercaptoethyl) ethylenediamine[22] (N_2S_2alkyl), *N*,*N*′-bis-2-methyl-mercaptopropyl-*N*,*N*′-dimethylethylenediamine[23] (N_2S_2alkylMe$_4$) and N_2S_2alkyl disulfide.[22]

Solvents either were dried with a system of drying columns from the Glass Contour Company (Et_2O, hexanes, pentane, toluene, benzene, tetrahydrofuran (THF)) or freshly distilled according to standard procedures (CH_3CN).[30] Other reagents were used as received from commercial sources.

All ^{1}H NMR spectra were recorded at 25 °C with a Varian Unity Inova spectrometer operating at 400 MHz and were referenced to the solvent residual. UV-vis spectra were recorded at ambient temperature with a Hewlett-Packard 8452A diode array spectrometer. Electrochemical measurements were performed using a CHI620C electrochemical analyzer workstation with a Ag/AgCl reference electrode, Pt-disk working electrode, and a Pt wire as auxiliary electrode. [^{n}Bu$_4$N][PF_6] was used as the electrolyte. Under these conditions, the Cp_2Fe^+/Cp_2Fe couple consistently occured at +0.50 V.

Molecular orbital calculations were performed at a B3LYP level of theory using the Gaussian 09 software package. Molecular orbitals were calculated for solid state crystal structures. Basis sets employed were the (6-311G) basis set for main group atoms except hydrogen, the (SDD) basis set for copper, and (6-31G) for hydrogen. The molecular rendering and visualization software ChemCraft was used to render molecular structures and orbital surfaces.

All crystals were coated with paratone oil and mounted on the end of a nylon loop attached to the end of the goniometer. Data were collected with a Bruker APEX CCD diffractometer equipped with a Kryoflex attachment supplying a nitrogen stream at 100 or 150 K. All data were collected under control of the *APEX2* software package. Raw data were reduced to F^2 values using the *SAINT* or *SAINT+* software, and a global refinement of unit cell parameters was performed using selected reflections representing ~ 25% of the full data set. Data for the all compounds were corrected for absorption on the basis of multiple measurements of symmetry equivalent reflections with the use of *SADABS*. All structure solutions were obtained by direct methods or intrinsic phasing using *SHELXS*, while refinements were accomplished by full-matrix least-squares procedures using *SHELXL*. Both the *SHELXS* and *SHELXL* programs are incorporated into the *SHELXTL* software suite. All hydrogen atoms were added in calculated positions and included as riding contributions with isotropic displacement parameters tied to those of the carbon atoms to which they were attached. All images were created with the use of *XP*, which also is part of the *SHELXTL* package. References for the crystallography software mentioned above can be found in Chapter 1 (references 79-87) of this dissertation. Final unit cell data and refinement statistics are collected in Table 4.1.

[(N_2S_2alkylMe$_4$)Cu)$_2$(μ-Cu$_2$)], **3**

To a clear, colorless solution of $H_2N_2S_2$alkylMe$_4$ (0.352 g, 1.33 mmol) in 20 mL of dry THF was added sodium triethylborohydride (1M in THF, 2.66 mL, 2 eq.) dropwise at room temperature via gas-tight syringe. Upon addition, bubbles (H_2) evolved from the stirring solution, and a white precipitate formed after 2 hr. The solvent was then removed *in vacuo* to give a sticky, white residue. [Cu(MeCN)$_4$]PF_6 (0.992 g, 2.66 mmol) in 25 mL of dry acetonitrile was then cannulated into the flask containing the residue to generate an orange solution which was stirred for 12 hr. Following removal of the solvent, 40 mL of dry toluene was added and the mixture stirred for 1 hr. The mixture was then filtered through celite anaerobically, and the solvent was evaporated to give 0.149 g of crude pale yellow product (29% yield). Crystalline material is obtained from ether/pentane at -30°C. ^{1}H NMR (δ, ppm in benzene): 1.52 (s, 12H), 1.83 (s, 12H), 1.88 (m, 4H), 2.04 (m, 8H), 2.14 (m, 4H), 2.35 (s, 12H). Electrochemistry (in THF): [(N_2S_2alkylMe$_4$)Cu)$_2$(μ-Cu$_2$)]$^+$/ [(N_2S_2alkylMe$_4$)Cu)$_2$(μ-Cu$_2$)] (quasireversible, $E_{1/2}$ = +10 mV *vs*. Ag/AgCl), [(N_2S_2alkylMe$_4$)Cu)$_2$(μ-Cu$_2$)]$^{2+}$/[(N_2S_2alkylMe$_4$)Cu)$_2$(μ-Cu$_2$)]$^+$ (quasireversible, $E_{1/2}$ = +380 mV *vs*. Ag/AgCl), and [(N_2S_2alkylMe$_4$)Cu)$_2$(μ-Cu$_2$)]$^{3+}$/[(N_2S_2alkylMe$_4$)Cu)$_2$(μ-Cu$_2$)]$^{2+}$ (irreversible anodic wave at + 650 mV *vs.* Ag/AgCl).

[Cu$_{10}$(S(CH$_2$)$_2$N(Me)CH$_2$−)$_4$(MeCN)$_8$][BF$_4$]$_6$, **4**

To a light yellow semi-suspension of N_2S_2alkyl disulfide (0.1089 g, 0.2638 mmol) in 35 mL of dry acetonitrile was added [Cu(MeCN)$_4$][PF_6] (0.2075 g, 0.6595

mmol) in one portion to generate a uniform, dark purple solution. This solution was stirred at room temperature for 2 hr, then evaporated to dryness. The crude dark purple resulting residue was washed with 2x 10 mL of diethyl ether and redissolved in 15 mL of dry acetonitrile. This concentrated acetonitrile solution was then filtered anaerobically through celite, and the filtrate evaporated to dryness to afford a deep purple crude solid (0.139 g, 91% yield based on copper). Large, deep purple slab crystals were grown by diffusing *tert*-butyl methyl ether vapor into a concentrated solution of the product. UV-vis (MeCN), λ_{max} nm (ε_M): 321 (shoulder, 4310), 365 (3830), 569 (1690).

References

1) Papini, G.; Alidori, S.; Lewis, J. S.; Reichert, D. E.; Pellei, M.; Gioia Lobbia, G.; Biddlecombe, G. B.; Anderson, C. J.; Santini, C., *J. Chem. Soc., Dalton Trans.* **2009**, 177-184.

2) Torelli, S.; Belle, C.; Philouze, C.; Pierre, J.-L.; Rammal, W.; Saint-Aman, E., *Eur. J. Inorg. Chem.* **2003**, *2003*, 2452-2457.

3) Sarkar, S.; Das, B., *Complex Metals*, **2014**, 80-87.

4) Dowerah, D.; Spence, J. T.; Singh, R.; Wedd, A. G.; Wilson, G. L.; Farchione, F.; Enemark, J. H.; Kristofzski, J.; Bruck, M., *J. Am. Chem. Soc.* **1987**, *109*, 5655-5665.

5) Barnard, K. R.; Bruck, M.; Huber, S.; Grittini, C.; Enemark, J. H.; Gable, R. W.; Wedd, A. G., *Inorg. Chem.* **1997**, *36*, 637-649.

6) Benoist, E.; Charbonnel-Jobic, G.; Courseille, C.; Gestin, J.-F.; Parrain, J.-L.; Chatal, J.-F.; Quintard, J.-P., *New J. Chem.* **1998**, *22*, 615-619.

7) Lipowska, M.; Hansen, L.; Cini, R.; Xu, X.; Choi, H.; Taylor, A. T.; Marzilli, L. G., *Inorg. Chim. Acta* **2002**, *339*, 327-340.

8) Mills, D. K.; Hsiao, Y. M.; Farmer, P. J.; Atnip, E. V.; Reibenspies, J. H.; Darensbourg, M. Y., *J. Am. Chem. Soc.* **1991**, *113*, 1421-1423.

9) Angamuthu, R.; Byers, P.; Lutz, M.; Spek, A. L.; Bouwman, E., *Science* **2010**, *327*, 313-315.

10) Solomon, E. I.; Szilagyi, R. K.; DeBeer George, S.; Basumallick, L., *Chem. Rev.* **2004**, *104*, 419-458.

11) Gray, H. B.; Malmström, B. G.; Williams, R. J. P., *JBIC J. Biol. Inorg. Chem.* **2000**, *5*, 551-559.

12) Malmström, B. G., *Eur. J. Biochem.* **1994**, *223*, 711-718.

13) Pomowski, A.; Zumft, W. G.; Kroneck, P. M. H.; Einsle, O., *Nature* **2011**, *477*, 234-237.

14) Pauleta, S. R.; Dell'Acqua, S.; Moura, I., *Coord. Chem. Rev.* **2013**, *257*, 332-349.

15) Solomon, E. I.; Heppner, D. E.; Johnston, E. M.; Ginsbach, J. W.; Cirera, J.; Qayyum, M.; Kieber-Emmons, M. T.; Kjaergaard, C. H.; Hadt, R. G.; Tian, L., *Chem. Rev.* **2014**, *114*, 3659-3853.

16) Neese, F.; Zumft, W. G.; Antholine, W. E.; Kroneck, P. M. H., *J. Am. Chem. Soc.* **1996**, *118*, 8692-8699.

17) Charnock, J. M.; Dreusch, A.; Korner, H.; Neese, F.; Nelson, J.; Kannt, A.; Michel, H.; Garner, C. D.; Kroneck, P. M. H.; Zumft, W. G. *Eur. J. Biochem.* **2000**, *267*, 1368-1381.

18) Rosenzweig, A. C., *Nat. Struct. Mol. Biol.* **2000**, *7*, 169-171.

19) York, J. T.; Bar-Nahum, I.; Tolman, W. B., *Inorg. Chim. Acta* **2008**, *361*, 885-893.

20) Brown, E. C.; York, J. T.; Antholine, W. E.; Ruiz, E.; Alvarez, S.; Tolman, W. B., *J. Am. Chem. Soc.* **2005**, *127*, 13752-13753.

21) Kuhl, K. P.; Cave, E. R.; Abram, D. N.; Jaramillo, T. F., *Energy & Environmental Science 5*, 7050-7059.

22) Karlin, K. D.; Lippard, S. J., *J. Am. Chem. Soc.* **1976**, *98*, 6951-7.

23) Grapperhaus, C. A.; Mullins, C. S.; Kozlowski, P. M.; Mashuta, M. S., *Inorg. Chem.* **2004**, *43*, 2859-2866.

24) Bharadwaj, P. K.; John, E.; Xie, C. L.; Zhang, D.; Hendrickson, D. N.; Potenza, J. A.; Schugar, H. J., *Inorg. Chem.* **1986**, *25*, 4541-4546.

25) Stibrany, R. T.; Fikar, R.; Brader, M.; Potenza, M. N.; Potenza, J. A.; Schugar, H. J., *Inorg. Chem.* **2002**, *41*, 5203-5215.

26) Fortman, G. C.; Slawin, A. M. Z.; Nolan, S. P., *Organometallics* **2010**, *29*, 3966-3972.

27) Howell, J. A. S., *Polyhedron* **2006**, *25*, 2993-3005.

28) Schneider, J.; Kockerling, M.; Kopitzky, R.; Henkel, G., *Eur. J. Inorg. Chem.* **2003**, 1727-1734.

29) Sukal, S.; Bradshaw, J. E.; He, J.; Yap, G. P. a.; Rheingold, A. L.; Kung, H. F.; Francesconi, L. C., *Polyhedron* **1998**, *18*, 7-17.

30) Armarego, W. L. F.; Chai, C. L. L., *Purification of Laboratory Chemicals*. Butterworth-Heinemann: 2003.

Chapter 1: Crystal Information

Structure Determination Summary

Crystal Data and Structure Refinement for ^{t}Bu-S-Trip, **8**

Identification code	jpd409_0m	
Empirical formula	$C_{24}H_{22}S$	
Formula weight	342.48	
Temperature	100(2) K	
Wavelength	0.71073 Å	
Crystal system	Orthorhombic	
Space group	$P2_12_12_1$	
Unit cell dimensions	a = 13.8394(7) Å	α = 90°
	b = 15.6605(8) Å	β = 90°
	c = 16.5178(9) Å	γ = 90°
Volume, Z	3579.9(3) Å^3, 8	
Density (calculated)	1.271 g/cm^3	
Absorption coefficient	0.184 mm^{-1}	
F(000)	1456	
Crystal size	0.29 x 0.18 x 0.08 mm	
θ range for data collection	1.92 to 28.34°	
Limiting indices	$-18 < h < 18$, $-20 < k < 20$, $-22 < l < 22$	
Reflections collected	63210	
Independent reflections	8914 (R_{int} = 0.0599)	
Completeness to θ = 28.34°	99.9 %	
Absorption correction	Semi-empirical from equivalents	
Max. and min. transmission	0.9855 and 0.9487	
Refinement method	Full-matrix least-squares on F^2	
Data / restraints / parameters	8914 / 0 / 457	
Goodness-of-fit on F^2	1.027	
Final R indices [I>2σ(I)]	R1 = 0.0374, wR2 = 0.0893	
R indices (all data)	R1 = 0.0443, wR2 = 0.0943	
Absolute structure parameter	0.07(4)	
Largest diff. peak and hole	0.327 and -0.235 e·Å^{-3}	

Table S1. Atomic coordinates (x 10^4) and equivalent isotropic displacement parameters ($Å^2$ x 10^3) for ^{t}Bu-S-Trip. U(eq) is defined as one third of the trace of the orthogonalized U_{ij} tensor.

Atom	x	y	z	U(eq)
S(1)	1239(1)	640(1)	8730(1)	17(1)
S(2)	3691(1)	8138(1)	8596(1)	18(1)
C(1)	274(1)	347(1)	8036(1)	14(1)
C(2)	717(1)	-277(1)	7407(1)	15(1)
C(3)	1657(1)	-574(1)	7378(1)	19(1)
C(4)	1932(1)	-1128(1)	6758(1)	22(1)
C(5)	1277(2)	-1380(1)	6179(1)	24(1)
C(6)	318(1)	-1098(1)	6214(1)	22(1)
C(7)	38(1)	-552(1)	6829(1)	17(1)
C(8)	-564(1)	-171(1)	8402(1)	16(1)
C(9)	-659(1)	-431(1)	9199(1)	18(1)
C(10)	-1425(1)	-961(1)	9424(1)	21(1)
C(11)	-2093(1)	-1230(1)	8854(1)	24(1)
C(12)	-2000(1)	-978(1)	8052(1)	22(1)
C(13)	-1236(1)	-458(1)	7825(1)	17(1)
C(14)	-157(1)	1060(1)	7496(1)	16(1)
C(15)	131(1)	1907(1)	7465(1)	19(1)
C(16)	-321(1)	2466(1)	6927(1)	22(1)
C(17)	-1048(1)	2180(1)	6421(1)	24(1)
C(18)	-1308(1)	1320(1)	6421(1)	21(1)
C(19)	-854(1)	761(1)	6951(1)	18(1)
C(20)	-980(1)	-203(1)	6968(1)	18(1)
C(21)	870(1)	1441(1)	9509(1)	18(1)
C(22)	1549(1)	2209(1)	9393(1)	25(1)
C(23)	1095(1)	1038(1)	10330(1)	22(1)
C(24)	-186(1)	1713(1)	9476(1)	18(1)
C(25)	4629(1)	7781(1)	7900(1)	14(1)
C(26)	5414(1)	7194(1)	8257(1)	15(1)
C(27)	5470(1)	6897(1)	9047(1)	17(1)
C(28)	6196(1)	6317(1)	9257(1)	20(1)
C(29)	6852(1)	6031(1)	8686(1)	21(1)
C(30)	6792(1)	6316(1)	7890(1)	18(1)
C(31)	6070(1)	6888(1)	7681(1)	16(1)
C(32)	5144(1)	8476(1)	7398(1)	16(1)
C(33)	4972(1)	9348(1)	7424(1)	19(1)
C(34)	5509(1)	9895(1)	6928(1)	22(1)
C(35)	6191(1)	9572(1)	6400(1)	22(1)
C(36)	6336(1)	8690(1)	6342(1)	19(1)
C(37)	5808(1)	8149(1)	6841(1)	15(1)

C(38)	4145(1)	7202(1)	7251(1)	16(1)

Table S1. Atomic coordinates (x 10^4) and equivalent isotropic displacement parameters ($Å^2$ x 10^3) for ^{t}Bu-S-Trip. U(eq) is defined as one third of the trace of the orthogonalized U_{ij} tensor.

Atom	x	y	z	U(eq)
C(39)	3182(1)	6967(1)	7204(1)	19(1)
C(40)	2880(1)	6408(1)	6596(1)	23(1)
C(41)	3534(1)	6086(1)	6042(1)	24(1)
C(42)	4502(1)	6330(1)	6082(1)	20(1)
C(43)	4806(1)	6886(1)	6681(1)	16(1)
C(44)	5844(1)	7179(1)	6826(1)	16(1)
C(45)	4163(1)	8825(1)	9443(1)	19(1)
C(46)	3912(1)	8362(1)	10233(1)	24(1)
C(47)	5237(1)	9025(1)	9420(1)	20(1)
C(48)	3557(1)	9645(1)	9400(1)	24(1)

Table S2. Bond lengths (Å) for ^{t}Bu-S-Trip. Symmetry transformations used to generate equivalent atoms:

S(1)-C(1)	1.8194(17)	C(9)-H(9)	0.9500
S(1)-C(21)	1.8672(17)	C(10)-C(11)	1.385(3)
S(2)-C(25)	1.8225(16)	C(10)-H(10)	0.9500
S(2)-C(45)	1.8814(18)	C(11)-C(12)	1.388(3)
C(1)-C(8)	1.539(2)	C(11)-H(11)	0.9500
C(1)-C(14)	1.548(2)	C(12)-C(13)	1.387(2)
C(1)-C(2)	1.552(2)	C(12)-H(12)	0.9500
C(2)-C(3)	1.382(2)	C(13)-C(20)	1.513(2)
C(2)-C(7)	1.407(2)	C(14)-C(15)	1.386(2)
C(3)-C(4)	1.396(2)	C(14)-C(19)	1.399(2)
C(3)-H(3)	0.9500	C(15)-C(16)	1.396(3)
C(4)-C(5)	1.376(3)	C(15)-H(15)	0.9500
C(4)-H(4)	0.9500	C(16)-C(17)	1.383(3)
C(5)-C(6)	1.400(3)	C(16)-H(16)	0.9500
C(5)-H(5)	0.9500	C(17)-C(18)	1.393(3)
C(6)-C(7)	1.384(2)	C(17)-H(17)	0.9500
C(6)-H(6)	0.9500	C(18)-C(19)	1.389(2)
C(7)-C(20)	1.528(2)	C(18)-H(18)	0.9500
C(8)-C(9)	1.384(2)	C(19)-C(20)	1.520(2)
C(8)-C(13)	1.405(2)	C(20)-H(20)	1.0000
C(9)-C(10)	1.397(2)	C(21)-C(24)	1.523(2)

C(21)-C(23)	1.528(2)
C(21)-C(22)	1.539(2)
C(22)-H(22A)	0.9800
C(22)-H(22B)	0.9800
C(22)-H(22C)	0.9800
C(23)-H(23A)	0.9800
C(23)-H(23B)	0.9800
C(23)-H(23C)	0.9800
C(24)-H(24A)	0.9800
C(24)-H(24B)	0.9800
C(24)-H(24C)	0.9800
C(25)-C(26)	1.539(2)
C(25)-C(32)	1.543(2)
C(25)-C(38)	1.556(2)
C(26)-C(27)	1.389(2)
C(26)-C(31)	1.399(2)
C(27)-C(28)	1.398(2)
C(27)-H(27)	0.9500
C(28)-C(29)	1.383(2)
C(28)-H(28)	0.9500
C(29)-C(30)	1.391(3)
C(29)-H(29)	0.9500
C(30)-C(31)	1.386(2)
C(30)-H(30)	0.9500
C(31)-C(44)	1.518(2)
C(32)-C(33)	1.386(2)
C(32)-C(37)	1.398(2)
C(33)-C(34)	1.399(3)
C(33)-H(33)	0.9500
C(34)-C(35)	1.381(3)
C(34)-H(34)	0.9500
C(35)-C(36)	1.399(2)
C(35)-H(35)	0.9500
C(36)-C(37)	1.389(2)
C(36)-H(36)	0.9500
C(37)-C(44)	1.521(2)
C(38)-C(39)	1.385(2)
C(38)-C(43)	1.402(2)
C(39)-C(40)	1.396(2)
C(39)-H(39)	0.9500
C(40)-C(41)	1.382(3)
C(40)-H(40)	0.9500
C(41)-C(42)	1.395(3)
C(41)-H(42)	0.95

Table S2. Bond lengths (Å) for ^{t}Bu-S-Trip. Symmetry transformations used to generate equivalent atoms:

C(42)-C(43)	1.383(2)
C(42)-H(43)	0.9500
C(43)-C(44)	1.527(2)
C(44)-H(44)	1.0000
C(45)-C(47)	1.520(2)
C(45)-C(46)	1.533(3)
C(45)-C(48)	1.535(2)
C(46)-H(46A)	0.9800
C(46)-H(46B)	0.9800
C(46)-H(46C)	0.9800
C(47)-H(47A)	0.9800
C(47)-H(47B)	0.9800
C(47)-H(47C)	0.9800
C(48)-H(48A)	0.9800
C(48)-H(48B)	0.9800
C(48)-H(48C)	0.9800

Table S3. Bond angles (deg.) for ^{t}Bu-S-Trip. Symmetry transformations used to generate equivalent atoms:

C(1)-S(1)-C(21)	113.80(8)	C(8)-C(13)-C(20)	113.24(15)
C(25)-S(2)-C(45)	113.38(8)	C(15)-C(14)-C(19)	119.63(16)
C(8)-C(1)-C(14)	108.39(13)	C(15)-C(14)-C(1)	126.91(15)
C(8)-C(1)-C(2)	103.21(12)	C(19)-C(14)-C(1)	113.24(14)
C(14)-C(1)-C(2)	102.77(13)	C(14)-C(15)-C(16)	119.70(17)
C(8)-C(1)-S(1)	116.01(12)	C(14)-C(15)-H(15)	120.2
C(14)-C(1)-S(1)	117.62(11)	C(16)-C(15)-H(15)	120.2
C(2)-C(1)-S(1)	106.95(11)	C(17)-C(16)-C(15)	120.45(16)
C(3)-C(2)-C(7)	120.18(15)	C(17)-C(16)-H(16)	119.8
C(3)-C(2)-C(1)	127.28(15)	C(15)-C(16)-H(16)	119.8
C(7)-C(2)-C(1)	112.53(14)	C(16)-C(17)-C(18)	120.08(16)
C(2)-C(3)-C(4)	119.41(17)	C(16)-C(17)-H(17)	120.0
C(2)-C(3)-H(3)	120.3	C(18)-C(17)-H(17)	120.0
C(4)-C(3)-H(3)	120.3	C(19)-C(18)-C(17)	119.53(17)
C(5)-C(4)-C(3)	120.57(17)	C(19)-C(18)-H(18)	120.2
C(5)-C(4)-H(4)	119.7	C(17)-C(18)-H(18)	120.2
C(3)-C(4)-H(4)	119.7	C(18)-C(19)-C(14)	120.41(16)
C(4)-C(5)-C(6)	120.38(16)	C(18)-C(19)-C(20)	125.89(16)
C(4)-C(5)-H(5)	119.8	C(14)-C(19)-C(20)	113.53(15)
C(6)-C(5)-H(5)	119.8	C(13)-C(20)-C(19)	107.84(14)
C(7)-C(6)-C(5)	119.38(17)	C(13)-C(20)-C(7)	105.24(14)
C(7)-C(6)-H(6)	120.3	C(19)-C(20)-C(7)	104.27(13)
C(5)-C(6)-H(6)	120.3	C(13)-C(20)-H(20)	112.9
C(6)-C(7)-C(2)	120.03(16)	C(19)-C(20)-H(20)	112.9
C(6)-C(7)-C(20)	126.13(16)	C(7)-C(20)-H(20)	112.9
C(2)-C(7)-C(20)	113.83(14)	C(24)-C(21)-C(23)	110.06(14)
C(9)-C(8)-C(13)	119.22(15)	C(24)-C(21)-C(22)	111.28(15)
C(9)-C(8)-C(1)	126.85(15)	C(23)-C(21)-C(22)	108.02(15)
C(13)-C(8)-C(1)	113.65(14)	C(24)-C(21)-S(1)	115.15(12)
C(8)-C(9)-C(10)	120.02(16)	C(23)-C(21)-S(1)	106.14(12)
C(8)-C(9)-H(9)	120.0	C(22)-C(21)-S(1)	105.81(12)
C(10)-C(9)-H(9)	120.0	C(21)-C(22)-H(22A)	109.5
C(11)-C(10)-C(9)	120.37(16)	C(21)-C(22)-H(22B)	109.5
C(11)-C(10)-H(10)	119.8	H(22A)-C(22)-H(22B)	109.5
C(9)-C(10)-H(10)	119.8	C(21)-C(22)-H(22C)	109.5
C(10)-C(11)-C(12)	120.07(16)	H(22A)-C(22)-H(22C)	109.5
C(10)-C(11)-H(11)	120.0	H(22B)-C(22)-H(22C)	109.5
C(12)-C(11)-H(11)	120.0	C(21)-C(23)-H(23A)	109.5
C(13)-C(12)-C(11)	119.70(17)	C(21)-C(23)-H(23B)	109.5
C(13)-C(12)-H(12)	120.1	H(23A)-C(23)-H(23B)	109.5
C(11)-C(12)-H(12)	120.1	C(21)-C(23)-H(23C)	109.5
C(12)-C(13)-C(8)	120.60(16)	H(23A)-C(23)-H(23C)	109.5
C(12)-C(13)-C(20)	125.96(15)	H(23B)-C(23)-H(23C)	109.5

Table S3. Bond angles (deg.) for ^{t}Bu-S-Trip. Symmetry transformations used to generate equivalent atoms:

C(21)-C(24)-H(24A)	109.5	C(37)-C(36)-H(36)	120.5
C(21)-C(24)-H(24B)	109.5	C(35)-C(36)-H(36)	120.5
H(24A)-C(24)-H(24B)	109.5	C(36)-C(37)-C(32)	120.90(15)
C(21)-C(24)-H(24C)	109.5	C(36)-C(37)-C(44)	125.60(15)
H(24A)-C(24)-H(24C)	109.5	C(32)-C(37)-C(44)	113.45(14)
H(24B)-C(24)-H(24C)	109.5	C(39)-C(38)-C(43)	119.73(16)
C(26)-C(25)-C(32)	107.56(13)	C(39)-C(38)-C(25)	127.45(15)
C(26)-C(25)-C(38)	102.72(12)	C(43)-C(38)-C(25)	112.79(14)
C(32)-C(25)-C(38)	103.83(13)	C(38)-C(39)-C(40)	119.68(17)
C(26)-C(25)-S(2)	116.39(11)	C(38)-C(39)-H(39)	120.2
C(32)-C(25)-S(2)	116.82(11)	C(40)-C(39)-H(39)	120.2
C(38)-C(25)-S(2)	107.85(11)	C(41)-C(40)-C(39)	120.56(17)
C(27)-C(26)-C(31)	119.16(15)	C(41)-C(40)-H(40)	119.7
C(27)-C(26)-C(25)	126.85(15)	C(39)-C(40)-H(40)	119.7
C(31)-C(26)-C(25)	113.72(14)	C(40)-C(41)-C(42)	119.88(16)
C(26)-C(27)-C(28)	119.43(16)	C(40)-C(41)-H(42)	120.1
C(26)-C(27)-H(27)	120.3	C(42)-C(41)-H(42)	120.1
C(28)-C(27)-H(27)	120.3	C(43)-C(42)-C(41)	119.87(17)
C(29)-C(28)-C(27)	120.87(16)	C(43)-C(42)-H(43)	120.1
C(29)-C(28)-H(28)	119.6	C(41)-C(42)-H(43)	120.1
C(27)-C(28)-H(28)	119.6	C(42)-C(43)-C(38)	120.28(16)
C(28)-C(29)-C(30)	120.10(16)	C(42)-C(43)-C(44)	125.94(15)
C(28)-C(29)-H(29)	120.0	C(38)-C(43)-C(44)	113.71(14)
C(30)-C(29)-H(29)	120.0	C(31)-C(44)-C(37)	106.95(13)
C(31)-C(30)-C(29)	119.06(16)	C(31)-C(44)-C(43)	104.47(13)
C(31)-C(30)-H(30)	120.5	C(37)-C(44)-C(43)	105.78(13)
C(29)-C(30)-H(30)	120.5	C(31)-C(44)-H(44)	113.0
C(30)-C(31)-C(26)	121.35(16)	C(37)-C(44)-H(44)	113.0
C(30)-C(31)-C(44)	125.09(15)	C(43)-C(44)-H(44)	113.0
C(26)-C(31)-C(44)	113.32(14)	C(47)-C(45)-C(46)	109.91(15)
C(33)-C(32)-C(37)	119.55(16)	C(47)-C(45)-C(48)	111.08(15)
C(33)-C(32)-C(25)	126.85(16)	C(46)-C(45)-C(48)	108.09(15)
C(37)-C(32)-C(25)	113.52(14)	C(47)-C(45)-S(2)	116.07(12)
C(32)-C(33)-C(34)	119.64(17)	C(46)-C(45)-S(2)	106.53(12)
C(32)-C(33)-H(33)	120.2	C(48)-C(45)-S(2)	104.74(12)
C(34)-C(33)-H(33)	120.2	C(45)-C(46)-H(46A)	109.5
C(35)-C(34)-C(33)	120.54(16)	C(45)-C(46)-H(46B)	109.5
C(35)-C(34)-H(34)	119.7	H(46A)-C(46)-H(46B)	109.5
C(33)-C(34)-H(34)	119.7	C(45)-C(46)-H(46C)	109.5
C(34)-C(35)-C(36)	120.18(16)	H(46A)-C(46)-H(46C)	109.5
C(34)-C(35)-H(35)	119.9	H(46B)-C(46)-H(46C)	109.5
C(36)-C(35)-H(35)	119.9	C(45)-C(47)-H(47A)	109.5
C(37)-C(36)-C(35)	119.08(16)	C(45)-C(47)-H(47B)	109.5

Table S3. Bond angles (deg.) for ^{t}Bu-S-Trip. Symmetry transformations used to generate equivalent atoms:

H(47A)-C(47)-H(47B)	109.5
C(45)-C(47)-H(47C)	109.5
H(47A)-C(47)-H(47C)	109.5
H(47B)-C(47)-H(47C)	109.5
C(45)-C(48)-H(48A)	109.5
C(45)-C(48)-H(48B)	109.5
H(48A)-C(48)-H(48B)	109.5
C(45)-C(48)-H(48C)	109.5
H(48A)-C(48)-H(48C)	109.5
H(48B)-C(48)-H(48C)	109.5

Table S4. Anisotropic displacement parameters ($Å^2$ x 10^3) for ^{t}Bu-S-Trip. The anisotropic displacement factor exponent takes the form: $-2\pi^2[(ha^*)^2U_{11} + ... + 2hka^*b^*U_{12}]$.

Atom	U_{11}	U_{22}	U_{33}	U_{23}	U_{13}	U_{12}
S(1)	15(1)	18(1)	17(1)	-3(1)	0(1)	0(1)
S(2)	14(1)	21(1)	19(1)	-4(1)	1(1)	2(1)
C(1)	16(1)	15(1)	13(1)	0(1)	0(1)	1(1)
C(2)	21(1)	12(1)	13(1)	1(1)	4(1)	-1(1)
C(3)	21(1)	16(1)	20(1)	4(1)	3(1)	-1(1)
C(4)	25(1)	16(1)	27(1)	2(1)	9(1)	2(1)
C(5)	35(1)	15(1)	23(1)	-3(1)	11(1)	-1(1)
C(6)	33(1)	17(1)	16(1)	-2(1)	1(1)	-5(1)
C(7)	22(1)	14(1)	16(1)	2(1)	2(1)	-1(1)
C(8)	15(1)	14(1)	19(1)	0(1)	2(1)	1(1)
C(9)	19(1)	17(1)	16(1)	-1(1)	-1(1)	1(1)
C(10)	23(1)	23(1)	17(1)	4(1)	3(1)	0(1)
C(11)	17(1)	24(1)	31(1)	3(1)	2(1)	-4(1)
C(12)	18(1)	24(1)	24(1)	0(1)	-4(1)	-2(1)
C(13)	17(1)	18(1)	17(1)	1(1)	-2(1)	1(1)
C(14)	18(1)	17(1)	14(1)	1(1)	2(1)	3(1)
C(15)	25(1)	16(1)	16(1)	-1(1)	4(1)	1(1)
C(16)	32(1)	16(1)	20(1)	1(1)	7(1)	4(1)
C(17)	29(1)	24(1)	20(1)	8(1)	6(1)	10(1)
C(18)	19(1)	28(1)	17(1)	3(1)	0(1)	3(1)
C(19)	18(1)	19(1)	16(1)	1(1)	2(1)	2(1)
C(20)	20(1)	19(1)	16(1)	0(1)	-3(1)	-2(1)
C(21)	20(1)	19(1)	16(1)	-3(1)	1(1)	-2(1)
C(22)	25(1)	23(1)	26(1)	-7(1)	3(1)	-7(1)
C(23)	21(1)	30(1)	16(1)	-1(1)	-3(1)	1(1)
C(24)	22(1)	18(1)	16(1)	-1(1)	2(1)	2(1)
C(25)	14(1)	15(1)	14(1)	0(1)	1(1)	3(1)
C(26)	15(1)	12(1)	18(1)	1(1)	-1(1)	1(1)
C(27)	19(1)	16(1)	17(1)	-2(1)	1(1)	0(1)
C(28)	23(1)	18(1)	18(1)	2(1)	-3(1)	1(1)
C(29)	19(1)	18(1)	25(1)	0(1)	-4(1)	6(1)
C(30)	17(1)	16(1)	22(1)	-3(1)	1(1)	2(1)
C(31)	16(1)	14(1)	18(1)	0(1)	0(1)	-1(1)
C(32)	17(1)	17(1)	14(1)	2(1)	-4(1)	-2(1)
C(33)	23(1)	18(1)	17(1)	0(1)	-4(1)	2(1)
C(34)	30(1)	14(1)	23(1)	1(1)	-8(1)	-1(1)
C(35)	25(1)	23(1)	18(1)	6(1)	-4(1)	-7(1)
C(36)	18(1)	22(1)	16(1)	2(1)	-3(1)	-1(1)
C(37)	16(1)	15(1)	16(1)	0(1)	-3(1)	0(1)
C(38)	17(1)	14(1)	16(1)	2(1)	-2(1)	2(1)

Table S4. Anisotropic displacement parameters ($Å^2$ x 10^3) for ^{t}Bu-S-Trip. The anisotropic displacement factor exponent takes the form: $-2\pi^2[(ha^*)^2U_{11} + ... + 2hka^*b^*U_{12}]$.

Atom	U_{11}	U_{22}	U_{33}	U_{23}	U_{13}	U_{12}
C(39)	18(1)	18(1)	19(1)	3(1)	-1(1)	-1(1)
C(40)	20(1)	22(1)	27(1)	4(1)	-4(1)	-5(1)
C(41)	33(1)	17(1)	21(1)	-1(1)	-6(1)	-6(1)
C(42)	28(1)	15(1)	18(1)	1(1)	-1(1)	1(1)
C(43)	19(1)	13(1)	15(1)	3(1)	0(1)	2(1)
C(44)	17(1)	15(1)	16(1)	-1(1)	2(1)	2(1)
C(45)	18(1)	22(1)	17(1)	-4(1)	-2(1)	3(1)
C(46)	23(1)	31(1)	18(1)	-3(1)	2(1)	3(1)
C(47)	20(1)	20(1)	19(1)	-3(1)	-2(1)	1(1)
C(48)	26(1)	24(1)	24(1)	-8(1)	-3(1)	8(1)

Table S5. Hydrogen coordinates (x 10^4) and isotropic displacement parameters ($Å^2$ x ^{103}) for ^{t}Bu-S-Trip.

H atom	x	y	z	U(eq)
H(3)	2111	-402	7778	23
H(4)	2578	-1333	6736	27
H(5)	1476	-1748	5753	29
H(6)	-137	-1280	5819	26
H(9)	-202	-250	9592	21
H(10)	-1488	-1137	9972	25
H(11)	-2615	-1587	9012	29
H(12)	-2458	-1162	7661	27
H(15)	633	2106	7809	23
H(16)	-128	3048	6908	27
H(17)	-1371	2569	6073	29
H(18)	-1792	1118	6062	25
H(20)	-1457	-413	6559	22
H(22A)	2222	2017	9423	37
H(22B)	1428	2631	9819	37
H(22C)	1430	2469	8863	37
H(23A)	656	557	10425	34
H(23B)	1009	1464	10758	34
H(23C)	1764	833	10334	34
H(24A)	-308	2146	9891	28
H(24B)	-600	1216	9574	28
H(24C)	-329	1951	8940	28
H(27)	5020	7086	9442	21
H(28)	6239	6116	9799	24
H(29)	7344	5640	8839	25
H(30)	7240	6121	7496	22
H(33)	4494	9572	7777	23
H(34)	5403	10494	6954	27
H(35)	6563	9949	6075	27
H(36)	6789	8464	5967	23
H(39)	2729	7185	7583	23
H(40)	2219	6246	6563	28
H(42)	3324	5700	5634	28
H(43)	4952	6114	5699	24
H(44)	6308	6950	6416	19
H(46A)	3227	8201	10228	36
H(46B)	4037	8742	10693	36
H(46C)	4310	7848	10284	36
H(47A)	5403	9396	9877	30
H(47B)	5393	9316	8911	30

Table S5. Hydrogen coordinates (x 10^4) and isotropic displacement parameters ($Å^2$ x ^{103}) for ^{t}Bu-S-Trip.

H atom	x	y	z	U(eq)
H(47C)	5607	8493	9456	30
H(48A)	3715	9956	8903	37
H(48B)	3701	10004	9870	37
H(48C)	2869	9497	9399	37

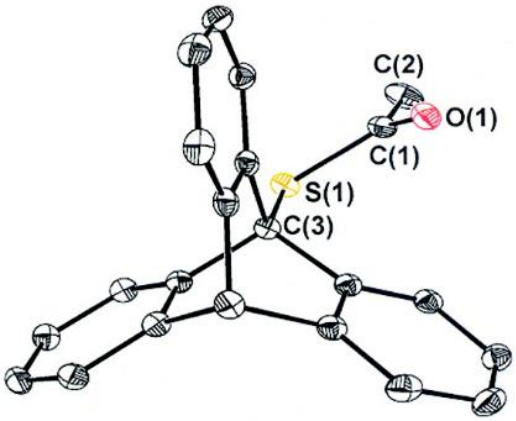

Structure Determination Summary

Crystal Data and Structure Refinement for Triptycyl Thiol *S*-Acetyl ester, **5**

Identification code	jpd383
Empirical formula	$C_{22}H_{16}OS$
Formula weight	328.41
Temperature	373(2) K
Wavelength	0.71073 Å
Crystal system	Monoclinic
Space group	$P2_1/c$
Unit cell dimensions	a = 27.442(9) Å α = 90° b = 13.748(4) Å β = 96.499(5)° c = 8.789(3) Å γ = 90°
Volume, Z	3294.6(18) $Å^3$, 8
Density (calculated)	1.324 g/cm^3
Absorption coefficient	0.201 mm^{-1}
F(000)	1376
Crystal size	0.29 x 0.18 x 0.09 mm
θ range for data collection	1.49 to 28.29°
Limiting indices	$-36 < h < 36$, $-18 < k < 18$, $-11 < l <$ 11
Reflections collected	29523
Independent reflections	7876 (R_{int} = 0.0301)
Completeness to θ = 28.29°	99.9 %
Absorption correction	Semi-empirical from equivalents
Max. and min. transmission	0.9829 and 0.9437
Refinement method	Full-matrix least-squares on F^2
Data / restraints / parameters	7876 / 0 / 435
Goodness-of-fit on F^2	1.031
Final R indices [I>2σ(I)]	R1 = 0.0412, wR2 = 0.1047
R indices (all data)	R1 = 0.0480, wR2 = 0.1092
Largest diff. peak and hole	0.458 and -0.268 $e \cdot Å^{-3}$

Table S1. Atomic coordinates (x 10^4) and equivalent isotropic displacement parameters ($Å^2$ x 10^3) for triptycyl thiol *S*-acetyl ester. U(eq) is defined as one third of the trace of the orthogonalized U_{ij} tensor.

Atom	x	y	z	U(eq)
S(1)	1584(1)	771(1)	205(1)	16(1)
S(2)	2858(1)	5757(1)	1210(1)	17(1)
O(1)	2176(1)	1093(1)	2764(1)	21(1)
O(2)	2615(1)	4078(1)	2413(1)	22(1)
C(1)	2089(1)	1295(1)	1427(2)	18(1)
C(2)	2380(1)	1987(1)	575(2)	28(1)
C(3)	1314(1)	-68(1)	1463(2)	13(1)
C(4)	892(1)	-1308(1)	3146(2)	15(1)
C(5)	1654(1)	-900(1)	2093(2)	14(1)
C(6)	1424(1)	-1556(1)	3004(2)	15(1)
C(7)	1676(1)	-2354(1)	3656(2)	20(1)
C(8)	2160(1)	-2504(1)	3387(2)	23(1)
C(9)	2388(1)	-1864(1)	2474(2)	21(1)
C(10)	2136(1)	-1057(1)	1826(2)	16(1)
C(11)	1108(1)	408(1)	2843(2)	14(1)
C(12)	885(1)	-269(1)	3741(2)	15(1)
C(13)	669(1)	32(1)	5011(2)	19(1)
C(14)	671(1)	1015(1)	5393(2)	21(1)
C(15)	890(1)	1686(1)	4504(2)	20(1)
C(16)	1107(1)	1386(1)	3221(2)	17(1)
C(17)	861(1)	-575(1)	594(2)	14(1)
C(18)	642(1)	-1244(1)	1513(2)	15(1)
C(19)	225(1)	-1748(1)	936(2)	17(1)
C(20)	18(1)	-1568(1)	-560(2)	18(1)
C(21)	229(1)	-896(1)	-1461(2)	17(1)
C(22)	656(1)	-402(1)	-896(2)	16(1)
C(23)	2470(1)	4805(1)	1744(2)	18(1)
C(24)	1941(1)	5025(1)	1239(2)	26(1)
C(25)	3470(1)	5316(1)	1803(2)	14(1)
C(26)	4379(1)	4802(1)	2559(2)	16(1)
C(27)	3843(1)	6089(1)	1396(2)	15(1)
C(28)	4332(1)	5806(1)	1814(2)	16(1)
C(29)	4714(1)	6418(1)	1552(2)	19(1)
C(30)	4608(1)	7321(1)	869(2)	23(1)
C(31)	4128(1)	7600(1)	444(2)	24(1)
C(32)	3742(1)	6983(1)	706(2)	20(1)
C(33)	3597(1)	5148(1)	3539(2)	15(1)
C(34)	4086(1)	4866(1)	3927(2)	16(1)
C(35)	4267(1)	4702(1)	5443(2)	19(1)

Table S1. Atomic coordinates (x 10^4) and equivalent isotropic displacement parameters ($Å^2$ x 10^3) for triptycyl thiol *S*-acetyl ester. U(eq) is defined as one third of the trace of the orthogonalized U_{ij} tensor.

Atom	x	y	z	U(eq)
C(36)	3961(1)	4825(1)	6589(2)	22(1)
C(37)	3479(1)	5119(1)	6211(2)	22(1)
C(38)	3295(1)	5283(1)	4685(2)	18(1)
C(39)	3614(1)	4384(1)	984(2)	15(1)
C(40)	4101(1)	4111(1)	1417(2)	16(1)
C(41)	4298(1)	3300(1)	781(2)	20(1)
C(42)	4007(1)	2763(1)	-313(2)	24(1)
C(43)	3526(1)	3035(1)	-762(2)	23(1)
C(44)	3325(1)	3849(1)	-113(2)	19(1)

Table S2. Bond lengths (Å) for triptycyl thiol *S*-acetyl ester. Symmetry transformations used to generate equivalent atoms:

S(1)-C(1)	1.8043(15)	C(31)-C(32)	1.398(2)
S(1)-C(3)	1.8131(14)	C(33)-C(38)	1.388(2)
S(2)-C(23)	1.7827(15)	C(33)-C(34)	1.400(2)
S(2)-C(25)	1.8077(15)	C(34)-C(35)	1.388(2)
O(1)-C(1)	1.2046(18)	C(35)-C(36)	1.393(2)
O(2)-C(23)	1.2051(19)	C(36)-C(37)	1.386(2)
C(1)-C(2)	1.496(2)	C(37)-C(38)	1.397(2)
C(3)-C(5)	1.5398(19)	C(39)-C(44)	1.387(2)
C(3)-C(11)	1.5416(18)	C(39)-C(40)	1.399(2)
C(3)-C(17)	1.5489(19)	C(40)-C(41)	1.385(2)
C(4)-C(6)	1.518(2)	C(41)-C(42)	1.390(2)
C(4)-C(18)	1.5214(19)	C(42)-C(43)	1.384(2)
C(4)-C(12)	1.522(2)	C(43)-C(44)	1.398(2)
C(5)-C(10)	1.387(2)		
C(5)-C(6)	1.4020(19)		
C(6)-C(7)	1.386(2)		
C(7)-C(8)	1.392(2)		
C(8)-C(9)	1.387(2)		
C(9)-C(10)	1.394(2)		
C(11)-C(16)	1.384(2)		
C(11)-C(12)	1.4045(19)		
C(12)-C(13)	1.3851(19)		
C(13)-C(14)	1.393(2)		
C(14)-C(15)	1.389(2)		
C(15)-C(16)	1.396(2)		
C(17)-C(22)	1.3861(19)		
C(17)-C(18)	1.4034(19)		
C(18)-C(19)	1.385(2)		
C(19)-C(20)	1.394(2)		
C(20)-C(21)	1.386(2)		
C(21)-C(22)	1.396(2)		
C(23)-C(24)	1.500(2)		
C(25)-C(33)	1.5435(19)		
C(25)-C(39)	1.5426(19)		
C(25)-C(27)	1.5453(19)		
C(26)-C(34)	1.522(2)		
C(26)-C(40)	1.522(2)		
C(26)-C(28)	1.5279(19)		
C(27)-C(32)	1.384(2)		
C(27)-C(28)	1.404(2)		
C(28)-C(29)	1.384(2)		
C(29)-C(30)	1.396(2)		
C(30)-C(31)	1.381(2)		

Table S3. Bond angles (deg.) for triptycyl thiol *S*-acetyl ester. Symmetry transformations used to generate equivalent atoms:

C(1)-S(1)-C(3)	103.31(7)	C(17)-C(22)-C(21)	119.16(13)
C(23)-S(2)-C(25)	103.98(7)	O(2)-C(23)-C(24)	124.61(14)
O(1)-C(1)-C(2)	125.18(14)	O(2)-C(23)-S(2)	124.24(12)
O(1)-C(1)-S(1)	122.91(11)	C(24)-C(23)-S(2)	111.15(11)
C(2)-C(1)-S(1)	111.90(11)	C(33)-C(25)-C(39)	107.25(11)
C(5)-C(3)-C(11)	107.11(11)	C(33)-C(25)-C(27)	104.50(11)
C(5)-C(3)-C(17)	105.22(11)	C(39)-C(25)-C(27)	104.67(11)
C(11)-C(3)-C(17)	103.48(11)	C(33)-C(25)-S(2)	115.69(10)
C(5)-C(3)-S(1)	114.77(10)	C(39)-C(25)-S(2)	114.98(10)
C(11)-C(3)-S(1)	114.98(10)	C(27)-C(25)-S(2)	108.71(9)
C(17)-C(3)-S(1)	110.26(9)	C(34)-C(26)-C(40)	106.72(11)
C(6)-C(4)-C(18)	105.72(11)	C(34)-C(26)-C(28)	105.02(11)
C(6)-C(4)-C(12)	106.83(11)	C(40)-C(26)-C(28)	105.62(11)
C(18)-C(4)-C(12)	104.34(11)	C(32)-C(27)-C(28)	119.94(13)
C(10)-C(5)-C(6)	119.81(13)	C(32)-C(27)-C(25)	127.35(13)
C(10)-C(5)-C(3)	127.25(13)	C(28)-C(27)-C(25)	112.71(12)
C(6)-C(5)-C(3)	112.93(12)	C(29)-C(28)-C(27)	120.51(13)
C(7)-C(6)-C(5)	120.65(13)	C(29)-C(28)-C(26)	126.26(13)
C(7)-C(6)-C(4)	125.65(13)	C(27)-C(28)-C(26)	113.23(12)
C(5)-C(6)-C(4)	113.68(12)	C(28)-C(29)-C(30)	119.15(14)
C(6)-C(7)-C(8)	119.17(14)	C(31)-C(30)-C(29)	120.59(14)
C(9)-C(8)-C(7)	120.44(14)	C(30)-C(31)-C(32)	120.34(14)
C(8)-C(9)-C(10)	120.39(14)	C(27)-C(32)-C(31)	119.46(14)
C(5)-C(10)-C(9)	119.53(14)	C(38)-C(33)-C(34)	119.66(13)
C(16)-C(11)-C(12)	119.74(13)	C(38)-C(33)-C(25)	127.68(13)
C(16)-C(11)-C(3)	127.70(12)	C(34)-C(33)-C(25)	112.60(12)
C(12)-C(11)-C(3)	112.51(12)	C(35)-C(34)-C(33)	120.54(13)
C(13)-C(12)-C(11)	120.55(13)	C(35)-C(34)-C(26)	125.80(13)
C(13)-C(12)-C(4)	125.50(13)	C(33)-C(34)-C(26)	113.63(12)
C(11)-C(12)-C(4)	113.92(12)	C(34)-C(35)-C(36)	119.62(14)
C(12)-C(13)-C(14)	119.54(14)	C(37)-C(36)-C(35)	119.94(14)
C(15)-C(14)-C(13)	119.98(13)	C(36)-C(37)-C(38)	120.59(14)
C(14)-C(15)-C(16)	120.59(14)	C(33)-C(38)-C(37)	119.63(14)
C(11)-C(16)-C(15)	119.59(13)	C(44)-C(39)-C(40)	120.02(13)
C(22)-C(17)-C(18)	120.10(13)	C(44)-C(39)-C(25)	127.48(13)
C(22)-C(17)-C(3)	127.29(12)	C(40)-C(39)-C(25)	112.45(12)
C(18)-C(17)-C(3)	112.54(11)	C(41)-C(40)-C(39)	120.67(13)
C(19)-C(18)-C(17)	120.51(13)	C(41)-C(40)-C(26)	125.45(13)
C(19)-C(18)-C(4)	125.62(12)	C(39)-C(40)-C(26)	113.83(12)
C(17)-C(18)-C(4)	113.82(12)	C(40)-C(41)-C(42)	119.17(14)
C(18)-C(19)-C(20)	119.20(13)	C(43)-C(42)-C(41)	120.50(14)
C(21)-C(20)-C(19)	120.36(13)	C(42)-C(43)-C(44)	120.52(14)
C(20)-C(21)-C(22)	120.64(13)	C(39)-C(44)-C(43)	119.11(14)

Table S4. Anisotropic displacement parameters ($Å^2$ x 10^3) for triptycyl thiol *S*-acetyl ester. The anisotropic displacement factor exponent takes the form: $-2\pi^2[(ha^*)^2U_{11} + ... + 2hka^*b^*U_{12}]$.

Atom	U_{11}	U_{22}	U_{33}	U_{23}	U_{13}	U_{12}
S(1)	19(1)	16(1)	12(1)	2(1)	3(1)	-3(1)
S(2)	14(1)	17(1)	21(1)	4(1)	0(1)	2(1)
O(1)	20(1)	23(1)	19(1)	-2(1)	1(1)	-2(1)
O(2)	25(1)	20(1)	22(1)	2(1)	1(1)	-4(1)
C(1)	18(1)	16(1)	20(1)	-4(1)	4(1)	-2(1)
C(2)	33(1)	25(1)	27(1)	-4(1)	10(1)	-14(1)
C(3)	15(1)	14(1)	11(1)	1(1)	2(1)	-1(1)
C(4)	17(1)	17(1)	12(1)	3(1)	2(1)	-1(1)
C(5)	18(1)	14(1)	11(1)	-1(1)	0(1)	0(1)
C(6)	19(1)	16(1)	12(1)	-1(1)	0(1)	-1(1)
C(7)	27(1)	17(1)	15(1)	2(1)	1(1)	0(1)
C(8)	28(1)	19(1)	19(1)	0(1)	-2(1)	8(1)
C(9)	19(1)	23(1)	21(1)	-5(1)	1(1)	4(1)
C(10)	18(1)	17(1)	14(1)	-4(1)	2(1)	-1(1)
C(11)	12(1)	18(1)	10(1)	0(1)	-1(1)	1(1)
C(12)	13(1)	19(1)	12(1)	1(1)	-2(1)	1(1)
C(13)	16(1)	27(1)	14(1)	3(1)	3(1)	1(1)
C(14)	19(1)	30(1)	15(1)	-3(1)	3(1)	6(1)
C(15)	19(1)	20(1)	19(1)	-4(1)	-1(1)	5(1)
C(16)	15(1)	18(1)	16(1)	0(1)	0(1)	2(1)
C(17)	15(1)	14(1)	12(1)	-1(1)	3(1)	0(1)
C(18)	16(1)	16(1)	12(1)	0(1)	2(1)	1(1)
C(19)	18(1)	17(1)	17(1)	2(1)	4(1)	-2(1)
C(20)	15(1)	21(1)	19(1)	-3(1)	2(1)	-2(1)
C(21)	18(1)	22(1)	12(1)	-1(1)	0(1)	0(1)
C(22)	18(1)	17(1)	13(1)	1(1)	3(1)	0(1)
C(23)	18(1)	23(1)	14(1)	-3(1)	2(1)	-4(1)
C(24)	17(1)	36(1)	23(1)	2(1)	0(1)	-4(1)
C(25)	13(1)	12(1)	16(1)	1(1)	1(1)	0(1)
C(26)	15(1)	13(1)	19(1)	2(1)	0(1)	1(1)
C(27)	16(1)	14(1)	16(1)	0(1)	3(1)	0(1)
C(28)	18(1)	13(1)	16(1)	0(1)	2(1)	1(1)
C(29)	16(1)	19(1)	23(1)	0(1)	4(1)	0(1)
C(30)	23(1)	18(1)	29(1)	2(1)	8(1)	-4(1)
C(31)	27(1)	14(1)	31(1)	6(1)	7(1)	1(1)
C(32)	19(1)	16(1)	24(1)	3(1)	4(1)	3(1)
C(33)	18(1)	9(1)	16(1)	0(1)	0(1)	-1(1)
C(34)	18(1)	10(1)	18(1)	0(1)	1(1)	-1(1)
C(35)	20(1)	14(1)	21(1)	2(1)	-3(1)	0(1)

C(36)	27(1)	22(1)	16(1)	2(1)	-1(1)	-2(1)

Table S4. Anisotropic displacement parameters ($Å^2$ x 10^3) for triptycyl thiol *S*-acetyl ester. The anisotropic displacement factor exponent takes the form: $-2\pi^2[(ha^*)^2U_{11} + ... + 2hka^*b^*U_{12}]$.

Atom	U_{11}	U_{22}	U_{33}	U_{23}	U_{13}	U_{12}
C(37)	26(1)	22(1)	18(1)	0(1)	7(1)	-2(1)
C(38)	17(1)	15(1)	21(1)	0(1)	2(1)	-2(1)
C(39)	19(1)	13(1)	14(1)	1(1)	3(1)	0(1)
C(40)	20(1)	12(1)	16(1)	2(1)	3(1)	-1(1)
C(41)	24(1)	16(1)	20(1)	3(1)	5(1)	4(1)
C(42)	37(1)	14(1)	22(1)	-2(1)	9(1)	2(1)
C(43)	33(1)	19(1)	18(1)	-3(1)	3(1)	-6(1)
C(44)	22(1)	18(1)	16(1)	2(1)	1(1)	-3(1)

Table S5. Hydrogen coordinates (x 10^4) and isotropic displacement parameters ($Å^2$ x 10^3) for triptycyl thiol *S*-acetyl ester.

H atom	x	y	z	U(eq)
H(2A)	2504	2502	1248	42
H(2B)	2173	2256	-276	42
H(2C)	2649	1648	207	42
H(4)	734	-1772	3779	19
H(7)	1523	-2785	4267	24
H(8)	2332	-3037	3822	27
H(9)	2711	-1973	2293	25
H(10)	2290	-626	1220	20
H(13)	523	-420	5605	22
H(14)	526	1223	6243	26
H(15)	892	2342	4765	24
H(16)	1250	1839	2625	20
H(19)	84	-2202	1539	20
H(20)	-263	-1900	-956	22
H(21)	85	-773	-2451	21
H(22)	801	37	-1512	19
H(24A)	1844	4714	274	38
H(24B)	1898	5716	1129	38
H(24C)	1742	4787	1989	38
H(26)	4720	4606	2844	19
H(29)	5037	6229	1828	23
H(30)	4863	7739	699	27
H(31)	4062	8201	-20	28
H(32)	3419	7172	421	24
H(35)	4592	4510	5694	22
H(36)	4080	4711	7607	26
H(37)	3277	5207	6980	26
H(38)	2972	5482	4439	21
H(41)	4621	3116	1081	24
H(42)	4136	2217	-747	29
H(43)	3336	2673	-1500	28
H(44)	3002	4031	-414	22

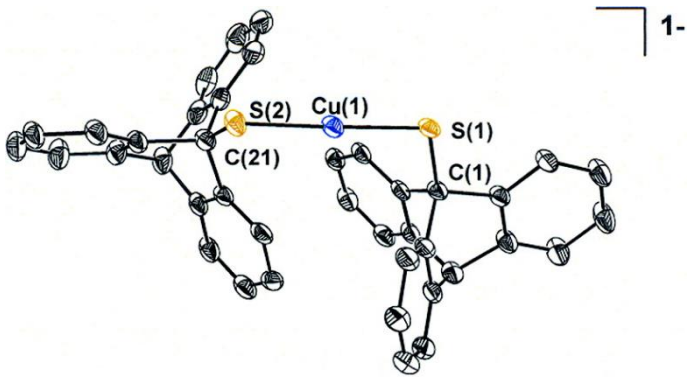

Structure Determination Summary

Crystal Data and Structure Refinement for $[Bu_4N][(Triptycyl\text{-}S)_2Cu]\cdot Et_2O$, **10**

Identification code	jpd425_0m
Empirical formula	$C_{60}H_{72}CuNOS_2$
Formula weight	950.85
Temperature	100(2) K
Wavelength	0.71073 Å
Crystal system	triclinic
Space group	*P*-1
Unit cell dimensions	*a* = 11.5110(7) Å α=100.892(1)°
	b = 16.0819(10) Å β=105.633(1)°
	c = 16.7584(11) Å γ=108.445(1)°
Volume, *Z*	2703.4(3) $Å^3$, 2
Density (calculated)	1.166 g/cm^3
Absorption coefficient	0.520 mm^{-1}
F(000)	1016
Crystal size	0.36 x 0.17 x 0.16 mm
θ range for data collection	1.94 to 28.31°
Limiting indices	$-15 < h < 15$, $-21 < k < 21$, $-21 < l <$ 22
Reflections collected	47339
Independent reflections	13166 (R_{int} = 0.0498)
Completeness to θ = 27.751°	99.1 %
Absorption correction	Semi-empirical from equivalents
Max. and min. transmission	0.9223 and 0.6876
Refinement method	Full-matrix least-squares on F^2
Data / restraints / parameters	13166 / 46 / 599
Goodness-of-fit on F^2	1.074
Final R indices [I>2σ(I)]	R1 = 0.0614, wR2 = 0.1828
R indices (all data)	R1 = 0.0832, wR2 = 0.1968
Largest diff. peak and hole	1.831 and -0.902 $e\cdot Å^{-3}$

Table S1. Atomic coordinates (x 10^4) and equivalent isotropic displacement parameters ($Å^2$ x 10^3) for $[Bu_4N][(Triptycyl\text{-}S)_2Cu]\cdot Et_2O$. U(eq) is defined as one third of the trace of the orthogonalized Uij tensor.

Atom	x	y	z	U(eq)
Cu(1)	2868(1)	5602(1)	2669(1)	27(1)
S(1)	1975(1)	5552(1)	3649(1)	26(1)
S(2)	3733(1)	5596(1)	1678(1)	31(1)
C(1)	2847(3)	6705(2)	4412(2)	26(1)
C(2)	4308(3)	6962(2)	4907(2)	29(1)
C(3)	4996(3)	6402(2)	4826(2)	33(1)
C(4)	6330(3)	6733(2)	5337(2)	40(1)
C(5)	6944(3)	7610(2)	5912(2)	44(1)
C(6)	6267(3)	8171(2)	5998(2)	40(1)
C(7)	4941(3)	7850(2)	5496(2)	34(1)
C(8)	4041(3)	8360(2)	5540(2)	34(1)
C(9)	2939(3)	7730(2)	5755(2)	35(1)
C(10)	2558(4)	7959(2)	6451(2)	47(1)
C(11)	1495(4)	7316(2)	6540(2)	52(1)
C(12)	831(3)	6450(2)	5933(2)	41(1)
C(13)	1218(3)	6214(2)	5229(2)	31(1)
C(14)	2282(3)	6846(2)	5138(2)	29(1)
C(15)	2807(2)	7491(2)	4017(2)	27(1)
C(16)	2249(3)	7402(2)	3144(2)	29(1)
C(17)	2272(3)	8185(2)	2880(2)	32(1)
C(18)	2843(3)	9041(2)	3494(2)	36(1)
C(19)	3418(3)	9141(2)	4369(2)	34(1)
C(20)	3418(3)	8368(2)	4629(2)	30(1)
C(21)	3900(3)	6671(2)	1420(2)	29(1)
C(22)	4573(3)	6780(2)	741(2)	31(1)
C(23)	5013(3)	6167(2)	349(2)	37(1)
C(24)	5589(3)	6363(2)	-261(2)	43(1)
C(25)	5722(4)	7164(2)	-484(2)	48(1)
C(26)	5269(4)	7784(2)	-99(2)	49(1)
C(27)	4709(3)	7592(2)	515(2)	38(1)
C(28)	4178(3)	8198(2)	994(2)	39(1)
C(29)	4893(3)	8365(2)	1948(2)	35(1)
C(30)	5640(3)	9220(2)	2565(2)	43(1)
C(31)	6217(3)	9272(2)	3429(2)	46(1)
C(32)	6032(3)	8481(2)	3675(2)	42(1)
C(33)	5287(3)	7611(2)	3048(2)	34(1)
C(34)	4735(3)	7562(2)	2195(2)	30(1)
C(35)	2607(3)	6786(2)	1024(2)	30(1)
C(36)	1352(3)	6166(2)	860(2)	35(1)

Table S1. Atomic coordinates (x 10^4) and equivalent isotropic displacement parameters ($Å^2$ x 10^3) for $[Bu_4N][(Triptycyl\text{-}S)_2Cu]\cdot Et_2O$. U(eq) is defined as one third of the trace of the orthogonalized Uij tensor.

Atom	x	y	z	U(eq)
C(37)	275(3)	6357(3)	489(2)	44(1)
C(38)	439(4)	7171(3)	279(2)	51(1)
C(39)	1689(4)	7794(3)	435(2)	46(1)
C(40)	2768(3)	7602(2)	808(2)	36(1)
N(1)	8285(2)	6542(2)	2945(2)	42(1)
C(41)	7803(15)	7171(10)	2482(10)	46(3)
C(42)	8838(10)	7803(8)	2219(7)	48(2)
C(43)	8296(11)	8400(8)	1739(9)	69(2)
C(44)	9361(14)	9034(11)	1530(9)	76(3)
C(41A)	7569(14)	6901(9)	2261(9)	46(3)
C(42A)	8388(9)	7515(6)	1849(7)	48(2)
C(43A)	8820(11)	8559(6)	2299(8)	69(2)
C(44A)	9602(14)	9199(10)	1911(8)	76(3)
C(45)	9420(3)	7221(2)	3751(3)	45(1)
C(46)	9089(3)	7844(2)	4370(3)	53(1)
C(47)	10300(4)	8634(3)	4999(3)	69(1)
C(48)	10066(4)	9206(3)	5712(3)	76(1)
C(49)	7198(3)	5956(2)	3200(2)	39(1)
C(50)	7597(3)	5417(2)	3791(2)	37(1)
C(51)	6393(3)	4713(2)	3850(2)	40(1)
C(52)	5739(4)	3851(3)	3087(3)	61(1)
C(53)	8823(3)	5939(2)	2456(2)	40(1)
C(54)	7857(3)	5247(3)	1607(2)	54(1)
C(55)	8407(4)	4551(3)	1292(2)	62(1)
C(56)	8354(4)	3834(3)	1771(3)	67(1)
O(1)	6687(5)	0(3)	9712(3)	115(1)
C(57)	7337(8)	241(5)	10633(4)	116(2)
C(58)	6886(7)	831(4)	11124(3)	101(2)
C(59)	7257(9)	-457(5)	9194(5)	130(3)
C(60)	6406(9)	-714(6)	8272(4)	142(3)

Table S2. Bond lengths (Å) for $[Bu_4N][(Triptycyl\text{-}S)_2Cu]\cdot Et_2O$. Symmetry transformations used to generate equivalent atoms:

Cu(1)-S(2)	2.1541(7)	C(21)-C(34)	1.553(3)
Cu(1)-S(1)	2.1605(7)	C(22)-C(23)	1.383(4)
S(1)-C(1)	1.821(2)	C(22)-C(27)	1.402(4)
S(2)-C(21)	1.824(3)	C(23)-C(24)	1.392(4)
C(1)-C(2)	1.538(4)	C(23)-H(23)	0.9500
C(1)-C(14)	1.540(4)	C(24)-C(25)	1.382(5)
C(1)-C(15)	1.541(4)	C(24)-H(24)	0.9500
C(2)-C(3)	1.387(4)	C(25)-C(26)	1.396(4)
C(2)-C(7)	1.401(4)	C(25)-H(25)	0.9500
C(3)-C(4)	1.405(4)	C(26)-C(27)	1.386(4)
C(3)-H(3)	0.9500	C(26)-H(26)	0.9500
C(4)-C(5)	1.381(5)	C(27)-C(28)	1.522(4)
C(4)-H(4)	0.9500	C(28)-C(40)	1.510(4)
C(5)-C(6)	1.377(5)	C(28)-C(29)	1.514(5)
C(5)-H(5)	0.9500	C(28)-H(28)	1.0000
C(6)-C(7)	1.396(4)	C(29)-C(30)	1.391(4)
C(6)-H(6)	0.9500	C(29)-C(34)	1.403(4)
C(7)-C(8)	1.520(4)	C(30)-C(31)	1.395(5)
C(8)-C(20)	1.507(4)	C(30)-H(30)	0.9500
C(8)-C(9)	1.528(4)	C(31)-C(32)	1.381(5)
C(8)-H(8)	1.0000	C(31)-H(31)	0.9500
C(9)-C(10)	1.380(4)	C(32)-C(33)	1.413(4)
C(9)-C(14)	1.416(4)	C(32)-H(32)	0.9500
C(10)-C(11)	1.394(4)	C(33)-C(34)	1.375(4)
C(10)-H(10)	0.9500	C(33)-H(33)	0.9500
C(11)-C(12)	1.390(4)	C(35)-C(36)	1.389(4)
C(11)-H(11)	0.9500	C(35)-C(40)	1.397(4)
C(12)-C(13)	1.398(4)	C(36)-C(37)	1.384(5)
C(12)-H(12)	0.9500	C(36)-H(36)	0.9500
C(13)-C(14)	1.389(4)	C(37)-C(38)	1.388(5)
C(13)-H(13)	0.9500	C(37)-H(37)	0.9500
C(15)-C(16)	1.389(4)	C(38)-C(39)	1.389(5)
C(15)-C(20)	1.404(3)	C(38)-H(38)	0.9500
C(16)-C(17)	1.407(4)	C(39)-C(40)	1.387(5)
C(16)-H(16)	0.9500	C(39)-H(39)	0.9500
C(17)-C(18)	1.383(4)	N(1)-C(45)	1.520(5)
C(17)-H(17)	0.9500	N(1)-C(49)	1.526(4)
C(18)-C(19)	1.391(4)	N(1)-C(41)	1.533(11)
C(18)-H(18)	0.9500	N(1)-C(53)	1.533(4)
C(19)-C(20)	1.393(4)	N(1)-C(41A)	1.540(11)
C(19)-H(19)	0.9500	C(41)-C(42)	1.528(11)
C(21)-C(35)	1.542(4)	C(41)-H(41A)	0.9900
C(21)-C(22)	1.546(4)	C(41)-H(41B)	0.9900

Table S2. Bond lengths (Å) for $[Bu_4N][(Triptycyl\text{-}S)_2Cu]\cdot Et_2O$. Symmetry transformations used to generate equivalent atoms:

C(42)-C(43)	1.534(11)	C(52)-H(52B)	0.9800
C(42)-H(42A)	0.9900	C(52)-H(52C)	0.9800
C(42)-H(42B)	0.9900	C(53)-C(54)	1.505(5)
C(43)-C(44)	1.498(12)	C(53)-H(53A)	0.9900
C(43)-H(43A)	0.9900	C(53)-H(53B)	0.9900
C(43)-H(43B)	0.9900	C(54)-C(55)	1.529(6)
C(44)-H(44A)	0.9800	C(54)-H(54A)	0.9900
C(44)-H(44B)	0.9800	C(54)-H(54B)	0.9900
C(44)-H(44C)	0.9800	C(55)-C(56)	1.520(6)
C(41A)-C(42A)	1.535(11)	C(55)-H(55A)	0.9900
C(41A)-H(41C)	0.9900	C(55)-H(55B)	0.9900
C(41A)-H(41D)	0.9900	C(56)-H(56A)	0.9800
C(42A)-C(43A)	1.558(11)	C(56)-H(56B)	0.9800
C(42A)-H(42C)	0.9900	C(56)-H(56C)	0.9800
C(42A)-H(42D)	0.9900	O(1)-C(57)	1.435(7)
C(43A)-C(44A)	1.509(11)	O(1)-C(59)	1.447(7)
C(43A)-H(43C)	0.9900	C(57)-C(58)	1.447(9)
C(43A)-H(43D)	0.9900	C(57)-H(57A)	0.9900
C(44A)-H(44D)	0.9800	C(57)-H(57B)	0.9900
C(44A)-H(44E)	0.9800	C(58)-H(58A)	0.9800
C(44A)-H(44F)	0.9800	C(58)-H(58B)	0.9800
C(45)-C(46)	1.513(5)	C(58)-H(58C)	0.9800
C(45)-H(45A)	0.9900	C(59)-C(60)	1.485(10)
C(45)-H(45B)	0.9900	C(59)-H(59A)	0.9900
C(46)-C(47)	1.500(6)	C(59)-H(59B)	0.9900
C(46)-H(46A)	0.9900	C(60)-H(60A)	0.9800
C(46)-H(46B)	0.9900	C(60)-H(60B)	0.9800
C(47)-C(48)	1.503(5)	C(60)-H(60C)	0.9800
C(47)-H(47A)	0.9900		
C(47)-H(47B)	0.9900		
C(48)-H(48A)	0.9800		
C(48)-H(48B)	0.9800		
C(48)-H(48C)	0.9800		
C(49)-C(50)	1.507(4)		
C(49)-H(49A)	0.9900		
C(49)-H(49B)	0.9900		
C(50)-C(51)	1.529(4)		
C(50)-H(50A)	0.9900		
C(50)-H(50B)	0.9900		
C(51)-C(52)	1.507(5)		
C(51)-H(51A)	0.9900		
C(51)-H(51B)	0.9900		
C(52)-H(52A)	0.9800		

Table S3. Bond angles (deg.) for $[Bu_4N][(Triptycyl\text{-}S)_2Cu]\cdot Et_2O$. Symmetry transformations used to generate equivalent atoms:

S(2)-Cu(1)-S(1)	177.80(3)	C(11)-C(12)-H(12)	119.7
C(1)-S(1)-Cu(1)	103.23(9)	C(13)-C(12)-H(12)	119.7
C(21)-S(2)-Cu(1)	106.12(9)	C(14)-C(13)-C(12)	119.9(2)
C(2)-C(1)-C(14)	103.7(2)	C(14)-C(13)-H(13)	120.1
C(2)-C(1)-C(15)	104.8(2)	C(12)-C(13)-H(13)	120.1
C(14)-C(1)-C(15)	104.3(2)	C(13)-C(14)-C(9)	118.9(2)
C(2)-C(1)-S(1)	115.48(19)	C(13)-C(14)-C(1)	127.0(2)
C(14)-C(1)-S(1)	111.95(17)	C(9)-C(14)-C(1)	114.1(2)
C(15)-C(1)-S(1)	115.33(18)	C(16)-C(15)-C(20)	119.5(3)
C(3)-C(2)-C(7)	120.0(3)	C(16)-C(15)-C(1)	126.4(2)
C(3)-C(2)-C(1)	126.1(2)	C(20)-C(15)-C(1)	114.1(2)
C(7)-C(2)-C(1)	113.8(2)	C(15)-C(16)-C(17)	120.0(2)
C(2)-C(3)-C(4)	119.4(3)	C(15)-C(16)-H(16)	120.0
C(2)-C(3)-H(3)	120.3	C(17)-C(16)-H(16)	120.0
C(4)-C(3)-H(3)	120.3	C(18)-C(17)-C(16)	119.7(3)
C(5)-C(4)-C(3)	120.0(3)	C(18)-C(17)-H(17)	120.1
C(5)-C(4)-H(4)	120.0	C(16)-C(17)-H(17)	120.1
C(3)-C(4)-H(4)	120.0	C(17)-C(18)-C(19)	120.8(3)
C(6)-C(5)-C(4)	121.0(3)	C(17)-C(18)-H(18)	119.6
C(6)-C(5)-H(5)	119.5	C(19)-C(18)-H(18)	119.6
C(4)-C(5)-H(5)	119.5	C(18)-C(19)-C(20)	119.5(3)
C(5)-C(6)-C(7)	119.6(3)	C(18)-C(19)-H(19)	120.3
C(5)-C(6)-H(6)	120.2	C(20)-C(19)-H(19)	120.3
C(7)-C(6)-H(6)	120.2	C(19)-C(20)-C(15)	120.4(3)
C(6)-C(7)-C(2)	120.0(3)	C(19)-C(20)-C(8)	126.2(2)
C(6)-C(7)-C(8)	126.3(3)	C(15)-C(20)-C(8)	113.4(2)
C(2)-C(7)-C(8)	113.7(2)	C(35)-C(21)-C(22)	104.2(2)
C(20)-C(8)-C(7)	106.6(2)	C(35)-C(21)-C(34)	104.0(2)
C(20)-C(8)-C(9)	105.7(2)	C(22)-C(21)-C(34)	104.4(2)
C(7)-C(8)-C(9)	104.7(2)	C(35)-C(21)-S(2)	115.59(19)
C(20)-C(8)-H(8)	113.0	C(22)-C(21)-S(2)	111.70(18)
C(7)-C(8)-H(8)	113.0	C(34)-C(21)-S(2)	115.6(2)
C(9)-C(8)-H(8)	113.0	C(23)-C(22)-C(27)	119.3(3)
C(10)-C(9)-C(14)	121.0(3)	C(23)-C(22)-C(21)	126.9(3)
C(10)-C(9)-C(8)	126.3(3)	C(27)-C(22)-C(21)	113.8(2)
C(14)-C(9)-C(8)	112.6(2)	C(22)-C(23)-C(24)	119.9(3)
C(9)-C(10)-C(11)	119.6(3)	C(22)-C(23)-H(23)	120.1
C(9)-C(10)-H(10)	120.2	C(24)-C(23)-H(23)	120.1
C(11)-C(10)-H(10)	120.2	C(25)-C(24)-C(23)	120.8(3)
C(12)-C(11)-C(10)	120.0(3)	C(25)-C(24)-H(24)	119.6
C(12)-C(11)-H(11)	120.0	C(23)-C(24)-H(24)	119.6
C(10)-C(11)-H(11)	120.0	C(24)-C(25)-C(26)	119.8(3)
C(11)-C(12)-C(13)	120.6(3)	C(24)-C(25)-H(25)	120.1

Table S3. Bond angles (deg.) for $[Bu_4N][(Triptycyl\text{-}S)_2Cu]\cdot Et_2O$. Symmetry transformations used to generate equivalent atoms:

C(26)-C(25)-H(25)	120.1	C(40)-C(39)-C(38)	119.7(3)
C(27)-C(26)-C(25)	119.3(3)	C(40)-C(39)-H(39)	120.2
C(27)-C(26)-H(26)	120.4	C(38)-C(39)-H(39)	120.2
C(25)-C(26)-H(26)	120.4	C(39)-C(40)-C(35)	120.6(3)
C(26)-C(27)-C(22)	120.9(3)	C(39)-C(40)-C(28)	125.7(3)
C(26)-C(27)-C(28)	125.6(3)	C(35)-C(40)-C(28)	113.6(3)
C(22)-C(27)-C(28)	113.5(2)	C(45)-N(1)-C(49)	110.4(3)
C(40)-C(28)-C(29)	106.0(2)	C(45)-N(1)-C(41)	102.9(6)
C(40)-C(28)-C(27)	105.8(2)	C(49)-N(1)-C(41)	109.3(6)
C(29)-C(28)-C(27)	104.9(3)	C(45)-N(1)-C(53)	107.2(2)
C(40)-C(28)-H(28)	113.1	C(49)-N(1)-C(53)	110.6(3)
C(29)-C(28)-H(28)	113.1	C(41)-N(1)-C(53)	116.1(7)
C(27)-C(28)-H(28)	113.1	C(45)-N(1)-C(41A)	119.6(6)
C(30)-C(29)-C(34)	120.0(3)	C(49)-N(1)-C(41A)	103.9(6)
C(30)-C(29)-C(28)	125.8(3)	C(53)-N(1)-C(41A)	104.9(7)
C(34)-C(29)-C(28)	114.2(2)	C(42)-C(41)-N(1)	113.3(10)
C(29)-C(30)-C(31)	119.6(3)	C(42)-C(41)-H(41A)	108.9
C(29)-C(30)-H(30)	120.2	N(1)-C(41)-H(41A)	108.9
C(31)-C(30)-H(30)	120.2	C(42)-C(41)-H(41B)	108.9
C(32)-C(31)-C(30)	120.3(3)	N(1)-C(41)-H(41B)	108.9
C(32)-C(31)-H(31)	119.8	H(41A)-C(41)-H(41B)	107.7
C(30)-C(31)-H(31)	119.8	C(41)-C(42)-C(43)	111.1(8)
C(31)-C(32)-C(33)	120.2(3)	C(41)-C(42)-H(42A)	109.4
C(31)-C(32)-H(32)	119.9	C(43)-C(42)-H(42A)	109.4
C(33)-C(32)-H(32)	119.9	C(41)-C(42)-H(42B)	109.4
C(34)-C(33)-C(32)	119.3(3)	C(43)-C(42)-H(42B)	109.4
C(34)-C(33)-H(33)	120.3	H(42A)-C(42)-H(42B)	108.0
C(32)-C(33)-H(33)	120.3	C(44)-C(43)-C(42)	109.0(10)
C(33)-C(34)-C(29)	120.5(3)	C(44)-C(43)-H(43A)	109.9
C(33)-C(34)-C(21)	126.5(3)	C(42)-C(43)-H(43A)	109.9
C(29)-C(34)-C(21)	113.0(3)	C(44)-C(43)-H(43B)	109.9
C(36)-C(35)-C(40)	119.2(3)	C(42)-C(43)-H(43B)	109.9
C(36)-C(35)-C(21)	126.7(3)	H(43A)-C(43)-H(43B)	108.3
C(40)-C(35)-C(21)	114.1(2)	C(43)-C(44)-H(44A)	109.5
C(37)-C(36)-C(35)	120.3(3)	C(43)-C(44)-H(44B)	109.5
C(37)-C(36)-H(36)	119.9	H(44A)-C(44)-H(44B)	109.5
C(35)-C(36)-H(36)	119.9	C(43)-C(44)-H(44C)	109.5
C(36)-C(37)-C(38)	120.4(3)	H(44A)-C(44)-H(44C)	109.5
C(36)-C(37)-H(37)	119.8	H(44B)-C(44)-H(44C)	109.5
C(38)-C(37)-H(37)	119.8	C(42A)-C(41A)-N(1)	117.6(10)
C(37)-C(38)-C(39)	119.9(3)	C(42A)-C(41A)-H(41C)	107.9
C(37)-C(38)-H(38)	120.1	N(1)-C(41A)-H(41C)	107.9
C(39)-C(38)-H(38)	120.1	C(42A)-C(41A)-H(41D)	107.9

Table S3. Bond angles (deg.) for $[Bu_4N][(Triptycyl\text{-}S)_2Cu]\cdot Et_2O$. Symmetry transformations used to generate equivalent atoms:

N(1)-C(41A)-H(41D)	107.9	H(48B)-C(48)-H(48C)	109.5
H(41C)-C(41A)-H(41D)	107.2	C(50)-C(49)-N(1)	115.4(2)
C(41A)-C(42A)-C(43A)	112.8(9)	C(50)-C(49)-H(49A)	108.4
C(41A)-C(42A)-H(42C)	109.0	N(1)-C(49)-H(49A)	108.4
C(43A)-C(42A)-H(42C)	109.0	C(50)-C(49)-H(49B)	108.4
C(41A)-C(42A)-H(42D)	109.0	N(1)-C(49)-H(49B)	108.4
C(43A)-C(42A)-H(42D)	109.0	H(49A)-C(49)-H(49B)	107.5
H(42C)-C(42A)-H(42D)	107.8	C(49)-C(50)-C(51)	110.7(3)
C(44A)-C(43A)-C(42A)	115.5(10)	C(49)-C(50)-H(50A)	109.5
C(44A)-C(43A)-H(43C)	108.4	C(51)-C(50)-H(50A)	109.5
C(42A)-C(43A)-H(43C)	108.4	C(49)-C(50)-H(50B)	109.5
C(44A)-C(43A)-H(43D)	108.4	C(51)-C(50)-H(50B)	109.5
C(42A)-C(43A)-H(43D)	108.4	H(50A)-C(50)-H(50B)	108.1
H(43C)-C(43A)-H(43D)	107.5	C(52)-C(51)-C(50)	113.1(3)
C(43A)-C(44A)-H(44D)	109.5	C(52)-C(51)-H(51A)	109.0
C(43A)-C(44A)-H(44E)	109.5	C(50)-C(51)-H(51A)	109.0
H(44D)-C(44A)-H(44E)	109.5	C(52)-C(51)-H(51B)	109.0
C(43A)-C(44A)-H(44F)	109.5	C(50)-C(51)-H(51B)	109.0
H(44D)-C(44A)-H(44F)	109.5	H(51A)-C(51)-H(51B)	107.8
H(44E)-C(44A)-H(44F)	109.5	C(51)-C(52)-H(52A)	109.5
C(46)-C(45)-N(1)	116.2(3)	C(51)-C(52)-H(52B)	109.5
C(46)-C(45)-H(45A)	108.2	H(52A)-C(52)-H(52B)	109.5
N(1)-C(45)-H(45A)	108.2	C(51)-C(52)-H(52C)	109.5
C(46)-C(45)-H(45B)	108.2	H(52A)-C(52)-H(52C)	109.5
N(1)-C(45)-H(45B)	108.2	H(52B)-C(52)-H(52C)	109.5
H(45A)-C(45)-H(45B)	107.4	C(54)-C(53)-N(1)	115.5(3)
C(47)-C(46)-C(45)	111.1(3)	C(54)-C(53)-H(53A)	108.4
C(47)-C(46)-H(46A)	109.4	N(1)-C(53)-H(53A)	108.4
C(45)-C(46)-H(46A)	109.4	C(54)-C(53)-H(53B)	108.4
C(47)-C(46)-H(46B)	109.4	N(1)-C(53)-H(53B)	108.4
C(45)-C(46)-H(46B)	109.4	H(53A)-C(53)-H(53B)	107.5
H(46A)-C(46)-H(46B)	108.0	C(53)-C(54)-C(55)	110.2(3)
C(46)-C(47)-C(48)	113.9(3)	C(53)-C(54)-H(54A)	109.6
C(46)-C(47)-H(47A)	108.8	C(55)-C(54)-H(54A)	109.6
C(48)-C(47)-H(47A)	108.8	C(53)-C(54)-H(54B)	109.6
C(46)-C(47)-H(47B)	108.8	C(55)-C(54)-H(54B)	109.6
C(48)-C(47)-H(47B)	108.8	H(54A)-C(54)-H(54B)	108.1
H(47A)-C(47)-H(47B)	107.7	C(56)-C(55)-C(54)	114.0(3)
C(47)-C(48)-H(48A)	109.5	C(56)-C(55)-H(55A)	108.7
C(47)-C(48)-H(48B)	109.5	C(54)-C(55)-H(55A)	108.7
H(48A)-C(48)-H(48B)	109.5	C(56)-C(55)-H(55B)	108.7
C(47)-C(48)-H(48C)	109.5	C(54)-C(55)-H(55B)	108.7
H(48A)-C(48)-H(48C)	109.5	H(55A)-C(55)-H(55B)	107.6

Table S3. Bond angles (deg.) for $[Bu_4N][(Triptycyl\text{-}S)_2Cu]\cdot Et_2O$. Symmetry transformations used to generate equivalent atoms:

C(55)-C(56)-H(56A)	109.5
C(55)-C(56)-H(56B)	109.5
H(56A)-C(56)-H(56B)	109.5
C(55)-C(56)-H(56C)	109.5
H(56A)-C(56)-H(56C)	109.5
H(56B)-C(56)-H(56C)	109.5
C(57)-O(1)-C(59)	114.4(6)
O(1)-C(57)-C(58)	112.6(6)
O(1)-C(57)-H(57A)	109.1
C(58)-C(57)-H(57A)	109.1
O(1)-C(57)-H(57B)	109.1
C(58)-C(57)-H(57B)	109.1
H(57A)-C(57)-H(57B)	107.8
C(57)-C(58)-H(58A)	109.5
C(57)-C(58)-H(58B)	109.5
H(58A)-C(58)-H(58B)	109.5
C(57)-C(58)-H(58C)	109.5
H(58A)-C(58)-H(58C)	109.5
H(58B)-C(58)-H(58C)	109.5
O(1)-C(59)-C(60)	106.8(6)
O(1)-C(59)-H(59A)	110.4
C(60)-C(59)-H(59A)	110.4
O(1)-C(59)-H(59B)	110.4
C(60)-C(59)-H(59B)	110.4
H(59A)-C(59)-H(59B)	108.6
C(59)-C(60)-H(60A)	109.5
C(59)-C(60)-H(60B)	109.5
H(60A)-C(60)-H(60B)	109.5
C(59)-C(60)-H(60C)	109.5
H(60A)-C(60)-H(60C)	109.5
H(60B)-C(60)-H(60C)	109.5

Table S4. Anisotropic displacement parameters ($Å^2$ x 10^3) for $[Bu_4N][(Triptycyl\text{-}S)_2Cu]\cdot Et_2O$. The anisotropic displacement factor exponent takes the form: $-2\pi^2[(ha^*)^2U_{11} + ... + 2hka^*b^*U_{12}]$.

Atom	U_{11}	U_{22}	U_{33}	U_{23}	U_{13}	U_{12}
Cu(1)	25(1)	22(1)	34(1)	1(1)	17(1)	6(1)
S(1)	22(1)	20(1)	31(1)	-2(1)	14(1)	1(1)
S(2)	33(1)	25(1)	42(1)	5(1)	25(1)	12(1)
C(1)	24(1)	21(1)	29(1)	-2(1)	14(1)	2(1)
C(2)	23(1)	29(1)	29(1)	1(1)	14(1)	1(1)
C(3)	26(1)	35(2)	33(1)	4(1)	15(1)	6(1)
C(4)	27(2)	55(2)	37(2)	11(1)	14(1)	12(1)
C(5)	25(1)	53(2)	40(2)	8(1)	11(1)	-1(1)
C(6)	33(2)	38(2)	30(1)	1(1)	13(1)	-5(1)
C(7)	30(1)	30(1)	30(1)	2(1)	17(1)	-3(1)
C(8)	35(2)	20(1)	34(1)	-4(1)	18(1)	-2(1)
C(9)	36(2)	25(1)	38(2)	0(1)	24(1)	2(1)
C(10)	59(2)	28(2)	45(2)	-4(1)	34(2)	0(1)
C(11)	65(2)	35(2)	54(2)	1(1)	47(2)	4(2)
C(12)	43(2)	30(2)	50(2)	5(1)	33(2)	5(1)
C(13)	31(1)	23(1)	38(2)	3(1)	21(1)	4(1)
C(14)	27(1)	24(1)	31(1)	1(1)	16(1)	5(1)
C(15)	22(1)	22(1)	34(1)	1(1)	18(1)	2(1)
C(16)	23(1)	26(1)	38(1)	4(1)	19(1)	6(1)
C(17)	29(1)	34(2)	37(1)	9(1)	19(1)	13(1)
C(18)	37(2)	29(1)	48(2)	10(1)	27(1)	11(1)
C(19)	32(2)	22(1)	45(2)	3(1)	22(1)	4(1)
C(20)	27(1)	25(1)	36(1)	0(1)	20(1)	2(1)
C(21)	27(1)	22(1)	35(1)	-2(1)	18(1)	6(1)
C(22)	28(1)	26(1)	36(1)	-1(1)	18(1)	5(1)
C(23)	35(2)	26(1)	45(2)	-2(1)	25(1)	5(1)
C(24)	39(2)	32(2)	51(2)	-5(1)	31(2)	5(1)
C(25)	54(2)	37(2)	51(2)	1(1)	39(2)	6(2)
C(26)	65(2)	35(2)	54(2)	7(1)	42(2)	15(2)
C(27)	45(2)	26(1)	40(2)	-2(1)	27(1)	8(1)
C(28)	52(2)	29(1)	44(2)	7(1)	32(2)	16(1)
C(29)	34(2)	26(1)	41(2)	-3(1)	27(1)	4(1)
C(30)	43(2)	27(2)	51(2)	-5(1)	33(2)	0(1)
C(31)	35(2)	33(2)	52(2)	-12(1)	28(2)	-5(1)
C(32)	22(1)	60(2)	32(1)	-9(1)	13(1)	9(1)
C(33)	19(1)	36(2)	40(2)	0(1)	17(1)	5(1)
C(34)	23(1)	26(1)	36(1)	-3(1)	18(1)	4(1)
C(35)	32(1)	32(1)	26(1)	-2(1)	16(1)	12(1)

C(36)	33(2)	37(2)	30(1)	-1(1)	15(1)	12(1)

Table S4. Anisotropic displacement parameters ($Å^2$ x 10^3) for $[Bu_4N][(Triptycyl\text{-}S)_2Cu]\cdot Et_2O$. The anisotropic displacement factor exponent takes the form: $-2\pi^2[(ha^*)^2U_{11} + ... + 2hka^*b^*U_{12}]$.

Atom	U_{11}	U_{22}	U_{33}	U_{23}	U_{13}	U_{12}
C(37)	32(2)	63(2)	34(2)	3(2)	14(1)	18(2)
C(38)	49(2)	83(3)	37(2)	21(2)	19(2)	41(2)
C(39)	65(2)	54(2)	37(2)	17(2)	29(2)	35(2)
C(40)	46(2)	36(2)	29(1)	4(1)	20(1)	19(1)
N(1)	29(1)	56(2)	63(2)	32(1)	28(1)	23(1)
C(41)	43(5)	60(7)	63(7)	34(6)	33(5)	34(5)
C(42)	38(5)	67(6)	62(6)	39(5)	26(4)	29(4)
C(43)	67(6)	70(4)	104(7)	46(6)	53(5)	40(4)
C(44)	79(4)	73(4)	91(7)	43(5)	37(5)	31(3)
C(41A)	43(5)	60(7)	63(7)	34(6)	33(5)	34(5)
C(42A)	38(5)	67(6)	62(6)	39(5)	26(4)	29(4)
C(43A)	67(6)	70(4)	104(7)	46(6)	53(5)	40(4)
C(44A)	79(4)	73(4)	91(7)	43(5)	37(5)	31(3)
C(45)	28(2)	41(2)	76(2)	19(2)	30(2)	15(1)
C(46)	38(2)	51(2)	83(3)	22(2)	40(2)	19(2)
C(47)	49(2)	43(2)	112(4)	3(2)	48(2)	10(2)
C(48)	59(3)	51(2)	109(4)	-1(2)	56(3)	3(2)
C(49)	23(1)	52(2)	48(2)	22(2)	18(1)	14(1)
C(50)	28(2)	41(2)	42(2)	14(1)	16(1)	10(1)
C(51)	34(2)	39(2)	46(2)	12(1)	22(1)	6(1)
C(52)	53(2)	51(2)	61(2)	0(2)	30(2)	-2(2)
C(53)	26(1)	56(2)	47(2)	22(2)	20(1)	20(1)
C(54)	32(2)	87(3)	43(2)	20(2)	16(2)	18(2)
C(55)	39(2)	95(3)	35(2)	0(2)	17(2)	13(2)
C(56)	74(3)	50(2)	64(2)	-8(2)	37(2)	9(2)
O(1)	172(4)	105(3)	88(3)	31(2)	50(3)	73(3)
C(57)	157(6)	107(4)	82(4)	30(3)	34(4)	55(4)
C(58)	153(5)	68(3)	54(2)	11(2)	50(3)	0(3)
C(59)	178(6)	126(5)	120(5)	24(4)	67(5)	98(5)
C(60)	213(7)	174(6)	72(3)	8(4)	57(4)	128(5)

Table S5. Hydrogen coordinates (x 10^4) and isotropic displacement parameters (Å^2 x 10^3) for $[Bu_4N][(Triptycyl\text{-}S)_2Cu]\cdot Et_2O$.

Atom	x	y	z	U(eq)
H(3)	4570	5799	4428	40
H(4)	6809	6353	5287	48
H(5)	7846	7830	6253	53
H(6)	6701	8773	6396	48
H(8)	4499	8988	5969	40
H(10)	3018	8550	6867	57
H(11)	1224	7471	7016	62
H(12)	108	6014	5997	49
H(13)	754	5622	4814	38
H(16)	1851	6812	2726	35
H(17)	1896	8126	2283	38
H(18)	2843	9568	3315	43
H(19)	3807	9732	4786	41
H(23)	4924	5613	495	44
H(24)	5893	5941	-527	51
H(25)	6122	7293	-899	58
H(26)	5344	8331	-256	58
H(28)	4284	8778	833	46
H(30)	5757	9765	2399	52
H(31)	6739	9855	3851	55
H(32)	6408	8522	4267	51
H(33)	5168	7066	3214	41
H(36)	1231	5607	1003	42
H(37)	-581	5930	378	53
H(38)	-302	7302	28	61
H(39)	1806	8350	288	55
H(41A)	7025	6786	1956	55
H(41B)	7530	7551	2871	55
H(42A)	9127	7428	1837	58
H(42B)	9608	8204	2744	58
H(43A)	7553	8004	1197	83
H(43B)	7976	8761	2109	83
H(44A)	9028	9428	1237	114
H(44B)	9653	8673	1148	114
H(44C)	10099	9417	2068	114
H(41C)	6871	6364	1787	55
H(41D)	7134	7251	2534	55
H(42C)	7870	7366	1227	58
H(42D)	9177	7377	1884	58
H(43C)	8027	8685	2279	83

Table S5. Hydrogen coordinates (x 10^4) and isotropic displacement parameters (Å^2 x 10^3) for $[Bu_4N][(Triptycyl\text{-}S)_2Cu]\cdot Et_2O$.

Atom	x	y	z	U(eq)
H(43D)	9349	8702	2918	83
H(44D)	9804	9837	2224	114
H(44E)	9092	9067	1298	114
H(44F)	10420	9111	1960	114
H(45A)	9829	6869	4074	54
H(45B)	10085	7610	3562	54
H(46A)	8488	8082	4035	63
H(46B)	8635	7488	4695	63
H(47A)	10680	9034	4675	82
H(47B)	10950	8392	5263	82
H(48A)	10893	9708	6095	113
H(48B)	9715	8820	6048	113
H(48C)	9437	9460	5458	113
H(49A)	6847	6362	3489	46
H(49B)	6479	5519	2663	46
H(50A)	8167	5844	4378	45
H(50B)	8103	5098	3566	45
H(51A)	6658	4546	4391	48
H(51B)	5754	4997	3886	48
H(52A)	4983	3424	3163	92
H(52B)	6363	3562	3052	92
H(52C)	5447	4008	2551	92
H(53A)	9570	6345	2342	47
H(53B)	9167	5607	2839	47
H(54A)	7672	5567	1167	65
H(54B)	7025	4924	1684	65
H(55A)	7909	4234	665	74
H(55B)	9329	4886	1359	74
H(56A)	8723	3415	1536	101
H(56B)	7442	3485	1694	101
H(56C)	8862	4139	2390	101
H(57A)	8291	557	10776	139
H(57B)	7188	-328	10807	139
H(58A)	7364	979	11746	152
H(58B)	5947	515	10998	152
H(58C)	7043	1399	10960	152
H(59A)	7294	-1012	9355	156
H(59B)	8157	-40	9288	156

H(60A)	6772	-1012	7897	213
H(60B)	6359	-160	8127	213

Table S5. Hydrogen coordinates (x 10^4) and isotropic displacement parameters ($Å^2$ x 10^3) for $[Bu_4N][(Triptycyl\text{-}S)_2Cu]\cdot Et_2O$.

Atom	x	y	z	U(eq)
H(60C)	5525	-1139	8185	213

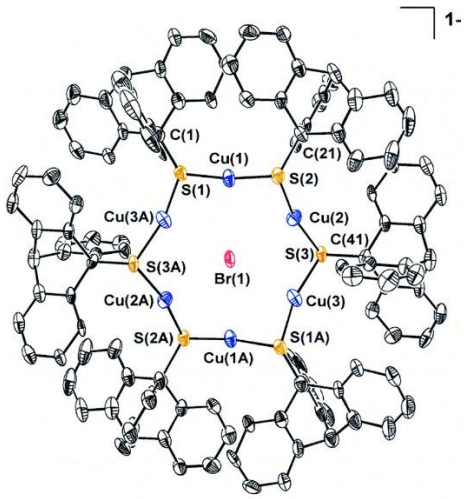

Structure Determination Summary

Crystal Data and Structure Refinement for $[Bu_4N][(triptycyl\text{-}S)_6Cu_6(\mu^6\text{-}Br)]\cdot[Bu_4N][PF_6]$, **14**

Identification code	jpd400_0m	
Empirical formula	$C_{152}H_{150}BrCu_6F_6N_2PS_6$	
Formula weight	2803.22	
Temperature	100(2) K	
Wavelength	0.71073 Å	
Crystal system	monoclinic	
Space group	*C*2/*c*	
Unit cell dimensions	*a* = 38.957(7) Å	*α* = 90°
	b = 28.740(5) Å	*β* = 91.710(2)°
	c = 11.982(2) Å	*γ* = 90°
Volume, *Z*	13410(4) Å^3, 4	
Density (calculated)	1.388 g/cm^3	
Absorption coefficient	1.398 mm^{-1}	
F(000)	5800	
Crystal size	0.30 x 0.20 x 0.03 mm	
θ range for data collection	1.05 to 23.33°	
Limiting indices	$-43 < h < 43$, $-31 < k < 31$, $-13 < l < 13$	
Reflections collected	41554	
Independent reflections	9670 (R_{int} = 0.1358)	
Completeness to θ = 23.33°	99.5 %	
Absorption correction	Semi-empirical from equivalents	
Max. and min. transmission	0.9593 and 0.5657	
Refinement method	Full-matrix least-squares on F^2	
Data / restraints / parameters	9670 / 0 / 823	
Goodness-of-fit on F^2	1.039	
Final R indices [I>2σ(I)]	R1 = 0.0810, wR2 = 0.2026	
R indices (all data)	R1 = 0.1552, wR2 = 0.2416	
Largest diff. peak and hole	1.323 and -0.956 e·Å^{-3}	

Table S1. Atomic coordinates (x 10^4) and equivalent isotropic displacement parameters ($Å^2$ x 10^3) for $[Bu_4N][(triptycyl\text{-}S)_6Cu_6(\mu^6\text{-}Br)]\cdot[Bu_4N][PF_6]$. U(eq) is defined as one third of the trace of the orthogonalized U_{ij} tensor.

Atom	x	y	z	U(eq)
Br(1)	2500	2500	5000	37(1)
Cu(1)	1705(1)	2514(1)	5001(1)	35(1)
Cu(2)	2120(1)	3345(1)	5664(1)	36(1)
Cu(3)	2913(1)	3336(1)	5620(1)	39(1)
S(1)	1646(1)	2022(1)	3646(2)	32(1)
S(2)	1690(1)	2990(1)	6384(2)	31(1)
S(3)	2513(1)	3834(1)	5159(2)	28(1)
C(1)	1250(3)	1692(4)	3803(9)	35(3)
C(2)	1208(3)	1317(3)	2886(9)	36(3)
C(3)	1451(3)	1193(4)	2134(9)	38(3)
C(4)	1377(3)	828(4)	1368(11)	57(4)
C(5)	1061(4)	600(5)	1402(13)	74(5)
C(6)	824(4)	723(5)	2151(13)	79(5)
C(7)	890(3)	1081(4)	2927(10)	49(3)
C(8)	667(3)	1245(4)	3835(12)	57(4)
C(9)	868(3)	1198(3)	4897(11)	44(3)
C(10)	774(4)	954(5)	5832(14)	71(5)
C(11)	977(5)	948(5)	6773(15)	85(6)
C(12)	1291(4)	1184(4)	6805(11)	63(4)
C(13)	1399(3)	1429(3)	5852(10)	48(3)
C(14)	1189(3)	1441(3)	4907(9)	36(3)
C(15)	927(3)	2019(4)	3660(8)	35(3)
C(16)	925(3)	2499(3)	3606(7)	30(2)
C(17)	604(3)	2732(4)	3560(9)	40(3)
C(18)	300(3)	2481(5)	3563(10)	54(3)
C(19)	306(3)	1999(4)	3610(10)	49(3)
C(20)	615(3)	1773(4)	3688(10)	43(3)
C(21)	1295(2)	3344(3)	6326(7)	25(2)
C(22)	1295(3)	3696(4)	7298(9)	38(3)
C(23)	1564(3)	3785(4)	8043(9)	48(3)
C(24)	1520(4)	4129(5)	8882(10)	67(4)
C(25)	1214(5)	4368(5)	8920(11)	69(4)
C(26)	950(4)	4287(4)	8165(11)	59(4)
C(27)	987(3)	3943(4)	7322(9)	47(3)
C(28)	726(3)	3820(4)	6440(9)	40(3)
C(29)	908(3)	3883(3)	5333(8)	33(3)
C(30)	785(3)	4151(4)	4436(10)	43(3)
C(31)	977(3)	4166(4)	3459(10)	44(3)

C(32)	1275(3)	3902(4)	3405(9)	40(3)

Table S1. Atomic coordinates (x 10^4) and equivalent isotropic displacement parameters ($Å^2$ x 10^3) for $[Bu_4N][(triptycyl\text{-}S)_6Cu_6(\mu^6\text{-}Br)]\cdot[Bu_4N][PF_6]$. U(eq) is defined as one third of the trace of the orthogonalized U_{ij} tensor.

Atom	x	y	z	U(eq)
C(33)	1395(3)	3637(3)	4292(8)	32(3)
C(34)	1215(3)	3623(3)	5270(8)	26(2)
C(35)	967(3)	3037(3)	6473(8)	31(3)
C(36)	950(3)	2559(3)	6464(8)	32(3)
C(37)	628(3)	2334(4)	6488(9)	43(3)
C(38)	331(3)	2599(4)	6552(10)	49(3)
C(39)	351(3)	3071(4)	6578(9)	39(3)
C(40)	667(3)	3292(4)	6512(8)	36(3)
C(41)	2532(2)	4265(3)	6298(8)	23(2)
C(42)	2844(3)	4588(3)	6194(8)	28(2)
C(43)	3110(3)	4551(3)	5449(8)	34(3)
C(44)	3385(3)	4862(4)	5500(9)	43(3)
C(45)	3399(3)	5206(4)	6299(9)	47(3)
C(46)	3133(3)	5249(4)	7048(9)	42(3)
C(47)	2861(3)	4942(3)	6991(8)	34(3)
C(48)	2560(3)	4921(3)	7798(8)	35(3)
C(49)	2230(3)	4926(3)	7117(8)	35(3)
C(50)	1947(3)	5206(4)	7297(9)	41(3)
C(51)	1653(3)	5141(4)	6662(10)	49(3)
C(52)	1634(3)	4802(3)	5832(9)	38(3)
C(53)	1917(3)	4521(3)	5647(8)	30(2)
C(54)	2213(3)	4576(3)	6301(8)	26(2)
C(55)	2565(2)	4084(3)	7509(8)	29(2)
C(56)	2576(3)	3620(3)	7871(9)	34(3)
C(57)	2619(3)	3528(4)	9015(9)	44(3)
C(58)	2655(3)	3877(4)	9773(10)	51(3)
C(59)	2635(3)	4336(4)	9417(9)	46(3)
C(60)	2591(3)	4443(4)	8309(8)	32(3)
N(1)	1181(2)	2523(3)	18(7)	42(2)
C(61)	959(3)	2097(4)	331(11)	55(4)
C(62)	696(3)	1949(4)	-552(11)	59(4)
C(63)	510(4)	1510(5)	-232(16)	90(6)
C(64)	222(4)	1378(5)	-1058(17)	103(6)
C(65)	1402(3)	2413(4)	-956(9)	43(3)
C(66)	1649(3)	2002(4)	-804(10)	51(3)
C(67)	1908(3)	2000(4)	-1763(9)	49(3)

C(68)	2188(3)	2363(4)	-1622(10)	51(3)
C(69)	1396(3)	2627(4)	1063(9)	48(3)
C(70)	1662(3)	3019(4)	954(9)	49(3)

Table S1. Atomic coordinates (x 10^4) and equivalent isotropic displacement parameters ($Å^2$ x 10^3) for $[Bu_4N][(triptycyl\text{-}S)_6Cu_6(\mu^6\text{-}Br)]\cdot[Bu_4N][PF_6]$. U(eq) is defined as one third of the trace of the orthogonalized U_{ij} tensor.

Atom	x	y	z	U(eq)
C(71)	1873(3)	3049(4)	2039(9)	43(3)
C(72)	2117(3)	3471(4)	2084(11)	58(4)
C(73)	963(3)	2937(4)	-312(10)	43(3)
C(74)	700(3)	3102(4)	520(11)	58(4)
C(75)	502(3)	3512(5)	112(13)	70(4)
C(76)	225(3)	3668(5)	895(13)	80(5)
P(1)	10000	0	5000	56(3)
F(1)	10118(9)	166(8)	6070(20)	197(14)
F(2)	9609(5)	122(5)	5610(20)	157(11)
F(3)	9988(5)	498(6)	4430(20)	127(8)
P(2)	0	4858(3)	7500	52(3)
F(4)	133(5)	4470(7)	8217(19)	129(8)
F(5)	295(5)	4889(5)	6650(20)	135(10)
F(6)	-135(5)	5221(7)	6790(20)	135(8)

Table S2. Bond lengths (Å) for $[Bu_4N][(triptycyl\text{-}S)_6Cu_6(\mu^6\text{-}Br)]\cdot[Bu_4N][PF_6]$. Symmetry transformations used to generate equivalent atoms: #1 -x + $^1/_2$, -y + $^1/_2$, -z + 1; #2 -x + 2, -y, -z + 1; #3 -x, y, -z + $^3/_2$.

Cu(1)-S(2)	2.150(3)	C(16)-C(17)	1.418(14)
Cu(1)-S(1)	2.161(3)	C(16)-H(16)	0.9500
Cu(1)-Cu(3)#1	2.9653(18)	C(17)-C(18)	1.388(16)
Cu(1)-Cu(2)	2.9775(18)	C(17)-H(17)	0.9500
Cu(2)-S(2)	2.165(3)	C(18)-C(19)	1.386(16)
Cu(2)-S(3)	2.178(3)	C(18)-H(18)	0.9500
Cu(3)-S(1)#1	2.167(3)	C(19)-C(20)	1.369(15)
Cu(3)-S(3)	2.176(3)	C(19)-H(19)	0.9500
Cu(3)-Cu(1)#1	2.9653(18)	C(21)-C(34)	1.523(13)
S(1)-C(1)	1.824(11)	C(21)-C(22)	1.543(14)
S(1)-Cu(3)#1	2.167(3)	C(21)-C(35)	1.567(14)
S(2)-C(21)	1.843(9)	C(22)-C(23)	1.378(15)
S(3)-C(41)	1.842(9)	C(22)-C(27)	1.395(16)
C(1)-C(14)	1.532(14)	C(23)-C(24)	1.423(16)
C(1)-C(2)	1.545(14)	C(23)-H(23)	0.9500
C(1)-C(15)	1.574(14)	C(24)-C(25)	1.38(2)
C(2)-C(3)	1.372(14)	C(24)-H(24)	0.9500
C(2)-C(7)	1.416(15)	C(25)-C(26)	1.369(19)
C(3)-C(4)	1.420(15)	C(25)-H(25)	0.9500
C(3)-H(3)	0.9500	C(26)-C(27)	1.425(16)
C(4)-C(5)	1.394(17)	C(26)-H(26)	0.9500
C(4)-H(4)	0.9500	C(27)-C(28)	1.487(16)
C(5)-C(6)	1.357(17)	C(28)-C(29)	1.533(14)
C(5)-H(5)	0.9500	C(28)-C(40)	1.537(14)
C(6)-C(7)	1.405(17)	C(28)-H(28)	1.0000
C(6)-H(6)	0.9500	C(29)-C(30)	1.395(14)
C(7)-C(8)	1.489(16)	C(29)-C(34)	1.414(14)
C(8)-C(9)	1.480(17)	C(30)-C(31)	1.408(15)
C(8)-C(20)	1.539(16)	C(30)-H(30)	0.9500
C(8)-H(8)	1.0000	C(31)-C(32)	1.387(15)
C(9)-C(10)	1.380(17)	C(31)-H(31)	0.9500
C(9)-C(14)	1.431(15)	C(32)-C(33)	1.379(14)
C(10)-C(11)	1.36(2)	C(32)-H(32)	0.9500
C(10)-H(10)	0.9500	C(33)-C(34)	1.385(13)
C(11)-C(12)	1.40(2)	C(33)-H(33)	0.9500
C(11)-H(11)	0.9500	C(35)-C(36)	1.375(13)
C(12)-C(13)	1.415(16)	C(35)-C(40)	1.384(14)
C(12)-H(12)	0.9500	C(36)-C(37)	1.409(14)
C(13)-C(14)	1.377(16)	C(36)-H(36)	0.9500
C(13)-H(13)	0.9500	C(37)-C(38)	1.388(15)
C(15)-C(16)	1.382(14)	C(37)-H(37)	0.9500
C(15)-C(20)	1.409(15)	C(38)-C(39)	1.359(15)

Table S2. Bond lengths (Å) for $[Bu_4N][(triptycyl\text{-}S)_6Cu_6(\mu^6\text{-}Br)]\cdot[Bu_4N][PF_6]$. Symmetry transformations used to generate equivalent atoms: #1 -x + $^1/_2$, -y + $^1/_2$, -z + 1; #2 -x + 2, -y, -z + 1; #3 -x, y, -z + $^3/_2$.

C(38)-H(38)	0.9500	N(1)-C(69)	1.514(14)
C(39)-C(40)	1.388(14)	N(1)-C(61)	1.552(14)
C(39)-H(39)	0.9500	C(61)-C(62)	1.513(17)
C(41)-C(54)	1.532(13)	C(61)-H(61A)	0.9900
C(41)-C(42)	1.537(13)	C(61)-H(61B)	0.9900
C(41)-C(55)	1.544(13)	C(62)-C(63)	1.510(17)
C(42)-C(43)	1.389(14)	C(62)-H(62A)	0.9900
C(42)-C(47)	1.395(13)	C(62)-H(62B)	0.9900
C(43)-C(44)	1.396(14)	C(63)-C(64)	1.52(2)
C(43)-H(43)	0.9500	C(63)-H(63A)	0.9900
C(44)-C(45)	1.376(15)	C(63)-H(63B)	0.9900
C(44)-H(44)	0.9500	C(64)-H(64A)	0.9800
C(45)-C(46)	1.397(15)	C(64)-H(64B)	0.9800
C(45)-H(45)	0.9500	C(64)-H(64C)	0.9800
C(46)-C(47)	1.380(14)	C(65)-C(66)	1.532(14)
C(46)-H(46)	0.9500	C(65)-H(65A)	0.9900
C(47)-C(48)	1.540(14)	C(65)-H(65B)	0.9900
C(48)-C(49)	1.503(15)	C(66)-C(67)	1.550(15)
C(48)-C(60)	1.508(13)	C(66)-H(66A)	0.9900
C(48)-H(48)	1.0000	C(66)-H(66B)	0.9900
C(49)-C(50)	1.389(15)	C(67)-C(68)	1.517(16)
C(49)-C(54)	1.402(13)	C(67)-H(67A)	0.9900
C(50)-C(51)	1.370(15)	C(67)-H(67B)	0.9900
C(50)-H(50)	0.9500	C(68)-H(68A)	0.9800
C(51)-C(52)	1.393(15)	C(68)-H(68B)	0.9800
C(51)-H(51)	0.9500	C(68)-H(68C)	0.9800
C(52)-C(53)	1.392(13)	C(69)-C(70)	1.539(15)
C(52)-H(52)	0.9500	C(69)-H(69A)	0.9900
C(53)-C(54)	1.384(13)	C(69)-H(69B)	0.9900
C(53)-H(53)	0.9500	C(70)-C(71)	1.519(15)
C(55)-C(56)	1.402(13)	C(70)-H(70A)	0.9900
C(55)-C(60)	1.409(14)	C(70)-H(70B)	0.9900
C(56)-C(57)	1.401(14)	C(71)-C(72)	1.542(15)
C(56)-H(56)	0.9500	C(71)-H(71A)	0.9900
C(57)-C(58)	1.357(16)	C(71)-H(71B)	0.9900
C(57)-H(57)	0.9500	C(72)-H(72A)	0.9800
C(58)-C(59)	1.388(16)	C(72)-H(72B)	0.9800
C(58)-H(58)	0.9500	C(72)-H(72C)	0.9800
C(59)-C(60)	1.368(14)	C(73)-C(74)	1.529(15)
C(59)-H(59)	0.9500	C(73)-H(73A)	0.9900
N(1)-C(73)	1.506(13)	C(73)-H(73B)	0.9900
N(1)-C(65)	1.504(13)	C(74)-C(75)	1.481(17)

Table S2. Bond lengths (Å) for $[Bu_4N][(triptycyl\text{-}S)_6Cu_6(\mu^6\text{-}Br)]\cdot[Bu_4N][PF_6]$. Symmetry transformations used to generate equivalent atoms: #1 -x + $^1/_2$, -y + $^1/_2$, -z + 1; #2 -x + 2, -y, -z + 1; #3 -x, y, -z + $^3/_2$.

C(74)-H(74A)	0.9900
C(74)-H(74B)	0.9900
C(75)-C(76)	1.520(17)
C(75)-H(75A)	0.9900
C(75)-H(75B)	0.9900
C(76)-H(76A)	0.9800
C(76)-H(76B)	0.9800
C(76)-H(76C)	0.9800
P(1)-F(1)#2	1.43(3)
P(1)-F(1)	1.43(3)
P(1)-F(3)#2	1.586(17)
P(1)-F(3)	1.586(17)
P(1)-F(2)	1.74(3)
P(1)-F(2)#2	1.74(3)
P(2)-F(6)#3	1.44(2)
P(2)-F(6)	1.44(2)
P(2)-F(4)#3	1.491(19)
P(2)-F(4)	1.491(19)
P(2)-F(5)	1.565(16)
P(2)-F(5)#3	1.565(16)

Table S3. Bond angles (deg.) for $[Bu_4N][(triptycyl\text{-}S)_6Cu_6(\mu^6\text{-}Br)]\cdot[Bu_4N][PF_6]$. Symmetry transformations used to generate equivalent atoms: #1 -x + $^1/_2$, -y + $^1/_2$, -z + 1; #2 -x + 2, -y, -z + 1; #3 -x, y, -z + $^3/_2$.

S(2)-Cu(1)-S(1)	171.98(12)	C(6)-C(7)-C(2)	118.1(11)
S(2)-Cu(1)-Cu(3)#1	138.00(9)	C(6)-C(7)-C(8)	128.0(12)
S(1)-Cu(1)-Cu(3)#1	46.85(8)	C(2)-C(7)-C(8)	113.8(10)
S(2)-Cu(1)-Cu(2)	46.57(8)	C(9)-C(8)-C(7)	107.2(11)
S(1)-Cu(1)-Cu(2)	140.43(9)	C(9)-C(8)-C(20)	104.8(10)
Cu(3)#1-Cu(1)-Cu(2)	117.09(6)	C(7)-C(8)-C(20)	107.8(10)
S(2)-Cu(2)-S(3)	167.06(12)	C(9)-C(8)-H(8)	112.2
S(2)-Cu(2)-Cu(1)	46.17(8)	C(7)-C(8)-H(8)	112.2
S(3)-Cu(2)-Cu(1)	145.51(9)	C(20)-C(8)-H(8)	112.2
S(1)#1-Cu(3)-S(3)	165.65(12)	C(10)-C(9)-C(14)	119.6(13)
S(1)#1-Cu(3)-Cu(1)#1	46.66(8)	C(10)-C(9)-C(8)	126.8(13)
S(3)-Cu(3)-Cu(1)#1	147.07(9)	C(14)-C(9)-C(8)	113.6(10)
C(1)-S(1)-Cu(1)	109.6(3)	C(11)-C(10)-C(9)	121.3(15)
C(1)-S(1)-Cu(3)#1	112.0(4)	C(11)-C(10)-H(10)	119.4
Cu(1)-S(1)-Cu(3)#1	86.49(11)	C(9)-C(10)-H(10)	119.4
C(21)-S(2)-Cu(1)	111.4(3)	C(10)-C(11)-C(12)	120.2(14)
C(21)-S(2)-Cu(2)	112.3(3)	C(10)-C(11)-H(11)	119.9
Cu(1)-S(2)-Cu(2)	87.26(11)	C(12)-C(11)-H(11)	119.9
C(41)-S(3)-Cu(3)	104.0(3)	C(11)-C(12)-C(13)	119.9(14)
C(41)-S(3)-Cu(2)	104.0(3)	C(11)-C(12)-H(12)	120.1
Cu(3)-S(3)-Cu(2)	90.46(10)	C(13)-C(12)-H(12)	120.1
C(14)-C(1)-C(2)	105.6(9)	C(14)-C(13)-C(12)	119.6(13)
C(14)-C(1)-C(15)	103.4(8)	C(14)-C(13)-H(13)	120.2
C(2)-C(1)-C(15)	105.8(8)	C(12)-C(13)-H(13)	120.2
C(14)-C(1)-S(1)	119.2(8)	C(13)-C(14)-C(9)	119.4(10)
C(2)-C(1)-S(1)	111.1(7)	C(13)-C(14)-C(1)	128.1(10)
C(15)-C(1)-S(1)	110.7(7)	C(9)-C(14)-C(1)	112.4(10)
C(3)-C(2)-C(7)	121.3(10)	C(16)-C(15)-C(20)	120.0(10)
C(3)-C(2)-C(1)	126.1(10)	C(16)-C(15)-C(1)	127.1(10)
C(7)-C(2)-C(1)	112.5(9)	C(20)-C(15)-C(1)	112.7(9)
C(2)-C(3)-C(4)	119.1(11)	C(15)-C(16)-C(17)	118.4(10)
C(2)-C(3)-H(3)	120.5	C(15)-C(16)-H(16)	120.8
C(4)-C(3)-H(3)	120.5	C(17)-C(16)-H(16)	120.8
C(5)-C(4)-C(3)	119.4(11)	C(18)-C(17)-C(16)	120.4(10)
C(5)-C(4)-H(4)	120.3	C(18)-C(17)-H(17)	119.8
C(3)-C(4)-H(4)	120.3	C(16)-C(17)-H(17)	119.8
C(6)-C(5)-C(4)	121.1(12)	C(19)-C(18)-C(17)	120.5(11)
C(6)-C(5)-H(5)	119.4	C(19)-C(18)-H(18)	119.8
C(4)-C(5)-H(5)	119.4	C(17)-C(18)-H(18)	119.8
C(5)-C(6)-C(7)	120.9(13)	C(20)-C(19)-C(18)	119.3(12)
C(5)-C(6)-H(6)	119.5	C(20)-C(19)-H(19)	120.3
C(7)-C(6)-H(6)	119.5	C(18)-C(19)-H(19)	120.3

Table S3. Bond angles (deg.) for $[Bu_4N][(triptycyl\text{-}S)_6Cu_6(\mu^6\text{-}Br)]\cdot[Bu_4N][PF_6]$. Symmetry transformations used to generate equivalent atoms: #1 -x + $^1/_2$, -y + $^1/_2$, -z + 1; #2 -x + 2, -y, -z + 1; #3 -x, y, -z + $^3/_2$.

C(19)-C(20)-C(15)	121.2(10)	C(33)-C(32)-C(31)	122.1(10)
C(19)-C(20)-C(8)	126.1(11)	C(33)-C(32)-H(32)	118.9
C(15)-C(20)-C(8)	112.7(10)	C(31)-C(32)-H(32)	118.9
C(34)-C(21)-C(22)	106.1(8)	C(32)-C(33)-C(34)	119.9(10)
C(34)-C(21)-C(35)	104.1(8)	C(32)-C(33)-H(33)	120.1
C(22)-C(21)-C(35)	105.5(8)	C(34)-C(33)-H(33)	120.1
C(34)-C(21)-S(2)	118.2(7)	C(33)-C(34)-C(29)	118.8(9)
C(22)-C(21)-S(2)	110.6(7)	C(33)-C(34)-C(21)	128.4(9)
C(35)-C(21)-S(2)	111.4(7)	C(29)-C(34)-C(21)	112.7(8)
C(23)-C(22)-C(27)	121.9(11)	C(36)-C(35)-C(40)	119.2(10)
C(23)-C(22)-C(21)	126.4(10)	C(36)-C(35)-C(21)	127.1(9)
C(27)-C(22)-C(21)	111.6(10)	C(40)-C(35)-C(21)	113.4(9)
C(22)-C(23)-C(24)	118.8(13)	C(35)-C(36)-C(37)	120.0(10)
C(22)-C(23)-H(23)	120.6	C(35)-C(36)-H(36)	120.0
C(24)-C(23)-H(23)	120.6	C(37)-C(36)-H(36)	120.0
C(25)-C(24)-C(23)	119.4(14)	C(38)-C(37)-C(36)	119.6(10)
C(25)-C(24)-H(24)	120.3	C(38)-C(37)-H(37)	120.2
C(23)-C(24)-H(24)	120.3	C(36)-C(37)-H(37)	120.2
C(26)-C(25)-C(24)	121.8(12)	C(39)-C(38)-C(37)	120.1(11)
C(26)-C(25)-H(25)	119.1	C(39)-C(38)-H(38)	120.0
C(24)-C(25)-H(25)	119.1	C(37)-C(38)-H(38)	120.0
C(25)-C(26)-C(27)	119.7(13)	C(38)-C(39)-C(40)	120.3(10)
C(25)-C(26)-H(26)	120.1	C(38)-C(39)-H(39)	119.8
C(27)-C(26)-H(26)	120.1	C(40)-C(39)-H(39)	119.8
C(22)-C(27)-C(26)	118.3(12)	C(35)-C(40)-C(39)	120.7(10)
C(22)-C(27)-C(28)	115.8(10)	C(35)-C(40)-C(28)	113.1(9)
C(26)-C(27)-C(28)	125.9(12)	C(39)-C(40)-C(28)	126.1(10)
C(27)-C(28)-C(29)	105.3(9)	C(54)-C(41)-C(42)	107.0(7)
C(27)-C(28)-C(40)	107.2(9)	C(54)-C(41)-C(55)	103.8(7)
C(29)-C(28)-C(40)	103.8(8)	C(42)-C(41)-C(55)	103.8(7)
C(27)-C(28)-H(28)	113.3	C(54)-C(41)-S(3)	112.2(7)
C(29)-C(28)-H(28)	113.3	C(42)-C(41)-S(3)	111.1(6)
C(40)-C(28)-H(28)	113.3	C(55)-C(41)-S(3)	118.0(6)
C(30)-C(29)-C(34)	121.3(9)	C(43)-C(42)-C(47)	118.5(9)
C(30)-C(29)-C(28)	125.2(10)	C(43)-C(42)-C(41)	127.7(9)
C(34)-C(29)-C(28)	113.4(9)	C(47)-C(42)-C(41)	113.8(9)
C(29)-C(30)-C(31)	118.7(10)	C(42)-C(43)-C(44)	120.5(10)
C(29)-C(30)-H(30)	120.6	C(42)-C(43)-H(43)	119.7
C(31)-C(30)-H(30)	120.6	C(44)-C(43)-H(43)	119.7
C(32)-C(31)-C(30)	119.1(10)	C(45)-C(44)-C(43)	120.3(11)
C(32)-C(31)-H(31)	120.5	C(45)-C(44)-H(44)	119.9
C(30)-C(31)-H(31)	120.5	C(43)-C(44)-H(44)	119.9

Table S3. Bond angles (deg.) for $[Bu_4N][(triptycyl\text{-}S)_6Cu_6(\mu^6\text{-}Br)]\cdot[Bu_4N][PF_6]$. Symmetry transformations used to generate equivalent atoms: #1 $-x + {}^1/_2, -y + {}^1/_2, -z + 1$; #2 $-x + 2, -y, -z + 1$; #3 $-x, y, -z + {}^3/_2$.

C(44)-C(45)-C(46)	119.7(10)	C(57)-C(58)-C(59)	119.5(11)
C(44)-C(45)-H(45)	120.1	C(57)-C(58)-H(58)	120.3
C(46)-C(45)-H(45)	120.1	C(59)-C(58)-H(58)	120.3
C(47)-C(46)-C(45)	119.7(10)	C(60)-C(59)-C(58)	121.0(11)
C(47)-C(46)-H(46)	120.2	C(60)-C(59)-H(59)	119.5
C(45)-C(46)-H(46)	120.2	C(58)-C(59)-H(59)	119.5
C(46)-C(47)-C(42)	121.3(10)	C(59)-C(60)-C(55)	120.0(10)
C(46)-C(47)-C(48)	126.1(9)	C(59)-C(60)-C(48)	127.1(10)
C(42)-C(47)-C(48)	112.5(9)	C(55)-C(60)-C(48)	112.8(8)
C(49)-C(48)-C(60)	106.5(8)	C(73)-N(1)-C(65)	107.0(8)
C(49)-C(48)-C(47)	108.2(8)	C(73)-N(1)-C(69)	110.8(9)
C(60)-C(48)-C(47)	103.8(8)	C(65)-N(1)-C(69)	111.7(9)
C(49)-C(48)-H(48)	112.6	C(73)-N(1)-C(61)	111.9(8)
C(60)-C(48)-H(48)	112.6	C(65)-N(1)-C(61)	110.8(9)
C(47)-C(48)-H(48)	112.6	C(69)-N(1)-C(61)	104.7(8)
C(50)-C(49)-C(54)	120.2(10)	C(62)-C(61)-N(1)	115.1(9)
C(50)-C(49)-C(48)	126.4(10)	C(62)-C(61)-H(61A)	108.5
C(54)-C(49)-C(48)	113.2(9)	N(1)-C(61)-H(61A)	108.5
C(51)-C(50)-C(49)	119.4(10)	C(62)-C(61)-H(61B)	108.5
C(51)-C(50)-H(50)	120.3	N(1)-C(61)-H(61B)	108.5
C(49)-C(50)-H(50)	120.3	H(61A)-C(61)-H(61B)	107.5
C(50)-C(51)-C(52)	121.2(11)	C(63)-C(62)-C(61)	112.3(12)
C(50)-C(51)-H(51)	119.4	C(63)-C(62)-H(62A)	109.1
C(52)-C(51)-H(51)	119.4	C(61)-C(62)-H(62A)	109.1
C(53)-C(52)-C(51)	119.6(11)	C(63)-C(62)-H(62B)	109.1
C(53)-C(52)-H(52)	120.2	C(61)-C(62)-H(62B)	109.1
C(51)-C(52)-H(52)	120.2	H(62A)-C(62)-H(62B)	107.9
C(54)-C(53)-C(52)	119.7(9)	C(62)-C(63)-C(64)	113.2(13)
C(54)-C(53)-H(53)	120.2	C(62)-C(63)-H(63A)	108.9
C(52)-C(53)-H(53)	120.2	C(64)-C(63)-H(63A)	108.9
C(53)-C(54)-C(49)	119.9(9)	C(62)-C(63)-H(63B)	108.9
C(53)-C(54)-C(41)	126.5(8)	C(64)-C(63)-H(63B)	108.9
C(49)-C(54)-C(41)	113.5(9)	H(63A)-C(63)-H(63B)	107.7
C(56)-C(55)-C(60)	119.0(9)	C(63)-C(64)-H(64A)	109.5
C(56)-C(55)-C(41)	127.8(9)	C(63)-C(64)-H(64B)	109.5
C(60)-C(55)-C(41)	113.2(8)	H(64A)-C(64)-H(64B)	109.5
C(55)-C(56)-C(57)	118.8(10)	C(63)-C(64)-H(64C)	109.5
C(55)-C(56)-H(56)	120.6	H(64A)-C(64)-H(64C)	109.5
C(57)-C(56)-H(56)	120.6	H(64B)-C(64)-H(64C)	109.5
C(58)-C(57)-C(56)	121.6(10)	N(1)-C(65)-C(66)	116.3(9)
C(58)-C(57)-H(57)	119.2	N(1)-C(65)-H(65A)	108.2
C(56)-C(57)-H(57)	119.2	C(66)-C(65)-H(65A)	108.2

Table S3. Bond angles (deg.) for $[Bu_4N][(triptycyl\text{-}S)_6Cu_6(\mu^6\text{-}Br)]\cdot[Bu_4N][PF_6]$. Symmetry transformations used to generate equivalent atoms: #1 $-x + {}^1/_2, -y + {}^1/_2, -z + 1$; #2 $-x + 2, -y, -z + 1$; #3 $-x, y, -z + {}^3/_2$.

N(1)-C(65)-H(65B)	108.2	C(71)-C(72)-H(72C)	109.5
C(66)-C(65)-H(65B)	108.2	H(72A)-C(72)-H(72C)	109.5
H(65A)-C(65)-H(65B)	107.4	H(72B)-C(72)-H(72C)	109.5
C(65)-C(66)-C(67)	109.7(9)	N(1)-C(73)-C(74)	117.3(9)
C(65)-C(66)-H(66A)	109.7	N(1)-C(73)-H(73A)	108.0
C(67)-C(66)-H(66A)	109.7	C(74)-C(73)-H(73A)	108.0
C(65)-C(66)-H(66B)	109.7	N(1)-C(73)-H(73B)	108.0
C(67)-C(66)-H(66B)	109.7	C(74)-C(73)-H(73B)	108.0
H(66A)-C(66)-H(66B)	108.2	H(73A)-C(73)-H(73B)	107.2
C(68)-C(67)-C(66)	113.4(10)	C(75)-C(74)-C(73)	112.6(10)
C(68)-C(67)-H(67A)	108.9	C(75)-C(74)-H(74A)	109.1
C(66)-C(67)-H(67A)	108.9	C(73)-C(74)-H(74A)	109.1
C(68)-C(67)-H(67B)	108.9	C(75)-C(74)-H(74B)	109.1
C(66)-C(67)-H(67B)	108.9	C(73)-C(74)-H(74B)	109.1
H(67A)-C(67)-H(67B)	107.7	H(74A)-C(74)-H(74B)	107.8
C(67)-C(68)-H(68A)	109.5	C(74)-C(75)-C(76)	113.8(12)
C(67)-C(68)-H(68B)	109.5	C(74)-C(75)-H(75A)	108.8
H(68A)-C(68)-H(68B)	109.5	C(76)-C(75)-H(75A)	108.8
C(67)-C(68)-H(68C)	109.5	C(74)-C(75)-H(75B)	108.8
H(68A)-C(68)-H(68C)	109.5	C(76)-C(75)-H(75B)	108.8
H(68B)-C(68)-H(68C)	109.5	H(75A)-C(75)-H(75B)	107.7
N(1)-C(69)-C(70)	115.6(9)	C(75)-C(76)-H(76A)	109.5
N(1)-C(69)-H(69A)	108.4	C(75)-C(76)-H(76B)	109.5
C(70)-C(69)-H(69A)	108.4	H(76A)-C(76)-H(76B)	109.5
N(1)-C(69)-H(69B)	108.4	C(75)-C(76)-H(76C)	109.5
C(70)-C(69)-H(69B)	108.4	H(76A)-C(76)-H(76C)	109.5
H(69A)-C(69)-H(69B)	107.5	H(76B)-C(76)-H(76C)	109.5
C(71)-C(70)-C(69)	108.6(9)	F(1)#2-P(1)-F(1)	180(4)
C(71)-C(70)-H(70A)	110.0	F(1)#2-P(1)-F(3)#2	95.1(12)
C(69)-C(70)-H(70A)	110.0	F(1)-P(1)-F(3)#2	84.9(12)
C(71)-C(70)-H(70B)	110.0	F(1)#2-P(1)-F(3)	84.9(12)
C(69)-C(70)-H(70B)	110.0	F(1)-P(1)-F(3)	95.1(12)
H(70A)-C(70)-H(70B)	108.4	F(3)#2-P(1)-F(3)	180.0(5)
C(70)-C(71)-C(72)	113.1(10)	F(1)#2-P(1)-F(2)	100.3(15)
C(70)-C(71)-H(71A)	109.0	F(1)-P(1)-F(2)	79.7(15)
C(72)-C(71)-H(71A)	109.0	F(3)#2-P(1)-F(2)	90.9(10)
C(70)-C(71)-H(71B)	109.0	F(3)-P(1)-F(2)	89.1(10)
C(72)-C(71)-H(71B)	109.0	F(1)#2-P(1)-F(2)#2	79.7(15)
H(71A)-C(71)-H(71B)	107.8	F(1)-P(1)-F(2)#2	100.3(15)
C(71)-C(72)-H(72A)	109.5	F(3)#2-P(1)-F(2)#2	89.1(10)
C(71)-C(72)-H(72B)	109.5	F(3)-P(1)-F(2)#2	90.9(10)
H(72A)-C(72)-H(72B)	109.5	F(2)-P(1)-F(2)#2	180.0(7)

Table S3. Bond angles (deg.) for $[Bu_4N][(triptycyl\text{-}S)_6Cu_6(\mu^6\text{-}Br)]\cdot[Bu_4N][PF_6]$. Symmetry transformations used to generate equivalent atoms: #1 $-x + {}^1/_2, -y + {}^1/_2, -z + 1$; #2 $-x + 2, -y, -z + 1$; #3 $-x, y, -z + {}^3/_2$.

F(6)#3-P(2)-F(6)	87(2)
F(6)#3-P(2)-F(4)#3	178.2(15)
F(6)-P(2)-F(4)#3	95.0(13)
F(6)#3-P(2)-F(4)	95.0(13)
F(6)-P(2)-F(4)	178.2(15)
F(4)#3-P(2)-F(4)	83(2)
F(6)#3-P(2)-F(5)	94.8(12)
F(6)-P(2)-F(5)	80.3(12)
F(4)#3-P(2)-F(5)	85.1(10)
F(4)-P(2)-F(5)	99.9(11)
F(6)#3-P(2)-F(5)#3	80.3(12)
F(6)-P(2)-F(5)#3	94.8(12)
F(4)#3-P(2)-F(5)#3	99.9(11)
F(4)-P(2)-F(5)#3	85.1(10)
F(5)-P(2)-F(5)#3	173.4(13)

Table S4. Anisotropic displacement parameters ($Å^2$ x 10^3) for $[Bu_4N][(triptycyl\text{-}S)_6Cu_6(\mu^6\text{-}Br)]\cdot[Bu_4N][PF_6]$. The anisotropic displacement factor exponent takes the form:$-2\pi^2[(ha^*)^2U_{11} + ... + 2hka^*b^*U_{12}]$.

Atom	U_{11}	U_{22}	U_{33}	U_{23}	U_{13}	U_{12}
Br(1)	40(1)	16(1)	56(1)	-9(1)	10(1)	0(1)
Cu(1)	48(1)	19(1)	39(1)	3(1)	6(1)	1(1)
Cu(2)	41(1)	28(1)	38(1)	6(1)	1(1)	-9(1)
Cu(3)	46(1)	32(1)	39(1)	2(1)	7(1)	12(1)
S(1)	37(2)	22(1)	39(2)	3(1)	7(1)	3(1)
S(2)	39(2)	19(1)	36(2)	4(1)	4(1)	-2(1)
S(3)	39(2)	15(1)	30(2)	-1(1)	5(1)	-1(1)
C(1)	39(6)	30(6)	35(6)	-2(5)	11(5)	0(5)
C(2)	47(7)	20(6)	40(7)	-11(5)	5(6)	3(5)
C(3)	44(7)	25(6)	44(7)	-5(5)	5(6)	9(5)
C(4)	58(9)	46(8)	67(9)	-21(7)	13(7)	16(7)
C(5)	64(10)	56(9)	103(12)	-47(9)	24(9)	-11(8)
C(6)	69(10)	52(9)	116(13)	-47(9)	28(9)	-11(7)
C(7)	59(8)	24(6)	65(9)	3(6)	15(7)	5(6)
C(8)	46(8)	36(7)	91(11)	-14(7)	25(8)	-8(6)
C(9)	55(8)	14(6)	65(9)	2(6)	28(7)	4(5)
C(10)	92(12)	40(8)	84(12)	19(8)	47(10)	15(8)
C(11)	126(16)	36(8)	98(14)	28(9)	89(12)	27(9)
C(12)	102(12)	38(8)	52(8)	21(6)	32(8)	42(8)
C(13)	67(9)	13(6)	66(9)	19(6)	37(7)	26(6)
C(14)	55(8)	11(5)	44(7)	7(5)	13(6)	4(5)
C(15)	46(7)	30(6)	28(6)	0(5)	2(5)	5(5)
C(16)	45(7)	26(6)	19(5)	-5(5)	0(5)	12(5)
C(17)	49(8)	31(6)	41(7)	-6(5)	1(6)	26(6)
C(18)	36(7)	65(9)	62(9)	-20(7)	-9(6)	22(7)
C(19)	49(8)	33(7)	65(9)	-18(6)	3(6)	8(6)
C(20)	49(8)	26(6)	54(8)	-16(5)	10(6)	0(6)
C(21)	36(6)	24(5)	17(5)	5(4)	8(4)	9(5)
C(22)	57(8)	24(6)	34(7)	3(5)	14(6)	3(6)
C(23)	69(9)	34(7)	43(7)	3(6)	6(6)	-20(6)
C(24)	120(14)	46(9)	35(8)	-17(7)	10(8)	-27(9)
C(25)	124(14)	41(9)	44(9)	-23(7)	24(9)	-21(9)
C(26)	90(11)	27(7)	63(9)	-8(6)	27(8)	4(7)
C(27)	77(9)	32(7)	33(7)	1(5)	22(6)	-6(6)
C(28)	61(8)	25(6)	36(7)	4(5)	23(6)	13(6)
C(29)	50(7)	18(5)	31(6)	0(5)	13(5)	0(5)
C(30)	45(7)	27(6)	59(8)	12(6)	8(6)	17(5)
C(31)	60(8)	22(6)	51(8)	13(5)	9(6)	2(6)
C(32)	47(7)	29(6)	44(7)	4(5)	15(6)	-1(5)

Table S4. Anisotropic displacement parameters ($Å^2$ x 10^3) for $[Bu_4N][(triptycyl\text{-}S)_6Cu_6(\mu^6\text{-}Br)]\cdot[Bu_4N][PF_6]$. The anisotropic displacement factor exponent takes the form:$-2\pi^2[(ha^*)^2U_{11} + ... + 2hka^*b^*U_{12}]$.

Atom	U_{11}	U_{22}	U_{33}	U_{23}	U_{13}	U_{12}
C(33)	46(7)	11(5)	39(7)	7(5)	7(5)	-1(5)
C(34)	39(6)	6(5)	33(6)	5(4)	7(5)	-6(4)
C(35)	44(7)	20(6)	29(6)	2(4)	8(5)	-6(5)
C(36)	39(7)	30(6)	27(6)	6(5)	6(5)	8(5)
C(37)	55(8)	31(6)	44(7)	10(5)	17(6)	-5(6)
C(38)	35(7)	54(9)	59(8)	8(6)	16(6)	0(6)
C(39)	38(7)	28(7)	53(8)	-1(5)	18(6)	-1(5)
C(40)	51(7)	25(6)	31(6)	3(5)	10(5)	7(5)
C(41)	32(6)	17(5)	21(5)	5(4)	5(4)	-10(4)
C(42)	43(7)	17(5)	25(6)	3(4)	3(5)	-1(5)
C(43)	45(7)	24(6)	32(6)	6(5)	2(5)	-6(5)
C(44)	44(7)	41(7)	43(7)	11(6)	1(6)	-11(6)
C(45)	61(8)	40(7)	41(7)	-7(6)	1(6)	-29(6)
C(46)	65(8)	19(6)	43(7)	1(5)	4(6)	-12(6)
C(47)	55(7)	17(6)	29(6)	-3(5)	4(5)	-4(5)
C(48)	69(8)	21(6)	16(6)	1(4)	3(5)	-4(5)
C(49)	51(7)	21(6)	32(6)	-1(5)	7(5)	4(5)
C(50)	66(9)	22(6)	35(7)	-6(5)	13(6)	2(6)
C(51)	60(9)	33(7)	53(8)	-11(6)	9(7)	14(6)
C(52)	45(7)	19(6)	49(7)	-3(5)	1(6)	9(5)
C(53)	46(7)	7(5)	37(6)	1(4)	2(5)	4(5)
C(54)	43(7)	10(5)	26(6)	6(4)	6(5)	-1(4)
C(55)	30(6)	21(6)	35(6)	5(5)	5(5)	-5(5)
C(56)	42(7)	18(6)	42(7)	7(5)	7(5)	2(5)
C(57)	53(8)	39(7)	38(7)	27(6)	-1(6)	2(6)
C(58)	63(9)	50(8)	41(7)	13(7)	3(6)	-12(7)
C(59)	59(8)	50(8)	29(7)	-3(6)	11(6)	-15(6)
C(60)	42(7)	32(6)	25(6)	2(5)	9(5)	-8(5)
N(1)	41(6)	46(6)	39(6)	11(5)	11(4)	3(5)
C(61)	39(7)	44(8)	84(10)	32(7)	21(7)	5(6)
C(62)	60(9)	43(8)	76(10)	23(7)	8(7)	-1(7)
C(63)	61(10)	45(9)	165(17)	39(10)	35(11)	12(8)
C(64)	56(10)	34(9)	220(20)	12(10)	16(12)	-13(7)
C(65)	45(7)	44(8)	41(7)	8(6)	11(6)	3(6)
C(66)	62(8)	43(7)	48(8)	23(6)	10(6)	18(6)
C(67)	53(8)	49(8)	45(8)	16(6)	18(6)	10(6)
C(68)	51(8)	59(9)	43(8)	20(6)	13(6)	0(6)

C(69)	58(8)	45(8)	41(7)	16(6)	20(6)	8(6)
C(70)	61(8)	47(8)	39(7)	12(6)	18(6)	-1(6)

Table S4. Anisotropic displacement parameters ($Å^2$ x 10^3) for $[Bu_4N][(triptycyl\text{-}S)_6Cu_6(\mu^6\text{-}Br)]\cdot[Bu_4N][PF_6]$. The anisotropic displacement factor exponent takes the form:$-2\pi^2[(ha^*)^2U_{11} + ... + 2hka^*b^*U_{12}]$.

Atom	U_{11}	U_{22}	U_{33}	U_{23}	U_{13}	U_{12}
C(71)	45(7)	33(7)	51(8)	-4(6)	9(6)	4(5)
C(72)	57(8)	61(9)	57(9)	-1(7)	16(7)	-13(7)
C(73)	37(7)	37(7)	54(8)	23(6)	8(6)	9(5)
C(74)	60(9)	44(8)	70(9)	18(7)	24(7)	6(7)
C(75)	61(9)	55(9)	94(12)	13(8)	14(8)	6(7)
C(76)	68(10)	41(8)	134(14)	2(8)	59(9)	16(7)
P(1)	63(7)	15(5)	87(9)	6(5)	-31(6)	-11(5)
F(1)	340(40)	80(17)	160(20)	35(16)	-40(30)	120(20)
F(2)	126(18)	9(8)	330(30)	34(12)	-110(20)	-20(10)
F(3)	115(16)	37(10)	220(20)	24(12)	-49(15)	1(10)
P(2)	43(6)	24(5)	89(8)	0	-14(5)	0
F(4)	99(16)	109(16)	180(20)	64(14)	64(14)	43(12)
F(5)	160(19)	30(9)	220(20)	-20(12)	137(18)	-28(11)
F(6)	107(17)	90(16)	210(30)	29(15)	20(15)	16(13)

Table S5. Hydrogen coordinates (x 10^4) and isotropic displacement parameters (Å^2 x 10^3) for $[Bu_4N][(triptycyl\text{-}S)_6Cu_6(\mu^6\text{-}Br)]\cdot[Bu_4N][PF_6]$.

H Atom	x	y	z	U(eq)
H(3)	1666	1350	2126	45
H(4)	1541	739	836	68
H(5)	1012	354	893	89
H(6)	609	566	2151	94
H(8)	445	1073	3848	69
H(10)	563	788	5817	85
H(11)	905	782	7412	102
H(12)	1432	1180	7466	76
H(13)	1614	1584	5864	58
H(16)	1134	2669	3601	36
H(17)	598	3062	3528	49
H(18)	86	2640	3532	65
H(19)	97	1828	3587	59
H(23)	1774	3620	7997	58
H(24)	1700	4193	9411	80
H(25)	1185	4595	9486	83
H(26)	743	4461	8202	71
H(28)	510	4005	6485	49
H(30)	577	4319	4482	52
H(31)	904	4354	2845	53
H(32)	1400	3905	2736	48
H(33)	1601	3463	4232	38
H(36)	1155	2380	6442	38
H(37)	615	2005	6460	51
H(38)	114	2450	6578	59
H(39)	148	3251	6641	47
H(43)	3103	4312	4901	41
H(44)	3563	4837	4980	51
H(45)	3589	5413	6341	57
H(46)	3139	5489	7594	51
H(48)	2572	5174	8370	42
H(50)	1957	5441	7855	49
H(51)	1458	5331	6790	58
H(52)	1428	4763	5394	45
H(53)	1907	4292	5075	36
H(56)	2556	3372	7349	41
H(57)	2622	3215	9267	52
H(58)	2694	3807	10542	62
H(59)	2652	4580	9951	55
H(61A)	1114	1831	494	66

Table S5. Hydrogen coordinates (x 10^4) and isotropic displacement parameters ($Å^2$ x 10^3) for $[Bu_4N][(triptycyl\text{-}S)_6Cu_6(\mu^6\text{-}Br)]\cdot[Bu_4N][PF_6]$.

H Atom	x	y	z	U(eq)
H(61B)	838	2170	1024	66
H(62A)	527	2202	-671	71
H(62B)	812	1896	-1265	71
H(63A)	412	1553	515	108
H(63B)	677	1251	-179	108
H(64A)	51	1628	-1095	155
H(64B)	113	1090	-812	155
H(64C)	316	1331	-1798	155
H(65A)	1538	2693	-1129	52
H(65B)	1249	2349	-1613	52
H(66A)	1519	1707	-809	61
H(66B)	1775	2029	-77	61
H(67A)	2015	1688	-1802	58
H(67B)	1781	2056	-2479	58
H(68A)	2084	2673	-1575	76
H(68B)	2338	2352	-2263	76
H(68C)	2324	2300	-936	76
H(69A)	1518	2339	1295	57
H(69B)	1239	2711	1667	57
H(70A)	1814	2952	326	58
H(70B)	1544	3318	804	58
H(71A)	2010	2760	2132	52
H(71B)	1715	3068	2670	52
H(72A)	2301	3425	1554	87
H(72B)	2218	3502	2840	87
H(72C)	1989	3753	1886	87
H(73A)	839	2861	-1022	51
H(73B)	1119	3200	-464	51
H(74A)	538	2845	668	69
H(74B)	820	3183	1234	69
H(75A)	394	3436	-623	84
H(75B)	663	3773	2	84
H(76A)	48	3427	934	120
H(76B)	121	3958	616	120
H(76C)	327	3721	1642	120

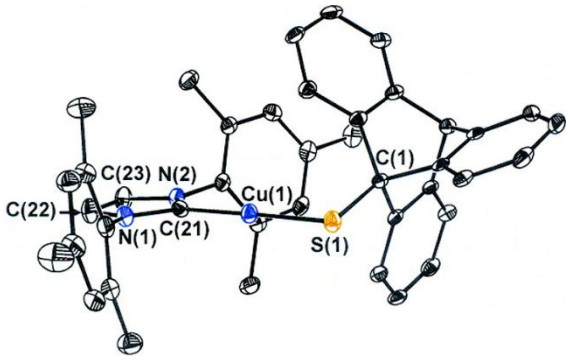

Structure Determination Summary

Crystal Data and Structure Refinement for [Cu(IMes)(STrip)], **13**

Identification code	jpd457_0m	
Empirical formula	$C_{41}H_{37}CuN_2S$	
Formula weight	653.33	
Temperature	100(2) K	
Wavelength	0.71073 Å	
Crystal system	Triclinic	
Space group	*P*-1	
Unit cell dimensions	*a* = 8.3547(15) Å	α = 78.984(2)°
	b = 9.8990(17) Å	β = 80.382(2)°
	c = 20.568(4) Å	γ = 80.950(2)°
Volume, *Z*	1632.3(5) $Å^3$, 2	
Density (calculated)	1.329 g/cm^3	
Absorption coefficient	0.765 mm^{-1}	
F(000)	684	
Crystal size	0.25 x 0.10 x 0.03 mm	
θ range for data collection	2.04 to 27.06°	
Limiting indices	$-10 < h < 10$, $-12 < k < 12$, $-26 < l < 26$	
Reflections collected	13657	
Independent reflections	7023 (R_{int} = 0.0345)	
Completeness to θ = 26.00°	99.1 %	
Absorption correction	Semi-empirical from equivalents	
Max. and min. transmission	0.9752 and 0.7234	
Refinement method	Full-matrix least-squares on F^2	
Data / restraints / parameters	7023 / 0 / 412	
Goodness-of-fit on F^2	1.023	
Final R indices [I>2σ(I)]	R1 = 0.0461, wR2 = 0.1072	
R indices (all data)	R1 = 0.0618, wR2 = 0.1160	
Largest diff. peak and hole	0.817 and -0.929 $e \cdot Å^{-3}$	

Table S1. Atomic coordinates (x 10^4) and equivalent isotropic displacement parameters ($Å^2$ x 10^3] for [Cu(IMes)(STrip)]. U(eq) is defined as one third of the trace of the orthogonalized U_{ij} tensor.

Atom	x	y	z	U(eq)
Cu(1)	6024(1)	1452(1)	3267(1)	17(1)
S(1)	7117(1)	-572(1)	3071(1)	18(1)
N(1)	5121(3)	3861(2)	3970(1)	19(1)
N(2)	4008(3)	4123(2)	3084(1)	18(1)
C(1)	7025(3)	-477(2)	2187(1)	13(1)
C(2)	8155(3)	-1678(2)	1893(1)	14(1)
C(3)	9130(3)	-2739(3)	2235(1)	18(1)
C(4)	10114(3)	-3728(3)	1892(1)	21(1)
C(5)	10126(3)	-3645(3)	1212(1)	21(1)
C(6)	9112(3)	-2598(3)	868(1)	19(1)
C(7)	8131(3)	-1623(2)	1209(1)	15(1)
C(8)	6952(3)	-437(3)	904(1)	16(1)
C(9)	7476(3)	872(3)	1041(1)	17(1)
C(10)	7897(3)	1991(3)	558(1)	21(1)
C(11)	8427(3)	3101(3)	753(2)	23(1)
C(12)	8557(3)	3069(3)	1414(2)	23(1)
C(13)	8128(3)	1937(3)	1904(1)	18(1)
C(14)	7558(3)	847(2)	1717(1)	15(1)
C(15)	5324(3)	-610(2)	2016(1)	14(1)
C(16)	3914(3)	-806(3)	2466(1)	18(1)
C(17)	2484(3)	-956(3)	2233(1)	20(1)
C(18)	2464(3)	-929(3)	1560(1)	21(1)
C(19)	3885(3)	-750(3)	1105(1)	19(1)
C(20)	5297(3)	-588(2)	1335(1)	15(1)
C(21)	5036(3)	3216(3)	3455(1)	16(1)
C(22)	4152(3)	5145(3)	3928(1)	25(1)
C(23)	3459(3)	5318(3)	3366(1)	24(1)
C(24)	6188(3)	3285(3)	4466(1)	19(1)
C(25)	5685(3)	2245(3)	4988(1)	21(1)
C(26)	6789(3)	1628(3)	5429(1)	22(1)
C(27)	8346(3)	2015(3)	5359(1)	23(1)
C(28)	8780(3)	3085(3)	4837(1)	25(1)
C(29)	7721(3)	3732(3)	4384(1)	23(1)
C(30)	4000(4)	1815(3)	5072(2)	29(1)
C(31)	9540(4)	1304(4)	5827(2)	36(1)
C(32)	8222(4)	4863(3)	3815(2)	32(1)
C(33)	3705(3)	3900(3)	2445(1)	16(1)
C(34)	2679(3)	2933(3)	2428(1)	18(1)
C(35)	2517(3)	2662(3)	1798(1)	20(1)

Table S1. Atomic coordinates (x 10^4) and equivalent isotropic displacement parameters ($Å^2$ x 10^3] for [Cu(IMes)(STrip)]. U(eq) is defined as one third of the trace of the orthogonalized U_{ij} tensor.

Atom	x	y	z	U(eq)
C(36)	3333(3)	3351(3)	1212(1)	20(1)
C(37)	4305(3)	4335(3)	1255(1)	20(1)
C(38)	4528(3)	4625(3)	1866(1)	17(1)
C(39)	1769(3)	2196(3)	3055(1)	25(1)
C(40)	3158(4)	3018(3)	543(2)	28(1)
C(41)	5614(3)	5683(3)	1901(2)	25(1)

Table S2. Bond lengths (Å) for [Cu(IMes)(STrip)]. Symmetry transformations used to generate equivalent atoms:

Cu(1)-C(21)	1.892(3)	C(18)-H(18)	0.9500
Cu(1)-S(1)	2.1491(8)	C(19)-C(20)	1.384(4)
S(1)-C(1)	1.817(3)	C(19)-H(19)	0.9500
N(1)-C(21)	1.353(3)	C(22)-C(23)	1.349(4)
N(1)-C(22)	1.392(3)	C(22)-H(22)	0.9500
N(1)-C(24)	1.443(3)	C(23)-H(23)	0.9500
N(2)-C(21)	1.357(3)	C(24)-C(29)	1.394(4)
N(2)-C(23)	1.395(3)	C(24)-C(25)	1.397(4)
N(2)-C(33)	1.442(3)	C(25)-C(26)	1.392(4)
C(1)-C(2)	1.549(3)	C(25)-C(30)	1.507(4)
C(1)-C(15)	1.551(3)	C(26)-C(27)	1.390(4)
C(1)-C(14)	1.552(3)	C(26)-H(26)	0.9500
C(2)-C(3)	1.380(4)	C(27)-C(28)	1.401(4)
C(2)-C(7)	1.401(3)	C(27)-C(31)	1.502(4)
C(3)-C(4)	1.396(4)	C(28)-C(29)	1.389(4)
C(3)-H(3)	0.9500	C(28)-H(28)	0.9500
C(4)-C(5)	1.384(4)	C(29)-C(32)	1.511(4)
C(4)-H(4)	0.9500	C(30)-H(30A)	0.9800
C(5)-C(6)	1.392(4)	C(30)-H(30B)	0.9800
C(5)-H(5)	0.9500	C(30)-H(30C)	0.9800
C(6)-C(7)	1.383(3)	C(31)-H(31A)	0.9800
C(6)-H(6)	0.9500	C(31)-H(31B)	0.9800
C(7)-C(8)	1.517(3)	C(31)-H(31C)	0.9800
C(8)-C(9)	1.520(3)	C(32)-H(32A)	0.9800
C(8)-C(20)	1.524(3)	C(32)-H(32B)	0.9800
C(8)-H(8)	1.0000	C(32)-H(32C)	0.9800
C(9)-C(10)	1.386(3)	C(33)-C(34)	1.391(4)
C(9)-C(14)	1.397(4)	C(33)-C(38)	1.400(4)
C(10)-C(11)	1.395(4)	C(34)-C(35)	1.403(4)
C(10)-H(10)	0.9500	C(34)-C(39)	1.503(4)
C(11)-C(12)	1.376(4)	C(35)-C(36)	1.394(4)
C(11)-H(11)	0.9500	C(35)-H(35)	0.9500
C(12)-C(13)	1.405(4)	C(36)-C(37)	1.386(4)
C(12)-H(12)	0.9500	C(36)-C(40)	1.508(4)
C(13)-C(14)	1.387(3)	C(37)-C(38)	1.390(4)
C(13)-H(13)	0.9500	C(37)-H(37)	0.9500
C(15)-C(16)	1.386(3)	C(38)-C(41)	1.508(4)
C(15)-C(20)	1.400(3)	C(39)-H(39A)	0.9800
C(16)-C(17)	1.398(4)	C(39)-H(39B)	0.9800
C(16)-H(16)	0.9500	C(39)-H(39C)	0.9800
C(17)-C(18)	1.383(4)	C(40)-H(40A)	0.9800
C(17)-H(17)	0.9500	C(40)-H(40B)	0.9800
C(18)-C(19)	1.395(4)	C(40)-H(40C)	0.9800

Table S2. Bond lengths (Å) for [Cu(IMes)(STrip)]. Symmetry transformations used to generate equivalent atoms:

C(41)-H(41A)	0.9800
C(41)-H(41B)	0.9800
C(41)-H(41C)	0.9800

Table S3. Bond angles (deg.) for [Cu(IMes)(STrip)]. Symmetry transformations used to generate equivalent atoms:

C(21)-Cu(1)-S(1)	178.83(8)	C(11)-C(10)-H(10)	120.5
C(1)-S(1)-Cu(1)	103.76(8)	C(12)-C(11)-C(10)	120.2(2)
C(21)-N(1)-C(22)	111.8(2)	C(12)-C(11)-H(11)	119.9
C(21)-N(1)-C(24)	122.3(2)	C(10)-C(11)-H(11)	119.9
C(22)-N(1)-C(24)	125.8(2)	C(11)-C(12)-C(13)	120.8(2)
C(21)-N(2)-C(23)	111.4(2)	C(11)-C(12)-H(12)	119.6
C(21)-N(2)-C(33)	122.2(2)	C(13)-C(12)-H(12)	119.6
C(23)-N(2)-C(33)	126.0(2)	C(14)-C(13)-C(12)	119.3(3)
C(2)-C(1)-C(15)	103.03(19)	C(14)-C(13)-H(13)	120.4
C(2)-C(1)-C(14)	103.72(18)	C(12)-C(13)-H(13)	120.4
C(15)-C(1)-C(14)	105.10(19)	C(13)-C(14)-C(9)	119.4(2)
C(2)-C(1)-S(1)	112.32(16)	C(13)-C(14)-C(1)	126.4(2)
C(15)-C(1)-S(1)	115.06(17)	C(9)-C(14)-C(1)	114.2(2)
C(14)-C(1)-S(1)	116.16(17)	C(16)-C(15)-C(20)	119.3(2)
C(3)-C(2)-C(7)	119.7(2)	C(16)-C(15)-C(1)	126.5(2)
C(3)-C(2)-C(1)	126.5(2)	C(20)-C(15)-C(1)	114.1(2)
C(7)-C(2)-C(1)	113.7(2)	C(15)-C(16)-C(17)	119.6(2)
C(2)-C(3)-C(4)	119.6(2)	C(15)-C(16)-H(16)	120.2
C(2)-C(3)-H(3)	120.2	C(17)-C(16)-H(16)	120.2
C(4)-C(3)-H(3)	120.2	C(18)-C(17)-C(16)	120.8(2)
C(5)-C(4)-C(3)	120.5(2)	C(18)-C(17)-H(17)	119.6
C(5)-C(4)-H(4)	119.7	C(16)-C(17)-H(17)	119.6
C(3)-C(4)-H(4)	119.7	C(17)-C(18)-C(19)	119.9(2)
C(4)-C(5)-C(6)	120.1(2)	C(17)-C(18)-H(18)	120.1
C(4)-C(5)-H(5)	120.0	C(19)-C(18)-H(18)	120.1
C(6)-C(5)-H(5)	120.0	C(20)-C(19)-C(18)	119.3(2)
C(7)-C(6)-C(5)	119.3(2)	C(20)-C(19)-H(19)	120.3
C(7)-C(6)-H(6)	120.3	C(18)-C(19)-H(19)	120.3
C(5)-C(6)-H(6)	120.3	C(19)-C(20)-C(15)	121.1(2)
C(6)-C(7)-C(2)	120.7(2)	C(19)-C(20)-C(8)	125.3(2)
C(6)-C(7)-C(8)	125.4(2)	C(15)-C(20)-C(8)	113.5(2)
C(2)-C(7)-C(8)	114.0(2)	N(1)-C(21)-N(2)	104.0(2)
C(7)-C(8)-C(9)	105.4(2)	N(1)-C(21)-Cu(1)	130.46(19)
C(7)-C(8)-C(20)	105.45(19)	N(2)-C(21)-Cu(1)	125.52(18)
C(9)-C(8)-C(20)	105.8(2)	C(23)-C(22)-N(1)	106.3(2)
C(7)-C(8)-H(8)	113.2	C(23)-C(22)-H(22)	126.8
C(9)-C(8)-H(8)	113.2	N(1)-C(22)-H(22)	126.8
C(20)-C(8)-H(8)	113.2	C(22)-C(23)-N(2)	106.4(2)
C(10)-C(9)-C(14)	121.2(2)	C(22)-C(23)-H(23)	126.8
C(10)-C(9)-C(8)	125.2(2)	N(2)-C(23)-H(23)	126.8
C(14)-C(9)-C(8)	113.5(2)	C(29)-C(24)-C(25)	122.4(2)
C(9)-C(10)-C(11)	119.0(3)	C(29)-C(24)-N(1)	118.6(2)
C(9)-C(10)-H(10)	120.5	C(25)-C(24)-N(1)	118.9(2)

Table S3. Bond angles (deg.) for [Cu(IMes)(STrip)]. Symmetry transformations used to generate equivalent atoms:

C(26)-C(25)-C(24)	117.7(2)	C(37)-C(36)-C(40)	121.0(3)
C(26)-C(25)-C(30)	121.3(2)	C(35)-C(36)-C(40)	120.1(2)
C(24)-C(25)-C(30)	121.0(2)	C(36)-C(37)-C(38)	122.0(2)
C(27)-C(26)-C(25)	122.0(2)	C(36)-C(37)-H(37)	119.0
C(27)-C(26)-H(26)	119.0	C(38)-C(37)-H(37)	119.0
C(25)-C(26)-H(26)	119.0	C(37)-C(38)-C(33)	117.4(2)
C(26)-C(27)-C(28)	118.2(3)	C(37)-C(38)-C(41)	121.0(2)
C(26)-C(27)-C(31)	121.1(3)	C(33)-C(38)-C(41)	121.6(2)
C(28)-C(27)-C(31)	120.6(3)	C(34)-C(39)-H(39A)	109.5
C(29)-C(28)-C(27)	121.9(3)	C(34)-C(39)-H(39B)	109.5
C(29)-C(28)-H(28)	119.0	H(39A)-C(39)-H(39B)	109.5
C(27)-C(28)-H(28)	119.0	C(34)-C(39)-H(39C)	109.5
C(28)-C(29)-C(24)	117.7(2)	H(39A)-C(39)-H(39C)	109.5
C(28)-C(29)-C(32)	121.3(3)	H(39B)-C(39)-H(39C)	109.5
C(24)-C(29)-C(32)	121.0(3)	C(36)-C(40)-H(40A)	109.5
C(25)-C(30)-H(30A)	109.5	C(36)-C(40)-H(40B)	109.5
C(25)-C(30)-H(30B)	109.5	H(40A)-C(40)-H(40B)	109.5
H(30A)-C(30)-H(30B)	109.5	C(36)-C(40)-H(40C)	109.5
C(25)-C(30)-H(30C)	109.5	H(40A)-C(40)-H(40C)	109.5
H(30A)-C(30)-H(30C)	109.5	H(40B)-C(40)-H(40C)	109.5
H(30B)-C(30)-H(30C)	109.5	C(38)-C(41)-H(41A)	109.5
C(27)-C(31)-H(31A)	109.5	C(38)-C(41)-H(41B)	109.5
C(27)-C(31)-H(31B)	109.5	H(41A)-C(41)-H(41B)	109.5
H(31A)-C(31)-H(31B)	109.5	C(38)-C(41)-H(41C)	109.5
C(27)-C(31)-H(31C)	109.5	H(41A)-C(41)-H(41C)	109.5
H(31A)-C(31)-H(31C)	109.5	H(41B)-C(41)-H(41C)	109.5
H(31B)-C(31)-H(31C)	109.5		
C(29)-C(32)-H(32A)	109.5		
C(29)-C(32)-H(32B)	109.5		
H(32A)-C(32)-H(32B)	109.5		
C(29)-C(32)-H(32C)	109.5		
H(32A)-C(32)-H(32C)	109.5		
H(32B)-C(32)-H(32C)	109.5		
C(34)-C(33)-C(38)	122.8(2)		
C(34)-C(33)-N(2)	119.1(2)		
C(38)-C(33)-N(2)	118.0(2)		
C(33)-C(34)-C(35)	117.4(2)		
C(33)-C(34)-C(39)	122.0(2)		
C(35)-C(34)-C(39)	120.6(2)		
C(36)-C(35)-C(34)	121.3(2)		
C(36)-C(35)-H(35)	119.3		
C(34)-C(35)-H(35)	119.3		
C(37)-C(36)-C(35)	118.9(2)		

Table S4. Anisotropic displacement parameters ($Å^2$ x 10^3) for [Cu(IMes)(STrip)]. The anisotropic displacement factor exponent takes the form: $-2\pi^2[(ha^*)^2U_{11} + ... + 2hka^*b^*U_{12}]$.

Atom	U_{11}	U_{22}	U_{33}	U_{23}	U_{13}	U_{12}
Cu(1)	19(1)	14(1)	18(1)	-3(1)	-3(1)	-1(1)
S(1)	22(1)	15(1)	17(1)	-3(1)	-4(1)	0(1)
N(1)	20(1)	18(1)	19(1)	-6(1)	-2(1)	-1(1)
N(2)	19(1)	16(1)	19(1)	-4(1)	-2(1)	-2(1)
C(1)	11(1)	11(1)	16(1)	0(1)	-1(1)	-2(1)
C(2)	11(1)	12(1)	21(1)	-2(1)	1(1)	-8(1)
C(3)	16(1)	16(1)	22(1)	-2(1)	-2(1)	-8(1)
C(4)	14(1)	12(1)	36(2)	-2(1)	-3(1)	-4(1)
C(5)	16(1)	17(1)	33(2)	-10(1)	3(1)	-6(1)
C(6)	16(1)	20(1)	22(1)	-8(1)	4(1)	-8(1)
C(7)	12(1)	15(1)	20(1)	-2(1)	1(1)	-8(1)
C(8)	15(1)	18(1)	17(1)	-2(1)	0(1)	-5(1)
C(9)	11(1)	14(1)	23(1)	1(1)	0(1)	-4(1)
C(10)	16(1)	20(1)	24(1)	2(1)	1(1)	-4(1)
C(11)	16(1)	17(1)	32(2)	3(1)	5(1)	-6(1)
C(12)	16(1)	15(1)	37(2)	-6(1)	3(1)	-8(1)
C(13)	13(1)	16(1)	25(1)	-4(1)	0(1)	-2(1)
C(14)	10(1)	13(1)	21(1)	0(1)	-1(1)	-2(1)
C(15)	13(1)	10(1)	21(1)	-2(1)	-2(1)	-3(1)
C(16)	19(1)	14(1)	21(1)	-1(1)	2(1)	-5(1)
C(17)	15(1)	16(1)	29(2)	-1(1)	2(1)	-7(1)
C(18)	14(1)	19(1)	32(2)	-4(1)	-6(1)	-7(1)
C(19)	20(1)	17(1)	21(1)	1(1)	-4(1)	-6(1)
C(20)	15(1)	11(1)	19(1)	0(1)	0(1)	-4(1)
C(21)	17(1)	18(1)	12(1)	-2(1)	-1(1)	-4(1)
C(22)	28(2)	20(1)	26(2)	-10(1)	-4(1)	3(1)
C(23)	26(1)	17(1)	29(2)	-8(1)	-5(1)	4(1)
C(24)	23(1)	18(1)	17(1)	-5(1)	-2(1)	-1(1)
C(25)	24(1)	22(1)	19(1)	-6(1)	0(1)	-6(1)
C(26)	28(1)	22(1)	16(1)	-2(1)	-1(1)	-6(1)
C(27)	23(1)	27(1)	19(1)	-3(1)	-2(1)	-3(1)
C(28)	20(1)	28(2)	26(2)	-3(1)	-1(1)	-7(1)
C(29)	25(1)	23(1)	18(1)	-3(1)	2(1)	-6(1)
C(30)	26(2)	34(2)	26(2)	-1(1)	-3(1)	-12(1)
C(31)	29(2)	47(2)	31(2)	6(1)	-9(1)	-7(1)
C(32)	31(2)	31(2)	29(2)	6(1)	-1(1)	-11(1)
C(33)	15(1)	14(1)	20(1)	-4(1)	-4(1)	1(1)
C(34)	15(1)	15(1)	22(1)	-2(1)	-2(1)	0(1)
C(35)	16(1)	16(1)	29(2)	-5(1)	-6(1)	-2(1)

C(36)	19(1)	18(1)	24(1)	-2(1)	-8(1)	3(1)

Table S4. Anisotropic displacement parameters ($Å^2$ x 10^3) for [Cu(IMes)(STrip)]. The anisotropic displacement factor exponent takes the form: $-2\pi^2[(ha^*)^2U_{11} + ... + 2hka^*b^*U_{12}]$.

Atom	U_{11}	U_{22}	U_{33}	U_{23}	U_{13}	U_{12}
C(37)	18(1)	18(1)	20(1)	1(1)	-2(1)	0(1)
C(38)	14(1)	13(1)	24(1)	-2(1)	-2(1)	0(1)
C(39)	25(1)	22(1)	28(2)	-1(1)	0(1)	-9(1)
C(40)	29(2)	28(2)	28(2)	-5(1)	-10(1)	0(1)
C(41)	23(1)	19(1)	34(2)	-4(1)	-2(1)	-7(1)

Table S5. Hydrogen coordinates (x 10^4) and isotropic displacement parameters (Å^2 x 10^3) for [Cu(IMes)(STrip)].

H atom	x	y	z	U(eq)
H(3)	9132	-2796	2702	21
H(4)	10781	-4463	2128	25
H(5)	10827	-4305	980	26
H(6)	9094	-2553	404	22
H(8)	6926	-424	419	20
H(10)	7825	2001	101	25
H(11)	8699	3882	429	28
H(12)	8942	3820	1541	27
H(13)	8227	1919	2360	22
H(16)	3920	-838	2930	22
H(17)	1514	-1078	2541	25
H(18)	1486	-1033	1407	25
H(19)	3883	-739	642	23
H(22)	4007	5775	4235	30
H(23)	2739	6098	3195	29
H(26)	6469	923	5789	27
H(28)	9830	3376	4791	30
H(30A)	3181	2642	5057	43
H(30B)	3794	1205	5504	43
H(30C)	3930	1319	4711	43
H(31A)	8947	827	6237	55
H(31B)	10123	1995	5939	55
H(31C)	10328	626	5610	55
H(32A)	9334	5034	3836	47
H(32B)	7463	5717	3851	47
H(32C)	8192	4573	3388	47
H(35)	1837	1997	1772	24
H(37)	4834	4825	855	23
H(39A)	2542	1519	3299	38
H(39B)	948	1714	2936	38
H(39C)	1225	2873	3338	38
H(40A)	2835	3878	244	42
H(40B)	2319	2398	605	42
H(40C)	4206	2562	347	42
H(41A)	6257	5928	1461	38
H(41B)	6355	5291	2232	38
H(41C)	4937	6515	2033	38

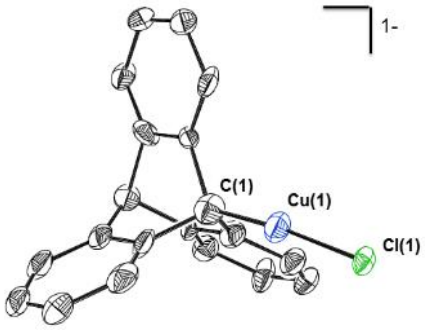

Table 1. Crystal data and structure refinement for jpd466_1m, **[Bu$_4$N][Cu(Trip)Cl]**

Identification code	jpd466_1m	
Empirical formula	C36 H49 Cl Cu N	
Formula weight	594.75	
Temperature	100(2) K	
Wavelength	0.71073 Å	
Crystal system	Orthorhombic	
Space group	$Pca2_1$	
Unit cell dimensions	a = 19.242(12) Å	a= 90°.
	b = 19.418(12) Å	b= 90°.
	c = 17.998(11) Å	g = 90°.
Volume	6725(7) $Å^3$	
Z	8	
Density (calculated)	1.175 Mg/m^3	
Absorption coefficient	0.752 mm^{-1}	
F(000)	2544	
Crystal size	0.30 x 0.17 x 0.10 mm^3	
Theta range for data collection	1.05 to 25.22°.	
Index ranges	-21<=h<=22, -22<=k<=23, -21<=l<=20	
Reflections collected	39711	
Independent reflections	11338 [R(int) = 0.2178]	
Completeness to theta = 25.22°	95.0 %	
Absorption correction	Semi-empirical from equivalents	
Max. and min. transmission	0.9286 and 0.8058	
Refinement method	Full-matrix least-squares on F^2	
Data / restraints / parameters	11338 / 1 / 712	
Goodness-of-fit on F^2	0.993	
Final R indices [I>2sigma(I)]	R1 = 0.1020, wR2 = 0.2417	
R indices (all data)	R1 = 0.1834, wR2 = 0.3129	
Absolute structure parameter	0.51(3)	
Largest diff. peak and hole	2.187 and -1.511 e.$Å^{-3}$	

Table 2. Atomic coordinates (x 10^4) and equivalent isotropic displacement parameters ($Å^2$x 10^3)
for jpd466_1m. U(eq) is defined as one third of the trace of the orthogonalized U^{ij} tensor.

	x	y	z	U(eq)
Cu(1)	6249(1)	1246(1)	10124(1)	37(1)
Cl(1)	5682(1)	828(1)	11083(1)	26(1)
C(1)	6897(7)	1633(7)	9392(7)	41(3)
C(2)	7243(7)	1112(7)	8850(6)	37(3)
C(3)	7075(7)	431(7)	8775(7)	44(3)
C(4)	7434(8)	-10(8)	8250(7)	52(4)
C(5)	7980(7)	276(8)	7810(6)	44(3)
C(6)	8132(7)	966(7)	7871(6)	42(3)
C(7)	7786(6)	1390(7)	8384(6)	40(3)
C(8)	7911(6)	2148(7)	8499(6)	35(3)
C(9)	7179(6)	2491(6)	8374(7)	36(3)
C(10)	7034(6)	2996(6)	7861(6)	34(3)
C(11)	6325(6)	3228(6)	7777(6)	33(3)
C(12)	5805(6)	2957(7)	8231(6)	37(3)
C(13)	5958(6)	2448(6)	8772(6)	35(3)
C(14)	6655(6)	2222(6)	8843(6)	31(3)
C(15)	7533(6)	1982(6)	9796(6)	35(3)
C(16)	7595(7)	2029(7)	10583(6)	38(3)
C(17)	8206(7)	2366(7)	10889(7)	45(3)
C(18)	8711(7)	2601(8)	10436(7)	44(3)
C(19)	8654(7)	2558(6)	9649(6)	34(3)
C(20)	8059(6)	2249(6)	9342(5)	28(3)
Cu(2)	3656(1)	3540(1)	-132(1)	39(1)
Cl(2)	4240(1)	3903(1)	-1106(1)	29(1)
C(21)	3035(6)	3300(6)	705(6)	33(3)
C(22)	2306(7)	3081(7)	468(7)	42(3)
C(23)	2072(7)	2995(6)	-272(7)	44(3)
C(24)	1364(7)	2789(7)	-413(8)	44(3)
C(25)	916(7)	2674(7)	167(8)	50(3)

C(26)	1130(7)	2738(7)	924(7)	45(3)
C(27)	1828(6)	2938(6)	1065(7)	37(3)
C(28)	2146(7)	3081(7)	1840(7)	46(3)
C(29)	2824(7)	2631(7)	1872(7)	43(3)
C(30)	2959(7)	2169(7)	2449(6)	41(3)
C(31)	3611(7)	1821(6)	2443(6)	39(3)
C(32)	4080(7)	1939(6)	1847(7)	39(3)
C(33)	3897(7)	2410(7)	1276(7)	47(4)
C(34)	3283(6)	2753(6)	1284(6)	34(3)
C(35)	2899(6)	3945(7)	1218(6)	40(3)
C(36)	3178(7)	4603(6)	1141(6)	37(3)
C(37)	2976(7)	5145(7)	1601(7)	45(3)
C(38)	2455(7)	5043(7)	2168(6)	42(3)
C(39)	2186(7)	4363(6)	2279(7)	40(3)
C(40)	2419(6)	3837(6)	1809(7)	35(3)
N(1)	1301(5)	84(5)	5459(5)	34(2)
C(41)	976(7)	-71(7)	6221(6)	46(3)
C(42)	1263(7)	-733(6)	6603(6)	36(3)
C(43)	806(7)	-934(7)	7277(7)	44(3)
C(44)	58(9)	-1169(10)	7061(8)	80(6)
C(45)	1179(6)	-530(6)	4886(7)	35(3)
C(46)	405(6)	-749(6)	4859(7)	41(3)
C(47)	216(8)	-1067(7)	4067(7)	50(3)
C(48)	80(7)	-502(7)	3491(7)	53(4)
C(49)	996(7)	743(6)	5164(7)	38(3)
C(50)	1332(6)	1084(7)	4491(6)	36(3)
C(51)	857(7)	1631(7)	4143(6)	46(3)
C(52)	1197(7)	2025(7)	3492(7)	46(3)
C(53)	2109(5)	155(7)	5524(7)	38(3)
C(54)	2347(6)	725(7)	6054(6)	41(3)
C(55)	3178(6)	815(6)	6047(7)	32(3)
C(56)	3456(8)	1044(8)	5285(9)	61(4)
N(2)	6254(5)	4681(5)	9812(5)	34(2)
C(57)	7051(6)	4794(6)	9809(6)	36(3)
C(58)	7480(7)	4402(7)	9198(6)	40(3)
C(59)	8252(6)	4425(7)	9376(7)	40(3)

C(60)	8714(7)	4159(7)	8730(7)	44(3)
C(61)	5945(6)	4811(6)	9013(6)	34(3)
C(62)	5996(7)	5548(7)	8720(7)	41(3)
C(63)	5644(7)	5584(7)	7942(6)	42(3)
C(64)	5612(7)	6318(7)	7628(8)	50(4)
C(65)	5957(6)	5197(7)	10374(6)	36(3)
C(66)	5158(6)	5146(6)	10527(7)	38(3)
C(67)	4907(7)	5770(7)	10969(8)	54(4)
C(68)	5259(8)	5832(9)	11749(8)	67(5)
C(69)	6070(6)	3950(6)	10010(6)	35(3)
C(70)	6294(7)	3682(6)	10788(6)	38(3)
C(71)	5915(7)	3025(6)	10982(6)	39(3)
C(72)	6107(7)	2740(7)	11758(7)	45(3)

Table 3. Bond lengths [Å] and angles [°] for jpd466_1m.

Cu(1)-C(1)	1.965(13)	C(17)-H(17)	0.9500
Cu(1)-Cl(1)	2.197(3)	C(18)-C(19)	1.423(17)
C(1)-C(2)	1.555(17)	C(18)-H(18)	0.9500
C(1)-C(15)	1.575(16)	C(19)-C(20)	1.407(16)
C(1)-C(14)	1.581(16)	C(19)-H(19)	0.9500
C(2)-C(3)	1.367(18)	Cu(2)-C(21)	1.978(11)
C(2)-C(7)	1.445(17)	Cu(2)-Cl(2)	2.198(3)
C(3)-C(4)	1.450(18)	C(21)-C(22)	1.525(17)
C(3)-H(3)	0.9500	C(21)-C(34)	1.564(15)
C(4)-C(5)	1.428(19)	C(21)-C(35)	1.577(16)
C(4)-H(4)	0.9500	C(22)-C(23)	1.416(17)
C(5)-C(6)	1.375(19)	C(22)-C(27)	1.442(17)
C(5)-H(5)	0.9500	C(23)-C(24)	1.442(18)
C(6)-C(7)	1.405(17)	C(23)-H(23)	0.9500
C(6)-H(6)	0.9500	C(24)-C(25)	1.372(19)
C(7)-C(8)	1.506(18)	C(24)-H(24)	0.9500
C(8)-C(20)	1.556(14)	C(25)-C(26)	1.429(18)
C(8)-C(9)	1.573(15)	C(25)-H(25)	0.9500
C(8)-H(8)	1.0000	C(26)-C(27)	1.421(17)
C(9)-C(10)	1.375(16)	C(26)-H(26)	0.9500
C(9)-C(14)	1.416(16)	C(27)-C(28)	1.548(17)
C(10)-C(11)	1.445(15)	C(28)-C(40)	1.559(19)
C(10)-H(10)	0.9500	C(28)-C(29)	1.571(17)
C(11)-C(12)	1.396(17)	C(28)-H(28)	1.0000
C(11)-H(11)	0.9500	C(29)-C(30)	1.398(17)
C(12)-C(13)	1.418(16)	C(29)-C(34)	1.398(17)
C(12)-H(12)	0.9500	C(30)-C(31)	1.425(17)
C(13)-C(14)	1.417(15)	C(30)-H(30)	0.9500
C(13)-H(13)	0.9500	C(31)-C(32)	1.420(18)
C(15)-C(20)	1.401(15)	C(31)-H(31)	0.9500
C(15)-C(16)	1.425(15)	C(32)-C(33)	1.421(18)
C(16)-C(17)	1.455(18)	C(32)-H(32)	0.9500
C(16)-H(16)	0.9500	C(33)-C(34)	1.356(18)
C(17)-C(18)	1.348(18)	C(33)-H(33)	0.9500

C(35)-C(36)	1.394(17)	C(48)-H(48B)	0.9800
C(35)-C(40)	1.426(17)	C(48)-H(48C)	0.9800
C(36)-C(37)	1.393(17)	C(49)-C(50)	1.524(16)
C(36)-H(36)	0.9500	C(49)-H(49A)	0.9900
C(37)-C(38)	1.443(18)	C(49)-H(49B)	0.9900
C(37)-H(37)	0.9500	C(50)-C(51)	1.535(19)
C(38)-C(39)	1.433(19)	C(50)-H(50A)	0.9900
C(38)-H(38)	0.9500	C(50)-H(50B)	0.9900
C(39)-C(40)	1.398(16)	C(51)-C(52)	1.545(17)
C(39)-H(39)	0.9500	C(51)-H(51A)	0.9900
N(1)-C(49)	1.506(15)	C(51)-H(51B)	0.9900
N(1)-C(41)	1.537(15)	C(52)-H(52A)	0.9800
N(1)-C(53)	1.565(14)	C(52)-H(52B)	0.9800
N(1)-C(45)	1.593(15)	C(52)-H(52C)	0.9800
C(41)-C(42)	1.559(18)	C(53)-C(54)	1.531(16)
C(41)-H(41A)	0.9900	C(53)-H(53A)	0.9900
C(41)-H(41B)	0.9900	C(53)-H(53B)	0.9900
C(42)-C(43)	1.548(16)	C(54)-C(55)	1.609(16)
C(42)-H(42A)	0.9900	C(54)-H(54A)	0.9900
C(42)-H(42B)	0.9900	C(54)-H(54B)	0.9900
C(43)-C(44)	1.56(2)	C(55)-C(56)	1.537(19)
C(43)-H(43A)	0.9900	C(55)-H(55A)	0.9900
C(43)-H(43B)	0.9900	C(55)-H(55B)	0.9900
C(44)-H(44A)	0.9800	C(56)-H(56A)	0.9800
C(44)-H(44B)	0.9800	C(56)-H(56B)	0.9800
C(44)-H(44C)	0.9800	C(56)-H(56C)	0.9800
C(45)-C(46)	1.551(16)	N(2)-C(69)	1.505(15)
C(45)-H(45A)	0.9900	N(2)-C(65)	1.534(15)
C(45)-H(45B)	0.9900	N(2)-C(57)	1.549(13)
C(46)-C(47)	1.596(17)	N(2)-C(61)	1.578(14)
C(46)-H(46A)	0.9900	C(57)-C(58)	1.572(16)
C(46)-H(46B)	0.9900	C(57)-H(57A)	0.9900
C(47)-C(48)	1.531(18)	C(57)-H(57B)	0.9900
C(47)-H(47A)	0.9900	C(58)-C(59)	1.521(18)
C(47)-H(47B)	0.9900	C(58)-H(58A)	0.9900
C(48)-H(48A)	0.9800	C(58)-H(58B)	0.9900

C(59)-C(60)	1.552(16)	C(71)-C(72)	1.546(16)
C(59)-H(59A)	0.9900	C(71)-H(71A)	0.9900
C(59)-H(59B)	0.9900	C(71)-H(71B)	0.9900
C(60)-H(60A)	0.9800	C(72)-H(72A)	0.9800
C(60)-H(60B)	0.9800	C(72)-H(72B)	0.9800
C(60)-H(60C)	0.9800	C(72)-H(72C)	0.9800
C(61)-C(62)	1.529(17)		
C(61)-H(61A)	0.9900	C(1)-Cu(1)-Cl(1)	169.7(4)
C(61)-H(61B)	0.9900	C(2)-C(1)-C(15)	103.8(10)
C(62)-C(63)	1.558(16)	C(2)-C(1)-C(14)	101.9(9)
C(62)-H(62A)	0.9900	C(15)-C(1)-C(14)	101.9(9)
C(62)-H(62B)	0.9900	C(2)-C(1)-Cu(1)	116.3(8)
C(63)-C(64)	1.533(18)	C(15)-C(1)-Cu(1)	110.3(8)
C(63)-H(63A)	0.9900	C(14)-C(1)-Cu(1)	120.5(9)
C(63)-H(63B)	0.9900	C(3)-C(2)-C(7)	118.4(11)
C(64)-H(64A)	0.9800	C(3)-C(2)-C(1)	126.2(11)
C(64)-H(64B)	0.9800	C(7)-C(2)-C(1)	115.4(11)
C(64)-H(64C)	0.9800	C(2)-C(3)-C(4)	121.5(13)
C(65)-C(66)	1.566(15)	C(2)-C(3)-H(3)	119.2
C(65)-H(65A)	0.9900	C(4)-C(3)-H(3)	119.2
C(65)-H(65B)	0.9900	C(5)-C(4)-C(3)	118.9(13)
C(66)-C(67)	1.529(18)	C(5)-C(4)-H(4)	120.6
C(66)-H(66A)	0.9900	C(3)-C(4)-H(4)	120.6
C(66)-H(66B)	0.9900	C(6)-C(5)-C(4)	119.3(12)
C(67)-C(68)	1.56(2)	C(6)-C(5)-H(5)	120.4
C(67)-H(67A)	0.9900	C(4)-C(5)-H(5)	120.4
C(67)-H(67B)	0.9900	C(5)-C(6)-C(7)	121.6(13)
C(68)-H(68A)	0.9800	C(5)-C(6)-H(6)	119.2
C(68)-H(68B)	0.9800	C(7)-C(6)-H(6)	119.2
C(68)-H(68C)	0.9800	C(6)-C(7)-C(2)	120.3(12)
C(69)-C(70)	1.556(16)	C(6)-C(7)-C(8)	126.0(12)
C(69)-H(69A)	0.9900	C(2)-C(7)-C(8)	113.7(10)
C(69)-H(69B)	0.9900	C(7)-C(8)-C(20)	106.6(10)
C(70)-C(71)	1.511(17)	C(7)-C(8)-C(9)	104.5(9)
C(70)-H(70A)	0.9900	C(20)-C(8)-C(9)	104.4(9)
C(70)-H(70B)	0.9900	C(7)-C(8)-H(8)	113.5

C(20)-C(8)-H(8)	113.5	C(15)-C(20)-C(8)	113.0(10)
C(9)-C(8)-H(8)	113.5	C(19)-C(20)-C(8)	125.9(10)
C(10)-C(9)-C(14)	121.2(10)	C(21)-Cu(2)-Cl(2)	172.5(4)
C(10)-C(9)-C(8)	125.4(11)	C(22)-C(21)-C(34)	106.1(10)
C(14)-C(9)-C(8)	113.4(10)	C(22)-C(21)-C(35)	103.5(10)
C(9)-C(10)-C(11)	119.0(11)	C(34)-C(21)-C(35)	101.5(8)
C(9)-C(10)-H(10)	120.5	C(22)-C(21)-Cu(2)	114.1(7)
C(11)-C(10)-H(10)	120.5	C(34)-C(21)-Cu(2)	118.9(8)
C(12)-C(11)-C(10)	119.9(11)	C(35)-C(21)-Cu(2)	111.0(8)
C(12)-C(11)-H(11)	120.0	C(23)-C(22)-C(27)	118.4(12)
C(10)-C(11)-H(11)	120.0	C(23)-C(22)-C(21)	126.1(11)
C(11)-C(12)-C(13)	121.0(11)	C(27)-C(22)-C(21)	115.6(10)
C(11)-C(12)-H(12)	119.5	C(22)-C(23)-C(24)	120.0(13)
C(13)-C(12)-H(12)	119.5	C(22)-C(23)-H(23)	120.0
C(14)-C(13)-C(12)	118.4(11)	C(24)-C(23)-H(23)	120.0
C(14)-C(13)-H(13)	120.8	C(25)-C(24)-C(23)	120.3(12)
C(12)-C(13)-H(13)	120.8	C(25)-C(24)-H(24)	119.8
C(9)-C(14)-C(13)	120.4(10)	C(23)-C(24)-H(24)	119.8
C(9)-C(14)-C(1)	115.4(9)	C(24)-C(25)-C(26)	122.0(12)
C(13)-C(14)-C(1)	124.1(11)	C(24)-C(25)-H(25)	119.0
C(20)-C(15)-C(16)	119.7(11)	C(26)-C(25)-H(25)	119.0
C(20)-C(15)-C(1)	116.8(10)	C(27)-C(26)-C(25)	117.8(12)
C(16)-C(15)-C(1)	123.5(11)	C(27)-C(26)-H(26)	121.1
C(15)-C(16)-C(17)	118.2(12)	C(25)-C(26)-H(26)	121.1
C(15)-C(16)-H(16)	120.9	C(26)-C(27)-C(22)	121.5(11)
C(17)-C(16)-H(16)	120.9	C(26)-C(27)-C(28)	125.7(11)
C(18)-C(17)-C(16)	120.4(11)	C(22)-C(27)-C(28)	112.6(10)
C(18)-C(17)-H(17)	119.8	C(27)-C(28)-C(40)	105.7(10)
C(16)-C(17)-H(17)	119.8	C(27)-C(28)-C(29)	105.1(10)
C(17)-C(18)-C(19)	121.7(13)	C(40)-C(28)-C(29)	104.2(10)
C(17)-C(18)-H(18)	119.1	C(27)-C(28)-H(28)	113.6
C(19)-C(18)-H(18)	119.1	C(40)-C(28)-H(28)	113.6
C(20)-C(19)-C(18)	118.7(11)	C(29)-C(28)-H(28)	113.6
C(20)-C(19)-H(19)	120.7	C(30)-C(29)-C(34)	123.5(12)
C(18)-C(19)-H(19)	120.7	C(30)-C(29)-C(28)	122.6(11)
C(15)-C(20)-C(19)	121.1(10)	C(34)-C(29)-C(28)	113.8(11)

C(29)-C(30)-C(31)	117.6(11)	C(49)-N(1)-C(45)	110.5(9)
C(29)-C(30)-H(30)	121.2	C(41)-N(1)-C(45)	111.8(9)
C(31)-C(30)-H(30)	121.2	C(53)-N(1)-C(45)	105.1(8)
C(32)-C(31)-C(30)	119.3(11)	N(1)-C(41)-C(42)	114.3(10)
C(32)-C(31)-H(31)	120.4	N(1)-C(41)-H(41A)	108.7
C(30)-C(31)-H(31)	120.4	C(42)-C(41)-H(41A)	108.7
C(31)-C(32)-C(33)	119.5(12)	N(1)-C(41)-H(41B)	108.7
C(31)-C(32)-H(32)	120.2	C(42)-C(41)-H(41B)	108.7
C(33)-C(32)-H(32)	120.2	H(41A)-C(41)-H(41B)	107.6
C(34)-C(33)-C(32)	121.6(12)	C(43)-C(42)-C(41)	110.6(10)
C(34)-C(33)-H(33)	119.2	C(43)-C(42)-H(42A)	109.5
C(32)-C(33)-H(33)	119.2	C(41)-C(42)-H(42A)	109.5
C(33)-C(34)-C(29)	118.5(12)	C(43)-C(42)-H(42B)	109.5
C(33)-C(34)-C(21)	126.3(11)	C(41)-C(42)-H(42B)	109.5
C(29)-C(34)-C(21)	115.2(11)	H(42A)-C(42)-H(42B)	108.1
C(36)-C(35)-C(40)	117.3(11)	C(42)-C(43)-C(44)	113.8(11)
C(36)-C(35)-C(21)	127.4(11)	C(42)-C(43)-H(43A)	108.8
C(40)-C(35)-C(21)	115.3(11)	C(44)-C(43)-H(43A)	108.8
C(37)-C(36)-C(35)	121.8(12)	C(42)-C(43)-H(43B)	108.8
C(37)-C(36)-H(36)	119.1	C(44)-C(43)-H(43B)	108.8
C(35)-C(36)-H(36)	119.1	H(43A)-C(43)-H(43B)	107.7
C(36)-C(37)-C(38)	120.6(12)	C(43)-C(44)-H(44A)	109.5
C(36)-C(37)-H(37)	119.7	C(43)-C(44)-H(44B)	109.5
C(38)-C(37)-H(37)	119.7	H(44A)-C(44)-H(44B)	109.5
C(39)-C(38)-C(37)	118.4(11)	C(43)-C(44)-H(44C)	109.5
C(39)-C(38)-H(38)	120.8	H(44A)-C(44)-H(44C)	109.5
C(37)-C(38)-H(38)	120.8	H(44B)-C(44)-H(44C)	109.5
C(40)-C(39)-C(38)	118.3(12)	C(46)-C(45)-N(1)	111.5(9)
C(40)-C(39)-H(39)	120.9	C(46)-C(45)-H(45A)	109.3
C(38)-C(39)-H(39)	120.9	N(1)-C(45)-H(45A)	109.3
C(39)-C(40)-C(35)	123.4(12)	C(46)-C(45)-H(45B)	109.3
C(39)-C(40)-C(28)	123.9(11)	N(1)-C(45)-H(45B)	109.3
C(35)-C(40)-C(28)	112.5(10)	H(45A)-C(45)-H(45B)	108.0
C(49)-N(1)-C(41)	108.8(9)	C(45)-C(46)-C(47)	110.6(10)
C(49)-N(1)-C(53)	109.8(10)	C(45)-C(46)-H(46A)	109.5
C(41)-N(1)-C(53)	110.8(9)	C(47)-C(46)-H(46A)	109.5

C(45)-C(46)-H(46B)	109.5	C(51)-C(52)-H(52C)	109.5
C(47)-C(46)-H(46B)	109.5	H(52A)-C(52)-H(52C)	109.5
H(46A)-C(46)-H(46B)	108.1	H(52B)-C(52)-H(52C)	109.5
C(48)-C(47)-C(46)	111.4(11)	C(54)-C(53)-N(1)	114.1(9)
C(48)-C(47)-H(47A)	109.3	C(54)-C(53)-H(53A)	108.7
C(46)-C(47)-H(47A)	109.3	N(1)-C(53)-H(53A)	108.7
C(48)-C(47)-H(47B)	109.3	C(54)-C(53)-H(53B)	108.7
C(46)-C(47)-H(47B)	109.3	N(1)-C(53)-H(53B)	108.7
H(47A)-C(47)-H(47B)	108.0	H(53A)-C(53)-H(53B)	107.6
C(47)-C(48)-H(48A)	109.5	C(53)-C(54)-C(55)	111.8(9)
C(47)-C(48)-H(48B)	109.5	C(53)-C(54)-H(54A)	109.3
H(48A)-C(48)-H(48B)	109.5	C(55)-C(54)-H(54A)	109.3
C(47)-C(48)-H(48C)	109.5	C(53)-C(54)-H(54B)	109.3
H(48A)-C(48)-H(48C)	109.5	C(55)-C(54)-H(54B)	109.3
H(48B)-C(48)-H(48C)	109.5	H(54A)-C(54)-H(54B)	107.9
N(1)-C(49)-C(50)	118.9(10)	C(56)-C(55)-C(54)	112.6(10)
N(1)-C(49)-H(49A)	107.6	C(56)-C(55)-H(55A)	109.1
C(50)-C(49)-H(49A)	107.6	C(54)-C(55)-H(55A)	109.1
N(1)-C(49)-H(49B)	107.6	C(56)-C(55)-H(55B)	109.1
C(50)-C(49)-H(49B)	107.6	C(54)-C(55)-H(55B)	109.1
H(49A)-C(49)-H(49B)	107.0	H(55A)-C(55)-H(55B)	107.8
C(49)-C(50)-C(51)	111.8(10)	C(55)-C(56)-H(56A)	109.5
C(49)-C(50)-H(50A)	109.3	C(55)-C(56)-H(56B)	109.5
C(51)-C(50)-H(50A)	109.3	H(56A)-C(56)-H(56B)	109.5
C(49)-C(50)-H(50B)	109.3	C(55)-C(56)-H(56C)	109.5
C(51)-C(50)-H(50B)	109.3	H(56A)-C(56)-H(56C)	109.5
H(50A)-C(50)-H(50B)	107.9	H(56B)-C(56)-H(56C)	109.5
C(50)-C(51)-C(52)	113.5(11)	C(69)-N(2)-C(65)	111.9(9)
C(50)-C(51)-H(51A)	108.9	C(69)-N(2)-C(57)	111.5(9)
C(52)-C(51)-H(51A)	108.9	C(65)-N(2)-C(57)	106.2(8)
C(50)-C(51)-H(51B)	108.9	C(69)-N(2)-C(61)	106.1(8)
C(52)-C(51)-H(51B)	108.9	C(65)-N(2)-C(61)	110.8(8)
H(51A)-C(51)-H(51B)	107.7	C(57)-N(2)-C(61)	110.4(9)
C(51)-C(52)-H(52A)	109.5	N(2)-C(57)-C(58)	116.9(9)
C(51)-C(52)-H(52B)	109.5	N(2)-C(57)-H(57A)	108.1
H(52A)-C(52)-H(52B)	109.5	C(58)-C(57)-H(57A)	108.1

N(2)-C(57)-H(57B)	108.1	C(64)-C(63)-H(63B)	109.0
C(58)-C(57)-H(57B)	108.1	C(62)-C(63)-H(63B)	109.0
H(57A)-C(57)-H(57B)	107.3	H(63A)-C(63)-H(63B)	107.8
C(59)-C(58)-C(57)	110.5(10)	C(63)-C(64)-H(64A)	109.5
C(59)-C(58)-H(58A)	109.5	C(63)-C(64)-H(64B)	109.5
C(57)-C(58)-H(58A)	109.5	H(64A)-C(64)-H(64B)	109.5
C(59)-C(58)-H(58B)	109.5	C(63)-C(64)-H(64C)	109.5
C(57)-C(58)-H(58B)	109.5	H(64A)-C(64)-H(64C)	109.5
H(58A)-C(58)-H(58B)	108.1	H(64B)-C(64)-H(64C)	109.5
C(58)-C(59)-C(60)	113.1(10)	N(2)-C(65)-C(66)	116.1(9)
C(58)-C(59)-H(59A)	109.0	N(2)-C(65)-H(65A)	108.3
C(60)-C(59)-H(59A)	109.0	C(66)-C(65)-H(65A)	108.3
C(58)-C(59)-H(59B)	109.0	N(2)-C(65)-H(65B)	108.3
C(60)-C(59)-H(59B)	109.0	C(66)-C(65)-H(65B)	108.3
H(59A)-C(59)-H(59B)	107.8	H(65A)-C(65)-H(65B)	107.4
C(59)-C(60)-H(60A)	109.5	C(67)-C(66)-C(65)	110.6(10)
C(59)-C(60)-H(60B)	109.5	C(67)-C(66)-H(66A)	109.5
H(60A)-C(60)-H(60B)	109.5	C(65)-C(66)-H(66A)	109.5
C(59)-C(60)-H(60C)	109.5	C(67)-C(66)-H(66B)	109.5
H(60A)-C(60)-H(60C)	109.5	C(65)-C(66)-H(66B)	109.5
H(60B)-C(60)-H(60C)	109.5	H(66A)-C(66)-H(66B)	108.1
C(62)-C(61)-N(2)	116.1(9)	C(66)-C(67)-C(68)	113.0(12)
C(62)-C(61)-H(61A)	108.3	C(66)-C(67)-H(67A)	109.0
N(2)-C(61)-H(61A)	108.3	C(68)-C(67)-H(67A)	109.0
C(62)-C(61)-H(61B)	108.3	C(66)-C(67)-H(67B)	109.0
N(2)-C(61)-H(61B)	108.3	C(68)-C(67)-H(67B)	109.0
H(61A)-C(61)-H(61B)	107.4	H(67A)-C(67)-H(67B)	107.8
C(61)-C(62)-C(63)	108.9(10)	C(67)-C(68)-H(68A)	109.5
C(61)-C(62)-H(62A)	109.9	C(67)-C(68)-H(68B)	109.5
C(63)-C(62)-H(62A)	109.9	H(68A)-C(68)-H(68B)	109.5
C(61)-C(62)-H(62B)	109.9	C(67)-C(68)-H(68C)	109.5
C(63)-C(62)-H(62B)	109.9	H(68A)-C(68)-H(68C)	109.5
H(62A)-C(62)-H(62B)	108.3	H(68B)-C(68)-H(68C)	109.5
C(64)-C(63)-C(62)	112.9(11)	N(2)-C(69)-C(70)	117.6(9)
C(64)-C(63)-H(63A)	109.0	N(2)-C(69)-H(69A)	107.9
C(62)-C(63)-H(63A)	109.0	C(70)-C(69)-H(69A)	107.9

N(2)-C(69)-H(69B)	107.9	C(72)-C(71)-H(71A)	108.9
C(70)-C(69)-H(69B)	107.9	C(70)-C(71)-H(71B)	108.9
H(69A)-C(69)-H(69B)	107.2	C(72)-C(71)-H(71B)	108.9
C(71)-C(70)-C(69)	110.9(10)	H(71A)-C(71)-H(71B)	107.7
C(71)-C(70)-H(70A)	109.4	C(71)-C(72)-H(72A)	109.5
C(69)-C(70)-H(70A)	109.4	C(71)-C(72)-H(72B)	109.5
C(71)-C(70)-H(70B)	109.4	H(72A)-C(72)-H(72B)	109.5
C(69)-C(70)-H(70B)	109.4	C(71)-C(72)-H(72C)	109.5
H(70A)-C(70)-H(70B)	108.0	H(72A)-C(72)-H(72C)	109.5
C(70)-C(71)-C(72)	113.2(10)	H(72B)-C(72)-H(72C)	109.5
C(70)-C(71)-H(71A)	108.9		

Table 4. Anisotropic displacement parameters ($Å^2 x\ 10^3$) for jpd466_1m. The anisotropic
displacement factor exponent takes the form: $-2p^2[\ h^2\ a^{*2}U^{11} + ... + 2\ h\ k\ a^*\ b^*\ U^{12}\ ]$

	U^{11}	U^{22}	U^{33}	U^{23}	U^{13}	U^{12}
Cu(1)	32(1)	50(1)	28(1)	4(1)	1(1)	1(1)
Cl(1)	16(1)	43(2)	20(1)	3(1)	4(1)	-4(1)
C(1)	34(8)	48(8)	39(7)	0(5)	-4(6)	-4(6)
C(2)	43(8)	54(8)	13(5)	5(5)	-1(5)	4(6)
C(3)	34(8)	69(10)	30(7)	4(6)	-12(6)	3(6)
C(4)	57(10)	69(10)	31(7)	-11(6)	-27(7)	12(8)
C(5)	42(8)	69(10)	20(6)	-5(6)	-8(6)	13(7)
C(6)	45(8)	62(9)	20(6)	1(5)	-7(5)	7(6)
C(7)	34(8)	66(9)	20(6)	-2(5)	-10(5)	19(6)
C(8)	19(6)	54(8)	33(6)	0(5)	-1(5)	5(5)
C(9)	22(7)	44(8)	41(7)	-12(5)	-3(5)	12(5)
C(10)	17(6)	60(8)	24(6)	0(5)	-5(5)	-1(5)
C(11)	32(7)	40(7)	27(6)	1(5)	-10(5)	6(5)
C(12)	28(7)	54(8)	30(6)	-5(5)	-9(5)	9(6)
C(13)	28(7)	62(8)	15(6)	-1(5)	-1(5)	-1(6)
C(14)	27(7)	47(7)	19(5)	-10(5)	-9(5)	19(5)
C(15)	32(7)	44(7)	28(6)	-3(5)	-7(5)	2(5)
C(16)	30(7)	58(8)	26(6)	4(5)	-4(5)	6(6)
C(17)	54(9)	57(9)	23(6)	-4(5)	-15(6)	11(7)
C(18)	35(8)	76(10)	20(6)	-7(6)	-3(5)	-6(7)
C(19)	37(7)	33(7)	31(7)	3(5)	0(5)	-1(5)
C(20)	25(6)	44(7)	15(5)	3(4)	6(4)	1(5)
Cu(2)	35(1)	55(1)	26(1)	-3(1)	5(1)	0(1)
Cl(2)	26(2)	40(2)	21(1)	-2(1)	10(1)	-2(1)
C(21)	31(7)	51(8)	19(5)	1(5)	-4(5)	4(6)
C(22)	36(8)	58(9)	30(6)	-2(6)	-10(5)	4(6)
C(23)	41(8)	48(8)	41(7)	-6(6)	-10(6)	7(6)
C(24)	46(9)	37(8)	49(8)	1(6)	-12(6)	7(6)
C(25)	30(7)	69(10)	51(8)	0(7)	-11(7)	-2(6)
C(26)	38(8)	66(10)	32(7)	-7(6)	1(6)	-9(6)

C(27)	28(7)	46(7)	37(7)	-14(6)	1(6)	0(6)
C(28)	29(7)	73(10)	35(7)	7(6)	0(6)	15(7)
C(29)	40(8)	43(8)	44(7)	-11(6)	4(6)	-8(6)
C(30)	37(8)	55(8)	30(7)	1(6)	3(5)	8(6)
C(31)	56(9)	35(7)	26(6)	1(5)	-13(6)	-13(6)
C(32)	37(8)	43(8)	38(7)	-6(5)	-11(6)	12(6)
C(33)	46(9)	67(10)	27(7)	-6(6)	9(6)	-26(7)
C(34)	36(7)	36(7)	29(6)	-5(5)	4(5)	4(6)
C(35)	29(7)	70(10)	22(6)	-6(6)	-5(5)	10(6)
C(36)	41(8)	42(8)	26(6)	-3(5)	-7(6)	8(6)
C(37)	45(9)	41(8)	47(8)	-3(6)	-8(6)	-9(6)
C(38)	36(8)	63(9)	29(6)	-11(5)	-8(6)	11(7)
C(39)	42(8)	47(8)	30(6)	-4(5)	4(6)	7(6)
C(40)	25(7)	42(7)	40(7)	-6(5)	-6(5)	4(6)
N(1)	27(6)	54(7)	21(5)	-3(4)	4(4)	-1(5)
C(41)	47(8)	70(10)	22(6)	-1(6)	12(6)	0(7)
C(42)	43(8)	35(7)	31(6)	0(5)	4(5)	4(6)
C(43)	45(9)	63(9)	26(6)	5(6)	0(6)	10(7)
C(44)	65(12)	141(17)	35(8)	20(9)	-4(8)	-22(11)
C(45)	34(7)	41(7)	30(6)	2(5)	0(6)	-13(5)
C(46)	36(7)	49(8)	38(6)	-6(6)	6(6)	-1(6)
C(47)	47(9)	70(9)	33(7)	-1(6)	5(6)	0(7)
C(48)	44(9)	64(10)	53(9)	7(7)	-7(7)	6(7)
C(49)	53(8)	32(7)	28(6)	6(5)	12(6)	13(6)
C(50)	35(8)	47(8)	26(6)	0(5)	0(5)	4(6)
C(51)	59(9)	53(9)	26(6)	-3(6)	-1(6)	-18(7)
C(52)	35(8)	72(10)	32(7)	3(6)	4(6)	3(7)
C(53)	10(6)	61(8)	42(7)	-7(6)	4(5)	-3(5)
C(54)	33(7)	61(9)	27(6)	-6(6)	-1(5)	5(6)
C(55)	33(7)	23(6)	40(6)	6(5)	-3(6)	-1(5)
C(56)	48(9)	70(10)	67(11)	0(8)	1(8)	1(8)
N(2)	31(6)	43(6)	27(5)	-3(4)	-3(5)	0(4)
C(57)	27(7)	54(8)	26(5)	-12(6)	3(5)	-8(5)
C(58)	39(8)	57(8)	24(6)	4(5)	1(5)	1(6)
C(59)	25(7)	54(8)	40(7)	-5(6)	2(5)	5(6)
C(60)	40(8)	53(9)	40(7)	-2(6)	12(6)	17(6)

C(61)	23(7)	45(8)	33(7)	-9(5)	-15(5)	5(5)
C(62)	31(7)	54(8)	37(7)	-1(6)	-8(6)	2(6)
C(63)	32(7)	70(9)	25(6)	0(6)	9(5)	-1(6)
C(64)	42(9)	54(9)	52(8)	-1(6)	-11(7)	-2(6)
C(65)	20(7)	54(8)	33(6)	1(5)	-8(5)	-9(6)
C(66)	25(7)	50(8)	39(7)	3(6)	8(5)	-3(6)
C(67)	36(8)	67(10)	59(9)	-3(7)	7(7)	6(7)
C(68)	35(9)	124(14)	43(8)	-11(8)	20(7)	-18(9)
C(69)	37(7)	40(7)	28(6)	-2(5)	1(5)	-3(5)
C(70)	43(8)	47(8)	23(6)	-2(5)	6(5)	4(6)
C(71)	48(8)	36(7)	32(6)	3(5)	-9(6)	-7(6)
C(72)	48(9)	59(9)	29(7)	3(6)	-3(6)	1(7)

Chapter 2: Crystal Information

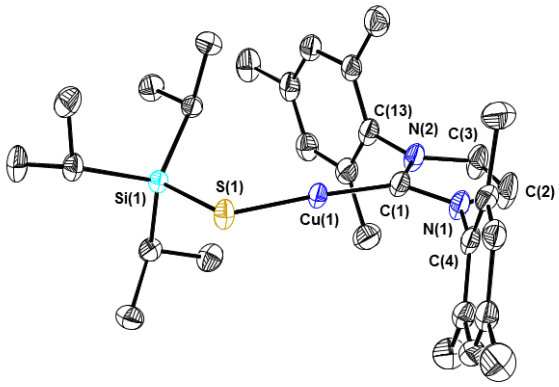

Structure Determination Summary
Crystal Data and Structure Refinement for [(IMes)Cu(SSi^{i}Pr$_3$)]

Identification code	jpd485_0m	
Empirical formula	$C_{30}H_{45}CuN_2SSi$	
Formula weight	557.37	
Temperature	150(2) K	
Wavelength	0.71073 Å	
Crystal system	monoclinic	
Space group	$P2_1/c$	
Unit cell dimensions	a = 19.4065(18) Å	α = 90°
	b = 10.8938(10) Å	β = 104.8340(10)°
	c = 15.2754(14) Å	γ = 90°
Volume, Z	3121.7(5) Å^3, 4	
Density (calculated)	1.186 g/cm^3	
Absorption coefficient	0.824 mm^{-1}	
F(000)	1192	
Crystal size	0.40 x 0.27 x 0.25 mm	
θ range for data collection	2.16 to 29.29°	
Limiting indices	$-26 < h < 26$, $-14 < k < 14$, $-20 < l < 20$	
Reflections collected	52949	
Independent reflections	8116 (R_{int} = 0.0465)	
Completeness to θ = 25.00°	100.0 %	
Absorption correction	Semi-empirical from equivalents	
Max. and min. transmission	0.8210 and 0.7360	
Refinement method	Full-matrix least-squares on F^2	
Data / restraints / parameters	8116 / 0 / 328	
Goodness-of-fit on F^2	1.048	
Final R indices [I>2σ(I)]	R1 = 0.0314, wR2 = 0.0823	
R indices (all data)	R1 = 0.0372, wR2 = 0.0884	
Largest diff. peak and hole	0.513 and -0.523 e·Å^{-3}	

Table S1. Atomic coordinates (x 10^4) and equivalent isotropic displacement parameters ($Å^2$ x 10^3) for [(IMes)Cu(SSi^{i}Pr$_3$)]. U(eq) is defined as one third of the trace of the orthogonalized U_{ij} tensor.

Atom	x	y	z	U(eq)
Cu(1)	1911(1)	1285(1)	26(1)	20(1)
S(1)	2015(1)	-147(1)	-885(1)	23(1)
Si(1)	3010(1)	-942(1)	-228(1)	17(1)
N(1)	1116(1)	3218(1)	631(1)	28(1)
N(2)	2148(1)	3034(1)	1551(1)	29(1)
C(1)	1732(1)	2564(1)	768(1)	25(1)
C(2)	1149(1)	4070(2)	1316(1)	39(1)
C(3)	1795(1)	3957(2)	1897(1)	39(1)
C(4)	515(1)	3029(1)	-138(1)	25(1)
C(5)	5(1)	2151(1)	-75(1)	26(1)
C(6)	-554(1)	1954(1)	-845(1)	27(1)
C(7)	-603(1)	2588(1)	-1649(1)	26(1)
C(8)	-88(1)	3468(1)	-1675(1)	26(1)
C(9)	474(1)	3718(1)	-918(1)	27(1)
C(10)	53(1)	1440(2)	784(1)	39(1)
C(11)	-1212(1)	2364(2)	-2472(1)	36(1)
C(12)	1002(1)	4725(2)	-940(1)	43(1)
C(13)	2858(1)	2602(1)	1982(1)	27(1)
C(14)	2939(1)	1719(2)	2657(1)	31(1)
C(15)	3628(1)	1312(1)	3064(1)	32(1)
C(16)	4219(1)	1774(1)	2814(1)	31(1)
C(17)	4114(1)	2659(1)	2143(1)	30(1)
C(18)	3435(1)	3096(1)	1709(1)	27(1)
C(19)	2308(1)	1224(2)	2953(1)	43(1)
C(20)	4957(1)	1300(2)	3267(1)	42(1)
C(21)	3334(1)	4056(2)	980(1)	36(1)
C(22)	3668(1)	277(1)	352(1)	22(1)
C(23)	3781(1)	1329(1)	-261(1)	31(1)
C(24)	4384(1)	-253(2)	887(1)	32(1)
C(25)	3300(1)	-1867(1)	-1134(1)	23(1)
C(26)	3494(1)	-1075(2)	-1864(1)	32(1)
C(27)	3895(1)	-2812(2)	-774(1)	36(1)
C(28)	2886(1)	-2054(1)	676(1)	24(1)
C(29)	2300(1)	-3003(1)	284(1)	34(1)
C(30)	2719(1)	-1374(2)	1481(1)	32(1)

Table S2. Bond lengths (Å) for [(IMes)Cu(SSi^{i}Pr$_3$)]. Symmetry transformations used to generate equivalent atoms:

Cu(1)-C(1)	1.8830(13)	C(17)-C(18)	1.398(2)
Cu(1)-S(1)	2.1336(4)	C(17)-H(17)	0.9300
S(1)-Si(1)	2.1207(5)	C(18)-C(21)	1.503(2)
Si(1)-C(22)	1.8975(13)	C(19)-H(19A)	0.9600
Si(1)-C(28)	1.8983(14)	C(19)-H(19B)	0.9600
Si(1)-C(25)	1.9079(13)	C(19)-H(19C)	0.9600
N(1)-C(1)	1.3615(17)	C(20)-H(20A)	0.9600
N(1)-C(2)	1.3878(19)	C(20)-H(20B)	0.9600
N(1)-C(4)	1.4421(17)	C(20)-H(20C)	0.9600
N(2)-C(1)	1.3605(17)	C(21)-H(21A)	0.9600
N(2)-C(3)	1.3935(18)	C(21)-H(21B)	0.9600
N(2)-C(13)	1.4450(17)	C(21)-H(21C)	0.9600
C(2)-C(3)	1.344(2)	C(22)-C(23)	1.531(2)
C(2)-H(2)	0.9300	C(22)-C(24)	1.5338(19)
C(3)-H(3)	0.9300	C(22)-H(22)	0.9800
C(4)-C(9)	1.393(2)	C(23)-H(23A)	0.9600
C(4)-C(5)	1.398(2)	C(23)-H(23B)	0.9600
C(5)-C(6)	1.3977(19)	C(23)-H(23C)	0.9600
C(5)-C(10)	1.506(2)	C(24)-H(24A)	0.9600
C(6)-C(7)	1.391(2)	C(24)-H(24B)	0.9600
C(6)-H(6)	0.9300	C(24)-H(24C)	0.9600
C(7)-C(8)	1.391(2)	C(25)-C(26)	1.532(2)
C(7)-C(11)	1.509(2)	C(25)-C(27)	1.5385(19)
C(8)-C(9)	1.398(2)	C(25)-H(25)	0.9800
C(8)-H(8)	0.9300	C(26)-H(26A)	0.9600
C(9)-C(12)	1.507(2)	C(26)-H(26B)	0.9600
C(10)-H(10A)	0.9600	C(26)-H(26C)	0.9600
C(10)-H(10B)	0.9600	C(27)-H(27A)	0.9600
C(10)-H(10C)	0.9600	C(27)-H(27B)	0.9600
C(11)-H(11A)	0.9600	C(27)-H(27C)	0.9600
C(11)-H(11B)	0.9600	C(28)-C(30)	1.539(2)
C(11)-H(11C)	0.9600	C(28)-C(29)	1.540(2)
C(12)-H(12A)	0.9600	C(28)-H(28)	0.9800
C(12)-H(12B)	0.9600	C(29)-H(29A)	0.9600
C(12)-H(12C)	0.9600	C(29)-H(29B)	0.9600
C(13)-C(14)	1.390(2)	C(29)-H(29C)	0.9600
C(13)-C(18)	1.399(2)	C(30)-H(30A)	0.9600
C(14)-C(15)	1.393(2)	C(30)-H(30B)	0.9600
C(14)-C(19)	1.509(2)	C(30)-H(30C)	0.9600
C(15)-C(16)	1.394(2)		
C(15)-H(15)	0.9300		
C(16)-C(17)	1.384(2)		
C(16)-C(20)	1.513(2)		

Table S3. Bond angles (deg.) for [(IMes)Cu(SSi^{i}Pr$_3$)]. Symmetry transformations used to generate equivalent atoms:

C(1)-Cu(1)-S(1)	174.77(4)	H(10A)-C(10)-H(10B)	109.5
Si(1)-S(1)-Cu(1)	102.556(17)	C(5)-C(10)-H(10C)	109.5
C(22)-Si(1)-C(28)	107.58(6)	H(10A)-C(10)-H(10C)	109.5
C(22)-Si(1)-C(25)	114.89(6)	H(10B)-C(10)-H(10C)	109.5
C(28)-Si(1)-C(25)	107.84(6)	C(7)-C(11)-H(11A)	109.5
C(22)-Si(1)-S(1)	110.92(4)	C(7)-C(11)-H(11B)	109.5
C(28)-Si(1)-S(1)	109.55(4)	H(11A)-C(11)-H(11B)	109.5
C(25)-Si(1)-S(1)	105.96(4)	C(7)-C(11)-H(11C)	109.5
C(1)-N(1)-C(2)	111.44(12)	H(11A)-C(11)-H(11C)	109.5
C(1)-N(1)-C(4)	123.02(11)	H(11B)-C(11)-H(11C)	109.5
C(2)-N(1)-C(4)	125.53(12)	C(9)-C(12)-H(12A)	109.5
C(1)-N(2)-C(3)	111.52(12)	C(9)-C(12)-H(12B)	109.5
C(1)-N(2)-C(13)	124.01(11)	H(12A)-C(12)-H(12B)	109.5
C(3)-N(2)-C(13)	124.45(12)	C(9)-C(12)-H(12C)	109.5
N(2)-C(1)-N(1)	103.72(11)	H(12A)-C(12)-H(12C)	109.5
N(2)-C(1)-Cu(1)	130.45(10)	H(12B)-C(12)-H(12C)	109.5
N(1)-C(1)-Cu(1)	125.81(10)	C(14)-C(13)-C(18)	122.68(13)
C(3)-C(2)-N(1)	106.93(13)	C(14)-C(13)-N(2)	118.50(13)
C(3)-C(2)-H(2)	126.5	C(18)-C(13)-N(2)	118.82(14)
N(1)-C(2)-H(2)	126.5	C(13)-C(14)-C(15)	117.72(14)
C(2)-C(3)-N(2)	106.38(13)	C(13)-C(14)-C(19)	121.49(15)
C(2)-C(3)-H(3)	126.8	C(15)-C(14)-C(19)	120.78(16)
N(2)-C(3)-H(3)	126.8	C(14)-C(15)-C(16)	121.77(15)
C(9)-C(4)-C(5)	122.73(13)	C(14)-C(15)-H(15)	119.1
C(9)-C(4)-N(1)	118.59(13)	C(16)-C(15)-H(15)	119.1
C(5)-C(4)-N(1)	118.67(13)	C(17)-C(16)-C(15)	118.56(14)
C(6)-C(5)-C(4)	117.29(13)	C(17)-C(16)-C(20)	121.33(15)
C(6)-C(5)-C(10)	121.01(14)	C(15)-C(16)-C(20)	120.11(16)
C(4)-C(5)-C(10)	121.70(13)	C(16)-C(17)-C(18)	122.12(14)
C(7)-C(6)-C(5)	121.92(13)	C(16)-C(17)-H(17)	118.9
C(7)-C(6)-H(6)	119.0	C(18)-C(17)-H(17)	118.9
C(5)-C(6)-H(6)	119.0	C(17)-C(18)-C(13)	117.15(14)
C(6)-C(7)-C(8)	118.74(13)	C(17)-C(18)-C(21)	121.07(14)
C(6)-C(7)-C(11)	121.10(14)	C(13)-C(18)-C(21)	121.78(13)
C(8)-C(7)-C(11)	120.14(14)	C(14)-C(19)-H(19A)	109.5
C(7)-C(8)-C(9)	121.58(14)	C(14)-C(19)-H(19B)	109.5
C(7)-C(8)-H(8)	119.2	H(19A)-C(19)-H(19B)	109.5
C(9)-C(8)-H(8)	119.2	C(14)-C(19)-H(19C)	109.5
C(4)-C(9)-C(8)	117.68(13)	H(19A)-C(19)-H(19C)	109.5
C(4)-C(9)-C(12)	121.34(15)	H(19B)-C(19)-H(19C)	109.5
C(8)-C(9)-C(12)	120.96(15)	C(16)-C(20)-H(20A)	109.5
C(5)-C(10)-H(10A)	109.5	C(16)-C(20)-H(20B)	109.5
C(5)-C(10)-H(10B)	109.5	H(20A)-C(20)-H(20B)	109.5

Table S3. Bond angles (deg.) for [(IMes)Cu(SSi^{i}Pr$_3$)]. Symmetry transformations used to generate equivalent atoms:

C(16)-C(20)-H(20C)	109.5	H(27A)-C(27)-H(27C)	109.5
H(20A)-C(20)-H(20C)	109.5	H(27B)-C(27)-H(27C)	109.5
H(20B)-C(20)-H(20C)	109.5	C(30)-C(28)-C(29)	110.35(12)
C(18)-C(21)-H(21A)	109.5	C(30)-C(28)-Si(1)	111.49(10)
C(18)-C(21)-H(21B)	109.5	C(29)-C(28)-Si(1)	111.31(10)
H(21A)-C(21)-H(21B)	109.5	C(30)-C(28)-H(28)	107.8
C(18)-C(21)-H(21C)	109.5	C(29)-C(28)-H(28)	107.8
H(21A)-C(21)-H(21C)	109.5	Si(1)-C(28)-H(28)	107.8
H(21B)-C(21)-H(21C)	109.5	C(28)-C(29)-H(29A)	109.5
C(23)-C(22)-C(24)	110.81(12)	C(28)-C(29)-H(29B)	109.5
C(23)-C(22)-Si(1)	115.02(10)	H(29A)-C(29)-H(29B)	109.5
C(24)-C(22)-Si(1)	113.23(10)	C(28)-C(29)-H(29C)	109.5
C(23)-C(22)-H(22)	105.6	H(29A)-C(29)-H(29C)	109.5
C(24)-C(22)-H(22)	105.6	H(29B)-C(29)-H(29C)	109.5
Si(1)-C(22)-H(22)	105.6	C(28)-C(30)-H(30A)	109.5
C(22)-C(23)-H(23A)	109.5	C(28)-C(30)-H(30B)	109.5
C(22)-C(23)-H(23B)	109.5	H(30A)-C(30)-H(30B)	109.5
H(23A)-C(23)-H(23B)	109.5	C(28)-C(30)-H(30C)	109.5
C(22)-C(23)-H(23C)	109.5	H(30A)-C(30)-H(30C)	109.5
H(23A)-C(23)-H(23C)	109.5	H(30B)-C(30)-H(30C)	109.5
H(23B)-C(23)-H(23C)	109.5		
C(22)-C(24)-H(24A)	109.5		
C(22)-C(24)-H(24B)	109.5		
H(24A)-C(24)-H(24B)	109.5		
C(22)-C(24)-H(24C)	109.5		
H(24A)-C(24)-H(24C)	109.5		
H(24B)-C(24)-H(24C)	109.5		
C(26)-C(25)-C(27)	109.58(12)		
C(26)-C(25)-Si(1)	113.77(10)		
C(27)-C(25)-Si(1)	115.31(10)		
C(26)-C(25)-H(25)	105.8		
C(27)-C(25)-H(25)	105.8		
Si(1)-C(25)-H(25)	105.8		
C(25)-C(26)-H(26A)	109.5		
C(25)-C(26)-H(26B)	109.5		
H(26A)-C(26)-H(26B)	109.5		
C(25)-C(26)-H(26C)	109.5		
H(26A)-C(26)-H(26C)	109.5		
H(26B)-C(26)-H(26C)	109.5		
C(25)-C(27)-H(27A)	109.5		
C(25)-C(27)-H(27B)	109.5		
H(27A)-C(27)-H(27B)	109.5		
C(25)-C(27)-H(27C)	109.5		

Table S4. Anisotropic displacement parameters [$Å^2$ x 10^3] for [(IMes)Cu(SSi^{i}Pr$_3$)]. The anisotropic displacement factor exponent takes the form: $-2\pi^2[(ha^*)^2U_{11} + ... + 2hka^*b^*U_{12}]$.

Atom	U_{11}	U_{22}	U_{33}	U_{23}	U_{13}	U_{12}
Cu(1)	16(1)	22(1)	21(1)	-5(1)	4(1)	3(1)
S(1)	21(1)	26(1)	20(1)	-5(1)	0(1)	6(1)
Si(1)	17(1)	19(1)	16(1)	-1(1)	3(1)	1(1)
N(1)	18(1)	32(1)	33(1)	-13(1)	5(1)	3(1)
N(2)	19(1)	34(1)	33(1)	-14(1)	4(1)	2(1)
C(1)	18(1)	28(1)	28(1)	-8(1)	5(1)	2(1)
C(2)	25(1)	44(1)	46(1)	-25(1)	5(1)	8(1)
C(3)	27(1)	44(1)	44(1)	-27(1)	6(1)	5(1)
C(4)	16(1)	28(1)	29(1)	-7(1)	5(1)	5(1)
C(5)	21(1)	28(1)	28(1)	0(1)	5(1)	3(1)
C(6)	21(1)	27(1)	32(1)	1(1)	5(1)	-1(1)
C(7)	23(1)	26(1)	28(1)	-2(1)	5(1)	5(1)
C(8)	28(1)	25(1)	28(1)	1(1)	12(1)	5(1)
C(9)	22(1)	26(1)	36(1)	-6(1)	14(1)	0(1)
C(10)	36(1)	45(1)	32(1)	8(1)	3(1)	-2(1)
C(11)	33(1)	38(1)	32(1)	1(1)	-2(1)	1(1)
C(12)	37(1)	40(1)	57(1)	-6(1)	21(1)	-12(1)
C(13)	19(1)	30(1)	29(1)	-13(1)	2(1)	1(1)
C(14)	29(1)	33(1)	30(1)	-12(1)	8(1)	-3(1)
C(15)	34(1)	31(1)	28(1)	-7(1)	3(1)	2(1)
C(16)	25(1)	32(1)	31(1)	-13(1)	-2(1)	2(1)
C(17)	20(1)	32(1)	35(1)	-11(1)	4(1)	-2(1)
C(18)	23(1)	27(1)	30(1)	-9(1)	4(1)	0(1)
C(19)	38(1)	48(1)	47(1)	-6(1)	18(1)	-6(1)
C(20)	29(1)	47(1)	41(1)	-10(1)	-7(1)	8(1)
C(21)	31(1)	35(1)	40(1)	-2(1)	7(1)	3(1)
C(22)	19(1)	23(1)	23(1)	-4(1)	5(1)	-1(1)
C(23)	33(1)	25(1)	37(1)	-1(1)	12(1)	-6(1)
C(24)	20(1)	35(1)	37(1)	-4(1)	0(1)	-1(1)
C(25)	22(1)	26(1)	21(1)	-4(1)	4(1)	3(1)
C(26)	35(1)	40(1)	26(1)	-4(1)	14(1)	1(1)
C(27)	34(1)	37(1)	36(1)	-8(1)	6(1)	15(1)
C(28)	23(1)	25(1)	24(1)	4(1)	6(1)	2(1)
C(29)	33(1)	25(1)	45(1)	3(1)	13(1)	-5(1)
C(30)	36(1)	38(1)	25(1)	6(1)	13(1)	3(1)

Table S5. Hydrogen coordinates (x 10^4) and isotropic displacement parameters (Å^2 x 10^3) for [(IMes)Cu(SSi^{i}Pr$_3$)].

H atom	x	y	z	U(eq)
H(2)	792	4616	1364	47
H(3)	1972	4405	2424	47
H(6)	-904	1381	-819	32
H(8)	-119	3899	-2209	32
H(10A)	435	855	869	58
H(10B)	-388	1016	741	58
H(10C)	143	1995	1288	58
H(11A)	-1421	1578	-2419	55
H(11B)	-1037	2378	-3005	55
H(11C)	-1565	2994	-2513	55
H(12A)	954	4977	-1555	64
H(12B)	1477	4428	-687	64
H(12C)	911	5413	-592	64
H(15)	3694	717	3514	38
H(17)	4507	2972	1975	36
H(19A)	2124	1852	3271	65
H(19B)	2455	531	3345	65
H(19C)	1944	974	2430	65
H(20A)	5022	1287	3911	63
H(20B)	5308	1827	3120	63
H(20C)	5011	483	3057	63
H(21A)	3788	4262	878	54
H(21B)	3124	4776	1166	54
H(21C)	3026	3741	430	54
H(22)	3456	655	804	27
H(23A)	4071	1953	99	47
H(23B)	3328	1672	-569	47
H(23C)	4016	1022	-699	47
H(24A)	4617	-645	478	48
H(24B)	4304	-844	1317	48
H(24C)	4680	397	1202	48
H(25)	2881	-2344	-1446	28
H(26A)	3937	-662	-1611	48
H(26B)	3126	-478	-2081	48
H(26C)	3540	-1587	-2357	48
H(27A)	3971	-3289	-1269	54
H(27B)	3757	-3344	-347	54
H(27C)	4327	-2391	-481	54
H(28)	3335	-2500	903	29
H(29A)	2232	-3525	761	51

Table S5. Hydrogen coordinates (x 10^4) and isotropic displacement parameters ($Å^2$ x 10^3) for [(IMes)Cu(SSi^{i}Pr$_3$)].

H atom	x	y	z	U(eq)
H(29B)	2440	-3491	-165	51
H(29C)	1863	-2584	11	51
H(30A)	2313	-851	1264	48
H(30B)	3123	-886	1780	48
H(30C)	2617	-1961	1900	48

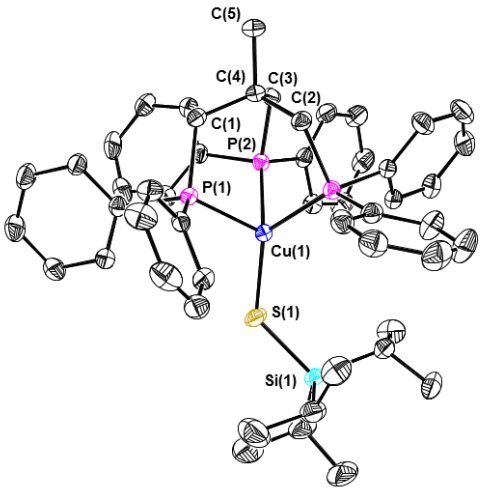

Structure Determination Summary

Crystal Data and Structure Refinement for [Cu(SSi^{i}Pr$_3$)((PPh$_2$CH$_2$CH$_2$)$_3$CCH$_3$)]

Identification code	jpd490_0m
Empirical formula	$C_{57}H_{68}CuP_3SSi$
Formula weight	969.71
Temperature	150(2) K
Wavelength	0.71073 Å
Crystal system	Monoclinic
Space group	$P2_1/n$
Unit cell dimensions	a = 14.5029(10) Å α = 90°
	b = 16.1500(11) Å β = 93.4550(10)°
	c = 22.0822(15) Å γ = 90°
Volume, Z	5162.7(6) Å^3, 4
Density (calculated)	1.248 g/cm^3
Absorption coefficient	0.616 mm^{-1}
F(000)	2056
Crystal size	0.29 x 0.24 x 0.22 mm
θ range for data collection	1.89 to 29.47°
Limiting indices	-19 < h < 19, -22 < k < 21, -30 < l < 30
Reflections collected	90914
Independent reflections	13576 (R_{int} = 0.0382)
Completeness to θ = 25.00°	100.0%
Absorption correction	Semi-empirical from equivalents
Max. and min. transmission	0.8738 and 0.8416
Refinement method	Full-matrix least-squares on F^2
Data / restraints / parameters	13576 / 0 / 576
Goodness-of-fit on F^2	1.010
Final R indices [I>2σ(I)]	R1 = 0.0321, wR2 = 0.0870
R indices (all data)	R1 = 0.0391, wR2 = 0.0923
Largest diff. peak and hole	0.624 and -0.400 e·Å^{-3}

Table S2. Atomic coordinates (x 10^4) and equivalent isotropic displacement parameters [$Å^2$ x 10^3) for [Cu(SSi^{i}Pr$_3$)((PPh$_2$CH$_2$CH$_2$)$_3$CCH$_3$)]. U(eq) is defined as one third of the trace of the orthogonalized U_{ij} tensor.

Atom	x	y	z	U(eq)
Cu(1)	3815(1)	2357(1)	3068(1)	20(1)
S(1)	4344(1)	3574(1)	2714(1)	39(1)
P(1)	3249(1)	1393(1)	2372(1)	20(1)
P(2)	2419(1)	2382(1)	3522(1)	19(1)
P(3)	4427(1)	1424(1)	3764(1)	21(1)
Si(1)	5684(1)	3964(1)	2996(1)	26(1)
C(1)	2520(1)	648(1)	2765(1)	24(1)
C(2)	2186(1)	1319(1)	3790(1)	22(1)
C(3)	3690(1)	489(1)	3681(1)	24(1)
C(4)	2659(1)	595(1)	3467(1)	21(1)
C(5)	2168(1)	-205(1)	3656(1)	28(1)
C(6)	2537(1)	1652(1)	1686(1)	22(1)
C(7)	1790(1)	1178(1)	1458(1)	28(1)
C(8)	1296(1)	1420(1)	929(1)	36(1)
C(9)	1545(1)	2121(1)	620(1)	36(1)
C(10)	2290(1)	2590(1)	839(1)	32(1)
C(11)	2780(1)	2359(1)	1373(1)	26(1)
C(12)	4152(1)	793(1)	2029(1)	21(1)
C(13)	4023(1)	9(1)	1779(1)	28(1)
C(14)	4729(1)	-380(1)	1493(1)	38(1)
C(15)	5577(1)	8(1)	1463(1)	38(1)
C(16)	5711(1)	792(1)	1700(1)	35(1)
C(17)	5003(1)	1186(1)	1981(1)	28(1)
C(18)	1405(1)	2637(1)	3019(1)	22(1)
C(19)	511(1)	2458(1)	3176(1)	29(1)
C(20)	-248(1)	2704(1)	2800(1)	36(1)
C(21)	-113(1)	3121(1)	2267(1)	38(1)
C(22)	771(1)	3301(1)	2106(1)	35(1)
C(23)	1529(1)	3069(1)	2484(1)	27(1)
C(24)	2198(1)	3045(1)	4166(1)	23(1)
C(25)	2543(1)	3851(1)	4137(1)	27(1)
C(26)	2408(1)	4412(1)	4599(1)	34(1)
C(27)	1942(1)	4168(1)	5098(1)	40(1)
C(28)	1609(1)	3370(1)	5134(1)	39(1)
C(29)	1725(1)	2808(1)	4668(1)	30(1)
C(30)	4280(1)	1773(1)	4540(1)	23(1)
C(31)	4230(1)	2622(1)	4640(1)	24(1)
C(32)	4112(1)	2936(1)	5215(1)	32(1)

C(33)	4048(1)	2402(1)	5698(1)	42(1)

Table S2. Atomic coordinates (x 10^4) and equivalent isotropic displacement parameters [$Å^2$ x 10^3) for [Cu(SSi^{i}Pr$_3$)((PPh$_2$CH$_2$CH$_2$)$_3$CCH$_3$)]. U(eq) is defined as one third of the trace of the orthogonalized U_{ij} tensor.

Atom	x	y	z	U(eq)
C(34)	4116(2)	1556(1)	5608(1)	48(1)
C(35)	4227(1)	1239(1)	5034(1)	37(1)
C(36)	5569(1)	931(1)	3838(1)	26(1)
C(37)	5854(1)	419(1)	3374(1)	30(1)
C(38)	6730(1)	66(1)	3412(1)	36(1)
C(39)	7329(1)	213(1)	3912(1)	44(1)
C(40)	7059(1)	720(1)	4370(1)	47(1)
C(41)	6188(1)	1080(1)	4335(1)	36(1)
C(42)	5723(1)	5111(1)	2779(1)	46(1)
C(43)	5464(2)	5275(1)	2117(1)	64(1)
C(44)	6618(2)	5564(1)	2980(1)	62(1)
C(45)	6638(1)	3351(1)	2644(1)	36(1)
C(46)	6504(2)	3275(2)	1952(1)	60(1)
C(47)	6752(1)	2484(1)	2924(1)	44(1)
C(48)	5907(1)	3880(1)	3849(1)	29(1)
C(49)	6918(1)	3982(1)	4086(1)	44(1)
C(50)	5298(1)	4471(1)	4193(1)	43(1)
C(51)	-703(1)	2770(1)	5084(1)	35(1)
C(52)	-938(1)	2469(1)	4507(1)	42(1)
C(53)	-795(2)	1652(1)	4364(1)	55(1)
C(54)	-424(2)	1120(1)	4787(1)	66(1)
C(55)	-189(2)	1402(1)	5370(1)	61(1)
C(56)	-327(1)	2224(1)	5516(1)	43(1)
C(57)	-860(1)	3663(1)	5236(1)	48(1)

Table S2. Bond lengths (Å) for [Cu(SSi^{i}Pr$_3$)((PPh$_2$CH$_2$CH$_2$)$_3$CCH$_3$)]. Symmetry transformations used to generate equivalent atoms.

Cu(1)-S(1)	2.2670(4)	C(13)-C(14)	1.385(2)
Cu(1)-P(3)	2.2921(4)	C(13)-H(13)	0.9300
Cu(1)-P(1)	2.3029(4)	C(14)-C(15)	1.386(2)
Cu(1)-P(2)	2.3124(4)	C(14)-H(14)	0.9300
S(1)-Si(1)	2.1019(5)	C(15)-C(16)	1.381(2)
P(1)-C(6)	1.8294(13)	C(15)-H(15)	0.9300
P(1)-C(12)	1.8293(14)	C(16)-C(17)	1.385(2)
P(1)-C(1)	1.8523(13)	C(16)-H(16)	0.9300
P(2)-C(24)	1.8247(13)	C(17)-H(17)	0.9300
P(2)-C(18)	1.8358(14)	C(18)-C(23)	1.3922(19)
P(2)-C(2)	1.8526(13)	C(18)-C(19)	1.393(2)
P(3)-C(30)	1.8286(14)	C(19)-C(20)	1.394(2)
P(3)-C(36)	1.8355(14)	C(19)-H(19)	0.9300
P(3)-C(3)	1.8531(13)	C(20)-C(21)	1.381(2)
Si(1)-C(48)	1.8968(15)	C(20)-H(20)	0.9300
Si(1)-C(45)	1.9044(18)	C(21)-C(22)	1.382(3)
Si(1)-C(42)	1.9141(17)	C(21)-H(21)	0.9300
C(1)-C(4)	1.5542(18)	C(22)-C(23)	1.390(2)
C(1)-H(1A)	0.9700	C(22)-H(22)	0.9300
C(1)-H(1B)	0.9700	C(23)-H(23)	0.9300
C(2)-C(4)	1.5511(18)	C(24)-C(29)	1.393(2)
C(2)-H(2A)	0.9700	C(24)-C(25)	1.3977(19)
C(2)-H(2B)	0.9700	C(25)-C(26)	1.386(2)
C(3)-C(4)	1.5511(18)	C(25)-H(25)	0.9300
C(3)-H(3A)	0.9700	C(26)-C(27)	1.384(2)
C(3)-H(3B)	0.9700	C(26)-H(26)	0.9300
C(4)-C(5)	1.5439(18)	C(27)-C(28)	1.381(2)
C(5)-H(5A)	0.9600	C(27)-H(27)	0.9300
C(5)-H(5B)	0.9600	C(28)-C(29)	1.390(2)
C(5)-H(5C)	0.9600	C(28)-H(28)	0.9300
C(6)-C(11)	1.3920(19)	C(29)-H(29)	0.9300
C(6)-C(7)	1.3952(18)	C(30)-C(31)	1.3907(19)
C(7)-C(8)	1.390(2)	C(30)-C(35)	1.3966(19)
C(7)-H(7)	0.9300	C(31)-C(32)	1.388(2)
C(8)-C(9)	1.380(2)	C(31)-H(31)	0.9300
C(8)-H(8)	0.9300	C(32)-C(33)	1.379(2)
C(9)-C(10)	1.382(2)	C(32)-H(32)	0.9300
C(9)-H(9)	0.9300	C(33)-C(34)	1.385(3)
C(10)-C(11)	1.390(2)	C(33)-H(33)	0.9300
C(10)-H(10)	0.9300	C(34)-C(35)	1.386(2)
C(11)-H(11)	0.9300	C(34)-H(34)	0.9300
C(12)-C(13)	1.3895(19)	C(35)-H(35)	0.9300
C(12)-C(17)	1.3980(18)	C(36)-C(41)	1.395(2)

Table S2. Bond lengths (Å) for [Cu(SSi^{i}Pr$_3$)((PPh$_2$CH$_2$CH$_2$)$_3$CCH$_3$)]. Symmetry transformations used to generate equivalent atoms.

C(36)-C(37)	1.398(2)	C(53)-H(53)	0.9300
C(37)-C(38)	1.391(2)	C(54)-C(55)	1.389(4)
C(37)-H(37)	0.9300	C(54)-H(54)	0.9300
C(38)-C(39)	1.385(3)	C(55)-C(56)	1.384(3)
C(38)-H(38)	0.9300	C(55)-H(55)	0.9300
C(39)-C(40)	1.376(3)	C(56)-H(56)	0.9300
C(39)-H(39)	0.9300	C(57)-H(57A)	0.9600
C(40)-C(41)	1.389(2)	C(57)-H(57B)	0.9600
C(40)-H(40)	0.9300	C(57)-H(57C)	0.9600
C(41)-H(41)	0.9300		
C(42)-C(43)	1.511(3)		
C(42)-C(44)	1.532(3)		
C(42)-H(42)	0.9800		
C(43)-H(43A)	0.9600		
C(43)-H(43B)	0.9600		
C(43)-H(43C)	0.9600		
C(44)-H(44A)	0.9600		
C(44)-H(44B)	0.9600		
C(44)-H(44C)	0.9600		
C(45)-C(46)	1.536(2)		
C(45)-C(47)	1.536(2)		
C(45)-H(45)	0.9800		
C(46)-H(46A)	0.9600		
C(46)-H(46B)	0.9600		
C(46)-H(46C)	0.9600		
C(47)-H(47A)	0.9600		
C(47)-H(47B)	0.9600		
C(47)-H(47C)	0.9600		
C(48)-C(50)	1.531(2)		
C(48)-C(49)	1.536(2)		
C(48)-H(48)	0.9800		
C(49)-H(49A)	0.9600		
C(49)-H(49B)	0.9600		
C(49)-H(49C)	0.9600		
C(50)-H(50A)	0.9600		
C(50)-H(50B)	0.9600		
C(50)-H(50C)	0.9600		
C(51)-C(56)	1.386(3)		
C(51)-C(52)	1.386(2)		
C(51)-C(57)	1.501(2)		
C(52)-C(53)	1.374(3)		
C(52)-H(52)	0.9300		
C(53)-C(54)	1.358(4)		

Table S3. Bond angles (deg.) for [Cu(SSi^{i}Pr$_3$)((PPh$_2$CH$_2$CH$_2$)$_3$CCH$_3$)]. Symmetry transformations used to generate equivalent atoms.

S(1)-Cu(1)-P(3)	132.490(14)	C(4)-C(3)-P(3)	118.71(9)
S(1)-Cu(1)-P(1)	118.050(16)	C(4)-C(3)-H(3A)	107.6
P(3)-Cu(1)-P(1)	96.418(14)	P(3)-C(3)-H(3A)	107.6
S(1)-Cu(1)-P(2)	117.236(16)	C(4)-C(3)-H(3B)	107.6
P(3)-Cu(1)-P(2)	91.994(13)	P(3)-C(3)-H(3B)	107.6
P(1)-Cu(1)-P(2)	90.871(13)	H(3A)-C(3)-H(3B)	107.1
Si(1)-S(1)-Cu(1)	118.93(2)	C(5)-C(4)-C(2)	106.49(11)
C(6)-P(1)-C(12)	99.27(6)	C(5)-C(4)-C(3)	106.09(11)
C(6)-P(1)-C(1)	103.06(6)	C(2)-C(4)-C(3)	112.83(10)
C(12)-P(1)-C(1)	107.01(6)	C(5)-C(4)-C(1)	106.33(10)
C(6)-P(1)-Cu(1)	123.99(4)	C(2)-C(4)-C(1)	112.50(11)
C(12)-P(1)-Cu(1)	113.54(4)	C(3)-C(4)-C(1)	112.01(11)
C(1)-P(1)-Cu(1)	108.46(4)	C(4)-C(5)-H(5A)	109.5
C(24)-P(2)-C(18)	99.65(6)	C(4)-C(5)-H(5B)	109.5
C(24)-P(2)-C(2)	104.51(6)	H(5A)-C(5)-H(5B)	109.5
C(18)-P(2)-C(2)	104.29(6)	C(4)-C(5)-H(5C)	109.5
C(24)-P(2)-Cu(1)	123.19(4)	H(5A)-C(5)-H(5C)	109.5
C(18)-P(2)-Cu(1)	115.58(5)	H(5B)-C(5)-H(5C)	109.5
C(2)-P(2)-Cu(1)	107.71(4)	C(11)-C(6)-C(7)	119.06(12)
C(30)-P(3)-C(36)	101.89(6)	C(11)-C(6)-P(1)	116.79(10)
C(30)-P(3)-C(3)	104.10(6)	C(7)-C(6)-P(1)	124.13(11)
C(36)-P(3)-C(3)	99.62(6)	C(8)-C(7)-C(6)	119.86(14)
C(30)-P(3)-Cu(1)	111.30(4)	C(8)-C(7)-H(7)	120.1
C(36)-P(3)-Cu(1)	131.00(5)	C(6)-C(7)-H(7)	120.1
C(3)-P(3)-Cu(1)	105.75(4)	C(9)-C(8)-C(7)	120.63(14)
C(48)-Si(1)-C(45)	106.45(7)	C(9)-C(8)-H(8)	119.7
C(48)-Si(1)-C(42)	108.21(8)	C(7)-C(8)-H(8)	119.7
C(45)-Si(1)-C(42)	111.56(8)	C(8)-C(9)-C(10)	119.94(14)
C(48)-Si(1)-S(1)	111.83(5)	C(8)-C(9)-H(9)	120.0
C(45)-Si(1)-S(1)	113.89(5)	C(10)-C(9)-H(9)	120.0
C(42)-Si(1)-S(1)	104.85(6)	C(9)-C(10)-C(11)	119.88(14)
C(4)-C(1)-P(1)	117.40(9)	C(9)-C(10)-H(10)	120.1
C(4)-C(1)-H(1A)	108.0	C(11)-C(10)-H(10)	120.1
P(1)-C(1)-H(1A)	108.0	C(6)-C(11)-C(10)	120.62(13)
C(4)-C(1)-H(1B)	108.0	C(6)-C(11)-H(11)	119.7
P(1)-C(1)-H(1B)	108.0	C(10)-C(11)-H(11)	119.7
H(1A)-C(1)-H(1B)	107.2	C(13)-C(12)-C(17)	118.83(13)
C(4)-C(2)-P(2)	117.19(9)	C(13)-C(12)-P(1)	124.39(10)
C(4)-C(2)-H(2A)	108.0	C(17)-C(12)-P(1)	116.61(10)
P(2)-C(2)-H(2A)	108.0	C(14)-C(13)-C(12)	120.55(14)
C(4)-C(2)-H(2B)	108.0	C(14)-C(13)-H(13)	119.7
P(2)-C(2)-H(2B)	108.0	C(12)-C(13)-H(13)	119.7
H(2A)-C(2)-H(2B)	107.2	C(13)-C(14)-C(15)	120.04(15)

Table S3. Bond angles (deg.) for [Cu(SSi^{i}Pr$_3$)((PPh$_2$CH$_2$CH$_2$)$_3$CCH$_3$)]. Symmetry transformations used to generate equivalent atoms.

C(13)-C(14)-H(14)	120.0	C(29)-C(28)-H(28)	119.7
C(15)-C(14)-H(14)	120.0	C(28)-C(29)-C(24)	119.80(14)
C(16)-C(15)-C(14)	120.05(15)	C(28)-C(29)-H(29)	120.1
C(16)-C(15)-H(15)	120.0	C(24)-C(29)-H(29)	120.1
C(14)-C(15)-H(15)	120.0	C(31)-C(30)-C(35)	118.62(13)
C(15)-C(16)-C(17)	120.04(15)	C(31)-C(30)-P(3)	117.59(10)
C(15)-C(16)-H(16)	120.0	C(35)-C(30)-P(3)	123.78(11)
C(17)-C(16)-H(16)	120.0	C(32)-C(31)-C(30)	121.09(13)
C(16)-C(17)-C(12)	120.46(14)	C(32)-C(31)-H(31)	119.5
C(16)-C(17)-H(17)	119.8	C(30)-C(31)-H(31)	119.5
C(12)-C(17)-H(17)	119.8	C(33)-C(32)-C(31)	119.79(15)
C(23)-C(18)-C(19)	118.97(13)	C(33)-C(32)-H(32)	120.1
C(23)-C(18)-P(2)	119.11(11)	C(31)-C(32)-H(32)	120.1
C(19)-C(18)-P(2)	121.79(11)	C(32)-C(33)-C(34)	119.80(16)
C(18)-C(19)-C(20)	120.41(14)	C(32)-C(33)-H(33)	120.1
C(18)-C(19)-H(19)	119.8	C(34)-C(33)-H(33)	120.1
C(20)-C(19)-H(19)	119.8	C(33)-C(34)-C(35)	120.62(16)
C(21)-C(20)-C(19)	119.90(15)	C(33)-C(34)-H(34)	119.7
C(21)-C(20)-H(20)	120.0	C(35)-C(34)-H(34)	119.7
C(19)-C(20)-H(20)	120.0	C(34)-C(35)-C(30)	120.05(16)
C(20)-C(21)-C(22)	120.18(14)	C(34)-C(35)-H(35)	120.0
C(20)-C(21)-H(21)	119.9	C(30)-C(35)-H(35)	120.0
C(22)-C(21)-H(21)	119.9	C(41)-C(36)-C(37)	118.24(13)
C(21)-C(22)-C(23)	120.10(14)	C(41)-C(36)-P(3)	121.95(12)
C(21)-C(22)-H(22)	119.9	C(37)-C(36)-P(3)	119.74(11)
C(23)-C(22)-H(22)	119.9	C(38)-C(37)-C(36)	120.58(14)
C(22)-C(23)-C(18)	120.41(14)	C(38)-C(37)-H(37)	119.7
C(22)-C(23)-H(23)	119.8	C(36)-C(37)-H(37)	119.7
C(18)-C(23)-H(23)	119.8	C(39)-C(38)-C(37)	120.24(16)
C(29)-C(24)-C(25)	119.17(13)	C(39)-C(38)-H(38)	119.9
C(29)-C(24)-P(2)	125.24(11)	C(37)-C(38)-H(38)	119.9
C(25)-C(24)-P(2)	115.59(10)	C(40)-C(39)-C(38)	119.71(15)
C(26)-C(25)-C(24)	120.53(14)	C(40)-C(39)-H(39)	120.1
C(26)-C(25)-H(25)	119.7	C(38)-C(39)-H(39)	120.1
C(24)-C(25)-H(25)	119.7	C(39)-C(40)-C(41)	120.47(16)
C(27)-C(26)-C(25)	119.85(15)	C(39)-C(40)-H(40)	119.8
C(27)-C(26)-H(26)	120.1	C(41)-C(40)-H(40)	119.8
C(25)-C(26)-H(26)	120.1	C(40)-C(41)-C(36)	120.74(16)
C(26)-C(27)-C(28)	120.06(14)	C(40)-C(41)-H(41)	119.6
C(26)-C(27)-H(27)	120.0	C(36)-C(41)-H(41)	119.6
C(28)-C(27)-H(27)	120.0	C(43)-C(42)-C(44)	110.66(17)
C(27)-C(28)-C(29)	120.57(15)	C(43)-C(42)-Si(1)	113.78(15)
C(27)-C(28)-H(28)	119.7	C(44)-C(42)-Si(1)	115.28(13)

Table S3. Bond angles (deg.) for [Cu(SSi^{i}Pr$_3$)((PPh$_2$CH$_2$CH$_2$)$_3$CCH$_3$)]. Symmetry transformations used to generate equivalent atoms.

C(43)-C(42)-H(42)	105.4	H(49A)-C(49)-H(49C)	109.5
C(44)-C(42)-H(42)	105.4	H(49B)-C(49)-H(49C)	109.5
Si(1)-C(42)-H(42)	105.4	C(48)-C(50)-H(50A)	109.5
C(42)-C(43)-H(43A)	109.5	C(48)-C(50)-H(50B)	109.5
C(42)-C(43)-H(43B)	109.5	H(50A)-C(50)-H(50B)	109.5
H(43A)-C(43)-H(43B)	109.5	C(48)-C(50)-H(50C)	109.5
C(42)-C(43)-H(43C)	109.5	H(50A)-C(50)-H(50C)	109.5
H(43A)-C(43)-H(43C)	109.5	H(50B)-C(50)-H(50C)	109.5
H(43B)-C(43)-H(43C)	109.5	C(56)-C(51)-C(52)	118.22(17)
C(42)-C(44)-H(44A)	109.5	C(56)-C(51)-C(57)	121.03(16)
C(42)-C(44)-H(44B)	109.5	C(52)-C(51)-C(57)	120.75(17)
H(44A)-C(44)-H(44B)	109.5	C(53)-C(52)-C(51)	121.14(19)
C(42)-C(44)-H(44C)	109.5	C(53)-C(52)-H(52)	119.4
H(44A)-C(44)-H(44C)	109.5	C(51)-C(52)-H(52)	119.4
H(44B)-C(44)-H(44C)	109.5	C(54)-C(53)-C(52)	120.5(2)
C(46)-C(45)-C(47)	109.34(15)	C(54)-C(53)-H(53)	119.8
C(46)-C(45)-Si(1)	113.36(15)	C(52)-C(53)-H(53)	119.8
C(47)-C(45)-Si(1)	111.95(12)	C(53)-C(54)-C(55)	119.7(2)
C(46)-C(45)-H(45)	107.3	C(53)-C(54)-H(54)	120.1
C(47)-C(45)-H(45)	107.3	C(55)-C(54)-H(54)	120.1
Si(1)-C(45)-H(45)	107.3	C(56)-C(55)-C(54)	119.9(2)
C(45)-C(46)-H(46A)	109.5	C(56)-C(55)-H(55)	120.0
C(45)-C(46)-H(46B)	109.5	C(54)-C(55)-H(55)	120.0
H(46A)-C(46)-H(46B)	109.5	C(55)-C(56)-C(51)	120.47(19)
C(45)-C(46)-H(46C)	109.5	C(55)-C(56)-H(56)	119.8
H(46A)-C(46)-H(46C)	109.5	C(51)-C(56)-H(56)	119.8
H(46B)-C(46)-H(46C)	109.5	C(51)-C(57)-H(57A)	109.5
C(45)-C(47)-H(47A)	109.5	C(51)-C(57)-H(57B)	109.5
C(45)-C(47)-H(47B)	109.5	H(57A)-C(57)-H(57B)	109.5
H(47A)-C(47)-H(47B)	109.5	C(51)-C(57)-H(57C)	109.5
C(45)-C(47)-H(47C)	109.5	H(57A)-C(57)-H(57C)	109.5
H(47A)-C(47)-H(47C)	109.5	H(57B)-C(57)-H(57C)	109.5
H(47B)-C(47)-H(47C)	109.5		
C(50)-C(48)-C(49)	109.30(14)		
C(50)-C(48)-Si(1)	112.23(11)		
C(49)-C(48)-Si(1)	115.63(11)		
C(50)-C(48)-H(48)	106.3		
C(49)-C(48)-H(48)	106.3		
Si(1)-C(48)-H(48)	106.3		
C(48)-C(49)-H(49A)	109.5		
C(48)-C(49)-H(49B)	109.5		
H(49A)-C(49)-H(49B)	109.5		
C(48)-C(49)-H(49C)	109.5		

Table S4. Anisotropic displacement parameters ($Å^2$ x 10^3) for [Cu(SSi^{i}Pr$_3$)((PPh$_2$CH$_2$CH$_2$)$_3$CCH$_3$)]. The anisotropic displacement factor exponent takes the form: $-2\pi^2[(ha^*)^2U_{11} + ... + 2hka^*b^*U_{12}]$.

Atom	U_{11}	U_{22}	U_{33}	U_{23}	U_{13}	U_{12}
Cu(1)	20(1)	20(1)	18(1)	0(1)	1(1)	-4(1)
S(1)	30(1)	37(1)	48(1)	22(1)	-16(1)	-16(1)
P(1)	20(1)	21(1)	18(1)	-1(1)	1(1)	-3(1)
P(2)	20(1)	20(1)	19(1)	0(1)	2(1)	-1(1)
P(3)	20(1)	19(1)	22(1)	2(1)	-1(1)	-2(1)
Si(1)	23(1)	24(1)	30(1)	6(1)	-4(1)	-8(1)
C(1)	23(1)	25(1)	22(1)	-2(1)	2(1)	-7(1)
C(2)	23(1)	22(1)	22(1)	3(1)	4(1)	-2(1)
C(3)	25(1)	18(1)	29(1)	2(1)	-1(1)	-2(1)
C(4)	21(1)	20(1)	23(1)	1(1)	1(1)	-4(1)
C(5)	29(1)	24(1)	32(1)	4(1)	3(1)	-8(1)
C(6)	21(1)	24(1)	20(1)	-3(1)	1(1)	2(1)
C(7)	28(1)	27(1)	29(1)	1(1)	-5(1)	-3(1)
C(8)	33(1)	38(1)	36(1)	1(1)	-13(1)	-4(1)
C(9)	37(1)	39(1)	30(1)	4(1)	-9(1)	5(1)
C(10)	37(1)	31(1)	28(1)	5(1)	2(1)	2(1)
C(11)	26(1)	28(1)	25(1)	0(1)	1(1)	-2(1)
C(12)	21(1)	25(1)	18(1)	2(1)	0(1)	0(1)
C(13)	30(1)	24(1)	32(1)	1(1)	6(1)	-2(1)
C(14)	47(1)	24(1)	43(1)	1(1)	14(1)	5(1)
C(15)	35(1)	41(1)	40(1)	8(1)	14(1)	14(1)
C(16)	24(1)	49(1)	34(1)	4(1)	4(1)	-2(1)
C(17)	25(1)	34(1)	27(1)	-1(1)	1(1)	-6(1)
C(18)	25(1)	21(1)	21(1)	-3(1)	-1(1)	0(1)
C(19)	27(1)	32(1)	28(1)	2(1)	-1(1)	-2(1)
C(20)	25(1)	40(1)	42(1)	-2(1)	-5(1)	-1(1)
C(21)	39(1)	37(1)	34(1)	-2(1)	-14(1)	8(1)
C(22)	49(1)	31(1)	24(1)	3(1)	-2(1)	8(1)
C(23)	34(1)	23(1)	25(1)	0(1)	3(1)	2(1)
C(24)	19(1)	27(1)	23(1)	-4(1)	0(1)	1(1)
C(25)	26(1)	26(1)	28(1)	-1(1)	1(1)	1(1)
C(26)	36(1)	26(1)	41(1)	-9(1)	2(1)	0(1)
C(27)	36(1)	46(1)	38(1)	-22(1)	6(1)	-3(1)
C(28)	33(1)	53(1)	31(1)	-15(1)	13(1)	-10(1)
C(29)	28(1)	36(1)	28(1)	-8(1)	7(1)	-9(1)
C(30)	22(1)	25(1)	22(1)	2(1)	-3(1)	-3(1)
C(31)	22(1)	26(1)	24(1)	2(1)	-3(1)	-2(1)
C(32)	30(1)	36(1)	28(1)	-6(1)	-4(1)	0(1)
C(33)	50(1)	56(1)	22(1)	-4(1)	1(1)	-7(1)

Table S4. Anisotropic displacement parameters ($Å^2$ x 10^3) for [Cu(SSi^{i}Pr$_3$)((PPh$_2$CH$_2$CH$_2$)$_3$CCH$_3$)]. The anisotropic displacement factor exponent takes the form: $-2\pi^2[(ha^*)^2U_{11} + ... + 2hka^*b^*U_{12}]$.

Atom	U_{11}	U_{22}	U_{33}	U_{23}	U_{13}	U_{12}
C(34)	70(1)	50(1)	24(1)	10(1)	0(1)	-15(1)
C(35)	53(1)	30(1)	28(1)	7(1)	-3(1)	-8(1)
C(36)	22(1)	23(1)	31(1)	5(1)	0(1)	-2(1)
C(37)	28(1)	31(1)	29(1)	5(1)	1(1)	1(1)
C(38)	31(1)	37(1)	41(1)	2(1)	8(1)	5(1)
C(39)	24(1)	49(1)	57(1)	2(1)	1(1)	6(1)
C(40)	26(1)	60(1)	52(1)	-9(1)	-10(1)	3(1)
C(41)	27(1)	40(1)	42(1)	-9(1)	-4(1)	0(1)
C(42)	39(1)	32(1)	65(1)	17(1)	-5(1)	-11(1)
C(43)	57(1)	52(1)	80(2)	35(1)	-11(1)	-8(1)
C(44)	61(1)	42(1)	82(2)	14(1)	-8(1)	-28(1)
C(45)	36(1)	37(1)	36(1)	-5(1)	7(1)	-12(1)
C(46)	86(2)	58(1)	36(1)	-5(1)	17(1)	-21(1)
C(47)	42(1)	35(1)	54(1)	-8(1)	3(1)	0(1)
C(48)	27(1)	29(1)	30(1)	-1(1)	0(1)	-3(1)
C(49)	34(1)	58(1)	37(1)	-4(1)	-10(1)	-7(1)
C(50)	46(1)	37(1)	48(1)	-7(1)	14(1)	-4(1)
C(51)	26(1)	42(1)	38(1)	-2(1)	8(1)	-2(1)
C(52)	37(1)	51(1)	38(1)	-3(1)	8(1)	-8(1)
C(53)	56(1)	55(1)	55(1)	-17(1)	19(1)	-21(1)
C(54)	70(2)	37(1)	93(2)	-11(1)	15(1)	-8(1)
C(55)	58(1)	44(1)	81(2)	14(1)	3(1)	2(1)
C(56)	36(1)	50(1)	44(1)	3(1)	3(1)	-1(1)
C(57)	50(1)	45(1)	48(1)	-5(1)	1(1)	9(1)

Table S5. Hydrogen coordinates (x 10^4) and isotropic displacement parameters (Å^2 x10^3) for [Cu(SSi^{i}Pr$_3$)((PPh$_2$CH$_2$CH$_2$)$_3$CCH$_3$)].

H atom	x	y	z	U(eq)
H(1A)	1878	787	2663	28
H(1B)	2626	102	2601	28
H(2A)	2372	1292	4219	27
H(2B)	1524	1230	3751	27
H(3A)	3969	121	3398	29
H(3B)	3714	210	4071	29
H(5A)	2174	-234	4090	42
H(5B)	2485	-677	3505	42
H(5C)	1541	-202	3490	42
H(7)	1623	700	1660	34
H(8)	793	1108	781	43
H(9)	1212	2278	266	43
H(10)	2463	3060	630	39
H(11)	3276	2680	1522	32
H(13)	3457	-257	1804	34
H(14)	4633	-901	1322	45
H(15)	6057	-261	1282	46
H(16)	6277	1056	1672	42
H(17)	5095	1716	2139	34
H(19)	419	2173	3533	35
H(20)	-844	2587	2909	43
H(21)	-619	3280	2015	45
H(22)	860	3579	1746	42
H(23)	2122	3202	2378	33
H(25)	2866	4013	3806	32
H(26)	2629	4950	4574	41
H(27)	1852	4542	5409	48
H(28)	1305	3206	5473	47
H(29)	1487	2275	4691	37
H(31)	4276	2985	4316	29
H(32)	4077	3505	5275	38
H(33)	3960	2609	6083	51
H(34)	4087	1197	5936	58
H(35)	4266	669	4977	45
H(37)	5454	314	3038	35
H(38)	6914	-271	3099	44
H(39)	7912	-29	3939	52
H(40)	7462	822	4705	56
H(41)	6015	1425	4646	44
H(42)	5239	5376	3002	55

Table S5. Hydrogen coordinates (x 10^4) and isotropic displacement parameters ($Å^2$ x10^3) for [Cu(SSi^{i}Pr$_3$)((PPh$_2$CH$_2$CH$_2$)$_3$CCH$_3$)].

H atom	x	y	z	U(eq)
H(43A)	5324	5852	2061	96
H(43B)	4933	4950	1990	96
H(43C)	5972	5129	1878	96
H(44A)	7128	5309	2795	93
H(44B)	6713	5534	3413	93
H(44C)	6572	6134	2857	93
H(45)	7218	3650	2734	43
H(46A)	6999	2955	1802	89
H(46B)	6502	3817	1773	89
H(46C)	5926	3006	1846	89
H(47A)	6175	2192	2879	66
H(47B)	6938	2532	3347	66
H(47C)	7214	2184	2720	66
H(48)	5724	3318	3960	35
H(49A)	7117	4538	4012	65
H(49B)	7298	3599	3881	65
H(49C)	6971	3873	4514	65
H(50A)	5344	4335	4617	65
H(50B)	4668	4418	4038	65
H(50C)	5503	5030	4138	65
H(52)	-1196	2825	4213	50
H(53)	-954	1463	3973	66
H(54)	-329	568	4688	79
H(55)	61	1039	5663	73
H(56)	-167	2412	5906	52
H(57A)	-684	3757	5656	71
H(57B)	-1502	3795	5159	71
H(57C)	-494	4008	4989	71

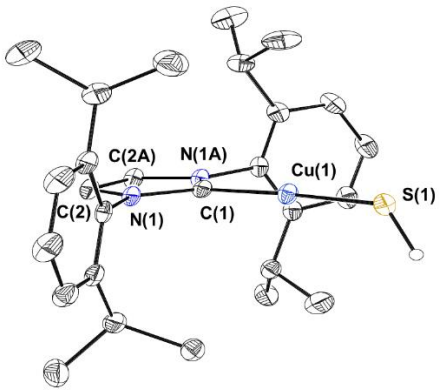

Structure Determination Summary

Crystal Data and Structure Refinement for [(IPr)Cu(SH)]

Identification code	JPD539_0m_a
Empirical formula	$C_{27}H_{37}CuN_2S$
Formula weight	486.19
Temperature	100(2) K
Wavelength	0.71073 Å
Crystal system	orthorhombic
Space group	*Pccn*
Unit cell dimensions	a = 10.6051(18) Å α = 90°
	b = 12.746(2) Å β = 90°
	c = 19.205(3) Å γ = 90°
Volume	2596.0(8) Å^3
Z	4
Density (calculated)	1.244 g/cm^3
Absorption coefficient	0.938 mm^{-1}
F(000)	1036
Crystal size	0.341 x 0.204 x 0.190 mm^3
θ range for data collection	2.121 to 26.365°
Index ranges	$-13 \le h \le 13$, $-15 \le k \le 15$, $-24 \le l \le 24$
Reflections collected	37834
Independent reflections	2655 [R(int) = 0.0357]
Completeness to θ = 25.242°	100.0 %
Absorption correction	Semi-empirical from equivalents
Max. and min. transmission	0.8435 and 0.7267
Refinement method	Full-matrix least-squares on F^2
Data / restraints / parameters	2655 / 42 / 154
Goodness-of-fit on F^2	1.125
Final R indices [I>2σ(I)]	R1 = 0.0387, wR2 = 0.1299
R indices (all data)	R1 = 0.0418, wR2 = 0.1330
Extinction coefficient	n/a
Largest diff. peak and hole	0.665 and -0.808 e·Å^{-3}

Table S1. Atomic coordinates (x 10^4) and equivalent isotropic displacement parameters ($Å^2$ x 10^3) for [(IPr)Cu(SH)]. U(eq) is defined as one third of the trace of the orthogonalized U^{ij} tensor.

Atom	x	y	z	U(eq)
Cu(1)	2500	2500	7233(1)	17(1)
S(1)	2606(3)	2397(4)	8323(1)	17(1)
N(1)	2807(2)	1699(1)	5812(1)	15(1)
C(1)	2500	2500	6248(2)	14(1)
C(2)	2697(2)	1995(2)	5120(1)	18(1)
C(3)	3242(2)	686(2)	6051(1)	16(1)
C(4)	2344(2)	-90(2)	6200(1)	18(1)
C(5)	2801(2)	-1047(2)	6455(1)	25(1)
C(6)	4079(2)	-1217(2)	6537(1)	27(1)
C(7)	4947(2)	-441(2)	6371(1)	25(1)
C(8)	4539(2)	534(2)	6125(1)	19(1)
C(9)	938(2)	77(2)	6103(1)	22(1)
C(10)	325(2)	-823(2)	5695(1)	30(1)
C(11)	282(2)	226(2)	6808(1)	35(1)
C(12)	5482(2)	1411(2)	5982(1)	23(1)
C(13)	5878(2)	1926(2)	6671(1)	34(1)
C(14)	6630(3)	1027(2)	5574(1)	37(1)

Table S2. Bond lengths (Å) and angles (deg.) for [(IPr)Cu(SH)]. Symmetry transformations used to generate equivalent atoms: #1 -x + ½, -y + ½, z.

Cu(1)-C(1)	1.893(3)	C(1)-Cu(1)-S(1)#1	175.29(12)
Cu(1)-S(1)#1	2.0991(12)	C(1)-Cu(1)-S(1)	175.29(12)
Cu(1)-S(1)	2.0991(12)	S(1)#1-Cu(1)-S(1)	9.4(2)
S(1)-S(1)#1	0.345(9)	S(1)#1-S(1)-Cu(1)	85.28(12)
S(1)-H(1)	1.2000(2)	S(1)#1-S(1)-H(1)	116.1(13)
N(1)-C(1)	1.360(2)	Cu(1)-S(1)-H(1)	125.36(9)
N(1)-C(2)	1.386(3)	C(1)-N(1)-C(2)	111.51(18)
N(1)-C(3)	1.447(2)	C(1)-N(1)-C(3)	123.39(17)
C(1)-N(1)#1	1.360(2)	C(2)-N(1)-C(3)	125.05(17)
C(2)-C(2)#1	1.354(4)	N(1)#1-C(1)-N(1)	103.9(2)
C(2)-H(2)	0.9500	N(1)#1-C(1)-Cu(1)	128.03(12)
C(3)-C(8)	1.396(3)	N(1)-C(1)-Cu(1)	128.03(12)
C(3)-C(4)	1.402(3)	C(2)#1-C(2)-N(1)	106.51(12)
C(4)-C(5)	1.401(3)	C(2)#1-C(2)-H(2)	126.7
C(4)-C(9)	1.518(3)	N(1)-C(2)-H(2)	126.7
C(5)-C(6)	1.382(3)	C(8)-C(3)-C(4)	123.39(19)
C(5)-H(5)	0.9500	C(8)-C(3)-N(1)	118.07(18)
C(6)-C(7)	1.389(3)	C(4)-C(3)-N(1)	118.54(19)
C(6)-H(6)	0.9500	C(5)-C(4)-C(3)	116.8(2)
C(7)-C(8)	1.398(3)	C(5)-C(4)-C(9)	120.30(19)
C(7)-H(7)	0.9500	C(3)-C(4)-C(9)	122.90(19)
C(8)-C(12)	1.525(3)	C(6)-C(5)-C(4)	121.0(2)
C(9)-C(10)	1.534(3)	C(6)-C(5)-H(5)	119.5
C(9)-C(11)	1.535(3)	C(4)-C(5)-H(5)	119.5
C(9)-H(9)	1.0000	C(5)-C(6)-C(7)	120.8(2)
C(10)-H(10A)	0.9800	C(5)-C(6)-H(6)	119.6
C(10)-H(10B)	0.9800	C(7)-C(6)-H(6)	119.6
C(10)-H(10C)	0.9800	C(6)-C(7)-C(8)	120.3(2)
C(11)-H(11A)	0.9800	C(6)-C(7)-H(7)	119.8
C(11)-H(11B)	0.9800	C(8)-C(7)-H(7)	119.8
C(11)-H(11C)	0.9800	C(3)-C(8)-C(7)	117.6(2)
C(12)-C(14)	1.528(3)	C(3)-C(8)-C(12)	121.75(19)
C(12)-C(13)	1.534(3)	C(7)-C(8)-C(12)	120.6(2)
C(12)-H(12)	1.0000	C(4)-C(9)-C(10)	111.99(19)
C(13)-H(13A)	0.9800	C(4)-C(9)-C(11)	110.73(19)
C(13)-H(13B)	0.9800	C(10)-C(9)-C(11)	110.6(2)
C(13)-H(13C)	0.9800	C(4)-C(9)-H(9)	107.8
C(14)-H(14A)	0.9800	C(10)-C(9)-H(9)	107.8
C(14)-H(14B)	0.9800	C(11)-C(9)-H(9)	107.8
C(14)-H(14C)	0.9800	C(9)-C(10)-H(10A)	109.5
		C(9)-C(10)-H(10B)	109.5
		H(10A)-C(10)-H(10B)	109.5
		C(9)-C(10)-H(10C)	109.5

Table S2. Bond lengths (Å) and angles (deg.) for [(IPr)Cu(SH)]. Symmetry transformations used to generate equivalent atoms: #1 -x + ½, -y + ½, z.

H(10A)-C(10)-H(10C)	109.5
H(10B)-C(10)-H(10C)	109.5
C(9)-C(11)-H(11A)	109.5
C(9)-C(11)-H(11B)	109.5
H(11A)-C(11)-H(11B)	109.5
C(9)-C(11)-H(11C)	109.5
H(11A)-C(11)-H(11C)	109.5
H(11B)-C(11)-H(11C)	109.5
C(8)-C(12)-C(14)	112.30(19)
C(8)-C(12)-C(13)	109.77(19)
C(14)-C(12)-C(13)	111.14(19)
C(8)-C(12)-H(12)	107.8
C(14)-C(12)-H(12)	107.8
C(13)-C(12)-H(12)	107.8
C(12)-C(13)-H(13A)	109.5
C(12)-C(13)-H(13B)	109.5
H(13A)-C(13)-H(13B)	109.5
C(12)-C(13)-H(13C)	109.5
H(13A)-C(13)-H(13C)	109.5
H(13B)-C(13)-H(13C)	109.5
C(12)-C(14)-H(14A)	109.5
C(12)-C(14)-H(14B)	109.5
H(14A)-C(14)-H(14B)	109.5
C(12)-C(14)-H(14C)	109.5
H(14A)-C(14)-H(14C)	109.5
H(14B)-C(14)-H(14C)	109.5

Table S3. Anisotropic displacement parameters ($Å^2$ x 10^3) for [(IPr)Cu(SH)]. The anisotropic displacement factor exponent takes the form: $-2\pi^2[h^2a^{*2}U^{11} + ... + 2hka^*b^*U^{12}]$.

Atom	U^{11}	U^{22}	U^{33}	U^{23}	U^{13}	U^{12}
Cu(1)	23(1)	17(1)	13(1)	0	0	-2(1)
S(1)	21(1)	16(2)	14(1)	3(1)	1(1)	4(1)
N(1)	21(1)	9(1)	14(1)	-1(1)	0(1)	-2(1)
C(1)	17(1)	11(1)	15(1)	0	0	-3(1)
C(2)	25(1)	14(1)	14(1)	-1(1)	0(1)	-4(1)
C(3)	25(1)	9(1)	14(1)	-2(1)	-2(1)	0(1)
C(4)	25(1)	12(1)	17(1)	0(1)	-2(1)	-2(1)

C(5)	34(1)	12(1)	28(1)	4(1)	-7(1)	-4(1)
C(6)	38(1)	12(1)	31(1)	1(1)	-12(1)	2(1)
C(7)	27(1)	18(1)	29(1)	-5(1)	-10(1)	4(1)
C(8)	24(1)	15(1)	19(1)	-5(1)	-4(1)	-1(1)
C(9)	24(1)	16(1)	26(1)	5(1)	-2(1)	-4(1)
C(10)	32(1)	23(1)	35(1)	5(1)	-11(1)	-7(1)
C(11)	31(1)	41(2)	34(1)	2(1)	5(1)	-3(1)
C(12)	22(1)	18(1)	29(1)	-6(1)	-1(1)	-2(1)
C(13)	24(1)	36(1)	40(1)	-21(1)	6(1)	-10(1)
C(14)	35(1)	34(1)	41(1)	-16(1)	11(1)	-9(1)

Table S4. Hydrogen coordinates (x 10^4) and isotropic displacement parameters ($Å^2$ x 10^3) for[(IPr)Cu(SH)].

H Atom	x	y	z	U(eq)
H(2)	2864	1571	4723	21
H(5)	2222	-1587	6573	30
H(6)	4367	-1873	6710	32
H(7)	5824	-573	6424	30
H(9)	820	736	5828	26
H(10A)	768	-919	5252	45
H(10B)	-562	-654	5604	45
H(10C)	375	-1471	5969	45
H(11A)	374	-413	7087	53
H(11B)	-616	371	6733	53
H(11C)	668	817	7056	53
H(12)	5048	1956	5694	28
H(13A)	5125	2113	6939	50
H(13B)	6370	2560	6573	50
H(13C)	6393	1433	6940	50
H(14A)	7114	535	5862	55
H(14B)	7162	1626	5450	55
H(14C)	6349	671	5149	55
H(1)	3543(3)	2519(16)	8663(1)	10(11)

Chapter 3: Crystal Information

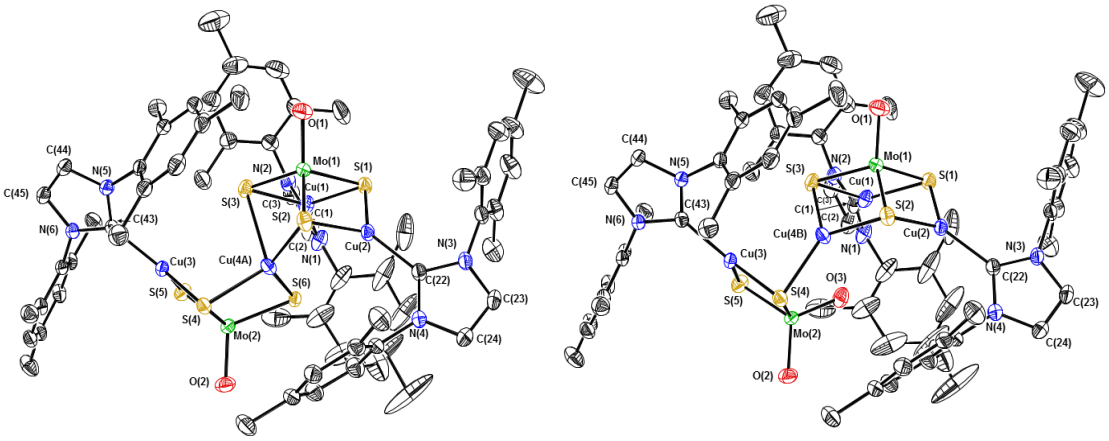

Structure Determination Summary
Crystal Data and Structure Refinement for
$\{[MoOS_3(CuIMes)](\mu^4\text{-}Cu)[MoOS_3(CuIMes)_2]\}_{0.36}$
$\{[MoO_2S_2(CuIMes)](\mu^3\text{-}Cu)[MoOS_3(CuIMes)_2]\}_{0.64}\cdot Ph_3SiOH\cdot 2½C_6H_6$, **1A + 1 B**

Identification code	jpd483_0m	
Empirical formula	$C_{96}H_{103}Cu_4Mo_2N_6O_{3.64}S_{5.36}Si$	
Formula weight	2044.98	
Temperature	150(2) K	
Wavelength	0.71073 Å	
Crystal system	triclinic	
Space group	*P*-1	
Unit cell dimensions	a = 15.106(5) Å	α = 100.487(5)°
	b = 18.635(7) Å	β = 107.454(5)°
	c = 19.062(7) Å	γ = 105.339(5)°
Volume, Z	4733(3) Å^3, 2	
Density (calculated)	1.435 g/cm^3	
Absorption coefficient	1.322 mm^{-1}	
F(000)	2100	
Crystal size	0.381 x 0.392 x 0.416 mm	
θ range for data collection	2.04 to 29.37°	
Limiting indices	$-20 < h < 20$, $-25 < k < 25$, $-26 < l < 26$	
Reflections collected	83802	
Independent reflections	23873 (R_{int} = 0.0335)	
Completeness to θ = 25.00°	99.7 %	
Absorption correction	Semi-empirical from equivalents	
Max. and min. transmission	0.9802 and 0.8443	
Refinement method	Full-matrix least-squares on F^2	
Data / restraints / parameters	23873 / 0 / 1060	
Goodness-of-fit on F^2	1.026	
Final R indices [I>2σ(I)]	R1 = 0.0368, wR2 = 0.0864	
R indices (all data)	R1 = 0.0443, wR2 = 0.0919	
Largest diff. peak and hole	2.516 and -2.097 e·Å^{-3}	

Table S1. Atomic coordinates (x 10^4) and equivalent isotropic displacement parameters [$Å^2$ x 10^3] for $\{[MoOS_3(CuIMes)](\mu^4\text{-}Cu)[MoOS_3(CuIMes)_2]\}_{0.36}\{[MoO_2S_2(CuIMes)](\mu^3\text{-}Cu)[MoOS_3(CuIMes)_2]\}_{0.64}\cdot Ph_3SiOH\cdot 2½C_6H_6$. U(eq) is defined as one third of the trace of the orthogonalized U_{ij} tensor.

Atom	x	y	z	U(eq)
Mo(1)	6044(1)	3489(1)	3310(1)	20(1)
Mo(2)	3482(1)	645(1)	1776(1)	22(1)
Cu(1)	6457(1)	2405(1)	2469(1)	26(1)
Cu(2)	6345(1)	2731(1)	4358(1)	21(1)
Cu(3)	2781(1)	1643(1)	1123(1)	21(1)
Cu(4A)	4416(1)	2022(1)	2926(1)	24(1)
S(6)	5039(2)	1072(1)	2596(1)	20(1)
Cu(4B)	4255(1)	2419(1)	2724(1)	24(1)
O(3)	4742(3)	914(3)	2325(2)	31(1)
S(1)	7331(1)	3048(1)	3714(1)	24(1)
S(2)	5039(1)	3107(1)	3961(1)	24(1)
S(3)	5212(1)	2856(1)	2056(1)	25(1)
S(4)	2793(1)	1490(1)	2268(1)	21(1)
S(5)	3349(1)	774(1)	606(1)	28(1)
Si(1)	-1919(1)	2583(1)	-1076(1)	22(1)
O(1)	6461(1)	4474(1)	3486(1)	37(1)
O(2)	2844(2)	-301(1)	1717(1)	35(1)
O(4)	-2257(1)	1802(1)	-810(1)	28(1)
N(1)	7106(2)	1196(1)	1680(1)	33(1)
N(2)	7167(2)	2160(1)	1218(1)	28(1)
N(3)	7516(1)	2533(1)	5811(1)	24(1)
N(4)	6028(1)	1749(1)	5372(1)	24(1)
N(5)	2412(1)	3081(1)	817(1)	23(1)
N(6)	1624(1)	2090(1)	-165(1)	22(1)
C(1)	6935(2)	1878(2)	1773(1)	27(1)
C(2)	7429(2)	1054(2)	1075(2)	37(1)
C(3)	7470(2)	1663(2)	788(1)	34(1)
C(4)	6979(3)	683(2)	2150(2)	44(1)
C(5)	6164(3)	15(2)	1845(2)	54(1)
C(6)	6073(4)	-485(2)	2315(3)	78(2)
C(7)	6783(5)	-305(3)	3048(3)	92(2)
C(8)	7567(5)	368(3)	3321(3)	84(2)
C(9)	7708(3)	888(3)	2896(2)	63(1)
C(10)	5400(3)	-160(2)	1055(2)	59(1)
C(11)	6631(7)	-875(4)	3526(4)	152(4)
C(12)	8573(3)	1627(3)	3222(2)	68(1)
C(13)	7128(2)	2903(2)	1119(1)	28(1)

C(14)	7927(2)	3566(2)	1582(2)	39(1)

Table S1. Atomic coordinates (x 10^4) and equivalent isotropic displacement parameters [$Å^2$ x 10^3] for $\{[MoOS_3(CuIMes)](\mu^4\text{-}Cu)[MoOS_3(CuIMes)_2]\}_{0.36}\{[MoO_2S_2(CuIMes)](\mu^3\text{-}Cu)[MoOS_3(CuIMes)_2]\}_{0.64}\cdot Ph_3SiOH\cdot 2½C_6H_6$. U(eq) is defined as one third of the trace of the orthogonalized U_{ij} tensor.

Atom	x	y	z	U(eq)
C(15)	7876(3)	4272(2)	1469(2)	51(1)
C(16)	7086(3)	4324(2)	910(2)	49(1)
C(17)	6296(2)	3652(2)	470(2)	42(1)
C(18)	6297(2)	2929(2)	568(2)	32(1)
C(19)	8813(2)	3509(2)	2172(2)	52(1)
C(20)	7078(4)	5091(2)	741(3)	76(1)
C(21)	5425(2)	2207(2)	116(2)	46(1)
C(22)	6644(2)	2318(1)	5216(1)	22(1)
C(23)	7441(2)	2104(2)	6330(1)	32(1)
C(24)	6506(2)	1612(2)	6054(2)	33(1)
C(25)	8387(2)	3150(1)	5899(1)	25(1)
C(26)	8461(2)	3916(2)	6175(1)	28(1)
C(27)	9314(2)	4497(2)	6252(2)	36(1)
C(28)	10071(2)	4328(2)	6066(2)	42(1)
C(29)	9966(2)	3556(2)	5790(2)	40(1)
C(30)	9125(2)	2953(2)	5698(1)	32(1)
C(31)	7642(2)	4125(2)	6362(2)	39(1)
C(32)	10985(3)	4975(2)	6154(2)	66(1)
C(33)	9010(2)	2115(2)	5381(2)	43(1)
C(34)	4998(2)	1366(1)	4896(1)	23(1)
C(35)	4733(2)	733(2)	4269(2)	30(1)
C(36)	3736(2)	387(2)	3809(2)	32(1)
C(37)	3026(2)	654(2)	3970(1)	29(1)
C(38)	3323(2)	1291(2)	4601(1)	28(1)
C(39)	4312(2)	1667(1)	5071(1)	24(1)
C(40)	5498(3)	432(2)	4089(2)	62(1)
C(41)	1951(2)	258(2)	3466(2)	44(1)
C(42)	4635(2)	2385(2)	5729(2)	36(1)
C(43)	2248(2)	2305(1)	580(1)	22(1)
C(44)	1906(2)	3336(1)	232(1)	29(1)
C(45)	1410(2)	2714(1)	-386(1)	29(1)
C(46)	2991(2)	3591(1)	1582(1)	22(1)
C(47)	3908(2)	4127(1)	1708(1)	26(1)
C(48)	4433(2)	4642(1)	2440(2)	31(1)
C(49)	4059(2)	4633(1)	3022(2)	32(1)
C(50)	3140(2)	4097(2)	2871(1)	30(1)

C(51)	2589(2)	3561(1)	2150(1)	26(1)
C(52)	4336(2)	4150(2)	1089(2)	36(1)

Table S1. Atomic coordinates (x 10^4) and equivalent isotropic displacement parameters [$Å^2$ x 10^3] for $\{[MoOS_3(CuIMes)](\mu^4\text{-}Cu)[MoOS_3(CuIMes)_2]\}_{0.36}\{[MoO_2S_2(CuIMes)](\mu^3\text{-}Cu)[MoOS_3(CuIMes)_2]\}_{0.64}\cdot Ph_3SiOH\cdot 2½C_6H_6$. U(eq) is defined as one third of the trace of the orthogonalized U_{ij} tensor.

Atom	x	y	z	U(eq)
C(53)	4651(2)	5191(2)	3819(2)	44(1)
C(54)	1606(2)	2967(2)	2017(2)	32(1)
C(55)	1204(2)	1308(1)	-665(1)	22(1)
C(56)	1688(2)	1070(1)	-1133(1)	24(1)
C(57)	1249(2)	323(2)	-1635(1)	27(1)
C(58)	361(2)	-176(1)	-1663(1)	28(1)
C(59)	-98(2)	85(1)	-1186(1)	27(1)
C(60)	313(2)	827(1)	-676(1)	24(1)
C(61)	2664(2)	1598(2)	-1085(2)	33(1)
C(62)	-85(2)	-993(2)	-2195(2)	41(1)
C(63)	-198(2)	1099(2)	-164(2)	29(1)
C(64)	-3014(2)	2825(1)	-1606(1)	25(1)
C(65)	-2963(2)	3369(2)	-2018(2)	36(1)
C(66)	-3751(2)	3621(2)	-2312(2)	37(1)
C(67)	-4623(2)	3320(2)	-2207(2)	38(1)
C(68)	-4707(3)	2759(3)	-1825(2)	61(1)
C(69)	-3908(2)	2516(2)	-1527(2)	51(1)
C(70)	-1164(2)	3416(1)	-189(1)	25(1)
C(71)	-1310(2)	4129(2)	-104(2)	38(1)
C(72)	-687(3)	4763(2)	527(2)	48(1)
C(73)	86(2)	4689(2)	1088(2)	37(1)
C(74)	236(2)	3993(2)	1016(2)	43(1)
C(75)	-385(2)	3363(2)	386(2)	43(1)
C(76)	-1114(2)	2484(1)	-1650(1)	22(1)
C(77)	-579(2)	3137(1)	-1800(1)	26(1)
C(78)	18(2)	3091(2)	-2224(1)	30(1)
C(79)	120(2)	2378(2)	-2490(1)	32(1)
C(80)	-382(2)	1724(1)	-2332(1)	27(1)
C(81)	-1005(2)	1778(1)	-1926(1)	24(1)
C(82A)	6972(2)	6472(2)	5472(3)	43(1)
C(83A)	7732(3)	7153(2)	5943(2)	44(1)
C(84A)	8707(2)	7180(2)	6148(2)	51(1)
C(85A)	8922(2)	6526(2)	5881(2)	43(1)
C(86A)	8162(3)	5845(2)	5410(2)	35(1)
C(87A)	7187(2)	5818(2)	5205(2)	42(1)
C(82B)	7432(3)	7071(2)	5849(3)	43(1)
C(83B)	8456(3)	7340(2)	6105(3)	44(1)
C(84B)	8950(3)	6846(2)	5918(4)	51(1)

Table S1. Atomic coordinates (x 10^4) and equivalent isotropic displacement parameters [$Å^2$ x 10^3] for $\{[MoOS_3(CuIMes)](\mu^4\text{-}Cu)[MoOS_3(CuIMes)_2]\}_{0.36}\{[MoO_2S_2(CuIMes)](\mu^3\text{-}Cu)[MoOS_3(CuIMes)_2]\}_{0.64}\cdot Ph_3SiOH\cdot 2½C_6H_6$. U(eq) is defined as one third of the trace of the orthogonalized U_{ij} tensor.

Atom	x	y	z	U(eq)
C(85B)	8419(3)	6083(2)	5476(3)	43(1)
C(86B)	7394(3)	5813(2)	5221(3)	35(1)
C(87B)	6901(3)	6307(2)	5408(4)	42(1)
C(88)	7622(3)	-2460(2)	3544(2)	51(1)
C(89)	7468(3)	-2520(2)	2781(2)	46(1)
C(90)	7217(2)	-3238(2)	2290(2)	48(1)
C(91)	7114(3)	-3885(2)	2570(2)	54(1)
C(92)	7263(3)	-3796(2)	3332(2)	56(1)
C(93)	7526(3)	-3082(2)	3822(2)	56(1)
C(94)	316(4)	718(4)	4895(4)	92(2)
C(95)	-25(4)	65(4)	4289(4)	95(2)
C(96)	-330(4)	-643(4)	4365(4)	100(2)

Table S2. Bond lengths (Å) for $\{[MoOS_3(CuIMes)](\mu^4\text{-}Cu)[MoOS_3(CuIMes)_2]\}_{0.36}\{[MoO_2S_2(CuIMes)](\mu^3\text{-}Cu)[MoOS_3(CuIMes)_2]\}_{0.64}\cdot Ph_3SiOH\cdot 2½C_6H_6$. Symmetry transformations used to generate equivalent atoms: #1 -x, -y, -z + 1.

Mo(1)-O(1)	1.7069(19)	N(3)-C(22)	1.356(3)
Mo(1)-S(3)	2.2514(9)	N(3)-C(23)	1.393(3)
Mo(1)-S(1)	2.2860(9)	N(3)-C(25)	1.442(3)
Mo(1)-S(2)	2.2883(8)	N(4)-C(22)	1.356(3)
Mo(1)-Cu(2)	2.6489(8)	N(4)-C(24)	1.390(3)
Mo(1)-Cu(4B)	2.6562(9)	N(4)-C(34)	1.443(3)
Mo(1)-Cu(1)	2.6703(7)	N(5)-C(43)	1.364(3)
Mo(1)-Cu(4A)	2.9481(12)	N(5)-C(44)	1.389(3)
Mo(2)-O(2)	1.7365(18)	N(5)-C(46)	1.444(3)
Mo(2)-O(3)	1.754(4)	N(6)-C(43)	1.362(3)
Mo(2)-S(6)	2.227(2)	N(6)-C(45)	1.390(3)
Mo(2)-S(5)	2.2409(10)	N(6)-C(55)	1.441(3)
Mo(2)-S(4)	2.3148(8)	C(2)-C(3)	1.342(4)
Mo(2)-Cu(3)	2.6865(7)	C(2)-H(2)	0.9300
Mo(2)-Cu(4A)	2.7489(11)	C(3)-H(3)	0.9300
Cu(1)-C(1)	1.928(2)	C(4)-C(5)	1.378(6)
Cu(1)-S(3)	2.2479(9)	C(4)-C(9)	1.422(5)
Cu(1)-S(1)	2.2489(9)	C(5)-C(6)	1.414(5)
Cu(2)-C(22)	1.916(2)	C(5)-C(10)	1.513(6)
Cu(2)-S(1)	2.2296(8)	C(6)-C(7)	1.398(8)
Cu(2)-S(2)	2.2319(9)	C(6)-H(6)	0.9300
Cu(3)-C(43)	1.933(2)	C(7)-C(8)	1.361(8)
Cu(3)-S(5)	2.2333(8)	C(7)-C(11)	1.536(5)
Cu(3)-S(4)	2.2469(10)	C(8)-C(9)	1.385(6)
Cu(3)-Cu(4B)	2.9953(10)	C(8)-H(8)	0.9300
Cu(4A)-S(4)	2.2319(12)	C(9)-C(12)	1.497(7)
Cu(4A)-S(6)	2.291(3)	C(10)-H(10A)	0.9600
Cu(4A)-S(2)	2.3014(12)	C(10)-H(10B)	0.9600
Cu(4A)-S(3)	2.7843(12)	C(10)-H(10C)	0.9600
Cu(4B)-S(4)	2.2145(9)	C(11)-H(11A)	0.9600
Cu(4B)-S(2)	2.2428(10)	C(11)-H(11B)	0.9600
Cu(4B)-S(3)	2.2878(9)	C(11)-H(11C)	0.9600
Si(1)-O(4)	1.6329(19)	C(12)-H(12A)	0.9600
Si(1)-C(64)	1.876(2)	C(12)-H(12B)	0.9600
Si(1)-C(70)	1.876(2)	C(12)-H(12C)	0.9600
Si(1)-C(76)	1.885(2)	C(13)-C(14)	1.392(4)
O(4)-H(4)	0.84(4)	C(13)-C(18)	1.393(4)
N(1)-C(1)	1.354(3)	C(14)-C(15)	1.390(5)
N(1)-C(2)	1.391(3)	C(14)-C(19)	1.511(4)
N(1)-C(4)	1.439(3)	C(15)-C(16)	1.379(5)
N(2)-C(1)	1.359(3)	C(15)-H(15)	0.930
N(2)-C(3)	1.384(3)		
N(2)-C(13)	1.444(3)		

Table S2. Bond lengths (Å) for $\{[MoOS_3(CuIMes)](\mu^4\text{-}Cu)[MoOS_3(CuIMes)_2]\}_{0.36}\{[MoO_2S_2(CuIMes)](\mu^3\text{-}Cu)[MoOS_3(CuIMes)_2]\}_{0.64}\cdot Ph_3SiOH\cdot 2½C_6H_6$. Symmetry transformations used to generate equivalent atoms: #1 -x, -y, -z + 1.

C(16)-C(17)	1.386(5)	C(36)-H(36)	0.9300
C(16)-C(20)	1.524(5)	C(37)-C(38)	1.390(4)
C(17)-C(18)	1.393(4)	C(37)-C(41)	1.509(3)
C(17)-H(17)	0.9300	C(38)-C(39)	1.393(3)
C(18)-C(21)	1.499(4)	C(38)-H(38)	0.9300
C(19)-H(19A)	0.9600	C(39)-C(42)	1.509(3)
C(19)-H(19B)	0.9600	C(40)-H(40A)	0.9600
C(19)-H(19C)	0.9600	C(40)-H(40B)	0.9600
C(20)-H(20A)	0.9600	C(40)-H(40C)	0.9600
C(20)-H(20B)	0.9600	C(41)-H(41A)	0.9600
C(20)-H(20C)	0.9600	C(41)-H(41B)	0.9600
C(21)-H(21A)	0.9600	C(41)-H(41C)	0.9600
C(21)-H(21B)	0.9600	C(42)-H(42A)	0.9600
C(21)-H(21C)	0.9600	C(42)-H(42B)	0.9600
C(23)-C(24)	1.344(4)	C(42)-H(42C)	0.9600
C(23)-H(23)	0.9300	C(44)-C(45)	1.344(3)
C(24)-H(24)	0.9300	C(44)-H(44)	0.9300
C(25)-C(26)	1.391(4)	C(45)-H(45)	0.9300
C(25)-C(30)	1.394(3)	C(46)-C(51)	1.395(3)
C(26)-C(27)	1.395(4)	C(46)-C(47)	1.399(3)
C(26)-C(31)	1.509(4)	C(47)-C(48)	1.394(3)
C(27)-C(28)	1.389(4)	C(47)-C(52)	1.507(4)
C(27)-H(27)	0.9300	C(48)-C(49)	1.388(4)
C(28)-C(29)	1.387(5)	C(48)-H(48)	0.9300
C(28)-C(32)	1.516(4)	C(49)-C(50)	1.389(4)
C(29)-C(30)	1.395(4)	C(49)-C(53)	1.519(4)
C(29)-H(29)	0.9300	C(50)-C(51)	1.396(3)
C(30)-C(33)	1.512(4)	C(50)-H(50)	0.9300
C(31)-H(31A)	0.9600	C(51)-C(54)	1.515(4)
C(31)-H(31B)	0.9600	C(52)-H(52A)	0.9600
C(31)-H(31C)	0.9600	C(52)-H(52B)	0.9600
C(32)-H(32A)	0.9600	C(52)-H(52C)	0.9600
C(32)-H(32B)	0.9600	C(53)-H(53A)	0.9600
C(32)-H(32C)	0.9600	C(53)-H(53B)	0.9600
C(33)-H(33A)	0.9600	C(53)-H(53C)	0.9600
C(33)-H(33B)	0.9600	C(54)-H(54A)	0.9600
C(33)-H(33C)	0.9600	C(54)-H(54B)	0.9600
C(34)-C(35)	1.390(3)	C(54)-H(54C)	0.9600
C(34)-C(39)	1.395(3)	C(55)-C(56)	1.395(3)
C(35)-C(36)	1.393(4)	C(55)-C(60)	1.398(3)
C(35)-C(40)	1.510(4)	C(56)-C(57)	1.393(3)
C(36)-C(37)	1.385(4)	C(56)-C(61)	1.507(3)

Table S2. Bond lengths (Å) for $\{[MoOS_3(CuIMes)](\mu^4\text{-}Cu)[MoOS_3(CuIMes)_2]\}_{0.36}\{[MoO_2S_2(CuIMes)](\mu^3\text{-}Cu)[MoOS_3(CuIMes)_2]\}_{0.64}\cdot Ph_3SiOH\cdot 2½C_6H_6$. Symmetry transformations used to generate equivalent atoms: #1 -x, -y, -z + 1.

C(57)-C(58)	1.394(4)	C(78)-C(79)	1.399(4)
C(57)-H(57)	0.9300	C(78)-H(78)	0.9300
C(58)-C(59)	1.392(4)	C(79)-C(80)	1.389(4)
C(58)-C(62)	1.512(4)	C(79)-H(79)	0.9300
C(59)-C(60)	1.392(3)	C(80)-C(81)	1.397(3)
C(59)-H(59)	0.9300	C(80)-H(80)	0.9300
C(60)-C(63)	1.511(3)	C(81)-H(81)	0.9300
C(61)-H(61A)	0.9600	C(82A)-C(83A)	1.3900
C(61)-H(61B)	0.9600	C(82A)-C(87A)	1.3900
C(61)-H(61C)	0.9600	C(82A)-H(82A)	0.9300
C(62)-H(62A)	0.9600	C(83A)-C(84A)	1.3900
C(62)-H(62B)	0.9600	C(83A)-H(83A)	0.9300
C(62)-H(62C)	0.9600	C(84A)-C(85A)	1.3900
C(63)-H(63A)	0.9600	C(84A)-H(84A)	0.9300
C(63)-H(63B)	0.9600	C(85A)-C(86A)	1.3900
C(63)-H(63C)	0.9600	C(85A)-H(85A)	0.9300
C(64)-C(69)	1.385(4)	C(86A)-C(87A)	1.3900
C(64)-C(65)	1.391(3)	C(86A)-H(86A)	0.9300
C(65)-C(66)	1.393(4)	C(87A)-H(87A)	0.9300
C(65)-H(65)	0.9300	C(82B)-C(83B)	1.3900
C(66)-C(67)	1.378(4)	C(82B)-C(87B)	1.3900
C(66)-H(66)	0.9300	C(82B)-H(82B)	0.9300
C(67)-C(68)	1.379(5)	C(83B)-C(84B)	1.3900
C(67)-H(67)	0.9300	C(83B)-H(83B)	0.9300
C(68)-C(69)	1.398(4)	C(84B)-C(85B)	1.3900
C(68)-H(68)	0.9300	C(84B)-H(84B)	0.9300
C(69)-H(69)	0.9300	C(85B)-C(86B)	1.3900
C(70)-C(75)	1.386(4)	C(85B)-H(85B)	0.9300
C(70)-C(71)	1.394(4)	C(86B)-C(87B)	1.3900
C(71)-C(72)	1.394(4)	C(86B)-H(86B)	0.9300
C(71)-H(71)	0.9300	C(87B)-H(87B)	0.9300
C(72)-C(73)	1.384(4)	C(88)-C(93)	1.352(5)
C(72)-H(72)	0.9300	C(88)-C(89)	1.380(5)
C(73)-C(74)	1.365(4)	C(88)-H(88)	0.9300
C(73)-H(73)	0.9300	C(89)-C(90)	1.368(5)
C(74)-C(75)	1.389(4)	C(89)-H(89)	0.9300
C(74)-H(74)	0.9300	C(90)-C(91)	1.395(5)
C(75)-H(75)	0.9300	C(90)-H(90)	0.9300
C(76)-C(81)	1.398(3)	C(91)-C(92)	1.373(5)
C(76)-C(77)	1.401(3)	C(91)-H(91)	0.9300
C(77)-C(78)	1.387(4)	C(92)-C(93)	1.359(6)
C(77)-H(77)	0.9300	C(92)-H(92)	0.930

Table S2. Bond lengths (Å) for {[$MoOS_3$(CuIMes)](μ^4-Cu)[$MoOS_3$($CuIMes)_2$]}$_{0.36}${[MoO_2S_2(CuIMes)](μ^3-Cu)[$MoOS_3$($CuIMes)_2$]}$_{0.64}$·Ph_3SiOH·2½C_6H_6. Symmetry transformations used to generate equivalent atoms: #1 -x, -y, -z + 1.

C(93)-H(93)	0.9300
C(94)-C(95)	1.371(8)
C(94)-C(96)#1	1.438(9)
C(94)-H(94)	0.9300
C(95)-C(96)	1.328(8)
C(95)-H(95)	0.9300
C(96)-C(94)#1	1.438(9)
C(96)-H(96)	0.9300

Table S3. Bond angles (deg.) for {[$MoOS_3$(CuIMes)](μ^4-Cu)[$MoOS_3$(CuIMes)$_2$]}$_{0.36}${[MoO_2S_2(CuIMes)](μ^3-Cu)[$MoOS_3$(CuIMes)$_2$]}$_{0.64}$·Ph_3SiOH·2½C_6H_6. Symmetry transformations used to generate equivalent atoms: #1 -x, -y, -z + 1.

O(1)-Mo(1)-S(3)	113.04(7)	S(6)-Mo(2)-Cu(4A)	53.59(7)
O(1)-Mo(1)-S(1)	110.68(7)	S(5)-Mo(2)-Cu(4A)	113.79(3)
S(3)-Mo(1)-S(1)	106.80(3)	S(4)-Mo(2)-Cu(4A)	51.44(3)
O(1)-Mo(1)-S(2)	111.73(8)	Cu(3)-Mo(2)-Cu(4A)	77.20(3)
S(3)-Mo(1)-S(2)	108.03(3)	C(1)-Cu(1)-S(3)	122.08(7)
S(1)-Mo(1)-S(2)	106.21(3)	C(1)-Cu(1)-S(1)	125.76(8)
O(1)-Mo(1)-Cu(2)	125.48(7)	S(3)-Cu(1)-S(1)	108.21(3)
S(3)-Mo(1)-Cu(2)	121.47(3)	C(1)-Cu(1)-Mo(1)	163.18(8)
S(1)-Mo(1)-Cu(2)	53.101(18)	S(3)-Cu(1)-Mo(1)	53.66(2)
S(2)-Mo(1)-Cu(2)	53.14(2)	S(1)-Cu(1)-Mo(1)	54.57(2)
O(1)-Mo(1)-Cu(4B)	133.41(7)	C(22)-Cu(2)-S(1)	125.30(7)
S(3)-Mo(1)-Cu(4B)	54.83(2)	C(22)-Cu(2)-S(2)	124.09(7)
S(1)-Mo(1)-Cu(4B)	115.87(3)	S(1)-Cu(2)-S(2)	110.16(3)
S(2)-Mo(1)-Cu(4B)	53.32(3)	C(22)-Cu(2)-Mo(1)	172.27(7)
Cu(2)-Mo(1)-Cu(4B)	83.50(2)	S(1)-Cu(2)-Mo(1)	55.08(2)
O(1)-Mo(1)-Cu(1)	129.81(8)	S(2)-Cu(2)-Mo(1)	55.120(19)
S(3)-Mo(1)-Cu(1)	53.53(2)	C(43)-Cu(3)-S(5)	122.98(7)
S(1)-Mo(1)-Cu(1)	53.29(2)	C(43)-Cu(3)-S(4)	128.46(7)
S(2)-Mo(1)-Cu(1)	118.40(3)	S(5)-Cu(3)-S(4)	108.20(3)
Cu(2)-Mo(1)-Cu(1)	85.30(3)	C(43)-Cu(3)-Mo(2)	175.73(7)
Cu(4B)-Mo(1)-Cu(1)	82.44(3)	S(5)-Cu(3)-Mo(2)	53.23(3)
O(1)-Mo(1)-Cu(4A)	150.17(7)	S(4)-Cu(3)-Mo(2)	55.098(18)
S(3)-Mo(1)-Cu(4A)	63.09(3)	C(43)-Cu(3)-Cu(4B)	116.35(7)
S(1)-Mo(1)-Cu(4A)	98.18(4)	S(5)-Cu(3)-Cu(4B)	105.46(3)
S(2)-Mo(1)-Cu(4A)	50.23(3)	S(4)-Cu(3)-Cu(4B)	47.37(3)
Cu(2)-Mo(1)-Cu(4A)	66.86(3)	Mo(2)-Cu(3)-Cu(4B)	67.65(2)
Cu(4B)-Mo(1)-Cu(4A)	18.524(18)	S(4)-Cu(4A)-S(6)	104.65(7)
Cu(1)-Mo(1)-Cu(4A)	73.87(3)	S(4)-Cu(4A)-S(2)	120.44(4)
O(2)-Mo(2)-O(3)	111.32(16)	S(6)-Cu(4A)-S(2)	131.73(7)
O(2)-Mo(2)-S(6)	112.75(9)	S(4)-Cu(4A)-Mo(2)	54.19(2)
O(3)-Mo(2)-S(6)	7.54(19)	S(6)-Cu(4A)-Mo(2)	51.47(6)
O(2)-Mo(2)-S(5)	110.62(7)	S(2)-Cu(4A)-Mo(2)	171.96(4)
O(3)-Mo(2)-S(5)	107.70(15)	S(4)-Cu(4A)-S(3)	106.84(4)
S(6)-Mo(2)-S(5)	113.05(7)	S(6)-Cu(4A)-S(3)	90.61(7)
O(2)-Mo(2)-S(4)	110.33(7)	S(2)-Cu(4A)-S(3)	91.99(4)
O(3)-Mo(2)-S(4)	111.08(15)	Mo(2)-Cu(4A)-S(3)	95.42(4)
S(6)-Mo(2)-S(4)	104.02(7)	S(4)-Cu(4A)-Mo(1)	139.70(4)
S(5)-Mo(2)-S(4)	105.61(3)	S(6)-Cu(4A)-Mo(1)	104.70(7)
O(2)-Mo(2)-Cu(3)	128.34(7)	S(2)-Cu(4A)-Mo(1)	49.84(3)
O(3)-Mo(2)-Cu(3)	120.32(15)		
S(6)-Mo(2)-Cu(3)	118.64(7)		
S(5)-Mo(2)-Cu(3)	52.969(18)		
S(4)-Mo(2)-Cu(3)	52.76(3)		
O(2)-Mo(2)-Cu(4A)	135.16(7)		
O(3)-Mo(2)-Cu(4A)	60.14(15)		

Table S3. Bond angles (deg.) for {[$MoOS_3$(CuIMes)](μ^4-Cu)[$MoOS_3$(CuIMes)$_2$]}$_{0.36}${[MoO_2S_2(CuIMes)](μ^3-Cu)[$MoOS_3$(CuIMes)$_2$]}$_{0.64}$·Ph_3SiOH·2½C_6H_6. Symmetry transformations used to generate equivalent atoms: #1 -x, -y, -z + 1.

Mo(2)-Cu(4A)-Mo(1)	138.20(3)	C(22)-N(3)-C(23)	111.3(2)
S(3)-Cu(4A)-Mo(1)	46.14(2)	C(22)-N(3)-C(25)	123.53(19)
Mo(2)-S(6)-Cu(4A)	74.94(8)	C(23)-N(3)-C(25)	125.14(19)
S(4)-Cu(4B)-S(2)	123.96(3)	C(22)-N(4)-C(24)	111.39(19)
S(4)-Cu(4B)-S(3)	127.69(3)	C(22)-N(4)-C(34)	123.24(19)
S(2)-Cu(4B)-S(3)	108.34(4)	C(24)-N(4)-C(34)	125.3(2)
S(4)-Cu(4B)-Mo(1)	177.17(3)	C(43)-N(5)-C(44)	111.60(19)
S(2)-Cu(4B)-Mo(1)	54.91(2)	C(43)-N(5)-C(46)	126.18(18)
S(3)-Cu(4B)-Mo(1)	53.55(3)	C(44)-N(5)-C(46)	122.15(19)
S(4)-Cu(4B)-Cu(3)	48.29(2)	C(43)-N(6)-C(45)	111.91(19)
S(2)-Cu(4B)-Cu(3)	164.97(3)	C(43)-N(6)-C(55)	124.75(19)
S(3)-Cu(4B)-Cu(3)	80.68(3)	C(45)-N(6)-C(55)	123.31(19)
Mo(1)-Cu(4B)-Cu(3)	133.52(2)	N(1)-C(1)-N(2)	103.7(2)
Cu(2)-S(1)-Cu(1)	107.16(4)	N(1)-C(1)-Cu(1)	133.04(18)
Cu(2)-S(1)-Mo(1)	71.82(3)	N(2)-C(1)-Cu(1)	123.29(19)
Cu(1)-S(1)-Mo(1)	72.14(2)	C(3)-C(2)-N(1)	106.5(2)
Cu(2)-S(2)-Cu(4B)	104.26(3)	C(3)-C(2)-H(2)	126.7
Cu(2)-S(2)-Mo(1)	71.74(3)	N(1)-C(2)-H(2)	126.7
Cu(4B)-S(2)-Mo(1)	71.77(3)	C(2)-C(3)-N(2)	106.6(2)
Cu(2)-S(2)-Cu(4A)	86.04(3)	C(2)-C(3)-H(3)	126.7
Mo(1)-S(2)-Cu(4A)	79.93(4)	N(2)-C(3)-H(3)	126.7
Cu(1)-S(3)-Mo(1)	72.81(2)	C(5)-C(4)-C(9)	123.8(3)
Cu(1)-S(3)-Cu(4B)	101.39(3)	C(5)-C(4)-N(1)	118.0(3)
Mo(1)-S(3)-Cu(4B)	71.62(3)	C(9)-C(4)-N(1)	118.2(3)
Cu(1)-S(3)-Cu(4A)	83.77(3)	C(4)-C(5)-C(6)	116.5(4)
Mo(1)-S(3)-Cu(4A)	70.77(3)	C(4)-C(5)-C(10)	121.3(3)
Cu(4B)-S(4)-Cu(3)	84.34(3)	C(6)-C(5)-C(10)	122.2(4)
Cu(4A)-S(4)-Cu(3)	98.44(3)	C(7)-C(6)-C(5)	121.1(5)
Cu(4B)-S(4)-Mo(2)	88.93(4)	C(7)-C(6)-H(6)	119.5
Cu(4A)-S(4)-Mo(2)	74.37(4)	C(5)-C(6)-H(6)	119.5
Cu(3)-S(4)-Mo(2)	72.14(2)	C(8)-C(7)-C(6)	119.7(4)
Cu(3)-S(5)-Mo(2)	73.80(3)	C(8)-C(7)-C(11)	122.3(6)
O(4)-Si(1)-C(64)	111.36(11)	C(6)-C(7)-C(11)	118.0(6)
O(4)-Si(1)-C(70)	108.03(11)	C(7)-C(8)-C(9)	122.7(5)
C(64)-Si(1)-C(70)	106.88(11)	C(7)-C(8)-H(8)	118.7
O(4)-Si(1)-C(76)	110.65(10)	C(9)-C(8)-H(8)	118.7
C(64)-Si(1)-C(76)	112.13(10)	C(8)-C(9)-C(4)	116.2(5)
C(70)-Si(1)-C(76)	107.56(11)	C(8)-C(9)-C(12)	121.0(4)
Si(1)-O(4)-H(4)	122(3)	C(4)-C(9)-C(12)	122.8(3)
C(1)-N(1)-C(2)	111.5(2)		
C(1)-N(1)-C(4)	124.5(2)		
C(2)-N(1)-C(4)	123.9(2)		
C(1)-N(2)-C(3)	111.7(2)		
C(1)-N(2)-C(13)	123.1(2)		
C(3)-N(2)-C(13)	125.1(2)		

Table S3. Bond angles (deg.) for {[$MoOS_3$(CuIMes)](μ^4-Cu)[$MoOS_3$(CuIMes)$_2$]}$_{0.36}${[MoO_2S_2(CuIMes)](μ^3-Cu)[$MoOS_3$(CuIMes)$_2$]}$_{0.64}$·Ph_3SiOH· 2½C_6H_6. Symmetry transformations used to generate equivalent atoms: #1 -x, -y, -z + 1.

C(5)-C(10)-H(10A)	109.5	C(16)-C(20)-H(20A)	109.5
C(5)-C(10)-H(10B)	109.5	C(16)-C(20)-H(20B)	109.5
H(10A)-C(10)-H(10B)	109.5	H(20A)-C(20)-H(20B)	109.5
C(5)-C(10)-H(10C)	109.5	C(16)-C(20)-H(20C)	109.5
H(10A)-C(10)-H(10C)	109.5	H(20A)-C(20)-H(20C)	109.5
H(10B)-C(10)-H(10C)	109.5	H(20B)-C(20)-H(20C)	109.5
C(7)-C(11)-H(11A)	109.5	C(18)-C(21)-H(21A)	109.5
C(7)-C(11)-H(11B)	109.5	C(18)-C(21)-H(21B)	109.5
H(11A)-C(11)-H(11B)	109.5	H(21A)-C(21)-H(21B)	109.5
C(7)-C(11)-H(11C)	109.5	C(18)-C(21)-H(21C)	109.5
H(11A)-C(11)-H(11C)	109.5	H(21A)-C(21)-H(21C)	109.5
H(11B)-C(11)-H(11C)	109.5	H(21B)-C(21)-H(21C)	109.5
C(9)-C(12)-H(12A)	109.5	N(4)-C(22)-N(3)	104.11(19)
C(9)-C(12)-H(12B)	109.5	N(4)-C(22)-Cu(2)	127.80(16)
H(12A)-C(12)-H(12B)	109.5	N(3)-C(22)-Cu(2)	128.09(17)
C(9)-C(12)-H(12C)	109.5	C(24)-C(23)-N(3)	106.6(2)
H(12A)-C(12)-H(12C)	109.5	C(24)-C(23)-H(23)	126.7
H(12B)-C(12)-H(12C)	109.5	N(3)-C(23)-H(23)	126.7
C(14)-C(13)-C(18)	122.6(3)	C(23)-C(24)-N(4)	106.6(2)
C(14)-C(13)-N(2)	118.3(2)	C(23)-C(24)-H(24)	126.7
C(18)-C(13)-N(2)	119.1(2)	N(4)-C(24)-H(24)	126.7
C(15)-C(14)-C(13)	117.2(3)	C(26)-C(25)-C(30)	122.4(2)
C(15)-C(14)-C(19)	122.1(3)	C(26)-C(25)-N(3)	119.2(2)
C(13)-C(14)-C(19)	120.7(3)	C(30)-C(25)-N(3)	118.4(2)
C(16)-C(15)-C(14)	122.2(3)	C(25)-C(26)-C(27)	117.6(2)
C(16)-C(15)-H(15)	118.9	C(25)-C(26)-C(31)	122.1(2)
C(14)-C(15)-H(15)	118.9	C(27)-C(26)-C(31)	120.3(3)
C(15)-C(16)-C(17)	118.9(3)	C(28)-C(27)-C(26)	122.0(3)
C(15)-C(16)-C(20)	121.9(3)	C(28)-C(27)-H(27)	119.0
C(17)-C(16)-C(20)	119.2(4)	C(26)-C(27)-H(27)	119.0
C(16)-C(17)-C(18)	121.4(3)	C(29)-C(28)-C(27)	118.6(3)
C(16)-C(17)-H(17)	119.3	C(29)-C(28)-C(32)	121.0(3)
C(18)-C(17)-H(17)	119.3	C(27)-C(28)-C(32)	120.4(3)
C(13)-C(18)-C(17)	117.6(3)	C(28)-C(29)-C(30)	121.7(3)
C(13)-C(18)-C(21)	120.9(3)	C(28)-C(29)-H(29)	119.2
C(17)-C(18)-C(21)	121.4(3)	C(30)-C(29)-H(29)	119.2
C(14)-C(19)-H(19A)	109.5	C(25)-C(30)-C(29)	117.8(3)
C(14)-C(19)-H(19B)	109.5	C(25)-C(30)-C(33)	121.0(2)
H(19A)-C(19)-H(19B)	109.5	C(29)-C(30)-C(33)	121.2(3)
C(14)-C(19)-H(19C)	109.5	C(26)-C(31)-H(31A)	109.5
H(19A)-C(19)-H(19C)	109.5	C(26)-C(31)-H(31B)	109.5
H(19B)-C(19)-H(19C)	109.5	H(31A)-C(31)-H(31B)	109.5

Table S3. Bond angles (deg.) for $\{[MoOS_3(CuIMes)](\mu^4\text{-}Cu)[MoOS_3(CuIMes)_2]\}_{0.36}\{[MoO_2S_2(CuIMes)](\mu^3\text{-}Cu)[MoOS_3(CuIMes)_2]\}_{0.64}\cdot Ph_3SiOH\cdot 2½C_6H_6$. Symmetry transformations used to generate equivalent atoms: #1 -x, -y, -z + 1.

C(26)-C(31)-H(31C)	109.5	C(37)-C(41)-H(41C)	109.5
H(31A)-C(31)-H(31C)	109.5	H(41A)-C(41)-H(41C)	109.5
H(31B)-C(31)-H(31C)	109.5	H(41B)-C(41)-H(41C)	109.5
C(28)-C(32)-H(32A)	109.5	C(39)-C(42)-H(42A)	109.5
C(28)-C(32)-H(32B)	109.5	C(39)-C(42)-H(42B)	109.5
H(32A)-C(32)-H(32B)	109.5	H(42A)-C(42)-H(42B)	109.5
C(28)-C(32)-H(32C)	109.5	C(39)-C(42)-H(42C)	109.5
H(32A)-C(32)-H(32C)	109.5	H(42A)-C(42)-H(42C)	109.5
H(32B)-C(32)-H(32C)	109.5	H(42B)-C(42)-H(42C)	109.5
C(30)-C(33)-H(33A)	109.5	N(6)-C(43)-N(5)	103.28(18)
C(30)-C(33)-H(33B)	109.5	N(6)-C(43)-Cu(3)	126.47(17)
H(33A)-C(33)-H(33B)	109.5	N(5)-C(43)-Cu(3)	130.21(16)
C(30)-C(33)-H(33C)	109.5	C(45)-C(44)-N(5)	106.8(2)
H(33A)-C(33)-H(33C)	109.5	C(45)-C(44)-H(44)	126.6
H(33B)-C(33)-H(33C)	109.5	N(5)-C(44)-H(44)	126.6
C(35)-C(34)-C(39)	122.8(2)	C(44)-C(45)-N(6)	106.4(2)
C(35)-C(34)-N(4)	118.9(2)	C(44)-C(45)-H(45)	126.8
C(39)-C(34)-N(4)	118.3(2)	N(6)-C(45)-H(45)	126.8
C(34)-C(35)-C(36)	117.6(2)	C(51)-C(46)-C(47)	122.8(2)
C(34)-C(35)-C(40)	121.3(2)	C(51)-C(46)-N(5)	118.9(2)
C(36)-C(35)-C(40)	121.1(2)	C(47)-C(46)-N(5)	118.2(2)
C(37)-C(36)-C(35)	121.7(2)	C(48)-C(47)-C(46)	117.4(2)
C(37)-C(36)-H(36)	119.2	C(48)-C(47)-C(52)	120.3(2)
C(35)-C(36)-H(36)	119.2	C(46)-C(47)-C(52)	122.3(2)
C(36)-C(37)-C(38)	118.8(2)	C(49)-C(48)-C(47)	121.6(2)
C(36)-C(37)-C(41)	120.2(3)	C(49)-C(48)-H(48)	119.2
C(38)-C(37)-C(41)	121.0(3)	C(47)-C(48)-H(48)	119.2
C(37)-C(38)-C(39)	121.8(2)	C(48)-C(49)-C(50)	119.1(2)
C(37)-C(38)-H(38)	119.1	C(48)-C(49)-C(53)	120.7(3)
C(39)-C(38)-H(38)	119.1	C(50)-C(49)-C(53)	120.1(3)
C(38)-C(39)-C(34)	117.3(2)	C(49)-C(50)-C(51)	121.6(3)
C(38)-C(39)-C(42)	121.5(2)	C(49)-C(50)-H(50)	119.2
C(34)-C(39)-C(42)	121.2(2)	C(51)-C(50)-H(50)	119.2
C(35)-C(40)-H(40A)	109.5	C(46)-C(51)-C(50)	117.4(2)
C(35)-C(40)-H(40B)	109.5	C(46)-C(51)-C(54)	122.6(2)
H(40A)-C(40)-H(40B)	109.5	C(50)-C(51)-C(54)	120.0(2)
C(35)-C(40)-H(40C)	109.5	C(47)-C(52)-H(52A)	109.5
H(40A)-C(40)-H(40C)	109.5	C(47)-C(52)-H(52B)	109.5
H(40B)-C(40)-H(40C)	109.5	H(52A)-C(52)-H(52B)	109.5
C(37)-C(41)-H(41A)	109.5	C(47)-C(52)-H(52C)	109.5
C(37)-C(41)-H(41B)	109.5	H(52A)-C(52)-H(52C)	109.5
H(41A)-C(41)-H(41B)	109.5	H(52B)-C(52)-H(52C)	109.5

Table S3. Bond angles (deg.) for $\{[MoOS_3(CuIMes)](\mu^4\text{-}Cu)[MoOS_3(CuIMes)_2]\}_{0.36}\{[MoO_2S_2(CuIMes)](\mu^3\text{-}Cu)[MoOS_3(CuIMes)_2]\}_{0.64}\cdot Ph_3SiOH\cdot 2½C_6H_6$. Symmetry transformations used to generate equivalent atoms: #1 -x, -y, -z + 1.

C(49)-C(53)-H(53A)	109.5	C(60)-C(63)-H(63A)	109.5
C(49)-C(53)-H(53B)	109.5	C(60)-C(63)-H(63B)	109.5
H(53A)-C(53)-H(53B)	109.5	H(63A)-C(63)-H(63B)	109.5
C(49)-C(53)-H(53C)	109.5	C(60)-C(63)-H(63C)	109.5
H(53A)-C(53)-H(53C)	109.5	H(63A)-C(63)-H(63C)	109.5
H(53B)-C(53)-H(53C)	109.5	H(63B)-C(63)-H(63C)	109.5
C(51)-C(54)-H(54A)	109.5	C(69)-C(64)-C(65)	116.6(2)
C(51)-C(54)-H(54B)	109.5	C(69)-C(64)-Si(1)	119.4(2)
H(54A)-C(54)-H(54B)	109.5	C(65)-C(64)-Si(1)	123.60(19)
C(51)-C(54)-H(54C)	109.5	C(64)-C(65)-C(66)	122.3(3)
H(54A)-C(54)-H(54C)	109.5	C(64)-C(65)-H(65)	118.8
H(54B)-C(54)-H(54C)	109.5	C(66)-C(65)-H(65)	118.8
C(56)-C(55)-C(60)	122.7(2)	C(67)-C(66)-C(65)	119.8(3)
C(56)-C(55)-N(6)	118.7(2)	C(67)-C(66)-H(66)	120.1
C(60)-C(55)-N(6)	118.5(2)	C(65)-C(66)-H(66)	120.1
C(57)-C(56)-C(55)	117.8(2)	C(66)-C(67)-C(68)	119.1(3)
C(57)-C(56)-C(61)	121.1(2)	C(66)-C(67)-H(67)	120.4
C(55)-C(56)-C(61)	121.1(2)	C(68)-C(67)-H(67)	120.4
C(56)-C(57)-C(58)	121.2(2)	C(67)-C(68)-C(69)	120.5(3)
C(56)-C(57)-H(57)	119.4	C(67)-C(68)-H(68)	119.8
C(58)-C(57)-H(57)	119.4	C(69)-C(68)-H(68)	119.8
C(59)-C(58)-C(57)	119.1(2)	C(64)-C(69)-C(68)	121.6(3)
C(59)-C(58)-C(62)	120.6(2)	C(64)-C(69)-H(69)	119.2
C(57)-C(58)-C(62)	120.2(2)	C(68)-C(69)-H(69)	119.2
C(60)-C(59)-C(58)	121.6(2)	C(75)-C(70)-C(71)	117.1(2)
C(60)-C(59)-H(59)	119.2	C(75)-C(70)-Si(1)	120.98(19)
C(58)-C(59)-H(59)	119.2	C(71)-C(70)-Si(1)	121.75(19)
C(59)-C(60)-C(55)	117.5(2)	C(72)-C(71)-C(70)	121.0(3)
C(59)-C(60)-C(63)	120.8(2)	C(72)-C(71)-H(71)	119.5
C(55)-C(60)-C(63)	121.7(2)	C(70)-C(71)-H(71)	119.5
C(56)-C(61)-H(61A)	109.5	C(73)-C(72)-C(71)	120.2(3)
C(56)-C(61)-H(61B)	109.5	C(73)-C(72)-H(72)	119.9
H(61A)-C(61)-H(61B)	109.5	C(71)-C(72)-H(72)	119.9
C(56)-C(61)-H(61C)	109.5	C(74)-C(73)-C(72)	119.5(3)
H(61A)-C(61)-H(61C)	109.5	C(74)-C(73)-H(73)	120.3
H(61B)-C(61)-H(61C)	109.5	C(72)-C(73)-H(73)	120.3
C(58)-C(62)-H(62A)	109.5	C(73)-C(74)-C(75)	120.2(3)
C(58)-C(62)-H(62B)	109.5	C(73)-C(74)-H(74)	119.9
H(62A)-C(62)-H(62B)	109.5	C(75)-C(74)-H(74)	119.9
C(58)-C(62)-H(62C)	109.5	C(70)-C(75)-C(74)	122.0(3)
H(62A)-C(62)-H(62C)	109.5	C(70)-C(75)-H(75)	119.0
H(62B)-C(62)-H(62C)	109.5	C(74)-C(75)-H(75)	119.0

Table S3. Bond angles (deg.) for {[$MoOS_3$(CuIMes)](μ^4-Cu)[$MoOS_3$(CuIMes)$_2$]}$_{0.36}${[MoO_2S_2(CuIMes)](μ^3-Cu)[$MoOS_3$(CuIMes)$_2$]}$_{0.64}$·Ph_3SiOH·
2½C_6H_6. Symmetry transformations used to generate equivalent atoms: #1 -x, -y, -z + 1.

C(81)-C(76)-C(77)	117.3(2)	C(84B)-C(83B)-H(83B)	120.0
C(81)-C(76)-Si(1)	122.58(18)	C(85B)-C(84B)-C(83B)	120.0
C(77)-C(76)-Si(1)	120.12(18)	C(85B)-C(84B)-H(84B)	120.0
C(78)-C(77)-C(76)	122.1(2)	C(83B)-C(84B)-H(84B)	120.0
C(78)-C(77)-H(77)	118.9	C(86B)-C(85B)-C(84B)	120.0
C(76)-C(77)-H(77)	118.9	C(86B)-C(85B)-H(85B)	120.0
C(77)-C(78)-C(79)	119.4(2)	C(84B)-C(85B)-H(85B)	120.0
C(77)-C(78)-H(78)	120.3	C(87B)-C(86B)-C(85B)	120.0
C(79)-C(78)-H(78)	120.3	C(87B)-C(86B)-H(86B)	120.0
C(80)-C(79)-C(78)	119.8(2)	C(85B)-C(86B)-H(86B)	120.0
C(80)-C(79)-H(79)	120.1	C(86B)-C(87B)-C(82B)	120.0
C(78)-C(79)-H(79)	120.1	C(86B)-C(87B)-H(87B)	120.0
C(79)-C(80)-C(81)	119.9(2)	C(82B)-C(87B)-H(87B)	120.0
C(79)-C(80)-H(80)	120.0	C(93)-C(88)-C(89)	122.6(3)
C(81)-C(80)-H(80)	120.0	C(93)-C(88)-H(88)	118.7
C(80)-C(81)-C(76)	121.5(2)	C(89)-C(88)-H(88)	118.7
C(80)-C(81)-H(81)	119.3	C(90)-C(89)-C(88)	118.5(3)
C(76)-C(81)-H(81)	119.3	C(90)-C(89)-H(89)	120.8
C(83A)-C(82A)-C(87A)	120.0	C(88)-C(89)-H(89)	120.8
C(83A)-C(82A)-H(82A)	120.0	C(89)-C(90)-C(91)	119.5(3)
C(87A)-C(82A)-H(82A)	120.0	C(89)-C(90)-H(90)	120.2
C(84A)-C(83A)-C(82A)	120.0	C(91)-C(90)-H(90)	120.2
C(84A)-C(83A)-H(83A)	120.0	C(92)-C(91)-C(90)	119.8(4)
C(82A)-C(83A)-H(83A)	120.0	C(92)-C(91)-H(91)	120.1
C(85A)-C(84A)-C(83A)	120.0	C(90)-C(91)-H(91)	120.1
C(85A)-C(84A)-H(84A)	120.0	C(93)-C(92)-C(91)	120.7(3)
C(83A)-C(84A)-H(84A)	120.0	C(93)-C(92)-H(92)	119.7
C(84A)-C(85A)-C(86A)	120.0	C(91)-C(92)-H(92)	119.7
C(84A)-C(85A)-H(85A)	120.0	C(88)-C(93)-C(92)	118.9(4)
C(86A)-C(85A)-H(85A)	120.0	C(88)-C(93)-H(93)	120.6
C(87A)-C(86A)-C(85A)	120.0	C(92)-C(93)-H(93)	120.6
C(87A)-C(86A)-H(86A)	120.0	C(95)-C(94)-C(96)#1	119.5(6)
C(85A)-C(86A)-H(86A)	120.0	C(95)-C(94)-H(94)	120.2
C(86A)-C(87A)-C(82A)	120.0	C(96)#1-C(94)-H(94)	120.2
C(86A)-C(87A)-H(87A)	120.0	C(96)-C(95)-C(94)	122.1(7)
C(82A)-C(87A)-H(87A)	120.0	C(96)-C(95)-H(95)	119.0
C(83B)-C(82B)-C(87B)	120.0	C(94)-C(95)-H(95)	119.0
C(83B)-C(82B)-H(82B)	120.0	C(95)-C(96)-C(94)#1	118.4(6)
C(87B)-C(82B)-H(82B)	120.0	C(95)-C(96)-H(96)	120.8
C(82B)-C(83B)-C(84B)	120.0	C(94)#1-C(96)-H(96)	120.8
C(82B)-C(83B)-H(83B)	120.0		

Table S4. Anisotropic displacement parameters ($Å^2$ x 10^3) for {[$MoOS_3$(CuIMes)](μ^4-Cu)[$MoOS_3$(CuIMes)$_2$]}$_{0.36}${[MoO_2S_2(CuIMes)](μ^3-Cu)[$MoOS_3$(CuIMes)$_2$]}$_{0.64}$·Ph_3SiOH· 2½C_6H_6. The anisotropic displacement factor exponent takes the form: $-2\pi^2[(ha^*)^2U_{11} + ... + 2hka^*b^*U_{12}]$.

Atom	U_{11}	U_{22}	U_{33}	U_{23}	U_{13}	U_{12}
Mo(1)	18(1)	18(1)	21(1)	6(1)	5(1)	3(1)
Mo(2)	23(1)	19(1)	21(1)	8(1)	6(1)	6(1)
Cu(1)	28(1)	35(1)	21(1)	12(1)	13(1)	15(1)
Cu(2)	19(1)	27(1)	16(1)	7(1)	5(1)	5(1)
Cu(3)	21(1)	20(1)	18(1)	6(1)	3(1)	6(1)
Cu(4A)	18(1)	25(1)	22(1)	3(1)	4(1)	2(1)
S(6)	18(1)	24(1)	19(1)	8(1)	5(1)	9(1)
Cu(4B)	18(1)	25(1)	22(1)	3(1)	4(1)	2(1)
O(3)	28(2)	41(2)	31(2)	16(2)	11(2)	20(2)
S(1)	18(1)	31(1)	23(1)	11(1)	7(1)	7(1)
S(2)	20(1)	32(1)	19(1)	4(1)	6(1)	8(1)
S(3)	26(1)	32(1)	20(1)	11(1)	8(1)	11(1)
S(4)	17(1)	24(1)	20(1)	5(1)	6(1)	4(1)
S(5)	38(1)	26(1)	23(1)	8(1)	13(1)	14(1)
Si(1)	27(1)	21(1)	19(1)	6(1)	9(1)	9(1)
O(1)	33(1)	21(1)	47(1)	9(1)	7(1)	3(1)
O(2)	43(1)	21(1)	35(1)	11(1)	12(1)	5(1)
O(4)	38(1)	24(1)	25(1)	9(1)	15(1)	11(1)
N(1)	40(1)	49(1)	27(1)	18(1)	20(1)	27(1)
N(2)	29(1)	36(1)	20(1)	8(1)	11(1)	10(1)
N(3)	19(1)	28(1)	20(1)	8(1)	4(1)	5(1)
N(4)	21(1)	25(1)	21(1)	8(1)	4(1)	5(1)
N(5)	24(1)	21(1)	19(1)	7(1)	3(1)	5(1)
N(6)	22(1)	21(1)	18(1)	6(1)	2(1)	5(1)
C(1)	26(1)	39(1)	21(1)	11(1)	11(1)	14(1)
C(2)	43(2)	53(2)	27(1)	14(1)	20(1)	26(1)
C(3)	37(1)	47(2)	22(1)	9(1)	16(1)	16(1)
C(4)	69(2)	63(2)	44(2)	37(2)	42(2)	52(2)
C(5)	89(3)	54(2)	72(2)	39(2)	62(2)	54(2)
C(6)	140(4)	60(2)	117(4)	56(3)	107(4)	75(3)
C(7)	198(6)	112(4)	93(3)	88(3)	121(4)	136(5)
C(8)	154(5)	128(4)	68(3)	72(3)	81(3)	125(4)
C(9)	99(3)	114(3)	45(2)	51(2)	53(2)	93(3)
C(10)	70(2)	35(2)	89(3)	16(2)	52(2)	21(2)
C(11)	339(11)	155(6)	170(6)	145(5)	212(7)	209(7)
C(12)	61(2)	132(4)	35(2)	23(2)	19(2)	68(3)
C(13)	30(1)	32(1)	21(1)	7(1)	13(1)	5(1)
C(14)	38(2)	43(2)	24(1)	6(1)	12(1)	-2(1)

Table S4. Anisotropic displacement parameters ($Å^2$ x 10^3) for {[$MoOS_3$(CuIMes)](μ^4-Cu)[$MoOS_3$(CuIMes)$_2$]}$_{0.36}${[MoO_2S_2(CuIMes)](μ^3-Cu)[$MoOS_3$(CuIMes)$_2$]}$_{0.64}$·Ph_3SiOH· 2½C_6H_6. The anisotropic displacement factor exponent takes the form: $-2\pi^2[(ha^*)^2U_{11} + ... + 2hka^*b^*U_{12}]$.

Atom	U_{11}	U_{22}	U_{33}	U_{23}	U_{13}	U_{12}
C(15)	64(2)	35(2)	36(2)	4(1)	18(2)	-7(1)
C(16)	71(2)	36(2)	50(2)	18(1)	34(2)	13(2)
C(17)	45(2)	51(2)	42(2)	25(1)	24(1)	18(1)
C(18)	30(1)	40(1)	30(1)	15(1)	15(1)	8(1)
C(19)	34(2)	70(2)	30(1)	9(1)	4(1)	-6(2)
C(20)	121(4)	44(2)	71(3)	28(2)	45(3)	24(2)
C(21)	32(1)	55(2)	37(2)	20(1)	3(1)	-3(1)
C(22)	19(1)	26(1)	18(1)	6(1)	6(1)	6(1)
C(23)	27(1)	40(1)	24(1)	16(1)	1(1)	7(1)
C(24)	30(1)	36(1)	29(1)	19(1)	5(1)	6(1)
C(25)	18(1)	32(1)	18(1)	7(1)	3(1)	3(1)
C(26)	23(1)	33(1)	26(1)	9(1)	8(1)	6(1)
C(27)	32(1)	31(1)	35(1)	4(1)	11(1)	1(1)
C(28)	31(1)	46(2)	37(2)	2(1)	16(1)	-3(1)
C(29)	25(1)	54(2)	34(1)	0(1)	15(1)	6(1)
C(30)	25(1)	40(1)	23(1)	2(1)	7(1)	7(1)
C(31)	34(1)	38(2)	49(2)	13(1)	19(1)	14(1)
C(32)	45(2)	60(2)	75(3)	-2(2)	36(2)	-14(2)
C(33)	39(2)	45(2)	40(2)	0(1)	15(1)	14(1)
C(34)	19(1)	22(1)	22(1)	6(1)	5(1)	3(1)
C(35)	31(1)	27(1)	29(1)	2(1)	8(1)	9(1)
C(36)	36(1)	22(1)	25(1)	0(1)	4(1)	1(1)
C(37)	24(1)	29(1)	26(1)	11(1)	4(1)	-1(1)
C(38)	22(1)	34(1)	30(1)	12(1)	11(1)	7(1)
C(39)	25(1)	24(1)	22(1)	7(1)	9(1)	5(1)
C(40)	44(2)	64(2)	58(2)	-21(2)	9(2)	25(2)
C(41)	26(1)	48(2)	38(2)	11(1)	1(1)	-7(1)
C(42)	35(1)	34(1)	32(1)	-1(1)	12(1)	9(1)
C(43)	20(1)	23(1)	18(1)	5(1)	3(1)	5(1)
C(44)	31(1)	23(1)	26(1)	12(1)	0(1)	7(1)
C(45)	30(1)	27(1)	23(1)	10(1)	-1(1)	8(1)
C(46)	23(1)	19(1)	18(1)	4(1)	0(1)	8(1)
C(47)	26(1)	22(1)	27(1)	10(1)	2(1)	9(1)
C(48)	26(1)	19(1)	34(1)	5(1)	-3(1)	6(1)
C(49)	38(1)	22(1)	28(1)	1(1)	-3(1)	15(1)
C(50)	39(1)	28(1)	24(1)	7(1)	7(1)	18(1)
C(51)	28(1)	23(1)	24(1)	7(1)	5(1)	11(1)
C(52)	31(1)	36(1)	38(1)	18(1)	10(1)	7(1)

Table S4. Anisotropic displacement parameters ($Å^2$ x 10^3) for {[$MoOS_3$(CuIMes)](μ^4-Cu)[$MoOS_3$(CuIMes)$_2$]}$_{0.36}${[MoO_2S_2(CuIMes)](μ^3-Cu)[$MoOS_3$(CuIMes)$_2$]}$_{0.64}$·Ph_3SiOH· 2½C_6H_6. The anisotropic displacement factor exponent takes the form: $-2\pi^2[(ha^*)^2U_{11} + ... + 2hka^*b^*U_{12}]$.

Atom	U_{11}	U_{22}	U_{33}	U_{23}	U_{13}	U_{12}
C(53)	47(2)	32(2)	33(1)	-8(1)	-6(1)	16(1)
C(54)	31(1)	32(1)	35(1)	11(1)	14(1)	12(1)
C(55)	21(1)	21(1)	17(1)	6(1)	0(1)	5(1)
C(56)	20(1)	29(1)	20(1)	8(1)	2(1)	7(1)
C(57)	22(1)	31(1)	26(1)	4(1)	4(1)	11(1)
C(58)	21(1)	24(1)	30(1)	1(1)	2(1)	8(1)
C(59)	18(1)	25(1)	33(1)	6(1)	4(1)	6(1)
C(60)	20(1)	26(1)	22(1)	7(1)	3(1)	8(1)
C(61)	26(1)	38(1)	28(1)	9(1)	9(1)	3(1)
C(62)	27(1)	31(1)	50(2)	-6(1)	8(1)	6(1)
C(63)	27(1)	29(1)	32(1)	8(1)	12(1)	9(1)
C(64)	28(1)	24(1)	23(1)	6(1)	9(1)	10(1)
C(65)	33(1)	42(2)	45(2)	24(1)	20(1)	18(1)
C(66)	43(2)	41(2)	41(2)	23(1)	18(1)	24(1)
C(67)	37(2)	51(2)	36(1)	16(1)	15(1)	27(1)
C(68)	36(2)	95(3)	80(3)	57(2)	31(2)	32(2)
C(69)	37(2)	70(2)	65(2)	48(2)	24(2)	24(2)
C(70)	29(1)	24(1)	21(1)	5(1)	11(1)	9(1)
C(71)	42(2)	30(1)	35(1)	2(1)	3(1)	17(1)
C(72)	58(2)	28(1)	45(2)	-1(1)	2(2)	20(1)
C(73)	44(2)	26(1)	29(1)	-1(1)	7(1)	7(1)
C(74)	47(2)	36(2)	31(1)	2(1)	-4(1)	19(1)
C(75)	53(2)	29(1)	36(2)	2(1)	-1(1)	22(1)
C(76)	23(1)	24(1)	17(1)	5(1)	3(1)	8(1)
C(77)	28(1)	24(1)	24(1)	5(1)	6(1)	9(1)
C(78)	24(1)	33(1)	25(1)	11(1)	5(1)	1(1)
C(79)	21(1)	47(2)	21(1)	2(1)	6(1)	7(1)
C(80)	22(1)	27(1)	23(1)	-4(1)	3(1)	7(1)
C(81)	22(1)	25(1)	20(1)	3(1)	3(1)	7(1)
C(88)	59(2)	49(2)	58(2)	20(2)	29(2)	25(2)
C(89)	52(2)	49(2)	58(2)	30(2)	31(2)	26(2)
C(90)	44(2)	52(2)	55(2)	20(2)	23(2)	16(2)
C(91)	43(2)	44(2)	68(2)	15(2)	19(2)	8(1)
C(92)	51(2)	50(2)	72(2)	35(2)	22(2)	12(2)
C(93)	64(2)	69(2)	56(2)	36(2)	30(2)	31(2)
C(94)	79(3)	97(4)	118(5)	35(4)	43(3)	45(3)
C(95)	68(3)	99(4)	139(5)	44(4)	50(3)	41(3)
C(96)	84(4)	89(4)	129(5)	15(4)	47(4)	35(3)

Table S5. Hydrogen coordinates (x 10^4) and isotropic displacement parameters (Å^2 x 10^3) for $\{[MoOS_3(CuIMes)](\mu^4\text{-}Cu)[MoOS_3(CuIMes)_2]\}_{0.36}\{[MoO_2S_2(CuIMes)](\mu^3\text{-}Cu)[MoOS_3(CuIMes)_2]\}_{0.64}\cdot Ph_3SiOH\cdot 2½C_6H_6$.

H atom	x	y	z	U(eq)
H(4)	-2450(30)	1350(20)	-1110(20)	57(11)
H(2)	7587	621	904	44
H(3)	7663	1736	379	40
H(6)	5533	-941	2134	94
H(8)	8027	483	3813	100
H(10A)	5282	308	982	88
H(10B)	4796	-537	1007	88
H(10C)	5636	-360	673	88
H(11A)	7175	-1064	3643	227
H(11B)	6028	-1303	3239	227
H(11C)	6593	-614	3993	227
H(12A)	8396	2031	3473	102
H(12B)	8765	1769	2816	102
H(12C)	9114	1554	3587	102
H(15)	8392	4725	1780	61
H(17)	5755	3684	100	50
H(19A)	8632	3356	2578	78
H(19B)	9332	4004	2378	78
H(19C)	9038	3130	1935	78
H(20A)	7160	5089	261	113
H(20B)	7608	5510	1143	113
H(20C)	6460	5157	714	113
H(21A)	5642	1813	-106	69
H(21B)	4967	2319	-284	69
H(21C)	5107	2026	449	69
H(23)	7940	2149	6781	39
H(24)	6232	1250	6275	39
H(27)	9377	5014	6434	43
H(29)	10469	3437	5663	48
H(31A)	7906	4637	6712	59
H(31B)	7350	3759	6593	59
H(31C)	7149	4112	5899	59
H(32A)	10798	5309	5853	99
H(32B)	11418	4757	5981	99
H(32C)	11319	5270	6683	99
H(33A)	8968	1846	5760	64
H(33B)	9569	2092	5249	64
H(33C)	8419	1875	4931	64
H(36)	3543	-34	3383	38

Table S5. Hydrogen coordinates (x 10^4) and isotropic displacement parameters (Å^2 x 10^3) for {[$MoOS_3$(CuIMes)](μ^4-Cu)[$MoOS_3$(CuIMes)$_2$]}$_{0.36}${[MoO_2S_2(CuIMes)](μ^3-Cu)[$MoOS_3$(CuIMes)$_2$]}$_{0.64}$·Ph_3SiOH·2½C_6H_6.

H atom	x	y	z	U(eq)
H(38)	2848	1472	4713	34
H(40A)	5983	842	4028	93
H(40B)	5185	13	3623	93
H(40C)	5813	248	4501	93
H(41A)	1891	100	2941	66
H(41B)	1599	611	3522	66
H(41C)	1680	-190	3616	66
H(42A)	4064	2481	5789	54
H(42B)	5023	2821	5625	54
H(42C)	5022	2309	6193	54
H(44)	1909	3841	262	34
H(45)	1004	2704	-867	35
H(48)	5049	5000	2541	37
H(50)	2885	4095	3258	36
H(52A)	4168	3631	779	53
H(52B)	5040	4387	1320	53
H(52C)	4070	4447	774	53
H(53A)	4930	4918	4157	66
H(53B)	4225	5404	4007	66
H(53C)	5171	5603	3796	66
H(54A)	1707	2505	2122	47
H(54B)	1176	2846	1493	47
H(54C)	1313	3175	2351	47
H(57)	1554	153	-1957	33
H(59)	-694	-245	-1209	33
H(61A)	2875	1345	-1457	49
H(61B)	3146	1717	-581	49
H(61C)	2592	2070	-1188	49
H(62A)	50	-996	-2657	61
H(62B)	-786	-1174	-2320	61
H(62C)	197	-1327	-1947	61
H(63A)	246	1269	361	44
H(63B)	-772	679	-230	44
H(63C)	-390	1522	-299	44
H(65)	-2383	3572	-2100	43
H(66)	-3688	3992	-2578	45
H(67)	-5148	3492	-2392	46
H(68)	-5299	2541	-1765	73
H(69)	-3978	2139	-1269	61

Table S5. Hydrogen coordinates (x 10^4) and isotropic displacement parameters (Å^2 x 10^3) for {[$MoOS_3$(CuIMes)](μ^4-Cu)[$MoOS_3$(CuIMes)$_2$]}$_{0.36}${[MoO_2S_2(CuIMes)](μ^3-Cu)[$MoOS_3$(CuIMes)$_2$]}$_{0.64}$·Ph_3SiOH·2½C_6H_6.

H atom	x	y	z	U(eq)
H(71)	-1833	4184	-475	46
H(72)	-790	5237	570	58
H(73)	499	5110	1511	44
H(74)	756	3940	1390	51
H(75)	-275	2892	348	52
H(77)	-625	3616	-1610	32
H(78)	348	3531	-2330	36
H(79)	522	2341	-2771	38
H(80)	-303	1252	-2496	33
H(81)	-1355	1333	-1839	29
H(82A)	6320	6454	5335	51
H(83A)	7589	7591	6121	53
H(84A)	9216	7636	6463	62
H(85A)	9574	6544	6019	52
H(86A)	8305	5407	5232	42
H(87A)	6678	5362	4890	51
H(82B)	7102	7401	5974	51
H(83B)	8812	7851	6401	53
H(84B)	9635	7027	6089	62
H(85B)	8749	5752	5352	52
H(86B)	7039	5303	4925	42
H(87B)	6215	6127	5237	51
H(88)	7799	-1972	3880	61
H(89)	7533	-2082	2604	56
H(90)	7116	-3294	1775	58
H(91)	6944	-4375	2240	64
H(92)	7183	-4230	3515	67
H(93)	7638	-3022	4340	68
H(94)	537	1207	4827	111
H(95)	-43	120	3810	114
H(96)	-548	-1079	3950	120

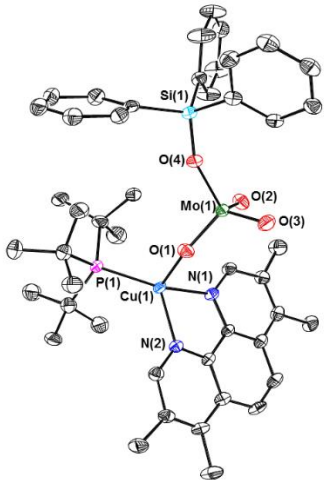

Table 1. Crystal data and structure refinement for jpd465_0m, **3**

Identification code	jpd465_0m	
Empirical formula	C46 H58 Cu Mo N2 O4 P Si	
Formula weight	921.48	
Temperature	100(2) K	
Wavelength	0.71073 Å	
Crystal system	Monoclinic	
Space group	C2/c	
Unit cell dimensions	a = 38.121(12) Å	a= 90°
	b = 9.499(3) Å	b= 116.922(4)°
	c = 30.459(10) Å	g = 90°
Volume	9834(5) $Å^3$	
Z	8	
Density (calculated)	1.245 Mg/m^3	
Absorption coefficient	0.784 mm^{-1}	
F(000)	3840	
Crystal size	0.25 x 0.11 x 0.09 mm^3	
Theta range for data collection	2.18 to 27.49°.	
Index ranges	-49<=h<=49, -12<=k<=11, -39<=l<=39	
Reflections collected	79577	
Independent reflections	11274 [R(int) = 0.0701]	
Completeness to theta = 27.49°	99.7 %	
Absorption correction	Semi-empirical from equivalents	
Max. and min. transmission	0.9300 and 0.7278	
Refinement method	Full-matrix least-squares on F^2	
Data / restraints / parameters	11274 / 0 / 518	
Goodness-of-fit on F^2	1.095	
Final R indices [I>2sigma(I)]	R1 = 0.0406, wR2 = 0.1028	
R indices (all data)	R1 = 0.0510, wR2 = 0.1081	
Largest diff. peak and hole	1.007 and -0.856 $e.Å^{-3}$	

Table 2. Atomic coordinates (x 10^4) and equivalent isotropic displacement parameters ($Å^2$x 10^3)
for jpd465_0m. U(eq) is defined as one third of the trace of the orthogonalized U^{ij} tensor.

	x	y	z	U(eq)
Mo(1)	1792(1)	9411(1)	10811(1)	19(1)
Cu(1)	1330(1)	10111(1)	9519(1)	18(1)
P(1)	705(1)	9542(1)	9178(1)	25(1)
Si(1)	1430(1)	7592(1)	11510(1)	19(1)
N(1)	1614(1)	12054(2)	9719(1)	19(1)
N(2)	1696(1)	9975(2)	9176(1)	19(1)
O(1)	1619(1)	9023(2)	10187(1)	25(1)
O(2)	1719(1)	11164(2)	10885(1)	28(1)
O(3)	2289(1)	9062(2)	11112(1)	31(1)
O(4)	1526(1)	8306(2)	11090(1)	23(1)
C(1)	1583(1)	13059(3)	10003(1)	22(1)
C(2)	1786(1)	14351(3)	10102(1)	24(1)
C(3)	2034(1)	14615(3)	9890(1)	26(1)
C(4)	2076(1)	13549(3)	9591(1)	23(1)
C(5)	2326(1)	13704(3)	9354(1)	29(1)
C(6)	2353(1)	12690(3)	9060(1)	30(1)
C(7)	2138(1)	11387(3)	8974(1)	24(1)
C(8)	2147(1)	10308(3)	8656(1)	26(1)
C(9)	1934(1)	9086(3)	8612(1)	24(1)
C(10)	1720(1)	8974(3)	8888(1)	22(1)
C(11)	1900(1)	11183(3)	9216(1)	20(1)
C(12)	1864(1)	12290(3)	9519(1)	18(1)
C(13)	1725(1)	15392(3)	10435(1)	36(1)
C(14)	2245(1)	16009(3)	9968(1)	32(1)
C(15)	2372(1)	10506(3)	8359(1)	40(1)
C(16)	1919(1)	7879(3)	8283(1)	32(1)
C(17)	442(1)	10525(4)	9488(1)	36(1)
C(18)	418(1)	12103(4)	9338(1)	43(1)
C(19)	701(1)	10527(3)	10043(1)	32(1)

C(20)	24(1)	10002(4)	9371(1)	42(1)
C(21)	637(1)	7550(3)	9250(1)	38(1)
C(22)	714(1)	7221(4)	9782(1)	43(1)
C(23)	227(1)	6963(4)	8897(1)	53(1)
C(24)	951(1)	6774(3)	9166(1)	40(1)
C(25)	471(1)	9981(4)	8504(1)	35(1)
C(26)	645(1)	11422(3)	8439(1)	36(1)
C(27)	597(1)	8869(4)	8222(1)	38(1)
C(28)	18(1)	10098(5)	8242(1)	52(1)
C(29)	1072(1)	6132(3)	11209(1)	22(1)
C(30)	1206(1)	4789(3)	11163(1)	27(1)
C(31)	944(1)	3737(3)	10884(1)	31(1)
C(32)	546(1)	4012(3)	10653(1)	32(1)
C(33)	404(1)	5317(3)	10695(1)	33(1)
C(34)	666(1)	6370(3)	10973(1)	28(1)
C(35)	1223(1)	8964(3)	11771(1)	22(1)
C(36)	1160(1)	8637(3)	12176(1)	44(1)
C(37)	1045(1)	9656(4)	12412(1)	42(1)
C(38)	985(1)	11012(3)	12246(1)	30(1)
C(39)	1040(1)	11358(3)	11843(1)	46(1)
C(40)	1160(1)	10341(3)	11612(1)	38(1)
C(41)	1886(1)	6920(3)	12030(1)	22(1)
C(42)	1874(1)	5962(3)	12375(1)	30(1)
C(43)	2210(1)	5641(3)	12805(1)	34(1)
C(44)	2567(1)	6251(3)	12897(1)	31(1)
C(45)	2589(1)	7183(3)	12562(1)	28(1)
C(46)	2251(1)	7513(3)	12132(1)	23(1)

Table 3. Bond lengths [Å] and angles [°] for jpd465_0m.

Mo(1)-O(2)	1.721(2)	C(8)-C(15)	1.513(4)
Mo(1)-O(3)	1.722(2)	C(9)-C(10)	1.414(3)
Mo(1)-O(1)	1.7451(19)	C(9)-C(16)	1.507(4)
Mo(1)-O(4)	1.9058(17)	C(10)-H(10)	0.9500
Cu(1)-N(1)	2.085(2)	C(11)-C(12)	1.448(3)
Cu(1)-N(2)	2.089(2)	C(13)-H(13A)	0.9800
Cu(1)-O(1)	2.0964(19)	C(13)-H(13B)	0.9800
Cu(1)-P(1)	2.1924(10)	C(13)-H(13C)	0.9800
P(1)-C(25)	1.880(3)	C(14)-H(14A)	0.9800
P(1)-C(17)	1.904(3)	C(14)-H(14B)	0.9800
P(1)-C(21)	1.936(3)	C(14)-H(14C)	0.9800
Si(1)-O(4)	1.6297(18)	C(15)-H(15A)	0.9800
Si(1)-C(41)	1.857(3)	C(15)-H(15B)	0.9800
Si(1)-C(29)	1.869(3)	C(15)-H(15C)	0.9800
Si(1)-C(35)	1.876(3)	C(16)-H(16A)	0.9800
N(1)-C(1)	1.328(3)	C(16)-H(16B)	0.9800
N(1)-C(12)	1.363(3)	C(16)-H(16C)	0.9800
N(2)-C(10)	1.326(3)	C(17)-C(19)	1.526(4)
N(2)-C(11)	1.361(3)	C(17)-C(20)	1.548(4)
C(1)-C(2)	1.409(3)	C(17)-C(18)	1.558(5)
C(1)-H(1)	0.9500	C(18)-H(18A)	0.9800
C(2)-C(3)	1.387(4)	C(18)-H(18B)	0.9800
C(2)-C(13)	1.509(4)	C(18)-H(18C)	0.9800
C(3)-C(4)	1.418(4)	C(19)-H(19A)	0.9800
C(3)-C(14)	1.512(4)	C(19)-H(19B)	0.9800
C(4)-C(12)	1.404(3)	C(19)-H(19C)	0.9800
C(4)-C(5)	1.440(3)	C(20)-H(20A)	0.9800
C(5)-C(6)	1.352(4)	C(20)-H(20B)	0.9800
C(5)-H(5)	0.9500	C(20)-H(20C)	0.9800
C(6)-C(7)	1.441(4)	C(21)-C(24)	1.522(4)
C(6)-H(6)	0.9500	C(21)-C(22)	1.542(4)
C(7)-C(11)	1.417(3)	C(21)-C(23)	1.545(4)
C(7)-C(8)	1.423(4)	C(22)-H(22A)	0.9800
C(8)-C(9)	1.387(4)	C(22)-H(22B)	0.9800

C(22)-H(22C)	0.9800	C(38)-C(39)	1.373(4)
C(23)-H(23A)	0.9800	C(38)-H(38)	0.9500
C(23)-H(23B)	0.9800	C(39)-C(40)	1.391(4)
C(23)-H(23C)	0.9800	C(39)-H(39)	0.9500
C(24)-H(24A)	0.9800	C(40)-H(40)	0.9500
C(24)-H(24B)	0.9800	C(41)-C(46)	1.400(4)
C(24)-H(24C)	0.9800	C(41)-C(42)	1.407(4)
C(25)-C(28)	1.544(4)	C(42)-C(43)	1.387(4)
C(25)-C(27)	1.566(4)	C(42)-H(42)	0.9500
C(25)-C(26)	1.571(5)	C(43)-C(44)	1.386(4)
C(26)-H(26A)	0.9800	C(43)-H(43)	0.9500
C(26)-H(26B)	0.9800	C(44)-C(45)	1.384(4)
C(26)-H(26C)	0.9800	C(44)-H(44)	0.9500
C(27)-H(27A)	0.9800	C(45)-C(46)	1.394(4)
C(27)-H(27B)	0.9800	C(45)-H(45)	0.9500
C(27)-H(27C)	0.9800	C(46)-H(46)	0.9500
C(28)-H(28A)	0.9800		
C(28)-H(28B)	0.9800	O(2)-Mo(1)-O(3)	108.75(10)
C(28)-H(28C)	0.9800	O(2)-Mo(1)-O(1)	110.10(9)
C(29)-C(34)	1.398(4)	O(3)-Mo(1)-O(1)	108.81(9)
C(29)-C(30)	1.404(4)	O(2)-Mo(1)-O(4)	108.83(9)
C(30)-C(31)	1.396(4)	O(3)-Mo(1)-O(4)	109.65(9)
C(30)-H(30)	0.9500	O(1)-Mo(1)-O(4)	110.67(8)
C(31)-C(32)	1.378(4)	N(1)-Cu(1)-N(2)	80.03(8)
C(31)-H(31)	0.9500	N(1)-Cu(1)-O(1)	100.25(8)
C(32)-C(33)	1.382(4)	N(2)-Cu(1)-O(1)	106.23(8)
C(32)-H(32)	0.9500	N(1)-Cu(1)-P(1)	131.64(6)
C(33)-C(34)	1.397(4)	N(2)-Cu(1)-P(1)	125.19(7)
C(33)-H(33)	0.9500	O(1)-Cu(1)-P(1)	108.50(6)
C(34)-H(34)	0.9500	C(25)-P(1)-C(17)	109.66(14)
C(35)-C(40)	1.378(4)	C(25)-P(1)-C(21)	108.55(14)
C(35)-C(36)	1.396(4)	C(17)-P(1)-C(21)	107.22(14)
C(36)-C(37)	1.390(4)	C(25)-P(1)-Cu(1)	109.80(9)
C(36)-H(36)	0.9500	C(17)-P(1)-Cu(1)	110.45(10)
C(37)-C(38)	1.365(4)	C(21)-P(1)-Cu(1)	111.10(10)
C(37)-H(37)	0.9500	O(4)-Si(1)-C(41)	110.84(11)

O(4)-Si(1)-C(29)	107.33(11)	C(7)-C(8)-C(15)	120.9(3)
C(41)-Si(1)-C(29)	110.89(12)	C(8)-C(9)-C(10)	118.4(2)
O(4)-Si(1)-C(35)	109.32(11)	C(8)-C(9)-C(16)	123.0(2)
C(41)-Si(1)-C(35)	106.77(12)	C(10)-C(9)-C(16)	118.6(2)
C(29)-Si(1)-C(35)	111.72(12)	N(2)-C(10)-C(9)	124.9(2)
C(1)-N(1)-C(12)	117.2(2)	N(2)-C(10)-H(10)	117.5
C(1)-N(1)-Cu(1)	129.81(16)	C(9)-C(10)-H(10)	117.5
C(12)-N(1)-Cu(1)	112.94(16)	N(2)-C(11)-C(7)	123.0(2)
C(10)-N(2)-C(11)	116.9(2)	N(2)-C(11)-C(12)	116.9(2)
C(10)-N(2)-Cu(1)	129.73(17)	C(7)-C(11)-C(12)	120.0(2)
C(11)-N(2)-Cu(1)	112.83(16)	N(1)-C(12)-C(4)	122.7(2)
Mo(1)-O(1)-Cu(1)	136.62(10)	N(1)-C(12)-C(11)	117.0(2)
Si(1)-O(4)-Mo(1)	158.99(12)	C(4)-C(12)-C(11)	120.3(2)
N(1)-C(1)-C(2)	124.3(2)	C(2)-C(13)-H(13A)	109.5
N(1)-C(1)-H(1)	117.8	C(2)-C(13)-H(13B)	109.5
C(2)-C(1)-H(1)	117.8	H(13A)-C(13)-H(13B)	109.5
C(3)-C(2)-C(1)	118.8(2)	C(2)-C(13)-H(13C)	109.5
C(3)-C(2)-C(13)	122.7(2)	H(13A)-C(13)-H(13C)	109.5
C(1)-C(2)-C(13)	118.6(2)	H(13B)-C(13)-H(13C)	109.5
C(2)-C(3)-C(4)	117.9(2)	C(3)-C(14)-H(14A)	109.5
C(2)-C(3)-C(14)	120.8(3)	C(3)-C(14)-H(14B)	109.5
C(4)-C(3)-C(14)	121.3(2)	H(14A)-C(14)-H(14B)	109.5
C(12)-C(4)-C(3)	118.9(2)	C(3)-C(14)-H(14C)	109.5
C(12)-C(4)-C(5)	118.3(2)	H(14A)-C(14)-H(14C)	109.5
C(3)-C(4)-C(5)	122.8(2)	H(14B)-C(14)-H(14C)	109.5
C(6)-C(5)-C(4)	121.7(2)	C(8)-C(15)-H(15A)	109.5
C(6)-C(5)-H(5)	119.1	C(8)-C(15)-H(15B)	109.5
C(4)-C(5)-H(5)	119.1	H(15A)-C(15)-H(15B)	109.5
C(5)-C(6)-C(7)	121.6(2)	C(8)-C(15)-H(15C)	109.5
C(5)-C(6)-H(6)	119.2	H(15A)-C(15)-H(15C)	109.5
C(7)-C(6)-H(6)	119.2	H(15B)-C(15)-H(15C)	109.5
C(11)-C(7)-C(8)	118.3(2)	C(9)-C(16)-H(16A)	109.5
C(11)-C(7)-C(6)	118.0(2)	C(9)-C(16)-H(16B)	109.5
C(8)-C(7)-C(6)	123.7(2)	H(16A)-C(16)-H(16B)	109.5
C(9)-C(8)-C(7)	118.3(2)	C(9)-C(16)-H(16C)	109.5
C(9)-C(8)-C(15)	120.8(3)	H(16A)-C(16)-H(16C)	109.5

H(16B)-C(16)-H(16C)	109.5	H(22B)-C(22)-H(22C)	109.5
C(19)-C(17)-C(20)	109.8(2)	C(21)-C(23)-H(23A)	109.5
C(19)-C(17)-C(18)	104.2(3)	C(21)-C(23)-H(23B)	109.5
C(20)-C(17)-C(18)	109.0(3)	H(23A)-C(23)-H(23B)	109.5
C(19)-C(17)-P(1)	109.1(2)	C(21)-C(23)-H(23C)	109.5
C(20)-C(17)-P(1)	116.6(2)	H(23A)-C(23)-H(23C)	109.5
C(18)-C(17)-P(1)	107.4(2)	H(23B)-C(23)-H(23C)	109.5
C(17)-C(18)-H(18A)	109.5	C(21)-C(24)-H(24A)	109.5
C(17)-C(18)-H(18B)	109.5	C(21)-C(24)-H(24B)	109.5
H(18A)-C(18)-H(18B)	109.5	H(24A)-C(24)-H(24B)	109.5
C(17)-C(18)-H(18C)	109.5	C(21)-C(24)-H(24C)	109.5
H(18A)-C(18)-H(18C)	109.5	H(24A)-C(24)-H(24C)	109.5
H(18B)-C(18)-H(18C)	109.5	H(24B)-C(24)-H(24C)	109.5
C(17)-C(19)-H(19A)	109.5	C(28)-C(25)-C(27)	108.4(3)
C(17)-C(19)-H(19B)	109.5	C(28)-C(25)-C(26)	108.0(3)
H(19A)-C(19)-H(19B)	109.5	C(27)-C(25)-C(26)	105.5(2)
C(17)-C(19)-H(19C)	109.5	C(28)-C(25)-P(1)	116.5(2)
H(19A)-C(19)-H(19C)	109.5	C(27)-C(25)-P(1)	109.7(2)
H(19B)-C(19)-H(19C)	109.5	C(26)-C(25)-P(1)	108.1(2)
C(17)-C(20)-H(20A)	109.5	C(25)-C(26)-H(26A)	109.5
C(17)-C(20)-H(20B)	109.5	C(25)-C(26)-H(26B)	109.5
H(20A)-C(20)-H(20B)	109.5	H(26A)-C(26)-H(26B)	109.5
C(17)-C(20)-H(20C)	109.5	C(25)-C(26)-H(26C)	109.5
H(20A)-C(20)-H(20C)	109.5	H(26A)-C(26)-H(26C)	109.5
H(20B)-C(20)-H(20C)	109.5	H(26B)-C(26)-H(26C)	109.5
C(24)-C(21)-C(22)	106.8(3)	C(25)-C(27)-H(27A)	109.5
C(24)-C(21)-C(23)	109.5(3)	C(25)-C(27)-H(27B)	109.5
C(22)-C(21)-C(23)	107.9(3)	H(27A)-C(27)-H(27B)	109.5
C(24)-C(21)-P(1)	107.40(19)	C(25)-C(27)-H(27C)	109.5
C(22)-C(21)-P(1)	110.2(2)	H(27A)-C(27)-H(27C)	109.5
C(23)-C(21)-P(1)	114.8(3)	H(27B)-C(27)-H(27C)	109.5
C(21)-C(22)-H(22A)	109.5	C(25)-C(28)-H(28A)	109.5
C(21)-C(22)-H(22B)	109.5	C(25)-C(28)-H(28B)	109.5
H(22A)-C(22)-H(22B)	109.5	H(28A)-C(28)-H(28B)	109.5
C(21)-C(22)-H(22C)	109.5	C(25)-C(28)-H(28C)	109.5
H(22A)-C(22)-H(22C)	109.5	H(28A)-C(28)-H(28C)	109.5

H(28B)-C(28)-H(28C)	109.5	C(39)-C(40)-H(40)	119.2
C(34)-C(29)-C(30)	117.6(2)	C(46)-C(41)-C(42)	117.4(2)
C(34)-C(29)-Si(1)	121.6(2)	C(46)-C(41)-Si(1)	120.23(19)
C(30)-C(29)-Si(1)	120.44(19)	C(42)-C(41)-Si(1)	121.7(2)
C(31)-C(30)-C(29)	121.3(3)	C(43)-C(42)-C(41)	121.3(3)
C(31)-C(30)-H(30)	119.4	C(43)-C(42)-H(42)	119.4
C(29)-C(30)-H(30)	119.4	C(41)-C(42)-H(42)	119.4
C(32)-C(31)-C(30)	119.6(3)	C(44)-C(43)-C(42)	120.0(3)
C(32)-C(31)-H(31)	120.2	C(44)-C(43)-H(43)	120.0
C(30)-C(31)-H(31)	120.2	C(42)-C(43)-H(43)	120.0
C(31)-C(32)-C(33)	120.7(3)	C(45)-C(44)-C(43)	120.1(3)
C(31)-C(32)-H(32)	119.7	C(45)-C(44)-H(44)	119.9
C(33)-C(32)-H(32)	119.7	C(43)-C(44)-H(44)	119.9
C(32)-C(33)-C(34)	119.6(3)	C(44)-C(45)-C(46)	119.9(3)
C(32)-C(33)-H(33)	120.2	C(44)-C(45)-H(45)	120.1
C(34)-C(33)-H(33)	120.2	C(46)-C(45)-H(45)	120.1
C(33)-C(34)-C(29)	121.3(3)	C(45)-C(46)-C(41)	121.3(2)
C(33)-C(34)-H(34)	119.4	C(45)-C(46)-H(46)	119.3
C(29)-C(34)-H(34)	119.4	C(41)-C(46)-H(46)	119.3
C(40)-C(35)-C(36)	116.8(3)		
C(40)-C(35)-Si(1)	123.3(2)		
C(36)-C(35)-Si(1)	119.6(2)		
C(37)-C(36)-C(35)	121.6(3)		
C(37)-C(36)-H(36)	119.2		
C(35)-C(36)-H(36)	119.2		
C(38)-C(37)-C(36)	120.3(3)		
C(38)-C(37)-H(37)	119.9		
C(36)-C(37)-H(37)	119.9		
C(37)-C(38)-C(39)	119.3(3)		
C(37)-C(38)-H(38)	120.3		
C(39)-C(38)-H(38)	120.3		
C(38)-C(39)-C(40)	120.4(3)		
C(38)-C(39)-H(39)	119.8		
C(40)-C(39)-H(39)	119.8		
C(35)-C(40)-C(39)	121.6(3)		
C(35)-C(40)-H(40)	119.2		

Table 4. Anisotropic displacement parameters ($Å^2 x\ 10^3$) for jpd465_0m. The anisotropic
displacement factor exponent takes the form: $-2p^2[\ h^2\ a^{*2}U^{11} + ...\ + 2\ h\ k\ a^*\ b^*\ U^{12}\ ]$

	U^{11}	U^{22}	U^{33}	U^{23}	U^{13}	U^{12}
Mo(1)	21(1)	18(1)	18(1)	1(1)	10(1)	-3(1)
Cu(1)	18(1)	18(1)	21(1)	-2(1)	12(1)	-4(1)
P(1)	20(1)	34(1)	24(1)	-9(1)	14(1)	-9(1)
Si(1)	21(1)	18(1)	21(1)	2(1)	12(1)	1(1)
N(1)	20(1)	17(1)	23(1)	2(1)	12(1)	-1(1)
N(2)	17(1)	21(1)	21(1)	1(1)	10(1)	1(1)
O(1)	34(1)	21(1)	22(1)	1(1)	14(1)	-2(1)
O(2)	37(1)	22(1)	22(1)	0(1)	11(1)	-4(1)
O(3)	25(1)	37(1)	32(1)	6(1)	15(1)	-2(1)
O(4)	25(1)	24(1)	22(1)	2(1)	13(1)	-2(1)
C(1)	25(1)	18(1)	25(1)	-1(1)	14(1)	-3(1)
C(2)	33(1)	15(1)	28(1)	0(1)	16(1)	-3(1)
C(3)	25(1)	19(1)	32(2)	2(1)	12(1)	-4(1)
C(4)	21(1)	21(1)	27(1)	2(1)	12(1)	-2(1)
C(5)	26(1)	27(2)	39(2)	5(1)	19(1)	-6(1)
C(6)	29(1)	32(2)	41(2)	5(1)	26(1)	-4(1)
C(7)	23(1)	24(1)	27(1)	4(1)	15(1)	1(1)
C(8)	28(1)	27(1)	32(2)	5(1)	21(1)	5(1)
C(9)	24(1)	27(1)	24(1)	2(1)	13(1)	6(1)
C(10)	20(1)	23(1)	22(1)	1(1)	10(1)	2(1)
C(11)	17(1)	20(1)	23(1)	1(1)	10(1)	-2(1)
C(12)	18(1)	18(1)	22(1)	4(1)	11(1)	-1(1)
C(13)	52(2)	21(2)	43(2)	-9(1)	29(2)	-10(1)
C(14)	38(2)	19(1)	43(2)	-1(1)	20(1)	-9(1)
C(15)	49(2)	40(2)	51(2)	1(2)	40(2)	0(1)
C(16)	32(2)	34(2)	34(2)	-5(1)	20(1)	5(1)
C(17)	22(1)	65(2)	24(1)	-8(1)	13(1)	-3(1)
C(18)	36(2)	53(2)	41(2)	-1(2)	18(2)	11(2)
C(19)	28(1)	44(2)	32(2)	-12(1)	19(1)	-7(1)
C(20)	23(1)	75(2)	34(2)	-7(2)	18(1)	-5(1)

C(21)	43(2)	40(2)	35(2)	-10(1)	22(1)	-21(1)
C(22)	55(2)	43(2)	39(2)	-4(2)	29(2)	-20(2)
C(23)	57(2)	60(2)	49(2)	-21(2)	29(2)	-37(2)
C(24)	63(2)	26(2)	46(2)	-10(1)	37(2)	-14(1)
C(25)	23(1)	54(2)	25(2)	-2(1)	9(1)	-4(1)
C(26)	29(2)	47(2)	29(2)	6(1)	9(1)	4(1)
C(27)	29(2)	67(2)	19(1)	-4(1)	12(1)	-6(1)
C(28)	27(2)	97(3)	30(2)	-6(2)	10(1)	-3(2)
C(29)	26(1)	23(1)	22(1)	1(1)	15(1)	-2(1)
C(30)	28(1)	26(1)	30(2)	2(1)	15(1)	1(1)
C(31)	42(2)	20(1)	35(2)	-2(1)	22(1)	-2(1)
C(32)	41(2)	26(2)	35(2)	-5(1)	22(1)	-11(1)
C(33)	24(1)	39(2)	36(2)	-4(1)	14(1)	-6(1)
C(34)	28(1)	25(1)	34(2)	-2(1)	17(1)	-1(1)
C(35)	22(1)	22(1)	25(1)	0(1)	13(1)	0(1)
C(36)	69(2)	32(2)	54(2)	16(2)	47(2)	19(2)
C(37)	60(2)	45(2)	42(2)	8(2)	40(2)	16(2)
C(38)	30(1)	30(2)	35(2)	-10(1)	18(1)	0(1)
C(39)	74(2)	23(2)	61(2)	5(2)	48(2)	10(2)
C(40)	62(2)	28(2)	39(2)	7(1)	37(2)	11(1)
C(41)	27(1)	19(1)	22(1)	2(1)	13(1)	4(1)
C(42)	33(2)	25(1)	34(2)	7(1)	16(1)	0(1)
C(43)	44(2)	28(2)	29(2)	11(1)	15(1)	7(1)
C(44)	34(2)	31(2)	23(1)	4(1)	9(1)	10(1)
C(45)	26(1)	35(2)	24(1)	0(1)	12(1)	5(1)
C(46)	26(1)	25(1)	22(1)	2(1)	13(1)	2(1)

Table 5. Hydrogen coordinates (x 10^4) and isotropic displacement parameters ($Å^2$x 10^3)
for jpd465_0m.

	x	y	z	U(eq)
H(1)	1413	12896	10148	26
H(5)	2476	14541	9407	35
H(6)	2517	12840	8905	36
H(10)	1584	8118	8865	26
H(13A)	1976	15560	10727	54
H(13B)	1534	15012	10537	54
H(13C)	1626	16280	10259	54
H(14A)	2204	16392	9650	48
H(14B)	2527	15869	10178	48
H(14C)	2141	16670	10128	48
H(15A)	2459	9588	8298	60
H(15B)	2602	11105	8543	60
H(15C)	2201	10954	8044	60
H(16A)	1843	8232	7950	47
H(16B)	1725	7186	8273	47
H(16C)	2179	7435	8412	47
H(18A)	332	12668	9541	65
H(18B)	230	12211	8990	65
H(18C)	679	12424	9389	65
H(19A)	582	11130	10201	49
H(19B)	963	10887	10116	49
H(19C)	725	9565	10170	49
H(20A)	42	9069	9517	63
H(20B)	-137	9942	9013	63
H(20C)	-98	10662	9508	63
H(22A)	683	6209	9815	64
H(22B)	525	7740	9857	64
H(22C)	982	7506	10011	64
H(23A)	173	7155	8556	80

H(23B)	27	7417	8966	80
H(23C)	223	5944	8946	80
H(24A)	1211	7147	9390	61
H(24B)	904	6909	8825	61
H(24C)	941	5768	9230	61
H(26A)	545	11626	8087	54
H(26B)	932	11364	8594	54
H(26C)	565	12174	8595	54
H(27A)	489	7946	8240	57
H(27B)	885	8812	8375	57
H(27C)	496	9152	7877	57
H(28A)	-73	10269	7890	78
H(28B)	-64	10880	8384	78
H(28C)	-97	9219	8286	78
H(30)	1480	4592	11325	33
H(31)	1040	2837	10853	37
H(32)	367	3297	10463	39
H(33)	129	5498	10536	39
H(34)	568	7265	11002	34
H(36)	1197	7696	12294	53
H(37)	1007	9408	12690	51
H(38)	906	11709	12406	36
H(39)	995	12296	11723	55
H(40)	1201	10604	11337	45
H(42)	1632	5527	12313	36
H(43)	2195	5004	13036	41
H(44)	2796	6029	13191	37
H(45)	2834	7598	12624	34
H(46)	2269	8153	11903	28

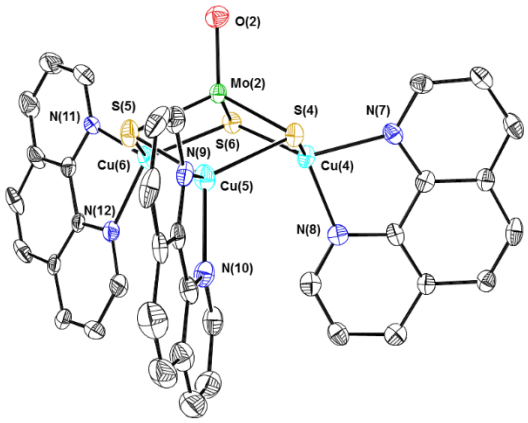

Structure Determination Summary

Crystal Data and Structure Refinement for $[Mo(O)(\mu\text{-}S)_3(Cu(phen))_3][PF_6]\cdot 2MeCN$, **5**

Identification code	jpd536_0m_a
Empirical formula	$C_{40}H_{30}Cu_3F_6MoN_8OPS_3$
Formula weight	1166.49
Temperature	100(2) K
Wavelength	0.71073 Å
Crystal system	monoclinic
Space group	$P2_1/c$
Unit cell dimensions	a = 15.1101(17) Å α = 90°
	b = 20.018(2) Å β = 102.9060(16)°
	c = 28.962(3) Å γ = 90°
Volume, Z	8538.9(17) Å^3, 8
Density (calculated)	1.815 g/cm^3
Absorption coefficient	2.016 mm^{-1}
F(000)	4640
Crystal size	0.29 x 0.03 x 0.02 mm
θ range for data collection	1.77 to 19.92°
Limiting indices	$-14 < h < 14$, $-19 < k < 19$, $-27 < l < 27$
Reflections collected	73828
Independent reflections	7864 (R_{int} = 0.0865)
Completeness to θ = 19.92°	99.8 %
Absorption correction	Semi-empirical from equivalent
Max. and min. transmission	0.9608 and 0.6335
Refinement method	Full-matrix least-squares on F^2
Data / restraints / parameters	7864 / 464 / 1139
Goodness-of-fit on F^2	1.042
Final R indices [I>2σ(I)]	R1 = 0.0318, wR2 = 0.0663
R indices (all data)	R1 = 0.0505, wR2 = 0.0754
Largest diff. peak and hole	0.467 and -0.395 eÅ^{-3}

Table S1. AtomicCoordinates (x 10^4) and equivalent isotropic displacement parameters (Å^2 x 10^3) for [Mo(O)(μ-S)$_3$(Cu(phen))$_3$][PF$_6$]·2MeCN. U(eq) is defined as one third of the trace of the orthogonalized U^{ij} tensor.

Atom	*x*	*y*	*z*	U(eq)
Mo(1)	-94(1)	5172(1)	2131(1)	16(1)
Mo(2)	4878(1)	5172(1)	2039(1)	17(1)
Cu(1)	-1536(1)	4443(1)	2162(1)	22(1)
Cu(2)	840(1)	4104(1)	1968(1)	24(1)
Cu(3)	-587(1)	5315(1)	1198(1)	23(1)
Cu(4)	3378(1)	5893(1)	1970(1)	22(1)
Cu(5)	5672(1)	6260(1)	1788(1)	26(1)
Cu(6)	4376(1)	4895(1)	1121(1)	26(1)
S(1)	-61(1)	4159(1)	2487(1)	21(1)
S(2)	835(1)	5113(1)	1614(1)	22(1)
S(3)	-1535(1)	5343(1)	1703(1)	20(1)
S(4)	4810(1)	6224(1)	2326(1)	21(1)
S(5)	5769(1)	5218(1)	1506(1)	26(1)
S(6)	3452(1)	4888(1)	1641(1)	21(1)
P(1)	2408(1)	7653(1)	-331(1)	32(1)
P(2)	-2642(1)	9194(1)	-130(1)	33(1)
F(1)	2801(2)	7117(2)	72(1)	37(1)
F(2)	1450(2)	7621(2)	-185(1)	35(1)
F(3)	2014(3)	8193(2)	-730(1)	51(1)
F(4)	3368(2)	7666(2)	-475(1)	49(1)
F(5)	2081(3)	7062(2)	-704(1)	48(1)
F(6)	2728(2)	8234(2)	46(1)	42(1)
F(7)	-2480(3)	8524(2)	165(1)	82(2)
F(8)	-3659(3)	9172(3)	-98(2)	88(2)
F(9)	-2831(4)	9864(2)	-419(1)	84(2)
F(10)	-1627(3)	9191(4)	-157(2)	134(2)
F(11)	-2882(4)	8772(2)	-603(1)	92(2)
F(12)	-2396(3)	9607(2)	345(1)	66(1)
O(1)	231(2)	5789(2)	2540(1)	26(1)
O(2)	5310(2)	4622(2)	2482(1)	26(1)
N(1)	-1970(3)	4552(2)	2826(2)	20(1)
N(2)	-2527(3)	3757(2)	2061(2)	22(1)
N(3)	2158(3)	3797(2)	2259(2)	22(1)
N(4)	859(3)	3212(2)	1601(2)	20(1)
N(5)	-806(3)	6212(2)	806(2)	18(1)
N(6)	-922(3)	4931(2)	524(2)	20(1)
N(7)	2665(3)	6133(2)	2497(2)	22(1)
N(8)	2485(3)	6583(2)	1603(2)	20(1)
N(9)	6952(3)	6678(2)	2026(2)	21(1)

Table S1. AtomicCoordinates (x 10^4) and equivalent isotropic displacement parameters ($Å^2$ x 10^3) for $[Mo(O)(\mu\text{-}S)_3(Cu(phen))_3][PF_6]\cdot 2MeCN$. U(eq) is defined as one third of the trace of the orthogonalized U^{ij} tensor.

Atom	*x*	*y*	*z*	U(eq)
N(10)	5547(3)	7095(2)	1347(2)	24(1)
N(11)	4218(3)	3926(2)	825(2)	20(1)
N(12)	4006(3)	5139(3)	417(2)	24(1)
N(13)	-38(5)	9307(3)	-732(3)	58(2)
N(14)	-221(4)	8959(3)	1151(2)	37(2)
N(15)	-3779(5)	9855(3)	1165(3)	61(2)
N(16)	-4788(4)	1466(3)	1396(2)	47(2)
C(1)	-1661(4)	4922(3)	3204(2)	25(2)
C(2)	-1909(4)	4830(3)	3635(2)	30(2)
C(3)	-2499(4)	4329(3)	3672(2)	30(2)
C(4)	-2838(4)	3918(3)	3284(2)	22(2)
C(5)	-2547(4)	4046(3)	2865(2)	21(1)
C(6)	-2861(4)	3633(3)	2454(2)	17(1)
C(7)	-3460(4)	3102(3)	2477(2)	19(1)
C(8)	-3746(4)	2716(3)	2062(2)	23(2)
C(9)	-3440(4)	2864(3)	1666(2)	27(2)
C(10)	-2820(4)	3384(3)	1679(2)	24(2)
C(11)	-3442(4)	3364(3)	3290(2)	25(2)
C(12)	-3729(4)	2972(3)	2911(2)	24(2)
C(13)	2773(5)	4073(3)	2602(2)	31(2)
C(14)	3654(5)	3833(4)	2748(2)	36(2)
C(15)	3901(4)	3297(4)	2518(2)	35(2)
C(16)	3269(4)	2970(3)	2158(2)	26(2)
C(17)	2389(4)	3254(3)	2041(2)	19(1)
C(18)	1701(4)	2936(3)	1692(2)	19(1)
C(19)	1892(4)	2345(3)	1471(2)	27(2)
C(20)	1183(5)	2027(3)	1157(2)	34(2)
C(21)	326(5)	2295(3)	1080(2)	36(2)
C(22)	190(4)	2889(3)	1304(2)	28(2)
C(23)	3453(5)	2391(3)	1913(2)	34(2)
C(24)	2811(5)	2090(3)	1583(2)	35(2)
C(25)	-783(4)	6844(3)	942(2)	25(2)
C(26)	-999(4)	7383(3)	632(2)	30(2)
C(27)	-1241(4)	7256(3)	160(2)	30(2)
C(28)	-1295(4)	6596(3)	-6(2)	22(2)
C(29)	-1070(4)	6089(3)	331(2)	17(1)
C(30)	-1122(4)	5404(3)	183(2)	17(1)
C(31)	-1381(4)	5245(3)	-301(2)	19(1)
C(32)	-1402(4)	4570(3)	-427(2)	29(2)

Table S1. AtomicCoordinates (x 10^4) and equivalent isotropic displacement parameters (Å^2 x 10^3) for [Mo(O)(μ-S)$_3$(Cu(phen))$_3$][PF$_6$]·2MeCN. U(eq) is defined as one third of the trace of the orthogonalized U^{ij} tensor.

Atom	*x*	*y*	*z*	U(eq)
C(33)	-1182(4)	4095(3)	-79(2)	32(2)
C(34)	-958(4)	4298(3)	392(2)	30(2)
C(35)	-1570(4)	6417(3)	-496(2)	27(2)
C(36)	-1613(4)	5778(3)	-638(2)	22(2)
C(37)	2792(4)	5940(3)	2946(2)	24(2)
C(38)	2358(4)	6231(3)	3271(2)	27(2)
C(39)	1756(4)	6741(3)	3128(2)	26(2)
C(40)	1607(4)	6974(3)	2659(2)	21(2)
C(41)	2084(4)	6657(3)	2355(2)	17(1)
C(42)	1976(4)	6883(3)	1877(2)	17(1)
C(43)	1395(4)	7424(3)	1715(2)	18(1)
C(44)	1329(4)	7640(3)	1246(2)	24(2)
C(45)	1824(4)	7322(3)	971(2)	27(2)
C(46)	2401(4)	6798(3)	1161(2)	25(2)
C(47)	1036(4)	7524(3)	2479(2)	25(2)
C(48)	929(4)	7739(3)	2031(2)	23(2)
C(49)	7633(4)	6458(3)	2363(2)	28(2)
C(50)	8479(4)	6775(3)	2481(2)	31(2)
C(51)	8598(4)	7330(3)	2232(2)	32(2)
C(52)	7905(4)	7568(3)	1868(2)	24(2)
C(53)	7081(4)	7225(3)	1777(2)	18(1)
C(54)	6337(4)	7451(3)	1418(2)	21(1)
C(55)	6438(4)	8018(3)	1147(2)	29(2)
C(56)	5695(5)	8223(3)	799(2)	38(2)
C(57)	4895(5)	7859(3)	725(2)	36(2)
C(58)	4859(4)	7308(3)	1009(2)	28(2)
C(59)	7988(5)	8146(3)	1587(2)	36(2)
C(60)	7292(5)	8360(3)	1240(2)	35(2)
C(61)	4313(4)	3337(4)	1028(2)	34(2)
C(62)	4112(5)	2737(3)	777(3)	44(2)
C(63)	3780(5)	2765(3)	301(3)	41(2)
C(64)	3655(4)	3379(3)	70(2)	29(2)
C(65)	3885(4)	3959(3)	350(2)	20(1)
C(66)	3772(4)	4604(3)	132(2)	20(1)
C(67)	3447(4)	4652(3)	-362(2)	24(2)
C(68)	3360(4)	5292(3)	-561(2)	35(2)
C(69)	3631(5)	5833(4)	-276(2)	42(2)
C(70)	3938(5)	5739(3)	210(2)	40(2)
C(71)	3207(4)	4058(4)	-634(2)	29(2)

Table S1. AtomicCoordinates (x 10^4) and equivalent isotropic displacement parameters ($Å^2$ x 10^3) for [Mo(O)(μ-S)$_3$(Cu(phen))$_3$][PF_6]·2MeCN. U(eq) is defined as one third of the trace of the orthogonalized U^{ij} tensor.

Atom	*x*	*y*	*z*	U(eq)
C(72)	3307(4)	3454(4)	-430(2)	31(2)
C(73)	305(5)	9232(4)	-338(3)	45(2)
C(74)	757(5)	9142(4)	153(3)	62(2)
C(75)	-623(5)	9395(4)	1238(2)	29(2)
C(76)	-1162(4)	9954(3)	1361(2)	39(2)
C(77)	-3898(5)	10203(4)	840(3)	49(2)
C(78)	-4050(5)	10667(4)	433(3)	58(2)
C(79)	-5192(5)	1000(4)	1425(2)	34(2)
C(80)	-5709(5)	401(3)	1471(3)	48(2)

Table S2. Bond lengths (Å) for [Mo(O)(μ-S)$_3$(Cu(phen))$_3$][PF$_6$]·2MeCN. Symmetry transformations used to generate equivalent atoms:

Mo(1)-O(1)	1.706(4)	P(1)-F(5)	1.604(4)
Mo(1)-S(1)	2.2709(16)	P(2)-F(10)	1.553(5)
Mo(1)-S(2)	2.2717(16)	P(2)-F(8)	1.561(5)
Mo(1)-S(3)	2.2782(15)	P(2)-F(9)	1.573(4)
Mo(1)-Cu(1)	2.6406(9)	P(2)-F(12)	1.575(4)
Mo(1)-Cu(3)	2.6533(9)	P(2)-F(7)	1.580(5)
Mo(1)-Cu(2)	2.6610(9)	P(2)-F(11)	1.582(4)
Mo(2)-O(2)	1.707(4)	N(1)-C(1)	1.318(7)
Mo(2)-S(5)	2.2649(16)	N(1)-C(5)	1.358(7)
Mo(2)-S(4)	2.2756(16)	N(2)-C(10)	1.326(7)
Mo(2)-S(6)	2.2776(16)	N(2)-C(6)	1.369(7)
Mo(2)-Cu(6)	2.6544(9)	N(3)-C(13)	1.319(7)
Mo(2)-Cu(4)	2.6570(9)	N(3)-C(17)	1.344(7)
Mo(2)-Cu(5)	2.6660(9)	N(4)-C(22)	1.338(7)
Cu(1)-N(2)	2.005(5)	N(4)-C(18)	1.357(7)
Cu(1)-N(1)	2.178(5)	N(5)-C(25)	1.324(7)
Cu(1)-S(3)	2.2398(17)	N(5)-C(29)	1.364(7)
Cu(1)-S(1)	2.2886(17)	N(6)-C(34)	1.321(7)
Cu(2)-N(3)	2.075(5)	N(6)-C(30)	1.353(7)
Cu(2)-N(4)	2.082(5)	N(7)-C(37)	1.330(7)
Cu(2)-S(1)	2.2456(17)	N(7)-C(41)	1.371(7)
Cu(2)-S(2)	2.2633(17)	N(8)-C(46)	1.329(7)
Cu(3)-N(6)	2.052(5)	N(8)-C(42)	1.362(7)
Cu(3)-N(5)	2.111(5)	N(9)-C(49)	1.325(7)
Cu(3)-S(2)	2.2531(17)	N(9)-C(53)	1.350(7)
Cu(3)-S(3)	2.2657(17)	N(10)-C(58)	1.328(7)
Cu(4)-N(8)	2.053(5)	N(10)-C(54)	1.366(7)
Cu(4)-N(7)	2.111(5)	N(11)-C(61)	1.310(7)
Cu(4)-S(6)	2.2404(17)	N(11)-C(65)	1.358(7)
Cu(4)-S(4)	2.2774(17)	N(12)-C(70)	1.337(8)
Cu(5)-N(9)	2.077(5)	N(12)-C(66)	1.351(7)
Cu(5)-N(10)	2.086(5)	N(13)-C(73)	1.153(9)
Cu(5)-S(4)	2.2440(17)	N(14)-C(75)	1.123(7)
Cu(5)-S(5)	2.2567(18)	N(15)-C(77)	1.153(9)
Cu(6)-N(12)	2.050(5)	N(16)-C(79)	1.128(8)
Cu(6)-N(11)	2.114(5)	C(1)-C(2)	1.393(8)
Cu(6)-S(5)	2.2465(17)	C(1)-H(1)	0.9500
Cu(6)-S(6)	2.2708(17)	C(2)-C(3)	1.361(8)
P(1)-F(6)	1.593(4)	C(2)-H(2)	0.9500
P(1)-F(4)	1.596(4)	C(3)-C(4)	1.395(8)
P(1)-F(3)	1.597(4)	C(3)-H(3)	0.9500
P(1)-F(2)	1.598(4)	C(4)-C(5)	1.403(8)
P(1)-F(1)	1.598(4)	C(4)-C(11)	1.439(8)

Table S2. Bond lengths (Å) for $[Mo(O)(\mu\text{-}S)_3(Cu(phen))_3][PF_6]\cdot 2MeCN$. Symmetry transformations used to generate equivalent atoms:

C(5)-C(6)	1.440(8)	C(31)-C(36)	1.436(8)
C(6)-C(7)	1.407(8)	C(32)-C(33)	1.370(8)
C(7)-C(8)	1.412(8)	C(32)-H(32)	0.9500
C(7)-C(12)	1.430(8)	C(33)-C(34)	1.391(8)
C(8)-C(9)	1.363(8)	C(33)-H(33)	0.9500
C(8)-H(8)	0.9500	C(34)-H(34)	0.9500
C(9)-C(10)	1.395(8)	C(35)-C(36)	1.341(8)
C(9)-H(9)	0.9500	C(35)-H(35)	0.9500
C(10)-H(10)	0.9500	C(36)-H(36)	0.9500
C(11)-C(12)	1.340(8)	C(37)-C(38)	1.389(8)
C(11)-H(11)	0.9500	C(37)-H(37)	0.9500
C(12)-H(12)	0.9500	C(38)-C(39)	1.369(8)
C(13)-C(14)	1.390(9)	C(38)-H(38)	0.9500
C(13)-H(13)	0.9500	C(39)-C(40)	1.406(8)
C(14)-C(15)	1.358(9)	C(39)-H(39)	0.9500
C(14)-H(14)	0.9500	C(40)-C(41)	1.408(8)
C(15)-C(16)	1.408(9)	C(40)-C(47)	1.424(8)
C(15)-H(15)	0.9500	C(41)-C(42)	1.432(8)
C(16)-C(17)	1.417(8)	C(42)-C(43)	1.407(8)
C(16)-C(23)	1.418(9)	C(43)-C(44)	1.408(8)
C(17)-C(18)	1.427(8)	C(43)-C(48)	1.420(8)
C(18)-C(19)	1.407(8)	C(44)-C(45)	1.365(8)
C(19)-C(20)	1.395(9)	C(44)-H(44)	0.9500
C(19)-C(24)	1.446(9)	C(45)-C(46)	1.396(8)
C(20)-C(21)	1.374(9)	C(45)-H(45)	0.9500
C(20)-H(20)	0.9500	C(46)-H(46)	0.9500
C(21)-C(22)	1.392(9)	C(47)-C(48)	1.343(8)
C(21)-H(21)	0.9500	C(47)-H(47)	0.9500
C(22)-H(22)	0.9500	C(48)-H(48)	0.9500
C(23)-C(24)	1.343(9)	C(49)-C(50)	1.399(8)
C(23)-H(23)	0.9500	C(49)-H(49)	0.9500
C(24)-H(24)	0.9500	C(50)-C(51)	1.359(9)
C(25)-C(26)	1.395(8)	C(50)-H(50)	0.9500
C(25)-H(25)	0.9500	C(51)-C(52)	1.394(8)
C(26)-C(27)	1.358(8)	C(51)-H(51)	0.9500
C(26)-H(26)	0.9500	C(52)-C(53)	1.395(8)
C(27)-C(28)	1.401(8)	C(52)-C(59)	1.434(9)
C(27)-H(27)	0.9500	C(53)-C(54)	1.423(8)
C(28)-C(29)	1.397(8)	C(54)-C(55)	1.407(8)
C(28)-C(35)	1.433(8)	C(55)-C(56)	1.393(9)
C(29)-C(30)	1.435(8)	C(55)-C(60)	1.432(9)
C(30)-C(31)	1.406(8)	C(56)-C(57)	1.387(9)
C(31)-C(32)	1.398(8)	C(56)-H(56)	0.9500

Table S2. Bond lengths (Å) for [Mo(O)(μ-S)$_3$(Cu(phen))$_3$][PF$_6$]·2MeCN. Symmetry transformations used to generate equivalent atoms:

C(57)-C(58)	1.385(9)
C(57)-H(57)	0.9500
C(58)-H(58)	0.9500
C(59)-C(60)	1.352(9)
C(59)-H(59)	0.9500
C(60)-H(60)	0.9500
C(61)-C(62)	1.400(9)
C(61)-H(61)	0.9500
C(62)-C(63)	1.360(9)
C(62)-H(62)	0.9500
C(63)-C(64)	1.391(9)
C(63)-H(63)	0.9500
C(64)-C(65)	1.413(8)
C(64)-C(72)	1.435(9)
C(65)-C(66)	1.430(8)
C(66)-C(67)	1.407(8)
C(67)-C(68)	1.399(9)
C(67)-C(71)	1.428(8)
C(68)-C(69)	1.367(9)
C(68)-H(68)	0.9500
C(69)-C(70)	1.393(9)
C(69)-H(69)	0.9500
C(70)-H(70)	0.9500
C(71)-C(72)	1.340(9)
C(71)-H(71)	0.9500
C(72)-H(72)	0.9500
C(73)-C(74)	1.446(11)
C(74)-H(74A)	0.9800
C(74)-H(74B)	0.9800
C(74)-H(74C)	0.9800
C(75)-C(76)	1.474(10)
C(76)-H(76A)	0.9800
C(76)-H(76B)	0.9800
C(76)-H(76C)	0.9800
C(77)-C(78)	1.477(11)
C(78)-H(78A)	0.9800
C(78)-H(78B)	0.9800
C(78)-H(78C)	0.9800
C(79)-C(80)	1.453(10)
C(80)-H(80A)	0.9800
C(80)-H(80B)	0.9800
C(80)-H(80C)	0.9800

Table S3. Bond angles (deg,) for $[Mo(O)(\mu\text{-}S)_3(Cu(phen))_3][PF_6]\cdot 2MeCN$. Symmetry transformations used to generate equivalent atoms:

O(1)-Mo(1)-S(1)	110.92(14)	N(1)-Cu(1)-S(1)	96.89(13)
O(1)-Mo(1)-S(2)	111.76(14)	S(3)-Cu(1)-S(1)	108.33(6)
S(1)-Mo(1)-S(2)	107.39(6)	N(2)-Cu(1)-Mo(1)	165.59(14)
O(1)-Mo(1)-S(3)	111.16(13)	N(1)-Cu(1)-Mo(1)	112.88(13)
S(1)-Mo(1)-S(3)	107.62(6)	S(3)-Cu(1)-Mo(1)	54.91(4)
S(2)-Mo(1)-S(3)	107.80(6)	S(1)-Cu(1)-Mo(1)	54.30(4)
O(1)-Mo(1)-Cu(1)	119.18(13)	N(3)-Cu(2)-N(4)	80.3(2)
S(1)-Mo(1)-Cu(1)	54.92(4)	N(3)-Cu(2)-S(1)	114.38(14)
S(2)-Mo(1)-Cu(1)	129.06(5)	N(4)-Cu(2)-S(1)	117.56(14)
S(3)-Mo(1)-Cu(1)	53.56(4)	N(3)-Cu(2)-S(2)	110.73(14)
O(1)-Mo(1)-Cu(3)	126.97(13)	N(4)-Cu(2)-S(2)	122.27(13)
S(1)-Mo(1)-Cu(3)	122.11(5)	S(1)-Cu(2)-S(2)	108.56(6)
S(2)-Mo(1)-Cu(3)	53.77(4)	N(3)-Cu(2)-Mo(1)	131.66(15)
S(3)-Mo(1)-Cu(3)	54.05(4)	N(4)-Cu(2)-Mo(1)	147.99(14)
Cu(1)-Mo(1)-Cu(3)	92.79(3)	S(1)-Cu(2)-Mo(1)	54.34(4)
O(1)-Mo(1)-Cu(2)	128.52(13)	S(2)-Cu(2)-Mo(1)	54.22(4)
S(1)-Mo(1)-Cu(2)	53.46(4)	N(6)-Cu(3)-N(5)	80.32(19)
S(2)-Mo(1)-Cu(2)	53.93(4)	N(6)-Cu(3)-S(2)	116.44(14)
S(3)-Mo(1)-Cu(2)	120.31(5)	N(5)-Cu(3)-S(2)	117.17(13)
Cu(1)-Mo(1)-Cu(2)	92.11(3)	N(6)-Cu(3)-S(3)	124.46(14)
Cu(3)-Mo(1)-Cu(2)	86.85(3)	N(5)-Cu(3)-S(3)	106.26(13)
O(2)-Mo(2)-S(5)	110.69(14)	S(2)-Cu(3)-S(3)	108.89(6)
O(2)-Mo(2)-S(4)	111.26(14)	N(6)-Cu(3)-Mo(1)	151.82(14)
S(5)-Mo(2)-S(4)	107.03(6)	N(5)-Cu(3)-Mo(1)	127.86(13)
O(2)-Mo(2)-S(6)	112.33(13)	S(2)-Cu(3)-Mo(1)	54.42(4)
S(5)-Mo(2)-S(6)	107.77(6)	S(3)-Cu(3)-Mo(1)	54.49(4)
S(4)-Mo(2)-S(6)	107.53(6)	N(8)-Cu(4)-N(7)	80.7(2)
O(2)-Mo(2)-Cu(6)	126.54(13)	N(8)-Cu(4)-S(6)	118.24(14)
S(5)-Mo(2)-Cu(6)	53.64(4)	N(7)-Cu(4)-S(6)	126.44(14)
S(4)-Mo(2)-Cu(6)	122.18(5)	N(8)-Cu(4)-S(4)	119.11(13)
S(6)-Mo(2)-Cu(6)	54.18(4)	N(7)-Cu(4)-S(4)	101.15(14)
O(2)-Mo(2)-Cu(4)	125.69(13)	S(6)-Cu(4)-S(4)	108.76(6)
S(5)-Mo(2)-Cu(4)	123.61(5)	N(8)-Cu(4)-Mo(2)	148.77(14)
S(4)-Mo(2)-Cu(4)	54.33(4)	N(7)-Cu(4)-Mo(2)	129.34(14)
S(6)-Mo(2)-Cu(4)	53.33(4)	S(6)-Cu(4)-Mo(2)	54.63(4)
Cu(6)-Mo(2)-Cu(4)	89.42(3)	S(4)-Cu(4)-Mo(2)	54.27(4)
O(2)-Mo(2)-Cu(5)	127.75(13)	N(9)-Cu(5)-N(10)	80.3(2)
S(5)-Mo(2)-Cu(5)	53.73(4)	N(9)-Cu(5)-S(4)	115.12(14)
S(4)-Mo(2)-Cu(5)	53.31(4)	N(10)-Cu(5)-S(4)	117.62(14)
S(6)-Mo(2)-Cu(5)	119.92(5)	N(9)-Cu(5)-S(5)	111.13(14)
Cu(6)-Mo(2)-Cu(5)	86.72(3)		
Cu(4)-Mo(2)-Cu(5)	87.91(3)		
N(2)-Cu(1)-N(1)	80.55(19)		
N(2)-Cu(1)-S(3)	124.29(14)		
N(1)-Cu(1)-S(3)	118.96(13)		
N(2)-Cu(1)-S(1)	121.12(14)		

Table S3. Bond angles (deg,) for $[Mo(O)(\mu\text{-}S)_3(Cu(phen))_3][PF_6]\cdot 2MeCN$. Symmetry transformations used to generate equivalent atoms:

N(10)-Cu(5)-S(5)	121.57(14)	F(2)-P(1)-F(1)	89.45(19)
S(4)-Cu(5)-S(5)	108.41(6)	F(6)-P(1)-F(5)	179.1(2)
N(9)-Cu(5)-Mo(2)	132.89(15)	F(4)-P(1)-F(5)	89.8(2)
N(10)-Cu(5)-Mo(2)	146.81(14)	F(3)-P(1)-F(5)	90.1(2)
S(4)-Cu(5)-Mo(2)	54.40(4)	F(2)-P(1)-F(5)	89.3(2)
S(5)-Cu(5)-Mo(2)	54.01(4)	F(1)-P(1)-F(5)	90.3(2)
N(12)-Cu(6)-N(11)	80.44(19)	F(10)-P(2)-F(8)	178.0(4)
N(12)-Cu(6)-S(5)	116.31(15)	F(10)-P(2)-F(9)	92.3(4)
N(11)-Cu(6)-S(5)	118.30(14)	F(8)-P(2)-F(9)	89.6(3)
N(12)-Cu(6)-S(6)	126.13(14)	F(10)-P(2)-F(12)	90.1(3)
N(11)-Cu(6)-S(6)	103.39(13)	F(8)-P(2)-F(12)	90.4(3)
S(5)-Cu(6)-S(6)	108.65(6)	F(9)-P(2)-F(12)	89.9(2)
N(12)-Cu(6)-Mo(2)	154.22(15)	F(10)-P(2)-F(7)	89.3(3)
N(11)-Cu(6)-Mo(2)	125.33(14)	F(8)-P(2)-F(7)	88.8(3)
S(5)-Cu(6)-Mo(2)	54.28(4)	F(9)-P(2)-F(7)	178.3(3)
S(6)-Cu(6)-Mo(2)	54.42(4)	F(12)-P(2)-F(7)	89.8(2)
Cu(2)-S(1)-Mo(1)	72.19(5)	F(10)-P(2)-F(11)	89.5(3)
Cu(2)-S(1)-Cu(1)	114.67(7)	F(8)-P(2)-F(11)	89.9(3)
Mo(1)-S(1)-Cu(1)	70.78(5)	F(9)-P(2)-F(11)	90.8(2)
Cu(3)-S(2)-Cu(2)	107.97(7)	F(12)-P(2)-F(11)	179.3(3)
Cu(3)-S(2)-Mo(1)	71.80(5)	F(7)-P(2)-F(11)	89.5(2)
Cu(2)-S(2)-Mo(1)	71.86(5)	C(1)-N(1)-C(5)	117.8(5)
Cu(1)-S(3)-Cu(3)	116.60(7)	C(1)-N(1)-Cu(1)	132.0(4)
Cu(1)-S(3)-Mo(1)	71.52(5)	C(5)-N(1)-Cu(1)	108.9(4)
Cu(3)-S(3)-Mo(1)	71.45(5)	C(10)-N(2)-C(6)	118.4(5)
Cu(5)-S(4)-Mo(2)	72.29(5)	C(10)-N(2)-Cu(1)	127.4(4)
Cu(5)-S(4)-Cu(4)	109.60(7)	C(6)-N(2)-Cu(1)	113.9(4)
Mo(2)-S(4)-Cu(4)	71.40(5)	C(13)-N(3)-C(17)	118.7(5)
Cu(6)-S(5)-Cu(5)	108.41(7)	C(13)-N(3)-Cu(2)	129.2(5)
Cu(6)-S(5)-Mo(2)	72.08(5)	C(17)-N(3)-Cu(2)	112.0(4)
Cu(5)-S(5)-Mo(2)	72.26(5)	C(22)-N(4)-C(18)	118.0(5)
Cu(4)-S(6)-Cu(6)	111.85(7)	C(22)-N(4)-Cu(2)	130.3(4)
Cu(4)-S(6)-Mo(2)	72.04(5)	C(18)-N(4)-Cu(2)	111.6(4)
Cu(6)-S(6)-Mo(2)	71.41(5)	C(25)-N(5)-C(29)	117.0(5)
F(6)-P(1)-F(4)	90.8(2)	C(25)-N(5)-Cu(3)	131.5(4)
F(6)-P(1)-F(3)	90.5(2)	C(29)-N(5)-Cu(3)	111.3(4)
F(4)-P(1)-F(3)	90.8(2)	C(34)-N(6)-C(30)	118.1(5)
F(6)-P(1)-F(2)	90.1(2)	C(34)-N(6)-Cu(3)	128.3(4)
F(4)-P(1)-F(2)	178.6(2)	C(30)-N(6)-Cu(3)	113.5(4)
F(3)-P(1)-F(2)	90.3(2)	C(37)-N(7)-C(41)	117.2(5)
F(6)-P(1)-F(1)	89.0(2)	C(37)-N(7)-Cu(4)	131.0(4)
F(4)-P(1)-F(1)	89.4(2)	C(41)-N(7)-Cu(4)	110.7(4)
F(3)-P(1)-F(1)	179.4(2)	C(46)-N(8)-C(42)	118.2(5)

Table S3. Bond angles (deg,) for $[Mo(O)(\mu\text{-}S)_3(Cu(phen))_3][PF_6]\cdot 2MeCN$. Symmetry transformations used to generate equivalent atoms:

C(46)-N(8)-Cu(4)	128.8(4)	C(9)-C(10)-H(10)	118.7
C(42)-N(8)-Cu(4)	112.8(4)	C(12)-C(11)-C(4)	122.1(6)
C(49)-N(9)-C(53)	118.7(5)	C(12)-C(11)-H(11)	119.0
C(49)-N(9)-Cu(5)	128.6(4)	C(4)-C(11)-H(11)	119.0
C(53)-N(9)-Cu(5)	112.6(4)	C(11)-C(12)-C(7)	120.8(6)
C(58)-N(10)-C(54)	117.2(5)	C(11)-C(12)-H(12)	119.6
C(58)-N(10)-Cu(5)	131.1(4)	C(7)-C(12)-H(12)	119.6
C(54)-N(10)-Cu(5)	111.6(4)	N(3)-C(13)-C(14)	123.4(6)
C(61)-N(11)-C(65)	118.4(5)	N(3)-C(13)-H(13)	118.3
C(61)-N(11)-Cu(6)	130.8(4)	C(14)-C(13)-H(13)	118.3
C(65)-N(11)-Cu(6)	110.4(4)	C(15)-C(14)-C(13)	118.2(6)
C(70)-N(12)-C(66)	117.1(5)	C(15)-C(14)-H(14)	120.9
C(70)-N(12)-Cu(6)	129.5(4)	C(13)-C(14)-H(14)	120.9
C(66)-N(12)-Cu(6)	113.3(4)	C(14)-C(15)-C(16)	121.1(6)
N(1)-C(1)-C(2)	123.6(6)	C(14)-C(15)-H(15)	119.5
N(1)-C(1)-H(1)	118.2	C(16)-C(15)-H(15)	119.5
C(2)-C(1)-H(1)	118.2	C(15)-C(16)-C(17)	115.8(6)
C(3)-C(2)-C(1)	118.7(6)	C(15)-C(16)-C(23)	125.1(6)
C(3)-C(2)-H(2)	120.7	C(17)-C(16)-C(23)	119.1(6)
C(1)-C(2)-H(2)	120.7	N(3)-C(17)-C(16)	122.7(6)
C(2)-C(3)-C(4)	120.0(6)	N(3)-C(17)-C(18)	118.0(5)
C(2)-C(3)-H(3)	120.0	C(16)-C(17)-C(18)	119.2(6)
C(4)-C(3)-H(3)	120.0	N(4)-C(18)-C(19)	122.2(5)
C(3)-C(4)-C(5)	117.3(6)	N(4)-C(18)-C(17)	117.4(5)
C(3)-C(4)-C(11)	124.4(6)	C(19)-C(18)-C(17)	120.4(6)
C(5)-C(4)-C(11)	118.3(6)	C(20)-C(19)-C(18)	118.3(6)
N(1)-C(5)-C(4)	122.6(5)	C(20)-C(19)-C(24)	123.0(6)
N(1)-C(5)-C(6)	117.4(5)	C(18)-C(19)-C(24)	118.7(6)
C(4)-C(5)-C(6)	120.1(6)	C(21)-C(20)-C(19)	119.1(6)
N(2)-C(6)-C(7)	122.4(5)	C(21)-C(20)-H(20)	120.5
N(2)-C(6)-C(5)	118.0(5)	C(19)-C(20)-H(20)	120.5
C(7)-C(6)-C(5)	119.5(5)	C(20)-C(21)-C(22)	119.4(6)
C(6)-C(7)-C(8)	116.9(5)	C(20)-C(21)-H(21)	120.3
C(6)-C(7)-C(12)	119.3(6)	C(22)-C(21)-H(21)	120.3
C(8)-C(7)-C(12)	123.8(6)	N(4)-C(22)-C(21)	122.8(6)
C(9)-C(8)-C(7)	120.0(6)	N(4)-C(22)-H(22)	118.6
C(9)-C(8)-H(8)	120.0	C(21)-C(22)-H(22)	118.6
C(7)-C(8)-H(8)	120.0	C(24)-C(23)-C(16)	122.1(6)
C(8)-C(9)-C(10)	119.5(6)	C(24)-C(23)-H(23)	118.9
C(8)-C(9)-H(9)	120.2	C(16)-C(23)-H(23)	118.9
C(10)-C(9)-H(9)	120.2	C(23)-C(24)-C(19)	120.4(6)
N(2)-C(10)-C(9)	122.6(6)	C(23)-C(24)-H(24)	119.8
N(2)-C(10)-H(10)	118.7	C(19)-C(24)-H(24)	119.8

Table S3. Bond angles (deg,) for [Mo(O)(μ-S)$_3$(Cu(phen))$_3$][PF$_6$]·2MeCN. Symmetry transformations used to generate equivalent atoms:

N(5)-C(25)-C(26)	124.1(6)	C(38)-C(39)-H(39)	120.3
N(5)-C(25)-H(25)	118.0	C(40)-C(39)-H(39)	120.3
C(26)-C(25)-H(25)	118.0	C(39)-C(40)-C(41)	117.5(6)
C(27)-C(26)-C(25)	118.3(6)	C(39)-C(40)-C(47)	124.3(6)
C(27)-C(26)-H(26)	120.8	C(41)-C(40)-C(47)	118.2(6)
C(25)-C(26)-H(26)	120.8	N(7)-C(41)-C(40)	122.8(5)
C(26)-C(27)-C(28)	120.3(6)	N(7)-C(41)-C(42)	117.3(5)
C(26)-C(27)-H(27)	119.8	C(40)-C(41)-C(42)	120.0(5)
C(28)-C(27)-H(27)	119.8	N(8)-C(42)-C(43)	122.5(5)
C(29)-C(28)-C(27)	117.2(5)	N(8)-C(42)-C(41)	117.9(5)
C(29)-C(28)-C(35)	118.8(6)	C(43)-C(42)-C(41)	119.5(5)
C(27)-C(28)-C(35)	124.0(6)	C(42)-C(43)-C(44)	117.5(5)
N(5)-C(29)-C(28)	123.0(5)	C(42)-C(43)-C(48)	119.3(5)
N(5)-C(29)-C(30)	117.2(5)	C(44)-C(43)-C(48)	123.2(6)
C(28)-C(29)-C(30)	119.7(5)	C(45)-C(44)-C(43)	119.3(6)
N(6)-C(30)-C(31)	122.5(5)	C(45)-C(44)-H(44)	120.3
N(6)-C(30)-C(29)	117.5(5)	C(43)-C(44)-H(44)	120.3
C(31)-C(30)-C(29)	120.0(5)	C(44)-C(45)-C(46)	119.7(6)
C(32)-C(31)-C(30)	117.6(6)	C(44)-C(45)-H(45)	120.2
C(32)-C(31)-C(36)	123.6(5)	C(46)-C(45)-H(45)	120.2
C(30)-C(31)-C(36)	118.8(6)	N(8)-C(46)-C(45)	122.7(6)
C(33)-C(32)-C(31)	119.5(6)	N(8)-C(46)-H(46)	118.6
C(33)-C(32)-H(32)	120.3	C(45)-C(46)-H(46)	118.6
C(31)-C(32)-H(32)	120.3	C(48)-C(47)-C(40)	122.2(6)
C(32)-C(33)-C(34)	118.9(6)	C(48)-C(47)-H(47)	118.9
C(32)-C(33)-H(33)	120.5	C(40)-C(47)-H(47)	118.9
C(34)-C(33)-H(33)	120.5	C(47)-C(48)-C(43)	120.8(6)
N(6)-C(34)-C(33)	123.4(6)	C(47)-C(48)-H(48)	119.6
N(6)-C(34)-H(34)	118.3	C(43)-C(48)-H(48)	119.6
C(33)-C(34)-H(34)	118.3	N(9)-C(49)-C(50)	123.2(6)
C(36)-C(35)-C(28)	121.8(6)	N(9)-C(49)-H(49)	118.4
C(36)-C(35)-H(35)	119.1	C(50)-C(49)-H(49)	118.4
C(28)-C(35)-H(35)	119.1	C(51)-C(50)-C(49)	117.5(6)
C(35)-C(36)-C(31)	120.8(6)	C(51)-C(50)-H(50)	121.3
C(35)-C(36)-H(36)	119.6	C(49)-C(50)-H(50)	121.3
C(31)-C(36)-H(36)	119.6	C(50)-C(51)-C(52)	121.1(6)
N(7)-C(37)-C(38)	123.7(6)	C(50)-C(51)-H(51)	119.5
N(7)-C(37)-H(37)	118.2	C(52)-C(51)-H(51)	119.5
C(38)-C(37)-H(37)	118.2	C(51)-C(52)-C(53)	117.5(6)
C(39)-C(38)-C(37)	119.4(6)	C(51)-C(52)-C(59)	124.0(6)
C(39)-C(38)-H(38)	120.3	C(53)-C(52)-C(59)	118.5(6)
C(37)-C(38)-H(38)	120.3	N(9)-C(53)-C(52)	121.9(6)
C(38)-C(39)-C(40)	119.4(6)	N(9)-C(53)-C(54)	117.6(5)

Table S3. Bond angles (deg,) for $[Mo(O)(\mu\text{-}S)_3(Cu(phen))_3][PF_6]\cdot 2MeCN$. Symmetry transformations used to generate equivalent atoms:

C(52)-C(53)-C(54)	120.5(6)	C(69)-C(68)-C(67)	119.2(6)
N(10)-C(54)-C(55)	122.5(6)	C(69)-C(68)-H(68)	120.4
N(10)-C(54)-C(53)	117.7(5)	C(67)-C(68)-H(68)	120.4
C(55)-C(54)-C(53)	119.8(6)	C(68)-C(69)-C(70)	119.4(6)
C(56)-C(55)-C(54)	118.1(6)	C(68)-C(69)-H(69)	120.3
C(56)-C(55)-C(60)	122.8(6)	C(70)-C(69)-H(69)	120.3
C(54)-C(55)-C(60)	119.1(6)	N(12)-C(70)-C(69)	123.2(6)
C(57)-C(56)-C(55)	119.4(6)	N(12)-C(70)-H(70)	118.4
C(57)-C(56)-H(56)	120.3	C(69)-C(70)-H(70)	118.4
C(55)-C(56)-H(56)	120.3	C(72)-C(71)-C(67)	121.2(6)
C(58)-C(57)-C(56)	118.4(6)	C(72)-C(71)-H(71)	119.4
C(58)-C(57)-H(57)	120.8	C(67)-C(71)-H(71)	119.4
C(56)-C(57)-H(57)	120.8	C(71)-C(72)-C(64)	121.3(6)
N(10)-C(58)-C(57)	124.4(6)	C(71)-C(72)-H(72)	119.3
N(10)-C(58)-H(58)	117.8	C(64)-C(72)-H(72)	119.3
C(57)-C(58)-H(58)	117.8	N(13)-C(73)-C(74)	178.5(9)
C(60)-C(59)-C(52)	121.7(6)	C(73)-C(74)-H(74A)	109.5
C(60)-C(59)-H(59)	119.2	C(73)-C(74)-H(74B)	109.5
C(52)-C(59)-H(59)	119.2	H(74A)-C(74)-H(74B)	109.5
C(59)-C(60)-C(55)	120.4(6)	C(73)-C(74)-H(74C)	109.5
C(59)-C(60)-H(60)	119.8	H(74A)-C(74)-H(74C)	109.5
C(55)-C(60)-H(60)	119.8	H(74B)-C(74)-H(74C)	109.5
N(11)-C(61)-C(62)	123.4(6)	N(14)-C(75)-C(76)	178.3(7)
N(11)-C(61)-H(61)	118.3	C(75)-C(76)-H(76A)	109.5
C(62)-C(61)-H(61)	118.3	C(75)-C(76)-H(76B)	109.5
C(63)-C(62)-C(61)	118.6(6)	H(76A)-C(76)-H(76B)	109.5
C(63)-C(62)-H(62)	120.7	C(75)-C(76)-H(76C)	109.5
C(61)-C(62)-H(62)	120.7	H(76A)-C(76)-H(76C)	109.5
C(62)-C(63)-C(64)	120.2(6)	H(76B)-C(76)-H(76C)	109.5
C(62)-C(63)-H(63)	119.9	N(15)-C(77)-C(78)	178.2(8)
C(64)-C(63)-H(63)	119.9	C(77)-C(78)-H(78A)	109.5
C(63)-C(64)-C(65)	117.4(6)	C(77)-C(78)-H(78B)	109.5
C(63)-C(64)-C(72)	123.9(6)	H(78A)-C(78)-H(78B)	109.5
C(65)-C(64)-C(72)	118.7(6)	C(77)-C(78)-H(78C)	109.5
N(11)-C(65)-C(64)	121.9(6)	H(78A)-C(78)-H(78C)	109.5
N(11)-C(65)-C(66)	118.2(5)	H(78B)-C(78)-H(78C)	109.5
C(64)-C(65)-C(66)	119.9(6)	N(16)-C(79)-C(80)	178.9(8)
N(12)-C(66)-C(67)	123.4(6)	C(79)-C(80)-H(80A)	109.5
N(12)-C(66)-C(65)	117.2(5)	C(79)-C(80)-H(80B)	109.5
C(67)-C(66)-C(65)	119.4(6)	H(80A)-C(80)-H(80B)	109.5
C(68)-C(67)-C(66)	117.5(6)	C(79)-C(80)-H(80C)	109.5
C(68)-C(67)-C(71)	123.0(6)	H(80A)-C(80)-H(80C)	109.5
C(66)-C(67)-C(71)	119.5(6)	H(80B)-C(80)-H(80C)	109.5

Table S4. Anisotropic displacement parameters ($Å^2$ x 10^3) for $[Mo(O)(\mu\text{-}S)_3(Cu(phen))_3][PF_6]\cdot 2MeCN$. The anisotropic displacement factor exponent takes the form: $-2\pi^2[(ha^*)^2U^{11} + ... + 2hka^*b^*U^{12}]$.

Atom	U^{11}	U^{22}	U^{33}	U^{23}	U^{13}	U^{12}
Mo(1)	15(1)	18(1)	16(1)	-1(1)	4(1)	-1(1)
Mo(2)	16(1)	18(1)	19(1)	-1(1)	5(1)	-1(1)
Cu(1)	18(1)	25(1)	23(1)	2(1)	7(1)	-4(1)
Cu(2)	22(1)	23(1)	29(1)	3(1)	11(1)	5(1)
Cu(3)	23(1)	28(1)	17(1)	2(1)	6(1)	0(1)
Cu(4)	18(1)	24(1)	25(1)	-4(1)	7(1)	1(1)
Cu(5)	25(1)	23(1)	32(1)	-3(1)	14(1)	-6(1)
Cu(6)	30(1)	28(1)	20(1)	-4(1)	10(1)	-4(1)
S(1)	19(1)	23(1)	22(1)	5(1)	6(1)	3(1)
S(2)	19(1)	25(1)	24(1)	4(1)	10(1)	0(1)
S(3)	15(1)	26(1)	19(1)	2(1)	4(1)	1(1)
S(4)	19(1)	21(1)	24(1)	-6(1)	8(1)	-2(1)
S(5)	24(1)	25(1)	33(1)	-7(1)	16(1)	-4(1)
S(6)	19(1)	22(1)	23(1)	-2(1)	6(1)	-4(1)
P(1)	33(1)	37(1)	26(1)	1(1)	10(1)	1(1)
P(2)	37(1)	39(1)	24(1)	-2(1)	8(1)	-1(1)
F(1)	39(2)	37(2)	36(2)	8(2)	11(2)	11(2)
F(2)	27(2)	50(3)	30(2)	6(2)	10(2)	2(2)
F(3)	59(3)	59(3)	35(2)	20(2)	12(2)	8(2)
F(4)	40(2)	59(3)	55(3)	3(2)	25(2)	-5(2)
F(5)	54(3)	54(3)	36(2)	-19(2)	13(2)	-9(2)
F(6)	44(3)	35(2)	45(2)	-6(2)	5(2)	-1(2)
F(7)	141(4)	42(3)	48(3)	0(2)	-10(3)	26(3)
F(8)	43(3)	98(4)	123(4)	17(3)	23(3)	-10(3)
F(9)	155(5)	51(3)	40(3)	16(2)	9(3)	-22(3)
F(10)	53(3)	202(7)	162(6)	-31(5)	55(3)	-3(4)
F(11)	152(5)	81(4)	35(3)	-24(2)	5(3)	13(3)
F(12)	102(4)	46(3)	39(2)	-13(2)	-10(2)	10(2)
O(1)	23(3)	25(3)	28(2)	-7(2)	2(2)	-4(2)
O(2)	20(2)	28(3)	29(2)	4(2)	4(2)	1(2)
N(1)	12(3)	24(3)	22(3)	-3(2)	2(2)	2(2)
N(2)	17(3)	28(3)	20(3)	-1(3)	2(2)	1(2)
N(3)	20(3)	25(3)	20(3)	3(2)	7(2)	-2(2)
N(4)	18(3)	22(3)	19(3)	8(2)	2(2)	0(2)
N(5)	21(3)	20(3)	17(3)	-4(2)	11(2)	3(2)
N(6)	20(3)	19(3)	22(3)	-2(2)	11(2)	-1(2)
N(7)	24(3)	24(3)	20(3)	-1(2)	7(2)	-4(2)
N(8)	16(3)	20(3)	23(3)	-3(2)	3(2)	-6(2)
N(9)	20(3)	23(3)	22(3)	-5(2)	7(2)	4(2)

Table S4. Anisotropic displacement parameters ($Å^2$ x 10^3) for $[Mo(O)(\mu\text{-}S)_3(Cu(phen))_3][PF_6]\cdot 2MeCN$. The anisotropic displacement factor exponent takes the form: $-2\pi^2[(ha^*)^2U^{11} + ... + 2hka^*b^*U^{12}]$.

Atom	U^{11}	U^{22}	U^{33}	U^{23}	U^{13}	U^{12}
N(10)	21(3)	25(3)	24(3)	-7(2)	4(2)	0(2)
N(11)	23(3)	23(3)	18(3)	3(2)	10(2)	3(2)
N(12)	32(3)	20(3)	23(3)	-2(3)	13(2)	3(3)
N(13)	57(5)	47(5)	72(5)	9(4)	14(4)	3(4)
N(14)	41(4)	26(4)	43(4)	2(3)	12(3)	0(3)
N(15)	78(5)	42(5)	64(5)	-5(4)	16(4)	4(4)
N(16)	54(5)	34(4)	47(4)	-11(3)	-2(3)	1(3)
C(1)	24(4)	31(4)	18(4)	3(3)	1(3)	6(3)
C(2)	39(5)	26(4)	23(4)	-6(3)	2(3)	1(3)
C(3)	31(4)	35(4)	29(4)	-4(3)	17(3)	4(3)
C(4)	21(4)	19(4)	27(4)	4(3)	9(3)	4(3)
C(5)	17(4)	23(4)	25(4)	0(3)	10(3)	1(3)
C(6)	13(4)	17(4)	23(3)	8(3)	4(3)	4(3)
C(7)	10(4)	19(4)	27(4)	6(3)	2(3)	5(3)
C(8)	10(4)	21(4)	35(4)	5(3)	-1(3)	-1(3)
C(9)	16(4)	31(4)	28(4)	-5(3)	-4(3)	0(3)
C(10)	18(4)	31(4)	22(4)	2(3)	0(3)	1(3)
C(11)	21(4)	31(4)	28(4)	8(3)	14(3)	3(3)
C(12)	18(4)	17(4)	38(4)	8(3)	8(3)	0(3)
C(13)	37(4)	33(4)	21(4)	7(3)	1(3)	-5(3)
C(14)	28(4)	52(5)	25(4)	7(3)	-2(3)	-20(4)
C(15)	15(4)	52(5)	36(5)	21(3)	4(3)	-4(3)
C(16)	24(4)	39(4)	16(4)	13(3)	7(3)	8(3)
C(17)	19(3)	26(4)	12(4)	13(3)	3(3)	4(3)
C(18)	19(3)	26(4)	13(4)	4(3)	5(3)	7(3)
C(19)	35(4)	32(4)	15(4)	4(3)	5(3)	12(3)
C(20)	47(4)	32(4)	24(4)	-3(3)	8(3)	8(3)
C(21)	40(4)	24(4)	41(5)	-4(3)	2(4)	-5(3)
C(22)	22(4)	24(4)	31(4)	3(3)	-4(3)	0(3)
C(23)	24(4)	48(5)	34(4)	14(3)	14(3)	14(3)
C(24)	45(4)	32(4)	31(4)	3(3)	17(3)	16(4)
C(25)	29(4)	33(4)	15(4)	-5(3)	8(3)	-3(3)
C(26)	44(5)	22(4)	29(4)	-1(3)	15(4)	4(3)
C(27)	42(5)	23(4)	30(4)	6(3)	20(4)	7(3)
C(28)	26(4)	22(4)	16(3)	1(3)	5(3)	7(3)
C(29)	16(4)	22(3)	14(3)	-1(3)	8(3)	3(3)
C(30)	15(4)	21(3)	17(3)	1(3)	7(3)	-2(3)
C(31)	13(4)	29(4)	17(3)	-1(3)	7(3)	-9(3)
C(32)	33(4)	38(4)	17(4)	-4(3)	9(3)	-18(3)

Table S4. Anisotropic displacement parameters ($Å^2$ x 10^3) for $[Mo(O)(\mu\text{-}S)_3(Cu(phen))_3][PF_6]\cdot 2MeCN$. The anisotropic displacement factor exponent takes the form: $-2\pi^2[(ha^*)^2U^{11} + ... + 2hka^*b^*U^{12}]$.

Atom	U^{11}	U^{22}	U^{33}	U^{23}	U^{13}	U^{12}
C(33)	43(5)	24(4)	34(4)	-10(3)	19(4)	-15(3)
C(34)	43(5)	27(4)	24(4)	6(3)	13(3)	-6(4)
C(35)	34(4)	30(4)	19(4)	9(3)	9(3)	4(3)
C(36)	19(4)	37(4)	13(3)	-2(3)	8(3)	-2(3)
C(37)	27(4)	21(4)	23(4)	2(3)	2(3)	-4(3)
C(38)	29(4)	33(4)	19(4)	-1(3)	6(3)	-8(3)
C(39)	16(4)	42(5)	21(4)	-4(3)	8(3)	-5(3)
C(40)	15(4)	23(4)	26(4)	-3(3)	8(3)	-3(3)
C(41)	8(3)	19(4)	23(3)	-7(3)	-2(3)	-7(3)
C(42)	10(4)	23(4)	17(3)	-8(3)	1(3)	-9(3)
C(43)	7(3)	22(4)	24(4)	-3(3)	5(3)	-6(3)
C(44)	18(4)	28(4)	24(4)	-3(3)	-4(3)	-2(3)
C(45)	24(4)	36(4)	20(4)	-2(3)	3(3)	-3(3)
C(46)	20(4)	30(4)	24(4)	-6(3)	1(3)	-4(3)
C(47)	12(4)	31(4)	31(4)	-14(3)	5(3)	-1(3)
C(48)	18(4)	25(4)	29(4)	-1(3)	9(3)	-1(3)
C(49)	33(4)	30(4)	23(4)	-5(3)	9(3)	8(3)
C(50)	26(4)	30(4)	34(4)	-10(3)	-2(3)	13(3)
C(51)	22(4)	33(4)	43(5)	-23(3)	8(3)	2(3)
C(52)	22(4)	30(4)	23(4)	-11(3)	13(3)	-1(3)
C(53)	21(3)	16(4)	22(4)	-9(3)	13(3)	-4(3)
C(54)	16(3)	28(4)	20(4)	-8(3)	8(3)	-7(3)
C(55)	35(4)	26(4)	29(4)	-9(3)	11(3)	-7(3)
C(56)	52(5)	32(4)	31(4)	0(3)	15(4)	-1(4)
C(57)	40(4)	39(5)	25(4)	-3(3)	-1(3)	12(4)
C(58)	22(4)	33(4)	27(4)	-10(3)	5(3)	-1(3)
C(59)	35(4)	35(4)	44(5)	-11(3)	17(3)	-18(3)
C(60)	43(4)	29(4)	38(4)	1(3)	22(3)	-10(3)
C(61)	44(5)	38(4)	22(4)	5(3)	14(3)	5(4)
C(62)	75(6)	24(4)	39(4)	7(3)	28(4)	7(4)
C(63)	65(6)	28(4)	40(4)	-9(3)	29(4)	-4(4)
C(64)	36(4)	30(4)	28(4)	-1(3)	20(3)	-7(3)
C(65)	16(4)	24(3)	22(4)	-3(3)	6(3)	2(3)
C(66)	19(4)	27(4)	17(3)	-1(3)	6(3)	10(3)
C(67)	20(4)	33(4)	21(4)	-1(3)	8(3)	13(3)
C(68)	44(5)	37(4)	27(4)	5(3)	16(3)	23(4)
C(69)	72(6)	32(4)	31(4)	12(3)	29(4)	17(4)
C(70)	78(6)	17(4)	35(4)	-5(3)	33(4)	9(4)
C(71)	26(4)	48(4)	14(4)	-2(3)	8(3)	-4(4)

Table S4. Anisotropic displacement parameters ($Å^2$ x 10^3) for [Mo(O)(μ-$S)_3(Cu(phen))_3][PF_6]\cdot$ 2MeCN. The anisotropic displacement factor exponent takes the form: $-2\pi^2[(ha^*)^2U^{11} + ... + 2hka^*b^*U^{12}]$.

Atom	U^{11}	U^{22}	U^{33}	U^{23}	U^{13}	U^{12}
C(72)	36(4)	41(4)	22(4)	-15(3)	16(3)	-15(4)
C(73)	49(6)	22(5)	69(5)	0(5)	25(5)	0(4)
C(74)	73(6)	53(6)	60(5)	-12(5)	14(5)	15(5)
C(75)	34(5)	25(5)	29(4)	1(4)	9(3)	-8(3)
C(76)	39(5)	44(5)	38(4)	-4(4)	14(4)	3(3)
C(77)	52(5)	34(5)	64(6)	-16(4)	22(5)	5(4)
C(78)	59(6)	42(5)	73(6)	4(4)	17(5)	-1(4)
C(79)	34(5)	29(5)	31(4)	2(4)	-9(4)	9(4)
C(80)	56(5)	37(5)	49(5)	-2(4)	5(4)	-5(4)

Table S5. Hydrogen coordinates (x 10^4) and isotropic displacement parameters (Å^2 x 10^3) for [Mo(O)(μ-S)$_3$(Cu(phen))$_3$][PF_6]·2MeCN.

H atom	x	y	z	U(eq)
H(1)	-1247	5271	3182	30
H(2)	-1671	5111	3898	36
H(3)	-2680	4260	3962	36
H(8)	-4151	2352	2060	27
H(9)	-3648	2616	1383	32
H(10)	-2599	3475	1403	29
H(11)	-3644	3273	3572	30
H(12)	-4115	2604	2932	29
H(13)	2605	4457	2756	37
H(14)	4072	4037	3003	44
H(15)	4509	3140	2601	41
H(20)	1291	1630	998	41
H(21)	-170	2077	877	43
H(22)	-404	3074	1243	33
H(23)	4049	2210	1984	41
H(24)	2961	1707	1422	42
H(25)	-610	6936	1272	30
H(26)	-976	7828	748	37
H(27)	-1375	7615	-58	36
H(32)	-1567	4441	-751	34
H(33)	-1182	3634	-159	38
H(34)	-824	3965	630	37
H(35)	-1726	6760	-727	33
H(36)	-1800	5677	-966	27
H(37)	3203	5584	3051	29
H(38)	2478	6078	3589	32
H(39)	1441	6936	3344	31
H(44)	945	8003	1122	29
H(45)	1776	7456	652	32
H(46)	2748	6587	967	30
H(47)	719	7747	2683	30
H(48)	538	8105	1924	28
H(49)	7543	6067	2532	34
H(50)	8952	6608	2727	38
H(51)	9162	7559	2307	39
H(56)	5736	8609	614	45
H(57)	4383	7985	486	43
H(58)	4306	7065	959	33
H(59)	8546	8384	1647	44
H(60)	7370	8740	1057	42

Table S5. Hydrogen coordinates (x 10^4) and isotropic displacement parameters ($Å^2$ x 10^3) for $[Mo(O)(\mu\text{-}S)_3(Cu(phen))_3][PF_6]\cdot 2MeCN$.

H atom	x	y	z	U(eq)
H(61)	4529	3316	1361	40
H(62)	4206	2320	937	53
H(63)	3633	2364	125	50
H(68)	3115	5350	-890	42
H(69)	3610	6268	-408	51
H(70)	4108	6121	404	49
H(71)	2972	4092	-966	35
H(72)	3144	3068	-621	38
H(74A)	1055	8704	194	94
H(74B)	311	9167	351	94
H(74C)	1214	9493	248	94
H(76A)	-1639	9778	1508	59
H(76B)	-1439	10201	1073	59
H(76C)	-765	10252	1584	59
H(78A)	-4662	10600	238	87
H(78B)	-3601	10580	243	87
H(78C)	-3987	11128	549	87
H(80A)	-5319	8	1481	73
H(80B)	-6226	367	1199	73
H(80C)	-5930	426	1764	73

Chapter 4: Crystal Information

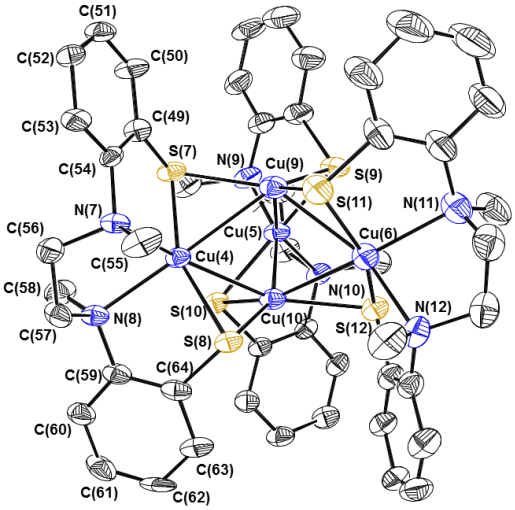

Structure Determination Summary

Crystal Data and Structure refinement for $[[Cu(L\text{-}N_2S^{Ar}{}_2)]_3Cu_2]$, **1**

Identification code	jpd513_0m_a	
Empirical formula	$C_{48}H_{54}Cu_5N_6S_6$	
Formula weight	1225.03	
Temperature	150(2) K	
Wavelength	0.71073 Å	
Crystal system	Triclinic	
Space group	*P*-1	
Unit cell dimensions	a = 11.840(2) Å	α = 85.228(2)°
	b = 20.650(4) Å	β = 89.839(2)°
	c = 20.801(4) Å	γ = 84.436(2)°
Volume, Z	5044.0(16) $Å^3$, 4	
Density (calculated)	1.613 g/cm^3	
Absorption coefficient	2.363 mm^{-1}	
F(000)	2500	
Crystal size	0.24 x 0.10 x 0.03 mm	
θ range for data collection	1.91 to 22.61°	
Limiting indices	$-12 < h < 12$, $-22 < k < 22$, $-22 < l < 22$	
Reflections collected	53618	
Independent reflections	13343 (R_{int} = 0.0739)	
Completeness to θ = 22.61°	99.7 %	
Absorption correction	Semi-empirical from equivalents	
Max. and min. transmission	0.9272 and 0.5986	
Refinement method	Full-matrix least-squares on F^2	
Data / restraints / parameters	13343 / 590 / 1183	
Goodness-of-fit on F^2	1.035	
Final R indices [I>2s(I)]	R1 = 0.0483, wR2 = 0.1041	
R indices (all data)	R1 = 0.0761, wR2 = 0.1134	
Largest diff. peak and hole	0.705 and -0.571 $e \cdot Å^{-3}$	

Table S1. Atomic coordinates (x 10^4) and equivalent isotropic displacement parameters ($Å^2$ x 10^3) for $[[Cu(L\text{-}N_2S^{Ar}{}_2)]_3Cu_2]$. U(eq) is defined as one third of the trace of the orthogonalized U^{ij} tensor.

Atom	x	y	z	U(eq)
Cu(1)	8212(1)	8695(1)	784(1)	27(1)
Cu(2)	8222(1)	6984(1)	1793(1)	26(1)
Cu(3)	10555(1)	7282(1)	527(1)	24(1)
Cu(4)	5381(1)	3261(1)	2899(1)	26(1)
Cu(5)	3012(1)	2155(1)	3513(1)	30(1)
Cu(6)	5151(1)	2677(1)	4754(1)	34(1)
Cu(7)	9553(1)	7899(1)	1466(1)	26(1)
Cu(8)	8349(1)	7374(1)	561(1)	27(1)
Cu(9)	5372(1)	2144(1)	3651(1)	33(1)
Cu(10)	3824(1)	3175(1)	3784(1)	29(1)
S(1)	9997(1)	8890(1)	984(1)	30(1)
S(2)	6801(1)	8075(1)	708(1)	28(1)
S(3)	8236(1)	7900(1)	2280(1)	30(1)
S(4)	8532(1)	6314(1)	1016(1)	28(1)
S(5)	11049(1)	7122(1)	1576(1)	27(1)
S(6)	9414(1)	7544(1)	-332(1)	26(1)
S(7)	5463(1)	2263(1)	2556(1)	30(1)
S(8)	4918(1)	4005(1)	3604(1)	30(1)
S(9)	4174(1)	1415(1)	4080(1)	37(1)
S(10)	2461(1)	3126(1)	3008(1)	28(1)
S(11)	6809(1)	2404(1)	4280(1)	39(1)
S(12)	3278(1)	2884(1)	4818(1)	33(1)
N(1)	7735(4)	9549(2)	1387(3)	30(1)
N(2)	7485(4)	9343(2)	-19(3)	31(1)
N(3)	8719(4)	6460(2)	2725(2)	29(1)
N(4)	6554(4)	6568(2)	1949(3)	28(1)
N(5)	12232(4)	7665(2)	370(2)	26(1)
N(6)	11263(4)	6423(2)	30(2)	24(1)
N(7)	7023(4)	3379(2)	2447(3)	26(1)
N(8)	4737(4)	4061(2)	2136(3)	29(1)
N(9)	2533(4)	1407(3)	2935(3)	36(1)
N(10)	1209(4)	2181(3)	3896(3)	30(1)
N(11)	5771(5)	1990(3)	5591(3)	46(1)
N(12)	5257(4)	3436(3)	5457(3)	38(1)
C(1)	9742(5)	9343(3)	1669(3)	30(2)
C(2)	10638(6)	9398(3)	2082(3)	38(2)
C(3)	10473(6)	9686(3)	2645(4)	48(2)
C(4)	9391(7)	9923(4)	2822(4)	50(2)

C(5) 8488(6) 9878(3) 2406(3) 41(2)

Table S1. Atomic coordinates (x 10^4) and equivalent isotropic displacement parameters ($Å^2$ x 10^3) for $[[Cu(L\text{-}N_2S^{Ar}{}_2)]_3Cu_2]$. U(eq) is defined as one third of the trace of the orthogonalized U^{ij} tensor.

Atom	x	y	z	U(eq)
C(6)	8647(5)	9601(3)	1831(3)	33(2)
C(7)	6624(5)	9500(3)	1701(4)	43(2)
C(8)	7664(5)	10086(3)	864(3)	35(2)
C(9)	6971(5)	9934(3)	282(3)	38(2)
C(10)	8421(6)	9514(3)	-466(4)	45(2)
C(11)	6629(5)	9018(3)	-341(3)	29(1)
C(12)	6133(5)	9286(3)	-913(3)	36(2)
C(13)	5368(5)	8953(4)	-1238(3)	41(2)
C(14)	5101(5)	8360(4)	-975(3)	36(2)
C(15)	5562(5)	8092(3)	-398(3)	33(2)
C(16)	6323(5)	8419(3)	-59(3)	27(1)
C(17)	9087(5)	7567(3)	2951(3)	32(2)
C(18)	9608(6)	7992(4)	3320(3)	41(2)
C(19)	10316(7)	7754(4)	3836(4)	54(2)
C(20)	10480(6)	7095(4)	3996(4)	50(2)
C(21)	9949(5)	6677(4)	3649(3)	39(2)
C(22)	9268(5)	6905(3)	3125(3)	32(2)
C(23)	9434(6)	5857(3)	2652(3)	42(2)
C(24)	7580(5)	6338(3)	2998(3)	36(2)
C(25)	6844(5)	6078(3)	2505(3)	36(2)
C(26)	5651(5)	7075(3)	2119(3)	39(2)
C(27)	6275(5)	6239(3)	1380(3)	28(1)
C(28)	5183(5)	6072(3)	1277(3)	32(2)
C(29)	4937(5)	5772(3)	729(3)	36(2)
C(30)	5776(5)	5640(3)	277(3)	38(2)
C(31)	6858(5)	5805(3)	385(3)	33(2)
C(32)	7126(5)	6102(3)	937(3)	26(1)
C(33)	12168(5)	7635(3)	1550(3)	28(1)
C(34)	12572(5)	7831(3)	2136(3)	33(2)
C(35)	13422(5)	8239(3)	2126(3)	36(2)
C(36)	13880(5)	8470(3)	1561(3)	38(2)
C(37)	13517(5)	8285(3)	988(3)	32(2)
C(38)	12655(5)	7866(3)	971(3)	26(1)
C(39)	12181(5)	8178(3)	-159(3)	30(2)
C(40)	12909(5)	7057(3)	205(3)	32(2)
C(41)	12301(5)	6684(3)	-262(3)	29(2)
C(42)	11556(5)	5845(3)	483(3)	31(2)
C(43)	10504(5)	6300(3)	-480(3)	24(1)

C(44) 10626(5) 5714(3) -781(3) 30(2)

Table S1. Atomic coordinates (x 10^4) and equivalent isotropic displacement parameters ($Å^2$ x 10^3) for [[Cu(L-$N_2S^{Ar}_2$)]$_3$Cu$_2$]. U(eq) is defined as one third of the trace of the orthogonalized U^{ij} tensor.

Atom	x	y	z	U(eq)
C(45)	9908(5)	5612(3)	-1283(3)	35(2)
C(46)	9060(5)	6087(3)	-1485(3)	35(2)
C(47)	8913(5)	6667(3)	-1185(3)	33(2)
C(48)	9626(5)	6779(3)	-679(3)	25(1)
C(49)	6914(5)	2202(3)	2330(3)	28(2)
C(50)	7439(5)	1608(3)	2154(3)	36(2)
C(51)	8534(5)	1552(3)	1935(3)	34(2)
C(52)	9146(5)	2085(3)	1871(3)	34(2)
C(53)	8653(5)	2682(3)	2045(3)	30(2)
C(54)	7555(5)	2745(3)	2283(3)	24(1)
C(55)	7752(5)	3677(4)	2897(3)	42(2)
C(56)	6757(5)	3806(3)	1854(3)	38(2)
C(57)	5813(5)	4337(3)	1964(3)	36(2)
C(58)	4224(6)	3795(4)	1590(3)	45(2)
C(59)	3989(5)	4544(3)	2433(3)	30(2)
C(60)	3250(5)	5002(3)	2068(4)	38(2)
C(61)	2570(6)	5473(4)	2352(4)	48(2)
C(62)	2590(6)	5492(3)	3004(4)	44(2)
C(63)	3283(5)	5042(3)	3382(4)	36(2)
C(64)	4012(5)	4561(3)	3095(3)	30(2)
C(65)	4209(6)	821(3)	3519(4)	39(2)
C(66)	5071(6)	298(4)	3565(4)	51(2)
C(67)	5122(7)	-176(4)	3140(4)	63(2)
C(68)	4299(7)	-168(4)	2691(4)	59(2)
C(69)	3413(7)	346(4)	2618(4)	51(2)
C(70)	3399(6)	840(3)	3029(4)	37(2)
C(71)	2417(6)	1676(4)	2251(3)	44(2)
C(72)	1426(5)	1244(3)	3202(4)	43(2)
C(73)	692(5)	1860(3)	3368(3)	37(2)
C(74)	1125(5)	1820(3)	4524(3)	39(2)
C(75)	749(5)	2863(3)	3875(3)	28(1)
C(76)	-187(5)	3051(3)	4247(3)	34(2)
C(77)	-621(5)	3706(3)	4230(3)	37(2)
C(78)	-144(5)	4169(3)	3827(3)	37(2)
C(79)	774(5)	3977(3)	3448(3)	32(2)
C(80)	1241(5)	3325(3)	3476(3)	28(2)
C(81)	7181(6)	1672(4)	4765(4)	45(2)
C(82)	8015(6)	1224(4)	4546(4)	65(2)

C(83)	8349(7)	647(5)	4906(5)	87(3)

Table S1. Atomic coordinates (x 10^4) and equivalent isotropic displacement parameters (Å^2 x 10^3) for [[Cu(L-$N_2S^{Ar}{}_2$)]$_3$$Cu_2$]. U(eq) is defined as one third of the trace of the orthogonalized U^{ij} tensor.

Atom	x	y	z	U(eq)
C(84)	7831(9)	501(5)	5492(5)	105(4)
C(85)	7013(7)	948(4)	5719(5)	77(3)
C(86)	6672(6)	1523(4)	5351(4)	50(2)
C(87)	4833(6)	1666(4)	5900(4)	61(2)
C(88)	6248(6)	2431(4)	6010(4)	55(2)
C(89)	5452(6)	3038(4)	6076(4)	52(2)
C(90)	6245(6)	3805(4)	5279(4)	54(2)
C(91)	4197(6)	3855(3)	5450(3)	37(2)
C(92)	4088(6)	4449(4)	5719(4)	46(2)
C(93)	3092(7)	4839(4)	5685(4)	49(2)
C(94)	2157(6)	4649(4)	5389(3)	44(2)
C(95)	2234(6)	4056(3)	5125(3)	38(2)
C(96)	3249(5)	3650(3)	5160(3)	35(2)

Table S2. Bond lengths (Å) and for [[Cu(L-$N_2S^{Ar}{}_2$)]$_3$Cu$_2$]. Symmetry transformations used to generate equivalent atoms:

Cu(1)-N(2)	2.176(5)	Cu(9)-S(11)	2.2801(19)
Cu(1)-S(2)	2.2145(17)	Cu(9)-S(7)	2.274(2)
Cu(1)-S(1)	2.2368(17)	Cu(9)-S(9)	2.2931(19)
Cu(1)-N(1)	2.274(5)	Cu(9)-Cu(10)	2.7032(11)
Cu(1)-Cu(7)	2.5195(11)	Cu(10)-S(8)	2.2532(18)
Cu(1)-Cu(8)	2.7934(12)	Cu(10)-S(12)	2.2926(19)
Cu(2)-N(3)	2.193(5)	Cu(10)-S(10)	2.3015(18)
Cu(2)-S(3)	2.2204(18)	S(1)-C(1)	1.777(6)
Cu(2)-S(4)	2.2199(18)	S(2)-C(16)	1.763(7)
Cu(2)-N(4)	2.242(5)	S(3)-C(17)	1.775(7)
Cu(2)-Cu(7)	2.6226(11)	S(4)-C(32)	1.773(6)
Cu(2)-Cu(8)	2.6304(12)	S(5)-C(33)	1.772(6)
Cu(3)-N(6)	2.221(5)	S(6)-C(48)	1.785(6)
Cu(3)-N(5)	2.220(5)	S(7)-C(49)	1.776(6)
Cu(3)-S(6)	2.2419(18)	S(8)-C(64)	1.775(7)
Cu(3)-S(5)	2.2480(19)	S(9)-C(65)	1.758(7)
Cu(3)-Cu(8)	2.6010(11)	S(10)-C(80)	1.775(6)
Cu(3)-Cu(7)	2.6361(11)	S(11)-C(81)	1.766(7)
Cu(4)-N(7)	2.183(5)	S(12)-C(96)	1.784(7)
Cu(4)-S(7)	2.2302(18)	N(1)-C(6)	1.442(8)
Cu(4)-S(8)	2.2408(18)	N(1)-C(7)	1.475(8)
Cu(4)-N(8)	2.270(5)	N(1)-C(8)	1.484(8)
Cu(4)-Cu(10)	2.6094(11)	N(2)-C(11)	1.462(8)
Cu(4)-Cu(9)	2.6784(12)	N(2)-C(9)	1.494(8)
Cu(5)-N(9)	2.153(5)	N(2)-C(10)	1.494(8)
Cu(5)-S(9)	2.218(2)	N(3)-C(23)	1.455(8)
Cu(5)-S(10)	2.2254(19)	N(3)-C(22)	1.484(8)
Cu(5)-N(10)	2.274(5)	N(3)-C(24)	1.497(7)
Cu(5)-Cu(10)	2.5046(11)	N(4)-C(27)	1.466(8)
Cu(5)-Cu(9)	2.8077(11)	N(4)-C(25)	1.489(8)
Cu(6)-S(12)	2.2231(18)	N(4)-C(26)	1.485(8)
Cu(6)-N(12)	2.241(5)	N(5)-C(38)	1.455(8)
Cu(6)-S(11)	2.2383(19)	N(5)-C(39)	1.460(8)
Cu(6)-N(11)	2.232(6)	N(5)-C(40)	1.488(8)
Cu(6)-Cu(9)	2.6277(12)	N(6)-C(43)	1.447(7)
Cu(6)-Cu(10)	2.6371(12)	N(6)-C(42)	1.471(8)
Cu(7)-S(5)	2.2704(18)	N(6)-C(41)	1.497(7)
Cu(7)-S(3)	2.2995(18)	N(7)-C(55)	1.484(8)
Cu(7)-S(1)	2.3087(19)	N(7)-C(56)	1.473(8)
Cu(7)-Cu(8)	2.7207(11)	N(7)-C(54)	1.461(7)
Cu(8)-S(2)	2.2594(17)	N(8)-C(59)	1.445(8)
Cu(8)-S(6)	2.2651(18)	N(8)-C(58)	1.461(8)
Cu(8)-S(4)	2.3021(19)	N(8)-C(57)	1.477(7)

Table S2. Bond lengths (Å) and for [[Cu(L-$N_2S^{Ar}{}_2$)]$_3$Cu$_2$]. Symmetry transformations used to generate equivalent atoms:

N(9)-C(71)	1.485(9)	C(17)-C(22)	1.381(9)
N(9)-C(70)	1.480(9)	C(17)-C(18)	1.400(9)
N(9)-C(72)	1.479(8)	C(18)-C(19)	1.390(10)
N(10)-C(75)	1.456(8)	C(18)-H(18)	0.9500
N(10)-C(74)	1.457(8)	C(19)-C(20)	1.369(11)
N(10)-C(73)	1.493(8)	C(19)-H(19)	0.9500
N(11)-C(86)	1.481(9)	C(20)-C(21)	1.369(10)
N(11)-C(88)	1.464(9)	C(20)-H(20)	0.9500
N(11)-C(87)	1.470(8)	C(21)-C(22)	1.380(9)
N(12)-C(90)	1.486(8)	C(21)-H(21)	0.9500
N(12)-C(91)	1.454(9)	C(23)-H(23A)	0.9800
N(12)-C(89)	1.475(9)	C(23)-H(23B)	0.9800
C(1)-C(2)	1.386(9)	C(23)-H(23C)	0.9800
C(1)-C(6)	1.404(9)	C(24)-C(25)	1.513(9)
C(2)-C(3)	1.363(9)	C(24)-H(24A)	0.9900
C(2)-H(2)	0.9500	C(24)-H(24B)	0.9900
C(3)-C(4)	1.386(10)	C(25)-H(25A)	0.9900
C(3)-H(3)	0.9500	C(25)-H(25B)	0.9900
C(4)-C(5)	1.393(10)	C(26)-H(26A)	0.9800
C(4)-H(4)	0.9500	C(26)-H(26B)	0.9800
C(5)-C(6)	1.372(9)	C(26)-H(26C)	0.9800
C(5)-H(5)	0.9500	C(27)-C(32)	1.389(8)
C(7)-H(7A)	0.9800	C(27)-C(28)	1.393(8)
C(7)-H(7B)	0.9800	C(28)-C(29)	1.386(9)
C(7)-H(7C)	0.9800	C(28)-H(28)	0.9500
C(8)-C(9)	1.535(9)	C(29)-C(30)	1.389(9)
C(8)-H(8A)	0.9900	C(29)-H(29)	0.9500
C(8)-H(8B)	0.9900	C(30)-C(31)	1.381(9)
C(9)-H(9A)	0.9900	C(30)-H(30)	0.9500
C(9)-H(9B)	0.9900	C(31)-C(32)	1.396(9)
C(10)-H(10A)	0.9800	C(31)-H(31)	0.9500
C(10)-H(10B)	0.9800	C(33)-C(38)	1.400(9)
C(10)-H(10C)	0.9800	C(33)-C(34)	1.414(9)
C(11)-C(12)	1.378(9)	C(34)-C(35)	1.374(9)
C(11)-C(16)	1.404(9)	C(34)-H(34)	0.9500
C(12)-C(13)	1.396(9)	C(35)-C(36)	1.364(9)
C(12)-H(12)	0.9500	C(35)-H(35)	0.9500
C(13)-C(14)	1.365(10)	C(36)-C(37)	1.364(9)
C(13)-H(13)	0.9500	C(36)-H(36)	0.9500
C(14)-C(15)	1.370(9)	C(37)-C(38)	1.403(8)
C(14)-H(14)	0.9500	C(37)-H(37)	0.9500
C(15)-C(16)	1.402(8)	C(39)-H(39A)	0.9800
C(15)-H(15)	0.9500	C(39)-H(39B)	0.9800

Table S2. Bond lengths (Å) and for [[Cu(L-$N_2S^{Ar}{}_2$)]$_3$Cu$_2$]. Symmetry transformations used to generate equivalent atoms:

C(39)-H(39C)	0.9800	C(60)-H(60)	0.9500
C(40)-C(41)	1.514(8)	C(61)-C(62)	1.360(10)
C(40)-H(40A)	0.9900	C(61)-H(61)	0.9500
C(40)-H(40B)	0.9900	C(62)-C(63)	1.374(9)
C(41)-H(41A)	0.9900	C(62)-H(62)	0.9500
C(41)-H(41B)	0.9900	C(63)-C(64)	1.420(9)
C(42)-H(42A)	0.9800	C(63)-H(63)	0.9500
C(42)-H(42B)	0.9800	C(65)-C(70)	1.397(10)
C(42)-H(42C)	0.9800	C(65)-C(66)	1.411(10)
C(43)-C(44)	1.403(8)	C(66)-C(67)	1.369(11)
C(43)-C(48)	1.400(8)	C(66)-H(66)	0.9500
C(44)-C(45)	1.391(9)	C(67)-C(68)	1.349(11)
C(44)-H(44)	0.9500	C(67)-H(67)	0.9500
C(45)-C(46)	1.374(9)	C(68)-C(69)	1.417(11)
C(45)-H(45)	0.9500	C(68)-H(68)	0.9500
C(46)-C(47)	1.392(9)	C(69)-C(70)	1.385(9)
C(46)-H(46)	0.9500	C(69)-H(69)	0.9500
C(47)-C(48)	1.400(8)	C(71)-H(71A)	0.9800
C(47)-H(47)	0.9500	C(71)-H(71B)	0.9800
C(49)-C(50)	1.397(9)	C(71)-H(71C)	0.9800
C(49)-C(54)	1.410(8)	C(72)-C(73)	1.533(9)
C(50)-C(51)	1.371(8)	C(72)-H(72A)	0.9900
C(50)-H(50)	0.9500	C(72)-H(72B)	0.9900
C(51)-C(52)	1.373(9)	C(73)-H(73A)	0.9900
C(51)-H(51)	0.9500	C(73)-H(73B)	0.9900
C(52)-C(53)	1.388(9)	C(74)-H(74A)	0.9800
C(52)-H(52)	0.9500	C(74)-H(74B)	0.9800
C(53)-C(54)	1.389(8)	C(74)-H(74C)	0.9800
C(53)-H(53)	0.9500	C(75)-C(80)	1.384(9)
C(55)-H(55A)	0.9800	C(75)-C(76)	1.392(8)
C(55)-H(55B)	0.9800	C(76)-C(77)	1.397(9)
C(55)-H(55C)	0.9800	C(76)-H(76)	0.9500
C(56)-C(57)	1.519(9)	C(77)-C(78)	1.381(9)
C(56)-H(56A)	0.9900	C(77)-H(77)	0.9500
C(56)-H(56B)	0.9900	C(78)-C(79)	1.387(9)
C(57)-H(57A)	0.9900	C(78)-H(78)	0.9500
C(57)-H(57B)	0.9900	C(79)-C(80)	1.401(9)
C(58)-H(58A)	0.9800	C(79)-H(79)	0.9500
C(58)-H(58B)	0.9800	C(81)-C(86)	1.383(10)
C(58)-H(59C)	0.9800	C(81)-C(82)	1.389(10)
C(59)-C(64)	1.382(9)	C(82)-C(83)	1.378(11)
C(59)-C(60)	1.400(9)	C(82)-H(82)	0.9500
C(60)-C(61)	1.372(9)	C(83)-C(84)	1.386(13)

Table S2. Bond lengths (Å) and for [[Cu(L-$N_2S^{Ar}{}_2$)]$_3$Cu$_2$]. Symmetry transformations used to generate equivalent atoms:

C(83)-H(83)	0.9500
C(84)-C(85)	1.382(12)
C(84)-H(84)	0.9500
C(85)-C(86)	1.385(11)
C(85)-H(85)	0.9500
C(87)-H(87A)	0.9800
C(87)-H(87B)	0.9800
C(87)-H(87C)	0.9800
C(88)-C(89)	1.509(10)
C(88)-H(88A)	0.9900
C(88)-H(88B)	0.9900
C(89)-H(89A)	0.9900
C(89)-H(89B)	0.9900
C(90)-H(90A)	0.9800
C(90)-H(90B)	0.9800
C(90)-H(90C)	0.9800
C(91)-C(92)	1.384(9)
C(91)-C(96)	1.394(9)
C(92)-C(93)	1.360(10)
C(92)-H(92)	0.9500
C(93)-C(94)	1.374(10)
C(93)-H(93)	0.9500
C(94)-C(95)	1.379(9)
C(94)-H(94)	0.9500
C(95)-C(96)	1.395(9)
C(95)-H(95)	0.9500

Table S3. Bond angles (deg.) for [[Cu(L-$N_2S^{Ar}{}_2$)]$_3$Cu$_2$]. Symmetry transformations used to generate equivalent atoms:

N(2)-Cu(1)-S(2)	89.46(14)	S(5)-Cu(3)-Cu(7)	54.71(5)
N(2)-Cu(1)-S(1)	111.12(14)	Cu(8)-Cu(3)-Cu(7)	62.59(3)
S(2)-Cu(1)-S(1)	155.12(7)	N(7)-Cu(4)-S(7)	88.66(13)
N(2)-Cu(1)-N(1)	85.04(19)	N(7)-Cu(4)-S(8)	112.53(14)
S(2)-Cu(1)-N(1)	112.03(13)	S(7)-Cu(4)-S(8)	153.82(7)
S(1)-Cu(1)-N(1)	84.50(13)	N(7)-Cu(4)-N(8)	83.79(18)
N(2)-Cu(1)-Cu(7)	162.01(13)	S(7)-Cu(4)-N(8)	113.33(14)
S(2)-Cu(1)-Cu(7)	98.67(5)	S(8)-Cu(4)-N(8)	85.21(14)
S(1)-Cu(1)-Cu(7)	57.71(5)	N(7)-Cu(4)-Cu(10)	160.44(14)
N(1)-Cu(1)-Cu(7)	106.38(14)	S(7)-Cu(4)-Cu(10)	100.49(5)
N(2)-Cu(1)-Cu(8)	113.66(14)	S(8)-Cu(4)-Cu(10)	54.73(5)
S(2)-Cu(1)-Cu(8)	52.09(5)	N(8)-Cu(4)-Cu(10)	107.81(12)
S(1)-Cu(1)-Cu(8)	104.97(5)	N(7)-Cu(4)-Cu(9)	112.79(14)
N(1)-Cu(1)-Cu(8)	152.94(14)	S(7)-Cu(4)-Cu(9)	54.27(5)
Cu(7)-Cu(1)-Cu(8)	61.35(3)	S(8)-Cu(4)-Cu(9)	101.60(6)
N(3)-Cu(2)-S(3)	87.06(14)	N(8)-Cu(4)-Cu(9)	157.08(12)
N(3)-Cu(2)-S(4)	109.38(14)	Cu(10)-Cu(4)-Cu(9)	61.47(3)
S(3)-Cu(2)-S(4)	157.44(7)	N(9)-Cu(5)-S(9)	89.58(17)
N(3)-Cu(2)-N(4)	85.58(19)	N(9)-Cu(5)-S(10)	108.71(17)
S(3)-Cu(2)-N(4)	110.21(13)	S(9)-Cu(5)-S(10)	156.12(7)
S(4)-Cu(2)-N(4)	87.01(14)	N(9)-Cu(5)-N(10)	85.52(18)
N(3)-Cu(2)-Cu(7)	111.66(13)	S(9)-Cu(5)-N(10)	111.61(15)
S(3)-Cu(2)-Cu(7)	55.95(5)	S(10)-Cu(5)-N(10)	85.72(14)
S(4)-Cu(2)-Cu(7)	102.52(5)	N(9)-Cu(5)-Cu(10)	158.68(15)
N(4)-Cu(2)-Cu(7)	155.44(14)	S(9)-Cu(5)-Cu(10)	99.88(6)
N(3)-Cu(2)-Cu(8)	158.44(13)	S(10)-Cu(5)-Cu(10)	57.87(5)
S(3)-Cu(2)-Cu(8)	103.63(6)	N(10)-Cu(5)-Cu(10)	108.20(13)
S(4)-Cu(2)-Cu(8)	55.90(5)	N(9)-Cu(5)-Cu(9)	112.95(14)
N(4)-Cu(2)-Cu(8)	107.49(14)	S(9)-Cu(5)-Cu(9)	52.71(5)
Cu(7)-Cu(2)-Cu(8)	62.39(3)	S(10)-Cu(5)-Cu(9)	104.69(5)
N(6)-Cu(3)-N(5)	86.57(17)	N(10)-Cu(5)-Cu(9)	153.50(14)
N(6)-Cu(3)-S(6)	87.07(13)	Cu(10)-Cu(5)-Cu(9)	60.86(3)
N(5)-Cu(3)-S(6)	111.31(14)	S(12)-Cu(6)-N(12)	86.40(14)
N(6)-Cu(3)-S(5)	108.66(14)	S(12)-Cu(6)-S(11)	156.31(8)
N(5)-Cu(3)-S(5)	86.19(14)	N(12)-Cu(6)-S(11)	113.17(14)
S(6)-Cu(3)-S(5)	157.55(6)	S(12)-Cu(6)-N(11)	109.24(15)
N(6)-Cu(3)-Cu(8)	111.87(12)	N(12)-Cu(6)-N(11)	83.5(2)
N(5)-Cu(3)-Cu(8)	154.61(13)	S(11)-Cu(6)-N(11)	87.03(15)
S(6)-Cu(3)-Cu(8)	55.17(5)	S(12)-Cu(6)-Cu(9)	101.74(6)
S(5)-Cu(3)-Cu(8)	103.11(5)	N(12)-Cu(6)-Cu(9)	157.72(15)
N(6)-Cu(3)-Cu(7)	156.20(13)	S(11)-Cu(6)-Cu(9)	55.18(5)
N(5)-Cu(3)-Cu(7)	107.15(13)	N(11)-Cu(6)-Cu(9)	112.48(17)
S(6)-Cu(3)-Cu(7)	105.03(5)	S(12)-Cu(6)-Cu(10)	55.51(5)

Table S3. Bond angles (deg.) for [[Cu(L-$N_2S^{Ar}_2$)]$_3$Cu$_2$]. Symmetry transformations used to generate equivalent atoms:

N(12)-Cu(6)-Cu(10)	108.83(15)	Cu(3)-Cu(8)-Cu(1)	92.38(3)
S(11)-Cu(6)-Cu(10)	103.60(6)	Cu(2)-Cu(8)-Cu(1)	93.60(3)
N(11)-Cu(6)-Cu(10)	158.12(15)	Cu(7)-Cu(8)-Cu(1)	54.36(3)
Cu(9)-Cu(6)-Cu(10)	61.79(3)	S(11)-Cu(9)-S(7)	121.46(7)
S(5)-Cu(7)-S(3)	116.79(7)	S(11)-Cu(9)-S(9)	118.59(8)
S(5)-Cu(7)-S(1)	114.12(6)	S(7)-Cu(9)-S(9)	116.02(7)
S(3)-Cu(7)-S(1)	118.45(6)	S(11)-Cu(9)-Cu(6)	53.70(5)
S(5)-Cu(7)-Cu(1)	151.57(6)	S(7)-Cu(9)-Cu(6)	149.31(6)
S(3)-Cu(7)-Cu(1)	89.43(5)	S(9)-Cu(9)-Cu(6)	85.90(6)
S(1)-Cu(7)-Cu(1)	54.99(5)	S(11)-Cu(9)-Cu(4)	92.22(6)
S(5)-Cu(7)-Cu(2)	88.14(5)	S(7)-Cu(9)-Cu(4)	52.76(5)
S(3)-Cu(7)-Cu(2)	53.14(5)	S(9)-Cu(9)-Cu(4)	141.83(6)
S(1)-Cu(7)-Cu(2)	155.49(5)	Cu(6)-Cu(9)-Cu(4)	96.63(4)
Cu(1)-Cu(7)-Cu(2)	100.55(4)	S(11)-Cu(9)-Cu(10)	100.44(6)
S(5)-Cu(7)-Cu(3)	53.91(5)	S(7)-Cu(9)-Cu(10)	96.65(5)
S(3)-Cu(7)-Cu(3)	147.84(5)	S(9)-Cu(9)-Cu(10)	92.48(5)
S(1)-Cu(7)-Cu(3)	90.86(5)	Cu(6)-Cu(9)-Cu(10)	59.28(3)
Cu(1)-Cu(7)-Cu(3)	98.12(4)	Cu(4)-Cu(9)-Cu(10)	58.01(3)
Cu(2)-Cu(7)-Cu(3)	94.70(3)	S(11)-Cu(9)-Cu(5)	145.57(6)
S(5)-Cu(7)-Cu(8)	98.92(5)	S(7)-Cu(9)-Cu(5)	87.28(5)
S(3)-Cu(7)-Cu(8)	98.79(5)	S(9)-Cu(9)-Cu(5)	50.33(5)
S(1)-Cu(7)-Cu(8)	105.24(5)	Cu(6)-Cu(9)-Cu(5)	91.87(3)
Cu(1)-Cu(7)-Cu(8)	64.29(3)	Cu(4)-Cu(9)-Cu(5)	91.50(3)
Cu(2)-Cu(7)-Cu(8)	58.95(3)	Cu(10)-Cu(9)-Cu(5)	54.02(3)
Cu(3)-Cu(7)-Cu(8)	58.07(3)	S(8)-Cu(10)-S(12)	119.22(7)
S(2)-Cu(8)-S(6)	118.78(7)	S(8)-Cu(10)-S(10)	114.74(7)
S(2)-Cu(8)-S(4)	122.58(6)	S(12)-Cu(10)-S(10)	114.79(6)
S(6)-Cu(8)-S(4)	114.30(6)	S(8)-Cu(10)-Cu(5)	154.30(6)
S(2)-Cu(8)-Cu(3)	143.02(5)	S(12)-Cu(10)-Cu(5)	84.91(5)
S(6)-Cu(8)-Cu(3)	54.34(5)	S(10)-Cu(10)-Cu(5)	54.97(5)
S(4)-Cu(8)-Cu(3)	86.54(5)	S(8)-Cu(10)-Cu(4)	54.28(5)
S(2)-Cu(8)-Cu(2)	87.18(5)	S(12)-Cu(10)-Cu(4)	151.14(6)
S(6)-Cu(8)-Cu(2)	149.44(5)	S(10)-Cu(10)-Cu(4)	90.69(5)
S(4)-Cu(8)-Cu(2)	52.99(5)	Cu(5)-Cu(10)-Cu(4)	100.44(4)
Cu(3)-Cu(8)-Cu(2)	95.36(3)	S(8)-Cu(10)-Cu(6)	90.26(5)
S(2)-Cu(8)-Cu(7)	91.99(5)	S(12)-Cu(10)-Cu(6)	53.05(5)
S(6)-Cu(8)-Cu(7)	101.74(5)	S(10)-Cu(10)-Cu(6)	153.67(6)
S(4)-Cu(8)-Cu(7)	97.47(5)	Cu(5)-Cu(10)-Cu(6)	98.89(4)
Cu(3)-Cu(8)-Cu(7)	59.34(3)	Cu(4)-Cu(10)-Cu(6)	98.11(4)
Cu(2)-Cu(8)-Cu(7)	58.67(3)	S(8)-Cu(10)-Cu(9)	100.52(5)
S(2)-Cu(8)-Cu(1)	50.65(4)	S(12)-Cu(10)-Cu(9)	97.70(5)
S(6)-Cu(8)-Cu(1)	91.73(5)	S(10)-Cu(10)-Cu(9)	105.86(5)
S(4)-Cu(8)-Cu(1)	146.18(6)	Cu(5)-Cu(10)-Cu(9)	65.12(3)

Table S3. Bond angles (deg.) for [[Cu(L-$N_2S^{Ar}_2$)]$_3$Cu$_2$]. Symmetry transformations used to generate equivalent atoms:

Cu(4)-Cu(10)-Cu(9)	60.52(3)	C(8)-N(1)-Cu(1)	98.9(4)
Cu(6)-Cu(10)-Cu(9)	58.94(3)	C(11)-N(2)-C(9)	111.6(5)
C(1)-S(1)-Cu(1)	98.7(2)	C(11)-N(2)-C(10)	111.8(5)
C(1)-S(1)-Cu(7)	96.8(2)	C(9)-N(2)-C(10)	110.7(5)
Cu(1)-S(1)-Cu(7)	67.30(5)	C(11)-N(2)-Cu(1)	109.1(4)
C(16)-S(2)-Cu(1)	96.0(2)	C(9)-N(2)-Cu(1)	104.8(4)
C(16)-S(2)-Cu(8)	107.6(2)	C(10)-N(2)-Cu(1)	108.5(4)
Cu(1)-S(2)-Cu(8)	77.27(5)	C(23)-N(3)-C(22)	112.3(5)
C(17)-S(3)-Cu(2)	97.0(2)	C(23)-N(3)-C(24)	112.3(5)
C(17)-S(3)-Cu(7)	101.3(2)	C(22)-N(3)-C(24)	109.7(5)
Cu(2)-S(3)-Cu(7)	70.91(5)	C(23)-N(3)-Cu(2)	112.2(4)
C(32)-S(4)-Cu(2)	98.1(2)	C(22)-N(3)-Cu(2)	109.1(4)
C(32)-S(4)-Cu(8)	101.0(2)	C(24)-N(3)-Cu(2)	100.7(4)
Cu(2)-S(4)-Cu(8)	71.11(6)	C(27)-N(4)-C(25)	110.1(5)
C(33)-S(5)-Cu(3)	97.6(2)	C(27)-N(4)-C(26)	113.2(5)
C(33)-S(5)-Cu(7)	99.1(2)	C(25)-N(4)-C(26)	111.5(5)
Cu(3)-S(5)-Cu(7)	71.38(5)	C(27)-N(4)-Cu(2)	109.2(3)
C(48)-S(6)-Cu(3)	97.5(2)	C(25)-N(4)-Cu(2)	100.6(3)
C(48)-S(6)-Cu(8)	106.3(2)	C(26)-N(4)-Cu(2)	111.4(4)
Cu(3)-S(6)-Cu(8)	70.49(6)	C(38)-N(5)-C(39)	113.5(5)
C(49)-S(7)-Cu(4)	97.2(2)	C(38)-N(5)-C(40)	109.3(5)
C(49)-S(7)-Cu(9)	108.3(2)	C(39)-N(5)-C(40)	112.5(5)
Cu(4)-S(7)-Cu(9)	72.96(6)	C(38)-N(5)-Cu(3)	110.1(4)
C(64)-S(8)-Cu(4)	98.4(2)	C(39)-N(5)-Cu(3)	111.2(4)
C(64)-S(8)-Cu(10)	100.8(2)	C(40)-N(5)-Cu(3)	99.4(3)
Cu(4)-S(8)-Cu(10)	70.99(5)	C(43)-N(6)-C(42)	113.0(5)
C(65)-S(9)-Cu(5)	96.0(3)	C(43)-N(6)-C(41)	109.2(5)
C(65)-S(9)-Cu(9)	103.9(2)	C(42)-N(6)-C(41)	111.5(5)
Cu(5)-S(9)-Cu(9)	76.96(6)	C(43)-N(6)-Cu(3)	110.2(3)
C(80)-S(10)-Cu(5)	98.2(2)	C(42)-N(6)-Cu(3)	112.3(4)
C(80)-S(10)-Cu(10)	98.5(2)	C(41)-N(6)-Cu(3)	99.9(3)
Cu(5)-S(10)-Cu(10)	67.16(5)	C(55)-N(7)-C(56)	112.2(5)
C(81)-S(11)-Cu(6)	97.2(2)	C(55)-N(7)-C(54)	110.8(5)
C(81)-S(11)-Cu(9)	103.1(2)	C(56)-N(7)-C(54)	109.8(5)
Cu(6)-S(11)-Cu(9)	71.11(6)	C(55)-N(7)-Cu(4)	109.1(4)
C(96)-S(12)-Cu(6)	97.9(2)	C(56)-N(7)-Cu(4)	104.8(3)
C(96)-S(12)-Cu(10)	100.6(2)	C(54)-N(7)-Cu(4)	109.9(3)
Cu(6)-S(12)-Cu(10)	71.44(6)	C(59)-N(8)-C(58)	113.6(5)
C(6)-N(1)-C(7)	113.7(5)	C(59)-N(8)-C(57)	109.2(5)
C(6)-N(1)-C(8)	111.6(5)	C(58)-N(8)-C(57)	112.5(5)
C(7)-N(1)-C(8)	110.9(5)	C(59)-N(8)-Cu(4)	109.3(4)
C(6)-N(1)-Cu(1)	109.0(4)	C(58)-N(8)-Cu(4)	111.6(4)
C(7)-N(1)-Cu(1)	111.8(4)	C(57)-N(8)-Cu(4)	99.8(4)

Table S3. Bond angles (deg.) for [[Cu(L-$N_2S^{Ar}_2$)]$_3$Cu$_2$]. Symmetry transformations used to generate equivalent atoms:

C(71)-N(9)-C(70)	112.9(5)	N(1)-C(7)-H(7B)	109.5
C(71)-N(9)-C(72)	111.1(5)	H(7A)-C(7)-H(7B)	109.5
C(70)-N(9)-C(72)	111.0(5)	N(1)-C(7)-H(7C)	109.5
C(71)-N(9)-Cu(5)	109.2(4)	H(7A)-C(7)-H(7C)	109.5
C(70)-N(9)-Cu(5)	108.1(4)	H(7B)-C(7)-H(7C)	109.5
C(72)-N(9)-Cu(5)	104.1(4)	C(9)-C(8)-N(1)	112.4(5)
C(75)-N(10)-C(74)	114.3(5)	C(9)-C(8)-H(8A)	109.1
C(75)-N(10)-C(73)	109.5(5)	N(1)-C(8)-H(8A)	109.1
C(74)-N(10)-C(73)	112.6(5)	C(9)-C(8)-H(8B)	109.1
C(75)-N(10)-Cu(5)	107.6(3)	N(1)-C(8)-H(8B)	109.1
C(74)-N(10)-Cu(5)	113.4(4)	H(8A)-C(8)-H(8B)	107.8
C(73)-N(10)-Cu(5)	98.2(3)	N(2)-C(9)-C(8)	112.0(5)
C(86)-N(11)-C(88)	111.0(6)	N(2)-C(9)-H(9A)	109.2
C(86)-N(11)-C(87)	112.9(6)	C(8)-C(9)-H(9A)	109.2
C(88)-N(11)-C(87)	112.2(6)	N(2)-C(9)-H(9B)	109.2
C(86)-N(11)-Cu(6)	107.5(4)	C(8)-C(9)-H(9B)	109.2
C(88)-N(11)-Cu(6)	101.6(4)	H(9A)-C(9)-H(9B)	107.9
C(87)-N(11)-Cu(6)	111.0(4)	N(2)-C(10)-H(10A)	109.5
C(90)-N(12)-C(91)	112.3(6)	N(2)-C(10)-H(10B)	109.5
C(90)-N(12)-C(89)	111.3(6)	H(10A)-C(10)-H(10B)	109.5
C(91)-N(12)-C(89)	112.2(5)	N(2)-C(10)-H(10C)	109.5
C(90)-N(12)-Cu(6)	108.2(4)	H(10A)-C(10)-H(10C)	109.5
C(91)-N(12)-Cu(6)	109.7(4)	H(10B)-C(10)-H(10C)	109.5
C(89)-N(12)-Cu(6)	102.6(4)	C(12)-C(11)-C(16)	120.1(6)
C(2)-C(1)-C(6)	119.0(6)	C(12)-C(11)-N(2)	121.3(6)
C(2)-C(1)-S(1)	118.8(5)	C(16)-C(11)-N(2)	118.7(6)
C(6)-C(1)-S(1)	122.0(5)	C(11)-C(12)-C(13)	120.9(7)
C(1)-C(2)-C(3)	121.3(7)	C(11)-C(12)-H(12)	119.6
C(1)-C(2)-H(2)	119.3	C(13)-C(12)-H(12)	119.6
C(3)-C(2)-H(2)	119.3	C(14)-C(13)-C(12)	119.0(7)
C(4)-C(3)-C(2)	120.3(7)	C(14)-C(13)-H(13)	120.5
C(4)-C(3)-H(3)	119.9	C(12)-C(13)-H(13)	120.5
C(2)-C(3)-H(3)	119.9	C(13)-C(14)-C(15)	121.1(7)
C(3)-C(4)-C(5)	118.8(7)	C(13)-C(14)-H(14)	119.5
C(3)-C(4)-H(4)	120.6	C(15)-C(14)-H(14)	119.5
C(5)-C(4)-H(4)	120.6	C(14)-C(15)-C(16)	121.1(7)
C(6)-C(5)-C(4)	121.5(7)	C(14)-C(15)-H(15)	119.5
C(6)-C(5)-H(5)	119.3	C(16)-C(15)-H(15)	119.5
C(4)-C(5)-H(5)	119.3	C(15)-C(16)-C(11)	117.8(6)
C(5)-C(6)-C(1)	119.1(6)	C(15)-C(16)-S(2)	118.6(5)
C(5)-C(6)-N(1)	123.0(6)	C(11)-C(16)-S(2)	123.5(5)
C(1)-C(6)-N(1)	117.8(6)	C(22)-C(17)-C(18)	118.2(6)
N(1)-C(7)-H(7A)	109.5	C(22)-C(17)-S(3)	123.0(5)

Table S3. Bond angles (deg.) for [[Cu(L-$N_2S^{Ar}_2$)]$_3$Cu$_2$]. Symmetry transformations used to generate equivalent atoms:

C(18)-C(17)-S(3)	118.8(5)	C(29)-C(28)-C(27)	120.2(6)
C(17)-C(18)-C(19)	121.0(7)	C(29)-C(28)-H(28)	119.9
C(17)-C(18)-H(18)	119.5	C(27)-C(28)-H(28)	119.9
C(19)-C(18)-H(18)	119.5	C(28)-C(29)-C(30)	120.3(6)
C(20)-C(19)-C(18)	119.5(7)	C(28)-C(29)-H(29)	119.9
C(20)-C(19)-H(19)	120.3	C(30)-C(29)-H(29)	119.9
C(18)-C(19)-H(19)	120.3	C(31)-C(30)-C(29)	119.1(6)
C(19)-C(20)-C(21)	120.0(7)	C(31)-C(30)-H(30)	120.4
C(19)-C(20)-H(20)	120.0	C(29)-C(30)-H(30)	120.4
C(21)-C(20)-H(20)	120.0	C(30)-C(31)-C(32)	121.5(6)
C(20)-C(21)-C(22)	121.2(7)	C(30)-C(31)-H(31)	119.2
C(20)-C(21)-H(21)	119.4	C(32)-C(31)-H(31)	119.2
C(22)-C(21)-H(21)	119.4	C(27)-C(32)-C(31)	118.7(5)
C(17)-C(22)-C(21)	120.1(6)	C(27)-C(32)-S(4)	123.4(5)
C(17)-C(22)-N(3)	117.6(6)	C(31)-C(32)-S(4)	117.8(5)
C(21)-C(22)-N(3)	122.3(6)	C(38)-C(33)-C(34)	118.5(6)
N(3)-C(23)-H(23A)	109.5	C(38)-C(33)-S(5)	122.7(5)
N(3)-C(23)-H(23B)	109.5	C(34)-C(33)-S(5)	118.8(5)
H(23A)-C(23)-H(23B)	109.5	C(35)-C(34)-C(33)	119.8(6)
N(3)-C(23)-H(23C)	109.5	C(35)-C(34)-H(34)	120.1
H(23A)-C(23)-H(23C)	109.5	C(33)-C(34)-H(34)	120.1
H(23B)-C(23)-H(23C)	109.5	C(34)-C(35)-C(36)	121.4(6)
N(3)-C(24)-C(25)	111.2(5)	C(34)-C(35)-H(35)	119.3
N(3)-C(24)-H(24A)	109.4	C(36)-C(35)-H(35)	119.3
C(25)-C(24)-H(24A)	109.4	C(37)-C(36)-C(35)	120.3(6)
N(3)-C(24)-H(24B)	109.4	C(37)-C(36)-H(36)	119.9
C(25)-C(24)-H(24B)	109.4	C(35)-C(36)-H(36)	119.9
H(24A)-C(24)-H(24B)	108.0	C(36)-C(37)-C(38)	120.6(6)
N(4)-C(25)-C(24)	112.0(5)	C(36)-C(37)-H(37)	119.7
N(4)-C(25)-H(25A)	109.2	C(38)-C(37)-H(37)	119.7
C(24)-C(25)-H(25A)	109.2	C(33)-C(38)-N(5)	118.2(5)
N(4)-C(25)-H(25B)	109.2	C(33)-C(38)-C(37)	119.5(6)
C(24)-C(25)-H(25B)	109.2	N(5)-C(38)-C(37)	122.3(6)
H(25A)-C(25)-H(25B)	107.9	N(5)-C(39)-H(39A)	109.5
N(4)-C(26)-H(26A)	109.5	N(5)-C(39)-H(39B)	109.5
N(4)-C(26)-H(26B)	109.5	H(39A)-C(39)-H(39B)	109.5
H(26A)-C(26)-H(26B)	109.5	N(5)-C(39)-H(39C)	109.5
N(4)-C(26)-H(26C)	109.5	H(39A)-C(39)-H(39C)	109.5
H(26A)-C(26)-H(26C)	109.5	H(39B)-C(39)-H(39C)	109.5
H(26B)-C(26)-H(26C)	109.5	N(5)-C(40)-C(41)	112.8(5)
C(32)-C(27)-C(28)	120.1(6)	N(5)-C(40)-H(40A)	109.0
C(32)-C(27)-N(4)	118.5(5)	C(41)-C(40)-H(40A)	109.0
C(28)-C(27)-N(4)	121.4(5)	N(5)-C(40)-H(40B)	109.0

Table S3. Bond angles (deg.) for [[Cu(L-$N_2S^{Ar}{}_2$)]$_3$Cu$_2$]. Symmetry transformations used to generate equivalent atoms:

C(41)-C(40)-H(40B)	109.0	C(51)-C(52)-H(52)	120.4
H(40A)-C(40)-H(40B)	107.8	C(52)-C(53)-C(54)	120.9(6)
N(6)-C(41)-C(40)	112.0(5)	C(52)-C(53)-H(53)	119.5
N(6)-C(41)-H(41A)	109.2	C(54)-C(53)-H(53)	119.5
C(40)-C(41)-H(41A)	109.2	C(53)-C(54)-C(49)	119.7(6)
N(6)-C(41)-H(41B)	109.2	C(53)-C(54)-N(7)	120.9(5)
C(40)-C(41)-H(41B)	109.2	C(49)-C(54)-N(7)	119.2(5)
H(41A)-C(41)-H(41B)	107.9	N(7)-C(55)-H(55A)	109.5
N(6)-C(42)-H(42A)	109.5	N(7)-C(55)-H(55B)	109.5
N(6)-C(42)-H(42B)	109.5	H(55A)-C(55)-H(55B)	109.5
H(42A)-C(42)-H(42B)	109.5	N(7)-C(55)-H(55C)	109.5
N(6)-C(42)-H(42C)	109.5	H(55A)-C(55)-H(55C)	109.5
H(42A)-C(42)-H(42C)	109.5	H(55B)-C(55)-H(55C)	109.5
H(42B)-C(42)-H(42C)	109.5	N(7)-C(56)-C(57)	111.4(5)
C(44)-C(43)-C(48)	119.3(6)	N(7)-C(56)-H(56A)	109.4
C(44)-C(43)-N(6)	121.6(5)	C(57)-C(56)-H(56A)	109.4
C(48)-C(43)-N(6)	119.1(5)	N(7)-C(56)-H(56B)	109.4
C(43)-C(44)-C(45)	120.8(6)	C(57)-C(56)-H(56B)	109.4
C(43)-C(44)-H(44)	119.6	H(56A)-C(56)-H(56B)	108.0
C(45)-C(44)-H(44)	119.6	N(8)-C(57)-C(56)	111.6(5)
C(46)-C(45)-C(44)	119.8(6)	N(8)-C(57)-H(57A)	109.3
C(46)-C(45)-H(45)	120.1	C(56)-C(57)-H(57A)	109.3
C(44)-C(45)-H(45)	120.1	N(8)-C(57)-H(57B)	109.3
C(45)-C(46)-C(47)	120.2(6)	C(56)-C(57)-H(57B)	109.3
C(45)-C(46)-H(46)	119.9	H(57A)-C(57)-H(57B)	108.0
C(47)-C(46)-H(46)	119.9	N(8)-C(58)-H(58A)	109.5
C(46)-C(47)-C(48)	120.9(6)	N(8)-C(58)-H(58B)	109.5
C(46)-C(47)-H(47)	119.6	H(58A)-C(58)-H(58B)	109.5
C(48)-C(47)-H(47)	119.6	N(8)-C(58)-H(59C)	109.5
C(43)-C(48)-C(47)	119.0(6)	H(58A)-C(58)-H(59C)	109.5
C(43)-C(48)-S(6)	122.5(5)	H(58B)-C(58)-H(59C)	109.5
C(47)-C(48)-S(6)	118.4(5)	C(64)-C(59)-C(60)	118.9(6)
C(50)-C(49)-C(54)	117.8(5)	C(64)-C(59)-N(8)	119.2(6)
C(50)-C(49)-S(7)	119.7(5)	C(60)-C(59)-N(8)	122.0(6)
C(54)-C(49)-S(7)	122.4(5)	C(59)-C(60)-C(61)	121.6(7)
C(49)-C(50)-C(51)	121.5(6)	C(59)-C(60)-H(60)	119.2
C(49)-C(50)-H(50)	119.2	C(61)-C(60)-H(60)	119.2
C(51)-C(50)-H(50)	119.2	C(62)-C(61)-C(60)	119.7(7)
C(50)-C(51)-C(52)	120.7(6)	C(62)-C(61)-H(61)	120.1
C(50)-C(51)-H(51)	119.6	C(60)-C(61)-H(61)	120.1
C(52)-C(51)-H(51)	119.6	C(61)-C(62)-C(63)	120.6(7)
C(53)-C(52)-C(51)	119.2(6)	C(61)-C(62)-H(62)	119.7
C(53)-C(52)-H(52)	120.4	C(63)-C(62)-H(62)	119.7

Table S3. Bond angles (deg.) for [[Cu(L-$N_2S^{Ar}{}_2$)]$_3$Cu$_2$]. Symmetry transformations used to generate equivalent atoms:

C(62)-C(63)-C(64)	120.4(7)	N(10)-C(74)-H(74B)	109.5
C(62)-C(63)-H(63)	119.8	H(74A)-C(74)-H(74B)	109.5
C(64)-C(63)-H(63)	119.8	N(10)-C(74)-H(74C)	109.5
C(59)-C(64)-C(63)	118.7(6)	H(74A)-C(74)-H(74C)	109.5
C(59)-C(64)-S(8)	122.7(5)	H(74B)-C(74)-H(74C)	109.5
C(63)-C(64)-S(8)	118.6(5)	C(80)-C(75)-C(76)	119.8(6)
C(70)-C(65)-C(66)	118.0(7)	C(80)-C(75)-N(10)	119.5(5)
C(70)-C(65)-S(9)	122.5(5)	C(76)-C(75)-N(10)	120.6(6)
C(66)-C(65)-S(9)	119.5(6)	C(77)-C(76)-C(75)	120.5(6)
C(67)-C(66)-C(65)	121.2(8)	C(77)-C(76)-H(76)	119.8
C(67)-C(66)-H(66)	119.4	C(75)-C(76)-H(76)	119.8
C(65)-C(66)-H(66)	119.4	C(76)-C(77)-C(78)	120.0(6)
C(68)-C(67)-C(66)	119.9(8)	C(76)-C(77)-H(77)	120.0
C(68)-C(67)-H(67)	120.0	C(78)-C(77)-H(77)	120.0
C(66)-C(67)-H(67)	120.0	C(79)-C(78)-C(77)	119.3(6)
C(67)-C(68)-C(69)	121.5(8)	C(79)-C(78)-H(78)	120.4
C(67)-C(68)-H(68)	119.2	C(77)-C(78)-H(78)	120.4
C(69)-C(68)-H(68)	119.2	C(78)-C(79)-C(80)	121.3(6)
C(70)-C(69)-C(68)	118.1(8)	C(78)-C(79)-H(79)	119.4
C(70)-C(69)-H(69)	120.9	C(80)-C(79)-H(79)	119.4
C(68)-C(69)-H(69)	120.9	C(75)-C(80)-C(79)	119.1(6)
C(69)-C(70)-C(65)	121.0(7)	C(75)-C(80)-S(10)	122.3(5)
C(69)-C(70)-N(9)	119.4(7)	C(79)-C(80)-S(10)	118.6(5)
C(65)-C(70)-N(9)	119.6(6)	C(86)-C(81)-C(82)	118.6(7)
N(9)-C(71)-H(71A)	109.5	C(86)-C(81)-S(11)	122.8(6)
N(9)-C(71)-H(71B)	109.5	C(82)-C(81)-S(11)	118.5(6)
H(71A)-C(71)-H(71B)	109.5	C(83)-C(82)-C(81)	121.1(8)
N(9)-C(71)-H(71C)	109.5	C(83)-C(82)-H(82)	119.4
H(71A)-C(71)-H(71C)	109.5	C(81)-C(82)-H(82)	119.4
H(71B)-C(71)-H(71C)	109.5	C(82)-C(83)-C(84)	119.8(9)
N(9)-C(72)-C(73)	111.1(5)	C(82)-C(83)-H(83)	120.1
N(9)-C(72)-H(72A)	109.4	C(84)-C(83)-H(83)	120.1
C(73)-C(72)-H(72A)	109.4	C(85)-C(84)-C(83)	119.6(9)
N(9)-C(72)-H(72B)	109.4	C(85)-C(84)-H(84)	120.2
C(73)-C(72)-H(72B)	109.4	C(83)-C(84)-H(84)	120.2
H(72A)-C(72)-H(72B)	108.0	C(84)-C(85)-C(86)	120.3(9)
N(10)-C(73)-C(72)	111.6(5)	C(84)-C(85)-H(85)	119.9
N(10)-C(73)-H(73A)	109.3	C(86)-C(85)-H(85)	119.9
C(72)-C(73)-H(73A)	109.3	C(81)-C(86)-C(85)	120.5(8)
N(10)-C(73)-H(73B)	109.3	C(81)-C(86)-N(11)	119.6(7)
C(72)-C(73)-H(73B)	109.3	C(85)-C(86)-N(11)	119.9(7)
H(73A)-C(73)-H(73B)	108.0	N(11)-C(87)-H(87A)	109.5
N(10)-C(74)-H(74A)	109.5	N(11)-C(87)-H(87B)	109.5

Table S3. Bond angles (deg.) for [[Cu(L-$N_2S^{Ar}_2$)]$_3$Cu$_2$]. Symmetry transformations used to generate equivalent atoms:

H(87A)-C(87)-H(87B)	109.5
N(11)-C(87)-H(87C)	109.5
H(87A)-C(87)-H(87C)	109.5
H(87B)-C(87)-H(87C)	109.5
N(11)-C(88)-C(89)	111.6(6)
N(11)-C(88)-H(88A)	109.3
C(89)-C(88)-H(88A)	109.3
N(11)-C(88)-H(88B)	109.3
C(89)-C(88)-H(88B)	109.3
H(88A)-C(88)-H(88B)	108.0
N(12)-C(89)-C(88)	112.4(6)
N(12)-C(89)-H(89A)	109.1
C(88)-C(89)-H(89A)	109.1
N(12)-C(89)-H(89B)	109.1
C(88)-C(89)-H(89B)	109.1
H(89A)-C(89)-H(89B)	107.9
N(12)-C(90)-H(90A)	109.5
N(12)-C(90)-H(90B)	109.5
H(90A)-C(90)-H(90B)	109.5
N(12)-C(90)-H(90C)	109.5
H(90A)-C(90)-H(90C)	109.5
H(90B)-C(90)-H(90C)	109.5
C(92)-C(91)-C(96)	118.6(7)
C(92)-C(91)-N(12)	123.0(6)
C(96)-C(91)-N(12)	118.5(6)
C(91)-C(92)-C(93)	121.3(7)
C(91)-C(92)-H(92)	119.3
C(93)-C(92)-H(92)	119.3
C(94)-C(93)-C(92)	120.8(7)
C(94)-C(93)-H(93)	119.6
C(92)-C(93)-H(93)	119.6
C(95)-C(94)-C(93)	119.3(7)
C(95)-C(94)-H(94)	120.4
C(93)-C(94)-H(94)	120.4
C(94)-C(95)-C(96)	120.5(7)
C(94)-C(95)-H(95)	119.8
C(96)-C(95)-H(95)	119.8
C(95)-C(96)-C(91)	119.5(6)
C(95)-C(96)-S(12)	117.9(5)
C(91)-C(96)-S(12)	122.6(5)

Table S4. Anisotropic displacement parameters (Å^2 x 10^3) for [[Cu(L-$N_2S^{Ar}{}_2$)]$_3$Cu$_2$]. The anisotropic displacement factor exponent takes the form: $-2\pi^2[(ha^*)^2U^{11} + ... + 2hka^*b^*U^{12}]$.

Atom	U^{11}	U^{22}	U^{33}	U^{23}	U^{13}	U^{12}
Cu(1)	20(1)	20(1)	40(1)	-4(1)	4(1)	-1(1)
Cu(2)	21(1)	22(1)	35(1)	-4(1)	7(1)	-3(1)
Cu(3)	16(1)	23(1)	34(1)	-6(1)	5(1)	-1(1)
Cu(4)	21(1)	24(1)	32(1)	-5(1)	6(1)	-2(1)
Cu(5)	24(1)	24(1)	42(1)	-6(1)	8(1)	-4(1)
Cu(6)	28(1)	38(1)	36(1)	1(1)	3(1)	-6(1)
Cu(7)	21(1)	21(1)	38(1)	-6(1)	5(1)	-2(1)
Cu(8)	19(1)	26(1)	38(1)	-6(1)	6(1)	-2(1)
Cu(9)	27(1)	29(1)	44(1)	-2(1)	7(1)	-1(1)
Cu(10)	23(1)	27(1)	36(1)	-5(1)	4(1)	-1(1)
S(1)	22(1)	22(1)	48(1)	-8(1)	7(1)	-4(1)
S(2)	20(1)	28(1)	35(1)	-4(1)	4(1)	-2(1)
S(3)	26(1)	25(1)	38(1)	-5(1)	5(1)	2(1)
S(4)	20(1)	24(1)	42(1)	-8(1)	8(1)	-3(1)
S(5)	22(1)	25(1)	35(1)	-4(1)	3(1)	-2(1)
S(6)	21(1)	22(1)	36(1)	-6(1)	4(1)	1(1)
S(7)	22(1)	26(1)	43(1)	-11(1)	7(1)	-4(1)
S(8)	28(1)	27(1)	36(1)	-10(1)	1(1)	-3(1)
S(9)	32(1)	25(1)	52(1)	0(1)	11(1)	0(1)
S(10)	19(1)	31(1)	34(1)	-5(1)	7(1)	-4(1)
S(11)	26(1)	44(1)	46(1)	4(1)	4(1)	-6(1)
S(12)	27(1)	36(1)	37(1)	-7(1)	3(1)	-5(1)
N(1)	23(3)	20(3)	45(3)	-5(2)	8(2)	1(2)
N(2)	31(3)	23(3)	37(3)	-6(2)	4(2)	2(2)
N(3)	22(3)	24(3)	39(3)	0(2)	5(2)	1(2)
N(4)	22(3)	24(3)	40(3)	-6(2)	9(2)	-4(2)
N(5)	19(2)	21(3)	38(3)	-5(2)	1(2)	0(2)
N(6)	20(3)	19(3)	32(3)	-4(2)	2(2)	0(2)
N(7)	18(2)	20(3)	41(3)	-5(2)	3(2)	-3(2)
N(8)	20(3)	25(3)	41(3)	-5(2)	3(2)	-2(2)
N(9)	34(3)	30(3)	49(4)	-16(3)	15(2)	-14(2)
N(10)	27(3)	28(3)	37(3)	-10(2)	9(2)	-13(2)
N(11)	34(3)	50(4)	50(4)	11(3)	6(3)	-4(3)
N(12)	36(3)	50(4)	32(3)	-6(3)	3(3)	-15(3)
C(1)	33(3)	19(4)	39(4)	-3(3)	2(3)	-5(3)
C(2)	34(4)	25(4)	55(5)	-10(3)	-7(3)	-6(3)
C(3)	53(4)	33(5)	61(5)	-8(4)	-13(4)	-10(4)
C(4)	70(5)	32(5)	51(5)	-17(4)	0(4)	-15(4)
C(5)	45(4)	28(4)	53(5)	-11(4)	8(3)	-5(3)
C(6)	38(3)	16(4)	45(4)	-11(3)	5(3)	-3(3)

Table S4. Anisotropic displacement parameters ($Å^2$ x 10^3) for [[Cu(L-$N_2S^{Ar}{}_2$)]$_3$Cu$_2$]. The anisotropic displacement factor exponent takes the form: $-2\pi^2[(ha^*)^2U^{11} + ... + 2hka^*b^*U^{12}]$

Atom	U^{11}	U^{22}	U^{33}	U^{23}	U^{13}	U^{12}
C(7)	31(4)	30(4)	67(5)	-11(4)	16(3)	-2(3)
C(8)	38(4)	17(4)	51(4)	-4(3)	7(3)	2(3)
C(9)	35(4)	23(4)	54(5)	-3(3)	-7(3)	5(3)
C(10)	39(4)	36(5)	59(5)	8(4)	13(3)	-10(3)
C(11)	19(3)	35(4)	32(4)	-11(3)	8(3)	1(3)
C(12)	34(4)	36(4)	36(4)	-2(3)	0(3)	8(3)
C(13)	32(4)	54(5)	36(4)	-11(3)	-1(3)	12(3)
C(14)	24(4)	48(5)	36(4)	-14(4)	8(3)	2(3)
C(15)	22(3)	43(4)	36(4)	-9(3)	10(3)	-2(3)
C(16)	18(3)	31(4)	32(4)	-10(3)	6(3)	3(3)
C(17)	26(3)	37(4)	34(4)	-6(3)	7(3)	-8(3)
C(18)	42(4)	45(4)	38(4)	-11(3)	6(3)	-8(3)
C(19)	63(5)	62(5)	41(5)	-16(4)	-2(4)	-13(4)
C(20)	46(5)	71(5)	32(5)	-7(4)	-1(3)	-1(4)
C(21)	37(4)	42(4)	37(4)	4(3)	4(3)	-8(3)
C(22)	23(3)	39(4)	34(4)	-1(3)	7(3)	-6(3)
C(23)	40(4)	34(4)	50(5)	-1(3)	-5(3)	7(3)
C(24)	33(4)	43(5)	34(4)	0(3)	8(3)	-10(3)
C(25)	23(3)	43(4)	41(4)	8(3)	7(3)	-14(3)
C(26)	18(3)	49(5)	52(5)	-9(4)	14(3)	0(3)
C(27)	26(3)	18(4)	40(4)	0(3)	4(3)	-8(3)
C(28)	20(3)	26(4)	48(4)	1(3)	5(3)	0(3)
C(29)	25(3)	28(4)	53(5)	1(3)	-5(3)	-4(3)
C(30)	39(4)	28(4)	50(5)	-8(4)	-1(3)	-9(3)
C(31)	32(3)	28(4)	41(4)	-8(3)	8(3)	-9(3)
C(32)	23(3)	15(3)	41(4)	-2(3)	6(3)	0(3)
C(33)	25(3)	19(4)	40(4)	-5(3)	0(3)	-2(3)
C(34)	24(3)	37(4)	38(4)	-8(3)	2(3)	-1(3)
C(35)	32(4)	43(5)	37(4)	-14(4)	1(3)	-2(3)
C(36)	21(3)	45(5)	52(5)	-19(4)	4(3)	-8(3)
C(37)	17(3)	38(4)	41(4)	-9(3)	8(3)	-2(3)
C(38)	14(3)	26(4)	40(4)	-9(3)	1(3)	3(3)
C(39)	28(4)	27(4)	35(4)	0(3)	2(3)	-8(3)
C(40)	20(3)	31(4)	45(5)	-5(3)	5(3)	-1(3)
C(41)	15(3)	32(4)	40(4)	-9(3)	8(3)	3(3)
C(42)	28(4)	24(4)	40(4)	-1(3)	4(3)	6(3)
C(43)	21(3)	25(4)	29(4)	-6(3)	6(3)	-6(3)
C(44)	27(3)	30(4)	34(4)	-5(3)	6(3)	-2(3)
C(45)	35(4)	24(4)	49(5)	-19(3)	7(3)	-7(3)
C(46)	25(3)	47(5)	36(4)	-9(3)	-1(3)	-12(3)

Table S4. Anisotropic displacement parameters (Å^2 x 10^3) for [[Cu(L-$N_2S^{Ar}{}_2$)]$_3$Cu$_2$]. The anisotropic displacement factor exponent takes the form: $-2\pi^2[(ha^*)^2U^{11} + ... + 2hka^*b^*U^{12}]$

Atom	U^{11}	U^{22}	U^{33}	U^{23}	U^{13}	U^{12}
C(47)	29(4)	35(4)	35(4)	-4(3)	4(3)	-7(3)
C(48)	19(3)	21(3)	37(4)	-7(3)	9(3)	-5(3)
C(49)	21(3)	26(4)	37(4)	-6(3)	4(3)	-8(3)
C(50)	29(3)	26(4)	56(5)	-17(4)	9(3)	-4(3)
C(51)	26(3)	31(4)	43(5)	-5(3)	2(3)	7(3)
C(52)	23(3)	39(4)	37(4)	-2(3)	7(3)	9(3)
C(53)	12(3)	31(4)	45(4)	2(3)	7(3)	4(3)
C(54)	20(3)	30(3)	22(4)	-5(3)	3(3)	3(3)
C(55)	22(3)	48(5)	59(5)	-25(4)	5(3)	-14(3)
C(56)	32(4)	36(4)	44(4)	0(3)	17(3)	-2(3)
C(57)	27(3)	29(4)	49(5)	9(3)	13(3)	-2(3)
C(58)	41(4)	51(5)	44(5)	-13(4)	-5(3)	8(4)
C(59)	19(3)	23(4)	47(4)	0(3)	6(3)	0(3)
C(60)	34(4)	28(4)	50(4)	3(3)	12(3)	4(3)
C(61)	35(4)	38(5)	63(5)	19(4)	13(4)	14(3)
C(62)	46(4)	16(4)	69(5)	-10(4)	6(4)	11(3)
C(63)	30(4)	27(4)	52(5)	-16(3)	5(3)	-4(3)
C(64)	23(3)	20(3)	47(4)	-6(3)	0(3)	-5(3)
C(65)	44(4)	20(4)	56(5)	-7(3)	18(3)	-10(3)
C(66)	47(4)	35(5)	69(6)	1(4)	23(4)	-1(3)
C(67)	65(5)	34(5)	89(7)	-7(4)	38(4)	3(4)
C(68)	75(6)	25(4)	80(6)	-19(4)	46(4)	-13(4)
C(69)	69(5)	36(4)	51(5)	-14(4)	28(4)	-16(4)
C(70)	40(4)	22(4)	51(5)	-6(3)	23(3)	-11(3)
C(71)	40(4)	45(5)	49(4)	-17(4)	13(3)	-7(3)
C(72)	40(4)	32(4)	61(5)	-20(4)	15(4)	-18(3)
C(73)	26(3)	41(4)	49(4)	-17(4)	7(3)	-14(3)
C(74)	32(4)	40(4)	46(4)	0(3)	12(3)	-7(3)
C(75)	16(3)	36(4)	31(4)	-8(3)	3(3)	1(3)
C(76)	30(4)	41(4)	33(4)	-6(3)	8(3)	-7(3)
C(77)	22(3)	44(4)	46(5)	-8(4)	8(3)	-1(3)
C(78)	31(4)	33(4)	45(5)	-8(3)	7(3)	3(3)
C(79)	26(3)	36(4)	34(4)	-2(3)	0(3)	1(3)
C(80)	21(3)	30(4)	32(4)	-7(3)	3(3)	-2(3)
C(81)	28(4)	52(5)	50(5)	16(4)	1(3)	-2(3)
C(82)	38(4)	66(6)	80(6)	27(5)	13(4)	14(4)
C(83)	61(6)	72(7)	116(8)	31(6)	27(5)	25(5)
C(84)	94(8)	84(8)	118(9)	53(7)	28(6)	42(6)
C(85)	73(6)	67(6)	78(7)	34(5)	14(5)	18(5)
C(86)	42(4)	50(5)	53(5)	15(3)	-1(3)	1(3)

Table S4. Anisotropic displacement parameters ($Å^2$ x 10^3) for [[Cu(L-$N_2S^{Ar}{}_2$)]$_3$$Cu_2$]. The anisotropic displacement factor exponent takes the form: $-2\pi^2[(ha^*)^2U^{11} + ... + 2hka^*b^*U^{12}]$

Atom	U^{11}	U^{22}	U^{33}	U^{23}	U^{13}	U^{12}
C(87)	51(5)	55(6)	71(6)	25(4)	14(4)	-1(4)
C(88)	39(4)	78(6)	47(5)	0(4)	-8(4)	2(4)
C(89)	51(5)	68(5)	37(4)	-3(4)	-2(4)	-8(4)
C(90)	43(4)	64(6)	60(6)	-16(4)	10(4)	-24(4)
C(91)	41(3)	38(4)	34(4)	-5(3)	8(3)	-10(3)
C(92)	48(4)	48(5)	47(5)	-14(4)	11(4)	-18(3)
C(93)	65(5)	31(4)	52(5)	-12(4)	20(4)	-8(3)
C(94)	53(4)	40(4)	39(5)	-7(4)	14(4)	5(4)
C(95)	37(4)	39(4)	38(4)	-11(3)	8(3)	-3(3)
C(96)	34(3)	39(4)	33(4)	-5(3)	7(3)	-8(3)

Table S5. Hydrogen coordinates (x 10^4) and isotropic displacement parameters ($Å^2$ x 10^3) for [[Cu(L-$N_2S^{Ar}_2$)]$_3$Cu$_2$].

H atom	x	y	z	U(eq)
H(2)	11383	9233	1969	45
H(3)	11101	9723	2918	58
H(4)	9268	10113	3220	60
H(5)	7745	10043	2522	50
H(7A)	6695	9152	2052	64
H(7B)	6069	9400	1384	64
H(7C)	6369	9916	1875	64
H(8A)	7311	10491	1035	42
H(8B)	8441	10165	720	42
H(9A)	6190	9863	423	46
H(9B)	6923	10314	-44	46
H(10A)	8694	9132	-692	67
H(10B)	9045	9652	-219	67
H(10C)	8136	9871	-782	67
H(12)	6313	9703	-1088	43
H(13)	5040	9137	-1636	50
H(14)	4587	8129	-1195	43
H(15)	5363	7678	-226	40
H(18)	9476	8450	3217	49
H(19)	10683	8046	4076	65
H(20)	10963	6928	4347	60
H(21)	10051	6221	3771	46
H(23A)	10182	5960	2496	63
H(23B)	9083	5605	2342	63
H(23C)	9518	5600	3070	63
H(24A)	7199	6750	3139	44
H(24B)	7679	6019	3381	44
H(25A)	7248	5681	2344	43
H(25B)	6135	5953	2713	43
H(26A)	5403	7351	1730	59
H(26B)	5949	7344	2433	59
H(26C)	5005	6864	2306	59
H(28)	4604	6164	1582	38
H(29)	4192	5656	662	43
H(30)	5608	5439	-101	46
H(31)	7434	5713	78	40
H(34)	12256	7680	2535	40
H(35)	13697	8363	2522	44
H(36)	14454	8761	1565	46
H(37)	13851	8441	596	38

Table S5. Hydrogen coordinates (x 10^4) and isotropic displacement parameters (Å^2 x 10^3) for [[Cu(L-$N_2S^{Ar}_2$)]$_3$Cu$_2$].

H atom	x	y	z	U(eq)
H(39A)	11762	8575	-20	45
H(39B)	11793	8035	-529	45
H(39C)	12952	8270	-282	45
H(40A)	13085	6772	606	38
H(40B)	13638	7171	13	38
H(41A)	12081	6977	-652	35
H(41B)	12824	6317	-396	35
H(42A)	10864	5646	613	47
H(42B)	11929	5977	864	47
H(42C)	12071	5529	272	47
H(44)	11208	5384	-641	36
H(45)	10002	5214	-1485	42
H(46)	8573	6019	-1830	42
H(47)	8322	6991	-1326	39
H(50)	7028	1234	2188	43
H(51)	8873	1139	1826	41
H(52)	9899	2045	1709	40
H(53)	9073	3052	2001	36
H(55A)	7933	3369	3275	62
H(55B)	7349	4079	3034	62
H(55C)	8455	3778	2678	62
H(56A)	6524	3541	1511	45
H(56B)	7446	4010	1706	45
H(57A)	6038	4594	2316	43
H(57B)	5698	4637	1568	43
H(58A)	3467	3672	1710	68
H(58B)	4701	3409	1471	68
H(59C)	4159	4125	1222	68
H(60)	3218	4987	1614	46
H(61)	2088	5785	2094	57
H(62)	2120	5818	3199	53
H(63)	3274	5053	3837	43
H(66)	5627	273	3897	61
H(67)	5736	-509	3160	76
H(68)	4313	-516	2418	70
H(69)	2844	351	2296	61
H(71A)	3160	1779	2087	66
H(71B)	1889	2073	2222	66
H(71C)	2125	1352	1994	66
H(72A)	1554	942	3595	51

Table S5. Hydrogen coordinates (x 10^4) and isotropic displacement parameters ($Å^2$ x 10^3) for $[[Cu(L\text{-}N_2S^{Ar}{}_2)]_3Cu_2]$.

H atom	x	y	z	U(eq)
H(72B)	1023	1020	2882	51
H(73A)	598	2172	2979	45
H(73B)	-70	1743	3502	45
H(74A)	1322	2092	4864	59
H(74B)	1651	1422	4543	59
H(74C)	348	1704	4588	59
H(76)	-534	2731	4514	41
H(77)	-1245	3832	4495	44
H(78)	-442	4614	3809	44
H(79)	1094	4294	3164	39
H(82)	8362	1317	4141	78
H(83)	8933	350	4754	105
H(84)	8037	97	5735	127
H(85)	6684	860	6131	92
H(87A)	4664	1302	5654	91
H(87B)	4159	1980	5909	91
H(87C)	5051	1500	6342	91
H(88A)	6978	2556	5830	66
H(88B)	6402	2201	6442	66
H(89A)	4716	2911	6246	62
H(89B)	5774	3305	6391	62
H(90A)	6059	4101	4893	81
H(90B)	6901	3499	5192	81
H(90C)	6425	4059	5636	81
H(92)	4721	4587	5931	55
H(93)	3043	5247	5869	59
H(94)	1464	4924	5366	53
H(95)	1592	3923	4917	45

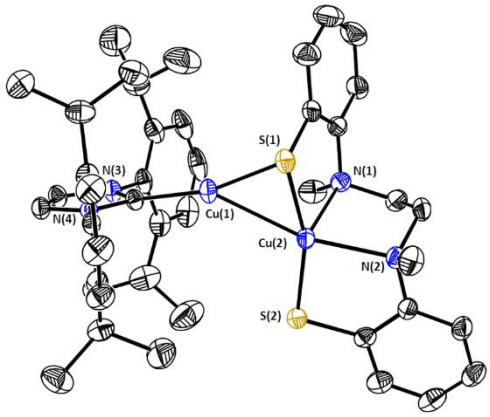

Structure Determination Summary

Crystal Data and Structure Refinement for [(L-$N_2S^{Ar}_2$)CuCu(IMes)]·C_6H_6, **2**

Identification code	jpd516_0m
Empirical formula	$C_{49}H_{60}Cu_2N_4S_2$
Formula weight	896.21
Temperature	150(2) K
Wavelength	0.71073 Å
Crystal system	monoclinic
Space group	$P2_1/c$
Unit cell dimensions	a = 12.8490(5) Å α = 90°
	b = 16.8154(7) Å β = 96.0220(10)°
	c = 23.0028(9) Å γ = 90°
Volume, Z	4942.6(3) $Å^3$, 4
Density (calculated)	1.204 g/cm^3
Absorption coefficient	0.980 mm^{-1}
F(000)	1888
Crystal size	0.18 x 0.08 x 0.06 mm
θ range for data collection	2.00 to 28.31°
Limiting indices	$-17 < h < 17$, $-21 < k < 22$, $-30 < l < 30$
Reflections collected	87896
Independent reflections	12269 (R_{int} = 0.0794)
Completeness to θ = 28.31°	99.9 %
Absorption correction	Semi-empirical from equivalents
Max. and min. transmission	0.9436 and 0.6968
Refinement method	Full-matrix least-squares on F^2
Data / restraints / parameters	12269 / 0 / 551
Goodness-of-fit on F^2	1.025
Final R indices [I>2σ(I)]	R1 = 0.0514, wR2 = 0.1514
R indices (all data)	R1 = 0.0785, wR2 = 0.1741
Largest diff. peak and hole	1.039 and -0.518 $e·Å^{-3}$

Table S1. Atomic coordinates (x 10^4) and equivalent isotropic displacement parameters [$Å^2$ x 10^3) for [(L-$N_2S^{Ar}_2$)CuCu(IMes)]·C_6H_6. U(eq) is defined as one third of the trace of the orthogonalized U^{ij} tensor.

Atom	x	y	z	U(eq)
Cu(1)	1267(1)	1142(1)	3519(1)	26(1)
Cu(2)	2336(1)	73(1)	3002(1)	25(1)
S(1)	2162(1)	166(1)	3945(1)	27(1)
S(2)	1938(1)	123(1)	2056(1)	31(1)
N(1)	3985(2)	596(2)	3213(1)	26(1)
N(2)	3237(2)	-1041(2)	2886(1)	26(1)
N(3)	538(2)	2786(2)	3232(1)	25(1)
N(4)	-681(2)	2024(1)	3456(1)	22(1)
C(1)	3403(2)	580(2)	4201(1)	28(1)
C(2)	3615(3)	738(2)	4796(2)	41(1)
C(3)	4583(4)	1015(3)	5024(2)	49(1)
C(4)	5360(3)	1145(2)	4669(2)	46(1)
C(5)	5162(3)	1006(2)	4079(2)	34(1)
C(6)	4189(2)	727(2)	3836(1)	26(1)
C(7)	4066(3)	1337(2)	2877(2)	40(1)
C(8)	4652(2)	-45(2)	3010(2)	32(1)
C(9)	4270(2)	-847(2)	3197(2)	32(1)
C(10)	2753(3)	-1721(2)	3161(2)	38(1)
C(11)	3287(2)	-1172(2)	2264(1)	26(1)
C(12)	3869(2)	-1799(2)	2071(2)	34(1)
C(13)	3962(3)	-1925(2)	1486(2)	39(1)
C(14)	3464(3)	-1412(2)	1085(2)	40(1)
C(15)	2871(3)	-786(2)	1267(2)	36(1)
C(16)	2753(2)	-650(2)	1856(1)	27(1)
C(17)	1540(2)	3066(2)	3081(2)	29(1)
C(18)	2260(2)	3351(2)	3526(2)	34(1)
C(19)	3221(3)	3602(2)	3367(2)	44(1)
C(20)	3430(3)	3579(2)	2796(2)	48(1)
C(21)	2704(3)	3294(2)	2362(2)	46(1)
C(22)	1725(3)	3029(2)	2491(2)	36(1)
C(23)	2041(3)	3374(2)	4158(2)	45(1)
C(24)	2385(4)	4151(3)	4473(2)	72(1)
C(25)	2559(4)	2656(3)	4499(2)	69(1)
C(26)	897(3)	2756(2)	2016(2)	47(1)
C(27)	1337(5)	2284(3)	1535(2)	78(2)
C(28)	256(3)	3466(3)	1756(2)	51(1)
C(29)	-352(2)	3254(2)	3227(1)	27(1)
C(30)	-1122(2)	2769(2)	3372(1)	26(1)
C(31)	351(2)	2020(2)	3373(1)	23(1)

Table S1. Atomic coordinates (x 10^4) and equivalent isotropic displacement parameters [$Å^2$ x 10^3) for [(L-$N_2S^{Ar}{}_2$)CuCu(IMes)]·C_6H_6. U(eq) is defined as one third of the trace of the orthogonalized U^{ij} tensor.

Atom	x	y	z	U(eq)
C(32)	-1236(2)	1326(2)	3618(1)	23(1)
C(33)	-1259(2)	1160(2)	4209(1)	28(1)
C(34)	-1787(3)	473(2)	4353(2)	37(1)
C(35)	-2269(3)	-10(2)	3922(2)	36(1)
C(36)	-2248(3)	175(2)	3341(2)	34(1)
C(37)	-1729(2)	853(2)	3172(1)	28(1)
C(38)	-732(3)	1689(2)	4692(1)	35(1)
C(39)	135(3)	1242(3)	5066(2)	48(1)
C(40)	-1536(3)	2027(3)	5063(2)	48(1)
C(41)	-1702(3)	1042(2)	2528(1)	34(1)
C(42)	-995(4)	461(3)	2244(2)	56(1)
C(43)	-2803(3)	1032(3)	2201(2)	50(1)
C(44)	4410(7)	1804(6)	1176(4)	57(2)
C(45)	4348(6)	997(5)	1166(3)	47(2)
C(46)	4960(7)	575(4)	861(3)	47(2)
C(47)	5670(7)	953(5)	538(3)	48(2)
C(48)	5761(9)	1700(6)	567(3)	67(3)
C(49)	5134(10)	2146(4)	875(4)	69(3)
C(50)	317(4)	10024(4)	590(2)	70(2)
C(51)	447(4)	9355(3)	278(2)	72(2)
C(52)	134(4)	9327(4)	-311(3)	76(2)

Table S2. Bond lengths (Å) for [(L-$N_2S^{Ar}{}_2$)CuCu(IMes)]·C_6H_6. Symmetry transformations used to generate equivalent atoms: #1 -x, -y + 2, -z.

Cu(1)-C(31)	1.895(3)	C(11)-C(16)	1.410(4)
Cu(1)-S(1)	2.1769(8)	C(12)-C(13)	1.379(5)
Cu(1)-Cu(2)	2.6231(5)	C(12)-H(12)	0.9500
Cu(2)-S(2)	2.1839(9)	C(13)-C(14)	1.371(6)
Cu(2)-S(1)	2.2103(8)	C(13)-H(13)	0.9500
Cu(2)-N(2)	2.233(2)	C(14)-C(15)	1.390(5)
Cu(2)-N(1)	2.298(3)	C(14)-H(14)	0.9500
S(1)-C(1)	1.783(3)	C(15)-C(16)	1.397(5)
S(2)-C(16)	1.759(3)	C(15)-H(15)	0.9500
N(1)-C(6)	1.446(4)	C(17)-C(18)	1.391(5)
N(1)-C(7)	1.476(4)	C(17)-C(22)	1.404(5)
N(1)-C(8)	1.482(4)	C(18)-C(19)	1.391(5)
N(2)-C(11)	1.454(4)	C(18)-C(23)	1.510(5)
N(2)-C(10)	1.475(4)	C(19)-C(20)	1.369(6)
N(2)-C(9)	1.477(4)	C(19)-H(19)	0.9500
N(3)-C(31)	1.356(4)	C(20)-C(21)	1.379(6)
N(3)-C(29)	1.387(4)	C(20)-H(20)	0.9500
N(3)-C(17)	1.447(4)	C(21)-C(22)	1.395(5)
N(4)-C(31)	1.360(3)	C(21)-H(21)	0.9500
N(4)-C(30)	1.381(4)	C(22)-C(26)	1.514(5)
N(4)-C(32)	1.441(4)	C(23)-C(24)	1.536(6)
C(1)-C(2)	1.392(5)	C(23)-C(25)	1.551(6)
C(1)-C(6)	1.402(4)	C(23)-H(23)	1.0000
C(2)-C(3)	1.379(6)	C(24)-H(24A)	0.9800
C(2)-H(2)	0.9500	C(24)-H(24B)	0.9800
C(3)-C(4)	1.372(6)	C(24)-H(24C)	0.9800
C(3)-H(3)	0.9500	C(25)-H(25A)	0.9800
C(4)-C(5)	1.374(5)	C(25)-H(25B)	0.9800
C(4)-H(4)	0.9500	C(25)-H(25C)	0.9800
C(5)-C(6)	1.396(4)	C(26)-C(27)	1.520(6)
C(5)-H(5)	0.9500	C(26)-C(28)	1.536(6)
C(7)-H(7A)	0.9800	C(26)-H(26)	1.0000
C(7)-H(7B)	0.9800	C(27)-H(27A)	0.9800
C(7)-H(7C)	0.9800	C(27)-H(27B)	0.9800
C(8)-C(9)	1.513(5)	C(27)-H(27C)	0.9800
C(8)-H(8A)	0.9900	C(28)-H(28A)	0.9800
C(8)-H(8B)	0.9900	C(28)-H(28B)	0.9800
C(9)-H(9A)	0.9900	C(28)-H(28C)	0.9800
C(9)-H(9B)	0.9900	C(29)-C(30)	1.351(4)
C(10)-H(10A)	0.9800	C(29)-H(29)	0.9500
C(10)-H(10B)	0.9800	C(30)-H(30)	0.9500
C(10)-H(10C)	0.9800	C(32)-C(33)	1.391(4)
C(11)-C(12)	1.393(4)	C(32)-C(37)	1.398(4)

Table S2. Bond lengths (Å) for [(L-$N_2S^{Ar}{}_2$)CuCu(IMes)]·C_6H_6. Symmetry transformations used to generate equivalent atoms: #1 -x, -y + 2, -z.

C(33)-C(34)	1.397(4)		
C(33)-C(38)	1.524(4)	C(51)-H(51)	0.9500
C(34)-C(35)	1.377(5)	C(52)-C(50)#1	1.365(7)
C(34)-H(34)	0.9500	C(52)-H(52)	0.9500
C(35)-C(36)	1.376(5)		
C(35)-H(35)	0.9500		
C(36)-C(37)	1.396(4)		
C(36)-H(36)	0.9500		
C(37)-C(41)	1.519(4)		
C(38)-C(40)	1.519(5)		
C(38)-C(39)	1.532(5)		
C(38)-H(38)	1.0000		
C(39)-H(39A)	0.9800		
C(39)-H(39B)	0.9800		
C(39)-H(39C)	0.9800		
C(40)-H(40A)	0.9800		
C(40)-H(40B)	0.9800		
C(40)-H(40C)	0.9800		
C(41)-C(42)	1.526(5)		
C(41)-C(43)	1.531(5)		
C(41)-H(41)	1.0000		
C(42)-H(42A)	0.9800		
C(42)-H(42B)	0.9800		
C(42)-H(42C)	0.9800		
C(43)-H(43A)	0.9800		
C(43)-H(43B)	0.9800		
C(43)-H(43C)	0.9800		
C(44)-C(49)	1.345(13)		
C(44)-C(45)	1.360(12)		
C(44)-H(44)	0.9500		
C(45)-C(46)	1.316(11)		
C(45)-H(45)	0.9500		
C(46)-C(47)	1.388(10)		
C(46)-H(46)	0.9500		
C(47)-C(48)	1.264(12)		
C(47)-H(47)	0.9500		
C(48)-C(49)	1.354(14)		
C(48)-H(48)	0.9500		
C(49)-H(49)	0.9500		
C(50)-C(51)	1.353(7)		
C(50)-C(52)#1	1.365(7)		
C(50)-H(50)	0.9500		
C(51)-C(52)	1.373(8)		

Table S3. Bond angles (deg.) for for [(L-$N_2S^{Ar}_2$)CuCu(IMes)]·C_6H_6. Symmetry transformations used to generate equivalent atoms: #1 -x, -y + 2, -z.

C(31)-Cu(1)-S(1)	162.88(9)	C(2)-C(3)-H(3)	119.6
C(31)-Cu(1)-Cu(2)	142.93(9)	C(3)-C(4)-C(5)	119.3(4)
S(1)-Cu(1)-Cu(2)	53.87(2)	C(3)-C(4)-H(4)	120.3
S(2)-Cu(2)-S(1)	159.75(4)	C(5)-C(4)-H(4)	120.3
S(2)-Cu(2)-N(2)	89.05(7)	C(4)-C(5)-C(6)	121.2(3)
S(1)-Cu(2)-N(2)	106.49(7)	C(4)-C(5)-H(5)	119.4
S(2)-Cu(2)-N(1)	108.09(7)	C(6)-C(5)-H(5)	119.4
S(1)-Cu(2)-N(1)	87.21(6)	C(5)-C(6)-C(1)	119.4(3)
N(2)-Cu(2)-N(1)	82.42(9)	C(5)-C(6)-N(1)	120.7(3)
S(2)-Cu(2)-Cu(1)	110.30(3)	C(1)-C(6)-N(1)	120.0(3)
S(1)-Cu(2)-Cu(1)	52.70(2)	N(1)-C(7)-H(7A)	109.5
N(2)-Cu(2)-Cu(1)	158.76(7)	N(1)-C(7)-H(7B)	109.5
N(1)-Cu(2)-Cu(1)	99.02(6)	H(7A)-C(7)-H(7B)	109.5
C(1)-S(1)-Cu(1)	105.46(10)	N(1)-C(7)-H(7C)	109.5
C(1)-S(1)-Cu(2)	99.96(11)	H(7A)-C(7)-H(7C)	109.5
Cu(1)-S(1)-Cu(2)	73.44(3)	H(7B)-C(7)-H(7C)	109.5
C(16)-S(2)-Cu(2)	98.54(11)	N(1)-C(8)-C(9)	110.1(2)
C(6)-N(1)-C(7)	112.0(2)	N(1)-C(8)-H(8A)	109.6
C(6)-N(1)-C(8)	111.9(2)	C(9)-C(8)-H(8A)	109.6
C(7)-N(1)-C(8)	111.9(3)	N(1)-C(8)-H(8B)	109.6
C(6)-N(1)-Cu(2)	109.60(18)	C(9)-C(8)-H(8B)	109.6
C(7)-N(1)-Cu(2)	109.1(2)	H(8A)-C(8)-H(8B)	108.2
C(8)-N(1)-Cu(2)	101.87(17)	N(2)-C(9)-C(8)	111.1(3)
C(11)-N(2)-C(10)	111.6(2)	N(2)-C(9)-H(9A)	109.4
C(11)-N(2)-C(9)	112.3(2)	C(8)-C(9)-H(9A)	109.4
C(10)-N(2)-C(9)	111.2(3)	N(2)-C(9)-H(9B)	109.4
C(11)-N(2)-Cu(2)	108.69(18)	C(8)-C(9)-H(9B)	109.4
C(10)-N(2)-Cu(2)	110.61(19)	H(9A)-C(9)-H(9B)	108.0
C(9)-N(2)-Cu(2)	102.00(18)	N(2)-C(10)-H(10A)	109.5
C(31)-N(3)-C(29)	112.1(2)	N(2)-C(10)-H(10B)	109.5
C(31)-N(3)-C(17)	123.4(2)	H(10A)-C(10)-H(10B)	109.5
C(29)-N(3)-C(17)	124.5(2)	N(2)-C(10)-H(10C)	109.5
C(31)-N(4)-C(30)	112.1(2)	H(10A)-C(10)-H(10C)	109.5
C(31)-N(4)-C(32)	123.3(2)	H(10B)-C(10)-H(10C)	109.5
C(30)-N(4)-C(32)	124.6(2)	C(12)-C(11)-C(16)	119.9(3)
C(2)-C(1)-C(6)	118.5(3)	C(12)-C(11)-N(2)	120.6(3)
C(2)-C(1)-S(1)	118.4(3)	C(16)-C(11)-N(2)	119.5(3)
C(6)-C(1)-S(1)	123.1(2)	C(13)-C(12)-C(11)	122.2(3)
C(3)-C(2)-C(1)	120.9(4)	C(13)-C(12)-H(12)	118.9
C(3)-C(2)-H(2)	119.6	C(11)-C(12)-H(12)	118.9
C(1)-C(2)-H(2)	119.6	C(14)-C(13)-C(12)	118.5(3)
C(4)-C(3)-C(2)	120.8(4)	C(14)-C(13)-H(13)	120.8
C(4)-C(3)-H(3)	119.6	C(12)-C(13)-H(13)	120.8

Table S3. Bond angles (deg.) for for [(L-$N_2S^{Ar}{}_2$)CuCu(IMes)]·C_6H_6. Symmetry transformations used to generate equivalent atoms: #1 -x, -y + 2, -z.

C(13)-C(14)-C(15)	120.4(3)	H(25A)-C(25)-H(25C)	109.5
C(13)-C(14)-H(14)	119.8	H(25B)-C(25)-H(25C)	109.5
C(15)-C(14)-H(14)	119.8	C(22)-C(26)-C(27)	113.4(4)
C(14)-C(15)-C(16)	122.3(3)	C(22)-C(26)-C(28)	110.7(3)
C(14)-C(15)-H(15)	118.9	C(27)-C(26)-C(28)	110.3(3)
C(16)-C(15)-H(15)	118.9	C(22)-C(26)-H(26)	107.4
C(15)-C(16)-C(11)	116.7(3)	C(27)-C(26)-H(26)	107.4
C(15)-C(16)-S(2)	120.1(3)	C(28)-C(26)-H(26)	107.4
C(11)-C(16)-S(2)	123.1(2)	C(26)-C(27)-H(27A)	109.5
C(18)-C(17)-C(22)	124.0(3)	C(26)-C(27)-H(27B)	109.5
C(18)-C(17)-N(3)	118.4(3)	H(27A)-C(27)-H(27B)	109.5
C(22)-C(17)-N(3)	117.6(3)	C(26)-C(27)-H(27C)	109.5
C(17)-C(18)-C(19)	116.8(3)	H(27A)-C(27)-H(27C)	109.5
C(17)-C(18)-C(23)	122.8(3)	H(27B)-C(27)-H(27C)	109.5
C(19)-C(18)-C(23)	120.4(3)	C(26)-C(28)-H(28A)	109.5
C(20)-C(19)-C(18)	120.9(4)	C(26)-C(28)-H(28B)	109.5
C(20)-C(19)-H(19)	119.6	H(28A)-C(28)-H(28B)	109.5
C(18)-C(19)-H(19)	119.6	C(26)-C(28)-H(28C)	109.5
C(19)-C(20)-C(21)	121.3(3)	H(28A)-C(28)-H(28C)	109.5
C(19)-C(20)-H(20)	119.4	H(28B)-C(28)-H(28C)	109.5
C(21)-C(20)-H(20)	119.4	C(30)-C(29)-N(3)	106.3(3)
C(20)-C(21)-C(22)	120.9(4)	C(30)-C(29)-H(29)	126.9
C(20)-C(21)-H(21)	119.6	N(3)-C(29)-H(29)	126.9
C(22)-C(21)-H(21)	119.6	C(29)-C(30)-N(4)	106.4(3)
C(21)-C(22)-C(17)	116.1(3)	C(29)-C(30)-H(30)	126.8
C(21)-C(22)-C(26)	121.6(3)	N(4)-C(30)-H(30)	126.8
C(17)-C(22)-C(26)	122.2(3)	N(3)-C(31)-N(4)	103.2(2)
C(18)-C(23)-C(24)	113.7(4)	N(3)-C(31)-Cu(1)	131.3(2)
C(18)-C(23)-C(25)	110.7(3)	N(4)-C(31)-Cu(1)	125.1(2)
C(24)-C(23)-C(25)	109.7(4)	C(33)-C(32)-C(37)	123.3(3)
C(18)-C(23)-H(23)	107.5	C(33)-C(32)-N(4)	118.5(3)
C(24)-C(23)-H(23)	107.5	C(37)-C(32)-N(4)	118.2(3)
C(25)-C(23)-H(23)	107.5	C(32)-C(33)-C(34)	117.2(3)
C(23)-C(24)-H(24A)	109.5	C(32)-C(33)-C(38)	122.7(3)
C(23)-C(24)-H(24B)	109.5	C(34)-C(33)-C(38)	120.0(3)
H(24A)-C(24)-H(24B)	109.5	C(35)-C(34)-C(33)	120.8(3)
C(23)-C(24)-H(24C)	109.5	C(35)-C(34)-H(34)	119.6
H(24A)-C(24)-H(24C)	109.5	C(33)-C(34)-H(34)	119.6
H(24B)-C(24)-H(24C)	109.5	C(36)-C(35)-C(34)	120.8(3)
C(23)-C(25)-H(25A)	109.5	C(36)-C(35)-H(35)	119.6
C(23)-C(25)-H(25B)	109.5	C(34)-C(35)-H(35)	119.6
H(25A)-C(25)-H(25B)	109.5	C(35)-C(36)-C(37)	121.0(3)
C(23)-C(25)-H(25C)	109.5	C(35)-C(36)-H(36)	119.5

Table S3. Bond angles (deg.) for for [(L-$N_2S^{Ar}{}_2$)CuCu(IMes)]·C_6H_6. Symmetry transformations used to generate equivalent atoms: #1 -x, -y + 2, -z.

C(37)-C(36)-H(36)	119.5	C(46)-C(45)-C(44)	120.7(6)
C(36)-C(37)-C(32)	116.9(3)	C(46)-C(45)-H(45)	119.6
C(36)-C(37)-C(41)	120.2(3)	C(44)-C(45)-H(45)	119.6
C(32)-C(37)-C(41)	122.8(3)	C(45)-C(46)-C(47)	120.1(6)
C(40)-C(38)-C(33)	110.6(3)	C(45)-C(46)-H(46)	120.0
C(40)-C(38)-C(39)	111.4(3)	C(47)-C(46)-H(46)	120.0
C(33)-C(38)-C(39)	111.4(3)	C(48)-C(47)-C(46)	119.4(7)
C(40)-C(38)-H(38)	107.8	C(48)-C(47)-H(47)	120.3
C(33)-C(38)-H(38)	107.8	C(46)-C(47)-H(47)	120.3
C(39)-C(38)-H(38)	107.8	C(47)-C(48)-C(49)	121.4(8)
C(38)-C(39)-H(39A)	109.5	C(47)-C(48)-H(48)	119.3
C(38)-C(39)-H(39B)	109.5	C(49)-C(48)-H(48)	119.3
H(39A)-C(39)-H(39B)	109.5	C(44)-C(49)-C(48)	121.0(7)
C(38)-C(39)-H(39C)	109.5	C(44)-C(49)-H(49)	119.5
H(39A)-C(39)-H(39C)	109.5	C(48)-C(49)-H(49)	119.5
H(39B)-C(39)-H(39C)	109.5	C(51)-C(50)-C(52)#1	119.1(5)
C(38)-C(40)-H(40A)	109.5	C(51)-C(50)-H(50)	120.5
C(38)-C(40)-H(40B)	109.5	C(52)#1-C(50)-H(50)	120.5
H(40A)-C(40)-H(40B)	109.5	C(50)-C(51)-C(52)	120.8(5)
C(38)-C(40)-H(40C)	109.5	C(50)-C(51)-H(51)	119.6
H(40A)-C(40)-H(40C)	109.5	C(52)-C(51)-H(51)	119.6
H(40B)-C(40)-H(40C)	109.5	C(50)#1-C(52)-C(51)	120.1(5)
C(37)-C(41)-C(42)	111.0(3)	C(50)#1-C(52)-H(52)	119.9
C(37)-C(41)-C(43)	111.2(3)	C(51)-C(52)-H(52)	119.9
C(42)-C(41)-C(43)	110.1(3)		
C(37)-C(41)-H(41)	108.1		
C(42)-C(41)-H(41)	108.1		
C(43)-C(41)-H(41)	108.1		
C(41)-C(42)-H(42A)	109.5		
C(41)-C(42)-H(42B)	109.5		
H(42A)-C(42)-H(42B)	109.5		
C(41)-C(42)-H(42C)	109.5		
H(42A)-C(42)-H(42C)	109.5		
H(42B)-C(42)-H(42C)	109.5		
C(41)-C(43)-H(43A)	109.5		
C(41)-C(43)-H(43B)	109.5		
H(43A)-C(43)-H(43B)	109.5		
C(41)-C(43)-H(43C)	109.5		
H(43A)-C(43)-H(43C)	109.5		
H(43B)-C(43)-H(43C)	109.5		
C(49)-C(44)-C(45)	117.3(8)		
C(49)-C(44)-H(44)	121.3		
C(45)-C(44)-H(44)	121.3		

Table S4. Anisotropic displacement parameters ($Å^2$ x 10^3) for [(L-$N_2S^{Ar}_2$)CuCu(IMes)]·C_6H_6. The anisotropic displacement factor exponent takes the form: $-2\pi^2[(ha^*)^2U^{11} + ... + 2hka^*b^*U^{12}]$.

Atom	U^{11}	U^{22}	U^{33}	U^{23}	U^{13}	U^{12}
Cu(1)	21(1)	22(1)	35(1)	2(1)	4(1)	3(1)
Cu(2)	22(1)	23(1)	29(1)	-2(1)	2(1)	4(1)
S(1)	26(1)	25(1)	30(1)	4(1)	4(1)	3(1)
S(2)	34(1)	27(1)	30(1)	-2(1)	-4(1)	6(1)
N(1)	26(1)	23(1)	27(1)	-1(1)	2(1)	-2(1)
N(2)	25(1)	19(1)	34(1)	-2(1)	1(1)	1(1)
N(3)	20(1)	20(1)	34(1)	1(1)	3(1)	0(1)
N(4)	20(1)	19(1)	27(1)	0(1)	1(1)	2(1)
C(1)	30(2)	22(2)	31(2)	0(1)	-2(1)	5(1)
C(2)	49(2)	46(2)	28(2)	4(2)	2(2)	1(2)
C(3)	61(3)	50(2)	33(2)	-2(2)	-12(2)	-2(2)
C(4)	39(2)	43(2)	52(2)	-3(2)	-16(2)	-4(2)
C(5)	27(2)	29(2)	45(2)	-4(1)	-4(1)	-3(1)
C(6)	28(2)	19(1)	30(2)	-2(1)	-2(1)	1(1)
C(7)	50(2)	33(2)	37(2)	6(2)	4(2)	-13(2)
C(8)	20(1)	38(2)	40(2)	-12(1)	4(1)	-3(1)
C(9)	24(2)	29(2)	40(2)	-6(1)	-3(1)	6(1)
C(10)	41(2)	28(2)	45(2)	5(2)	11(2)	-2(2)
C(11)	18(1)	23(2)	37(2)	-6(1)	4(1)	-3(1)
C(12)	25(2)	26(2)	49(2)	-9(1)	2(1)	-1(1)
C(13)	32(2)	39(2)	48(2)	-15(2)	14(2)	-3(2)
C(14)	40(2)	42(2)	41(2)	-14(2)	16(2)	-12(2)
C(15)	37(2)	34(2)	36(2)	-3(1)	6(1)	-10(2)
C(16)	26(2)	25(2)	32(2)	-4(1)	4(1)	-8(1)
C(17)	22(1)	20(1)	45(2)	6(1)	5(1)	2(1)
C(18)	25(2)	24(2)	51(2)	3(1)	-2(1)	0(1)
C(19)	22(2)	35(2)	74(3)	10(2)	-2(2)	-3(1)
C(20)	23(2)	37(2)	86(3)	20(2)	12(2)	2(2)
C(21)	47(2)	34(2)	60(2)	17(2)	22(2)	3(2)
C(22)	38(2)	26(2)	46(2)	11(1)	10(2)	1(1)
C(23)	38(2)	42(2)	53(2)	-9(2)	-6(2)	-8(2)
C(24)	63(3)	60(3)	91(4)	-27(3)	-3(3)	-10(2)
C(25)	92(4)	62(3)	49(3)	6(2)	-14(2)	-6(3)
C(26)	65(3)	42(2)	37(2)	5(2)	12(2)	-17(2)
C(27)	130(5)	49(3)	54(3)	-5(2)	7(3)	10(3)
C(28)	42(2)	71(3)	40(2)	0(2)	1(2)	-5(2)
C(29)	27(2)	20(1)	35(2)	2(1)	1(1)	3(1)
C(30)	24(1)	25(2)	31(2)	0(1)	2(1)	4(1)
C(31)	19(1)	22(1)	28(1)	2(1)	2(1)	0(1)

Table S4. Anisotropic displacement parameters ($Å^2$ x 10^3) for [(L-$N_2S^{Ar}_2$)CuCu(IMes)]·C_6H_6. The anisotropic displacement factor exponent takes the form: $-2\pi^2[(ha^*)^2U^{11} + ... + 2hka^*b^*U^{12}]$.

Atom	U^{11}	U^{22}	U^{33}	U^{23}	U^{13}	U^{12}
C(32)	18(1)	21(1)	30(2)	0(1)	3(1)	0(1)
C(33)	27(2)	25(2)	34(2)	0(1)	5(1)	-1(1)
C(34)	42(2)	35(2)	35(2)	5(1)	11(2)	-4(2)
C(35)	40(2)	28(2)	44(2)	-2(1)	12(2)	-13(1)
C(36)	36(2)	30(2)	38(2)	-5(1)	6(1)	-9(1)
C(37)	25(2)	25(2)	35(2)	-3(1)	6(1)	-2(1)
C(38)	40(2)	33(2)	30(2)	0(1)	0(1)	-9(2)
C(39)	39(2)	64(3)	38(2)	-8(2)	-6(2)	2(2)
C(40)	49(2)	49(2)	46(2)	-15(2)	2(2)	7(2)
C(41)	39(2)	32(2)	31(2)	-5(1)	4(1)	-6(1)
C(42)	60(3)	75(3)	34(2)	-1(2)	16(2)	16(2)
C(43)	52(2)	48(2)	47(2)	8(2)	-11(2)	-1(2)
C(44)	52(5)	67(6)	53(5)	-9(4)	12(4)	13(4)
C(45)	60(5)	55(5)	29(3)	-12(3)	20(3)	-46(4)
C(46)	75(6)	14(3)	54(5)	3(3)	19(4)	-15(3)
C(47)	59(5)	40(4)	49(4)	-8(3)	26(4)	7(4)
C(48)	108(8)	76(6)	19(3)	-2(4)	23(4)	-54(6)
C(49)	149(10)	12(3)	43(5)	7(3)	-7(5)	-11(5)
C(50)	63(3)	108(5)	36(2)	2(3)	-15(2)	-3(3)
C(51)	62(3)	71(4)	76(3)	29(3)	-18(3)	2(3)
C(52)	70(3)	73(4)	80(4)	-22(3)	-17(3)	1(3)

Table S5. Hydrogen coordinates (x 10^4) and isotropic displacement parameters (Å^2 x 10^3) for [(L-$N_2S^{Ar}_2$)CuCu(IMes)]·C_6H_6.

H atom	x	y	z	U(eq)
H(2)	3085	654	5048	50
H(3)	4713	1117	5431	59
H(4)	6028	1329	4829	55
H(5)	5696	1103	3832	41
H(7A)	3705	1767	3062	60
H(7B)	3742	1259	2476	60
H(7C)	4805	1477	2870	60
H(8A)	5386	36	3177	39
H(8B)	4628	-27	2578	39
H(9A)	4782	-1262	3115	38
H(9B)	4219	-843	3624	38
H(10A)	2078	-1845	2941	57
H(10B)	2645	-1585	3564	57
H(10C)	3215	-2185	3160	57
H(12)	4213	-2152	2351	40
H(13)	4363	-2357	1364	47
H(14)	3524	-1485	681	48
H(15)	2534	-438	981	43
H(19)	3740	3792	3659	53
H(20)	4088	3762	2697	58
H(21)	2873	3278	1970	55
H(23)	1267	3324	4166	54
H(24A)	3147	4202	4493	108
H(24B)	2170	4144	4869	108
H(24C)	2056	4603	4256	108
H(25A)	2314	2161	4308	104
H(25B)	2371	2662	4901	104
H(25C)	3322	2693	4505	104
H(26)	407	2399	2203	57
H(27A)	1735	2639	1303	117
H(27B)	761	2043	1281	117
H(27C)	1799	1864	1709	117
H(28A)	-48	3752	2069	77
H(28B)	-306	3274	1469	77
H(28C)	713	3825	1563	77
H(29)	-408	3805	3140	33
H(30)	-1827	2912	3408	32
H(34)	-1814	338	4752	44
H(35)	-2621	-477	4028	44
H(36)	-2590	-164	3051	41

Table S5. Hydrogen coordinates (x 10^4) and isotropic displacement parameters ($Å^2$ x 10^3) for [(L-$N_2S^{Ar}_2$)CuCu(IMes)]·C_6H_6.

H atom	x	y	z	U(eq)
H(38)	-401	2145	4501	42
H(39A)	-165	781	5248	72
H(39B)	461	1597	5370	72
H(39C)	664	1062	4818	72
H(40A)	-1879	1591	5252	73
H(40B)	-2061	2330	4815	73
H(40C)	-1187	2379	5363	73
H(41)	-1408	1589	2496	41
H(42A)	-289	481	2451	84
H(42B)	-967	609	1834	84
H(42C)	-1275	-79	2266	84
H(43A)	-3080	489	2193	75
H(43B)	-2773	1220	1799	75
H(43C)	-3262	1382	2400	75
H(44)	3959	2115	1387	68
H(45)	3859	735	1382	56
H(46)	4916	11	861	56
H(47)	6082	652	298	57
H(48)	6281	1955	368	80
H(49)	5206	2708	878	83
H(50)	537	10041	997	84
H(51)	759	8900	469	86
H(52)	232	8854	-524	91

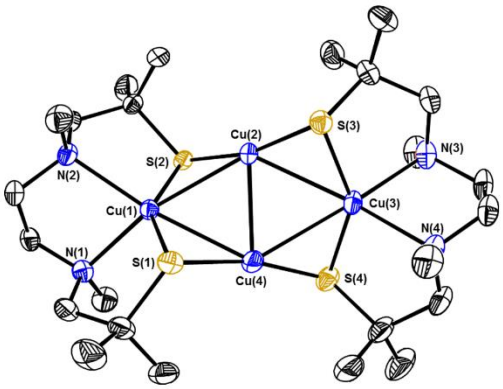

Structure Determination Summary

Crystal Data and Structure Refinement for [(L-N_2S_2-Cu)$_2$(μ-Cu_2)]·½Et_2O, **3**

Identification code	jpd572_0m_a	
Empirical formula	$C_{26}H_{57}Cu_4N_4O_{0.50}S_4$	
Formula weight	816.15	
Temperature	150(2) K	
Wavelength	0.71073 Å	
Crystal system	monoclinic	
Space group	$P2_1/c$	
Unit cell dimensions	a = 13.1795(15) Å	α= 90°
	b = 13.1678(15) Å	β= 103.5610(16)°
	c = 21.683(3) Å	γ = 90°
Volume	3658.0(7) $Å^3$	
Z	4	
Density (calculated)	1.482 g/cm^3	
Absorption coefficient	2.545 mm^{-1}	
F(000)	1700	
Crystal size	0.140 x 0.140 x 0.100 mm^3	
Theta range for data collection	1.932 to 28.771°	
Index ranges	$-17 \le h \le 17$, $-17 \le k \le 17$, $-28 \le l \le 29$	
Reflections collected	63078	
Independent reflections	9431 [R(int) = 0.0590]	
Completeness to θ = 28.770°	99.1 %	
Absorption correction	Semi-empirical from equivalents	
Max. and min. transmission	0.79 and 0.59	
Refinement method	Full-matrix least-squares on F^2	
Data / restraints / parameters	9431 / 182 / 382	
Goodness-of-fit on F^2	1.037	
Final R indices [I>2σ(I)]	R1 = 0.0365, wR2 = 0.0862	
R indices (all data)	R1 = 0.0524, wR2 = 0.0957	
Extinction coefficient	n/a	
Largest diff. peak and hole	0.902 and -0.635 e·$Å^{-3}$	

Table S1. Atomic coordinates (x 10^4) and equivalent isotropic displacement parameters ($Å^2$·x 10^3) for [(L-N_2S_2-Cu)$_2$(μ-Cu_2)]·½Et_2O. U(eq) is defined as one third of the trace of the orthogonalized U^{ij} tensor.

Atom	x	y	z	U(eq)
Cu(1)	3669(1)	-870(1)	7553(1)	22(1)
Cu(2)	2317(1)	401(1)	6934(1)	25(1)
Cu(3)	1423(1)	1646(1)	7569(1)	26(1)
Cu(4)	2782(1)	368(1)	8205(1)	27(1)
S(1)	2805(1)	-1292(1)	8301(1)	27(1)
S(2)	3907(1)	240(1)	6806(1)	24(1)
S(3)	630(1)	579(1)	6789(1)	28(1)
S(4)	2853(1)	2023(1)	8334(1)	31(1)
N(1)	5123(2)	-1421(2)	8187(1)	26(1)
N(2)	3957(2)	-2121(2)	6922(1)	24(1)
N(3)	682(2)	2933(2)	6964(1)	33(1)
N(4)	444(2)	2190(2)	8204(1)	32(1)
C(1)	3924(2)	-1657(2)	8960(1)	32(1)
C(2)	4224(3)	-783(3)	9436(2)	44(1)
C(3)	3564(3)	-2567(3)	9295(2)	49(1)
C(4)	4847(2)	-2033(2)	8693(1)	30(1)
C(5)	5850(2)	-589(2)	8440(2)	37(1)
C(6)	5595(2)	-2073(2)	7773(1)	27(1)
C(7)	4788(2)	-2731(2)	7335(1)	27(1)
C(8)	3036(2)	-2769(2)	6688(2)	38(1)
C(9)	4350(2)	-1672(2)	6398(1)	27(1)
C(10)	3875(2)	-647(2)	6137(1)	29(1)
C(11)	4594(3)	-192(3)	5743(2)	43(1)
C(12)	2781(3)	-735(3)	5716(2)	41(1)
C(13)	189(2)	1515(2)	6141(2)	36(1)
C(14)	998(3)	1635(3)	5740(2)	50(1)
C(15)	-819(3)	1089(3)	5715(2)	59(1)
C(16)	-96(2)	2515(2)	6425(2)	37(1)
C(17)	1440(3)	3595(3)	6760(2)	48(1)
C(18)	150(2)	3528(2)	7377(2)	40(1)
C(19)	-333(2)	2857(2)	7795(2)	38(1)
C(20)	-110(3)	1357(3)	8440(2)	44(1)
C(21)	1117(2)	2769(2)	8721(2)	38(1)
C(22)	2232(2)	2370(3)	8991(2)	41(1)
C(23)	2862(3)	3259(3)	9347(2)	64(1)
C(24)	2287(3)	1483(3)	9454(2)	53(1)
O(1)	-67(7)	9722(8)	-125(6)	120(3)
C(25)	1039(10)	9794(11)	324(7)	113(4)
C(26)	1692(11)	8910(12)	82(7)	125(5)
C(27)	-720(11)	10606(12)	63(8)	120(4)
C(28)	-1836(10)	10503(11)	-436(7)	111(4)

Table S2. Bond lengths (Å) for [(L-N_2S_2-Cu)$_2$(μ-Cu_2)]·½Et_2O. Symmetry transformations used to generate equivalent atoms:

Cu(1)-N(1)	2.203(2)	C(4)-H(4B)	0.9900
Cu(1)-N(2)	2.230(2)	C(5)-H(5A)	0.9800
Cu(1)-S(2)	2.2565(8)	C(5)-H(5B)	0.9800
Cu(1)-S(1)	2.2593(8)	C(5)-H(5C)	0.9800
Cu(1)-Cu(2)	2.5799(5)	C(6)-C(7)	1.520(4)
Cu(1)-Cu(4)	2.6078(5)	C(6)-H(6A)	0.9900
Cu(2)-S(3)	2.1836(8)	C(6)-H(6B)	0.9900
Cu(2)-S(2)	2.1873(8)	C(7)-H(7A)	0.9900
Cu(2)-Cu(3)	2.5940(5)	C(7)-H(7B)	0.9900
Cu(2)-Cu(4)	2.6802(6)	C(8)-H(8A)	0.9800
Cu(3)-N(4)	2.215(2)	C(8)-H(8B)	0.9800
Cu(3)-N(3)	2.223(3)	C(8)-H(8C)	0.9800
Cu(3)-S(4)	2.2553(8)	C(9)-C(10)	1.539(4)
Cu(3)-S(3)	2.2568(8)	C(9)-H(9A)	0.9900
Cu(3)-Cu(4)	2.6042(5)	C(9)-H(9B)	0.9900
Cu(4)-S(1)	2.1958(8)	C(10)-C(12)	1.518(4)
Cu(4)-S(4)	2.1965(9)	C(10)-C(11)	1.538(4)
S(1)-C(1)	1.859(3)	C(11)-H(11A)	0.9800
S(2)-C(10)	1.856(3)	C(11)-H(11B)	0.9800
S(3)-C(13)	1.857(3)	C(11)-H(11C)	0.9800
S(4)-C(22)	1.858(3)	C(12)-H(12A)	0.9800
N(1)-C(5)	1.474(4)	C(12)-H(12B)	0.9800
N(1)-C(4)	1.475(4)	C(12)-H(12C)	0.9800
N(1)-C(6)	1.480(4)	C(13)-C(14)	1.533(5)
N(2)-C(8)	1.473(4)	C(13)-C(15)	1.535(5)
N(2)-C(9)	1.478(4)	C(13)-C(16)	1.538(4)
N(2)-C(7)	1.479(3)	C(14)-H(14A)	0.9800
N(3)-C(16)	1.470(4)	C(14)-H(14B)	0.9800
N(3)-C(17)	1.471(4)	C(14)-H(14C)	0.9800
N(3)-C(18)	1.483(4)	C(15)-H(15A)	0.9800
N(4)-C(21)	1.470(4)	C(15)-H(15B)	0.9800
N(4)-C(20)	1.475(4)	C(15)-H(15C)	0.9800
N(4)-C(19)	1.475(4)	C(16)-H(16A)	0.9900
C(1)-C(2)	1.534(4)	C(16)-H(16B)	0.9900
C(1)-C(3)	1.535(4)	C(17)-H(17A)	0.9800
C(1)-C(4)	1.546(4)	C(17)-H(17B)	0.9800
C(2)-H(2A)	0.9800	C(17)-H(17C)	0.9800
C(2)-H(2B)	0.9800	C(18)-C(19)	1.509(5)
C(2)-H(2C)	0.9800	C(18)-H(18A)	0.9900
C(3)-H(3A)	0.9800	C(18)-H(18B)	0.9900
C(3)-H(3B)	0.9800	C(19)-H(19A)	0.9900
C(3)-H(3C)	0.9800	C(19)-H(19B)	0.9900
C(4)-H(4A)	0.9900	C(20)-H(20A)	0.9800

C(20)-H(20B)	0.9800
C(20)-H(20C)	0.9800
C(21)-C(22)	1.542(4)
C(21)-H(21A)	0.9900
C(21)-H(21B)	0.9900
C(22)-C(24)	1.530(6)
C(22)-C(23)	1.534(5)
C(23)-H(23A)	0.9800
C(23)-H(23B)	0.9800
C(23)-H(23C)	0.9800
C(24)-H(24A)	0.9800
C(24)-H(24B)	0.9800
C(24)-H(24C)	0.9800
O(1)-C(25)	1.555(14)
O(1)-C(27)	1.558(13)
C(25)-C(26)	1.607(14)
C(25)-H(25A)	0.9600
C(25)-H(25B)	0.9600

Table S2. Bond lengths (Å) for [(L-N_2S_2-Cu)$_2$(μ-Cu_2)]·½Et_2O. Symmetry transformations used to generate equivalent atoms:

C(26)-H(26A)	0.9600
C(26)-H(26B)	0.9599
C(26)-H(26C)	0.9601
C(27)-C(28)	1.614(15)
C(27)-H(27A)	0.9601
C(27)-H(27B)	0.9600
C(28)-H(28A)	0.9601
C(28)-H(28B)	0.9599
C(28)-H(28C)	0.9602

Table S3. Bond angles (deg.) for $[(L\text{-}N_2S_2\text{-}Cu)_2(\mu\text{-}Cu_2)]\cdot\frac{1}{2}Et_2O$. Symmetry transformations used to generate equivalent atoms:

N(1)-Cu(1)-N(2)	83.74(8)	S(1)-Cu(4)-Cu(1)	55.31(2)
N(1)-Cu(1)-S(2)	114.50(6)	S(4)-Cu(4)-Cu(1)	132.69(3)
N(2)-Cu(1)-S(2)	88.06(6)	Cu(3)-Cu(4)-Cu(1)	117.161(18)
N(1)-Cu(1)-S(1)	88.95(6)	S(1)-Cu(4)-Cu(2)	96.21(2)
N(2)-Cu(1)-S(1)	116.44(6)	S(4)-Cu(4)-Cu(2)	96.18(3)
S(2)-Cu(1)-S(1)	148.51(3)	Cu(3)-Cu(4)-Cu(2)	58.777(13)
N(1)-Cu(1)-Cu(2)	158.78(6)	Cu(1)-Cu(4)-Cu(2)	58.384(13)
N(2)-Cu(1)-Cu(2)	110.87(6)	C(1)-S(1)-Cu(4)	108.70(10)
S(2)-Cu(1)-Cu(2)	53.27(2)	C(1)-S(1)-Cu(1)	99.95(10)
S(1)-Cu(1)-Cu(2)	97.48(2)	Cu(4)-S(1)-Cu(1)	71.64(2)
N(1)-Cu(1)-Cu(4)	107.62(6)	C(10)-S(2)-Cu(2)	108.24(10)
N(2)-Cu(1)-Cu(4)	163.11(6)	C(10)-S(2)-Cu(1)	99.88(10)
S(2)-Cu(1)-Cu(4)	98.03(2)	Cu(2)-S(2)-Cu(1)	70.96(2)
S(1)-Cu(1)-Cu(4)	53.05(2)	C(13)-S(3)-Cu(2)	107.87(11)
Cu(2)-Cu(1)-Cu(4)	62.212(15)	C(13)-S(3)-Cu(3)	99.29(11)
S(3)-Cu(2)-S(2)	164.90(3)	Cu(2)-S(3)-Cu(3)	71.47(2)
S(3)-Cu(2)-Cu(1)	134.44(3)	C(22)-S(4)-Cu(4)	109.16(12)
S(2)-Cu(2)-Cu(1)	55.77(2)	C(22)-S(4)-Cu(3)	100.17(10)
S(3)-Cu(2)-Cu(3)	55.58(2)	Cu(4)-S(4)-Cu(3)	71.59(2)
S(2)-Cu(2)-Cu(3)	134.11(2)	C(5)-N(1)-C(4)	112.4(2)
Cu(1)-Cu(2)-Cu(3)	118.552(18)	C(5)-N(1)-C(6)	109.2(2)
S(3)-Cu(2)-Cu(4)	97.40(2)	C(4)-N(1)-C(6)	110.3(2)
S(2)-Cu(2)-Cu(4)	97.69(2)	C(5)-N(1)-Cu(1)	112.43(18)
Cu(1)-Cu(2)-Cu(4)	59.404(13)	C(4)-N(1)-Cu(1)	108.31(16)
Cu(3)-Cu(2)-Cu(4)	59.148(14)	C(6)-N(1)-Cu(1)	103.91(16)
N(4)-Cu(3)-N(3)	83.10(10)	C(8)-N(2)-C(9)	112.1(2)
N(4)-Cu(3)-S(4)	88.81(7)	C(8)-N(2)-C(7)	109.1(2)
N(3)-Cu(3)-S(4)	116.19(7)	C(9)-N(2)-C(7)	109.9(2)
N(4)-Cu(3)-S(3)	115.59(7)	C(8)-N(2)-Cu(1)	113.17(18)
N(3)-Cu(3)-S(3)	88.35(7)	C(9)-N(2)-Cu(1)	108.47(16)
S(4)-Cu(3)-S(3)	148.06(3)	C(7)-N(2)-Cu(1)	103.75(16)
N(4)-Cu(3)-Cu(2)	159.62(7)	C(16)-N(3)-C(17)	112.3(3)
N(3)-Cu(3)-Cu(2)	111.13(7)	C(16)-N(3)-C(18)	109.8(2)
S(4)-Cu(3)-Cu(2)	97.17(2)	C(17)-N(3)-C(18)	108.6(3)
S(3)-Cu(3)-Cu(2)	52.95(2)	C(16)-N(3)-Cu(3)	108.12(18)
N(4)-Cu(3)-Cu(4)	107.94(7)	C(17)-N(3)-Cu(3)	113.2(2)
N(3)-Cu(3)-Cu(4)	163.17(6)	C(18)-N(3)-Cu(3)	104.6(2)
S(4)-Cu(3)-Cu(4)	53.16(2)	C(21)-N(4)-C(20)	112.3(3)
S(3)-Cu(3)-Cu(4)	97.75(2)	C(21)-N(4)-C(19)	111.0(2)
Cu(2)-Cu(3)-Cu(4)	62.074(15)	C(20)-N(4)-C(19)	108.7(2)
S(1)-Cu(4)-S(4)	167.60(3)	C(21)-N(4)-Cu(3)	107.90(17)
S(1)-Cu(4)-Cu(3)	133.32(2)	C(20)-N(4)-Cu(3)	112.59(19)
S(4)-Cu(4)-Cu(3)	55.26(2)	C(19)-N(4)-Cu(3)	104.06(19)

C(2)-C(1)-C(3)	109.1(3)
C(2)-C(1)-C(4)	113.0(3)
C(3)-C(1)-C(4)	106.5(3)
C(2)-C(1)-S(1)	110.9(2)
C(3)-C(1)-S(1)	106.8(2)
C(4)-C(1)-S(1)	110.3(2)
C(1)-C(2)-H(2A)	109.5
C(1)-C(2)-H(2B)	109.5
H(2A)-C(2)-H(2B)	109.5
C(1)-C(2)-H(2C)	109.5
H(2A)-C(2)-H(2C)	109.5
H(2B)-C(2)-H(2C)	109.5
C(1)-C(3)-H(3A)	109.5
C(1)-C(3)-H(3B)	109.5
H(3A)-C(3)-H(3B)	109.5
C(1)-C(3)-H(3C)	109.5
H(3A)-C(3)-H(3C)	109.5
H(3B)-C(3)-H(3C)	109.5

Table S3. Bond angles (deg.) for [(L-N_2S_2-Cu)$_2$(μ-Cu_2)]·½Et_2O. Symmetry transformations used to generate equivalent atoms:

N(1)-C(4)-C(1)	117.2(2)	C(10)-C(11)-H(11B)	109.5
N(1)-C(4)-H(4A)	108.0	H(11A)-C(11)-H(11B)	109.5
C(1)-C(4)-H(4A)	108.0	C(10)-C(11)-H(11C)	109.5
N(1)-C(4)-H(4B)	108.0	H(11A)-C(11)-H(11C)	109.5
C(1)-C(4)-H(4B)	108.0	H(11B)-C(11)-H(11C)	109.5
H(4A)-C(4)-H(4B)	107.3	C(10)-C(12)-H(12A)	109.5
N(1)-C(5)-H(5A)	109.5	C(10)-C(12)-H(12B)	109.5
N(1)-C(5)-H(5B)	109.5	H(12A)-C(12)-H(12B)	109.5
H(5A)-C(5)-H(5B)	109.5	C(10)-C(12)-H(12C)	109.5
N(1)-C(5)-H(5C)	109.5	H(12A)-C(12)-H(12C)	109.5
H(5A)-C(5)-H(5C)	109.5	H(12B)-C(12)-H(12C)	109.5
H(5B)-C(5)-H(5C)	109.5	C(14)-C(13)-C(15)	108.3(3)
N(1)-C(6)-C(7)	112.1(2)	C(14)-C(13)-C(16)	114.0(3)
N(1)-C(6)-H(6A)	109.2	C(15)-C(13)-C(16)	107.2(3)
C(7)-C(6)-H(6A)	109.2	C(14)-C(13)-S(3)	111.2(2)
N(1)-C(6)-H(6B)	109.2	C(15)-C(13)-S(3)	106.6(3)
C(7)-C(6)-H(6B)	109.2	C(16)-C(13)-S(3)	109.1(2)
H(6A)-C(6)-H(6B)	107.9	C(13)-C(14)-H(14A)	109.5
N(2)-C(7)-C(6)	112.3(2)	C(13)-C(14)-H(14B)	109.5
N(2)-C(7)-H(7A)	109.1	H(14A)-C(14)-H(14B)	109.5
C(6)-C(7)-H(7A)	109.1	C(13)-C(14)-H(14C)	109.5
N(2)-C(7)-H(7B)	109.1	H(14A)-C(14)-H(14C)	109.5
C(6)-C(7)-H(7B)	109.1	H(14B)-C(14)-H(14C)	109.5
H(7A)-C(7)-H(7B)	107.9	C(13)-C(15)-H(15A)	109.5
N(2)-C(8)-H(8A)	109.5	C(13)-C(15)-H(15B)	109.5
N(2)-C(8)-H(8B)	109.5	H(15A)-C(15)-H(15B)	109.5
H(8A)-C(8)-H(8B)	109.5	C(13)-C(15)-H(15C)	109.5
N(2)-C(8)-H(8C)	109.5	H(15A)-C(15)-H(15C)	109.5
H(8A)-C(8)-H(8C)	109.5	H(15B)-C(15)-H(15C)	109.5
H(8B)-C(8)-H(8C)	109.5	N(3)-C(16)-C(13)	116.7(2)
N(2)-C(9)-C(10)	116.6(2)	N(3)-C(16)-H(16A)	108.1
N(2)-C(9)-H(9A)	108.1	C(13)-C(16)-H(16A)	108.1
C(10)-C(9)-H(9A)	108.1	N(3)-C(16)-H(16B)	108.1
N(2)-C(9)-H(9B)	108.1	C(13)-C(16)-H(16B)	108.1
C(10)-C(9)-H(9B)	108.1	H(16A)-C(16)-H(16B)	107.3
H(9A)-C(9)-H(9B)	107.3	N(3)-C(17)-H(17A)	109.5
C(12)-C(10)-C(11)	108.6(3)	N(3)-C(17)-H(17B)	109.5
C(12)-C(10)-C(9)	113.7(3)	H(17A)-C(17)-H(17B)	109.5
C(11)-C(10)-C(9)	107.2(2)	N(3)-C(17)-H(17C)	109.5
C(12)-C(10)-S(2)	111.2(2)	H(17A)-C(17)-H(17C)	109.5
C(11)-C(10)-S(2)	106.5(2)	H(17B)-C(17)-H(17C)	109.5
C(9)-C(10)-S(2)	109.37(19)	N(3)-C(18)-C(19)	112.2(2)
C(10)-C(11)-H(11A)	109.5	N(3)-C(18)-H(18A)	109.2

C(19)-C(18)-H(18A)	109.2
N(3)-C(18)-H(18B)	109.2
C(19)-C(18)-H(18B)	109.2
H(18A)-C(18)-H(18B)	107.9
N(4)-C(19)-C(18)	112.2(2)
N(4)-C(19)-H(19A)	109.2
C(18)-C(19)-H(19A)	109.2
N(4)-C(19)-H(19B)	109.2
C(18)-C(19)-H(19B)	109.2
H(19A)-C(19)-H(19B)	107.9
N(4)-C(20)-H(20A)	109.5
N(4)-C(20)-H(20B)	109.5
H(20A)-C(20)-H(20B)	109.5
N(4)-C(20)-H(20C)	109.5
H(20A)-C(20)-H(20C)	109.5
H(20B)-C(20)-H(20C)	109.5
N(4)-C(21)-C(22)	117.7(2)
N(4)-C(21)-H(21A)	107.9

Table S3. Bond angles (deg.) for [(L-N_2S_2-Cu)$_2$(μ-Cu_2)]·½Et_2O. Symmetry transformations used to generate equivalent atoms:

C(22)-C(21)-H(21A)	107.9	H(28A)-C(28)-H(28B)	109.5
N(4)-C(21)-H(21B)	107.9	C(27)-C(28)-H(28C)	109.0
C(22)-C(21)-H(21B)	107.9	H(28A)-C(28)-H(28C)	109.5
H(21A)-C(21)-H(21B)	107.2	H(28B)-C(28)-H(28C)	109.5
C(24)-C(22)-C(23)	108.4(3)		
C(24)-C(22)-C(21)	113.8(3)		
C(23)-C(22)-C(21)	106.6(3)		
C(24)-C(22)-S(4)	110.7(2)		
C(23)-C(22)-S(4)	106.9(3)		
C(21)-C(22)-S(4)	110.2(2)		
C(22)-C(23)-H(23A)	109.5		
C(22)-C(23)-H(23B)	109.5		
H(23A)-C(23)-H(23B)	109.5		
C(22)-C(23)-H(23C)	109.5		
H(23A)-C(23)-H(23C)	109.5		
H(23B)-C(23)-H(23C)	109.5		
C(22)-C(24)-H(24A)	109.5		
C(22)-C(24)-H(24B)	109.5		
H(24A)-C(24)-H(24B)	109.5		
C(22)-C(24)-H(24C)	109.5		
H(24A)-C(24)-H(24C)	109.5		
H(24B)-C(24)-H(24C)	109.5		
C(25)-O(1)-C(27)	106.6(8)		
O(1)-C(25)-C(26)	104.3(9)		
O(1)-C(25)-H(25A)	110.8		
C(26)-C(25)-H(25A)	110.0		
O(1)-C(25)-H(25B)	111.6		
C(26)-C(25)-H(25B)	111.1		
H(25A)-C(25)-H(25B)	108.9		
C(25)-C(26)-H(26A)	110.2		
C(25)-C(26)-H(26B)	109.6		
H(26A)-C(26)-H(26B)	109.5		
C(25)-C(26)-H(26C)	108.5		
H(26A)-C(26)-H(26C)	109.5		
H(26B)-C(26)-H(26C)	109.5		
O(1)-C(27)-C(28)	103.5(10)		
O(1)-C(27)-H(27A)	111.5		
C(28)-C(27)-H(27A)	110.2		
O(1)-C(27)-H(27B)	111.6		
C(28)-C(27)-H(27B)	111.1		
H(27A)-C(27)-H(27B)	108.8		
C(27)-C(28)-H(28A)	109.4		
C(27)-C(28)-H(28B)	109.9		

Table S4. Anisotropic displacement parameters ($Å^2 x\ 10^3$) for $[(L\text{-}N_2S_2\text{-}Cu)_2(\mu\text{-}Cu_2)]\cdot\frac{1}{2}Et_2O$. The anisotropic displacement factor exponent takes the form: $-2\pi^2[h^2a^{*2}U^{11} + ... + 2hk\ a^*b^*U^{12}]$.

Atom	U^{11}	U^{22}	U^{33}	U^{23}	U^{13}	U^{12}
Cu(1)	21(1)	20(1)	24(1)	0(1)	6(1)	3(1)
Cu(2)	25(1)	23(1)	28(1)	-2(1)	6(1)	7(1)
Cu(3)	22(1)	22(1)	35(1)	-6(1)	8(1)	3(1)
Cu(4)	26(1)	29(1)	28(1)	-4(1)	8(1)	4(1)
S(1)	23(1)	32(1)	27(1)	1(1)	8(1)	-2(1)
S(2)	27(1)	20(1)	25(1)	-2(1)	8(1)	1(1)
S(3)	25(1)	24(1)	34(1)	-2(1)	5(1)	1(1)
S(4)	23(1)	33(1)	39(1)	-12(1)	10(1)	-3(1)
N(1)	23(1)	22(1)	31(1)	1(1)	6(1)	0(1)
N(2)	25(1)	18(1)	31(1)	-4(1)	7(1)	1(1)
N(3)	27(1)	24(1)	51(2)	2(1)	14(1)	4(1)
N(4)	26(1)	28(1)	46(2)	-9(1)	15(1)	-1(1)
C(1)	32(1)	36(2)	27(1)	5(1)	5(1)	3(1)
C(2)	41(2)	58(2)	29(2)	-8(2)	2(1)	7(2)
C(3)	54(2)	53(2)	43(2)	18(2)	20(2)	5(2)
C(4)	30(1)	31(2)	29(2)	6(1)	4(1)	4(1)
C(5)	29(1)	35(2)	45(2)	-7(1)	5(1)	-5(1)
C(6)	20(1)	24(1)	36(2)	1(1)	7(1)	4(1)
C(7)	26(1)	20(1)	37(2)	1(1)	11(1)	4(1)
C(8)	31(2)	31(2)	51(2)	-8(1)	5(1)	-4(1)
C(9)	28(1)	26(1)	28(1)	-4(1)	9(1)	5(1)
C(10)	37(2)	28(1)	24(1)	-2(1)	10(1)	9(1)
C(11)	61(2)	41(2)	36(2)	10(1)	29(2)	15(2)
C(12)	46(2)	41(2)	30(2)	-10(1)	-3(1)	16(2)
C(13)	31(2)	39(2)	36(2)	3(1)	2(1)	13(1)
C(14)	61(2)	51(2)	40(2)	15(2)	18(2)	28(2)
C(15)	49(2)	57(2)	56(2)	-12(2)	-17(2)	18(2)
C(16)	29(1)	33(2)	47(2)	3(1)	8(1)	11(1)
C(17)	40(2)	38(2)	72(3)	8(2)	23(2)	-4(2)
C(18)	31(2)	23(1)	67(2)	-6(1)	16(2)	5(1)
C(19)	26(1)	30(2)	59(2)	-8(1)	16(1)	3(1)
C(20)	37(2)	39(2)	58(2)	-3(2)	17(2)	-5(1)
C(21)	32(2)	36(2)	52(2)	-19(1)	19(1)	0(1)
C(22)	34(2)	47(2)	43(2)	-23(2)	9(1)	-1(1)
C(23)	43(2)	76(3)	71(3)	-49(2)	10(2)	-5(2)
C(24)	50(2)	73(3)	39(2)	-10(2)	16(2)	15(2)
O(1)	127(5)	116(7)	116(6)	-12(5)	24(5)	3(5)
C(25)	112(6)	116(7)	113(7)	10(6)	29(6)	-10(5)

C(26)	121(7)	128(8)	122(8)	-4(6)	18(6)	3(6)
C(27)	117(6)	120(8)	128(8)	-3(6)	38(6)	9(6)
C(28)	117(6)	109(7)	112(7)	11(6)	38(5)	8(6)

Table S5. Hydrogen coordinates (x 10^4) and isotropic displacement parameters ($Å^2$x 10^3) for $[(L\text{-}N_2S_2\text{-}Cu)_2(\mu\text{-}Cu_2)]\cdot½Et_2O$.

H atom	x	y	z	U(eq)
H(2A)	4841	-976	9764	66
H(2B)	3643	-640	9633	66
H(2C)	4381	-175	9214	66
H(3A)	4144	-2806	9635	73
H(3B)	3337	-3116	8989	73
H(3C)	2981	-2362	9477	73
H(4A)	5471	-2078	9050	36
H(4B)	4684	-2730	8529	36
H(5A)	5522	-130	8692	55
H(5B)	6020	-213	8088	55
H(5C)	6490	-872	8710	55
H(6A)	6130	-2515	8040	32
H(6B)	5948	-1638	7514	32
H(7A)	5139	-3149	7068	33
H(7B)	4469	-3197	7594	33
H(8A)	2484	-2370	6412	58
H(8B)	2785	-3028	7049	58
H(8C)	3227	-3340	6449	58
H(9A)	4227	-2165	6044	32
H(9B)	5114	-1583	6546	32
H(11A)	4608	-642	5385	65
H(11B)	5301	-122	6011	65
H(11C)	4331	477	5583	65
H(12A)	2776	-1247	5387	62
H(12B)	2567	-78	5516	62
H(12C)	2296	-938	5974	62
H(14A)	790	2194	5438	75
H(14B)	1038	1004	5507	75
H(14C)	1682	1784	6018	75
H(15A)	-1107	1582	5381	88
H(15B)	-1328	961	5970	88
H(15C)	-665	452	5521	88
H(16A)	-239	3032	6084	44
H(16B)	-753	2406	6563	44
H(17A)	1806	3208	6492	72

H(17B)	1946	3851	7133	72
H(17C)	1073	4169	6517	72
H(18A)	-401	3951	7109	47
H(18B)	662	3988	7647	47
H(19A)	-667	3287	8066	45
H(19B)	-883	2433	7526	45
H(20A)	399	890	8695	66
H(20B)	-544	990	8080	66
H(20C)	-554	1639	8703	66
H(21A)	760	2807	9075	46
H(21B)	1171	3471	8569	46
H(23A)	2552	3473	9695	96
H(23B)	2851	3828	9055	96
H(23C)	3584	3043	9520	96
H(24A)	3018	1336	9656	80

Table S5. Hydrogen coordinates (x 10^4) and isotropic displacement parameters ($Å^2$x 10^3) for $[(L\text{-}N_2S_2\text{-}Cu)_2(\mu\text{-}Cu_2)]\cdot\frac{1}{2}Et_2O$.

H atom	x	y	z	U(eq)
H(24B)	1964	881	9223	80
H(24C)	1913	1663	9780	80
H(25A)	1011	9670	756	136
H(25B)	1351	10446	298	136
H(26A)	2394	8893	337	188
H(26B)	1363	8266	108	188
H(26C)	1704	9046	-351	188
H(27A)	-413	11255	18	144
H(27B)	-791	10537	492	144
H(28A)	-2296	11025	-354	166
H(28B)	-1749	10570	-861	166
H(28C)	-2128	9849	-385	166

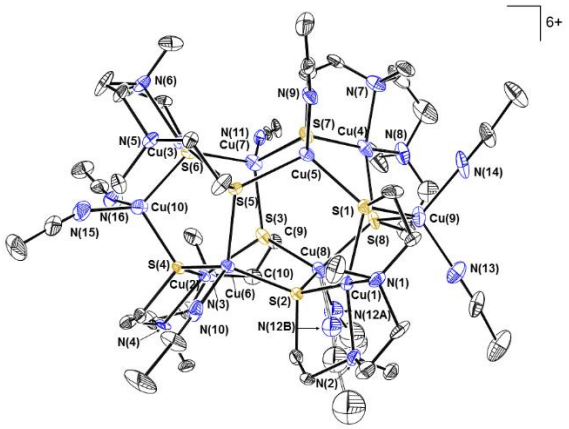

Structure Determination Summary

Crystal Data and Structure Refinement for jpd501_a, **4**

Identification code	$[Cu_{10}(S(CH_2)_2N(Me)CH_2-)_2(MeCN)_8][BF_4]_6\cdot(MeCN)_{2.25}$	
Empirical formula	$C_{52.50}H_{102.75}B_6Cu_{10}F_{24}N_{18.25}S_8$	
Formula weight	2402.51	
Temperature	150(2) K	
Wavelength	0.71073 Å	
Crystal system	monoclinic	
Space group	*Pn*	
Unit cell dimensions	a = 14.014(3) Å	α= 90°
	b = 31.074(6) Å	β= 90.39(3)°
	c = 21.818(4) Å	γ = 90°
Volume	9501(3) $Å^3$	
Z	4	
Density (calculated)	1.680 g/cm^3	
Absorption coefficient	2.457 mm^{-1}	
F(000)	4838	
Crystal size	0.422 x 0.365 x 0.342 mm^3	
θ range for data collection	1.842 to 26.373°	
Index ranges	$-17 \le h \le 17$, $-38 \le k \le 38$, $-27 \le l \le 27$	
Reflections collected	142127	
Independent reflections	38673 [R(int) = 0.0444]	
Completeness to θ = 25.242°	99.9 %	
Absorption correction	Semi-empirical from equivalents	
Max. and min. transmission	0.487 and 0.362	
Refinement method	Full-matrix least-squares on F^2	
Data / restraints / parameters	38673 / 44 / 2063	
Goodness-of-fit on F^2	1.137	
Final R indices [I > 2σ(I)]	R1 = 0.0750, wR2 = 0.1672	
R indices (all data)	R1 = 0.0799, wR2 = 0.1692	
Absolute structure parameter	0.836(18)	
Extinction coefficient	n/a	
Largest diff. peak and hole	1.337 and -1.442 $e\cdot Å^{-3}$	

Table S1. Atomic coordinates (x 10^4) and equivalent isotropic displacement parameters (Å^2 x 10^3) for $[Cu_{10}(S(CH_2)_2N(Me)CH_2-)_2(MeCN)_8][BF_4]_6\cdot(MeCN)_{2.25}$. U(eq) is defined as one third of the trace of the orthogonalized U^{ij} tensor.

Atom	x	y	z	U(eq)
Cu(1)	9980(5)	-3140(1)	-1518(3)	20(1)
Cu(2)	10770(5)	-4807(1)	-3279(3)	19(1)
Cu(3)	7289(5)	-4745(1)	-2174(3)	17(1)
Cu(4)	8130(5)	-3135(1)	-3924(3)	30(1)
Cu(5)	7623(5)	-3548(1)	-2299(3)	23(1)
Cu(6)	9759(5)	-4298(1)	-1767(3)	20(1)
Cu(7)	8354(5)	-4272(1)	-3725(3)	31(1)
Cu(8)	10547(5)	-3580(1)	-3132(3)	29(1)
Cu(9)	9174(5)	-2538(1)	-2769(3)	34(1)
Cu(10)	8936(5)	-5329(1)	-2769(3)	34(1)
Cu(11)	2328(5)	-267(1)	1460(3)	18(1)
Cu(12)	5814(5)	-220(1)	2560(3)	19(1)
Cu(13)	5007(5)	-1864(1)	743(3)	18(1)
Cu(14)	3263(5)	-1925(1)	3144(3)	30(1)
Cu(15)	4776(5)	-710(1)	1028(3)	21(1)
Cu(16)	2663(5)	-1470(1)	1543(3)	23(1)
Cu(17)	3449(5)	-784(1)	3001(3)	31(1)
Cu(18)	5641(5)	-1447(1)	2370(3)	28(1)
Cu(19)	3970(5)	288(1)	2090(3)	34(1)
Cu(20)	4255(5)	-2484(1)	1961(3)	34(1)
S(1)	8611(5)	-2989(1)	-2013(3)	23(1)
S(2)	10521(5)	-3684(1)	-2095(3)	23(1)
S(3)	10002(6)	-4207(1)	-3610(3)	25(1)
S(4)	10104(5)	-4894(1)	-2364(3)	18(1)
S(5)	8145(5)	-4182(1)	-1832(3)	18(1)
S(6)	7856(5)	-4837(1)	-3123(3)	23(1)
S(7)	7597(6)	-3666(1)	-3328(3)	24(1)
S(8)	9583(6)	-3035(1)	-3501(3)	26(1)
S(9)	3174(5)	-832(1)	1098(3)	16(1)
S(10)	2901(5)	-214(1)	2423(3)	24(1)
S(11)	5089(5)	-835(1)	2873(3)	23(1)
S(12)	5131(5)	-123(1)	1646(3)	18(1)
S(13)	5572(5)	-1327(1)	1334(3)	21(1)
S(14)	3640(5)	-2017(1)	1231(3)	20(1)
S(15)	2698(5)	-1380(1)	2575(3)	25(1)
S(16)	4699(6)	-2006(1)	2716(3)	30(1)
N(1)	9491(10)	-2797(4)	-782(7)	26(3)
N(2)	11316(11)	-3066(4)	-1146(7)	26(3)
N(3)	11208(10)	-4905(4)	-4154(6)	24(3)

Table S1. Atomic coordinates (x 10^4) and equivalent isotropic displacement parameters ($Å^2$ x 10^3) for $[Cu_{10}(S(CH_2)_2N(Me)CH_2-)_2(MeCN)_8][BF_4]_6\cdot(MeCN)_{2.25}$. U(eq) is defined as one third of the trace of the orthogonalized U^{ij} tensor.

Atom	x	y	z	U(eq)
N(4)	11793(10)	-5233(4)	-3008(7)	23(3)
N(5)	6919(10)	-4853(4)	-1293(6)	23(3)
N(6)	6136(11)	-5125(5)	-2423(7)	30(3)
N(7)	6778(12)	-3027(5)	-4205(7)	36(3)
N(8)	8546(14)	-2810(5)	-4678(7)	42(4)
N(9)	6316(11)	-3449(4)	-1961(7)	30(3)
N(10)	10263(12)	-4486(4)	-932(7)	32(3)
N(11)	8119(11)	-4327(4)	-4627(7)	30(3)
N(13)	10331(13)	-2183(5)	-2644(8)	46(4)
N(14)	8104(15)	-2115(5)	-2874(8)	50(4)
N(15)	8716(13)	-5767(6)	-2087(9)	48(4)
N(16)	9075(13)	-5755(5)	-3463(8)	44(4)
N(17)	1952(10)	-129(4)	583(6)	21(3)
N(18)	1225(10)	107(4)	1717(7)	25(3)
N(19)	6244(10)	-130(5)	3426(7)	30(3)
N(20)	6837(10)	218(4)	2312(6)	25(3)
N(21)	6338(11)	-1914(4)	370(7)	31(3)
N(22)	4526(10)	-2187(4)	-5(6)	23(3)
N(23)	1927(12)	-2055(4)	3447(7)	34(3)
N(24)	3727(15)	-2268(6)	3873(8)	55(5)
N(25)	5246(12)	-512(5)	215(7)	41(4)
N(26)	1366(10)	-1555(4)	1193(7)	29(3)
N(27)	3263(13)	-745(6)	3903(7)	44(4)
N(28)	7048(14)	-1550(6)	2552(10)	61(5)
N(29)	3690(13)	750(5)	1473(10)	56(5)
N(30)	4108(12)	707(6)	2820(9)	49(4)
N(31)	5447(12)	-2830(4)	1837(7)	34(3)
N(32)	3211(14)	-2913(5)	2086(8)	43(4)
N(33)	9043(17)	988(6)	1809(10)	63(5)
N(34)	-888(15)	5978(6)	2424(9)	55(5)
N(35)	-900(30)	7751(14)	3699(19)	65(11)
N(36)	6186(15)	-1137(8)	-1346(10)	72(6)
N(37)	-3814(17)	3873(8)	5598(10)	75(6)
C(1)	8039(12)	-2684(6)	-1402(8)	33(4)
C(2)	8796(11)	-2487(5)	-996(8)	24(3)
C(3)	9075(17)	-3112(6)	-355(8)	44(5)
C(4)	10340(12)	-2588(6)	-497(9)	34(4)
C(5)	11184(14)	-2905(6)	-518(9)	38(4)
C(6)	11859(13)	-2760(5)	-1536(10)	38(4)

Table S1. Atomic coordinates (x 10^4) and equivalent isotropic displacement parameters (Å^2 x 10^3) for $[Cu_{10}(S(CH_2)_2N(Me)CH_2-)_2(MeCN)_8][BF_4]_6\cdot(MeCN)_{2.25}$. U(eq) is defined as one third of the trace of the orthogonalized U^{ij} tensor.

Atom	x	y	z	U(eq)
C(7)	11798(12)	-3506(5)	-1146(9)	34(4)
C(8)	11747(12)	-3684(5)	-1788(9)	32(4)
C(9)	10498(13)	-4198(6)	-4376(8)	32(4)
C(10)	11399(13)	-4467(6)	-4417(8)	34(4)
C(11)	10449(14)	-5117(6)	-4490(9)	41(5)
C(12)	12101(14)	-5164(6)	-4116(9)	38(4)
C(13)	12027(14)	-5479(5)	-3581(8)	33(4)
C(14)	12641(12)	-4973(6)	-2798(9)	33(4)
C(15)	11459(13)	-5503(5)	-2530(8)	32(4)
C(16)	11001(11)	-5256(4)	-2015(7)	22(3)
C(17)	7720(13)	-4178(6)	-1039(7)	32(4)
C(18)	6817(11)	-4430(5)	-996(7)	21(3)
C(19)	7671(13)	-5123(5)	-991(8)	31(4)
C(20)	5984(12)	-5098(5)	-1296(8)	28(3)
C(21)	5946(16)	-5371(6)	-1860(8)	47(5)
C(22)	5358(14)	-4837(7)	-2565(10)	48(5)
C(23)	6399(13)	-5391(6)	-2937(8)	33(4)
C(24)	6850(12)	-5135(6)	-3453(8)	31(4)
C(25)	6329(14)	-3651(6)	-3580(9)	40(4)
C(26)	6256(13)	-3428(6)	-4194(9)	35(4)
C(27)	6347(14)	-2699(6)	-3796(10)	46(5)
C(28)	6817(19)	-2833(8)	-4825(10)	58(6)
C(29)	7670(20)	-2572(10)	-4893(11)	72(8)
C(30)	8830(20)	-3134(9)	-5173(10)	85(11)
C(31)	9379(19)	-2540(8)	-4529(12)	63(6)
C(32)	10146(16)	-2756(7)	-4155(10)	52(6)
C(33)	5635(12)	-3424(5)	-1692(9)	30(4)
C(34)	4755(14)	-3394(6)	-1344(12)	55(6)
C(35)	10688(14)	-4646(7)	-577(7)	40(5)
C(36)	11258(18)	-4892(10)	-137(10)	77(9)
C(37)	8203(12)	-4312(4)	-5143(8)	26(3)
C(38)	8313(14)	-4298(5)	-5800(8)	33(4)
N(12A)	11761(18)	-3500(14)	-3597(11)	50(6)
C(39A)	12510(30)	-3350(20)	-3889(11)	89(13)
C(40A)	13070(16)	-3420(30)	-4491(9)	150(20)
N(12B)	11960(20)	-3495(11)	-3289(16)	50(6)
C(39B)	12720(40)	-3468(18)	-3250(30)	89(13)
C(40B)	13840(60)	-3340(30)	-3210(40)	150(20)
C(41)	11033(17)	-1993(6)	-2657(10)	48(5)

Table S1. Atomic coordinates (x 10^4) and equivalent isotropic displacement parameters ($Å^2$ x 10^3) for $[Cu_{10}(S(CH_2)_2N(Me)CH_2-)_2(MeCN)_8][BF_4]_6\cdot(MeCN)_{2.25}$. U(eq) is defined as one third of the trace of the orthogonalized U^{ij} tensor.

Atom	x	y	z	U(eq)
C(42)	11950(20)	-1781(8)	-2638(12)	74(8)
C(43)	7474(17)	-1876(6)	-2853(9)	45(5)
C(44)	6638(18)	-1610(8)	-2827(11)	63(7)
C(45)	8834(14)	-5962(6)	-1651(12)	48(5)
C(46)	9004(18)	-6186(9)	-1057(13)	81(10)
C(47)	8935(13)	-5982(6)	-3852(9)	36(4)
C(48)	8727(15)	-6274(7)	-4360(10)	52(5)
C(49)	2701(11)	-823(5)	304(7)	18(3)
C(50)	1817(11)	-551(4)	266(7)	18(3)
C(51)	2729(14)	136(5)	295(8)	35(4)
C(52)	1065(14)	123(6)	598(8)	38(4)
C(53)	1026(13)	381(6)	1182(9)	36(4)
C(54)	398(14)	-175(8)	1837(10)	50(5)
C(55)	1449(13)	367(5)	2270(8)	33(4)
C(56)	1910(12)	87(6)	2754(7)	34(4)
C(57)	5619(15)	-860(5)	3639(8)	35(4)
C(58)	6485(14)	-558(6)	3685(8)	37(4)
C(59)	5494(13)	66(5)	3796(7)	30(4)
C(60)	7119(12)	142(6)	3410(9)	35(4)
C(61)	7011(14)	470(6)	2883(8)	36(4)
C(62)	7669(14)	1(7)	2108(9)	43(5)
C(63)	6473(13)	507(5)	1827(8)	26(3)
C(64)	5999(12)	248(5)	1316(7)	27(3)
C(65)	6804(12)	-1314(6)	1000(9)	33(4)
C(66)	6802(13)	-1503(7)	380(9)	41(4)
C(67)	6868(14)	-2240(6)	728(9)	36(4)
C(68)	6182(12)	-2079(6)	-273(8)	33(4)
C(69)	5349(14)	-2390(6)	-290(9)	38(4)
C(70)	4059(13)	-1873(6)	-421(8)	34(4)
C(71)	3797(12)	-2526(5)	197(8)	28(3)
C(72)	3079(11)	-2334(5)	623(8)	23(3)
C(73)	1455(13)	-1392(7)	2850(9)	40(4)
C(74)	1410(15)	-1630(7)	3452(9)	50(6)
C(75)	1411(15)	-2352(6)	3029(9)	41(4)
C(76)	2007(17)	-2241(8)	4061(9)	58(6)
C(77)	2877(18)	-2532(8)	4061(11)	63(7)
C(78)	4018(19)	-1965(8)	4365(10)	68(8)
C(79)	4557(17)	-2547(8)	3692(11)	57(6)
C(80)	5279(15)	-2293(7)	3355(9)	47(5)

Table S1. Atomic coordinates (x 10^4) and equivalent isotropic displacement parameters ($Å^2$ x 10^3) for $[Cu_{10}(S(CH_2)_2N(Me)CH_2-)_2(MeCN)_8][BF_4]_6\cdot(MeCN)_{2.25}$. U(eq) is defined as one third of the trace of the orthogonalized U^{ij} tensor.

Atom	x	y	z	U(eq)
C(81)	5722(14)	-344(5)	-147(8)	33(4)
C(82)	6277(16)	-120(9)	-592(11)	66(7)
C(83)	693(13)	-1586(5)	901(9)	34(4)
C(84)	-185(13)	-1594(6)	540(11)	46(5)
C(85)	3293(13)	-730(5)	4424(8)	31(4)
C(86)	3367(16)	-733(6)	5086(8)	44(5)
C(87)	7838(19)	-1580(8)	2511(17)	84(10)
C(88)	8856(19)	-1581(12)	2409(18)	108(13)
C(89A)	3860(30)	937(10)	938(10)	36(6)
C(90A)	4030(30)	1205(10)	350(10)	41(6)
C(89B)	3720(20)	1039(7)	1285(12)	36(6)
C(90B)	3930(20)	1453(7)	914(12)	41(6)
C(91)	3989(14)	938(7)	3193(10)	48(5)
C(92)	3713(16)	1254(7)	3657(11)	57(6)
C(93)	6133(16)	-3007(6)	1841(8)	41(4)
C(94)	7071(17)	-3227(8)	1862(10)	58(6)
C(95)	2555(16)	-3123(6)	2094(8)	40(4)
C(96)	1719(18)	-3410(7)	2084(10)	57(6)
C(97)	9091(16)	1304(7)	1580(11)	52(5)
C(98)	9160(20)	1705(9)	1271(11)	72(7)
C(99)	-834(15)	6320(7)	2661(10)	51(6)
C(100)	-756(16)	6715(8)	2971(10)	55(5)
C(101)	-1090(30)	8071(13)	3903(19)	45(9)
C(102)	-1390(40)	8501(15)	4110(20)	62(12)
C(103)	5406(16)	-1057(7)	-1443(9)	48(5)
C(104)	4399(16)	-977(8)	-1572(13)	68(7)
C(105)	-4632(16)	3936(7)	5697(10)	46(5)
C(106)	-5609(16)	4015(9)	5814(12)	65(7)
F(1)	1669(10)	-1712(4)	-444(7)	59(4)
F(2)	924(10)	-1691(4)	-1357(6)	52(3)
F(3)	879(13)	-1131(5)	-726(9)	96(6)
F(4)	2238(11)	-1276(6)	-1170(7)	92(6)
F(5)	8237(11)	4126(4)	4299(7)	63(4)
F(6)	8970(11)	4757(4)	4393(8)	74(4)
F(7)	9090(13)	4367(6)	3544(9)	93(5)
F(8)	7717(10)	4689(4)	3774(7)	68(4)
F(9)	5934(10)	6706(4)	566(6)	53(3)
F(10)	6689(10)	6718(4)	-324(7)	63(4)
F(11)	5800(12)	6164(5)	-84(9)	97(6)

Table S1. Atomic coordinates (x 10^4) and equivalent isotropic displacement parameters ($Å^2$ x 10^3) for $[Cu_{10}(S(CH_2)_2N(Me)CH_2-)_2(MeCN)_8][BF_4]_6\cdot(MeCN)_{2.25}$. U(eq) is defined as one third of the trace of the orthogonalized U^{ij} tensor.

Atom	x	y	z	U(eq)
F(12)	7202(12)	6264(5)	392(7)	80(5)
F(13)	8221(12)	9154(5)	-28(7)	75(4)
F(14)	9035(12)	9778(4)	-109(10)	94(6)
F(15)	7771(11)	9719(5)	528(7)	71(4)
F(16)	9104(14)	9359(6)	744(10)	103(6)
F(17)	9599(12)	-68(5)	3259(8)	76(4)
F(18)	10336(11)	-656(5)	3578(8)	80(4)
F(19)	9034(13)	-411(7)	4067(7)	98(6)
F(20)	8826(12)	-693(6)	3113(9)	91(5)
F(21)	5418(12)	3794(5)	-886(7)	80(5)
F(22)	6273(19)	3292(6)	-463(11)	157(12)
F(23)	6607(14)	3468(6)	-1398(7)	99(6)
F(24)	6876(15)	3921(6)	-674(11)	115(7)
F(25)	5440(11)	-1218(5)	5159(7)	72(4)
F(26)	6959(13)	-1094(5)	5056(10)	99(6)
F(27)	6362(13)	-1711(5)	4706(9)	90(6)
F(28)	6509(14)	-1604(7)	5719(8)	103(6)
F(29)	4113(18)	2489(8)	6016(12)	136(8)
F(30)	5045(15)	2508(7)	6870(10)	107(6)
F(31)	4506(14)	3098(6)	6483(9)	100(5)
F(32)	5560(20)	2664(9)	5994(13)	162(10)
F(33)	10271(14)	4371(6)	662(9)	96(5)
F(34)	9556(15)	4946(6)	961(9)	105(6)
F(36)	8968(14)	4605(6)	177(9)	98(5)
F(35)	8814(15)	4344(6)	1125(9)	102(6)
F(37)	-2768(12)	6333(5)	3249(7)	72(4)
F(38)	-3628(14)	6333(6)	4098(9)	103(6)
F(39)	-3070(15)	6953(7)	3694(10)	109(6)
F(40)	-4235(14)	6579(6)	3207(9)	99(5)
F(41)	4437(16)	8117(7)	7753(10)	115(6)
F(42)	4098(16)	7535(7)	8245(11)	119(7)
F(43)	4950(19)	7506(9)	7352(13)	144(8)
F(44)	5570(20)	7676(10)	8184(15)	180(11)
B(1)	1449(18)	-1446(6)	-936(10)	39(5)
B(2)	8508(15)	4502(8)	4006(11)	39(5)
B(3)	6395(15)	6453(6)	137(11)	35(4)
B(4)	8520(15)	9495(7)	279(13)	45(6)
B(5)	9448(17)	-470(8)	3511(13)	48(6)
B(6)	6291(15)	3597(7)	-848(10)	36(4)

Table S1. Atomic coordinates (x 10^4) and equivalent isotropic displacement parameters ($Å^2$ x 10^3) for $[Cu_{10}(S(CH_2)_2N(Me)CH_2-)_2(MeCN)_8][BF_4]_6 \cdot (MeCN)_{2.25}$. U(eq) is defined as one third of the trace of the orthogonalized U^{ij} tensor.

Atom	x	y	z	U(eq)
B(7)	6258(17)	-1434(7)	5156(10)	39(5)
B(8)	4730(30)	2668(9)	6367(16)	73(9)
B(9)	9370(20)	4513(10)	694(12)	60(7)
B(10)	-3520(20)	6544(12)	3579(14)	75(10)
B(11)	4620(30)	7666(13)	7822(19)	84(10)
B(12A)	1463(8)	-1652(4)	5534(5)	81(11)
F(45A)	2291(9)	-1608(8)	5210(8)	74(5)
F(47A)	725(10)	-1740(8)	5138(8)	87(7)
F(46A)	1560(19)	-1984(6)	5944(8)	166(15)
F(48A)	1278(16)	-1279(5)	5845(9)	106(8)
B(12B)	1597(8)	-1602(4)	5657(5)	81(11)
F(45B)	2062(15)	-1981(5)	5540(11)	74(5)
F(46B)	770(11)	-1686(9)	5966(10)	166(15)
F(47B)	1387(17)	-1399(7)	5116(6)	87(7)
F(48B)	2171(14)	-1342(6)	6009(9)	106(8)

Table S2. Bond lengths (Å) for $[Cu_{10}(S(CH_2)_2N(Me)CH_2-)_2(MeCN)_8][BF_4]_6\cdot(MeCN)_{2.25}$. Symmetry transformations used to generate equivalent atoms:

Cu(1)-N(2)	2.049(13)	Cu(11)-S(10)	2.250(4)
Cu(1)-N(1)	2.050(13)	Cu(11)-S(9)	2.264(4)
Cu(1)-S(2)	2.243(4)	Cu(12)-N(19)	2.000(14)
Cu(1)-S(1)	2.245(4)	Cu(12)-N(20)	2.053(13)
Cu(2)-N(3)	2.033(12)	Cu(12)-S(12)	2.226(4)
Cu(2)-N(4)	2.036(11)	Cu(12)-S(11)	2.271(4)
Cu(2)-S(4)	2.226(4)	Cu(13)-N(22)	2.026(12)
Cu(2)-S(3)	2.269(4)	Cu(13)-N(21)	2.046(13)
Cu(3)-N(5)	2.022(13)	Cu(13)-S(13)	2.249(4)
Cu(3)-N(6)	2.070(13)	Cu(13)-S(14)	2.250(4)
Cu(3)-S(6)	2.242(4)	Cu(14)-N(24)	2.016(16)
Cu(3)-S(5)	2.245(4)	Cu(14)-N(23)	2.030(15)
Cu(4)-N(7)	2.016(14)	Cu(14)-S(16)	2.239(5)
Cu(4)-N(8)	2.019(15)	Cu(14)-S(15)	2.243(4)
Cu(4)-S(7)	2.233(4)	Cu(15)-N(25)	1.995(14)
Cu(4)-S(8)	2.252(5)	Cu(15)-S(9)	2.283(4)
Cu(5)-N(9)	2.003(14)	Cu(15)-S(13)	2.314(4)
Cu(5)-S(7)	2.274(4)	Cu(15)-S(12)	2.320(4)
Cu(5)-S(1)	2.304(4)	Cu(16)-N(26)	1.985(13)
Cu(5)-S(5)	2.335(4)	Cu(16)-S(15)	2.268(4)
Cu(6)-N(10)	2.036(14)	Cu(16)-S(14)	2.289(4)
Cu(6)-S(5)	2.293(4)	Cu(16)-S(9)	2.323(4)
Cu(6)-S(2)	2.302(4)	Cu(17)-N(27)	1.992(15)
Cu(6)-S(4)	2.318(4)	Cu(17)-S(10)	2.302(5)
Cu(7)-N(11)	2.000(15)	Cu(17)-S(15)	2.321(4)
Cu(7)-S(6)	2.304(5)	Cu(17)-S(11)	2.321(4)
Cu(7)-S(3)	2.330(5)	Cu(18)-N(28)	2.033(17)
Cu(7)-S(7)	2.331(4)	Cu(18)-S(13)	2.293(4)
Cu(8)-N(12A)	2.00(2)	Cu(18)-S(16)	2.310(4)
Cu(8)-N(12B)	2.02(3)	Cu(18)-S(11)	2.332(4)
Cu(8)-S(2)	2.287(4)	Cu(19)-N(29)	2.007(18)
Cu(8)-S(8)	2.307(4)	Cu(19)-N(30)	2.066(15)
Cu(8)-S(3)	2.336(5)	Cu(19)-S(10)	2.285(4)
Cu(9)-N(13)	1.981(16)	Cu(19)-S(12)	2.288(4)
Cu(9)-N(14)	2.006(16)	Cu(20)-N(32)	1.999(17)
Cu(9)-S(8)	2.296(4)	Cu(20)-N(31)	2.008(15)
Cu(9)-S(1)	2.306(4)	Cu(20)-S(16)	2.299(5)
Cu(10)-N(16)	2.019(15)	Cu(20)-S(14)	2.315(4)
Cu(10)-N(15)	2.043(18)	S(1)-C(1)	1.825(16)
Cu(10)-S(6)	2.284(4)	S(2)-C(8)	1.839(16)
Cu(10)-S(4)	2.296(4)	S(3)-C(9)	1.815(17)
Cu(11)-N(18)	2.015(12)	S(4)-C(16)	1.847(15)
Cu(11)-N(17)	2.027(12)	S(5)-C(17)	1.834(15)

Table S2. Bond lengths (Å) for $[Cu_{10}(S(CH_2)_2N(Me)CH_2-)_2(MeCN)_8][BF_4]_6\cdot(MeCN)_{2.25}$. Symmetry transformations used to generate equivalent atoms:

S(6)-C(24)	1.831(15)	N(17)-C(50)	1.494(18)
S(7)-C(25)	1.858(17)	N(17)-C(51)	1.51(2)
S(8)-C(32)	1.850(18)	N(18)-C(53)	1.47(2)
S(9)-C(49)	1.852(13)	N(18)-C(54)	1.48(2)
S(10)-C(56)	1.829(16)	N(18)-C(55)	1.49(2)
S(11)-C(57)	1.826(17)	N(19)-C(59)	1.46(2)
S(12)-C(64)	1.829(15)	N(19)-C(58)	1.48(2)
S(13)-C(65)	1.878(16)	N(19)-C(60)	1.490(19)
S(14)-C(72)	1.825(15)	N(20)-C(62)	1.42(2)
S(15)-C(73)	1.847(17)	N(20)-C(63)	1.477(19)
S(16)-C(80)	1.841(18)	N(20)-C(61)	1.49(2)
N(1)-C(2)	1.45(2)	N(21)-C(66)	1.43(2)
N(1)-C(3)	1.48(2)	N(21)-C(67)	1.48(2)
N(1)-C(4)	1.488(19)	N(21)-C(68)	1.51(2)
N(2)-C(5)	1.47(2)	N(22)-C(69)	1.46(2)
N(2)-C(6)	1.49(2)	N(22)-C(70)	1.48(2)
N(2)-C(7)	1.527(19)	N(22)-C(71)	1.535(19)
N(3)-C(11)	1.45(2)	N(23)-C(76)	1.46(2)
N(3)-C(12)	1.49(2)	N(23)-C(75)	1.48(2)
N(3)-C(10)	1.50(2)	N(23)-C(74)	1.51(3)
N(4)-C(15)	1.42(2)	N(24)-C(78)	1.48(3)
N(4)-C(13)	1.503(19)	N(24)-C(77)	1.51(3)
N(4)-C(14)	1.506(19)	N(24)-C(79)	1.51(3)
N(5)-C(18)	1.473(19)	N(25)-C(81)	1.16(2)
N(5)-C(19)	1.50(2)	N(26)-C(83)	1.14(2)
N(5)-C(20)	1.514(18)	N(27)-C(85)	1.14(2)
N(6)-C(23)	1.44(2)	N(28)-C(87)	1.12(3)
N(6)-C(22)	1.44(2)	N(29)-C(89B)	0.99(2)
N(6)-C(21)	1.47(2)	N(29)-C(89A)	1.33(3)
N(7)-C(26)	1.45(2)	N(30)-C(91)	1.10(2)
N(7)-C(28)	1.48(2)	N(31)-C(93)	1.11(2)
N(7)-C(27)	1.49(2)	N(32)-C(95)	1.13(3)
N(8)-C(31)	1.47(3)	N(33)-C(97)	1.10(3)
N(8)-C(29)	1.51(3)	N(34)-C(99)	1.18(3)
N(8)-C(30)	1.53(3)	N(35)-C(101)	1.12(5)
N(9)-C(33)	1.13(2)	N(36)-C(103)	1.14(3)
N(10)-C(35)	1.09(2)	N(37)-C(105)	1.18(3)
N(11)-C(37)	1.13(2)	C(1)-C(2)	1.51(2)
N(13)-C(41)	1.15(2)	C(4)-C(5)	1.54(3)
N(14)-C(43)	1.16(2)	C(7)-C(8)	1.51(3)
N(15)-C(45)	1.14(3)	C(9)-C(10)	1.52(2)
N(16)-C(47)	1.12(2)	C(12)-C(13)	1.53(2)
N(17)-C(52)	1.470(18)	C(15)-C(16)	1.51(2)

Table S2. Bond lengths (Å) for $[Cu_{10}(S(CH_2)_2N(Me)CH_2-)_2(MeCN)_8][BF_4]_6\cdot(MeCN)_{2.25}$. Symmetry transformations used to generate equivalent atoms:

C(17)-C(18)	1.49(2)	F(1)-B(1)	1.39(2)
C(20)-C(21)	1.50(2)	F(2)-B(1)	1.40(2)
C(23)-C(24)	1.52(2)	F(3)-B(1)	1.35(3)
C(25)-C(26)	1.51(2)	F(4)-B(1)	1.33(3)
C(28)-C(29)	1.45(4)	F(5)-B(2)	1.39(3)
C(31)-C(32)	1.50(3)	F(6)-B(2)	1.32(2)
C(33)-C(34)	1.46(2)	F(7)-B(2)	1.37(3)
C(35)-C(36)	1.46(2)	F(8)-B(2)	1.35(2)
C(37)-C(38)	1.44(2)	F(9)-B(3)	1.39(2)
N(12A)-C(39A)	1.32(4)	F(10)-B(3)	1.37(2)
C(39A)-C(40A)	1.5500(9)	F(11)-B(3)	1.31(3)
N(12B)-C(39B)	1.07(6)	F(12)-B(3)	1.39(2)
C(39B)-C(40B)	1.62(9)	F(13)-B(4)	1.32(3)
C(41)-C(42)	1.44(3)	F(14)-B(4)	1.42(3)
C(43)-C(44)	1.43(3)	F(15)-B(4)	1.37(2)
C(45)-C(46)	1.49(3)	F(16)-B(4)	1.37(3)
C(47)-C(48)	1.46(2)	F(17)-B(5)	1.38(3)
C(49)-C(50)	1.502(17)	F(18)-B(5)	1.38(3)
C(52)-C(53)	1.51(2)	F(19)-B(5)	1.36(3)
C(55)-C(56)	1.51(2)	F(20)-B(5)	1.41(3)
C(57)-C(58)	1.54(2)	F(21)-B(6)	1.37(2)
C(60)-C(61)	1.54(3)	F(22)-B(6)	1.26(3)
C(63)-C(64)	1.52(2)	F(23)-B(6)	1.34(2)
C(65)-C(66)	1.47(2)	F(24)-B(6)	1.35(3)
C(68)-C(69)	1.51(2)	F(25)-B(7)	1.33(3)
C(71)-C(72)	1.50(2)	F(26)-B(7)	1.46(3)
C(73)-C(74)	1.51(3)	F(27)-B(7)	1.31(3)
C(76)-C(77)	1.52(4)	F(28)-B(7)	1.38(2)
C(79)-C(80)	1.48(3)	F(29)-B(8)	1.28(4)
C(81)-C(82)	1.43(2)	F(30)-B(8)	1.28(3)
C(83)-C(84)	1.46(2)	F(31)-B(8)	1.40(3)
C(85)-C(86)	1.45(2)	F(32)-B(8)	1.42(4)
C(87)-C(88)	1.45(4)	F(33)-B(9)	1.33(3)
C(89A)-C(90A)	1.5500(8)	F(34)-B(9)	1.49(4)
C(89B)-C(90B)	1.5500(8)	F(36)-B(9)	1.29(3)
C(91)-C(92)	1.47(2)	F(35)-B(9)	1.34(3)
C(93)-C(94)	1.48(3)	F(37)-B(10)	1.44(4)
C(95)-C(96)	1.47(3)	F(38)-B(10)	1.32(3)
C(97)-C(98)	1.42(3)	F(39)-B(10)	1.44(4)
C(99)-C(100)	1.41(3)	F(40)-B(10)	1.29(3)
C(101)-C(102)	1.48(6)	F(41)-B(11)	1.43(4)
C(103)-C(104)	1.46(3)	F(42)-B(11)	1.25(4)
C(105)-C(106)	1.42(3)	F(43)-B(11)	1.23(4)

Table S2. Bond lengths (Å) for $[Cu_{10}(S(CH_2)_2N(Me)CH_2-)_2(MeCN)_8][BF_4]_6\cdot(MeCN)_{2.25}$. Symmetry transformations used to generate equivalent atoms:

F(44)-B(11)	1.55(5)
B(12A)-F(48A)	1.3700(8)
B(12A)-F(46A)	1.3700(8)
B(12A)-F(45A)	1.3700(8)
B(12A)-F(47A)	1.3700(8)
B(12B)-F(45B)	1.3700(8)
B(12B)-F(47B)	1.3700(8)
B(12B)-F(48B)	1.3700(8)
B(12B)-F(46B)	1.3700(8)

Table S2. Bond angles (deg.) for $[Cu_{10}(S(CH_2)_2N(Me)CH_2-)_2(MeCN)_8][BF_4]_6\cdot(MeCN)_{2.25}$. Symmetry transformations used to generate equivalent atoms:

N(2)-Cu(1)-N(1)	86.6(5)	N(9)-Cu(5)-S(1)	109.5(4)
N(2)-Cu(1)-S(2)	89.8(4)	S(7)-Cu(5)-S(1)	113.20(16)
N(1)-Cu(1)-S(2)	161.4(4)	N(9)-Cu(5)-S(5)	104.7(4)
N(2)-Cu(1)-S(1)	160.6(4)	S(7)-Cu(5)-S(5)	107.29(15)
N(1)-Cu(1)-S(1)	88.8(4)	S(1)-Cu(5)-S(5)	109.47(15)
S(2)-Cu(1)-S(1)	100.30(15)	N(10)-Cu(6)-S(5)	115.9(4)
N(3)-Cu(2)-N(4)	87.6(5)	N(10)-Cu(6)-S(2)	110.9(4)
N(3)-Cu(2)-S(4)	162.8(4)	S(5)-Cu(6)-S(2)	108.08(14)
N(4)-Cu(2)-S(4)	87.7(4)	N(10)-Cu(6)-S(4)	101.5(4)
N(3)-Cu(2)-S(3)	88.3(4)	S(5)-Cu(6)-S(4)	107.45(14)
N(4)-Cu(2)-S(3)	163.4(4)	S(2)-Cu(6)-S(4)	112.89(15)
S(4)-Cu(2)-S(3)	100.63(14)	N(11)-Cu(7)-S(6)	116.6(4)
N(5)-Cu(3)-N(6)	87.1(5)	N(11)-Cu(7)-S(3)	105.7(4)
N(5)-Cu(3)-S(6)	162.2(4)	S(6)-Cu(7)-S(3)	107.94(15)
N(6)-Cu(3)-S(6)	88.0(4)	N(11)-Cu(7)-S(7)	111.3(4)
N(5)-Cu(3)-S(5)	87.4(4)	S(6)-Cu(7)-S(7)	105.25(15)
N(6)-Cu(3)-S(5)	161.0(4)	S(3)-Cu(7)-S(7)	110.07(16)
S(6)-Cu(3)-S(5)	102.32(15)	N(12A)-Cu(8)-S(2)	122.6(9)
N(7)-Cu(4)-N(8)	86.9(7)	N(12B)-Cu(8)-S(2)	102.0(10)
N(7)-Cu(4)-S(7)	89.0(5)	N(12A)-Cu(8)-S(8)	103.3(11)
N(8)-Cu(4)-S(7)	160.7(5)	N(12B)-Cu(8)-S(8)	114.6(10)
N(7)-Cu(4)-S(8)	161.3(5)	S(2)-Cu(8)-S(8)	115.84(16)
N(8)-Cu(4)-S(8)	90.0(5)	N(12A)-Cu(8)-S(3)	98.9(12)
S(7)-Cu(4)-S(8)	99.69(16)	N(12B)-Cu(8)-S(3)	110.5(10)
N(9)-Cu(5)-S(7)	112.3(4)	S(2)-Cu(8)-S(3)	108.39(15)

S(8)-Cu(8)-S(3)	105.51(16)
N(13)-Cu(9)-N(14)	105.1(7)
N(13)-Cu(9)-S(8)	105.2(5)
N(14)-Cu(9)-S(8)	123.5(5)
N(13)-Cu(9)-S(1)	121.6(5)
N(14)-Cu(9)-S(1)	102.7(5)
S(8)-Cu(9)-S(1)	100.26(14)
N(16)-Cu(10)-N(15)	97.3(7)
N(16)-Cu(10)-S(6)	104.6(5)
N(15)-Cu(10)-S(6)	126.1(5)
N(16)-Cu(10)-S(4)	127.1(5)
N(15)-Cu(10)-S(4)	102.8(5)
S(6)-Cu(10)-S(4)	101.78(14)
N(18)-Cu(11)-N(17)	86.9(5)
N(18)-Cu(11)-S(10)	88.2(4)
N(17)-Cu(11)-S(10)	162.8(4)
N(18)-Cu(11)-S(9)	161.4(4)
N(17)-Cu(11)-S(9)	88.1(3)
S(10)-Cu(11)-S(9)	101.39(14)
N(19)-Cu(12)-N(20)	87.0(5)
N(19)-Cu(12)-S(12)	162.2(4)
N(20)-Cu(12)-S(12)	88.4(3)
N(19)-Cu(12)-S(11)	88.1(4)
N(20)-Cu(12)-S(11)	162.2(4)
S(12)-Cu(12)-S(11)	101.11(14)
N(22)-Cu(13)-N(21)	86.6(5)
N(22)-Cu(13)-S(13)	160.5(4)
N(21)-Cu(13)-S(13)	88.1(4)
N(22)-Cu(13)-S(14)	89.8(4)
N(21)-Cu(13)-S(14)	162.5(4)
S(13)-Cu(13)-S(14)	100.58(14)
N(24)-Cu(14)-N(23)	86.1(7)
N(24)-Cu(14)-S(16)	89.1(6)
N(23)-Cu(14)-S(16)	161.4(4)
N(24)-Cu(14)-S(15)	161.1(6)
N(23)-Cu(14)-S(15)	90.4(4

Table S2. Bond angles (deg.) for $[Cu_{10}(S(CH_2)_2N(Me)CH_2-)_2(MeCN)_8][BF_4]_6\cdot(MeCN)_{2.25}$. Symmetry transformations used to generate equivalent atoms:

S(16)-Cu(14)-S(15)	99.66(16)	C(8)-S(2)-Cu(1)	96.6(6)
N(25)-Cu(15)-S(9)	116.2(5)	C(8)-S(2)-Cu(8)	109.8(6)
N(25)-Cu(15)-S(13)	110.5(5)	Cu(1)-S(2)-Cu(8)	117.11(17)
S(9)-Cu(15)-S(13)	108.44(14)	C(8)-S(2)-Cu(6)	108.7(5)
N(25)-Cu(15)-S(12)	101.8(5)	Cu(1)-S(2)-Cu(6)	106.96(17)
S(9)-Cu(15)-S(12)	107.40(14)	Cu(8)-S(2)-Cu(6)	115.83(17)
S(13)-Cu(15)-S(12)	112.48(14)	C(9)-S(3)-Cu(2)	97.0(6)
N(26)-Cu(16)-S(15)	114.3(4)	C(9)-S(3)-Cu(7)	106.7(6)
N(26)-Cu(16)-S(14)	109.5(4)	Cu(2)-S(3)-Cu(7)	115.52(19)
S(15)-Cu(16)-S(14)	112.18(16)	C(9)-S(3)-Cu(8)	105.8(6)
N(26)-Cu(16)-S(9)	103.7(4)	Cu(2)-S(3)-Cu(8)	113.02(18)
S(15)-Cu(16)-S(9)	107.74(14)	Cu(7)-S(3)-Cu(8)	116.19(17)
S(14)-Cu(16)-S(9)	108.87(14)	C(16)-S(4)-Cu(2)	98.9(5)
N(27)-Cu(17)-S(10)	116.6(5)	C(16)-S(4)-Cu(10)	106.3(5)
N(27)-Cu(17)-S(15)	112.5(5)	Cu(2)-S(4)-Cu(10)	91.60(14)
S(10)-Cu(17)-S(15)	104.21(15)	C(16)-S(4)-Cu(6)	113.6(5)
N(27)-Cu(17)-S(11)	105.0(5)	Cu(2)-S(4)-Cu(6)	119.79(17)
S(10)-Cu(17)-S(11)	108.27(16)	Cu(10)-S(4)-Cu(6)	122.46(16)
S(15)-Cu(17)-S(11)	110.15(16)	C(17)-S(5)-Cu(3)	98.2(5)
N(28)-Cu(18)-S(13)	104.6(7)	C(17)-S(5)-Cu(6)	105.6(6)
N(28)-Cu(18)-S(16)	112.0(6)	Cu(3)-S(5)-Cu(6)	115.04(16)
S(13)-Cu(18)-S(16)	115.10(15)	C(17)-S(5)-Cu(5)	107.6(6)
N(28)-Cu(18)-S(11)	111.1(5)	Cu(3)-S(5)-Cu(5)	110.38(16)
S(13)-Cu(18)-S(11)	108.63(15)	Cu(6)-S(5)-Cu(5)	117.70(16)
S(16)-Cu(18)-S(11)	105.46(17)	C(24)-S(6)-Cu(3)	98.7(6)
N(29)-Cu(19)-N(30)	94.7(7)	C(24)-S(6)-Cu(10)	107.5(6)
N(29)-Cu(19)-S(10)	125.2(5)	Cu(3)-S(6)-Cu(10)	90.67(16)
N(30)-Cu(19)-S(10)	104.1(5)	C(24)-S(6)-Cu(7)	113.4(6)
N(29)-Cu(19)-S(12)	104.6(6)	Cu(3)-S(6)-Cu(7)	122.74(18)
N(30)-Cu(19)-S(12)	128.0(5)	Cu(10)-S(6)-Cu(7)	120.06(18)
S(10)-Cu(19)-S(12)	102.86(14)	C(25)-S(7)-Cu(4)	97.6(6)
N(32)-Cu(20)-N(31)	105.7(6)	C(25)-S(7)-Cu(5)	107.3(7)
N(32)-Cu(20)-S(16)	121.9(5)	Cu(4)-S(7)-Cu(5)	116.96(19)
N(31)-Cu(20)-S(16)	102.8(5)	C(25)-S(7)-Cu(7)	110.3(7)
N(32)-Cu(20)-S(14)	104.0(5)	Cu(4)-S(7)-Cu(7)	102.97(17)
N(31)-Cu(20)-S(14)	123.3(4)	Cu(5)-S(7)-Cu(7)	119.53(17)
S(16)-Cu(20)-S(14)	100.70(14)	C(32)-S(8)-Cu(4)	97.9(7)
C(1)-S(1)-Cu(1)	97.7(5)	C(32)-S(8)-Cu(9)	109.3(8)
C(1)-S(1)-Cu(5)	108.8(6)	Cu(4)-S(8)-Cu(9)	98.53(17)
Cu(1)-S(1)-Cu(5)	118.83(17)	C(32)-S(8)-Cu(8)	111.2(7)
C(1)-S(1)-Cu(9)	111.3(7)	Cu(4)-S(8)-Cu(8)	124.57(19)
Cu(1)-S(1)-Cu(9)	100.11(16)	Cu(9)-S(8)-Cu(8)	113.51(19)
Cu(5)-S(1)-Cu(9)	118.14(18)	C(49)-S(9)-Cu(11)	97.5(4)

Table S2. Bond angles (deg.) for $[Cu_{10}(S(CH_2)_2N(Me)CH_2-)_2(MeCN)_8][BF_4]_6\cdot(MeCN)_{2.25}$. Symmetry transformations used to generate equivalent atoms:

C(49)-S(9)-Cu(15)	106.3(5)	Cu(14)-S(16)-Cu(20)	97.51(17)
Cu(11)-S(9)-Cu(15)	114.32(15)	C(80)-S(16)-Cu(18)	111.2(6)
C(49)-S(9)-Cu(16)	107.1(5)	Cu(14)-S(16)-Cu(18)	124.8(2)
Cu(11)-S(9)-Cu(16)	110.65(15)	Cu(20)-S(16)-Cu(18)	113.84(19)
Cu(15)-S(9)-Cu(16)	118.39(16)	C(2)-N(1)-C(3)	112.3(14)
C(56)-S(10)-Cu(11)	98.0(5)	C(2)-N(1)-C(4)	112.4(12)
C(56)-S(10)-Cu(19)	106.1(6)	C(3)-N(1)-C(4)	110.0(14)
Cu(11)-S(10)-Cu(19)	89.06(15)	C(2)-N(1)-Cu(1)	108.7(9)
C(56)-S(10)-Cu(17)	115.4(6)	C(3)-N(1)-Cu(1)	106.6(10)
Cu(11)-S(10)-Cu(17)	124.84(18)	C(4)-N(1)-Cu(1)	106.5(10)
Cu(19)-S(10)-Cu(17)	118.81(18)	C(5)-N(2)-C(6)	112.5(13)
C(57)-S(11)-Cu(12)	97.5(5)	C(5)-N(2)-C(7)	111.4(13)
C(57)-S(11)-Cu(17)	106.9(6)	C(6)-N(2)-C(7)	110.1(13)
Cu(12)-S(11)-Cu(17)	115.11(18)	C(5)-N(2)-Cu(1)	106.7(10)
C(57)-S(11)-Cu(18)	105.2(6)	C(6)-N(2)-Cu(1)	108.3(10)
Cu(12)-S(11)-Cu(18)	113.17(18)	C(7)-N(2)-Cu(1)	107.6(9)
Cu(17)-S(11)-Cu(18)	116.35(16)	C(11)-N(3)-C(12)	113.4(13)
C(64)-S(12)-Cu(12)	98.9(5)	C(11)-N(3)-C(10)	110.6(13)
C(64)-S(12)-Cu(19)	106.9(5)	C(12)-N(3)-C(10)	111.0(13)
Cu(12)-S(12)-Cu(19)	89.95(14)	C(11)-N(3)-Cu(2)	108.6(10)
C(64)-S(12)-Cu(15)	114.1(5)	C(12)-N(3)-Cu(2)	106.7(10)
Cu(12)-S(12)-Cu(15)	120.23(17)	C(10)-N(3)-Cu(2)	106.2(9)
Cu(19)-S(12)-Cu(15)	122.31(16)	C(15)-N(4)-C(13)	112.8(13)
C(65)-S(13)-Cu(13)	96.6(5)	C(15)-N(4)-C(14)	110.9(13)
C(65)-S(13)-Cu(18)	110.6(6)	C(13)-N(4)-C(14)	110.5(13)
Cu(13)-S(13)-Cu(18)	117.15(17)	C(15)-N(4)-Cu(2)	111.2(10)
C(65)-S(13)-Cu(15)	108.3(6)	C(13)-N(4)-Cu(2)	104.2(9)
Cu(13)-S(13)-Cu(15)	106.38(16)	C(14)-N(4)-Cu(2)	107.0(10)
Cu(18)-S(13)-Cu(15)	115.85(17)	C(18)-N(5)-C(19)	112.2(12)
C(72)-S(14)-Cu(13)	97.7(5)	C(18)-N(5)-C(20)	111.3(12)
C(72)-S(14)-Cu(16)	111.2(5)	C(19)-N(5)-C(20)	109.1(12)
Cu(13)-S(14)-Cu(16)	119.74(16)	C(18)-N(5)-Cu(3)	107.2(9)
C(72)-S(14)-Cu(20)	108.6(5)	C(19)-N(5)-Cu(3)	109.0(9)
Cu(13)-S(14)-Cu(20)	98.31(15)	C(20)-N(5)-Cu(3)	107.9(9)
Cu(16)-S(14)-Cu(20)	118.76(17)	C(23)-N(6)-C(22)	112.6(14)
C(73)-S(15)-Cu(14)	97.7(7)	C(23)-N(6)-C(21)	113.6(15)
C(73)-S(15)-Cu(16)	107.8(6)	C(22)-N(6)-C(21)	111.1(16)
Cu(14)-S(15)-Cu(16)	117.48(19)	C(23)-N(6)-Cu(3)	109.2(10)
C(73)-S(15)-Cu(17)	108.2(6)	C(22)-N(6)-Cu(3)	106.9(12)
Cu(14)-S(15)-Cu(17)	102.92(17)	C(21)-N(6)-Cu(3)	102.8(10)
Cu(16)-S(15)-Cu(17)	120.17(17)	C(26)-N(7)-C(28)	112.8(16)
C(80)-S(16)-Cu(14)	97.5(7)	C(26)-N(7)-C(27)	111.9(15)
C(80)-S(16)-Cu(20)	110.2(7)	C(28)-N(7)-C(27)	106.7(16)

Table S2. Bond angles (deg.) for $[Cu_{10}(S(CH_2)_2N(Me)CH_2-)_2(MeCN)_8][BF_4]_6\cdot(MeCN)_{2.25}$. Symmetry transformations used to generate equivalent atoms:

C(26)-N(7)-Cu(4)	109.1(10)	C(66)-N(21)-Cu(13)	109.9(10)
C(28)-N(7)-Cu(4)	107.7(13)	C(67)-N(21)-Cu(13)	107.4(10)
C(27)-N(7)-Cu(4)	108.5(11)	C(68)-N(21)-Cu(13)	105.6(10)
C(31)-N(8)-C(29)	115.7(19)	C(69)-N(22)-C(70)	111.7(13)
C(31)-N(8)-C(30)	109(2)	C(69)-N(22)-C(71)	110.8(12)
C(29)-N(8)-C(30)	108.5(18)	C(70)-N(22)-C(71)	109.6(12)
C(31)-N(8)-Cu(4)	109.8(14)	C(69)-N(22)-Cu(13)	107.4(10)
C(29)-N(8)-Cu(4)	105.0(12)	C(70)-N(22)-Cu(13)	108.1(9)
C(30)-N(8)-Cu(4)	108.9(12)	C(71)-N(22)-Cu(13)	109.1(9)
C(33)-N(9)-Cu(5)	169.2(14)	C(76)-N(23)-C(75)	110.5(15)
C(35)-N(10)-Cu(6)	161.6(15)	C(76)-N(23)-C(74)	112.0(16)
C(37)-N(11)-Cu(7)	162.9(13)	C(75)-N(23)-C(74)	108.5(14)
C(41)-N(13)-Cu(9)	170.1(16)	C(76)-N(23)-Cu(14)	108.1(12)
C(43)-N(14)-Cu(9)	171.1(17)	C(75)-N(23)-Cu(14)	111.8(12)
C(45)-N(15)-Cu(10)	160.2(17)	C(74)-N(23)-Cu(14)	105.9(10)
C(47)-N(16)-Cu(10)	164.4(16)	C(78)-N(24)-C(77)	111.2(18)
C(52)-N(17)-C(50)	111.9(13)	C(78)-N(24)-C(79)	110.2(19)
C(52)-N(17)-C(51)	109.4(13)	C(77)-N(24)-C(79)	111.8(18)
C(50)-N(17)-C(51)	112.1(12)	C(78)-N(24)-Cu(14)	108.8(13)
C(52)-N(17)-Cu(11)	107.8(9)	C(77)-N(24)-Cu(14)	104.6(13)
C(50)-N(17)-Cu(11)	106.5(8)	C(79)-N(24)-Cu(14)	110.1(12)
C(51)-N(17)-Cu(11)	109.0(10)	C(81)-N(25)-Cu(15)	159.9(15)
C(53)-N(18)-C(54)	109.8(13)	C(83)-N(26)-Cu(16)	168.4(15)
C(53)-N(18)-C(55)	111.5(13)	C(85)-N(27)-Cu(17)	170.3(16)
C(54)-N(18)-C(55)	109.9(14)	C(87)-N(28)-Cu(18)	164(3)
C(53)-N(18)-Cu(11)	104.8(10)	C(89B)-N(29)-Cu(19)	157(2)
C(54)-N(18)-Cu(11)	108.2(11)	C(89A)-N(29)-Cu(19)	150(2)
C(55)-N(18)-Cu(11)	112.4(10)	C(91)-N(30)-Cu(19)	165.8(16)
C(59)-N(19)-C(58)	109.1(13)	C(93)-N(31)-Cu(20)	171.2(15)
C(59)-N(19)-C(60)	111.9(13)	C(95)-N(32)-Cu(20)	170.2(16)
C(58)-N(19)-C(60)	109.4(13)	C(2)-C(1)-S(1)	109.2(10)
C(59)-N(19)-Cu(12)	111.5(9)	N(1)-C(2)-C(1)	112.9(12)
C(58)-N(19)-Cu(12)	107.4(10)	N(1)-C(4)-C(5)	108.8(13)
C(60)-N(19)-Cu(12)	107.5(10)	N(2)-C(5)-C(4)	110.3(14)
C(62)-N(20)-C(63)	110.2(13)	C(8)-C(7)-N(2)	108.2(13)
C(62)-N(20)-C(61)	112.4(13)	C(7)-C(8)-S(2)	112.1(11)
C(63)-N(20)-C(61)	109.5(13)	C(10)-C(9)-S(3)	111.7(12)
C(62)-N(20)-Cu(12)	110.1(11)	N(3)-C(10)-C(9)	109.1(13)
C(63)-N(20)-Cu(12)	110.7(9)	N(3)-C(12)-C(13)	109.1(13)
C(61)-N(20)-Cu(12)	103.8(10)	N(4)-C(13)-C(12)	109.1(13)
C(66)-N(21)-C(67)	112.1(14)	N(4)-C(15)-C(16)	113.1(13)
C(66)-N(21)-C(68)	112.4(14)	C(15)-C(16)-S(4)	107.2(11)
C(67)-N(21)-C(68)	109.1(13)	C(18)-C(17)-S(5)	109.7(10)

Table S2. Bond angles (deg.) for $[Cu_{10}(S(CH_2)_2N(Me)CH_2-)_2(MeCN)_8][BF_4]_6\cdot(MeCN)_{2.25}$. Symmetry transformations used to generate equivalent atoms:

N(5)-C(18)-C(17)	110.9(12)	N(24)-C(77)-C(76)	108.2(19)
C(21)-C(20)-N(5)	108.3(13)	C(80)-C(79)-N(24)	110.7(18)
N(6)-C(21)-C(20)	112.8(14)	C(79)-C(80)-S(16)	109.6(14)
N(6)-C(23)-C(24)	112.8(14)	N(25)-C(81)-C(82)	177(2)
C(23)-C(24)-S(6)	107.2(10)	N(26)-C(83)-C(84)	175.8(19)
C(26)-C(25)-S(7)	109.4(13)	N(27)-C(85)-C(86)	177(2)
N(7)-C(26)-C(25)	112.3(14)	N(28)-C(87)-C(88)	174(4)
C(29)-C(28)-N(7)	110.8(19)	N(29)-C(89A)-C(90A)	173(3)
C(28)-C(29)-N(8)	111(2)	N(29)-C(89B)-C(90B)	168(3)
N(8)-C(31)-C(32)	115(2)	N(30)-C(91)-C(92)	173(2)
C(31)-C(32)-S(8)	108.8(15)	N(31)-C(93)-C(94)	177(2)
N(9)-C(33)-C(34)	179.6(19)	N(32)-C(95)-C(96)	177(2)
N(10)-C(35)-C(36)	175(2)	N(33)-C(97)-C(98)	179(2)
N(11)-C(37)-C(38)	179.5(16)	N(34)-C(99)-C(100)	177(2)
C(39A)-N(12A)-Cu(8)	166(4)	N(35)-C(101)-C(102)	174(5)
N(12A)-C(39A)-C(40A)	140(5)	N(36)-C(103)-C(104)	177(3)
C(39B)-N(12B)-Cu(8)	166(4)	N(37)-C(105)-C(106)	180(3)
N(12B)-C(39B)-C(40B)	170(6)	F(4)-B(1)-F(3)	109.9(19)
N(13)-C(41)-C(42)	175(3)	F(4)-B(1)-F(1)	110.6(18)
N(14)-C(43)-C(44)	175(2)	F(3)-B(1)-F(1)	107.4(18)
N(15)-C(45)-C(46)	176(3)	F(4)-B(1)-F(2)	113.5(18)
N(16)-C(47)-C(48)	178(2)	F(3)-B(1)-F(2)	108.0(18)
C(50)-C(49)-S(9)	110.4(9)	F(1)-B(1)-F(2)	107.2(15)
N(17)-C(50)-C(49)	111.6(11)	F(6)-B(2)-F(8)	112.3(18)
N(17)-C(52)-C(53)	109.7(14)	F(6)-B(2)-F(7)	111.2(18)
N(18)-C(53)-C(52)	110.8(14)	F(8)-B(2)-F(7)	110.4(19)
N(18)-C(55)-C(56)	109.9(13)	F(6)-B(2)-F(5)	110.2(18)
C(55)-C(56)-S(10)	109.9(10)	F(8)-B(2)-F(5)	108.0(16)
C(58)-C(57)-S(11)	110.5(11)	F(7)-B(2)-F(5)	104.3(18)
N(19)-C(58)-C(57)	110.2(14)	F(11)-B(3)-F(10)	110(2)
N(19)-C(60)-C(61)	108.4(13)	F(11)-B(3)-F(9)	109.7(16)
N(20)-C(61)-C(60)	106.9(14)	F(10)-B(3)-F(9)	107.3(15)
N(20)-C(63)-C(64)	110.5(12)	F(11)-B(3)-F(12)	111.8(18)
C(63)-C(64)-S(12)	109.4(10)	F(10)-B(3)-F(12)	107.6(16)
C(66)-C(65)-S(13)	110.6(11)	F(9)-B(3)-F(12)	110.6(18)
N(21)-C(66)-C(65)	111.5(15)	F(13)-B(4)-F(16)	108.3(19)
N(21)-C(68)-C(69)	110.3(14)	F(13)-B(4)-F(15)	111.4(17)
N(22)-C(69)-C(68)	108.9(13)	F(16)-B(4)-F(15)	109(2)
C(72)-C(71)-N(22)	110.9(12)	F(13)-B(4)-F(14)	111(2)
C(71)-C(72)-S(14)	112.2(10)	F(16)-B(4)-F(14)	109.3(19)
C(74)-C(73)-S(15)	109.8(14)	F(15)-B(4)-F(14)	108.5(17)
N(23)-C(74)-C(73)	113.6(15)	F(19)-B(5)-F(18)	111(2)
N(23)-C(76)-C(77)	107.0(18)	F(19)-B(5)-F(17)	108(2)

Table S2. Bond angles (deg.) for $[Cu_{10}(S(CH_2)_2N(Me)CH_2-)_2(MeCN)_8][BF_4]_6\cdot(MeCN)_{2.25}$. Symmetry transformations used to generate equivalent atoms:

F(18)-B(5)-F(17)	106.3(19)	F(33)-B(9)-F(34)	99(2)
F(19)-B(5)-F(20)	110(2)	F(35)-B(9)-F(34)	100(2)
F(18)-B(5)-F(20)	114.3(19)	F(40)-B(10)-F(38)	119(3)
F(17)-B(5)-F(20)	107(2)	F(40)-B(10)-F(37)	107(3)
F(22)-B(6)-F(23)	112(2)	F(38)-B(10)-F(37)	107(2)
F(22)-B(6)-F(24)	113(2)	F(40)-B(10)-F(39)	112(2)
F(23)-B(6)-F(24)	105.6(19)	F(38)-B(10)-F(39)	110(3)
F(22)-B(6)-F(21)	110.7(18)	F(37)-B(10)-F(39)	100(2)
F(23)-B(6)-F(21)	112.2(19)	F(43)-B(11)-F(42)	135(4)
F(24)-B(6)-F(21)	102.9(18)	F(43)-B(11)-F(41)	112(3)
F(27)-B(7)-F(25)	115.8(19)	F(42)-B(11)-F(41)	107(3)
F(27)-B(7)-F(28)	112.7(19)	F(43)-B(11)-F(44)	96(3)
F(25)-B(7)-F(28)	113.8(19)	F(42)-B(11)-F(44)	98(3)
F(27)-B(7)-F(26)	106.6(19)	F(41)-B(11)-F(44)	101(3)
F(25)-B(7)-F(26)	102.4(17)	F(48A)-B(12A)-F(46A)	109.4(3)
F(28)-B(7)-F(26)	104.0(19)	F(48A)-B(12A)-F(45A)	109.5(3)
F(29)-B(8)-F(30)	125(3)	F(46A)-B(12A)-F(45A)	109.4(3)
F(29)-B(8)-F(31)	112(2)	F(48A)-B(12A)-F(47A)	109.6(3)
F(30)-B(8)-F(31)	107(3)	F(46A)-B(12A)-F(47A)	109.5(3)
F(29)-B(8)-F(32)	102(3)	F(45A)-B(12A)-F(47A)	109.5(3)
F(30)-B(8)-F(32)	102(3)	F(45B)-B(12B)-F(47B)	109.5(3)
F(31)-B(8)-F(32)	107(3)	F(45B)-B(12B)-F(48B)	109.4(3)
F(36)-B(9)-F(33)	116(2)	F(47B)-B(12B)-F(48B)	109.5(3)
F(36)-B(9)-F(35)	116(3)	F(45B)-B(12B)-F(46B)	109.5(4)
F(33)-B(9)-F(35)	118(2)	F(47B)-B(12B)-F(46B)	109.5(3)
F(36)-B(9)-F(34)	102(2)	F(48B)-B(12B)-F(46B)	109.5(3)

Table S4. Anisotropic displacement parameters ($Å^2$ x 10^3) for $[Cu_{10}(S(CH_2)_2N(Me)CH_2-)_2(MeCN)_8][BF_4]_6\cdot(MeCN)_{2.25}$. The anisotropic displacement factor exponent takes the form: $-2\pi^2[h^2a^{*2}U^{11} + ... + 2hka^*b^*U^{12}]$.

Atom	U^{11}	U^{22}	U^{33}	U^{23}	U^{13}	U^{12}
Cu(1)	19(1)	16(1)	26(1)	-2(1)	-2(1)	0(1)
Cu(2)	20(1)	20(1)	18(1)	-3(1)	1(1)	6(1)
Cu(3)	18(1)	18(1)	16(1)	-3(1)	-1(1)	0(1)
Cu(4)	37(1)	32(1)	20(1)	7(1)	5(1)	16(1)
Cu(5)	20(1)	27(1)	21(1)	1(1)	2(1)	6(1)
Cu(6)	20(1)	20(1)	20(1)	-2(1)	-2(1)	3(1)
Cu(7)	35(1)	38(1)	20(1)	-4(1)	2(1)	10(1)
Cu(8)	29(1)	27(1)	32(1)	3(1)	5(1)	6(1)
Cu(9)	41(1)	21(1)	40(1)	3(1)	11(1)	2(1)

Cu(10)	29(1)	29(1)	42(1)	-16(1)	-5(1)	3(1)
Cu(11)	19(1)	17(1)	18(1)	-3(1)	1(1)	1(1)
Cu(12)	20(1)	21(1)	16(1)	-3(1)	-1(1)	-6(1)
Cu(13)	17(1)	15(1)	24(1)	-2(1)	0(1)	1(1)
Cu(14)	40(1)	27(1)	23(1)	7(1)	-6(1)	-17(1)
Cu(15)	22(1)	22(1)	20(1)	-4(1)	-1(1)	-3(1)
Cu(16)	19(1)	24(1)	24(1)	1(1)	-2(1)	-5(1)
Cu(17)	34(1)	38(1)	23(1)	-4(1)	-1(1)	-8(1)
Cu(18)	30(1)	25(1)	29(1)	2(1)	-7(1)	-5(1)
Cu(19)	29(1)	33(1)	41(1)	-17(1)	7(1)	-2(1)
Cu(20)	38(1)	24(1)	41(1)	4(1)	-10(1)	-2(1)
S(1)	20(2)	24(2)	24(2)	1(2)	3(1)	2(1)
S(2)	18(2)	18(2)	32(2)	-2(2)	-3(2)	2(1)
S(3)	33(2)	28(2)	15(2)	3(1)	4(2)	10(2)
S(4)	18(2)	18(2)	17(2)	-5(1)	0(1)	6(1)
S(5)	15(2)	21(2)	19(2)	-1(1)	1(1)	-3(1)
S(6)	22(2)	30(2)	18(2)	-10(2)	-1(1)	3(2)
S(7)	31(2)	24(2)	19(2)	0(1)	2(2)	8(2)
S(8)	35(2)	17(2)	27(2)	4(1)	11(2)	8(2)
S(9)	18(2)	13(2)	17(2)	-2(1)	1(1)	-1(1)
S(10)	22(2)	27(2)	22(2)	-9(2)	3(1)	-1(1)
S(11)	26(2)	22(2)	21(2)	0(1)	-5(1)	-10(1)
S(12)	18(2)	19(2)	18(2)	-3(1)	0(1)	-3(1)
S(13)	18(2)	19(2)	25(2)	-2(1)	-2(1)	-4(1)
S(14)	21(2)	15(2)	23(2)	1(1)	-3(1)	-4(1)
S(15)	26(2)	26(2)	24(2)	3(2)	1(2)	-7(2)
S(16)	34(2)	25(2)	31(2)	11(2)	-8(2)	-12(2)
N(1)	23(7)	25(7)	28(7)	-8(5)	-1(5)	-6(5)
N(2)	30(7)	21(6)	27(7)	3(5)	-4(5)	-8(5)
N(3)	24(7)	25(7)	23(6)	-13(5)	3(5)	14(5)

Table S4. Anisotropic displacement parameters ($Å^2$ x 10^3) for $[Cu_{10}(S(CH_2)_2N(Me)CH_2-)_2(MeCN)_8][BF_4]_6\cdot(MeCN)_{2.25}$. The anisotropic displacement factor exponent takes the form: $-2\pi^2[h^2a^{*2}U^{11} + ... + 2hka^*b^*U^{12}]$.

Atom	U^{11}	U^{22}	U^{33}	U^{23}	U^{13}	U^{12}
N(4)	14(6)	24(6)	30(7)	-11(5)	-6(5)	15(5)
N(5)	21(6)	28(7)	21(6)	-3(5)	2(5)	-9(5)
N(6)	30(7)	34(8)	27(7)	-5(6)	-1(6)	-15(6)
N(7)	35(8)	51(9)	21(7)	3(6)	-1(6)	14(7)
N(8)	65(11)	31(8)	31(8)	7(6)	17(7)	11(7)
N(9)	27(7)	25(7)	36(8)	2(6)	4(6)	10(5)
N(10)	51(9)	23(7)	23(7)	-3(6)	-3(6)	-13(6)
N(11)	34(8)	15(6)	41(9)	-8(6)	-5(6)	-1(5)
N(13)	48(10)	46(10)	43(9)	-1(7)	11(7)	-20(8)

N(14)	83(13)	19(7)	46(10)	3(7)	0(9)	18(8)
N(15)	36(9)	43(10)	64(12)	5(9)	13(8)	-6(7)
N(16)	50(10)	37(9)	45(9)	-24(7)	-17(8)	-2(7)
N(17)	24(6)	20(6)	21(6)	9(5)	1(5)	19(5)
N(18)	20(6)	18(6)	39(8)	-10(5)	1(5)	0(5)
N(19)	10(6)	45(8)	35(8)	0(6)	0(5)	-6(6)
N(20)	18(6)	39(8)	18(6)	-4(5)	-11(5)	-12(5)
N(21)	27(7)	34(8)	31(7)	-2(6)	7(6)	11(6)
N(22)	20(6)	20(6)	29(7)	-6(5)	3(5)	3(5)
N(23)	42(8)	26(7)	35(8)	4(6)	-8(6)	-10(6)
N(24)	80(13)	59(11)	25(8)	22(8)	-17(8)	-40(10)
N(25)	48(9)	60(10)	14(7)	0(7)	-4(6)	3(8)
N(26)	23(7)	29(7)	35(7)	-5(6)	-10(6)	-4(5)
N(27)	51(10)	61(11)	20(8)	12(7)	-11(6)	-20(8)
N(28)	37(10)	57(11)	88(15)	-18(10)	-33(10)	4(8)
N(29)	40(9)	19(8)	109(16)	-1(9)	-21(10)	-2(7)
N(30)	38(9)	52(10)	58(11)	-30(9)	-9(8)	-2(8)
N(31)	44(9)	18(6)	38(8)	12(6)	1(7)	7(6)
N(32)	59(11)	30(8)	40(9)	16(7)	7(8)	-3(8)
N(33)	74(14)	49(11)	66(13)	-17(10)	11(11)	-1(10)
N(34)	52(11)	44(10)	70(14)	-6(9)	0(9)	6(9)
N(36)	51(12)	108(18)	56(12)	4(12)	-5(9)	16(12)
N(37)	72(15)	93(17)	60(13)	10(12)	16(11)	4(13)
C(1)	15(7)	46(10)	37(9)	-15(8)	1(6)	5(7)
C(2)	13(6)	23(7)	36(8)	-22(6)	9(6)	-1(5)
C(3)	76(14)	36(10)	19(8)	-1(7)	-2(8)	-20(9)
C(4)	23(8)	35(9)	45(10)	-17(8)	5(7)	-16(7)
C(5)	35(9)	39(10)	40(10)	-4(8)	-6(8)	-11(8)
C(6)	22(8)	23(8)	69(13)	-13(8)	0(8)	-1(6)
C(7)	12(7)	23(8)	67(12)	-2(8)	-9(7)	6(6)

Table S4. Anisotropic displacement parameters ($Å^2$ x 10^3) for $[Cu_{10}(S(CH_2)_2N(Me)CH_2-)_2(MeCN)_8][BF_4]_6\cdot(MeCN)_{2.25}$. The anisotropic displacement factor exponent takes the form: $-2\pi^2[h^2a^{*2}U^{11} + ... + 2hka^*b^*U^{12}]$.

Atom	U^{11}	U^{22}	U^{33}	U^{23}	U^{13}	U^{12}
C(8)	21(8)	23(8)	53(11)	9(7)	0(7)	1(6)
C(10)	35(9)	50(11)	16(8)	-4(7)	4(6)	1(8)
C(11)	43(11)	46(11)	35(10)	-17(8)	1(8)	20(9)
C(12)	35(10)	44(10)	36(10)	-5(8)	19(8)	15(8)
C(13)	36(9)	28(8)	34(9)	-8(7)	9(7)	17(7)
C(14)	16(7)	36(9)	47(10)	-6(8)	-2(7)	-3(6)
C(15)	24(8)	33(9)	38(9)	-12(7)	-1(7)	-3(7)
C(16)	23(7)	15(7)	27(8)	-4(6)	3(6)	3(6)
C(17)	41(10)	42(9)	15(7)	-8(7)	8(6)	-22(8)

C(18)	19(7)	22(7)	22(7)	-5(6)	12(6)	0(6)
C(19)	41(10)	24(8)	27(8)	4(7)	1(7)	6(7)
C(20)	26(8)	27(8)	32(9)	5(7)	5(7)	-13(6)
C(21)	65(13)	49(11)	27(9)	5(8)	-1(9)	-45(10)
C(22)	23(9)	68(14)	53(12)	-8(10)	3(8)	7(9)
C(23)	27(8)	38(9)	33(9)	-12(7)	-4(7)	-9(7)
C(24)	24(8)	40(9)	27(8)	-18(7)	-12(6)	2(7)
C(25)	29(9)	43(11)	49(11)	11(9)	-19(8)	-7(8)
C(26)	29(9)	37(9)	38(9)	-11(8)	-15(7)	17(7)
C(27)	34(10)	42(11)	63(13)	-17(10)	-10(9)	18(8)
C(28)	75(16)	67(15)	30(10)	1(10)	-1(10)	40(13)
C(29)	79(18)	90(20)	44(13)	42(13)	11(12)	27(15)
C(30)	130(20)	90(20)	38(12)	38(13)	41(14)	72(18)
C(32)	43(11)	58(13)	56(13)	28(10)	25(10)	6(10)
C(33)	26(8)	15(7)	50(10)	-9(7)	6(7)	0(6)
C(34)	35(10)	32(10)	99(18)	3(10)	45(11)	-1(8)
C(35)	42(10)	74(14)	5(7)	11(8)	2(7)	18(9)
C(36)	66(16)	130(20)	33(11)	46(14)	-11(10)	26(15)
C(37)	33(8)	9(6)	37(9)	-4(6)	-10(7)	7(6)
C(38)	56(11)	12(7)	32(9)	-3(6)	-6(8)	9(7)
C(41)	68(14)	27(9)	49(12)	-12(8)	18(10)	-14(9)
C(42)	86(19)	69(16)	69(16)	-1(13)	37(14)	-50(14)
C(43)	75(14)	29(9)	33(10)	-16(7)	-16(9)	21(9)
C(44)	69(16)	60(14)	61(14)	-5(11)	-1(12)	41(12)
C(45)	24(9)	36(10)	85(16)	5(10)	32(10)	5(8)
C(46)	56(15)	100(20)	91(19)	75(17)	23(13)	14(14)
C(47)	23(8)	37(10)	49(11)	-15(8)	6(7)	8(7)
C(48)	38(11)	63(14)	53(12)	-28(11)	4(9)	-8(10)
C(49)	19(7)	23(7)	14(6)	2(5)	-7(5)	11(6)
C(50)	17(7)	18(7)	20(7)	3(5)	-13(5)	7(5)

Table S4. Anisotropic displacement parameters ($Å^2$ x 10^3) for $[Cu_{10}(S(CH_2)_2N(Me)CH_2-)_2(MeCN)_8][BF_4]_6\cdot(MeCN)_{2.25}$. The anisotropic displacement factor exponent takes the form: $-2\pi^2[h^2a^{*2}U^{11} + ... + 2hka^*b^*U^{12}]$.

Atom	U^{11}	U^{22}	U^{33}	U^{23}	U^{13}	U^{12}
C(51)	47(11)	27(8)	30(9)	5(7)	4(8)	-14(8)
C(52)	41(10)	51(11)	24(8)	0(8)	-1(7)	29(9)
C(53)	28(9)	33(9)	48(11)	2(8)	1(8)	12(7)
C(54)	27(9)	77(15)	46(11)	10(11)	-9(8)	-10(9)
C(55)	32(9)	30(9)	36(9)	-10(7)	9(7)	4(7)
C(56)	27(8)	55(11)	19(8)	-16(7)	13(6)	-1(8)
C(57)	59(12)	21(8)	25(8)	8(6)	-2(8)	-24(8)
C(58)	42(10)	53(11)	14(7)	-5(7)	-2(7)	4(8)
C(59)	36(9)	36(9)	17(7)	-8(6)	-5(6)	-10(7)

C(60)	19(8)	47(10)	38(10)	-15(8)	-14(7)	-9(7)
C(61)	45(10)	43(10)	20(8)	-4(7)	-2(7)	-11(8)
C(62)	34(10)	61(13)	34(10)	4(9)	10(8)	-6(9)
C(63)	36(9)	14(7)	29(8)	6(6)	-5(7)	-6(6)
C(64)	28(8)	32(8)	22(8)	9(6)	6(6)	-3(7)
C(65)	21(8)	34(9)	43(10)	-4(7)	2(7)	-10(7)
C(66)	22(8)	55(12)	46(11)	-12(9)	21(8)	-6(8)
C(67)	38(10)	29(9)	39(10)	0(7)	3(8)	6(7)
C(68)	27(8)	37(9)	35(9)	-8(7)	14(7)	13(7)
C(69)	41(10)	27(9)	45(10)	-13(8)	3(8)	8(7)
C(70)	24(8)	43(10)	33(9)	-4(8)	-9(7)	11(7)
C(71)	25(8)	21(7)	37(9)	1(7)	-9(7)	-7(6)
C(72)	15(7)	16(7)	36(9)	2(6)	-7(6)	-1(5)
C(73)	28(9)	57(12)	36(10)	-6(8)	8(7)	-14(8)
C(74)	39(11)	79(15)	32(10)	-15(10)	16(8)	-34(10)
C(75)	51(11)	32(9)	42(10)	-8(8)	-9(9)	-13(8)
C(76)	68(15)	76(16)	30(10)	18(10)	-7(9)	-36(13)
C(77)	64(15)	76(16)	50(13)	29(12)	-11(11)	-26(13)
C(78)	85(18)	82(17)	37(11)	35(12)	-30(11)	-32(14)
C(79)	61(14)	57(14)	54(13)	36(11)	4(11)	-4(11)
C(80)	48(11)	56(12)	37(10)	18(9)	-23(9)	-21(9)
C(81)	56(11)	15(7)	29(9)	-2(6)	5(8)	0(7)
C(82)	40(12)	100(20)	55(13)	37(13)	20(10)	-11(12)
C(83)	31(9)	28(9)	44(10)	-5(7)	1(8)	-5(7)
C(84)	28(9)	41(10)	70(14)	-10(10)	-25(9)	1(8)
C(85)	44(10)	28(8)	22(8)	5(6)	3(7)	-23(7)
C(86)	63(13)	49(11)	19(8)	0(7)	2(8)	-23(10)
C(87)	48(15)	59(16)	140(30)	-38(17)	-28(16)	5(12)
C(88)	44(16)	130(30)	150(30)	-30(20)	-25(18)	11(17)
C(91)	32(10)	56(12)	55(12)	-31(10)	-1(8)	-14(9)

Table S4. Anisotropic displacement parameters ($Å^2$ x 10^3) for $[Cu_{10}(S(CH_2)_2N(Me)CH_2-)_2(MeCN)_8][BF_4]_6\cdot(MeCN)_{2.25}$. The anisotropic displacement factor exponent takes the form: $-2\pi^2[h^2a^{*2}U^{11} + ... + 2hka^*b^*U^{12}]$.

Atom	U^{11}	U^{22}	U^{33}	U^{23}	U^{13}	U^{12}
C(92)	50(12)	57(13)	63(14)	-50(11)	12(10)	-2(10)
C(93)	56(12)	43(10)	23(8)	-15(8)	-15(8)	6(9)
C(94)	63(14)	74(16)	38(11)	7(10)	-5(10)	38(12)
C(95)	64(13)	28(9)	27(9)	4(7)	9(8)	15(9)
C(96)	75(16)	43(12)	54(13)	-11(10)	11(11)	-39(11)
C(97)	44(12)	48(13)	64(14)	-17(11)	24(10)	-5(10)
C(98)	90(20)	82(19)	43(13)	-6(12)	10(12)	-6(15)
C(99)	43(11)	57(13)	54(13)	33(11)	-6(9)	16(10)
C(100)	45(12)	70(15)	49(12)	-4(11)	-5(9)	5(10)

C(103)	56(13)	46(11)	40(11)	23(9)	-1(9)	9(9)
C(104)	43(12)	67(15)	93(19)	31(14)	22(12)	18(11)
C(105)	46(12)	49(12)	43(11)	-2(9)	-8(9)	16(9)
C(106)	39(12)	83(17)	75(16)	-28(14)	-1(11)	12(11)
F(1)	54(7)	56(8)	67(8)	23(6)	-34(6)	-22(6)
F(2)	61(7)	49(7)	46(7)	-16(5)	-13(5)	-14(6)
F(3)	92(11)	57(9)	138(14)	-62(9)	-56(10)	35(8)
F(4)	59(9)	146(16)	72(10)	49(10)	3(7)	-47(10)
F(5)	69(8)	38(6)	84(9)	8(6)	2(7)	-25(6)
F(6)	59(8)	61(9)	100(11)	-14(8)	-39(8)	3(7)
F(7)	94(12)	86(11)	99(12)	-9(9)	49(10)	-17(9)
F(8)	56(8)	66(8)	80(9)	-7(7)	-38(7)	15(6)
F(9)	62(8)	49(7)	47(7)	-18(5)	6(6)	6(6)
F(10)	57(8)	63(8)	69(9)	21(7)	30(6)	19(6)
F(11)	73(11)	70(10)	150(16)	-61(11)	27(10)	-22(8)
F(12)	93(11)	83(10)	64(9)	22(8)	-6(8)	50(9)
F(13)	81(10)	71(9)	73(9)	1(7)	-3(8)	-44(8)
F(14)	71(10)	31(7)	182(18)	-8(8)	63(11)	-14(6)
F(15)	56(8)	74(9)	84(10)	10(8)	33(7)	20(7)
F(16)	97(13)	75(11)	137(16)	-30(10)	-63(12)	20(9)
F(17)	72(10)	60(9)	98(11)	0(8)	-1(8)	-15(7)
F(18)	50(8)	83(10)	106(12)	-13(9)	-9(8)	26(7)
F(19)	85(11)	165(18)	44(8)	10(9)	25(7)	50(11)
F(20)	71(10)	94(12)	108(13)	-8(10)	-33(9)	-3(9)
F(21)	71(10)	94(11)	73(10)	6(8)	10(7)	46(8)
F(22)	200(20)	96(14)	180(20)	81(14)	130(19)	90(15)
F(23)	107(13)	136(16)	53(9)	-23(9)	13(8)	48(12)
F(24)	105(15)	84(13)	154(19)	-25(12)	-2(13)	-30(11)
F(25)	65(9)	81(10)	71(9)	-4(8)	1(7)	26(8)
F(26)	75(11)	63(10)	160(18)	6(10)	33(11)	-16(8)

Table S4. Anisotropic displacement parameters ($Å^2$ x 10^3) for $[Cu_{10}(S(CH_2)_2N(Me)CH_2-)_2(MeCN)_8][BF_4]_6\cdot(MeCN)_{2.25}$. The anisotropic displacement factor exponent takes the form: $-2\pi^2[h^2a^{*2}U^{11} + ... + 2hka^*b^*U^{12}]$.

Atom	U^{11}	U^{22}	U^{33}	U^{23}	U^{13}	U^{12}
F(27)	93(11)	61(9)	116(13)	-47(9)	-38(10)	31(8)
F(28)	103(14)	144(17)	62(10)	27(10)	-16(9)	16(12)
B(1)	57(14)	27(10)	32(11)	-2(8)	-8(9)	-11(9)
B(2)	22(9)	52(13)	44(12)	-12(10)	-2(8)	-8(9)
B(3)	28(10)	23(9)	55(13)	1(8)	15(9)	8(7)
B(4)	19(9)	36(11)	81(17)	-4(11)	9(10)	-4(8)
B(5)	30(11)	46(13)	69(16)	-11(12)	-14(10)	3(9)

B(6)	27(10)	32(10)	49(12)	-4(9)	11(9)	-9(8)
B(7)	49(13)	31(10)	35(11)	4(8)	-4(9)	2(9)
B(8)	90(20)	52(16)	80(20)	-1(14)	-43(18)	24(15)
B(9)	65(17)	78(19)	39(13)	12(13)	19(12)	10(15)
B(10)	48(15)	110(30)	65(18)	59(18)	2(13)	14(16)

Table S5. Hydrogen coordinates (x 10^4) and isotropic displacement parameters (Å^2 x 10^3) for $[Cu_{10}(S(CH_2)_2N(Me)CH_2-)_2(MeCN)_8][BF_4]_6\cdot(MeCN)_{2.25}$.

H atom	x	y	z	U(eq)
H(1A)	7632	-2455	-1580	40
H(1B)	7629	-2878	-1157	40
H(2A)	9128	-2258	-1227	29
H(2B)	8486	-2352	-638	29
H(3A)	8460	-3213	-517	65
H(3B)	8980	-2976	45	65
H(3C)	9510	-3357	-309	65
H(4A)	10200	-2511	-66	41
H(4B)	10501	-2322	-722	41
H(5A)	11773	-2758	-378	46
H(5B)	11062	-3149	-239	46
H(6A)	12478	-2698	-1343	57
H(6B)	11497	-2492	-1581	57
H(6C)	11960	-2888	-1940	57
H(7A)	12472	-3478	-1014	41
H(7B)	11470	-3702	-859	41
H(8A)	11995	-3982	-1788	39
H(8B)	12158	-3509	-2059	39
H(9A)	10018	-4309	-4671	38
H(9B)	10645	-3897	-4491	38
H(10A)	11596	-4494	-4850	40
H(10B)	11922	-4326	-4186	40
H(11A)	10652	-5167	-4913	62
H(11B)	9880	-4934	-4491	62
H(11C)	10302	-5392	-4295	62
H(12A)	12656	-4971	-4054	46
H(12B)	12195	-5325	-4503	46
H(13A)	11522	-5693	-3667	39
H(13B)	12639	-5633	-3527	39
H(14A)	13175	-5167	-2706	50
H(14B)	12473	-4811	-2429	50
H(14C)	12826	-4773	-3123	50
H(15A)	12002	-5671	-2363	38
H(15B)	10990	-5709	-2702	38
H(16A)	11487	-5087	-1788	26
H(16B)	10691	-5457	-1726	26
H(17A)	8210	-4306	-765	39
H(17B)	7606	-3878	-906	39
H(18A)	6649	-4470	-560	26
H(18B)	6292	-4268	-1197	26

Table S5. Hydrogen coordinates (x 10^4) and isotropic displacement parameters (Å^2 x 10^3) for $[Cu_{10}(S(CH_2)_2N(Me)CH_2-)_2(MeCN)_8][BF_4]_6\cdot(MeCN)_{2.25}$.

H atom	x	y	z	U(eq)
H(19A)	8296	-5052	-1164	46
H(19B)	7533	-5428	-1064	46
H(19C)	7678	-5066	-550	46
H(20A)	5942	-5281	-926	34
H(20B)	5442	-4894	-1294	34
H(21A)	6422	-5605	-1822	56
H(21B)	5307	-5505	-1893	56
H(22A)	5461	-4706	-2967	72
H(22B)	5326	-4611	-2252	72
H(22C)	4757	-4999	-2570	72
H(23A)	5822	-5538	-3096	39
H(23B)	6853	-5614	-2796	39
H(24A)	6379	-4933	-3634	37
H(24B)	7075	-5331	-3779	37
H(25A)	6078	-3948	-3615	48
H(25B)	5942	-3495	-3274	48
H(26A)	6507	-3621	-4515	42
H(26B)	5576	-3371	-4289	42
H(27A)	5676	-2657	-3910	70
H(27B)	6693	-2427	-3837	70
H(27C)	6388	-2799	-3370	70
H(28A)	6816	-3064	-5138	69
H(28B)	6243	-2653	-4894	69
H(29A)	7595	-2304	-4652	87
H(29B)	7740	-2491	-5329	87
H(30A)	9115	-2980	-5518	128
H(30B)	8259	-3288	-5315	128
H(30C)	9289	-3339	-5003	128
H(31A)	9156	-2283	-4303	75
H(31B)	9664	-2439	-4917	75
H(32A)	10606	-2538	-4002	63
H(32B)	10495	-2965	-4411	63
H(34A)	4434	-3122	-1440	83
H(34B)	4903	-3406	-905	83
H(34C)	4336	-3635	-1454	83
H(36A)	11451	-5166	-323	115
H(36B)	10879	-4949	230	115
H(36C)	11828	-4727	-23	115
H(38A)	7943	-4531	-5988	50
H(38B)	8989	-4332	-5903	50

Table S5. Hydrogen coordinates (x 10^4) and isotropic displacement parameters (Å^2 x 10^3) for $[Cu_{10}(S(CH_2)_2N(Me)CH_2-)_2(MeCN)_8][BF_4]_6\cdot(MeCN)_{2.25}$.

H atom	x	y	z	U(eq)
H(38C)	8083	-4021	-5956	50
H(40A)	13554	-3190	-4533	229
H(40B)	12628	-3402	-4841	229
H(40C)	13381	-3698	-4481	229
H(40D)	14220	-3605	-3178	229
H(40E)	13948	-3162	-2849	229
H(40F)	14019	-3183	-3580	229
H(42A)	12124	-1718	-2212	112
H(42B)	11917	-1512	-2871	112
H(42C)	12434	-1970	-2819	112
H(44A)	6071	-1792	-2788	95
H(44B)	6588	-1439	-3204	95
H(44C)	6685	-1417	-2473	95
H(46A)	8636	-6044	-734	122
H(46B)	9685	-6174	-953	122
H(46C)	8802	-6487	-1092	122
H(48A)	8814	-6572	-4225	77
H(48B)	9161	-6214	-4700	77
H(48C)	8066	-6232	-4498	77
H(49A)	3191	-706	25	22
H(49B)	2550	-1120	171	22
H(50A)	1652	-500	-169	22
H(50B)	1280	-707	457	22
H(51A)	2581	181	-140	53
H(51B)	3340	-16	335	53
H(51C)	2772	415	503	53
H(52A)	509	-73	574	46
H(52B)	1039	319	241	46
H(53A)	1500	616	1166	43
H(53B)	385	511	1224	43
H(54A)	-166	2	1918	75
H(54B)	534	-357	2194	75
H(54C)	277	-358	1479	75
H(55A)	855	495	2433	39
H(55B)	1887	605	2160	39
H(56A)	1432	-116	2921	40
H(56B)	2147	269	3095	40
H(57A)	5139	-775	3947	42
H(57B)	5822	-1159	3728	42
H(58A)	6680	-526	4119	44

Table S5. Hydrogen coordinates (x 10^4) and isotropic displacement parameters (Å^2 x 10^3) for $[Cu_{10}(S(CH_2)_2N(Me)CH_2-)_2(MeCN)_8][BF_4]_6\cdot(MeCN)_{2.25}$.

H atom	x	y	z	U(eq)
H(58B)	7028	-683	3457	44
H(59A)	5555	-32	4221	45
H(59B)	4868	-18	3632	45
H(59C)	5555	380	3781	45
H(60A)	7688	-41	3342	42
H(60B)	7202	295	3805	42
H(61A)	6469	665	2963	43
H(61B)	7599	644	2845	43
H(62A)	7517	-164	1737	64
H(62B)	7896	-195	2429	64
H(62C)	8167	212	2017	64
H(63A)	7006	678	1658	32
H(63B)	6004	710	2004	32
H(64A)	6489	84	1089	33
H(64B)	5675	445	1025	33
H(65A)	7033	-1013	981	39
H(65B)	7246	-1479	1268	39
H(66A)	6469	-1305	94	49
H(66B)	7467	-1536	239	49
H(67A)	7537	-2243	598	53
H(67B)	6585	-2524	658	53
H(67C)	6836	-2168	1165	53
H(68A)	6766	-2227	-415	40
H(68B)	6053	-1835	-552	40
H(69A)	5195	-2467	-720	45
H(69B)	5518	-2657	-67	45
H(70A)	4541	-1678	-589	51
H(70B)	3586	-1707	-193	51
H(70C)	3743	-2028	-757	51
H(71A)	3466	-2644	-168	33
H(71B)	4133	-2765	406	33
H(72A)	2699	-2568	809	27
H(72B)	2638	-2147	386	27
H(73A)	1219	-1094	2904	48
H(73B)	1043	-1537	2543	48
H(74A)	1689	-1446	3777	60
H(74B)	732	-1681	3555	60
H(75A)	1501	-2649	3169	62
H(75B)	1661	-2321	2613	62
H(75C)	729	-2282	3029	62

Table S5. Hydrogen coordinates (x 10^4) and isotropic displacement parameters (Å^2 x 10^3) for $[Cu_{10}(S(CH_2)_2N(Me)CH_2-)_2(MeCN)_8][BF_4]_6\cdot(MeCN)_{2.25}$.

H atom	x	y	z	U(eq)
H(76A)	1427	-2409	4158	69
H(76B)	2082	-2011	4371	69
H(77A)	2983	-2653	4476	76
H(77B)	2780	-2773	3771	76
H(78A)	4487	-2105	4634	102
H(78B)	3458	-1882	4604	102
H(78C)	4303	-1707	4182	102
H(79A)	4853	-2673	4064	69
H(79B)	4327	-2786	3430	69
H(80A)	5779	-2487	3195	57
H(80B)	5587	-2084	3636	57
H(82A)	6081	183	-605	99
H(82B)	6177	-251	-996	99
H(82C)	6954	-138	-480	99
H(84A)	-612	-1365	682	69
H(84B)	-499	-1874	589	69
H(84C)	-36	-1548	107	69
H(86A)	3766	-976	5218	65
H(86B)	2729	-763	5262	65
H(86C)	3654	-463	5227	65
H(88A)	9026	-1339	2142	162
H(88B)	9042	-1852	2213	162
H(88C)	9192	-1552	2802	162
H(90A)	4376	1470	456	62
H(90B)	3416	1279	162	62
H(90C)	4410	1037	60	62
H(90D)	4609	1520	942	62
H(90E)	3557	1693	1081	62
H(90F)	3748	1407	483	62
H(92A)	3082	1371	3556	85
H(92B)	4181	1489	3667	85
H(92C)	3693	1115	4060	85
H(94A)	7582	-3011	1860	87
H(94B)	7133	-3414	1504	87
H(94C)	7118	-3399	2237	87
H(96A)	1821	-3641	1785	86
H(96B)	1149	-3246	1969	86
H(96C)	1631	-3536	2492	86
H(98A)	9789	1834	1356	108
H(98B)	8661	1899	1416	108

Table S5. Hydrogen coordinates (x 10^4) and isotropic displacement parameters (Å^2 x 10^3) for $[Cu_{10}(S(CH_2)_2N(Me)CH_2-)_2(MeCN)_8][BF_4]_6\cdot(MeCN)_{2.25}$.

H atom	x	y	z	U(eq)
H(98C)	9088	1660	829	108
H(10C)	-1383	6800	3126	82
H(10D)	-522	6936	2689	82
H(10E)	-307	6685	3315	82
H(10F)	-947	8718	3957	93
H(10G)	-1395	8509	4560	93
H(10H)	-2034	8561	3954	93
H(10I)	4049	-1250	-1565	101
H(10J)	4332	-844	-1977	101
H(10K)	4141	-783	-1260	101
H(10L)	-5733	4325	5796	98
H(10M)	-5770	3907	6223	98
H(10N)	-6001	3868	5505	98